

# Foreword

The book is meant primarily for physicists, but it will also appeal to workers in chemistry, biology, medicine, and related fields. It is written by Vladimir N. Binhi, a well-known expert in magnetobiology and a member of the American Bioelectromagnetics Society.

Electromagnetobiology is a fast-developing field of research, its practical and environmental aspects being a topic of ever-increasing number of books. At the same time, physically, the biological effects of weak magnetic fields are still regarded as a paradox. The book comes to grips with that problem and fills in a theoretical gap. It reviews and analyzes the experimental evidence that yields some insights into the primary physical processes of magnetoreception and the frequency and amplitude spectra of the action of weak magnetic fields. Also, the book reviews the available hypothetical mechanisms for that action.

The methodology used in the book enables any physical idea to be quickly

assessed in terms of its value for magnetobiology. The author proposes a unified foundation to account for the biological effects of magnetic fields. Of especial interest is his hypothesis of the interference of quantum states of ions and molecules put forth to explain the paradoxes of the non-thermal action of electromagnetic fields.

Binhi draws on fundamental physical principles to derive a reasonable model for the interaction of electromagnetic fields with biological systems. The model agrees well with experiment and is essentially a thorough formulation of this interaction problem. The theory awaits elaboration, a fact that is bound to attract to that field new workers to whom the book could be recommended as a proper introduction.

The subject of the book could also be referred to as magnetobiological spectroscopy, in which data on physical processes in biophysical structures are derived by physical as well as biological means. It is safe to say that a new field, magnetobiology, has made its appearance in theoretical biophysics. This field still continues to cause much discussion, but it calls for more sophisticated studies to be carried out using rigorous mathematical and physical tools.

A. M. Prokhorov  
member of the Russian Academy of Sciences  
winner of the Nobel Prize for Physics

A handwritten signature in black ink, appearing to be 'A. M. Prokhorov', written in a cursive style.

# Acknowledgements

It is a pleasure to express my deep sense of obligation to A. M. Prokhorov who has found time to go over the book and make valuable comments. I am grateful to E. E. Fesenko. His support of original studies and discussions of the issue influenced the structure of the book and the interplay of its parts. I also thank V. A. Milyaev for useful discussions and for making my cooperation with the Institute of General Physics possible.

I thank H. Berg, F. Bersani, C. Blackman, R. Fitzsimmons, R. Goldman, B. Greenebaum, Yu. G. Grigoriev, A. Liboff, V. P. Makarov, S. D. Zakharov, and A. V. Zolotaryuk for their reviews, comments, and assistance.

Discussions with colleagues and friends have always been an invaluable source of new insights. I record my thanks to A. E. Akimov, I. Ya. Belyaev, O. V. Betskii, L. A. Blumenfeld, M. Fillion-Robin, R. Goldman, Yu. I. Gurfinkel, A. P. Dubrov, A. A. Konradov, V. K. Konyukhov, A. N. Kozlov, V. V. Lednev, V. I. Lobyshev, A. V. Savin, S. E. Shnoll, I. M. Shvedov, and E. V. Stepanov.

Translators A. Repiev and M. Edelev, two bilingual physicists, deserve particular credit for the fact that the English version of the book is more readable than its Russian original.

At various times I received much assistance from my parents and relatives. Their generous encouragement made the book possible. Special thanks are due to E. Tourantaeva, who has taken immense pains in the production of this work and whose skill and forbearance have greatly eased my task.

Vladimir Binhi

# Physical notation

$m_e, m_p$	masses of the electron and proton, respectively
$M, q$	mass and electric charge of a particle
$S, \mu$	spin in units of $\hbar$ and magnetic moment of a particle
$\gamma = \mu/\hbar S$	gyromagnetic ratio
$I$	moment of inertia
$\chi$	magnetic susceptibility
$\mathbf{A}, A_0$	vector and scalar potentials of an EM field
$\mathbf{H}, \mathbf{B}$	strength and induction of a magnetic field
$\mathbf{E}, \mathbf{D}$	strength and displacement of an electric field
$H_{\text{DC}}, H_{\text{AC}}$	strength of DC and AC magnetic fields
$h' = H_{\text{AC}}/H_{\text{DC}}$	relative amplitude of a magnetic field
$\Omega$	circular frequency of an external field
$\Omega_c = qH_{\text{DC}}/Mc$	cyclotron frequency
$f' = \Omega/\Omega_c$	relative frequency of a magnetic field
$\Omega_N = \gamma H_{\text{DC}}$	NMR frequency
$\Omega_R = \gamma H_{\text{AC}}$	Rabi frequency
$\Gamma = \Omega_N/\Omega_c = \gamma Mc/q$	ion–isotope constant
$\omega_0 = \Omega_c/2$	Larmor frequency
$\omega_1 = qH_{\text{AC}}/2Mc$	Larmor frequency in terms of the amplitude of a magnetic field
$L, H$	Lagrange and Hamilton functions
$\mathcal{H}$	Hamiltonian operator
$\mathbf{P}, \mathcal{P}, p, \mathbf{L}, \mathcal{L}, l$	vector and scalar operators of the momentum and angular momentum and their eigenvalues
$\mathbf{S} = \boldsymbol{\sigma}/2, \mathcal{S}$	vector and scalar spin operators
$\mathbf{I}, \mathcal{I}$	same for the nuclear spin
$\mathcal{M} = \mu\mathbf{S}/S$	magnetic moment operator
$\boldsymbol{\sigma} = (\sigma_1, \sigma_2, \sigma_3)$	Pauli matrices
$\Psi$	wave function
$\psi_i, \varepsilon_i$	eigenfunctions and eigenvalues of the Hamiltonian
$m$	magnetic quantum number
$\mathcal{T}$	absolute temperature

# Mathematical notation

$\mathbf{a}\mathbf{b}$	scalar product of vectors
$\mathbf{a} \times \mathbf{b}$	vector product
$\langle \dots \rangle$	quantum-mechanical averaging
$\{ , \}$	commutation operator
$E[\dots]$	mathematical expectation
$\sim$	equal in order of magnitude
$\Re, \Im$	real and imaginary parts
$\delta$	delta function

# Fundamental constants

$e = 4.803 \cdot 10^{-10}$	electron charge (CGS system)
$\hbar = 1.055 \cdot 10^{-27} \text{ erg s}$	Planck constant
$c = 2.998 \cdot 10^{10} \text{ cm s}^{-1}$	velocity of light in a vacuum
$m_e = 9.109 \cdot 10^{-28} \text{ g}$	electron mass
$m_p = 1.673 \cdot 10^{-24} \text{ g}$	proton mass
$\mu_B = e\hbar/2m_e c = 9.274 \cdot 10^{-21} \text{ erg G}^{-1}$	Bohr magneton
$\mu_N = e\hbar/2m_p c = 5.051 \cdot 10^{-24} \text{ erg G}^{-1}$	nuclear magneton
$\mu_p = 2.7928 \mu_N$	proton magnetic moment
$\kappa = 1.3807 \cdot 10^{-16} \text{ erg K}^{-1}$	Boltzmann constant
$N_A = 6.022 \cdot 10^{23} \text{ mol}^{-1}$	Avogadro number

# Some physical quantities

$\kappa T \approx 4.6 \cdot 10^{-14} \text{ erg}$	thermal energy at $T = 300 \text{ K}$
$1 \text{ amu} = 1.661 \cdot 10^{-24} \text{ g}$	atomic mass
$1 \text{ A/m} = 1.26 \cdot 10^{-2} \text{ Oe}$	magnetic field strength
$1 \text{ V/m} = 0.333 \cdot 10^{-4} \text{ CGS units}$	electric field strength
$1 \text{ D} = e \cdot 1 \text{ \AA} = 3.336 \cdot 10^{-30} \text{ C m}$	electric dipole moment
$= 10^{-18} \text{ CGS units}$	
$1 \text{ ohm} = 1.11 \cdot 10^{-12} \text{ CGS units}$	electric resistance
$1 \text{ mW/cm}^2 = 10^4 \text{ erg/(m}^2\text{s)}$	energy flux
$1 \text{ cm}^{-1} = 30 \text{ GHz}$	frequency ( $f/c = \lambda^{-1}$ )
$1 \text{ eV} = 1.602 \cdot 10^{-12} \text{ erg}$	energy

# 1

---

## INTRODUCTION

There were also two choruses, one of which somehow managed to represent the de Broglie's waves and the logic of history, while the other chorus, the good one, argued with it.

V. Nabokov, *The Gift*

Magnetobiology is a new multidisciplinary domain with contributions coming from fields as diverse as physics and medicine. Its mainstay, however, is biophysics. Magnetobiology has only received a remarkable impetus in the recent two decades. At the same time magnetobiology is a subject matter that during the above relatively long time span failed to receive a satisfactory explanation. There is still no magnetobiological theory, or rather its general physical treatments, or predictive theoretical models. This is all due to the paradoxical nature of the biological action of weak low-frequency magnetic fields, whose energy is incomparable by far with the characteristic energy of biochemical transformations. This all makes the very existence of the domain quite dubious with most of the scientific community, despite a wealth of experimental evidence.

A large body of observational evidence gleaned over years strongly suggests that some electromagnetic fields pose a potential hazard to human health and are a climatic factor that is of no less significance than temperature, pressure, and humidity. As more and more scientists become aware of that fact, studies of the mechanisms of the biological action of electromagnetic fields become an increasingly more topical issue.

There being no biological magnetoreceptors in nature, it is important to perceive the way in which the signal of a magnetic field is transformed into a response of a biological system. A low-frequency magnetic field permeates a living matter without any apparent hindrances. It affects all the particles of the tissue, but not all of the particles are involved in the process of the transferring of information about the magnetic field to the biological level. Primary processes of the interaction of a magnetic field with matter particles, such as electrons, atoms, and molecules, are purely physical processes. Charged particles of living matter, ions, that take part in biophysical and biochemical processes seem to be intermediaries in the transfer of magnetic field signals to the next biochemical level. Such a subtle regulation of the activity of proteins of enzyme type, affected via biophysical mechanisms involving

interim ions, shifts the metabolic processes. Beginning with that level one can gauge the action of a magnetic field from the changes in metabolic product densities.

The biological effects of a magnetic field are often observed from the life-support parameters and the behavior of individuals and populations. Experiments, as a rule, boil down to the observation of relations between an external magnetic field and the biological effects it causes. Intermediary levels of the organization of a living system, such as biophysical, biochemical, and physiological ones, appear to lie outside the experimental range, but anyway they affect the experimental results. We thus end up having a kind of a cause-and-effect black box with properties beyond our control. This does not allow any cause-effect relations to be worked out completely. At the same time, there is no practical way to observe the result of the action of weak magnetic fields at the level of individual biochemical reactions or biophysical structures using physical or chemical methods. Magnetobiology is thus fraught with practical difficulties caused by the fact that it necessarily combines issues of physics, biophysics, biochemistry, and biology.

In addition to an analytical review of magnetobiological studies, the book also provides the first detailed description of the effect of the interference of quantum ion states within protein cavities. Using the Schrödinger and Pauli equations, a treatment is given of ion dynamics for idealized conditions and for parallel magnetic fields, as well as for a series of other combinations of magnetic and electric fields. The treatment takes into consideration the ion nuclear spin and the non-linear response of a protein to the redistribution of ion probability density. Formulas are obtained for the magnetic-field-dependent component of the dissociation probability for an ion-protein complex. The principal formula that gives possible magnetobiological effects in parallel DC  $H_{DC}$  and AC  $H_{AC}$  magnetic fields has the form<sup>1</sup>

$$P = \sum_{m \neq m'; n} |a_{mm'}|^2 \frac{\sin^2 A}{A^2} J_n^2 \left( \frac{\Delta m h'}{2 f'} \right), \quad A = \left( \frac{1}{2} \Delta m + n f' \right) \Xi.$$

Here  $m$  is the magnetic quantum number,  $\Delta m = m - m'$ ,  $\Xi = T\Omega_c$  is a dimensionless parameter that depends on the properties of an ion-protein complex,  $\Omega_c = qH_{DC}/Mc$  is the cyclotron frequency of an ion,  $f' = \Omega/\Omega_s$  and  $h' = H_{AC}/H_{DC}$  are the dimensionless frequency and amplitude of the variable components of a magnetic field, and  $J_n$  is the  $n$ th order Bessel function. The elements  $a_{mm'}$  are constant coefficients that define the initial conditions for an ion to stay in a cavity. The natural frequency and amplitude interference spectra are worked out for a wide variety of magnetic conditions, including those of pulsed magnetic fields (MFs), for a “magnetic vacuum”, subjected to natural rotations of macromolecules, etc. They show a high level of agreement with available experimental data.

---

<sup>1</sup>The book provides formulas to compute probable biologically active regimes of exposure to an EMF. We note that their practical application is fraught with unpredictable consequences, specifically with risks to human health.

The interference of quantum states of the molecules rotating inside protein cavities, i.e., the interference of molecular gyroscopes, is considered. The properties of molecular gyroscopes are a consistent basis for explaining the physical mechanism of the non-thermal resonance-like biological effects of EMFs, and for solving the so-called “kT problem”.

## 1.1 AN OVERVIEW OF MAGNETOBIOLOGICAL ISSUES

Unlike biomagnetism, which studies the MFs produced by various biological systems (Vvedenskii and Ozhgin, 1986; Kholodov *et al.*, 1990; Hämäläinen *et al.*, 1993; Baumgartner *et al.*, 1995), magnetobiology addresses the biological reactions and mechanisms of the action of primarily weak, lower than 1 mT, magnetic fields. Recent years have seen a growing interest in the biological actions of weak magnetic and electromagnetic fields. “Microwave News”, published in the USA, provides a catalogue of hundreds of Internet links to organizations that are directly concerned with electromagnetobiological studies, <http://www.microwavenews.com/www.html>.

Electromagnetobiology is a part of a more general issue of the biological effectiveness of weak and hyperweak physico-chemical factors. It is believed that the action of such factors lies below the trigger threshold for protective biological mechanisms and is therefore prone to accumulating at the subcellular level and is likely at the level of genetic processes.

Electromagnetobiological research received an impetus in the 1960s when Devyatkov’s school developed and produced generators of microwave EM radiations. Almost immediately it was found that microwaves caused noticeable biological effects (Devyatkov, 1973). Those works were reproduced elsewhere. Of much interest was the fact that more often than not the radiations concerned had a power too low to cause any significant heating of tissues. At the same time, the radiation energy quantum was two orders of magnitude lower than the characteristic energy of chemical transformations  $\kappa\mathcal{T}$ . Also, the effects were only observed at some, not all, frequencies, which pointed to a non-thermal nature of the effects. The action of microwaves was also dependent on the frequency of low-frequency modulation. Therefore, as early as the 1980s reliable observations of bioeffects of low-frequency 10–100 Hz magnetic fields themselves were obtained. This is important, since that frequency range covers frequencies of industrial and household electric appliances.

Interest in magnetobiology stems predominantly from ecological considerations. The intrusion of man into natural processes has reached a dangerous level. The environment is polluted with the wastes of industrial and household activities. We are also witnessing a fast buildup of electromagnetic pollution. In addition, there is still no clear understanding of the physico-chemical mechanisms for the biological action of hyperweak natural and artificial agents. We have thus a paradox on our hands. That is to say, these phenomena are not just unaccountable, they seem to be at variance with the current scientific picture of the world. At the same time, a wealth of observational and experimental data has been accumulated, thus

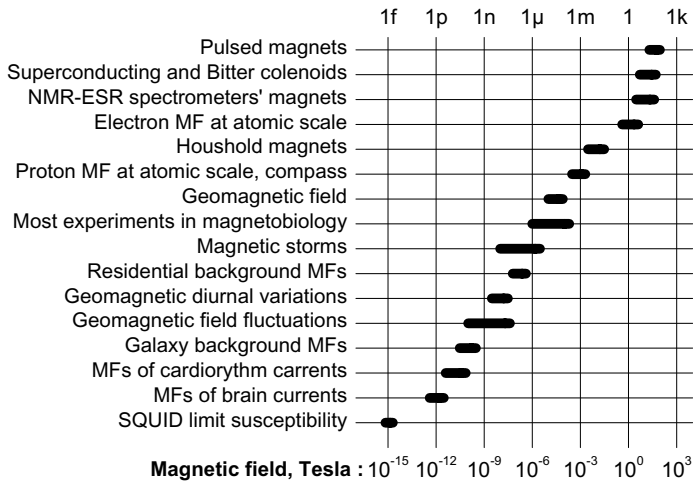


**Figure 1.1.** Levels of various natural and man-made sources; approximate boundaries are indicated.

pointing to the real nature of the phenomenon. It follows that the biological action of hyperweak agents is a fundamental scientific problem with a host of applications.

What factors can be called hyperweak? An intuitively acceptable threshold is dictated by common sense. If an effect, or rather a correlation, observed when exposed to some small signal is inconsistent with current views, i.e., we have a that-is-impossible situation, then the signal can be referred to as hyperweak. For electromagnetic fields (EMFs) within a low-frequency range it is a background level, which is engendered by industrial or even household electric devices (Grigoriev, 1994). The diagram in Fig. 1.1 shows the relative level of magnetic fields that characterize their sources and application fields. Figure 1.2 contains information on the spectral composition of a low-frequency MF of natural origins. The spectrum, especially its part below 1 kHz, is strongly dependent on the place of measurement, weather, season, etc.; therefore it is only conventional in nature. Municipal magnetic noise in the same spectral range, except for its discrete components 50 Hz and harmonics, is one or two orders of magnitude higher than the natural background.

Earlier on it had been believed that weak low-frequency MFs and EMFs of non-thermal intensity were safe for humans, and a biological action of such fields had seemed to be impossible in terms of physics. With time, experimental evidence has been gleaned that pointed to a potential danger of those fields and radiations (Pool, 1990a; Nakagawa, 1997), and the often-concealed nature of their action. Consequences may show themselves months or even years later. The ecological pertinence of magnetic fields becomes a subject of investigations. Sanitary norms, prognostication, and control of and protection against electromagnetic smog are important

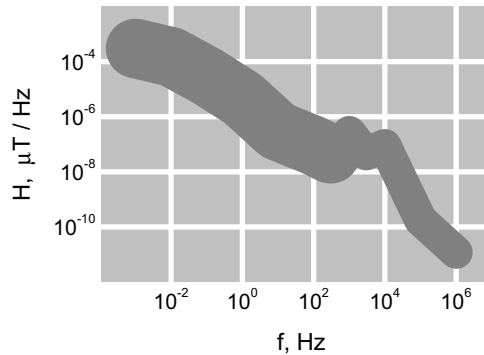


**Figure 1.2.** Spectral density of fluctuations of low-frequency MFs from natural sources; adapted from Vladimirskii (1971).

aspects of electromagnetic ecology. Standards of electromagnetic safety are worked out by various national and international organizations, such as Comité Européen de Normalisation Electrotechnique (CENELEC), Deutsche Institut für Normung (DIN), American National Standards Institute (ANSI), International Non-Ionising Radiation Committee of International Radiation Protection Association (INIRC IRPA), and Occupational Health Institute of the Russian Academy of Sciences. The World Health Organization (WHO) coordinates that activity with a view to achieve unified world standards. At present, safety norms for various ranges may differ tens or even hundreds of times, which strongly suggests that this domain awaits in-depth scientific studies.

The biological action of interest is that produced by systems and devices whose “services” are hard to do without: power transmission lines, cars, TV sets, background radiations of dwellings, and manufacturing facilities. Special culprits of late are computers and radio telephones (Carlo, 2000). A quantitative indication of the power-frequency EMF level coming from power transmission lines is given in Fig. 1.3, which provides the theoretical distribution of electric and magnetic fields with the distance from a line.

Radiations produced by household appliances have been measured many times. For instance, measurements of the 50-Hz MF conducted by Conti *et al.* (1997) within half a meter from household appliances yielded the following roughly averaged data: a washing machine —  $5 \mu\text{T}$ , a refrigerator —  $0.1 \mu\text{T}$ , a conditioner —  $1 \mu\text{T}$ , an electric meat grinder —  $2 \mu\text{T}$ , a vacuum cleaner —  $2 \mu\text{T}$ . The range of  $\sim 0.1\text{--}1 \mu\text{T}$  is characteristic of the majority of office and public premises and vehicles, although peak values may be three orders of magnitude higher.

Intensity distributions of background magnetic fields in the range of 30–2000 Hz in town (Göteborg City, Sweden) were studied by Lindgren *et al.* (2001). It appeared that up to 50% of the population were exposed to MFs higher than

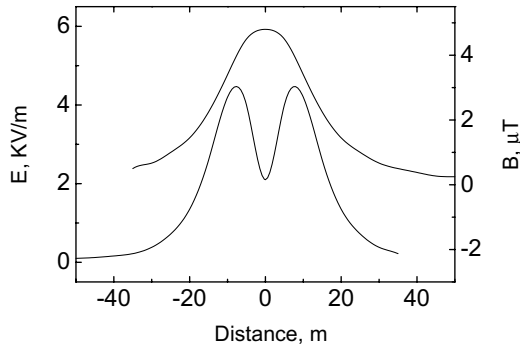


**Figure 1.3.** Mean EMF profiles 1 m from the ground for a standard 380-kV, 50-Hz line at 400 A, according to Conti *et al.* (1997).

0.2  $\mu\text{T}$ , and around 5% were exposed to 1  $\mu\text{T}$ .

The biological significance of such electric and magnetic fields has been revealed in many epidemiological studies (e.g., Tenforde, 1992) initiated by the work of Milham, Jr (1982) on the mortality of workers with higher EMF exposures. One of the last reviews on the subject (Nakagawa, 1997) contains an analysis of 31 positive and 13 negative results pointing to doubled cancer risks for populations living near electric transmission lines and workers in energy-intensive industries. In all the cases, the mean MF level lay in the interval 0.1–10  $\mu\text{T}$ . Grigoriev (1994) pointed out that it is necessary to continually monitor background ambient electromagnetic fields.

“Electromagnetic weather”, i.e., exposure to space and geophysical electromagnetic factors, such as magnetic storms (0.1–1  $\mu\text{T}$ ), has long become an indispensable topic at International Biometeorology Congresses.

The EMF of electric household appliances can also inflict its harmful action in an indirect manner. It is common knowledge that under normal conditions the ambient air inside dwellings contains some natural aeroions due to the ionization of the air by decay products of radioactive radon. Its concentration is about several thousand ions per cubic centimeter. That fact of nature is not indifferent for the vital activity (Andreeva *et al.*, 1989). The screen of a standard monitor, which normally possesses a high positive potential, attracts negative aeroions and repulses positive ones.<sup>2</sup> Aeroions are thus totally removed from the area around the computer operator (Akimenko and Voznesenskii, 1997). WHO experts regard work with a computer monitor, which in addition to its indirect actions emits EMFs within a wide frequency range, as a stress factor.

---

<sup>2</sup>Modern monitors have applied onto their screens special-purpose layers that reduce the electrostatic potential.

The correlation of EMFs with cardio-vascular incidences is a subject of many studies. In that respect, also of significance are EMFs of natural origins, specifically the geomagnetic field (GMF).

The most extensively studied issue is cancer risks (Wilson *et al.*, 1990; Pool, 1990b; Goodman and Henderson, 1990; Stevens *et al.*, 1997), a topic of hundreds of publications (Nakagawa, 1997). The American Journal of Epidemiology has recently devoted a collection of materials just to one concern — EMFs and brain tumors in children (Preston-Martin *et al.*, 1996). Some works maintain that findings do not support the hypothesis of carcinogenic effects of the magnetic fields of high-voltage lines, electric heaters, and other household appliances (Verreault *et al.*, 1990). Others stress the primitive nature of the techniques used to gauge the results of exposure to magnetic fields, the possible systematic control errors and the preliminary nature of those works, and the need for further discussions (Gurney *et al.*, 1995; Lacy-Hulbert *et al.*, 1995).

Long-term exposures to even weak fields are believed to be able to suppress the activity of some clones of the cells of the immune system, thereby impairing the defences of the organism against the multiplication of “foreign” cells (Adey, 1988; Lyle *et al.*, 1988). Another possible mechanism is related to genetic changes induced by an MF (Goodman *et al.*, 1989). There is also evidence that low-frequency MFs are able to affect the synthesis of some peptides that in the organism play the role of some internal biological signals (Goodman and Henderson, 1988; Novikov, 1994). Coghill (1996) indicated that levels of power-frequency EMFs (both electric and magnetic) near beds of children are 1.3–2 times higher for leukemia cases than for healthy children. Recent studies in the UK (documents<sup>3</sup> of the National Radiological Protection Board, 12(1), 2001) provided evidence that relatively heavy average exposures of  $0.4\ \mu\text{T}$  or more are associated with a doubling of the risk of leukemia in children under 15 years of age. Novikov *et al.* (1996) report that under certain conditions weak MFs, in contrast, retard the cancer-producing process.

The *European Journal of Cancer* published a paper by Feychting *et al.* (1995) with the results of extensive long-term studies of cancer in children of Sweden and Denmark. The authors came to the conclusion that their data support the hypothesis of a correlation between the magnetic fields of high-voltage lines and leukemia in children. One of the interested consulting companies has recently issued a comprehensive analysis of the literature on epidemiological investigations concerned with the level of electromagnetic pollution. Their manual, (Sage and Sampson, 1996), contains more than 500 (!) observations and risk assessments related to cancers and pregnancy disorders as a result of exposures to EMFs under household and professional conditions.

Twenty percent of the works at the III Congress of the European Bioelectromagnetics Association in 1996 addressed, to some degree or other, the interrelation between cancer incidence and electromagnetic radiations. On the one hand, it is well established that EMFs in certain cases enhance the carcinogenic effect of some detri-

---

<sup>3</sup>[http://www.nrpb.org.uk/publications/documents\\_of\\_nrpb/abstracts/absd12-1.htm](http://www.nrpb.org.uk/publications/documents_of_nrpb/abstracts/absd12-1.htm)

mental chemical substances and other factors (Wilson *et al.*, 1990). For instance, Juutilainen *et al.* (1996) found that a 50-Hz MF accelerates the development of skin cancer on exposure to UV radiation. It is well known that an MF changes the activity of melatonin enzyme, which is responsible for the fine regulation of the immune system (Wilson *et al.*, 1981; Cremer-Bartels *et al.*, 1984; Lerchl *et al.*, 1991; Kato *et al.*, 1993, 1994; Loscher *et al.*, 1994; Kato and Shigemitsu, 1996; Stevens *et al.*, 1997; Harland and Liburdy, 1997; Blackman *et al.*, 2001). On the other hand, there is no hard correlation with exposure to an MF, and no correlation between a 60-Hz MF and the melatonin level has been found by Lee *et al.* (1995). Juutilainen *et al.* (2000) believe that the effects manifest themselves especially distinctly with long-term exposures to both an EM radiation and chemical carcinogens. Much remains unclear so far, and further studies are in order (Reiter and Robinson, 1993; Taubes, 1993).

We note that such investigations, especially epidemiological ones, are quite active (Aldrich *et al.*, 1992; Theriault *et al.*, 1994). Scientific societies that enjoy governmental support have been established. Also, electromagnetobiological projects have attracted the interest and financial support of manufacturers of radiotelephones and computers. Even realtor brokers have begun to take into consideration the electromagnetic factor in their financial estimations of real estate objects (Lathrop, 1996). At the same time, the American Cancer Society has published in its journal a paper by Heath (1996) with an overview of the findings of epidemiological studies over the past 20 years, which pronounces the epidemiological evidence on the correlation of EMFs with cancer incidence to be “weak, inconsistent, and inconclusive”. Note also the special issue of *Bioelectromagnetics, Supplement 5, 2001*, which summarizes the state of the art of studies on the cancer hazard of background EMFs.

Despite the still negative attitude of physicists to the issues under consideration, the last issue of the *Physical Encyclopedia* contains the following statement (Golovkov, 1990): “Some variations of the geomagnetic field can affect living organisms.” Although this statement is not quite correct,<sup>4</sup> the fact that this phenomenon has been recognized is of importance. Fairly recently, in 1981, M. V. Volkenstein in his monograph *Biofizika* wrote: “there are almost no sound data to date on the action of a DC magnetic field on biological phenomena.” Ten to fifteen years later we have a large body of data on magnetobiology. We should note, by the way, that some works on magnetobiology were published at the turn of the 20th century, see, e.g., a concise overview by Warnke and Popp (1979).

The controversy is fuelled by negative statements made by some members of the international scientific community. So, in the leading American physical journal *Physical Review A* **43**, 1039, 1991, one reads “any biological effects of weak low-frequency fields at the cellular level must be outside of the framework of traditional

---

<sup>4</sup>In the absence of a large body of direct experimental evidence that would provide a reliable confirmation of the biological action of a weakly fluctuating component of an MF, we should speak about a *correlation* of the variation of the GMF and the vital activity of some organisms.

physics.” The American Physical Society has issued a resume (APS Statement, 1995) that doubts the expediency of governmental financing of these investigations. The US National Academy striving to arrive at some final conclusion on this question established an ad hoc commission. A report of the commission (NRC, 1997), which is basically an overview of a voluminous literature on the topic, has instead given rise to a host of questions. Even the members of that commission had different opinions on the report’s conclusions. A year later, on completion of its 5-year research program RAPID<sup>5</sup> concerned with EMFs, the US National Institute of Environmental and Health Studies (NIEHS) published an extensive report to the US Congress (Portier and Wolfe, 1998) that covered about a dozen aspects of the problem. Reading the section on biophysical mechanisms for magnetoreception leaves one in no doubt that professional physicists were largely excluded from the implementation of the program. According to the report, low-frequency MFs can cause cancer in men; there is also another conclusion that animal studies do not support cancer risks (Boorman *et al.*, 2000).

One reason behind such a confounding situation is that the physical mechanisms for the biochemical action of hyperweak EMFs are yet unclear.

The current status of electromagnetobiology, its “nerve”, so to speak, was appropriately addressed in a memorandum of the 1996–1998 presidents R. A. Luben, K. H. Mild, and M. Blank of the American Bioelectromagnetics Society<sup>6</sup> to officers of the House of Representatives and the Senate responsible for budgeting and scientific and technological policy making (Luben *et al.*, 1996). Specifically, the presidents wrote

A wealth of published, peer-reviewed scientific evidence indicates that exposure to different combinations of electric and magnetic fields consistently affects biological systems in living body as well as in laboratories. . . . There is a potential for benefits from these fields as well as the possibility of adverse public health consequences. Understanding their biological effects may allow us to increase the benefits as well as mitigate the possible hazards. (page 4)

The number of overviews of experimental work, all sorts of guidelines, reports, and books in the field of magnetobiology is large and continues to grow. The following is just a short and incomplete list: Presman (1970); Piruzyan and Kuznetsov (1983); Wilson *et al.* (1990); Luben (1991); Polk (1991); Simon (1992); Berg and Zhang (1993); Adey (1993); Bates (1994); Blank (1995); Hitchcock and Patterson (1995); Goodman *et al.* (1995); Hafemeister (1996); Hughes (1996); Sagan (1996); Ueno (1996); Adey (1997); Gandhi (1997); Lin and Chou (1997); Mahlum (1997); Stevens *et al.* (1997), and Repacholi and Greenebaum (1999). Even academic reviews make their appearance (Carpenter and Ayrapetyan, 1994).

A good introduction to electromagnetobiology is a huge tome of the proceedings of the Second World Congress for Electricity and Magnetism in Biology and

---

<sup>5</sup>Research and Public Information Dissemination Program (e.g., Moulder, 2000).

<sup>6</sup>The society has more than 700 members from more than 30 countries.

Medicine edited by Bersani (1999). This book contains more than 230 papers covering a wide variety of aspects, from fundamental physical and biological to socio-political ones. There exists a data base, <http://infoventures.com>, on all the aspects of electromagnetobiology, scientific, medical, and social, which includes as much as 30,000 bibliographic units. Addresses of open bibliographic data bases on individual domains of magnetobiology can be found at <http://www.biomagneti.com>. An interesting assay of the history of electromagnetobiology is given in a monograph by Kholodov (1982). As early as 1986 there was an analysis of more than 6000 literature sources (Kholodov, 1986). Now several thousand papers on electromagnetobiology are published each year, see Fig. 5.19. A historical overview of Russian, mostly experimental, works is contained in a recent publication by Zhadin (2001).

At the same time, there are almost no critical reviews of theoretical work, if only because there are no theoretical works as such. Some papers contain critical reviews in terms of physics of well-known ideas on the mechanisms of exposure to an MF (Kuznetsov and Vanag, 1987; Vanag and Kuznetsov, 1988; Adair, 1991; Binhi, 2001). The available reviews for the most part are concerned with recording ideas (Adey and Sheppard, 1987; Polk, 1991; Grundler *et al.*, 1992; Berg and Zhang, 1993). Several provocative works are attempts at a physical substantiation of some reliably reproducible experiments with weak MFs (Moggia *et al.*, 1997; Binhi, 1997c). These models, at least on the surface of it, contradict neither orthodox physics nor common sense.

Investigations into how to protect against harmful EMF actions are exploding. The most complete protection is only possible under natural conditions, in the country, where the level of “electromagnetic smog” is about three orders of magnitude smaller than in town, Fig. 1.4. Maximal magnetic variations of a technogenic nature are observed on the  $z$ -component of an MF within trams, trains, and near other power-intensive rigs (Tyasto *et al.*, 1995). These variations within the range of 0.05–0.2 Hz can exceed the amplitude of a strong magnetic storm thousandfold.

General measures are known to reduce the risks of diseases due to EMF over-exposures. They boil down to reducing the level of electromagnetic pollution. One snag here is that biological systems themselves are sources of electromagnetic fields (Kholodov *et al.*, 1990); for millennia they have evolved against a background of the Earth’s natural electromagnetic field. Certain fields of natural levels and spectra are useful and even necessary for normal vital activity. Furthermore, there are many efficient therapeutic techniques using EM radiations (Congress WRBM, 1997). Purely practical and perceived uses of electricity and magnetism can be traced down to 1270 (Stillings, 1997). Fundamental works by Devyatkov and Betskii (1994) on microwave technologies paved the way for remedial applications of these electromagnetic radiations. In Russia alone, more than a thousand medical establishments employ about one hundred modifications of EHF devices. For several decades more than a million cases for up to 50 disorders have been successfully treated.

There has been an extensive growth in magnetotherapy worldwide (Bassett, 1984; Congress EMBM, 1997). Low-frequency EM fields are known, e.g., to promote

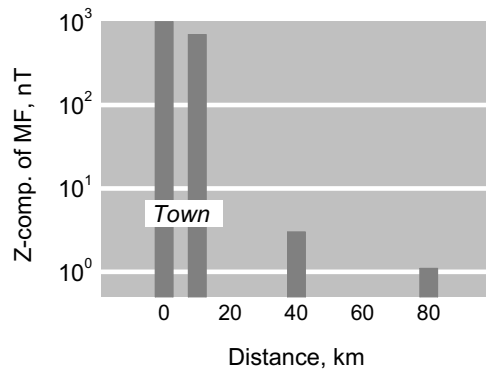


**Figure 1.4.** Mean intensity of the variations of the  $z$ -component of a  $10^{-3}$ -10 Hz magnetic field at St. Petersburg and its environs along the NW-SE line. According to Tyasto *et al.* (1995).

fracture healing in difficult cases (Ryaby, 1998). In a number of cases, a pre-exposure of an organism to a weak low-frequency MF enables its resistance to unfavorable external factors to be drastically improved (Kopylov and Troitskii, 1982). At the same time, the high curative efficiency of EMFs also points to their potential hazard. Here we have an analogy with the uses of chemical preparations. While useful in certain quantities, medicinal preparations may become dangerous if used without control for a long time. Therefore, reducing the risks of diseases due to EM pollution is a complicated scientific and technological problem. The sanitary safety norms for electromagnetic radiations are regulated in Russia by GOST 50949-96 and SNiP 2.2.2.542-96. Internationally known standards are MPR-II, MPR-III, TCO 95-96, and some others.

One promising area of research, in addition to the general reduction in the pollution level, is the use of ... electromagnetic fields! That is no mistake. Just as very small homeopathic doses of drugs are able to compensate for a biological action of the same substances in normal doses, so the action of weak deleterious EMFs can be offset by similar fields, only much weaker ones. Devices based on that principle were shown at the 1996 Congress of the European Bioelectromagnetics Association at Nancy. Works of some scientific groups coordinated by M. Fillion-Robin have shown that these devices reduce the risk of diseases in users of computer monitors and mobile phones (Hyland *et al.*, 1999).

There is some direct evidence suggesting that special-purpose experimental MFs are able to retard the growth and even cause a dissolution of cancer tumors (Muzalevskaya and Uritskii, 1997). Garkavi *et al.* (1990) report a retardation of sarcoma growth in rats exposed to a low-frequency MF, Fig. 1.5.

Hopefully, it will soon become possible to account for the action of low-frequency EMFs at a geomagnetic level, although we are not any closer to an understanding of the biological effects of the geomagnetic field fluctuations, to put it mildly.

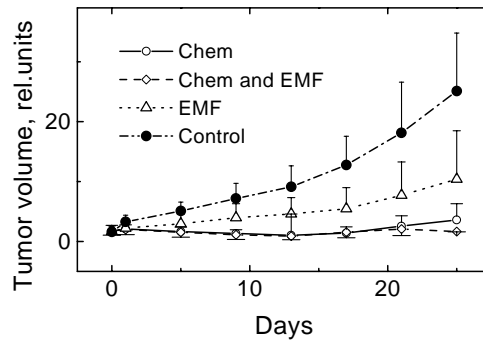


**Figure 1.5.** Sarcoma growth in rat males exposed separately and jointly to cyclophosphamide and a 1-mT MF. According to Garkavi *et al.* (1990).

## 1.2 STATISTICS

The statistics of investigations into magnetobiology, and its integral part electromagnetobiology, is quite interesting. Throughout the decades of the development of the science, the body of publications has grown manifold and its annual vintage now amounts to thousands of papers and reports. To gain an understanding of the world spread of those works, and also of the intrinsic structure of the studies, an analysis is in order of proceedings of major symposia, congresses, and conferences devoted to electromagnetobiology.

The Third International Congress of the EBEA, held in the spring of 1996 at Nancy, France, enjoyed an attendance from 27 countries. Presented were more than two hundred works. Contributions from various nations varied widely, such that Fig. 1.6 gives an indication of the intensity of work in electromagnetobiology throughout the world. The figures are absolute, i.e., numbers of papers presented, and relative, in relation to a country's population in millions. An average input was one report per two million of population. It is noteworthy that the relative figures are roughly similar. This is indicative of the fact that the potential dangers of "electromagnetic smog", the interaction of EMFs with the biosphere as a whole, are concerns of global proportions.

Shown in Fig. 1.7 is the percentage of works on respective topics in electromagnetobiology. Experiments were conducted in fairly equal proportions on prepared living tissues, cells, proteins, and whole biological and social cohorts, including humans. Theoretical works are clearly dominated by engineering calculations of distributions of EMFs in man-made and natural environments. Especially prolific are studies of emissions of mobile phones near the user's head. The absence of

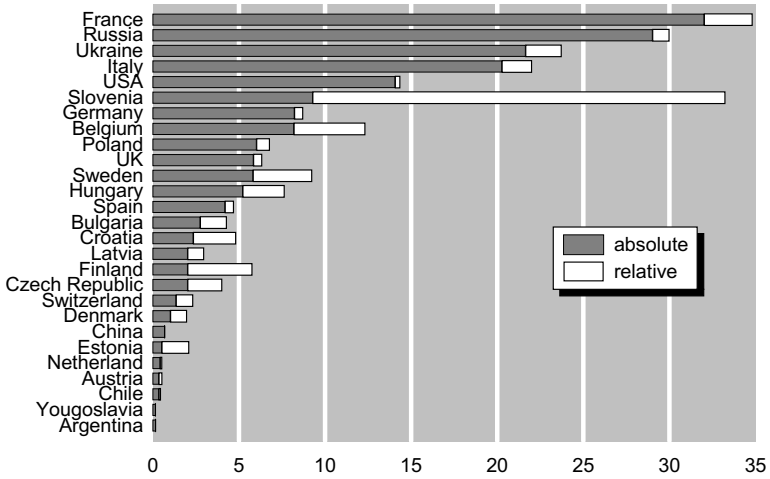


**Figure 1.6.** Absolute numbers of reports and relative contributions of nations to the proceedings of the III EBEA Congress, 1996.

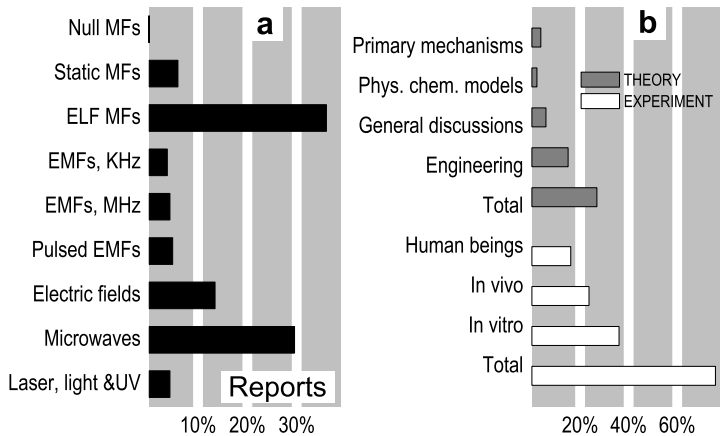


**Figure 1.7.** The structure of the reports presented at the III EBEA Congress. Percentages of the number of works presented: (a) the range of electromagnetic fields; (b) the nature of the works.

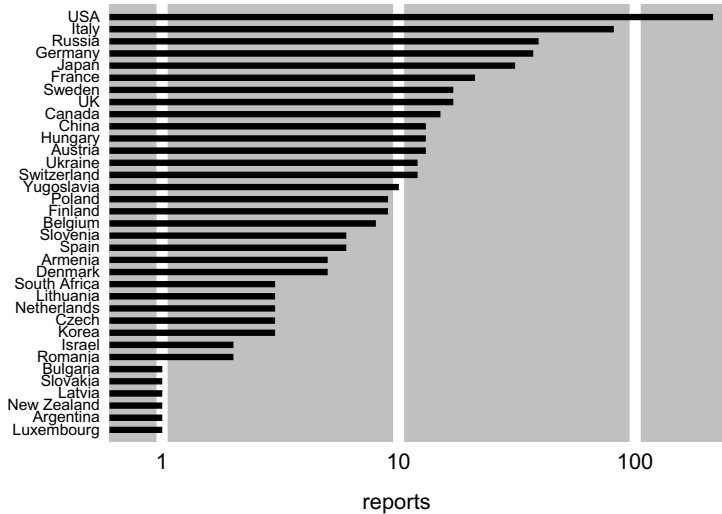


**Figure 1.8.** Distribution of reports at the Second World Congress for Electricity and Magnetism in Biology and Medicine, Bologna, 1997.

productive physical ideas on the primary magnetoreception mechanisms<sup>7</sup> explains the small number of works on the nature of biomagnetic reception, which is a matter of principle for magnetobiology. This was said to be due to the paradoxical nature of magnetobiological effects. The paradox stands out with especial clarity in experiments with low-frequency EMFs, where the field energy quantum is approximately ten orders of magnitude smaller than the characteristic energy of chemical bonds.<sup>8</sup> We have no universally accepted mechanism to date for the biological actions of such fields. It is obvious that this, along with the relative ease of generation of artificial low-frequency fields, accounts for the relatively large number of experiments in this area.

Since 1983 at Pushchino, Russia, symposia for the correlation of a variety of physico-chemical and biological processes with space-physical processes have been held (Shnoll, 1995a). It is to be noted that out of the 57 papers published as proceedings of the 1990 symposium (Pushchino, 1992), 40 % contain discussions of the relation between biospheric processes with geomagnetic perturbations. Out of the 65 contributions to the 1993 symposium, the percentage of such works grew to 55 % (Pushchino, 1995).

<sup>7</sup>The term magnetoreception is used throughout the book in a wide sense as the ability of living systems to respond to changes in magnetic conditions.

<sup>8</sup> Such a comparison however is only of limited use as the interaction of low-frequency EMFs with biophysical targets may be a multiquantum process, see Section 3.12.

**Table 1.1.** Reports of the international congress in St.Petersburg, 1997

---

hyperlow field intensities	3
DC fields	13
electric fields	3
ELF EMFs	41
combined AC–DC fields	5
extreme dose dependences	3
MHz	4
UHF–EHF, microwaves	41
IR, optical and UV	20
EMF target indicated	1
computer models	3
analytical models and estimates	9
water systems	10
engineering R&D	38
general ideas, hypotheses	19
reports with deviations from scientific methodology	59

---

The Second World Congress for Electricity and Magnetism in Biology and Medicine was attended by researchers drawn from 35 countries and had more than 600 contributions, Fig. 1.8. The Congress covered the issues of biology, medicine, technologies, and physics concerned with a variety of manifestations of electromagnetobiology. Discussions centered around several topics: biophysical mechanisms, bioenergetics and electron transport, transfer of biological signals, sensor physiology, microwave effects, electromagnetic epidemiology, radiation level gauges, mobile phone bioeffects, bioelectron devices and biocomputers, EMF treatment of bones and cartilages, electroinjuries and electrotreatments, electroinduced transport of drugs and genes, thermal effects of EMFs, melatonin secretion and EMF action on immune and nerve systems, electric transmission lines and permissible radiation doses, effects of a DC magnetic field, and learning and memory for electromagnetic exposures. Among the co-sponsors of the Congress, in addition to governmental institutions of the USA and Italy, were some industrial corporations concerned with the production and distribution of electric power and well-known manufacturers of mobile phones.

Another remarkable event was the International Congress for “Weak and Hyper-weak Fields and Radiations in Biology and Medicine” that took place in the summer of 1997 in St.Petersburg, Russia (Congress WRBM, 1997). Among the 352 reports presented at the congress, 223 were concerned with electromagnetobiology. Table 1.1 is a breakdown of the reports by topics.

Some reports (about 2-3%) were classed fairly arbitrarily, and there were relatively few analytical studies of EMF action mechanisms. This seems to be due to the uncertainty of targets of that action — only one paper discussed a possible MF target in a living tissue. There were almost no reports wherein static MF was under control, with the natural exception of papers on the bioaction of DC fields themselves. At the same time, there were works galore that contained just speculations unsupported by any factual evidence or statements that could not be proven in principle.

Significantly, there were virtually no reports under the heading of analytical reviews provided in Chapters 2 and 3. Most of the experimental works were not concerned with testing any hypothesis, although nearly always they stressed the unclear nature of the mechanisms involved. As a result, there were many, often similar, works that defied any comments in terms of physics. In substance, they only confirmed the existence of EMF-induced biological effects. Admittedly, it is important to amass a body of factual evidence, especially medical, but the wealth of material available in the world already enables one to plan special-purpose experiments to reveal the primary mechanisms of electro- and magnetoreception.

### 1.3 METHODOLOGICAL NOTES AND TERMS

In order to describe real quantum physical processes they employ the well-established tool kit of quantum mechanics (QM) and quantum electrodynamics (QED). Different processes call for QM and QED mathematical tools of different caliber. Phenomena considered in this work do not require any special mathematical techniques. This is because the subject under study — primary mechanisms for biomagnetic reception — is a relatively new domain of physics, which awaits further elaboration. Therefore, at the first stage of the investigation into magnetobiological effects it is sufficient to employ QM mathematical tools at the level of complexity of most university QM courses, such as laid down in the well-known monographs by Landau and Lifshitz (1977), Blokhintsev (1983), and Davydov (1973).

Discourses on the physical nature of the biological efficiency of an MF use the terms “mechanism” and “model”, the meanings of which are close but still slightly different. The term “mechanism” is used to describe a concept, physical processes, or their progression that may underlie a phenomenon. If it is stressed that a given mechanism is realized via some equations or mathematical relationships that feature a predictive power, the term “model” is used. Cases are possible where there are no models at all, or in contrast, several mathematical models for the same mechanism of biological effectiveness of an MF.

In certain cases, the term “atom” is used for short to designate a charged particle in a central potential, rather than electrons in the field of a nucleus. An analogy is apparent here.

Graphs with reference to earlier works were constructed or adapted from the results of those works and are no direct reproduction of the graphs published previously.

### 1.3.1 Notation and terms for magnetic fields

In the literature, the conditions of magnetobiological experiments are described using both the MF strength  $\mathbf{H}$ , and the MF induction  $\mathbf{B}$ . The latter quantity is related to  $\mathbf{H}$  by the relationship  $\mathbf{B} = \mu\mathbf{H}$ . Here the permeability  $\mu$  of the medium, generally speaking, is essentially averaged over a physically small volume of the medium. That is so because  $\mathbf{B}$ , in addition to  $\mathbf{H}$ , contains a contribution of the medium's magnetization induced by  $\mathbf{H}$ . The magnetization is only referred to as an average over a sufficiently large volume, when the local inhomogeneities of MFs of atomic sources are largely ironed out, i.e., those due to orbital magnetic moments of atomic electrons, and also of unpaired electron and nuclear spins.

Clearly, when considering the primary magnetoreception mechanisms involving the motion of particles precisely on an atomic scale, it is more correct to use  $\mathbf{H}$ , rather than  $\mathbf{B}$ . Considering that in the Gaussian system the permeability of biological tissues is close to unity (Pavlovich, 1985), the atomic field  $\mathbf{H}$  averaged over a physically small volume is nearly coincident with the exogenous field — with given external sources: permanent magnets, Helmholtz coils, etc.

Some authors, however, make use of the MKS system, in which vacuum possesses a permeability. Therefore, even to describe the motion of particles in a vacuum, e.g., on interatomic scales, one has to apply the magnetic induction  $\mathbf{B}$ . In that system, the unit of  $\mathbf{B}$  is Tesla (T), related to the unit of  $\mathbf{B}$  in the Gauss system (G) by the relationship  $1 \text{ G} = 10^{-4} \text{ T}$ . In the Gaussian system the MF strength  $\mathbf{H}$  is measured in Oersteds (Oe). Since in that system  $\mu$  is unity and, moreover, dimensionless, the units Oe and G in fact coincide:  $1 \text{ Oe} = 1 \text{ G} = 1 \text{ cm}^{-1/2} \text{ g}^{1/2} \text{ s}^{-1}$ .

In this connection, throughout the book we will characterize an MF using both  $\mathbf{H}$  and  $\mathbf{B}$ . It is to be stressed that in the latter case we do not imply the presence of some macroscopic magnetization in a living tissue, but rather our desire to make use of MKS units, T and  $\mu\text{T}$ , which are convenient for a number of reasons. In actual fact, more often than not we deal with a magnetic field engendered by external sources in a vacuum. Relationships between physical quantities in the book are given in the Gauss system.

Some organisms are not indifferent to the compensation of a natural local DC MF down to the level of  $\ll 1 \text{ G}$ . To deal with a situation where a DC MF takes on values that are sufficiently small to cause a biological response and that have no distinct boundary, we will utilize terms that are current in the literature, such as “magnetic vacuum” and “zero field”, and use them without inverted commas. We will take the formal definitions of a magnetic vacuum in biological terms to be the inequalities

$$H_{\text{AC}} \ll H_{\text{DC}} \ll H_{\text{geo}} ,$$

where  $H_{\text{geo}}$  is a natural magnetic biological reference, i.e., the local geomagnetic field.

One of the MF configurations most popular in experiment is a superposition of collinear DC and AC magnetic fields. The MF vector axis being time-independent, such a configuration is conditionally referred to as a “uniaxial MF”. In the more

general case of the superposition of arbitrarily oriented DC and AC magnetic fields we will talk about a “combined MF”.

In the literature, for frequency ranges of fields they employ the following nomenclature: low frequency (LF) 30–300 kHz, very low frequencies (VLF) 3–30 kHz, ultralow frequencies (ULF) 0.3–3 kHz, superlow frequencies (SLF) 30–300 Hz, and extremely low frequencies (ELF) 3–30 Hz. Since there are no significant differences between these ranges in terms of primary physical mechanisms, the book uses for convenience one general term “low-frequency MFs”.

The values of magnetic fields are defined below in relation to the biologically natural level of the geomagnetic field  $\sim 50 \mu\text{T}$ . There being no clear-cut boundaries, for such fields in the literature they use the term “weak MFs”. Fields higher than 1 mT will be defined as “strong MFs”. Correspondingly, fields under  $1 \mu\text{T}$  are called “superweak MFs”. In the magnetobiological literature they often use the term “amplitude” in relation to a sinusoidal signal at large, always pointing out what specifically is meant: the peak value, the rms (root-mean-square) value, or the peak-to-peak value. In the book the term is taken to mean strictly the peak value.

In certain cases the term “power” is utilized to mean the relative energetic characteristic of electromagnetic radiation, which will become apparent from the context.

## 1.4 MAGNETOBIOLOGICAL EFFECT

The term “magnetobiological effect”, or MBE for short, used in the book has the following meanings.

On the one hand, the term implies any change in any variables of a biological system caused by a change in the magnetic conditions of its occurrence. Those may be biological properties of an organism *in vivo* or biochemical parameters of a living system *in vitro*.

At the microscopic level, biological structures are common for most of the living systems — these are proteins, membranes, etc. Clearly, the primary mechanism of magnetoreception realized at the level of biophysical structures displays the same level of generality, but one and the same primary mechanism in various biological systems can manifest itself through changes in a wide variety of properties.

For a researcher of the primary mechanism, biological systems are just special tools. In a sense, all the biological systems that display a measure of magnetosensitivity are the same. It is important that the way some property varies with changeable magnetic conditions would enable one to derive information on the nature of primary magnetoreception. Also which variable in particular in a biological system is being changed is immaterial. Therefore, it would be convenient to view a “magnetobiological effect” just as a dependence of the system’s behaviour on MF variables, whatever the biological nature of that dependence.

On the other hand, physically, that term singles out magnetic conditions from a general electromagnetic situation. Some comments are in order. Electromagnetic

fields are known to cause biological effects within a wide range of amplitudes, frequencies, etc. For instance, sufficiently intensive EMFs engender conduction currents, heat biological tissues, and cause rotations of molecular dipoles. They give rise to noticeable shifts in many reactions and spectacular biological effects. Thermal and electrochemical effects are widely used in practice, including in medicine: UVF treatments, electrophoresis, and so on. These phenomena are no paradox. In contrast, paradoxical are the bioaction of DC MFs, low-frequency AC MFs, and centimeter and millimeter waves of nonthermal intensities. At the same time, both AC low-frequency MFs and microwave radiations may have a meaningful electric component. The question of its role in the biological effects of an EMF in those ranges is not that simple. In experiment and theoretical treatments of effects of weak low-frequency MFs, an electric component is normally ignored.

As the frequency of a low-frequency MF is increased, sooner or later one will have to take into consideration the induced electric component, because it varies with the field frequency. Whether it is possible to ignore the electric component is also dependent on the specific experimental realizations of an EMF source, and the presence of the configuration of the “near” zone or “far” zone in relation to the source. As the EMF intensity is decreased or the frequency increased, a moment comes when it can only be described in QED terms. The language of electromagnetic waves is replaced by that of field quanta. It becomes impossible to break down an EMF into magnetic and electric components. The criteria of the “magnetism” of an electromagnetic field define the confines of magnetobiology as such, and are therefore in need of clarification.

### 1.4.1 Evaluation of the thermal action of eddy currents

Temporal variations of an MF induce an electric field. If we expose to an MF an electroconductive medium, e.g., a biological system, it develops macroscopic currents. Their electrochemical effects, — i.e., those on a phase boundary and involving charge carriers, — can cause a biological reaction. A reaction can also occur owing to the Joule heating of tissues. In the latter case, the biological response has nothing to do with magnetobiology, since an MF here is just one of the possible heating factors or sources of electromotive force (e.m.f.) On the other hand, it is clear that such a response is a biological effect of an MF. What is thus of importance here is the difference between MF biological effects in general and magnetobiological effects, the latter appealing to special non-thermal and non-electrochemical mechanisms for the interaction of an MF and living matter.

Let us identify the boundary between magnetobiological and thermal effects of an MF. Biological tissues being macroscopically neutral, the Maxwell equations for an electric field look like

$$\begin{aligned} \operatorname{rot}\mathbf{E} &= -\frac{1}{c}\frac{\partial}{\partial t}\mathbf{B}, & \operatorname{div}\mathbf{D} &= 0, & \mathbf{D} &= \varepsilon\mathbf{E} \\ \operatorname{rot}\mathbf{H} &= \frac{4\pi}{c}\mathbf{j}, & \operatorname{div}\mathbf{B} &= 0, & \mathbf{B} &= \mu\mathbf{H}, & \mathbf{j} &= \sigma\mathbf{E}. \end{aligned}$$

We re-write them as

$$\begin{aligned} \operatorname{rot}\mathbf{E} &= -\frac{1}{c}\frac{\partial}{\partial t}(\mathbf{B} + \mathbf{B}_{\text{ind}}) , & \operatorname{div}\mathbf{E} &= 0 \\ \operatorname{rot}(\mathbf{B} + \mathbf{B}_{\text{ind}}) &= \frac{\mu 4\pi}{c}\mathbf{j} , & \mathbf{j} &= \sigma\mathbf{E} , \end{aligned}$$

where  $\mathbf{B}$  is an external homogeneous MF, and  $\mathbf{B}_{\text{ind}}$  is an MF induced by eddy currents.

It is seen from the equations that the electric field induced by a sinusoidal field  $\mathbf{B}$  is about  $r\Omega B/c$ . The electric field produces a current density of  $\sigma r\Omega B/c$ , which in turn engenders an MF equal to

$$B_{\text{ind}} \sim \frac{4\pi r^2 \mu \sigma \Omega}{c^2} B .$$

The proportionality coefficient for “biological” values of the parameters  $r \sim 1$  cm and  $\sigma \sim 9 \cdot 10^9$  CGS units is much smaller than unity up to megahertz frequencies. Therefore, we will later use the equations

$$\operatorname{rot}\mathbf{E} = -\frac{1}{c}\frac{\partial}{\partial t}\mathbf{B} , \quad \operatorname{div}\mathbf{E} = 0$$

and ignore the effects, e.g., the skin-effect, concerned with MF induction by eddy currents. The last equation suggests that the field  $\mathbf{E}$  is solenoidal. It can then be represented as the rotor of a certain vector field (Korn and Korn, 1961),

$$\mathbf{E}(\mathbf{r}) = \frac{1}{4\pi} \operatorname{rot} \int \frac{\operatorname{rot}\mathbf{E}(\mathbf{r}')}{|\mathbf{r} - \mathbf{r}'|} dv ,$$

integrating over all the points  $\mathbf{r}'$ . The relationship defines the induced field  $\mathbf{E}$  from its rotor in an arbitrary coordinate system up to the gradient of some potential  $\varphi$ , which meets the condition  $\operatorname{div}(\operatorname{grad}\varphi) = 0$ . It is easier, however, to work out the field  $\mathbf{E}$  from symmetry considerations and suitable potentials of an EMF.

Let a homogeneous MF  $\mathbf{B}$  be aligned along the  $z$ -axis and limited by the dimensions of an infinitely long solenoid — an idealization that is often used in calculations. The field  $\mathbf{E}$  then possesses only an angular (tangential) component. The potentials can be taken to be

$$\mathbf{A}(\mathbf{r}) = \frac{1}{2}\mathbf{B} \times \mathbf{r} , \quad A_0 = 0 .$$

It is easily seen that  $\mathbf{B} = \operatorname{rot}\mathbf{A}$ , as the case should be. Since  $\mathbf{E}(\mathbf{r}) = -\operatorname{grad}A_0 - \frac{1}{c}\frac{\partial}{\partial t}\mathbf{A}(\mathbf{r})$ , then, in a cylindrical coordinate system, we find<sup>9</sup>

$$E_\varphi = -\frac{r}{2c}\frac{\partial}{\partial t}B(t) .$$

Note that for the chosen potential gauge  $\mathbf{E}(0) = 0$ . That is to say that such gauging is only possible in the coordinate system of the symmetry center of MF sources,

---

<sup>9</sup>In convenient units this relationship can be written (Misakian and Kaune, 1990) as  $E_{\text{peak}}[\mu\text{V/m}] = 0.01\pi r[\text{cm}] f[\text{Hz}] B_{\text{peak}}[\mu\text{T}]$ .

and that the MF homogeneity condition alone is insufficient to arrive at  $E_\varphi$ . Here  $r$  is the distance to the solenoid center.

On the other hand, the Joule thermal energy of the current with density  $j = \sigma E$ , emitted per unit time per unit volume is

$$w = \sigma E^2 ,$$

where  $\sigma$  is the specific electric conductivity of the medium. Hence we can readily arrive at the mean energy per unit time within a macroscopic volume of radius  $R$  and height  $a$ , which is placed at the center of the solenoid. That will be a model of a biological body. We write

$$\int \overline{w} dv = a \int \sigma \overline{E_\varphi^2} 2\pi r dr = \frac{\pi a \sigma R^4}{8} \overline{\left( \frac{\partial}{\partial t} B(t) \right)^2} = \frac{\pi a \sigma R^4}{16} B^2 \Omega^2 .$$

The last equality is derived considering that the MF is sinusoidal,  $B(t) = B \cos(\Omega t)$ , and we have  $\overline{\sin^2(\Omega t)} = \frac{1}{2}$ . It follows that on average, per unit body volume ( $V = a\pi R^2$ ), we get the power

$$P = \frac{\sigma R^2}{16c^2} B^2 \Omega^2 .$$

It is conditioned by the body dimensions, a corollary of  $E_\varphi$  being proportional to the distance  $r$  to the solenoid center.

The increase in the temperature  $T$  of the body due to heat  $Q$  will be

$$dT = \frac{1}{c_Q} dQ ,$$

where  $c_Q$  is the heat capacity of a volume unit. Taking the time derivative we get

$$T'_t = \frac{1}{c_Q} P ,$$

which, after the substitution of the expression for  $P$ , yields the frequency dependence of the MF amplitude, which defines the boundary of thermal effects on the amplitude–frequency plane, Fig. 3.1.

$$B = \frac{4c}{R} \sqrt{\frac{T'_t c_Q}{\sigma}} \frac{1}{\Omega} . \quad (1.4.1)$$

We note that for bodies with a fairly complicated geometry and inhomogeneous distributions of conductivities and heat capacities over the volume, which is nearly always the case in experiments, the appropriate computations are more complicated by far and require special numerical techniques (e.g., Gandhi *et al.*, 2001). Therefore, rough estimations of the orders of magnitude in this case are quite justified.

We will apply the following values of the variables of a biological tissue and the specimen dimensions:  $\sigma \sim 1 \text{ S/m} = 9 \cdot 10^9 \text{ CGS units}$  (Mazzoleni *et al.*,

1986; Foster and Schwan, 1996; Gabriel *et al.*, 1996),  $c_Q \sim 1 \text{ cal}/(\text{cm}^3 \text{ }^\circ\text{C}) \approx 4.2 \cdot 10^7 \text{ erg}/(\text{cm}^3 \text{ }^\circ\text{C})$ ,  $R \sim 1 \text{ cm}$ . We take a tissue-heating criterion of biological significance to be the temperature growth at a rate of  $T'_t \sim 0.1 \text{ }^\circ\text{C}/\text{min}$  (in the absence of a heat sink). Then the proportionality between  $B$  and  $f^{-1} = 2\pi/\Omega$  in Gaussian units will be

$$B \sim 10^8 / f . \quad (1.4.2)$$

The relationship holds well until the conductivity can be regarded as frequency independent. As the frequency is increased, we have a contribution to conductivity and Joule heat owing to the imaginary component of the complex permittivity of the medium, i.e., to polarization currents. The conductivity grows; therefore the boundary of thermal values of the amplitude  $B$  declines in comparison with the predictions (1.4.2). This drop can set in at frequencies  $\sim 1 \text{ kHz}$ . Since the static permittivity of a biological tissue is under 100, the above drop is below one or two orders and on the scale of Fig. 3.1 is nearly imperceptible. Note that the dependence (1.4.2) yields only an approximate indication of the boundary of thermal effects, to within two or three orders of magnitude. Therefore, in each specific case it may be required to be estimated individually.

Sometimes for a of biological significance criterion of eddy currents they take the current density  $\sim 1 \text{ mA}/\text{m}^2$  (Nakagawa, 1997), of the order of natural biological electric currents, above which electrochemical reactions in a living tissue set in. The MF amplitude vs frequency dependence, worked out similarly to (1.4.2), will then have the form

$$B \sim 6 \cdot 10^2 \frac{1}{f} , \quad (1.4.3)$$

i.e., five orders below the specified thermal threshold. That dependence, a section of the broken curve in Fig. 3.1, is accepted by the American Conference of Governmental Industrial Hygienists as the safety boundary for a low-frequency MF. Specifically, at 50 Hz it gives the threshold level about 12 G. It is to be noted that this value is one or two orders higher than the levels of a number of magnetobiological effects established with certainty in laboratory assays. Similar values of norms have also been established by other organizations (Suvorov *et al.*, 1998).

### 1.4.2 Criterion for classical EMF

Berestetskii *et al.* (1982) gives a criterion for the applicability of the classical treatment of an EMF. It relies on the large-numbers requirement for the filling of the levels of elementary EMF oscillators in a quantum treatment. The criterion relates the frequency  $f$  to the amplitude of an AC field,<sup>10</sup>

$$H \gg \sqrt{\hbar c} \left( \frac{2\pi}{c} \right)^2 f^2 \sim 10^{-30} f^2 , \quad (1.4.4)$$

---

<sup>10</sup>The estimate holds well for the electric field  $E$  as well. In the Gaussian system physical dimensions of  $E$  and  $H$  are the same  $\text{g}^{1/2} \text{cm}^{-1/2} \text{s}^{-1}$ .

where the numerical coefficient is in the CGS system. That can be readily perceived from general considerations. The energy flux of an EMF plane wave is related to the MF strength as (1.4.8)  $S = cH^2/4\pi$ . Hence the volume  $\lambda^3$ , where  $\lambda = c/f$  is the wavelength, contains about  $S\lambda^2\frac{\lambda}{c}$  of energy. At the same time,  $\lambda^3$  is the characteristic volume of a quantum of EM radiation with the wavelength  $\lambda$ . The classical description is clearly valid if the number of quanta of the field  $2\pi\hbar f$  in the volume  $\lambda^3$  is much larger than unity. That is,  $S\lambda^3/c \gg 2\pi\hbar f$ . From this we can easily derive the inequality, which will, up to a numerical factor of about unity, repeat (1.4.4).

It is seen that in the range of low-frequency magnetic fields down to infinitesimal amplitudes the classical treatment of an electromagnetic field is applicable. Dependence (1.4.4), which defines the ranges for the classical and quantum descriptions of an EMF in the amplitude–frequency plane, is also shown in Fig. 3.1. Together with the curve (1.4.2), it identifies the area of magnetobiology that by definition must be the area of non-thermal effects and, at the same time, the area of the classical treatment of an EMF, where it is possible to single out the magnetic component of the field.

The quantum dynamics of particles in a classical EMF constitutes the so-called semiclassical approximation. In that approximation, the dynamic equation of a particle has the form of the Schrödinger equation, in a broad sense, and the EMF enters into the equation as a vector  $\mathbf{A}$  and a scalar  $A_0$  potentials of the field. The potentials are defined accurate to the gauge transformation: for the important special cases of an external homogeneous AC MF and a plane electromagnetic wave, the fields  $\mathbf{H}$  and  $\mathbf{E}$  can be defined just in terms of the vector potential, by putting  $A_0 = 0$ . Then the question of which field, magnetic or electric, determines the motion of a particle no longer makes sense. From the general point of view, the governing factor here is the vector potential of an EMF, and there are no constraints on the frequency or amplitude of the field, besides the specified QED one. If, however, we take into consideration some mechanisms defined below, they will define on the frequency–amplitude plane some areas of their possible effectiveness.

For a non-plane wave, in the vicinity of an emitter, it is sometimes possible to create a purely electric or purely magnetic AC field, to within some accuracy. So, Broers *et al.* (1992) employed a cavity for 150 MHz of cylindrical shape about half a meter in size. In such a cavity, standing electric and magnetic waves form nodes and crests. To place the cellular culture of *M. africana* fungus in the cavity, locations were chosen either with a purely magnetic wave (1.2 nT at maximum), within experimental accuracy, or with a purely electric (0.91 V/m) wave. The findings, shown in Fig. 1.9, indicate that, unlike the electric field, the magnetic field produced a statistically significant biological effect.

It would be of interest to plot on the graph of Fig. 3.1 areas of the variation of EMF parameters as a classical wave that correspond to some processes and experiments.

The human eye is known to have a sensitivity threshold of about  $N = 10$  photons during the eye response time  $\tau \sim 0.1$  s (Aho *et al.*, 1988). We take it that the photon

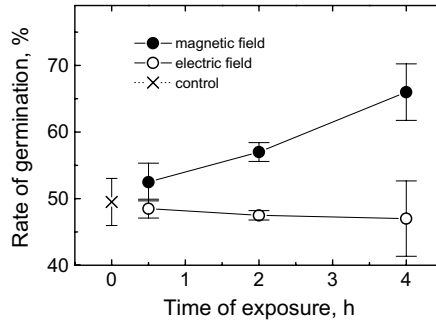


**Figure 1.9.** Germination of fungus cells in the magnetic and electric fields of an EMF that is frequency-modulated (10 Hz) 150 MHz depending on exposure time.

energy or frequency corresponds to a maximum of eye spectral sensitivity; i.e., the wavelength is  $\lambda = 55.5 \cdot 10^{-6}$  cm. We can then readily work out the energy quantum to be  $2\pi\hbar s/\lambda$ , and the energy flux through the pupil of area  $\varrho \sim 1$  cm<sup>2</sup> will be

$$\frac{1}{\tau} N 2\pi\hbar \frac{c}{\lambda} \frac{1}{\varrho} .$$

On the other hand, the energy flux of a plane wave is related to the amplitude of its magnetic component by the relationship (1.4.8). Equating these quantities gives the MF amplitude  $H$  of the EMF classical wave, which corresponds to the eye sensitivity. Its order of magnitude is

$$H = 2\pi \sqrt{\frac{2N\hbar}{\tau\lambda\varrho}} \sim 4 \cdot 10^{-10} \text{ G} .$$

As is seen in Fig. 3.1, the EMF of this, optical, section of the spectrum at such a low intensity is in fact a quantum object.

We now find the equivalent amplitude of an optical range MF produced by a household light source, e.g., by a 100-W incandescent lamp. The optical part of the spectrum only makes up several percents of power, i.e., about  $P \sim 5$  W. At a distance of  $R \sim 1$  m the optical radiation flux will be  $P/4\pi R^2$ ; hence we get  $H \sim 0.3 \cdot 10^{-2}$  G. Obviously, there are more grounds to regard such as radiation as a classical wave. It falls somewhere between a classical and a quantum description. In fact, the optical radiation of that power displays properties both of waves (interference) and of quanta (photoelectric phenomena).

### 1.4.3 Some limitations on an electric field

Interaction of an EMF with bound charged particles seems to be the only criterion in the search for primary magnetoreception mechanisms. When a quantum particle

is exposed to a field with some binding highly symmetric, e.g., central, potential, its initially degenerate energy levels split. It is natural, therefore, to compare splitting amounts caused by magnetic and electric fields. This gives a smallness criterion for an electric field in relation to an atomic system exposed to a magnetic field. This does not exhaust, of course, all the possible situations, but still gives some estimates of value for magnetobiology.

To arrive at proper estimates we assume that a particle is exposed to some central potential. A charge  $q$  of mass  $M$  exposed to a magnetic field  $H$  has its levels split (Zeeman effect) as follows:

$$\mathcal{E} \sim \frac{\hbar q}{2Mc} H . \quad (1.4.5)$$

In an electric field  $E$ , a system acquires a dipole moment  $d \sim \alpha E$ , where  $\alpha$  is a polarizability of the system. The moment energy  $-dE = -\alpha E^2$  varies with the squared electric field. A perturbation operator in the field  $\mathbf{E}$  is  $\mathcal{V} = -\mathbf{d}\mathbf{E}$ , where  $\mathbf{d} = q\mathbf{r}$  is the operator of the ion dipole moment. We take the  $z$ -axis to be in the  $\mathbf{E}$  direction, then

$$\mathcal{V} = -q\mathbf{r}\mathbf{E} = -qzE .$$

In the first order of perturbation theory, the energy shift for a non-degenerate level, e.g., where  $H \neq 0$ , in a homogeneous field  $E$  is (in terms of the notation of (Landau and Lifshitz, 1977))

$$\mathcal{E}_n^{(1)} = \mathcal{V}_{nn} = \langle \psi_n | \mathcal{V} | \psi_n \rangle = -q\mathbf{E} \langle \psi_n | \mathbf{r} | \psi_n \rangle = 0,$$

where  $\psi_n$  is an unperturbed wave function of the  $n$ th level, and  $n$  is a set of quantum numbers. The splitting of a degenerate level, in the absence of an MF, is dictated by the solution to the secular equation

$$\|\mathcal{V}_{nn'} - \mathcal{E}_n^{(1)}\delta_{nn'}\| = 0 ,$$

where  $n$  and  $n'$  refer to the states of a degenerate level, and have the same parity. It follows that irrespective of an MF, corrections to energy are dependent on matrix elements of the vector  $\mathbf{r}$  or pseudoscalar  $z$ , between functions of like parity.<sup>11</sup> But such matrix elements are zero. Therefore, the level splitting is determined by second-order approximation corrections (quadratic Stark effect)

$$\mathcal{E}_n^{(2)} = \sum_m \frac{|(\mathbf{d}\mathbf{E})_{nm}|^2}{\varepsilon_n - \varepsilon_m} = q^2 E^2 \sum_m \frac{|(z)_{nm}|^2}{\varepsilon_n - \varepsilon_m} , \quad m \neq n ,$$

where the denominator contains the difference of energies of unperturbed states. The main contribution to  $\mathcal{E}_n^{(2)}$  is made by terms with the smallest values of energy difference. States of a Zeeman multiplet in a central potential have the same parity,

---

<sup>11</sup>Except for cases of Coulomb and harmonic potentials, where the functions of stationary states may have no parities.

and appropriate matrix elements are zero. Therefore, the smallest energy difference values correspond to various values of the radial or azimuthal quantum numbers. The splitting is around

$$\mathcal{E}_n^{(2)} = q^2 E^2 \frac{|(z)_{10}|^2}{\varepsilon_{10}} .$$

Considering that the transition energy is  $\varepsilon_{10} \sim \hbar^2 / MR^2$ , where  $R$  is the size of the area where a particle stays, and subject to  $(z)_{nm} \sim R$ , we obtain the following relationship for the corrections to energies in an electric field:

$$\mathcal{E} \sim \frac{q^2 MR^4}{\hbar^2} E^2 . \quad (1.4.6)$$

We can estimate, for instance, the true order of polarizability of  $\alpha \sim \partial^2 \mathcal{E} / \partial E^2 \sim q^2 MR^4 / \hbar^2$  of the ground state of the hydrogen atom.

Equating the splittings (1.4.5) and (1.4.6) yields an estimate of the electric field, where perturbations introduced into an atom-like system in a magnetic field become significant

$$E \sim \frac{\hbar}{MR^2} \sqrt{\frac{\hbar H}{2cq}} .$$

The following sections provide evidence that the biologically significant ions of calcium, magnesium, etc., are primary targets for an MF in biological systems. Considering that a typical laboratory level of an MF is about 0.5 G and substituting approximate values for the  $^{40}\text{Ca}^{2+}$  calcium ion in a capsule with an effective radius potential of 0.7 Å give  $E \sim 10^{-3}$  CGS units or  $\sim 30$  V/m.

A biological tissue is 60–95% water. It possesses a relatively high permittivity for quasi-static electric fields  $\varepsilon \approx 80$ . Therefore, in an external electric field, an ion in a biological tissue has acting on it a field that is  $\varepsilon$  times smaller. Thus, the estimate

$$E \sim 100\text{--}1000 \text{ V/m}$$

is acceptable for the highest permissible electric fields in the above sense. Note that for dwellings the standard level is 5–20 V/m at frequency 50 Hz. The estimate is valid for quasi-static fields, when the field frequency is much lower than that of transitions  $\sim \hbar / MR^2$  with a change in the radial quantum number. For the specified system, that equals  $10^{10}$  Hz.

Note that here we deal with electric fields produced by external sources. Electric fields induced by an AC MF are said to be included in the dynamic equation alongside the MF via the vector potential.

#### 1.4.4 Limitations on plane waves

We have considered so far mainly homogeneous MFs and the electric fields they engender. That is to say we have dealt with fields in the so-called near zone, where the distance to an emitter is comparable with its size. To be more exact, if  $d$  is

the emitter size and  $\lambda$  is the EM wavelength, then the near zone occurs within a distance  $r$  to the emitter, approximately not father than

$$r_0 \sim \begin{cases} d^2/\lambda, & d \gg \lambda \\ \lambda, & d < \lambda. \end{cases} \quad (1.4.7)$$

For the near zone, the EMF configuration is mainly determined by the distribution of currents and charges on the emitter. If the distance to the emitter is much larger than  $r_0$ , we have the far zone. In the latter case, an EMF, with small scales, is close to the plane wave, and the field strengths are related by

$$\mathbf{H} = \mathbf{n} \times \mathbf{E},$$

where  $\mathbf{n}$  is the unit vector in the direction of wave propagation. From this we can readily find the energy flux in the plane wave

$$\mathbf{S} = \frac{c}{4\pi} \mathbf{E} \times \mathbf{H} = \frac{c}{4\pi} H^2 \mathbf{n}. \quad (1.4.8)$$

For instance, the far zone conditions are met by an EMF acting on some areas of the human body when using a mobile phone. Also, far zone situations are staged specially when conducting experiments with microwave radiations. In such cases the plane wave idealization is quite justified and mathematically convenient.

Relationships (1.4.5) and (1.4.6), which determine the splitting of atomic levels in magnetic and electric fields, for a plane EM wave, yield estimates of radiation power levels, where either electric or magnetic effects prevail.

We derive the ratio of (1.4.5) and (1.4.6), considering that for the plane wave  $E = H$ ,

$$\frac{\mathcal{E}_{\text{mag}}}{\mathcal{E}_{\text{el}}} = \frac{\hbar^3}{2M^2 R^4 c q H}.$$

We introduce the convenient quantities

$$\epsilon_a = \hbar^2 / MR^2, \quad \epsilon_p = m_p c^2,$$

which are the characteristic scale of the vibrational energy of an ion in the cavity with the effective potential of radius  $R$  and the rest energy of a proton, respectively. The desired relationship will then assume the convenient form

$$\frac{\mathcal{E}_{\text{mag}}}{\mathcal{E}_{\text{el}}} = \frac{\epsilon_a^2}{4q' \epsilon_p \mu_N H},$$

where  $q' = q/e$  is the ion relative charge. We can rewrite that relationship in a still more convenient form, subject to the definition (1.4.8) of the energy flux of a plane wave:

$$\frac{\mathcal{E}_{\text{mag}}}{\mathcal{E}_{\text{el}}} = \sqrt{\frac{S_0}{S}}, \quad S_0 = \frac{c}{\pi} \left( \frac{\epsilon_a^2}{8q' \epsilon_p \mu_N} \right)^2. \quad (1.4.9)$$

It is clear that the quantity  $S_0$  defines the same threshold level of the radiation power density, where magnetic and electric effects are potentially identical. We can readily arrive at

$$S_0 \sim 8.8 \cdot 10^{-10} \text{ W/cm}^2$$

for calcium in the binding cavity of calmodulin with potential radius  $R \sim 0.7 \text{ \AA}$ . As follows from (1.4.8), corresponding to that quantity is the amplitude of the magnetic component  $H_0 \sim 2\sqrt{\pi S_0/s} \sim 2 \cdot 10^{-6} \text{ G}$ .

In the diagram in Fig. 3.1 that level separates the lower part in the high-frequency range, i.e., in the range where the plane wave approximation is valid and where the EMF electric component can be ignored. As is seen in the diagram, the power range of microwaves effective in relation to *E. coli* cells studied by Belyaev *et al.* (1996) nearly wholly lies within the range of the action of the magnetic component.

The power of microwave radiation, e.g., of mobile phones, falls off exponentially penetrating biological tissues. Therefore, there is always a tissue layer where magnetic effects are more probable. As will become clear later in the book, magnetic fields in comparison with electric ones feature definite advantages from the point of view of the probability of the biological effects they will produce.

## 2

---

# OVERVIEW OF EXPERIMENTAL FINDINGS

Some law of logic should fix the number of coincidences, in a given domain, after which they cease to be coincidences, and form, instead, the living organism of a new truth.

V. Nabokov, *Ada or Ardor: A Family Chronicle*

This overview encompasses just a small part of the published work on magnetobiology. It does not cover many remarkable results because they are not concerned with the physical nature of magnetobiological effects, although they may be unique in their own right and be of significant scientific value. One example is works of an epidemiological nature, which look into correlations between the intensity of power-frequency electromagnetic noise and incidences for some diseases. It is clear that the presence of a correlation between these factors does not suggest their cause-effect links and can hardly give us any helpful insights into the nature of the effect. At the same time, these findings are an important social and political factor.

The scope of this book warrants our concern only with those ideas that lie within the mainstream of traditional physics and raise no doubts as to their validation. This gives some indication of criteria followed in selecting experimental evidence. So, the selection was guided by a possibility of commenting in terms of physics. Findings had to contain dependences, functions, and correlations that could be coupled with various physical mechanisms that were likely to underlie the effects observed. We have focused on experimental observations of multipeak dependences of MBEs with magnetic conditions properly described. Such observations are especially paradoxical and, at the same time, they are on a par with mechanisms of MF non-thermal effects, in particular, with ion interference, which is a focus of the book. We generally overlooked work on actions of AC MFs that did not indicate the amount and orientation of a DC MF on samples. The yardstick of completeness of information on the magnetic situation comes also to be employed by specialized journals when reviewing submissions.

MF exposure time is an important parameter dictating the amount and sometimes the direction of a biological response. Studies of MBE temporal variations are the core of a half of the works on electromagnetobiology. These data are impor-

tant in yielding a wider understanding of the biochemistry and physiology of EMF reception by living systems. At the same time, temporal variations, which as a rule are relatively slow, with characteristic times of 10 minutes or longer, carry virtually no information on the primary physical process of the transformation of an EMF signal into a biochemical response. This book concentrates primarily on magnetoreception processes. Therefore, a wealth of results involving temporal dependences are outside the scope of this review.

We only note that in the majority of cases exposure times from several minutes to several months were used. Typical here are two types of dependences of the measurable variables on exposure times: a *s*-shaped curve with a saturation and a bell-type dependence (e.g., Byus *et al.*, 1984; Lin *et al.*, 1996). The first type is defined by the balance of processes of accumulation and decay of products of biochemical reactions that accompany primary reception processes. The bell-shaped-type dependence reflects the additional involvement of adaptive mechanisms that hinder the shift of homeostasis and enhance the stability of living systems under changed external conditions. At the same time, in the organism there is a whole spectrum of topical time scales of biochemical and physiological processes, including natural biorhythms. Therefore, measurable temporal dependences are often curves that are more complex than the aforementioned ones.

Nearly 5–10% of papers on magnetobiology report failures to observe any MBEs. These works are also excluded from the overview because these data are impossible to analyze. The chain of processes involved in the transformation of an MF signal into an observable biological parameter is very long and beyond control, and so the fact that many experiments show no effect is quite normal. As is shown in Ho *et al.* (1992); McLeod *et al.* (1992a); Berg and Zhang (1993); Ružič *et al.* (1998), reproducible MBEs can only be obtained when “electromagnetic” windows coincide with “physiological” windows. For instance, Blank and Soo (1996) observed that sign of the EMF response changed when Na,K-ATPase enzyme initial activity was varied. That implies that within some range of initial activities there was no EMF effect, whatever the kind of EMF stimulation, magnetic or electric, and its variables.

Also observed are temporal windows, i.e., time intervals where a biological system is able to be sensitive to an MF. Such windows have been found for various time scales, from minutes and hours (Ho *et al.*, 1992) to seasons (Ružič *et al.*, 1992, 1998). Importantly, reasons for magnetobiological assays being not quite reproducible may be quite exotic. So, Simkó *et al.* (1998) report that whether a biological reaction appeared in human amnion cells was dictated by which magnetic system — Helmholtz or Merritt rings — was used to produce an AC MF, the field amplitude in both cases being the same. In experiments on biological effects of microwaves the result may be significantly dependent on the distance to an emitter, the energy flux density being equal (Gapeyev *et al.*, 1996).

Researchers often took pains seeking relatively rare successful combinations of electromagnetic and physiological conditions. Nevertheless, biological systems were found to be influenced by weak MFs in a host of experimental configurations. The following is a concise catalogue of them.

Some important experimental works are described or commented on later in the book when comparing findings with theory.

This author could not find in the libraries accessible to him some important works dating from the turn of the 20th century to the late 1970s. However, there are reviews of such works (Kholodov, 1975; Warnke and Popp, 1979) that point to the therapeutic uses of MFs and discuss investigations into physiological and tissue responses to weak DC, AC and pulsed MFs, magnetic vacuum, and geomagnetic fluctuations. The main “set” of magnetic configurations studied remained essentially the same.

It would be of interest to point to some “pioneer” works on magnetobiology from the turn of the 20th century and earlier.<sup>12</sup>

- E.K. O’Jasti (1798). *Magic Magnet Mystery*. “Hibernia”, Dublin.
- W. Waldmann (1878). Der Magnetismus in der Heilkunde. *Deutsch. Arch. Geschichte Med. Med. Geographie* **1**, 320.
- N.I. Grigoriev (1881). *Metalloscopy and Metallotherapy*. St.Petersburg, (in Russian).
- V.Ya. Danilevsky (1900–1901). *Research into the Physiological Action of Electricity at a Distance*. V.1–2. Kharkov, (in Russian).
- B. Beer (1901). Über das Auftreten einer subjektiven Licht-empfindung im magnetischen Feld. *Wiener klin. Wochenschr.* **4**.
- C. Lilienfeld (1902). Der Elektromagnetismus als Heilfaktor. *Therapie Gegenwart* Sept., 390.
- P. Rodari (1903). Die Physikalischen und physiologisch-therapeutischen Einflüsse des magnetischen Feldes auf den menschlichen Organismus. *Correspond. Schweiz. Ärzte* **4**, 114.
- S.P. Thompson (1910). A physiological effect of an alternating magnetic field. *R. Soc.* **82**, 396.
- G. Durvil (1913). *Treatment of Diseases by Magnets*. Kiev, (in Russian).
- C.E. Magnussen and H.C. Stevens (1914). Visual sensations caused by a magnetic field. *Philos. Mag.* **28**, 188.
- H.B. Barlow, H.J. Kohn and G. Walsh (1917). Visual sensations aroused by magnetic fields. *Am. J. Physiol.* **148**, 372.

Many magnetobiological assays still await confirmations by other laboratories. It might appear that there is no evidence reliable enough for theoretical models to be constructed. However, when pooled (e.g., Bersani, 1999), these findings show a measure of commonness in what concerns manifestations of MBEs under various conditions and on various biological objects. It is these common elements that serve as a foundation for our further theorizing.

---

<sup>12</sup>This author is grateful to S.N. Uferom of Leeds University who introduced him to a curiosity by O’Jasti. Other publications are borrowed from bibliographies available in Warnke and Popp (1979) and Kholodov and Lebedeva (1992).

## 2.1 A POTPOURRI OF EXPERIMENTAL WORK

The following is a summary of experimental findings that are primarily discussed in the book. For convenience, works are grouped by (1) research objects, (2) parameters observable in experiment, (3) frequency ranges, and (4) configurations of electromagnetic fields to which organisms were subjected.

### 2.1.1 Objects studied

Among the commonest objects studied are:

- biochemical reactions (Jafary-Asl *et al.*, 1983; Litovitz *et al.*, 1991; Shuvalova *et al.*, 1991; Markov *et al.*, 1992; Novikov, 1994; Markov *et al.*, 1998; Blank and Soo, 1998; Ramundo-Orlando *et al.*, 2000),<sup>13</sup>
- DNA damage and repair processes (Whitson *et al.*, 1986; Nordensen *et al.*, 1994),
- DNA–RNA synthesis (Liboff *et al.*, 1984; Takahashi *et al.*, 1986; Goodman and Henderson, 1991; Phillips *et al.*, 1992; Goodman *et al.*, 1993a; Lin and Goodman, 1995; Blank and Goodman, 1997),
- enzymes — membrane ion pumps (Blank and Soo, 1996),
- cells (Spadinger *et al.*, 1995; Alipov and Belyaev, 1996; Sisken *et al.*, 1996):
  - \* amoeba cells (Berk *et al.*, 1997),
  - \* bacterial cells (Moore, 1979; Alexander, 1996),
  - \* *E. coli* (Aarholt *et al.*, 1982; Dutta *et al.*, 1994; Alipov *et al.*, 1994; Nazar *et al.*, 1996),
  - \* yeast cells (Jafary-Asl *et al.*, 1983),
  - \* *Candida* (Moore, 1979),
  - \* cells of plants (Fomicheva *et al.*, 1992a,b; Belyavskaya *et al.*, 1992),
  - \* fungi (Broers *et al.*, 1992),
  - \* algae (Smith *et al.*, 1987; Reese *et al.*, 1991) and
  - \* insects (Goodman and Henderson, 1991).
  - \* animal cells (Takahashi *et al.*, 1986):
    - fibroblasts (Whitson *et al.*, 1986; Ross, 1990; Matronchik *et al.*, 1996b; Katsir *et al.*, 1998),
    - mouse epidermis (West *et al.*, 1996),
    - erythrocytes (Serpensu and Tsong, 1983; Mooney *et al.*, 1986; Shiga *et al.*, 1996),
    - lymphocytes (Conti *et al.*, 1985; Rozek *et al.*, 1987; Lyle *et al.*, 1988; Goodman and Henderson, 1991; Lyle *et al.*, 1991; Walleczek, 1992; Yost and Liburdy, 1992; Coulton and Barker, 1993; Lindstrom *et al.*, 1995; Tofani *et al.*, 1995),

---

<sup>13</sup>Evidence is scarce. Actions of a low-frequency MF on biochemical reactions *in vitro* have been comparatively little studied.

- leucocytes (Barnothy, 1956; Goodman *et al.*, 1989; Picazo *et al.*, 1994; Sontag, 2000),
- osteoblasts (Luben *et al.*, 1982),
- neoblasts (Lednev *et al.*, 1996b,a),
- endothelia (Yen-Patton *et al.*, 1988),
- of salivary glands (Goodman *et al.*, 1983; Goodman and Henderson, 1988),
- thymocytes (Walleczek and Budinger, 1992; Matronchik *et al.*, 1996b),
- amniotic (Simkó *et al.*, 1998),
- bone cells (Fitzsimmons *et al.*, 1989).
- \* tumor cells (Phillips *et al.*, 1986b; Wilson *et al.*, 1990; Lyle *et al.*, 1991):
  - Ehrlich carcinoma (Garcia-Sancho *et al.*, 1994; Muzalevskaya and Uritskii, 1997),
  - breast cancer MCF-7 (Harland and Liburdy, 1997; Blackman *et al.*, 2001),
  - pheochromocytoma (Blackman *et al.*, 1993),
  - leukemia in humans U937 (Smith *et al.*, 1991; Garcia-Sancho *et al.*, 1994; Eremenko *et al.*, 1997),
  - E6.1 (Galvanovskis *et al.*, 1999),
  - carcinoma of mouse embryo F9 (Akimine *et al.*, 1985),
  - glioma N6 (Ruhstroth-Bauer *et al.*, 1994),
  - human osteosarcoma TE-85 (Fitzsimmons *et al.*, 1995).
- \* tissues of the brain (Bawin and Adey, 1976; Blackman *et al.*, 1979; Dutta *et al.*, 1984; Blackman *et al.*, 1988, 1990; Martynyuk, 1992; Agadzhanian and Vlasova, 1992; Espinar *et al.*, 1997; Lai and Carino, 1999),
- \* nerve (Semm and Beason, 1990),
- \* intestine (Liboff and Parkinson, 1991),
- \* bone (Reinbold and Pollack, 1997).
- organs:
  - \* brain (Kholodov, 1982; Richards *et al.*, 1996),
  - \* heart (Kuznetsov *et al.*, 1990).
- physiological systems:
  - \* central nervous (Bawin *et al.*, 1975; Kholodov, 1982; Lerchl *et al.*, 1990),
  - \* neuroendocrine (Reiter, 1992),
  - \* immune (Lyle *et al.*, 1988).
- organisms:
  - \* plants (Pittman and Ormrod, 1970; Kato, 1988; Kato *et al.*, 1989; Govorun *et al.*, 1992; Sapogov, 1992; Smith *et al.*, 1995),
  - \* plant seeds (Ružič and Jerman, 1998; Ružič *et al.*, 1998),
  - \* kidneys (Ružič *et al.*, 1992),

- \* insects (Ho *et al.*, 1992),
  - \* rats (Wilson *et al.*, 1981; Ossenkopp and Ossenkopp, 1983; Thomas *et al.*, 1986; Sidyakin, 1992; Temuriyants *et al.*, 1992a; Pestryaev, 1994; Kato *et al.*, 1994; Kato and Shigemitsu, 1996; Deryugina *et al.*, 1996; Nikollskaya *et al.*, 1996) and
  - \* embryos of rats (Delgado *et al.*, 1982; McGivern *et al.*, 1990),
  - \* mice (Barnothy, 1956; Kavaliers and Ossenkopp, 1985, 1986; Picazo *et al.*, 1994),
  - \* newts (Asashima *et al.*, 1991),
  - \* worms (Jenrow *et al.*, 1995; Lednev *et al.*, 1996a,b),
  - \* pigeons (Sidyakin, 1992),
  - \* chickens (Saali *et al.*, 1986),
  - \* snails (Prato *et al.*, 1993, 1995),
  - \* human organism (Akerstedt *et al.*, 1997; Sastre *et al.*, 1998).
- ecosystems and bio-geocenosis (Uffen, 1963; Opdyke *et al.*, 1966; Hays, 1971; Valet and Meynadier, 1993; Feychting *et al.*, 1995; Belyaev *et al.*, 1997),
  - solutions of amino acids — although they are no biological objects, they display MF effects that are very close in essence to those discussed — (Novikov and Zhadin, 1994; Novikov, 1994, 1996).

### 2.1.2 Observables

The observable parameters were:

- physical:
  - \* dimensions and weight of an object (Saali *et al.*, 1986; Kato, 1988; Kato *et al.*, 1989; Sapogov, 1992; Smith *et al.*, 1995),
  - \* viscosity of cell suspension (Alipov *et al.*, 1994; Alipov and Belyaev, 1996),
  - \* rheological properties of cells (Shiga *et al.*, 1996),
  - \* number of cells (Broers *et al.*, 1992; Picazo *et al.*, 1994; Tofani *et al.*, 1995; Alexander, 1996; West *et al.*, 1996; Eremenko *et al.*, 1997; Berk *et al.*, 1997) and
  - \* subcellular structures (Simkó *et al.*, 1998),
  - \* surface electric change (Smith *et al.*, 1991; Muzalevskaya and Uritskii, 1997),
  - \* transmembrane potential (Liboff and Parkinson, 1991),
  - \* structure of images of electron and other microscopies (Goodman *et al.*, 1983; Belyavskaya *et al.*, 1992; Blackman *et al.*, 1993; Espinar *et al.*, 1997),
  - \* current through electrochemical cell with an object (Novikov and Zhadin, 1994; Novikov, 1994, 1996),
  - \* photoprotein luminescence (Sisken *et al.*, 1996),
  - \* intensity of radioactive tracer emission (Liboff *et al.*, 1984; Fitzsimmons *et al.*, 1989; Markov *et al.*, 1992; Fitzsimmons *et al.*, 1995; Markov *et al.*, 1998; Katsir *et al.*, 1998),

- \* DNA mobility (Lai and Singh, 1997a),
- \* parameters analyzed:
  - chromatographic (Novikov and Zhadin, 1994; Novikov, 1994),
  - fluorescent (Fitzsimmons *et al.*, 1989; Katsir *et al.*, 1998)
  - microfluorescent (Walleczek, 1992; Walleczek and Budinger, 1992; Lindstrom *et al.*, 1995; Muzalevskaya and Uritskii, 1997; Reinbold and Pollack, 1997),
  - spectrophotometric (Blank and Soo, 1998; Ramundo-Orlando *et al.*, 2000),
  - gel-electrophoresis (Goodman and Henderson, 1988; Lin and Goodman, 1995),
  - radiographic (Goodman *et al.*, 1983; Mooney *et al.*, 1986; Goodman and Henderson, 1991),
  - ECG, EEG, ECoG (Kholodov and Lebedeva, 1992; Pestryaev, 1994; Sastre *et al.*, 1998).
- biochemical:
  - \* activity and level of an enzyme in the transcription of a  $\beta$ -galactosidase gene (Aarholt *et al.*, 1982),
  - \* adenylate cyclase (Luben *et al.*, 1982),
  - \* lysozyme (Jafary-Asl *et al.*, 1983),
  - \* protein-kinase (Byus *et al.*, 1984),
  - \* Na,K-ATPase (Serpersu and Tsong, 1983; Blank and Soo, 1990, 1996),
  - \* acetylcholinesterase (Dutta *et al.*, 1992),
  - \* enolase (Dutta *et al.*, 1994; Nazar *et al.*, 1996),
  - \* melatonin (Wilson *et al.*, 1981; Lerchl *et al.*, 1991; Reiter, 1992; Kato *et al.*, 1993, 1994; Loscher *et al.*, 1994; Lee *et al.*, 1995; Kato and Shigemitsu, 1996),
  - \* noradrenaline and adrenaline (Temuriyants *et al.*, 1992a),
  - \* phosphorylation of light myosin chains (Markov *et al.*, 1992),
  - \* choline (Lai and Carino, 1999),
  - \* ornithine-decarboxylase (Litovitz *et al.*, 1991, 1997b),
  - \* cytochrome-oxidase (Blank and Soo, 1998),
  - \* N-acetyl-serotonin transferase (Cremer-Bartels *et al.*, 1984).
  - \* Calcium efflux (Bawin *et al.*, 1975; Dutta *et al.*, 1984; Smith *et al.*, 1987; Blackman *et al.*, 1988, 1990; Schwartz *et al.*, 1990; Blackman *et al.*, 1991; Adey, 1992; Dutta *et al.*, 1992),
  - \* intra- and extracellular ion concentration (Liboff, 1985; Galvanovskis *et al.*, 1999),
  - \* concentration of peroxide lipid oxygenation products and of total thiol groups (Martynyuk, 1992),
  - \* uptake of radioactive tracers (Serpersu and Tsong, 1983; Takahashi *et al.*, 1986; Lyle *et al.*, 1991; Fomicheva *et al.*, 1992a; Garcia-Sancho *et al.*, 1994),
  - \* level of ribonucleic acids (mRNA) (Goodman *et al.*, 1989; Fomicheva *et al.*, 1992b).

- biological:
  - \* pulsed activity of neurons (Semm and Beason, 1990; Agadzhanian and Vlasova, 1992),
  - \* stability of biological rhythm (Kuznetsov *et al.*, 1990),
  - \* parameters of morphogenesis and development (Asashima *et al.*, 1991; Ho *et al.*, 1992; Ružič *et al.*, 1992, 1998),
  - \* seed germination rate (Ružič and Jerman, 1998),
  - \* mobility and morphology of cells (Smith *et al.*, 1987; Spadinger *et al.*, 1995; Reese *et al.*, 1991),
  - \* proliferation of cells (Akimine *et al.*, 1985; Whitson *et al.*, 1986; Ross, 1990; Fomicheva *et al.*, 1992a; Ruhestroth-Bauer *et al.*, 1994; Lednev *et al.*, 1996b; Muzalevskaya and Uritskii, 1997; Harland and Liburdy, 1997; Katsir *et al.*, 1998; Blackman *et al.*, 2001),
  - \* expression of genes (Goodman and Henderson, 1988; Phillips *et al.*, 1992),
  - \* behavior of individuals and cohorts:
    - conditional-reflex activity (Kholodov, 1982; Ossenkopp and Ossenkopp, 1983; Thomas *et al.*, 1986; Sidiyakin, 1992),
    - time of reaction (Kavaliers and Ossenkopp, 1986; Prato *et al.*, 1995) and regeneration (Jenrow *et al.*, 1995),
    - motive and exploratory activity (Deryugina *et al.*, 1996; Nikollskaya *et al.*, 1996),
    - memory (Richards *et al.*, 1996),
    - physiological parameters of sleep (Akerstedt *et al.*, 1997).

### 2.1.3 EMF ranges

Observed is the behavior of biological systems in electromagnetic fields of various ranges:

- DC fields (Barnothy, 1956; Ramirez *et al.*, 1983; Strand *et al.*, 1983; Cremer-Bartels *et al.*, 1984; Persson and Stahlberg, 1989; Kato, 1988; Kato *et al.*, 1989; Semm and Beason, 1990; Luben, 1991; Ho *et al.*, 1992; Ružič *et al.*, 1992; Malko *et al.*, 1994; Nikollskaya *et al.*, 1996; Shiga *et al.*, 1996; Espinar *et al.*, 1997; Berk *et al.*, 1997; Markov *et al.*, 1998),
- geomagnetic fields (Yeagley, 1947; Lindauer and Martin, 1968; Blakemore, 1975; Bookman, 1977; Martin and Lindauer, 1977; Kalmijn, 1978; Gould *et al.*, 1980; Frankel *et al.*, 1981; Mather and Baker, 1981; Quinn *et al.*, 1981; Bingman, 1983; Ossenkopp *et al.*, 1983; Chew and Brown, 1989),
- range < 1 Hz (Kavaliers and Ossenkopp, 1986; Semm and Beason, 1990; Muzalevskaya and Uritskii, 1997),
- range 1–100 Hz (Delgado *et al.*, 1982; Goodman *et al.*, 1983; Akimine *et al.*, 1985; Whitson *et al.*, 1986; Saali *et al.*, 1986; Takahashi *et al.*, 1986; Smith *et al.*, 1987; Lyle *et al.*, 1988; Fitzsimmons *et al.*, 1989; Kuznetsov *et al.*,

- 1990; Ross, 1990; Wilson *et al.*, 1990; Lyle *et al.*, 1991; Reese *et al.*, 1991; Agadzhanyan and Vlasova, 1992; Martynyuk, 1992; Sidyakin, 1992; Reiter, 1992; Temuriyants *et al.*, 1992a; Walleczek and Budinger, 1992; Coulton and Barker, 1993; Blackman *et al.*, 1993; Alipov *et al.*, 1994; Kato *et al.*, 1994; Novikov and Zhadin, 1994; Novikov, 1994; Dutta *et al.*, 1994; Fitzsimmons *et al.*, 1995; Jenrow *et al.*, 1995; Lindstrom *et al.*, 1995; Prato *et al.*, 1995; Smith *et al.*, 1995; Spadinger *et al.*, 1995; Tofani *et al.*, 1995; Blank and Soo, 1996; Kato and Shigemitsu, 1996; Novikov, 1996; Alipov and Belyaev, 1996; Nazar *et al.*, 1996; West *et al.*, 1996; Akerstedt *et al.*, 1997; Harland and Liburdy, 1997; Reinbold and Pollack, 1997; Litovitz *et al.*, 1997b; Katsir *et al.*, 1998; Ružič and Jerman, 1998; Ružič *et al.*, 1998; Sastre *et al.*, 1998; Simkó *et al.*, 1998; Galvanovskis *et al.*, 1999; Lai and Carino, 1999; Ramundo-Orlando *et al.*, 2000; Blackman *et al.*, 2001),
- range  $10^2$ – $10^3$  Hz (Saali *et al.*, 1986; Blackman *et al.*, 1988, 1990; Blank and Soo, 1990; Liboff and Parkinson, 1991; Deryugina *et al.*, 1996; Blank and Soo, 1998),
  - range  $1$ – $10^3$  kHz (Serpersu and Tsong, 1983; Liboff *et al.*, 1984; Blank and Soo, 1990; Ruhenstroth-Bauer *et al.*, 1994; Lednev *et al.*, 1996b; Blank and Soo, 1998; Sontag, 2000),
  - range  $1$ – $100$  MHz (Aarholt *et al.*, 1988; Alexander, 1996),
  - range  $10^2$ – $10^3$  MHz (Bawin *et al.*, 1975; Byus *et al.*, 1984; Dutta *et al.*, 1984; Broers *et al.*, 1992; Dutta *et al.*, 1994),
  - more than  $1$  GHz (Smolyanskaya *et al.*, 1979; Webb, 1979; Adey, 1980; Bannikov and Ryzhov, 1980; Grundler and Keilmann, 1983; Dutta *et al.*, 1984; Andreev *et al.*, 1985; Aarholt *et al.*, 1988; Didenko *et al.*, 1989; Grundler *et al.*, 1992; Grundler and Kaiser, 1992; Belyaev *et al.*, 1993; Kataev *et al.*, 1993; Gapeyev *et al.*, 1994; Belyaev *et al.*, 1996),
  - narrow-band noise and broad-band MFs (Smith *et al.*, 1991; Pestryaev, 1994; Ruhenstroth-Bauer *et al.*, 1994; Lin and Goodman, 1995; Litovitz *et al.*, 1997b; Muzalevskaya and Uritskii, 1997).

#### 2.1.4 Field configurations

They use various combinations and orientations of fields:

- parallel DC and AC MFs (Thomas *et al.*, 1986; Smith *et al.*, 1987; Liboff *et al.*, 1987a; Liboff and Parkinson, 1991; Reese *et al.*, 1991; Prato *et al.*, 1995; Smith *et al.*, 1995; Tofani *et al.*, 1995; Lednev *et al.*, 1996a,b; Deryugina *et al.*, 1996; Reinbold and Pollack, 1997; Ramundo-Orlando *et al.*, 2000),
- perpendicular DC and AC MFs (Thomas *et al.*, 1986; Blackman *et al.*, 1990; Picazo *et al.*, 1994; Blackman *et al.*, 1996; Ružič *et al.*, 1998),
- tilted fields (Ross, 1990; Kuznetsov *et al.*, 1990; Lyle *et al.*, 1991; Blackman *et al.*, 1993; Alipov *et al.*, 1994; Fitzsimmons *et al.*, 1995; Lindstrom *et al.*, 1995; Alipov and Belyaev, 1996; Blackman *et al.*, 1996;

- West *et al.*, 1996; Litovitz *et al.*, 1997b; Muzalevskaya and Uritskii, 1997; Ružič and Jerman, 1998; Galvanovskis *et al.*, 1999),
- rotating MFs (Ossenkopp and Ossenkopp, 1983; Kavaliers and Ossenkopp, 1985, 1986; Kato *et al.*, 1994; Sastre *et al.*, 1998),
  - near-zero MFs (Becker, 1965; Beischer, 1965; Halpern and Van Dyke, 1966; Busby, 1968; Lindauer and Martin, 1968; Conley, 1969; Dubrov, 1969; Beischer, 1971; Gleizer and Khodorkovskii, 1971; Khodorkovskii and Polonnikov, 1971; Wever, 1973; Edmiston, 1975; Pavlovich and Sluvko, 1975; Semikin and Golubeva, 1975; Sluvko, 1975; Chew and Brown, 1989; Kato *et al.*, 1989; Asashima *et al.*, 1991; Kashulin and Pershakov, 1995; Eremenko *et al.*, 1997),
  - electric fields, also in combination with MFs (Wilson *et al.*, 1981; Jafary-Asl *et al.*, 1983; Serpersu and Tsong, 1983; Whitson *et al.*, 1986; Phillips *et al.*, 1986b; Blackman *et al.*, 1988; Lyle *et al.*, 1988; Fitzsimmons *et al.*, 1989; Blackman *et al.*, 1990; Blank and Soo, 1990; Nazar *et al.*, 1996; Huang *et al.*, 1997; Schimmelpfeng and Dertinger, 1997; Sontag, 1998, 2000),
  - parallel MF and a perpendicular electric field (Novikov and Zhadin, 1994; Novikov, 1994, 1996),
  - pulses and pulse bursts of MFs of various shapes (Aarholt *et al.*, 1982; Goodman *et al.*, 1983; Mooney *et al.*, 1986; Takahashi *et al.*, 1986; Goodman and Henderson, 1988; Semm and Beason, 1990; Luben, 1991; Smith *et al.*, 1991; Walleczek and Budinger, 1992; Ruhenstroth-Bauer *et al.*, 1994; Pestryaev, 1994; Richards *et al.*, 1996),
  - with low-frequency EMF modulation (Bawin *et al.*, 1975; Lin and Goodman, 1995; Litovitz *et al.*, 1997b),
  - motion of biosystems in a modulated MF (Sapogov, 1992; Nikollskaya *et al.*, 1996),
  - low-frequency MFs of super-low  $< 1\mu\text{T}$  intensity (Delgado *et al.*, 1982; Takahashi *et al.*, 1986; Berman *et al.*, 1990; Kato *et al.*, 1993; Ruhenstroth-Bauer *et al.*, 1994; Kato *et al.*, 1994; Loscher *et al.*, 1994; Feychting *et al.*, 1995; Blank and Soo, 1996; Novikov, 1996; Richards *et al.*, 1996; West *et al.*, 1996; Akerstedt *et al.*, 1997; Harland and Liburdy, 1997; Farrell *et al.*, 1997),
  - millimeter-wavelength radiation of super-low intensity (Aarholt *et al.*, 1988; Grundler and Kaiser, 1992; Belyaev *et al.*, 1996; Gapeyev *et al.*, 1996; Kuznetsov *et al.*, 1997).

Unfortunately, a number of interesting works are fairly difficult to be classed with any of the above combinations, since, as is very often the case, no indication is given in them of the DC MF level involved. That variable is as important as the frequency and amplitude of an AC field.

The works cited above are only provided here by way of example to illustrate the variety, completeness, and generality of magnetobiological effects. These quali-

ties alone strongly suggest that biological actions of electromagnetic fields are not exotic highly specialized effects, but rather common phenomena, refined regulatory mechanisms, perhaps used by nature on a global scale. Anyway, not all share that point of view (Garcia-Sancho *et al.*, 1994; Gustavsson *et al.*, 1999). The last work concludes, by the way, that there is perhaps no common cellular effect for low-frequency MFs. That inference was prompted by low reproducibility of findings in various laboratories, except for melatonin assays (e.g., Reiter, 1998). However whether uses of statistical tools are legitimate here is questionable. We might as well believe that science as a whole does not exist because only a small proportion of people are involved in scientific activities. Low reproducibility of results on various cohorts, with high reproducibility in each cohort, for more than a decade is indicative of the fact that it is just the experimental *conditions* that have not been adequately reproducible.

Information on the plausible physical nature of observed magnetobiological effects is primarily contained in the “physical part” of experiments, i.e., in the details of effective MFs. Emphasis, therefore, has been placed on MF configuration details, which are crucial for the outcome of an experiment. The “biological part”, the preparation of biological systems, supporting preparations and adequate conditions, as well as procedures for measuring the final variable — which are often sophisticated and artful experimental techniques — lie outside the scope of the discussion. Selection of an appropriate low-frequency MF range is dictated, as stated above, by the possibility of ignoring an induced electric field, which varies with the frequency, and mainly by the fact that in that range EMF biological effects are especially paradoxical. Uses of DC MFs and combined DC and low-frequency fields are detailed below.

In our descriptions of experiments we will make use of a unified scheme, or formula, of an experiment. It will contain controllable MF parameters, intervals of their variations, and some statistical data. Units of measurement are those often employed in experiments of that nature: for MF induction  $B$  —  $\mu\text{T}$ , for frequency  $f$  — Hz, for time intervals  $T, \tau$  — s. For instance, the formula

$$B(45 \pm 5)b(0-12/1)f(50, 60)B_p(!)n(5-8)g(?) \quad (2.1.1)$$

implies that the DC MF  $B$  (we will also denote it  $B_{\text{DC}}$  or  $H_{\text{DC}}$  depending on the context) is  $45 \mu\text{T}$  to within  $5 \mu\text{T}$ ; a parallel field with an *amplitude*, i.e., peak value,  $b$  (or  $B_{\text{AC}}$ ) varied from 0 to  $12 \mu\text{T}$  with an increment of  $1 \mu\text{T}$ . Various trials used two fixed frequencies, either 50 or 60 Hz, the value of the perpendicular component of DC MF  $B_p$  was not controlled (!), and the number of repeats  $n$  (experimental points) for each set of MF variables was from 5 to 8, the MF gradient being unknown (?). With pulsed MFs,  $b$  meant the pulse height. The order of parameter listing is arbitrary.

## 2.2 BIOLOGICAL EFFECTS OF DC MAGNETIC FIELDS

The behavior of living systems exposed to DC MFs has been discussed for quite a long time. The biological effect of DC MFs, unlike that of low-frequency ones, does not seem to be paradoxical on the face of it, since there are no EMF quanta whose energy could be compared with the energy of biochemical transformations. It seems plausible that a DC MF acts following another mechanism and is able to accumulate at some biological level, bypassing the state of primary physical oscillators. However, in this case as well, there are no reliably established mechanisms of primary reception of weak fields, except for those connected with the so-called biogenic magnetite (Simon, 1992).

Malko *et al.* (1994) deem it generally accepted that DC MFs exert no marked adverse biological action, which is confirmed by a rich experience of magnetic resonance tomography (Persson and Stahlberg, 1989). They addressed the multiplication of *S. cerevisiae* yeast cells exposed to a static MF of 1.5 T, produced by a clinical NMR tomograph. Exposed and control cells were allowed to multiply in a broth for 15 hours, which corresponded to seven cell divisions cycles. The DC and AC 60-Hz fields were under 50 and 3  $\mu$ T (rms), respectively. Data processing unearthed no statistically reliable effect.

The authors thus assumed that a given MF would not affect mammal cells as well, since most of the chemical reactions involving these cells and those of unicellular organisms are identical. They challenged reports of adverse actions of a DC MF on the blood in mice (Barnothy, 1956), *Drosophila* larvae (Ramirez *et al.*, 1983), and trout (Strand *et al.*, 1983). However, that inference is hard to accept considering a wealth of data on biological efficiency of both strong and weak static MFs, including changes in enzyme activity (e.g., Wiltschko *et al.*, 1986; Polk and Postow, 1997; Moses and Basak, 1996).

Constant exposure to a 20-mT field in Espinar *et al.* (1997) produced a 25% change in the histological parameters of chicken cerebellum tissue. Fields of about 71 and 107 mT, investigated in Berk *et al.* (1997), retarded the growth of an amoeba population by 9–72%. Also, stimulation was observed (Moore, 1979) at 15 mT and inhibition at 30–60 mT in various bacteria and fungi. Furthermore, from the viewpoint of the most likely interference MBE mechanisms, in certain cases strong MFs are less effective than weak fields, comparable with the geomagnetic field.

With the exception of relatively strong MFs, more than 1 mT, the question of possible adverse consequences of exposure to an MF different from the Earth's also awaits its solution. The issue is important because the level of a DC MF of technogenic origin and its gradient strongly vary from place to place. In given production premises a DC MF may be as low as several percent of the geomagnetic field, or as high as tens of oersteds near massive iron structures, and it may take on those extreme values within meters. The action of DC MFs on the human health and international programs in that field were discussed in a review by Repacholi and Greenebaum (1999).

### 2.2.1 Biological effects of weak magnetic fields

Leucht (1987) investigated the dissipation of melanophore pigments in tadpole skin samples subjected to a stimulating hormone and their aggregation under light. These processes appeared to have different rates, depending on the value of a DC MF. Doubling the field, from 42 to 84  $\mu\text{T}$ , reduced the dissipation rate by 22–24%. In these assays, the MBE was largely independent of the hormone density and illumination intensity, a fact that, according to the author, points to modulation of secondary signaling processes involving calcium by a magnetic field.

Belyaev *et al.* (1994) and Matronchik *et al.* (1996a) studied the influence of a 15-min exposure of *E. coli* cells to an MF, modified in comparison with the Earth's field, on the viscosity of cell suspension. The MF varied within 0–110  $\mu\text{T}$ . The absolute maximum of the MBE was about  $25 \pm 2\%$  in a near-zero MF. The dependence of the MBE on  $H_{\text{DC}}$  displayed several extrema with their sign alternating, Fig. 4.48.

Markov *et al.* (1998) found that the rate of  $\text{Ca}^{2+}$ -calmodulin-dependent phosphorylation of myosin light chains in a cell-free reaction mixture was strongly dependent on the DC MF level. The rate, worked out using the  $^{32}\text{P}$  radioactive tracer, grew monotonously from 80 to 280% as the MF was varied from  $0 \pm 0.1$  to 200  $\mu\text{T}$ .

### 2.2.2 Orientation in the Earth's magnetic field

Worthy of special attention are effects involving the orientation of living organisms in a weak MF, specifically in the geomagnetic field (GMF). Many biological systems have been found to “see” magnetic lines of force and employ this faculty for navigation (Kirschvink *et al.*, 1985; Beason, 1989). Biosystems can thus respond not only to the value of an MF, but also to changes in its direction. In this case, however, magnetosensitivity is no paradox. Kirschvink *et al.* (1985) came up with more or less satisfactory insights into the nature of that phenomenon. The magazines *Nature* and *Science* publish editorials on that topic with amazing constancy, overlooking at the same time to give to the general physical issues of the paradoxical biological action of EMFs a positive treatment.

Some navigational capabilities in a weak MF are displayed by bacteria (Blakemore, 1975; Frankel *et al.*, 1981), birds (Yeagley, 1947; Bookman, 1977; Bingman, 1983; Wiltschko *et al.*, 1986; Beason, 1989), fishes (Kalmijn, 1978; Quinn *et al.*, 1981; Chew and Brown, 1989), insects (Lindauer and Martin, 1968; Martin and Lindauer, 1977; Gould *et al.*, 1980), and mammals (Mather and Baker, 1981; Zoeger *et al.*, 1981).

Large-scale orientation using a “compass” requires a conjunction of a magnetic chart to a geographic chart. To us humans such a conjunction is our knowledge that the magnetic meridian is approximately aligned along the geographic one. Birds have no such knowledge, and so they have to adjust or to learn by coordinating their magnetic “feel” with their innate navigational means, e.g., those relying on the polarization distribution of daylight. After some learning, birds do not need daylight anymore, and so some of them are able to perform seasonal migrations

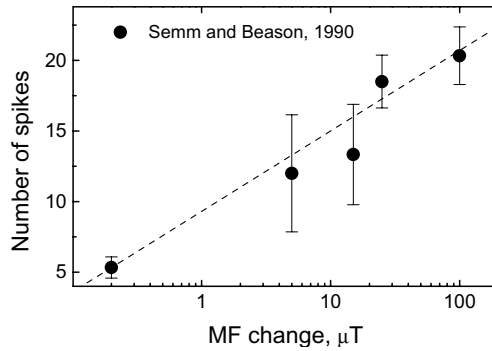


**Figure 2.1.** Changes in the vertical component of a local MF within 0.2 s bring about some heightened spike activity of the trigeminal ganglion cells, according to Semm and Beason (1990).

by night. Able and Able (1995) exposed sparrows in open cages for four days to a local MF oriented at  $90^\circ$  relative to the natural geomagnetic field. This tended to change the predominant direction, also by  $90^\circ$ , of night flights both in young and adult individuals.

Collett and Baron (1994) found that bees remember and then recognize the visual picture of some place, taking bearings using the lines of force of the geomagnetic field, i.e., using them as a reference. This markedly simplifies the retention and retrieval of information from memory.

Compass-type magnetic orientation is also inherent in newts in the daylight, but not by night. Orientation nature varies depending on the spectral composition of the light. It is believed therefore that photoreceptors of the retina can be suitable targets for a DC MF since their orientation is linked with the body stance. At the same time, Lohmann (1993) has shown that there exists light-independent compass-type orientation in some invertebrates, fishes, and mammals.

Semm and Beason (1990) studied the optic nerve and trigeminal ganglion in bobolinks exposed to short-term variations of a local DC MF. Their goal was to identify field-sensitive fibers of the nerve and to find out whether their sensitivity is high enough for a kind of “magnetic map” to be realized. The spontaneous activity of some areas or cells of the nerve (studied were 182 cells in 23 birds) was registered using micropipets–electrodes  $1\text{--}5\ \mu\text{m}$  in diameter. An inclinable couple of Helmholtz rings was used.

Only 14% of cells with a spontaneous activity appeared to be sensitive to MF variations. These cells did not respond to vibrations and mechanical stimulation of a bird’s body. Different cells responded differently. Some only responded to an increase, others to a decrease in the MF. Some cells appeared to be sensitive to hyperweak,  $\sim 200\ \text{nT}$ , variations within an interval from 0.2 to 4 s, the pulse front

being 6 ms. The variation of the number of activity spikes with the stimulus intensity for one of the cells is given in Fig. 2.1. Biological systems' sensitivity to stimulus typically shows a logarithmic dependence. This suggests that this dependence reflects secondary biochemical processes, rather than primary biophysical reception of an MF. Another evidence of that is the relatively large time, 10–20 s, of the recovery of initial cell activity after the removal of a weak magnetic stimulus. The authors believe that the “magnetic map” in birds, which responds to variations about 100 nT (Wiltschko *et al.*, 1986), could be due to the magnetic sensitivity of neurons.

### 2.2.3 Effects of a near-zero magnetic field

It has long been noticed that living organisms are not indifferent to changes in a DC MF level. Life on Earth has always existed under a weak (but not zero) geomagnetic field. It is widely believed that during the many millennia biological systems have somehow adjusted to the natural level of the magnetic field. Therefore, any MF changes can cause some infirmities and disorders. Some researchers maintain that an inversion of the Earth's magnetic poles could bring about changes of global proportions (Uffen, 1963; Opdyke *et al.*, 1966; Hays, 1971; Valet and Meynadier, 1993; Belyaev *et al.*, 1997). Specifically, a correlation of the emergence and disappearance of biological species with the average frequency of GMF inversions was found, Fig. 2.2.

The Earth's magnetic field changes its orientation approximately every 200 thousand years (ranging from 10 to 730 thousand years) and lasts for about 4–5 thousand years, with the result that living organisms find themselves for a long time in changed magnetic conditions, specifically exposed to a markedly reduced (to 10%) geomagnetic field (e.g., Skiles, 1985). Skiles provides arguments that we now witness a GMF inversion. Since during an inversion the geomagnetic field is different from a dipole field, local magnetic conditions may include values that are yet closer to zero (Valet and Meynadier, 1993).

Liboff (1997) believes that perturbations in biological species in a changing geomagnetic field are rather associated with cyclotron resonance conditions for some ions in the GMF and in the endogenous electric field of organisms. Unlike the already established fact of biological activity of a zero field, this hypothesis does not lend itself to easy verification, unfortunately. What is more, the very idea of cyclotron resonance in biology has not yet received any physical substantiation.

The relative simplicity of the realization of conditions of a near-zero MF, the presence of such a field in the working conditions of some professions, e.g., astronauts and submariners, predicated scientific research of biological effects of a magnetic vacuum, or a zero MF. A review of such works till 1976 is given in a monograph by Dubrov (1978) and till 1985 in a monograph by Kopanev and Shakula (1986). It is generally possible to reduce the value of an MF within an experimental space by two or three orders of magnitude as compared to that of the GMF. There are also sophisticated magnetic vacuum systems with a passive or active

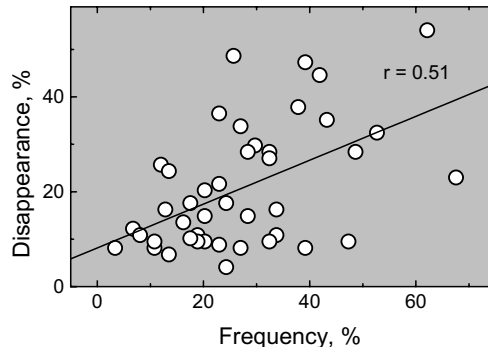


**Figure 2.2.** Correlation diagram: the  $x$ -axis, index of GMF inversion frequency;  $y$ -axis, index of the vanishing of biological species. Processing of data in Fig.24 from Dubrov (1978).

compensation to reduce the field  $10^5$ – $10^6$  times (Govorun *et al.*, 1992) and more (Vvedenskii and Ozhgin, 1986).

Biological effects of a magnetic vacuum are displayed by plants (Dubrov, 1969; Edmiston, 1975; Semikin and Golubeva, 1975; Kato *et al.*, 1989; Govorun *et al.*, 1992; Fomicheva *et al.*, 1992a,b; Belyavskaya *et al.*, 1992; Kashulin and Pershakov, 1995), microorganisms (Pavlovich and Sluvko, 1975; Sluvko, 1975), insects (Becker, 1965; Lindauer and Martin, 1968), worms (Lednev *et al.*, 1996a), newts (Asashima *et al.*, 1991), fishes (Gleizer and Khodorkovskii, 1971; Khodorkovskii and Polonnikov, 1971; Chew and Brown, 1989), mammals (Halpern and Van Dyke, 1966; Busby, 1968; Conley, 1969; Beischer, 1971), various cells (Belyaev *et al.*, 1997), and the human organism (Beischer, 1965, 1971; Wever, 1973).

No response of plants to a zero MF was found in Dyke and Halpern (1965). Different responses were observed (Shrager, 1975) in right and left isomer forms of onion seeds.

Kato *et al.* (1989) studied in a magnetic vacuum  $\sim 5$  nT the growth of “pilose roots” on carrot and belladonna induced by some genetic methods. The growth of roots on belladonna in the field  $50 \mu\text{T}$  was enhanced by 40–56% as compared with controls. The carrot root growth remained nearly unchanged. At the same time a DC field  $\sim 0.5$  T, strong as compared with the control field  $\sim 10^{-3}$  T, caused a  $\sim 25\%$  enhancement of root growth in both plants. It was shown that a changed DC MF in those assays acts precisely on plant roots, since a pre-treatment of the medium where the plants grew under similar magnetic conditions did not result in any changes. It was concluded that a strong MF and a magnetic vacuum might have different targets in plants, i.e., different mechanisms of biological action. The authors also refer to a work where identical conditions,  $H_{\text{DC}} \sim 5$  nT, resulted in the death of newt embryos within several days.

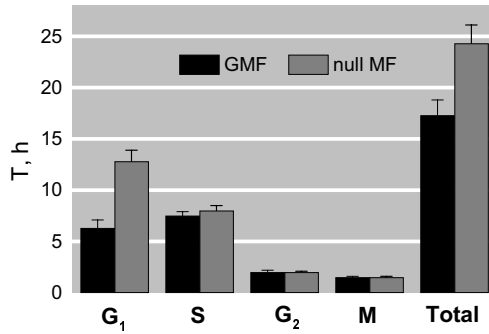


**Figure 2.3.** Influence of an MF on reproduction cycle phases of pea root meristematic cells. Phase G<sub>1</sub>, RNA and protein synthesis; S, DNA synthesis; G<sub>2</sub>, post-synthesis; M, mitosis phase; Total, entire cycle; according to data (Fomicheva *et al.*, 1992a).

Many hours of exposure of oats plants at the early stages of ontogenesis under hypomagnetic conditions, with the GMF compensated down to 1% of its local value, stimulated plant growth (Kashulin and Pershakov, 1995).

Bacterial cultures respond to screening from the GMF in a wide variety of ways, by changes at the phenotype and genotype levels, which manifest themselves both in metabolic and physiological processes (Dubrov, 1978). Hypomagnetic conditions, up to 0.1  $\mu$ T, brought about an increase in cellular nuclei size and a marked reduction in mitosis intensity in mouse and hamster cells *in vitro* (Sushkov, 1975). At the same time, hypomagnetic conditions (Green and Halpern, 1966) have not produced any changes in isolated cells of some mammals.

GMF screening is often performed using protective boxes from non-retentive, magnetically soft materials. Such a screening always leaves one wondering whether an effect observed could be due to changed levels of AC MFs and electric fields. Therefore, the findings were compared with a control group of biological objects held in metal non-magnetic containers (Halpern and Van Dyke, 1966; Busby, 1968; Govorun *et al.*, 1992; Fomicheva *et al.*, 1992a,b; Belyavskaya *et al.*, 1992).

In a series of works Govorun *et al.* (1992), Fomicheva *et al.* (1992a,b), and Belyavskaya *et al.* (1992) addressed the vital activity of germinating pea, lentil, and flax seeds. A multilayer permalloy screen box was used to produce a magnetic vacuum of about  $10^{-5}$ – $10^{-6}$  GMF. It was shown that the predominant response to a magnetic vacuum was a decline in seed germination rate by 30–50% (Govorun *et al.*, 1992). The proliferative pool of root meristem cells dropped from 90–96% to 68–75% with consistent statistics (Fomicheva *et al.*, 1992a); the evidence for changes in activities of various phases of the reproduction cycle is shown in Fig. 2.3. Radioactive tracing here was done using a  $^3$ H hydrogen isotope. The authors assumed that responses to a zero MF in these plants are associated with the synthesis of

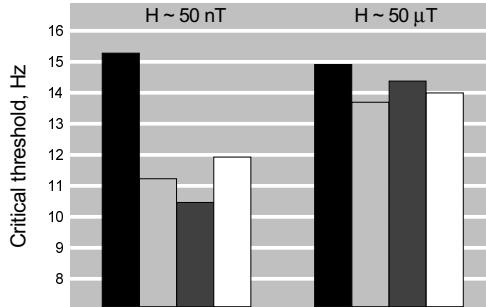


**Figure 2.4.** A response of one of the rhythms in men to a zero MF on four human volunteers. Averaging: on the left, during the exposure; on the right, 3 days before and 3 days after it. According to Beischer (1965).

RNA and proteins, rather than with the synthesis of DNA or mitosis. RNA synthesis dynamics in some proteins of meristem cells was studied (Fomicheva *et al.*, 1992b) by fluorescent spectroscopy to reveal some details of transcription processes in cells of a variety of plants. Electron microscopy of sections of root meristem cells revealed some structural functional changes in the state of the cells, primarily Ca-homeostasis (Belyavskaya *et al.*, 1992). Under a zero MF, free and weakly bound calcium made its appearance in cellular hyaloplasm, whereas it was absent during the growth in the GMF.

Also, many experiments in Becker (1965), Beischer (1965), Lindauer and Martin (1968), Conley (1969), Dubrov (1969), Gleizer and Khodorkovskii (1971), Khodorkovskii and Polonnikov (1971), including the relatively recent work by Kashulin and Pershakov (1995), were conducted with the GMF compensated by man-made MF sources, such as Helmholtz rings. Beischer (1965) used an 8-m ring system to cope with four volunteers at the same time. Figure 2.4 shows the response of a functional characteristic of the central nervous system after a 10-day exposure to a magnetic vacuum measured under these conditions. It is well seen that the mean frequency of the rhythm drops markedly for three out of four volunteers.

Unfortunately, with very few exceptions, the literature on biological effects of a zero MF contains no dependences of an effect on the field magnitude. Such dependences are of interest, because they carry information on magnetoreception primary processes.

Asashima *et al.* (1991) exposed Japanese newt larvae in development phase to a magnetic vacuum 5 nT for five days. On the 20th day of their development the authors observed distorted spines, irregular eye formation, general retardation of development, and even the appearance of two-headed individuals. Vacuum exposure turned out to be effective in the early phases of larvae development, including the

gastrula phase, the effect being 100–200%.

Belyaev *et al.* (1997) measured the abnormal viscosity of a suspension of *E. coli* cells after a 15-min exposure to an MF changed in relation to the geomagnetic field. As the field was decreased from 2 to  $0 \pm 0.1 \mu\text{T}$  a 5% MBE growth was observed. Similar effects under these conditions have also been found in other cells, e.g., in rat thymocytes and human fibroblasts.

Lednev *et al.* (1996a) observed a zero MF effect in the mitosis of neoplast cells of regenerating planaria. A DC field was varied from 200 to  $0 \mu\text{T}$  to within  $0.06 \mu\text{T}$ . The mitotic index increased by  $37 \pm 12\%$  in going over from a field of  $0.2 \mu\text{T}$  to zero, Fig. 4.47.

Measurements of some parameters of biological systems indicate that not all of those systems show evidence of effective influences of magnetic vacuum conditions. Proliferation of leukemia cells was studied (Eremenko *et al.*, 1997) in a residual (after magnetic screening) field of 20 nT. Although some statistically significant difference from control samples, outside of the chamber, was registered, the effect was fairly small,  $< 5\%$ .

We note that biological effects of a magnetic vacuum are circumstantial evidence for the quantum nature of MBEs. In terms of the classical dynamics of relatively free charges, e.g., of ions in a solution, an MF decrease is not accompanied by any qualitative changes. The geomagnetic field, let alone yet lower fields, exerts virtually no influence on a particle's trajectory within its mean free path. So, a relative deviation of an ion with charge  $q$  and mass  $M$  in an MF  $H \sim H_{\text{geo}}$  during the time of a mean-free path at room temperature,  $t \sim 10^{-11}$  s, will be  $\Omega_c t \sim 10^{-9}$ , where  $\Omega_c = qH/Mc$  is an ion cyclotron frequency. However, bound particles, such as ions and electrons, oscillating in an MF are subject to the so-called Zeeman splitting of energy levels — a quantum phenomenon at the microscopic scale of oscillations. In the absence of an MF, the splitting vanishes, and the levels become degenerated. It is immaterial that the splitting amount had the same order of smallness  $\sim 10^{-9}$  as compared with  $\kappa\mathcal{T}$ . It is important that the symmetry of the particle wave function changes, which is a qualitative change. Other qualitative changes that accompany the deprivation of an MF are not observed, which is an indirect indication to the quantum nature of MBEs.

## 2.2.4 Biological effects of gradient magnetic fields

During the past decade some companies were manufacturing all sorts of magnetic bracelets, necklaces, pads, etc. They sell well but have no adequate scientific underpinnings. In this case, MF sources lie outside of biological receptors, and so it is not to be excluded that any possible action of such devices is due to spatial inhomogeneity of an MF. Descriptions of such devices used in magnetotherapy and popular publications on the topic are available on the Internet, see, e.g., [www.biomagnetics.com](http://www.biomagnetics.com), [www.painreliever.com](http://www.painreliever.com), and [www.magnetease.com](http://www.magnetease.com).

Medical practitioners also use so-called magnetophores (Fefer, 1967). These are basically flexible rubber applications several millimeters thick, which are cut out

to size from a roll. The rubber incorporates some magnetically rigid filler magnetized following a definite pattern with alternating magnetic poles on the sheet surface. Such an MF source produces an MF that is strongly inhomogeneous near the surface.

Very few research works are known that address the biological action of such devices.

Therapeutic actions of magnetophores, in particular the enhanced repair of tissues after skin plastic surgery, is discussed in the monograph by Usacheva (1981). That evidence is confirmed by Shilov *et al.* (1983), who investigated into the influence of a magnetophore applicator on the rate of lipid peroxide oxidation in human skin. The induction and gradient of an MF on the applicator surface were 30 mT and 5 mT/mm, respectively. An index of oxidation rate was the behavior of the hyperweak chemiluminescence of skin homogenates. An MF of specified configuration would totally remove the effect of a 20% activation of lipid free-radical oxidation due to hypoxia.

Clinical data of Lin *et al.* (1985) show that matrices of 0.3-T permanent magnets have some neurological action on humans, but do not remove inflammations and do not abate pain.

Krylov and Tarakanova (1960) report their findings of different biological actions caused by the opposite poles of permanent magnets, with the south pole MF exerting a stimulating action on plant growth. Davis and Rawls (1987) reported that plants were growing faster in the field of a magnet's north pole. The evidence was confirmed by Ružič *et al.* (1993), although stimulation here was provided by the south pole.

Kogan and Tikhonova (1965) addressed the motion of *Paramecium caudatum* infusoria in a 0.5-mm dia capillary 50–70 mm long with a nutrient solution. The motion of Paramecia in the control was fairly regular in nature. An infusorium periodically moved from one edge of a capillary to the other; the mean residence time at some half of the capillary ranged from 17 to 50 s, depending on the individual properties of an animal. The capillary was then brought to a pole of a permanent magnet of 160 Oe or, in another experiment, about 700 Oe. It appeared that Paramecia are quite pole-sensitive. They stayed for a long time near the south pole and avoided the north pole, as if they contained a Dirac monopole. The asymmetry attained 300% and was on the whole proportional to the magnet force.

Cavopol *et al.* (1995) observed the reaction of sensory neurons in a cell culture to the MF gradient. Such an MF affected the probability of "firing" of the neuron action potential (AP). A gradient of 1 mT/mm blocked 70% of the AP; 1.5 mT/mm, 80%. At the same time, a DC field of 0.2 mT with a gradient of 0.02 mT/mm caused no changes.

It is to be noted that the physical mechanism for the detection of MF orientation by biological systems is yet unclear. What we need here is a reference vector in relation to which we could discriminate MF direction. One such vector is the gradient of the MF absolute value, Fig. 2.5. The figure shows that the MF and its gradient are oriented in the same direction near the magnet's south pole, and in

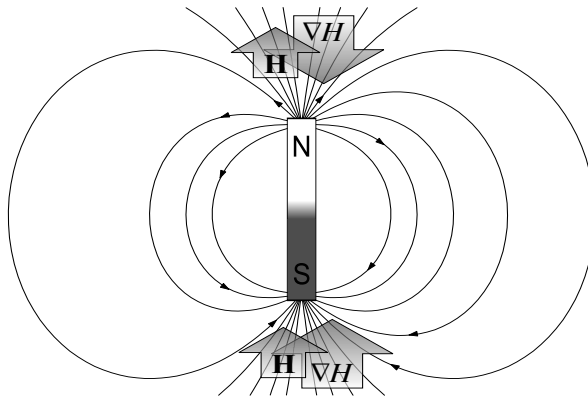


**Figure 2.5.** Magnetic lines of force of a permanent magnet and the relative orientations of MFs and their gradients near magnet poles.

opposite directions near the north pole. No data are yet available on similar effects in cellular cultures with randomly oriented cells. For plants, a vector that orients cells and can therefore be taken to be a reference for MF orientation detection is the gravity vector. We note that in the experimental works just described it is maintained that a magnet's poles have different actions. That would be so if the authors had shown that an MF with a specified direction and magnitude, produced in two different manners, say, by putting the north pole of a bar magnet to the right of a symmetrical object, or the south pole to the left, would produce different biological effects.

It is interesting that Yano *et al.* (2001) described exactly such an experiment. They placed tubes with radish seedlings in a gel horizontally on a platform. By slowly rotating the platform around a horizontal axis they eliminated the action of gravitation on the seedlings. Illuminating the tubes along their axes would set the direction for root growth. In the middle of each tube a disk-shaped axially magnetized permanent magnet was attached. Some magnets had their north poles pointing to the tube axis, others in the opposite direction. For controls, they used brass disks of the same shape and size. With such an arrangement, a root grew in a permanent MF gradient pointing to the magnet at all times, and also in a DC MF whose sense was conditioned by the magnet orientations. It appeared that magnetotropism is dictated by magnet orientation. The seedling root deflected away from the magnet if the latter had its south pole pointing at the plant. Approximate mean daily deflections are as follows: controls,  $-0.01 \pm 0.09$  mm; the north pole,  $0.05 \pm 0.08$  mm; the south pole,  $0.14 \pm 0.1$  mm. At the tube center, where it intersects the magnet axis, the MF was about 40 mT for a gradient of 10 mT/mm. That experiment shows that it makes sense to talk about biosystems that detect the direction of an MF relative to its gradient.

Rai *et al.* (1996) and Pandey *et al.* (1996) observed different actions on water samples of MFs produced by the north and south poles of permanent magnets. The samples were tested using different biological reactions. However, in that case no reliable conclusions were made, since the experiments were staged with other objectives in mind.

It is shown later in the book that biological actions of low-frequency MFs and microwaves have a measure of similarity and, probably, in certain cases the physical processes underlying such actions have a general nature. It would be of interest, therefore, to cite the work Gapeyev *et al.* (1996) concerned with frequency spectra of the action of microwave radiation on cells of the immune system in mice. Both near and far zone radiation conditions, see Section 1.4.4, were utilized to obtain equal energy flux densities at samples. It appeared that the far-zone radiation had a pronounced resonance-like action on cells; i.e., the spectrum had a maximum. At the same time, the far-zone radiation had only a frequency-independent action. Note that the far-zone radiation had relatively small field gradients, suggesting that the plane waves approximation often appears to be insufficient. At the same time, in the near zone, in the immediate vicinity of the emitter, field gradients are large.

We also note a work by Makarevich (1999), which focuses on the influence on microorganism growth of magnetoplasts — ferrite-containing magnetized polymer composites. On the surface of magnetoplast samples the residual induction was 0.1–1 mT. Microbial strains were incubated in Petri dishes that also contained cylindrical magnetoplast samples. After two days of incubation, around the samples they observed ring areas of enhanced and retarded growth, depending on the magnetization of the samples. In some assays, growth enhancement was observed near the north pole of a magnetoplast magnetized along its axis. In contrast, near the south pole, the microbial growth was retarded. The possible role of MF gradients was not discussed in that work.

No special studies to separate the effects of a homogeneous and a gradient MF are known. Also, in the literature there are no discussions of possible physical mechanisms for the biological reception of the aligning of an MF relative to its gradient — i.e., of mechanisms of biological sensitivity to the sign of the scalar product  $\mathbf{B} \nabla B$ .

### 2.3 BIOLOGICAL EFFECTS OF AC MAGNETIC FIELDS

Biological effects of AC MFs have for a long time been studied ignoring the DC MF level at site. It was supposed that the amplitude and frequency of an AC MF, or the shape and frequency of pulses for pulsed action, are in themselves sufficient to completely characterize the magnetic conditions involved. Studies of amplitude dependences were in turn restrained by our intuitive understanding of the resonance mechanism for MF reception by biological objects where the main parameter is the field frequency, although amplitude–frequency windows in EMF biological effects were observed by Bawin *et al.* (1975), Bawin and Adey (1976), and Blackman *et al.* (1979). Plekhanov (1990), who has reviewed the impressive body of experimental

evidence due to the Tomsk group of magnetobiologists, also points to the existence of MF effectiveness windows.

This section focuses primarily on experiments that reveal complex frequency and amplitude MBE spectra (Adey, 1980). It is spectral curves that bear especially much information on the physics of magnetoreception primary processes.

### 2.3.1 Effects of combined AC–DC fields

A series of fundamental works by Blackman *et al.* and Liboff *et al.* revealed in the 1980s that in certain biological systems the DC MF level would define the position of maxima in MBE frequency spectra (Blackman *et al.*, 1985; Liboff, 1985; McLeod *et al.*, 1987a; Liboff *et al.*, 1987a,b). The importance of taking into consideration the permanent geomagnetic field in experiments with biosystems exposed to an EMF was also noted by Cremer-Bartels *et al.* (1984) and Blackman *et al.* (1985). A dependence of AC MF effects on the magnitude of the DC component was pointed out by Lednev (1991) and Lyskov *et al.* (1996). The DC MF level was a significant parameter also in early theoretical MBE models of Chiabrera and Bianco (1987). Bowman *et al.* (1995) noted a correlation between definite “resonant” DC MF magnitudes and the childhood leukemia risk in an epidemiological study.

It has taken more than a decade for the involvement of DC fields in the shaping of experimental conditions to become a criterion of scientific value in magnetobiology. It is now clear why magnetobiological experiments used to exhibit such a low reproducibility, a fact that has been continually stressed by opponents. Special-purpose studies have been undertaken to reveal biologically meaningful elements in the organization of the electromagnetic environment (Valberg, 1995). It has gradually become clear that the AC MF amplitude, which may not necessarily be large, may also play a decisive role in observing the effect. That sets the behavior of biological systems in an MF apart from that of oscillators in the standard spectroscopy of physical systems. It is this involved behavior of biosystems, which was one of the reasons for the poor reproducibility, that supplies ample information on the physical nature of the primary processes of MF reception.

- <sup>14</sup> The action of an MF on the weight of a chicken on the 10th day of its development was studied by Saali *et al.* (1986) under the conditions

$$B(?)B_p(?)b(0-125)f(50, 1000)n(14-28) ,$$

and also under pulsed MF conditions. They found that both pulsed and sinusoidal MFs cause some MBEs. In the latter case, an MBE was observed with statistical confidence at various AC MF amplitudes. Figure 2.6 shows results depending on the field amplitude variations relative to a local DC MF, whose magnitude is taken to be 50  $\mu$ T. It is seen that at 50 Hz an MBE occurs when the field amplitude becomes

---

<sup>14</sup>In what follows this symbol marks works or groups of works that are arranged in chronological order.

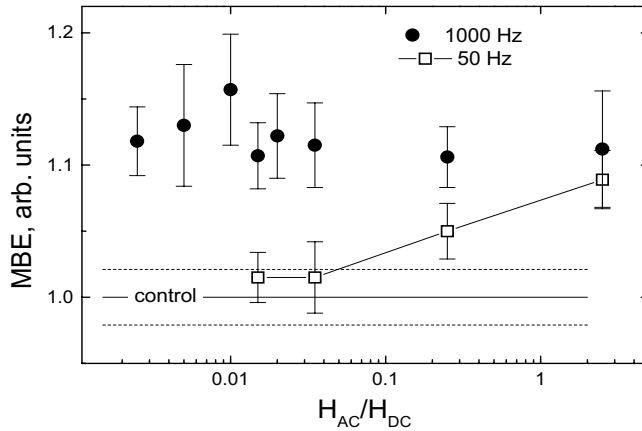


**Figure 2.6.** Dependence of the weight of a 10-day chicken embryo on the amplitude of a 60-min exposure to an AC MF at the early development stage for various field frequencies, according to Saali *et al.* (1986).

comparable with a local field. At 1 kHz, the MBE shows no definite dependence and, on the whole, remains unchanged within a wide amplitude range.

- Smith *et al.* (1987) measured the mobility of diatomic algae cells in agar with a low content of  $^{40}\text{Ca}$  as a function of the frequency of an AC MF with an amplitude of  $20\ \mu\text{T}$ , a parallel DC field being  $21\ \mu\text{T}$ . They found a resonance-like mobility growth by  $35 \pm 4\%$  at 16 Hz, which corresponded to a cyclotron frequency of  $^{40}\text{Ca}^{2+}$  ions, Fig. 2.21.

A detailed study of the mobility of diatomic algae subjected to an MF under various conditions corresponding to a cyclotron resonance (CR) frequency and its harmonics was conducted in McLeod *et al.* (1987a). The diagram of the experiment

$$B(kf)B_p(?)b(15)f(8, 12, 16, 23, 31, 32, 46, 64)n(> 500)$$

was selected so that the magnetic conditions corresponded to a cyclotron resonance of  $\text{Ca}^{2+}$  ions:  $k = 1.31\ \mu\text{T}/\text{Hz}$ . Under all conditions, a statistically significant MBE was found that was similar to that in a control exposed to a  $B(55.7 \pm 0.1)$  DC field. For conditions  $f(8, 12, 16, 23, 31)$ , bell-shaped frequency spectra were found near respective central frequencies.

- Kuznetsov *et al.* (1990) studied the probability of arrhythmia in frog auricle preparations as a function of the MF frequency and amplitude. Experiments were conducted following the scheme

$$B(?)B_p(?)b(0-750)f(0-100)t(30\ \text{min})n(7) .$$

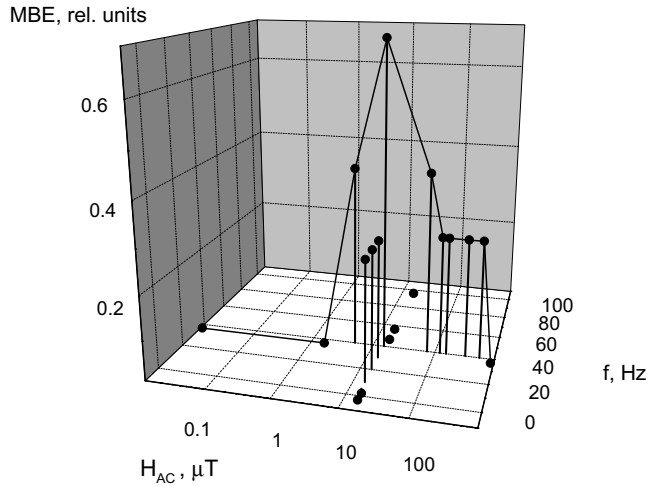


**Figure 2.7.** Myocardium arrhythmia incidence in frogs as a function of the AC MF frequency and amplitude, according to Kuznetsov *et al.* (1990).

The effect appeared to have a quasi-resonance behavior in both frequency and amplitude. It had a maximum at  $H_{AC} = 15 \mu\text{T}$ ,  $f = 40 \text{ Hz}$ , Fig. 2.7. A relatively large increment of changes of MF variables, and also the absence of information on the magnitude and direction of a local DC MF, hinders the interpretation of data, although the general nature of the window structure of the response is quite obvious. It is supposed that the effect is produced by AC MF-induced electric fields.

- Reese *et al.* (1991) reproduced and confirmed the assays of Smith *et al.* (1987). They measured the mobility of unicellular algae *Amphora coffeaformis* in agar enriched by calcium ions in concentrations 0.0, 0.25, and 2.5 mM. The experimental setup was like that in Smith *et al.* (1987)

$$B(21)b(21)B_p(\sim 0)f(16)n(19)B_{\text{sham}}(43)b_{\text{sham}}(< 0.2) .$$

A wide spread of data did not enable the frequency spectrum of the effect to be measured. The results (Smith *et al.*, 1987; Reese *et al.*, 1991), as is seen in Fig. 2.8, agree quite well. These experiments show that for effects to be observed requires a measure of non-equilibrium in calcium. At the same time, in the intercellular medium a large calcium density, 5 mM, “switched off” the calcium-related MBE, but caused an MBE to occur under other magnetic conditions, concerned perhaps with potassium (McLeod *et al.*, 1987a).

- Goodman and Henderson (1991) also observed frequency, amplitude, and temporal windows when transcription processes in human lymphocytes and *Drosophila*

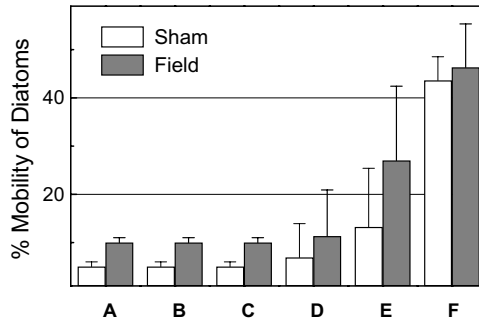


**Figure 2.8.** The variation of the algae cell mobility in parallel MFs at concentrations (mM) of calcium ions in agar 0.0, A,D; 0.25, B,E; 2.5, C,F. According to Smith *et al.* (1987) (A,B,C) and Reese *et al.* (1991) (D,E,F).

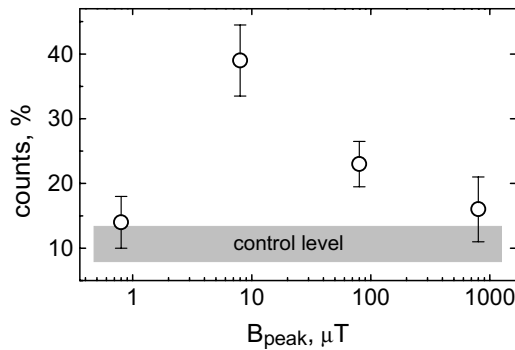


**Figure 2.9.** Influence of a 20-min exposure to a 60-Hz magnetic field of various amplitudes on the transcription process in HL-60 cells, according to Goodman and Henderson (1991).

saliva glands were exposed to low-frequency MFs. One experiment with amplitude variations was performed using the formula

$$b(0.8-800)B(?)B_p(?)f(60,72)t(10,20,40 \text{ min}) .$$

The level of some transcripts in chromosomes was measured using the radioactive tracer  $^{35}S$ .

Figure 2.9 displays the variation of the tracer reference level with the MF amplitude. The effect is seen to be especially significant where the AC MF amplitude compares with the geomagnetic field. Maximal values occurred at a 20-min exposure.

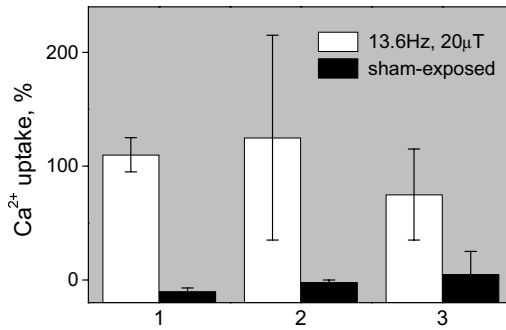


**Figure 2.10.** Influence of inclined low-frequency and DC MFs on  $^{45}\text{Ca}^{2+}$  uptake by lymphocytes of various types — 1,2,3, according to Lyle *et al.* (1991).

- Lyle *et al.* (1991) investigated the calcium radioactive tracer uptake by lymphocytes exposed to an AC field at an angle to a DC one. Cells of various lines were used, including cancer ones. The magnetic field had the configuration

$$B(16.5 \pm 0.5)b(20)b_{\text{sham}}(\sim 0)f(13.6)B_p(? > 20) .$$

The authors observed a significant effect, Fig. 2.10, on exposure to a parallel AC field against the background of an inclined geomagnetic one. Somewhat smaller, but also statistically significant, changes were observed at 60 Hz. Data on DC field values are contradictory. Its magnitude was reported to be  $384 \mu\text{T}$ , its slope to the horizontal being  $57 \pm 2^\circ$ . Even if we take account of the probable error in the indication of the field value, there is still no computing the true angle between the fields. It is interesting that if a 30-min MF exposure was conducted before a tracer was introduced, rather than immediately after it, no effect was observed. This may be due to the fact that a combination of MF variables corresponded exactly to the  $^{45}\text{Ca}$  isotope. The authors believed that the frequency they used corresponded to a cyclotron one for calcium in a  $16.5\text{-}\mu\text{T}$  field, although they did not cite the isotope number. By the same token, it hardly makes sense to work out the frequency using only one MF component along some axis, because in the general case the other MF component also affects the dynamics of a particle.

- Experiments of Prato *et al.* (1993) addressed the dependence of MBEs on the amplitude of the AC MF component. They placed *Cepaea nemoralis* snails on a warm surface and measured the time it took a snail to raise its leg. Before the assay, the snails were treated with an inhibitor to increase the response time. Exposure to an MF reduced the inhibition effect. The arrangement of the experiment

$$B(78)b(18-547)f(60)B_p(\pm 0.8)$$

was chosen to correspond to a cyclotron frequency of  $^{40}\text{Ca}^{2+}$  ions. The magnetic effect appeared to be as high as 80% of the relative amount of inhibition by a bioactive preparation, the data spread being 10-20%. The behavior of the amplitude  $B_{AC}$  displayed several extrema, Fig. 4.39. The data were then confirmed and refined in later works of the group (Prato *et al.*, 1995, 1996) using a double-blind technique. The procedures of (1) preparation, placement, and transportation of the animals, (2) exposure to an MF, and (3) taking the reaction time were conducted by mutually uninitiated workers. In Prato *et al.* (1995) a multipeak frequency spectrum of an MBE is provided, Fig. 4.36, along with a dependence on DC MF with the frequency and amplitude of the DC MF component fixed.

- Blackman *et al.* (1994) carried out some assays to capture the dependence of biological response on the ratio of the DC MF amplitude to the magnitude of DC collinear MFs. The quantity measured was the inhibition degree of neurite outgrowth in PC-12 cells. The outgrowth was induced by a biological stimulator. The temperature was sustained to within 0.1 °C. Control was performed in the same thermostat in a passively screened section, which reduced the MF level by two orders of magnitude. There were two types of controls, with and without the outgrowth stimulator. Experimental data were normalized using a technique commonly employed for two different exposure factors; in this case these factors were the outgrowth stimulator and the MF. The relative MF effect was worked out by

$$\%NO = \frac{R - Z}{N - Z} 100\% ,$$

where  $Z$  is the relative number of neurite-containing cells in an assay without MF and stimulator (control 1),  $N$  is the same with an MF but without a stimulator (control 2), and  $R$  is the same with an MF and a stimulator. The results 0 and 100% thus corresponded to the effect value when the cells were treated in the absence of an MF, with or without stimulator. Exposure to an MF yielded intermediate values. For the formula of the experiment

$$B(36.6)b(10.8-66.2/\sim 5)f(45)B_p(< 0.2)n(3-4)g(!) \quad (2.3.1)$$

results were obtained that are depicted in Fig. 2.11<sup>15</sup> by open circles, the quantity  $100\% - \%NO$  is shown. Maximal effect was confidently observed with intermediary AC MF amplitudes. Magnetic layout

$$B(2)b(1.1-2.9/\sim 0.4)f(45)B_p(< 0.2)n(3)g(!) \quad (2.3.2)$$

yielded points that grouped closely around 100%, i.e., a zero effect.

Studies of amplitude spectra of neurite outgrowth inhibition for large relative MF amplitudes were continued in Blackman *et al.* (1995b). These data, shown in Fig. 2.11 by solid circles, attest to the multipeak nature of the amplitude spectra.

---

<sup>15</sup>This author is grateful to C. Blackman for the file of data.

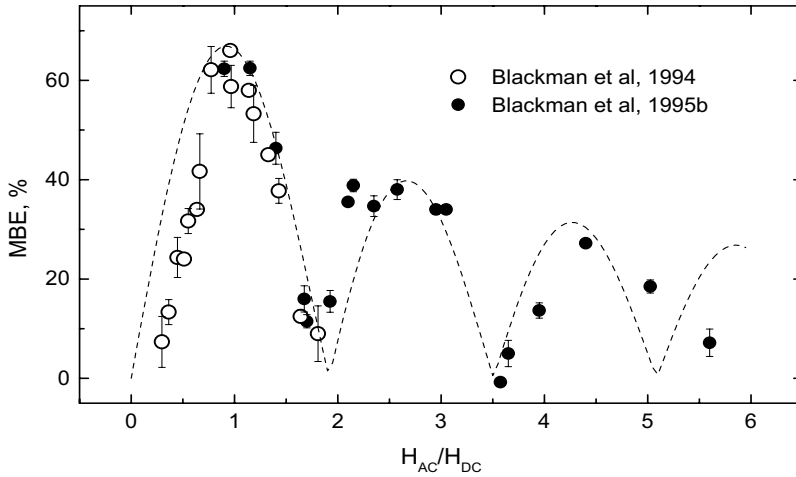


**Figure 2.11.** Variation of MBE in PC-12 cells with the amplitude of the AC component in a uniaxial MF, according to Blackman *et al.* (1994, 1995b). The line depicts the function  $|J_1(2H_{AC}/H_{DC})|$ .

Plotted in the figure is also the magnitude of the function  $J_1(2H_{AC}/H_{DC})$ . It is a fairly good approximation of the findings; therefore the authors carry on their search for a physical substantiation of that dependence (Machlup and Blackman, 1997).

The authors assumed that Mn(4), V(4), and Mg(2) ions<sup>16</sup> and also, with a smaller probability, Li(1) and H(1) ions can be responsible for magnetoreception in PC-12 cells. It is precisely with these ions that, for the DC MF  $B_{DC}$  and AC field frequency  $f$  specified by the experiment formula (2.3.1), the cyclotron frequencies  $\Omega_c = qB_{DC}/Mc$  approximately obey the relation  $\Omega_c = n\Omega$ ,  $\Omega = 2\pi f$ .

The group also researched the MBE frequency spectra of neurite outgrowth inhibition in the same cells (Blackman *et al.*, 1995a). The main departure was the presence of the DC MF perpendicular component

$$B(37)b(5.3-12.5/\sim 1.5)B_p(19)f(15-70/5).$$

MBE frequency windows were found near 40 and 60 Hz and higher, Fig. 2.12; i.e., the MBE frequency spectra had several extrema.

In parallel fields no effects were captured at 45 Hz, and the authors concluded therefore that a DC MF component normal to the AC field was an essential factor. It is interesting that an opposite conclusion was reached after an investigation

<sup>16</sup>Shown in parentheses is the ion valence.

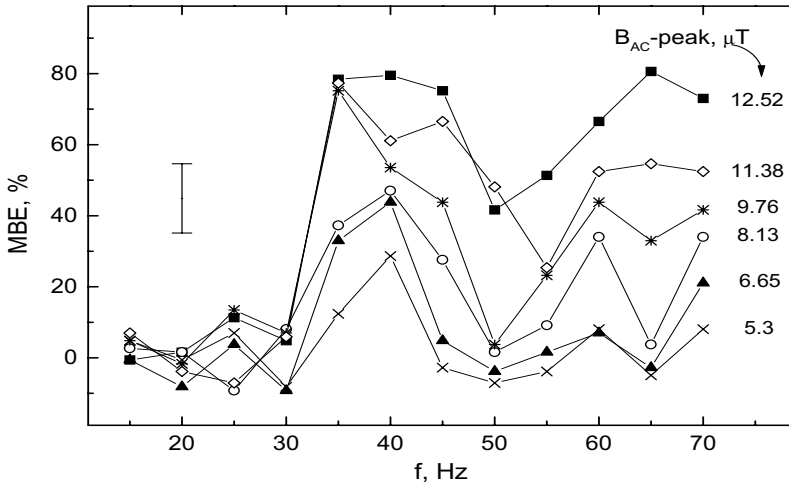


**Figure 2.12.** Inhibition of stimulated neurite outgrowths in PC-12 cells with DC and AC fields oriented at an angle; points for different AC MF amplitudes are shown, according to Blackman *et al.* (1995a).

(Belyaev *et al.*, 1994) into the role of a perpendicular DC field in another biological system, *E. coli* cells. McLeod *et al.* (1987a) also reported that the perpendicular component was insignificant in experiments on the mobility of diatomic algae in an MF. On the other hand, it was shown (Blackman *et al.*, 1996) that parallel and perpendicular orientations of fields result in opposite effects, and that MBEs may vanish at some of their combinations. It will be shown in what follows that such complicated dependences on field orientations are characteristic of the interference of ions bound in macromolecular capsules.

We note that Blackman *et al.* (1994, 1995a) used a horizontal ring coil for an AC MF source. At various separations from the ring, they could thus get a number of AC MF amplitudes at the same time. Such an arrangement of a field source produced relatively strong MF gradients in the vicinity of biological samples. There is evidence of biological activity in certain cases precisely due to MF gradients. It would be difficult to comment on the findings if it were not for good agreement in these works of the effect for similar MF amplitude values with different gradients. That is indicative of an insignificant role played by MF gradients in assays under considerations. Overall, in the absence of well-established MF exposure mechanisms, the question of whether it is admissible to employ gradient fields in such experiments is open.

- Lindstrom *et al.* (1995) found that a sinusoidal MF induced cytosol calcium density variations in human leukemia T-cell line. The experimental setup was

$$B(50)B_p(53)[B(60)B_p(22)]b(40, 80, 150, 300)f(5, 25, 50, 75, 100) .$$

The variations looked like records of a random process, but some processing of those curves suggested that the maximal response to fields belonging to the set in the diagram was a concentration growth by a factor of 5–8, which was observed for a 50-Hz, 150- $\mu$ T exposure in a parallel field of 50–60  $\mu$ T. Unfortunately, the authors did not indicate which of the AC MF characteristics, root-mean-square or peak ones, they employed; also the parameters' increment was fairly large. It was therefore fairly hard to identify an MF target, although assays revealed a distinct amplitude–frequency window.

- Tofani *et al.* (1995) undertook to evaluate the oncogenic potential of low-frequency fields. They visually found the rate of intracellular nuclei formation in human peripheral lymphocytes. The formation of such nuclei under special conditions is a marker of chromosomal damages. Experimental setups

$$B(\pm 0.1)b(150_{\text{rms}})f(50)[b(75_{\text{rms}})f(32)] \\ B(42)B_p(\pm 0.1)b(75_{\text{rms}}, 150_{\text{rms}})f(32)$$

made it possible to single out the permanent MF component that is parallel to the variable component. Adapted data are given in Fig. 2.13. The authors noticed a statistically significant MBE in the presence of a parallel DC MF, namely points in the middle of the plot. At the same time, overall, the findings are hard to interpret, since experimental points are few. The fact that these results are not as remarkable as those obtained in other cases can be attributed to the fact that the second of the MF diagrams provided here did not meet the condition that the interference has a maximum at  $H_{\text{AC}}/H_{\text{DC}} \approx 1.8$ . Indeed, that quantity was 2.5 and 5, since the authors erroneously used the root-mean-square value  $H_{\text{AC}}$ , rather than the peak one.

- A cycle of works (Alipov *et al.*, 1994; Belyaev *et al.*, 1995; Alipov and Belyaev, 1996) is devoted to effects of a combined MF on the conformational state of the genome of *E. coli* K12 AB1157 cells under various magnetic conditions. Specially treated cell suspensions were subjected to lysis after exposure to an MF. A rotational viscosimeter was used to measure viscosity of the suspensions. The observable here was the rotation period of the viscosimeter rotor. That variable is connected with the conformational state of the cell genome prior to lysis. The MBE in cells was thus determined from the relative rotation period for exposed and intact cells. Measurements were conducted 1 h after a 15-min cell exposure, when the effect was especially robust.

Alipov *et al.* (1994) observed at 8.6–8.9 Hz a distinct 25% peak on the MBE curve with a width of around 1.6 Hz for the arrangement

$$B(43.6)B_p(19.7)b(30)f(7-12) .$$

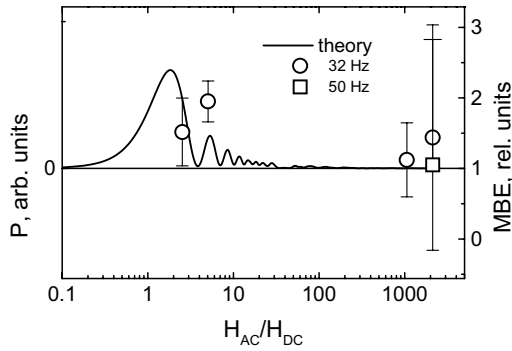


**Figure 2.13.** Occurrences of markers of chromosomal damages in HPL cells in parallel low-frequency MFs. The curve is a typical curve from the theory of ion interference.

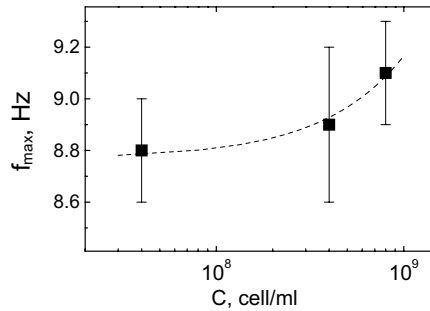


**Figure 2.14.** The shift of an MBE maximum in *E. coli* cells depending on the cell density, according to Belyaev *et al.* (1995).

A DC field here was the Earth's field. Under these magnetic conditions, less pronounced changes in the bacterial titer and intensity of DNA and protein synthesis were obtained using other techniques.

It was also shown that varying the orthogonal component in the range  $B_p(0-148/4)$  changed the peak height only by  $\pm 5\%$ , and that those changes as a function of  $B_p$  were sporadic (Belyaev *et al.*, 1994). In those trials, the orthogonal field did not play any noticeable role. At the same time, varying the parallel field within the range  $B(126-133/1)$  removed the peak, MBE being at a level of  $99 \pm 4\%$  within the entire range. The observed frequency of peak at 8.9 Hz was around the fourth subharmonic of the cyclotron frequency of  $^{40}\text{Ca}$  ions, if we ignore the orthogonal MF component.

Belyaev *et al.* (1995) studied the variation of MBEs with cell density in the range  $10^7$ – $10^9$  ml<sup>-1</sup> following the scheme

$$B(44 \pm 1)B_p(20 \pm 1)b(30)f(7.4-10.4)$$

and found that MBE peaks shift positively with cell concentration, Fig. 2.14. The authors account for that by the fact that intercellular interactions, whose role grows with cell density, encourage the formation of a cell population response to a combined MF.

Alipov and Belyaev (1996) showed several well-defined MBE frequency windows in the range 6–69 Hz for the same MF strengths as above, Fig. 4.32. Importantly, MBE frequency spectra for standard and mutant lines of *E. coli* cells appeared to be different. A 16-Hz peak was only observed for mutant cells. The authors suppose that the genome structure and DNA-involving processes are involved in the magnetoreception of those cells.

- Garcia-Sancho *et al.* (1994) studied the action of low-frequency MFs on ion transport in several mammal cell types. The effect was assessed via uptake of a <sup>42</sup>K radioactive tracer at a cyclotron resonance frequency (15.5 Hz for an ion of a given potassium isotope in a field of 41 μT) only by cancer Ehrlich cells and human leukemia cells U937. The <sup>45</sup>Ca tracer uptake was observed at an appropriate MF frequency, but it was not statistically significant and was never observed for <sup>22</sup>Na tracers. The experimental setup was

$$B(41)b(25-1000 \pm 5\%)B_p(\sim 0)f(13.5-16.5/1)n(8-24) .$$

The findings are plotted in Fig. 2.15. The plot displays a non-monotonous dependence on the frequency and amplitude of the AC MF component, which makes the results suitable for comparison with computations.

Note that the non-monotonous amplitude dependence of the effect poorly agrees with the generally recognized hypothesis on the excitation by AC MFs of quantum transitions against the background of a DC field. It is common for transition excitation to be accompanied by a saturation of transition intensity with the MF amplitude.

- Perpendicular MF combinations were employed by Picazo *et al.* (1994) when observing MBEs in chronically, for 3 months, irradiated mice

$$B(40)B_p(141)f(50) .$$

The leukocyte count in the blood of exposed,  $9.3_{-2.8}^{+6.2}$  thousand/mm<sup>3</sup>, and control ( $B_p = 0$ ),  $13.3_{-3.3}^{+5.7}$  thousand/mm<sup>3</sup>, groups differed with a statistical significance. Both qualitative and quantitative changes in the leukocyte compositions were associated with MF-induced leukemia.

- Spadinger *et al.* (1995) took into account the fact that the cytoskeleton responsible for the shape and mobility of cells contains molecules changed by a Ca<sup>2+</sup>

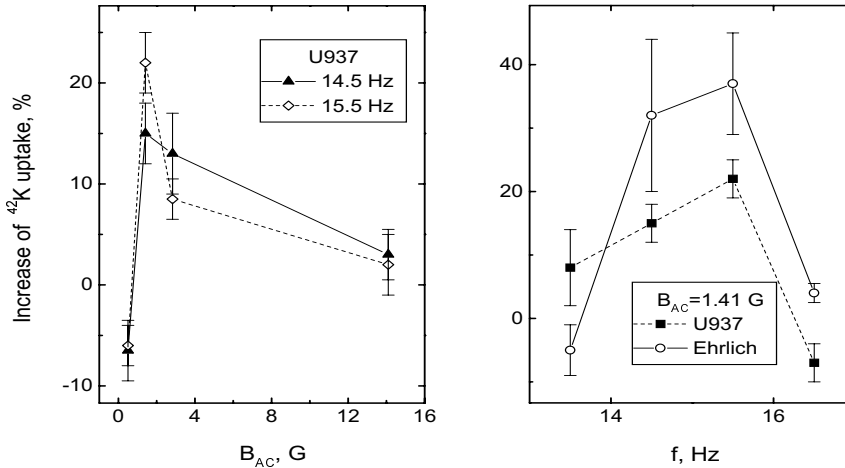


**Figure 2.15.** The influence of a 1-h exposure of cancer cells to magnetic fields of various amplitudes and frequencies on the uptake of radioactive  $^{42}\text{K}$  ions, according to Garcia-Sancho *et al.* (1994).

mediator. Since an MF acts on calcium transport *in vitro*, the field can also change the cell mobility. The authors studied the mobility and morphology of fibroblasts before, during, and after a 4-h exposure to a low-frequency MF. The measurements were performed using a computerized microscope equipped to produce an MF by a ring coil that fitted around a Petri dish. Experimental setup was as follows:

$$B(28.3)b(141 \pm 21)B_p(6.4)f(10-63/2)n(\sim 80)g(< 10 \mu\text{T}/\text{cm}) .$$

No statistically significant differences between exposed and sham cells were found for those frequencies.

The authors believe that underlying this negative result could be unaccounted parameters of ambient humidity and of uneven illuminations of cells by the microscope lamp, as well as the fact that the metabolic state of cells was inadequate.

Observation of such effects does require that MF parameters be fine-tuned or that different parameters form specific combinations concurrently, these parameters being the value of a DC MF, the amplitude of a uniaxial AC field, the perpendicular component, the frequency, and also the smallness of background variations of the field and its gradients. Therefore, the absence of an effect here could also be accounted for by a relatively large DC MF gradient, so that the field difference in one cell sampling was consistently as high as 30%.

- Novikov and Zhadin (1994) reported to have found an effect caused by parallel fields at a frequency scanning of 0.1 Hz/s on *L*-forms of solutions of asparagine,

arginine, glutamine acid, and tyrosine in a redistillate. They observed the current in an electrochemical cell. The effect consisted in the appearance on the current vs frequency plot of a single 30-50% maximum near cyclotron frequencies for appropriate molecules. The results are given in Table 2.1, where MF values are in  $\mu\text{T}$ .

The authors underscore the unclear nature of the physical mechanism for current growth at cyclotron frequencies corresponding to appropriate molecules of given amino acids containing ionizing amino groups. Note that resonance-like responses in a similar “electrochemical” configuration have been observed in yeast cell suspension in the geomagnetic field as the electric field frequency (Jafary-Asl *et al.*, 1983; Aarholt *et al.*, 1988) was scanned. In the latter case, the frequencies of maxima corresponded not to cyclotron frequencies, but to NMR ones.

A more thorough research was conducted (Novikov, 1994) in the Glu solution. Some Glu molecules were ionized by adding some hydrochloric acid to the solution. For controls, they used a solution without Glu and a solution at an acid concentration, such that it provided a zero electrokinetic Glu potential, i.e., their immobility. They used slow frequency scanning 0.01 Hz/s at

$$B(30)b(0.025)B_p(< 1)E_p(8 \text{ V/m})f(1-10) .$$

A current maximum was observed near a cyclotron frequency of 3.11 Hz, for Glu in a field of  $B = 30 \mu\text{T}$ . The maximum had a width of about 0.05–0.1 Hz. The author also performed a gel-chromatographic measurement on a solution exposed to an MF with effective parameters to notice the formation of Glu polymeric molecules. Chromatographic results obviously suggested that the effects observed were governed by the behavior of Glu molecules in a solution, rather than on the surface of electrodes. To account for the effect, it was assumed that a target for an MF were clusters or polymeric ions of amino acids with a cyclotron frequency like that of an individual molecule.

Solutions of L-asparagine Asn  $7.57 \cdot 10^{-3} \text{ M/l}$  in acidified redistillate at pH 3.2,  $T = 18 \pm 0.1^\circ\text{C}$  were studied in Novikov (1996) following the scheme

$$B(30.34 \pm 0.16)b((20 \pm 2) \cdot 10^{-3})E_p(5 \text{ mV/cm})f(3.38-3.62/0.01) .$$

**Table 2.1.** The action of an MF on the conductivity of amino acid solutions

Frequency	<i>b</i>	<i>B</i>	<i>B<sub>p</sub></i>	Solution	Frequency max., Hz
0.1–40	0.05	25	0	Asn	$2.9 \pm 0.1$
				Arg	$4.4 \pm 0.1$
				Glu	$2.5 \pm 0.1$
				Tyr	$4.4 \pm 0.1$
				H <sub>2</sub> O	no effect
		0	25		no effect
			0		no effect
	5	25	0		no effect

According to Novikov and Zhadin (1994).

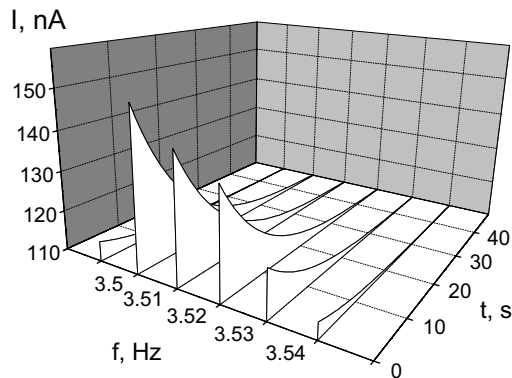


**Figure 2.16.** Current pulses in an electrochemical cell with asparagine solution in a DC MF of  $30.34 \mu\text{T}$  induced by switching on a parallel AC MF with an amplitude of 20 nT, according to Novikov (1996).

When an AC MF was switched on, a current pulse in the cell was observed, which took 50s to relax. The field was then switched off, the frequency readjusted to 0.01 Hz, and the field switched again. The findings are plotted in Fig. 2.16 using the data of Novikov (1996). We note the smallness of the AC MF, around 20 nT, and the non-steady-state nature of the response, thus suggesting that the molecular structure of the solution changed. In that experiment the electric field was an order of magnitude smaller than that in Novikov and Zhadin (1994) and Novikov (1994), without any noticeable consequences for the effect observed. That shows that in these experiments an electric field is only of significance for the measurement of an effect. As the solution temperature was increased to  $36^\circ\text{C}$ , the value of current pulse decreased.

The works do not answer some questions that are important for gaining insights into the physical nature of the phenomenon. In particular, it was of interest to find out (a) whether an electric field was applied to a solution when the formation of polymer molecules was studied, and (b) whether the frequency of a maximum of the effect was dependent on the solution pH. The charge of an amino acid zwitterion varies, depending on the medium acidity.

- The influence of a pulsed MF on an enzyme system of *lac operon* NCTC9001 line *E. coli* was studied by Aarholt *et al.* (1982). They measured the gene transcription rate for the  $\beta$ -galactosidase suppressed by a repressor protein, which hinders the approach of polymerase to an appropriate DNA section. Control cells were held in a container made of soft-magnetic metal. Experimental cells were exposed for 2 h to square 50-Hz MF pulses. Recorded was the synthesis rate vs pulse height dependence in the range of 200–660  $\mu\text{T}$ .

The exposed cell synthesis rate deviated from controls in the following manner: for pulse magnitudes around  $300 \mu\text{T}$  it dropped fourfold; at  $550 \mu\text{T}$  it increased 2.5 times, Fig. 4.46. The MBE variation with the cell density in suspension had an extremum. MBE observations were performed in the range  $2.5\text{--}5.5 \cdot 10^7 \text{ ml}^{-1}$ ; i.e., the separation between bacteria was about  $30 \mu\text{m}$ , which is more than 15 times larger than their size. The authors stressed the importance of intercellular interaction and supposed that the observed MBE is concerned with a change in the activity of a repressor protein.

- Reinbold and Pollack (1997) used modulated MFs,  $B(20)b(20)f(76.6)$  with a frequency close to a double cyclotron frequency for  $^{39}\text{K}$  and a treble one for Mg, and also an MF with a calcium cyclotron frequency,  $B(130)b(250, 500)f(100)$ . For bone cells in rats, these fields increased calcium density peaks 2–2.5 times ( $P < 0.05$ ), as measured using fluorescent microscopy techniques. It is interesting that the effect was conditioned by MF orientation, horizontal or vertical, and by the presence of calcium serum in a cell culture.

- Litovitz *et al.* (1997b) considered the role of the invariability of MF signal parameters in a cell response. They observed ornithine decarboxylase activity in a L929 cell culture. They did not measure the DC field, but conducted assays in a mu-metallic box that reduced an external MF fivefold, so that an approximate value could be around  $10 \mu\text{T}$ . Magnetic fields with frequencies of 55, 60, and 65 Hz ( $10 \mu\text{T}$ ) produced approximately similar effects of doubling the activity. However, a regime with 55/65 Hz frequency switching appeared to be effective only if the retention time for each of the frequencies was longer than 10 s. Amplitude switching from 0/10 to 5/15  $\mu\text{T}$  was also effective, beginning with 10 s within the switching interval. On the other hand, if a 60-Hz,  $10\text{-}\mu\text{T}$  MF signal was interrupted each second for more than 0.1 s, no biological effect was revealed. The dependence of the enzyme activity on the pause duration and the MF switching interval is shown in Fig. 2.17 and Fig. 2.18.

The authors thus conclude that in a cellular system there are two time scales, 10 and 0.1 s, which characterize the cell memory of the invariability of action conditions and the MF signal detection time respectively.

- A 2-h exposure to an MF with a  $1/f$  spectrum in the range of  $10^{-3}\text{--}10\text{ Hz}$  definitely reduced the cell adhesion index, which was proportional to the surface negative cell charge, by 30% as compared with controls (Muzalevskaya and Uritskii, 1997). That also enhanced cell sedimentation and increased the density of nuclear DNA super-spiral packing. At the same time, MFs of similar intensity, but different spectral composition (white noise, 0.8 Hz meander, and sine field 50 Hz), caused no biological effects.

The authors assumed that the  $1/f$  spectrum shape of an MF is a significant asset, because it was responsible for the emergence of an effect. They meant a “resonance” with a natural  $1/f$ -type process in cells, e.g., with ion currents. They did not discuss the primary biophysical processes of magnetoreception. As it will

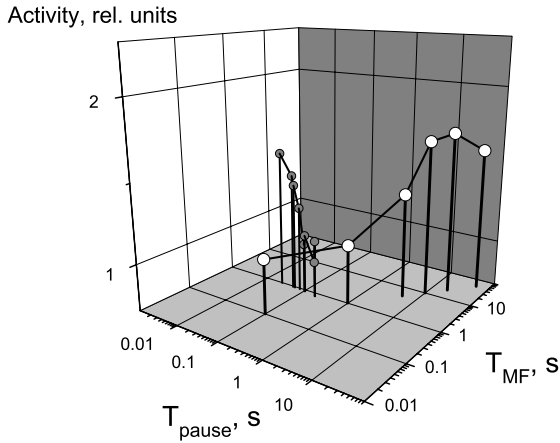


**Figure 2.17.** Activity of ornithine decarboxylase in a L929 cell culture as a function of parameters of an interrupted sinusoidal MF, according to Litovitz *et al.* (1997b).

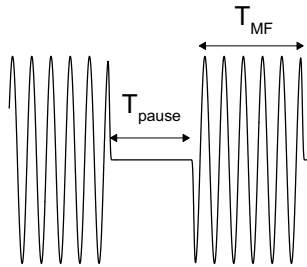


**Figure 2.18.** Parameters of the interrupted 60-Hz, 10- $\mu$ T magnetic field: pause duration and MF switching interval.

become clear from the results of Chapter 4, these findings could be described using an ion interference mechanism.

- Variation of the mobility of DNA brain cells in rats with the MF amplitude  $B(?)B_p(?)b(100, 250, 500)f(60)$  for a 2-h exposure against a background of uncontrolled local static MF was observed in Lai and Singh (1997a).
- Katsir *et al.* (1998) researched the proliferation of fibroblast embryo cells in chickens under the magnetic conditions

$$B(?)B_p(?)b(60-700)f(50, 60, 100)n(\sim 100)$$

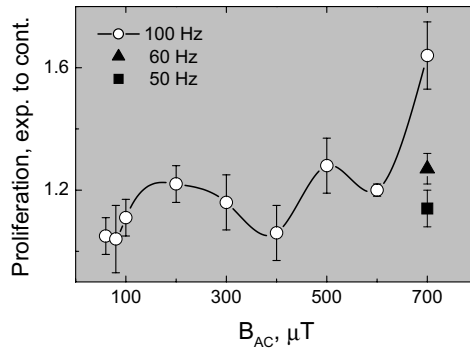


**Figure 2.19.** Amplitude dependence of fibroblast cell proliferation in MFs of various frequencies.

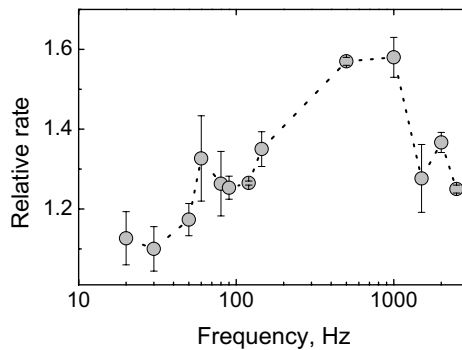


**Figure 2.20.** The frequency spectrum of the activity of liver cytochrome oxidase in rats in an MF of  $10\ \mu\text{T}$ . Averaged results of Blank and Soo (1998).

and found the multippeak dependence of the response to a 24-h exposure, Fig. 2.19.

Various proliferation measurement techniques, using a hemocytometer, spectrophotometer, or radioactive tracer, have led to similar results. The growth of the effect at large amplitudes and frequencies seems to be associated with induced currents, since the product  $bf$  exceeds the established limit (1.4.3). Data on the magnitude and direction of a DC MF are not provided; therefore it would be fairly difficult to comment of the possible ion target for an MF, but an extremum at about  $200\ \mu\text{T}$  is largely in sympathy with an ion interference mechanism.

- The frequency spectrum for the action of a  $10\text{-}\mu\text{T}$  MF on the activity of cytochrome oxidase, a membrane enzyme, was measured by Blank and Soo (1998).

The activity was measured spectrophotometrically from the density of an oxidized form of C cytochrome. Local DC MF data are not provided. The frequency dependence of the effect exhibited a maximum at around 500–1000 Hz, Fig. 2.20. That spectrum seems to be at variance with natural ion frequencies. It is assumed that an MF acts on a traveling charge within an enzyme, the position of a maximum on the frequency spectrum corresponding to the unit cycle time of the enzyme reaction.

### 2.3.2 Participation of some ions in magnetoreception

It has been established ever since that biologically effective MF frequencies approximately correspond to cyclotron frequencies of various ions, their harmonics and subharmonics, and they move proportionally to the magnitude of a DC magnetic field (Liboff, 1985; Liboff *et al.*, 1987b). The participation of ions in the formation of the response of a biological system is discussed in many works on magnetobiology. The wealth of experimental evidence makes the important role of  $\text{Ca}^{2+}$  ions as good as universally recognized.

The contribution of other ions is not that clear and gives rise to a discussion, since one effective frequency can at the same time correspond to various harmonics/subharmonics of different ions. It is then impossible to identify an ion from the shift of a frequency maximum depending on a DC MF, since both hypotheses yield similar predictions. It is clear that an isotopic shift of maxima is a regular way to identify ions; however such experiments are expensive and not always possible. Only some works are known where a calcium ion was identified as a target for an MF from a shift of MBE peaks with  $^{40}\text{Ca}$  (Smith *et al.*, 1987) and  $^{45}\text{Ca}$  (Liboff *et al.*, 1987b) isotopes, Fig. 2.21. The ratio of maxima frequencies 16/14.3 is close to the ratio 44.95/40.08 of  $^{45}\text{Ca}$  and  $^{40}\text{Ca}$  isotope masses. The value of that result was somewhat reduced by the fact that MBE spectra of different biological systems were compared.

Generally they use radioactive isotopes as tracers to take account of the intensity of exchange processes involving substances marked by that tracer. The isotopes used were  $^3\text{H}$  (Liboff *et al.*, 1984; Fomicheva *et al.*, 1992a; Alipov *et al.*, 1994; Ruhstroth-Bauer *et al.*, 1994; Fitzsimmons *et al.*, 1995),  $^{32}\text{P}$  (Markov *et al.*, 1992),  $^{35}\text{S}$  (Goodman and Henderson, 1991),  $^{45}\text{Ca}$  (Bawin *et al.*, 1975, 1978; Conti *et al.*, 1985; Rozek *et al.*, 1987; Blackman *et al.*, 1988; Yost and Liburdy, 1992),  $^{22}\text{Na}$  and  $^{86}\text{Rb}$  (Serpersu and Tsong, 1984), and  $^{125}\text{I}$  (Phillips *et al.*, 1986a).

Unfortunately, even if some MBE is observed in the processes, the fact in itself does not prove that given isotopes are targets for a magnetic field. To indirectly identify the ions, attempts have been made to observe changes in the conductivity of appropriate ion channels in an MF (Serpersu and Tsong, 1984; Blank and Soo, 1996).

#### 2.3.2.1 Calcium

Calcium ions are known to contribute to many biological processes, such as synaptic transmission, secretion, ciliary motility, enzyme activation, muscular contraction

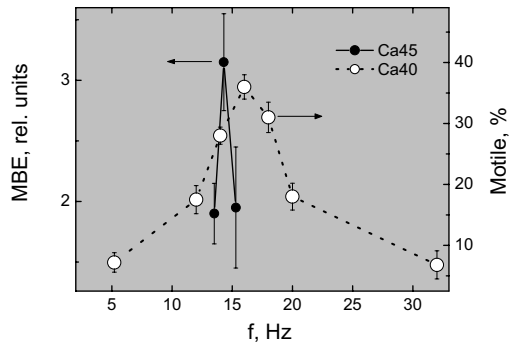


**Figure 2.21.** 1, incorporation of  $^{45}\text{Ca}$  tracer in human lymphocytes (Liboff *et al.*, 1987a); 2, motility of diatomic cells in agar low in  $^{40}\text{Ca}$  (Smith *et al.*, 1987), as a function of the AC MF frequency at an amplitude of  $20\ \mu\text{T}$ , the parallel DC field being  $21\ \mu\text{T}$ .

processes, multiplication, growth, and development. Intracellular calcium density  $\sim 10^{-8}$ – $10^{-6}\ \text{M}$  is four orders of magnitude smaller than in the environment and is sustained by membrane mechanisms. This takes care of the workings of fast signal mechanisms for response to external conditions. Especially sensitive to intercellular calcium density is calmodulin protein that affects the activity of many enzymes.

Kislovsky (1971) supposed that calcium plays an important role in biological effects of EMFs. The works of Bawin *et al.* (1975) and Bawin and Adey (1976) seem to have been the first assays to reveal a connection between EMF biological effects and calcium ions. They studied the rate of calcium ions efflux from brain tissues under low-frequency, RF, and microwave EMFs. Later on these data have been independently confirmed. Calcium binding with calmodulin as a primary target for the biological action of microwaves and the biochemical analysis of the hypothesis were discussed by Arber (1985).

- Höjerik *et al.* (1995) performed experiments to test the hypothesis that an MF interacts with the organism via calcium ion channels. They measured the total  $\text{Ca}^{2+}$  flux through micropatches of cellular membranes where clonal insulin-producing  $\beta$ -cells were subjected to combined AC–DC magnetic fields within the frequency range 10–60 Hz, including the cyclotron frequency 16 Hz (for  $\text{Ca}^{2+}$  in a field of  $B_{\text{DC}} = 20.9\ \mu\text{T}$ ,  $H_{\text{ACpeak}} = H_{\text{DC}}$ ,  $H_{\text{DC}} \parallel H_{\text{AC}} \parallel z$ ). This field was chosen because it was found to be effective. A 50-Hz background field was not higher than 70 nT; the geomagnetic field was compensated. The transport of  $\text{Ca}^{2+}$  ions through protein channels exhibited no resonance behavior within the frequency range at hand. This suggests that with magnetosensitive calcium processes an MF does not affect ion channels, but rather other biophysical systems.
- Jenrow *et al.* (1995) found a further biological system that could be successfully

employed to observe a magnetobiological effect. They studied the regeneration of the severed head of the Planarian *Dugesia tigrina*. Underlying the regeneration are many cell signaling processes involving  $\text{Ca}^{2+}$  ions, a fact that makes them, according to the authors, a convenient experimental model. The observable was the regeneration time recorded when pigmentation patches appeared at sites where eyes would later develop. Exposure to an MF sometimes increased regeneration time from 140 to 180 h. The experiments were staged to test the hypothesis that electric currents induced by an AC MF was a physical reason for MBEs, see Liboff *et al.* (1987b) and Tenforde and Kaune (1987).

The first experiment was performed simultaneously using the two schemes

$$\begin{aligned} \text{(A1)} \quad & B(78.42 \pm 0.18)b(10)f(60)B_p(10^{-2} \pm 10^{-1})N(69) \\ \text{(A2)} \quad & B(10^{-2} \pm 5 \cdot 10^{-2})b(10)f(60)B_p(10^{-2} \pm 10^{-1})N(70) . \end{aligned}$$

The second experiment followed two other schemes

$$\begin{aligned} \text{(B1)} \quad & B(51.13 \pm 0.12)b(51.1)f(60)B_p(5 \cdot 10^{-2} \pm 5 \cdot 10^{-1})N(92) \\ \text{(B2)} \quad & B(10^{-2} \pm 2 \cdot 10^{-2})b(51.1)f(60)B_p(10^{-2} \pm 5 \cdot 10^{-2})N(91) . \end{aligned}$$

The third experiment involved exposure to a local geomagnetic field with the power frequency background controlled

$$\text{(C)} \quad B(18.2 \pm 10^{-2})b(5 \cdot 10^{-3})f(60)B_p(53.5 \pm 10^{-2}) .$$

In these experiments, the MF gradient did not exceed  $10^{-2} \mu\text{T}/\text{cm}$ .

Schemes A1 and B1 corresponded to CR conditions for  $\text{Ca}^{2+}$  and  $\text{K}^{+}$  ions, respectively. The temperature was maintained to within  $\sim 0.05^\circ\text{C}$ . The findings for all the schemes are given in Fig. 2.22.

It was concluded that there is, probably, a delay in the early regeneration stage, before proliferation and differentiation processes set in, and it is due to  $\text{Ca}^{2+}$  ions. It was shown that an induced electric field and eddy currents are not responsible for the observed MBE. This follows from the fact that (1) the MBEs found in schemes A1 and A2 had different levels, whereas the level of the induced electric field is the same, (2) the MBEs for schemes A2 and C were identical, whereas the electric field levels were different, (3) the MBE for A1 was larger than that for B1, whereas the electric fields involved had opposite relations, and (4) direct computations of the induced electric field in oriented planaria yielded a value three orders of magnitude smaller than the known threshold value.

- Smith *et al.* (1995) tested the hypothesis that various cations, such as Ca, Mg, and K, are responsible for changes in the growth of *Raphanus sativus* var. *Cherry Belle* garden radish when continuously exposed to parallel MFs. Exposure by the scheme

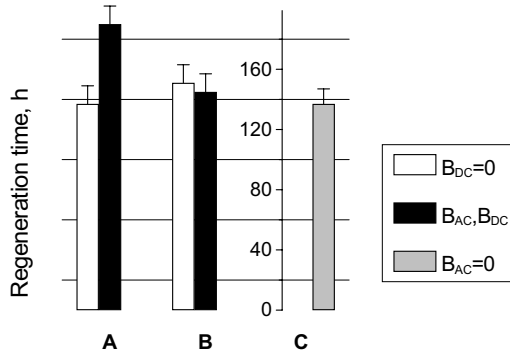


**Figure 2.22.** Mean regeneration time in planaria exposed to parallel magnetic fields at various temperatures: A, 22°C; B, 20°C; C, 22°C. According to Jenrow *et al.* (1995).

$$\begin{aligned}
 \text{Ca} & \quad N = 1, 2, 3 \quad B(78.4, 39.2, 26.1)b(20)f(60) & (2.3.3) \\
 \text{K} & \quad N = 1, 2, 3 \quad B(153.3, 76.6, 51.1)b(20)f(60) \\
 \text{Mg} & \quad N = 1, 5 \quad B(47.5, 9.5)b(20)f(60) \\
 \text{controls} & \quad B(0)b(20)f(60) , \quad B(\text{geo})b(0) ,
 \end{aligned}$$

where  $N$  is the number of a cyclotron frequency harmonic, enabled inputs of ions to growth variables to be identified. The strongest, 70–80%, changes in comparison with the controls were displayed by the weight of the root on a 21-day exposure. Other parameters displayed lesser, although statistically significant, changes. Fine-tuning to a cyclotron frequency and its harmonics appeared to be efficient for all the above-mentioned ions, the most pronounced effect being observed on fine-tuning to calcium. Fine-tunings to odd harmonics appeared to be more effective in comparison with the second harmonic.

The sign of the effect, i.e., increase or decrease, depended both on the type of the exposed ion and on the variable selected (stem length, leaf width, etc.). No pattern was found here, however.

The authors believe that these experiments provide supporting evidence for the cyclotron resonance mechanism in magnetobiology. Unfortunately, these experiments are hard to interpret in terms of an ion interference mechanism, to be discussed later, since the variable  $b/B$ , which was important for that mechanism, changed significantly in the experiments just described.

- Sisken *et al.* (1996) measured the luminescence of photoprotein introduced to cells before, during, and after 2 or 3 h of exposure to an MF

$$B(?)B_p(?)b(300-71700)f(16-180) .$$

Intercellular calcium density and other calcium-dependent processes in ROS 17/2.8 cells remained unchanged when subjected to an MF. The absence of an MBE seems

to be due to the fact that the variable field was large: its lower value was six times larger than that of the geomagnetic one. Nothing was said about DC MF variables, which were important indeed. Moreover, AC MFs were obtained using ferromagnetic concentrators, which normally produce large MF gradients.

The role of calcium processes was also discussed in several works (Conti *et al.*, 1985; Kavaliers and Ossenkopp, 1986; McLeod *et al.*, 1987a; Lyle *et al.*, 1991; Reese *et al.*, 1991; Belyavskaya *et al.*, 1992; Walleczek, 1992; Yost and Liburdy, 1992; Coulton and Barker, 1993; Garcia-Sancho *et al.*, 1994; Spadinger *et al.*, 1995; Deryugina *et al.*, 1996; Reinbold and Pollack, 1997; Ružič and Jerman, 1998). It was reported (Grundler *et al.*, 1992) that by 1992 at least 11 research centers observed calcium regulatory processes influenced by low-frequency MFs.

### 2.3.2.2 Magnesium

Some calcium-binding proteins are also able to bind magnesium, see for example Lester and Blumfeld (1991), and calcium and magnesium can have the same binding sites (Wolff *et al.*, 1977). Therefore, in addition to calcium ions,  $Mg^{2+}$  ions are regarded as potential targets for an MF.

A long exposure to parallel MFs tuned to a magnesium cyclotron frequency and its fifth harmonic resulted in 10–70% changes in garden radish growth variables (Smith *et al.*, 1995), see (2.3.3).

- Deryugina *et al.* (1996) studied the motive and exploratory activities in rats exposed to an “open field”. The animals were subjected to parallel DC and AC fields. AC MF frequency was chosen from among cyclotron and Larmor frequencies for magnesium, calcium, sodium, potassium, chlorine, lithium, and zinc ions

$$B(500)b(250)f(380, 630)B_p(< 50) .$$

The effect was only found at magnesium’s and calcium’s cyclotron frequencies.

- A magnetobiological effect on Planarian worms at the cyclotron frequency of magnesium ions was observed by Lednev *et al.* (1996a) using the scheme

$$B(20.9 \pm 0.1)b(38.4 \pm 0.1)f(20.4-32.4) .$$

A characteristic bell-shaped MBE spectrum is given in Fig. 4.35.

### 2.3.2.3 Sodium

Liboff and Parkinson (1991) made an attempt at observing an MBE in intestine tissue of a *Pseudemys scripta* tortoise for a parallel arrangement of DC and AC fields at cyclotron frequencies of  $^{23}Na$  and other ions. They measured the transepithelium potential at fixed MF values in a wide range of frequencies and fields:

$$B(10-220)b(1-20)f(3-770) .$$

No changes in the potential were found. The authors explained that by a number of reasons including the absence of artificial imbalance in ion density, which was a condition for a reliable observation of an MBE involving calcium.

### 2.3.2.4 Potassium and rubidium

Obviously, the first observation of an extremal MBE at a potassium cyclotron frequency was made by McLeod *et al.* (1987a). In the experiment

$$B(41)B_p(?)b(15)f(16)n(> 300)$$

they observed a reduction in the mobility of diatomic algae cells in agar with a high calcium density, which provided for initially maximal mobility. Controls were exposed to a  $55.7\text{-}\mu\text{T}$  DC MF. Some responses were also found at 3, 5, and 15 harmonics of a cyclotron frequency and were not found for the remaining harmonics with numbers from 1 to 17.

Later on that group of authors confirmed the efficiency of exposure of radish seeds to parallel MFs fine-tuned to 1 and 3 harmonics of the potassium cyclotron frequency (Smith *et al.*, 1995), see (2.3.3).

- Statistically significant changes in the trapping of  $^{42}\text{K}$  isotope ions in mammal cells both for parallel and for perpendicular orientations of magnetic fields were observed (Garcia-Sancho *et al.*, 1994) for a certain value of the field amplitude, Fig. 4.42. The frequency of a maximum corresponded to a cyclotron frequency for a given ion, which betokens possible involvement of potassium processes in certain magnetobiological effects.
- Experiment (Jenrow *et al.*, 1995) has not confirmed the input of  $\text{K}^+$  ions as targets for an MF in the regeneration of Planarian worms, although their probable involvement in MBEs with regenerating planaria is discussed (Lednev *et al.*, 1996b).
- Kavaliers *et al.* (1996) studied the variation of opioid-induced analgesia in land snails on a 15-min exposure to parallel MFs at a cyclotron frequency of  $\text{K}^+$  ions

$$B(76.1)f(30)b(0 \pm 0.2, 38.1, 114.2, 190.3, 213.1)n(23-46) .$$

The effect attained  $27 \pm 4.2\%$ . At  $b(190.3)$ , the MBE vanished when the snails were treated with glibenclamide, an antagonist of potassium channels. The authors note that a potassium cyclotron frequency was very close to the second subharmonic of the calcium cyclotron frequency, which makes it difficult to differentiate effects between those ions.

- In some experiments the  $^{86}\text{Rb}$  radioactive isotope is used. The properties of the  $\text{Rb}^+$  rubidium ion are close to those of the  $\text{K}^+$  ion. Their ion radii are equal to 1.49 and  $1.33 \text{ \AA}$  respectively, and differ noticeably from that of  $\text{Na}^+$ ,  $0.98 \text{ \AA}$ . Therefore, when investigating into the behavior of a membrane ion pump, Na,K-ATPase protein, in an AC electric field (Serpescu and Tsong, 1984) some  $\text{K}^+$  ions were replaced for  $\text{Rb}^+$ . That made it possible to show that in an AC electric field only the  $\text{K}^+$  part of the pump is activated and the protein can work as two independent pumps.

The authors employed an electric field of  $e(20 \text{ V/cm})f(1000)$ . It would be of interest to assume that in such tests a combined MF could affect ions and rubidium isotopes, since potassium ions as targets for an MF were an object of experimental studies.

- Ramundo-Orlando *et al.* (2000) observed a non-living system exposed to a low-frequency MF using a suspension of liposomes, artificial cells that model erythrocytes. The diffusion rate of *p*-nitrophenyl acetate (*p*-NPA) was measured spectrophotometrically. The diffusion rate was connected with the enzyme activity of carbonic anhydrase trapped by liposomes as they were prepared. The liposomes also contained stearylamine, a lipid interacting with other proteins of the system. The exposure scheme included parallel DC and AC MFs:

$$B(50 \pm 0.5)b(25-75)f(4-16)n(15)g(< 1\%) .$$

Control measurements were performed in a geomagnetic field  $B(22.4)b(< 0.5)$ . The experiments were repeated using two sets of equipment in two different premises. A 60-min exposure to a 7-Hz,  $B(50)b(50)$  field caused the *p*-NPA diffusion rate to rise from the control level of  $17 \pm 3$  to  $80 \pm 9\%$  (100% for destroyed liposomes). The frequency spectrum of the effect contained pronounced maxima at 7 (main) and 14 Hz. The effect disappeared on exposure to either a DC or an AC MF.

The authors believe that targets for an external MF here are positive charges of stearylamine on the surface of liposomes. The effect disappeared when the medium was alkalized from pH 7.55 to 8.95 to bind the charges.

Note that in a 50- $\mu$ T DC MF the frequency of 7 Hz is close to the rubidium cyclotron frequency and the potassium Larmor frequency; the frequency 14 Hz is close to the potassium cyclotron frequency.

- It was shown (Miyamoto *et al.*, 1996) that the trapping of potassium and rubidium tracers changes when subjected to electromagnetic fields. Possible MBEs involving potassium were also discussed (Lednev, 1996).

### 2.3.2.5 Lithium

Thomas *et al.* (1986) used mutually perpendicular DC and AC MFs. Five rats were pretreated for several months to develop a conditional reflex. The assay consisted of the rats being made to perform that standard procedure immediately upon a 30-min MF exposure. The MF variables were selected assuming that they had been adjusted to a cyclotron frequency of  $\text{Li}^+$  ions

$$B(26.1)b_p(\sim 70)b(?)f(60) .$$

A small  $B_{AC}$  component parallel to the DC field was found. Some aspect of the rats' behavior, which was connected with the conditional reflex being developed, changed when exposed to an MF; Fig. 2.23 depicts data averaged over five rats. It is seen that significant changes only occur when the DC and AC fields act jointly.

- Blackman *et al.* (1996) observed an MBE by the formula

$$b(18.7-48.6)B_p(36.6)B(< 0.2)f(45) .$$

In terms of resonance interference of bound ions (interference in perpendicular fields), the effect is possible at a Larmor frequency. In the specified DC MF it is

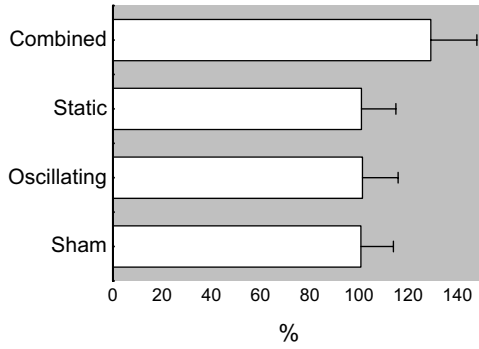


**Figure 2.23.** Index of response to a 30-min exposure to an MF in rats, according to Thomas *et al.* (1986). Levels: control — GMF; only  $B_{AC}$  60 Hz; only  $B_{DC} = 27.1 \mu\text{T}$ ; joint action of  $B_{AC} + B_{DC}$ .

only the Larmor frequency of lithium ions, 40.5 Hz, that is close to the one used in experiments.

- Ružič *et al.* (1998) addressed the effect of physiological stress factors (lack of water) on the spruce seed germination sensitivity to a combined perpendicularly oriented MF

$$B(46 \pm 4)b_p(26 \pm 4, 105 \pm 10)f(50) .$$

They observed a 10–50% drop in germination rate due to an MF under stress or the absence or a minor enhancement of the effect without stress. We note that the MF frequency used equaled the Larmor frequency of lithium ions at a given level of DC MF.

- It is also possible to account for the form of MBE amplitude spectra obtained in Blackman *et al.* (1994, 1995b) with the first amplitude maximum near  $H_{AC}/H_{DC} \sim 0.9$ , assuming that lithium ions are involved in the magnetoreception of PC–12 cells (Binhi, 2000), see Section 4.5.

The possible role of lithium ions in MBE was discussed in Smith (1988) and Blackman *et al.* (1990).

### 2.3.2.6 Hydrogen

Trillo *et al.* (1996) observed the variation of neurite outgrowth rate in PC–12 cells with magnetic conditions corresponding to a CR of a proton or  $^1\text{H}^+$  ions. MBE amplitude spectra were studied for various DC field values and AC frequencies

- (1)  $B(2.96)f(45)b(0.41-5.81)B_p(< 0.2)$
- (2)  $B(1.97)f(30)b(1.12-2.9)$
- (3)  $B(1.97)f(45)b(1.12-2.9) .$

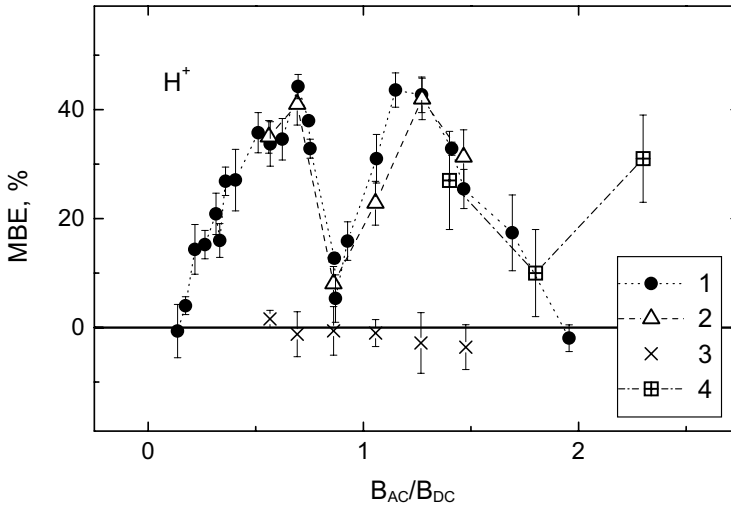


**Figure 2.24.** Magnetobiological effect at the cyclotron resonance conditions of hydrogen ions: in PC-12 cells, 1, 2 (out of resonance conditions, 3), according to Trillo *et al.* (1996); in regenerating planaria, 4, according to Lednev *et al.* (1997).

For comparison a spectrum was also measured under conditions that did not correspond to cyclotron resonance.

The measurement results are provided in Fig. 2.24. It is seen that the cells really respond when the frequency is fine-tuned to  $\Omega_c$ . A good agreement of points 1 and 2, obtained at different levels of a DC MF that were “in resonance”, indicated that the MF gradients, which were varied both from group to group, 1 and 2, and for different points within one group, were not a biotropic factor here.

On the curve there are three points for mitoses intensity measured in regenerating planaria cells under CR conditions in significantly larger MFs,  $B(44)$  (Lednev *et al.*, 1997).

It is assumed (Trillo *et al.*, 1996) that the location of the points attests to the presence of two different MBE mechanisms. One is responsible for the relatively slow rise and fall of the MBE with the relative MF amplitude from 0 to 2, and it can largely be approximated by the Bessel function  $J_1(2B_{AC}/B_{DC})$ . The other is responsible for the sharp “drop” in the MBE at the center of the graph. Adey and Bowin (1982) believe that at binding sites hydrogen ions could be substituted for by calcium.

- Action of parallel MFs at a proton magnetic resonance frequency on the proliferation of neoblast cells in regenerating planaria was observed by Lednev *et al.*

(1996b). Planaria with their head sections severed were exposed for 24 h to an MF, whereas controls were exposed to an MF that contained no variable components. Thereupon the number of mitoses in cells removed from the regenerating tissue was measured. To clarify the variation of the magnetobiological effect with the amplitude and frequency of the variable MF component the assays were performed by the schemes

$$B(20.87 \pm 0.01)b(0-80/\sim 20)f(889) ,$$

$$B(42.74 \pm 0.01)b(78.6 \pm 0.8)f(1808-1830/\sim 3) .$$

The frequency dependence had a resonance shape with a 10-Hz-wide maximum at a proton NMR frequency. The amplitude dependence also had a maximum at an AC-to-DC field ratio of 1.8. The effect at maximum was about  $47 \pm 10\%$ , Figs. 4.33 and 4.43. The authors took pains to take account of the daily course of the geomagnetic field. Note that the magnetic conditions in that experiment excluded an NMR, since the variable and DC fields were coaxial.

It was assumed that MF targets in those experiments were spins of hydrogen nuclei that enter into the composition of intra-protein hydrogen bonds. The earlier assumption that hydrogen atoms played an important role in magnetodependent biological reactions in yeast cells was made in Jafary-Asl *et al.* (1983) and Aarholt *et al.* (1988), where they observed biological effects at frequencies corresponding to the NMR of  $^1\text{H}$  in the geomagnetic field. A theoretical treatment of such effects is given in Polk (1989) and Binhi (1995b).

- Blackman *et al.* (1999) reproduced the data of Trillo *et al.* (1996) and also determined the frequency dependence near an MBE maximum (neurite outgrowth on PC-12 cells) at a proton cyclotron frequency. The experiment formula was

$$b(1.67-4.36)B(2.97)f(40-50) .$$

The findings are represented in Fig. 2.25 as amplitude dependences at various frequencies. The window structure of the response is clearly apparent in both the frequency and the amplitude of an MF. A sharp “drop” at the center, exactly where a maximum effect is expected, supports the data of Trillo *et al.* (1996), although there is no reliable accounting for that so far.

The proton seems to be the only more or less reliably established target for an MF, since the proton cyclotron frequency is a couple of orders of magnitude different from frequencies of other ions of biological significance.

### 2.3.2.7 Zinc

Thomas *et al.* (1986) supposed that zinc ions can contribute to the behavioral response of rats to perpendicular DC and AC MFs. Blackman *et al.* (1990) discussed the involvement of zinc ions in the removal of calcium from brain tissues exposed to combined MFs.

Binhi *et al.* (2001) studied processes concerned with conformational restructuring of *E. coli* genome exposed for 1 h to a changed DC MF  $B(0-110 \pm 1/1)$ . The

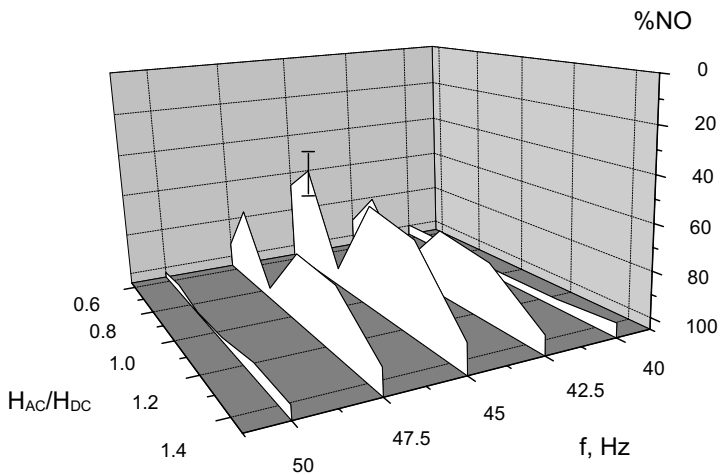


**Figure 2.25.** The influence of a 24-h exposure to a uniaxial MF on the neurite outgrowth in a nerve cell culture at a proton cyclotron frequency. According to Blackman *et al.* (1999).

dependence of the viscosity of lysed cell suspension on the magnitude of a DC field to which they were exposed is quite complicated and has several extrema, Fig. 4.48. To account for the dependence they used the ion interference mechanism involving calcium and zinc that respond in a cymbate manner and magnesium that responds oppositely. Such a combination was unique; i.e., no biologically important ions or their combination yielded such a good agreement of experimental and theoretical curves. That points to a possible input of zinc ions to magnetoreception by *E. coli* cells.

### 2.3.2.8 Other elements

It was assumed (Blackman *et al.*, 1988) that responsible for a statically significant MBE caused by combined magnetic and electric fields and observed at a frequency of 405 Hz at a DC MF  $B_{DC} = 38 \mu\text{T}$  were  $^{13}\text{C}$  atoms. The NMR frequency of this isotope in this field is 406.9 Hz, which is close to the specified value. The natural content of that isotope in a biological system, 1.1%, is sufficient for it to be a potential target for an MF.

- Smith *et al.* (1992) studied the multiplication of N-18 neuroblastoma cells exposed to parallel AC–DC MFs

$$B(15-40/5)b(20)f(16) .$$

They observed in a  $B(30)$  DC field the proliferation stimulated by 60%. These conditions were noted by the authors as being close to cyclotron ones for Co ions,  $30.7 \mu\text{T}$ , and  $\text{Fe}^{2+}$ ,  $29.1 \mu\text{T}$ , Fig. 2.26.

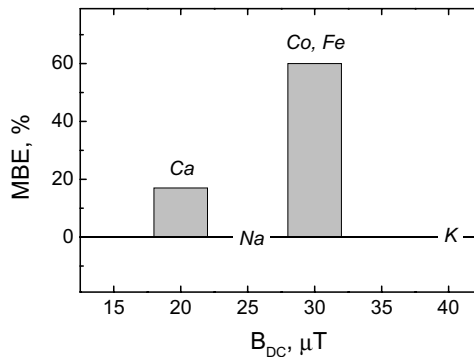


**Figure 2.26.** Variation of the rate of neuroblastoma cell proliferation at  $B_{AC} = 20 \mu T$ ,  $f = 16$  Hz, and a comparison with cyclotron ion regimes; according to Smith *et al.* (1992).

- Piruzyan *et al.* (1984) demonstrated the action of a variable MF on the sodium current in myocardium cells.

Manganese, zinc, cobalt, vanadium, cesium, selenium, iodine, molybdenum, and copper trace elements are present in the most important proteins, which control the biochemical equilibrium of organisms. They are scant, on average  $10^{-3}$  to  $10^{-6}$  %. Nevertheless, a shortage of those trace elements causes serious maladies. Therefore, generally speaking, these atoms may also be targets for weak EMFs.

## 2.4 CORRELATION OF BIOLOGICAL PROCESSES WITH GMF VARIATIONS

One feature of the geomagnetic field (GMF) is the fact that both DC and variable components are important. On the one hand, the magnitude of a local GMF to within a good accuracy,  $\sim 10^{-2}$ , is constant within time spans up to several days. In some experiments involving those times, the DC component is of importance. For larger times, several months or years, the GMF varies widely. Since the course of various biological processes and the slow variation of the GMF are often correlated, the very fact of GMF variation is important. In this case, however, the GMF can be regarded to be quasi-static in the sense that MBE physical models may ignore the time derivative of the GMF. It is to be noted that so far there are no physically justified frequency criteria for a varying MF to be viewed as constant in relation to biological effects. That is because there are no workable MBE models whose analysis could give such a criterion.

On the other hand, with shorter time intervals, under 24 h, as well, the GMF vector undergoes insignificant variations that correlate with the course of some biological processes. The GMF variation times are here shorter than the characteristic times of bioprocesses that correlated with them. In that case, the variable

GMF component should be regarded as more significant than the level of the DC component.

The characteristics of the geomagnetic field and their correlation with processes on the Sun have been described many times (e.g., Akasofu and Chapman, 1972; Guliyellmi and Troitskaya, 1973; Stern, 1996), and so we here just summarize them. The GMF shape is close to that of a dipole field whose axis is oriented at an angle of  $11.5^\circ$  to the Earth's rotation axis. The GMF strength declines from the magnetic poles to the magnetic equator from about 0.7 to 0.4 Oe, the GMF vector in the north hemisphere pointing down. It is widely believed that the GMF is a result of hydrodynamic flow within the Earth's liquid core.

Along with the solar wind — a supersonic flux of hydrogen ions that envelops the Earth — the GMF forms the magnetosphere, i.e., a complicated system of electromagnetic fields and charged particle fluxes. The magnetosphere is compressed by the solar wind on the diurnal side and strongly extended on the nocturnal side. The electric processes in the magnetosphere produce a variable GMF component of under  $10^{-2}$  Oe during times of seconds and longer, except for paleomagnetic periods. The Sun's own electromagnetic emission is nearly totally absorbed by the ionosphere, the ionized layer of the Earth's atmosphere, except for the narrow band from near ultraviolet to near IR range. The corpuscular solar emission that shapes the solar wind is subject to random fluctuations due to flares in the Sun's active regions.

The Sun possesses its own MF, which, unlike the Earth's field, does not look like a dipole one. Solar wind fluxes capture the MF from the Sun's surface and carry it to the Earth. In the Earth's orbit that field, referred to as the interplanetary MF, is only several nT and points either to or away from the Sun, thus breaking down the interplanetary MF into sectors. Since the Sun's equator area, with which its MF is associated, rotates with a period of about 27 days, during that time on Earth we can observe several alternations of the sectors of the interplanetary MF, i.e., alternations of the field direction. Normally, the number of sectors, which is even of course, is not higher than 4.

It takes the Earth several minutes to cross a sector boundary. Thereafter, marked changes in the magnetosphere may occur. If the component of the interplanetary MF is aligned along the Earth's axis from north to south ( $B_z < 0$ ), then the interplanetary and geomagnetic fields in most of the magnetosphere compensate for each other. As a result, penetration of the solar wind into the magnetosphere becomes deeper and more inhomogeneous, a fact which causes heightened electromagnetic perturbations on Earth.

GMF variations are conventionally divided into quiet and perturbed ones. Quiet variations are due to the daily and seasonal motion of the Earth, and also to the motion of the Moon; they also include effects of the sectoring of the interplanetary MF. Quiet daily GMF variations do not exceed 60–70 nT. Perturbed variations — quasi-periodic and irregular pulsations from split seconds to minutes, or magnetic storms — are caused by random processes on the Sun, which affect the magnetosphere via the solar wind. Therefore, perturbed variations occur approximately

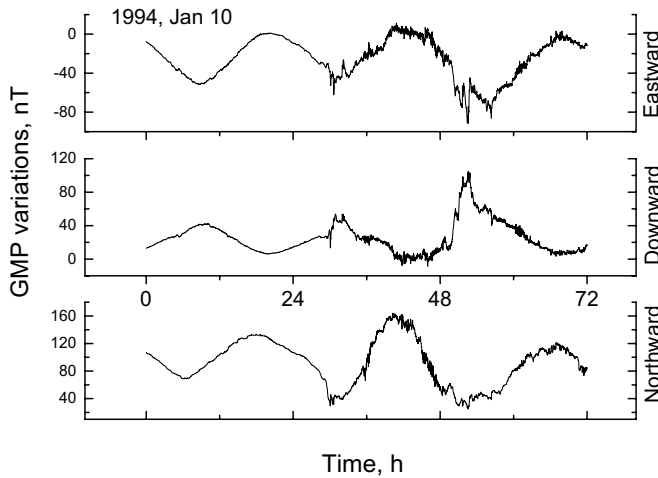


**Figure 2.27.** Variations of GMF components according to the data supplied by a geostationary satellite, 10–13.01.1994. Measurements were taken at 1-min intervals. Daily variations of the components and the geomagnetic perturbations from 6 a.m. of January 11 are clearly seen.

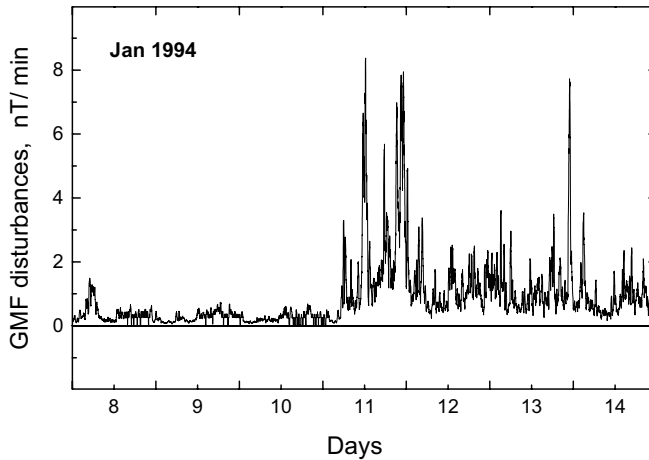
four days after solar “cataclysms”. This is the time taken by solar hydrogen ions to reach the Earth. Perturbed variations attain  $1 \mu\text{T}$  and last from hours to days.

Figure 2.27 shows variations of GMF components recorded by a geostationary satellite, <http://spidr.ngdc.noaa.gov>. The satellite revolved together with the Earth at a height of several Earth’s radii above a meridian, so that its terrestrial coordinates remained almost unchanged during a long time. The figure shows both quiet and perturbed variations. It is these latter that correlate with the state of the biosphere. In order to get an insight into the nature of those perturbations, i.e., to single out a “useful signal”, such data are processed.

Figure 2.28 provides the result of the consecutive procedure of differentiating, squaring, and sliding (15 min) averaging of similar data for the GMF vector module within several days, including the interval in Fig. 2.27. Shown is the absolute rate of the GMF variation, or rather the course of its root-mean-square deviation. The curve is made up of points

$$\left(\frac{\partial B}{\partial t}\right)_n = \left[ \frac{1}{\Delta t N} \sum_{i=n}^{n+N} (B_i - B_{i+1})^2 \right]^{\frac{1}{2}}, \quad \Delta t = 1 \text{ min}, \quad N = 15.$$

It is seen that relatively quiet days alternate with days with pronounced perturbations of the GMF variation rate. It is not clear yet which of the two perturbations, that of the field or that of the field variation rate, is more concerned with the course of biological processes.



**Figure 2.28.** Perturbations in the GMF magnitude variation rate during a geomagnetic storm. Processed 1-min measurements of GMF  $B_n$ , 8–14.01.1994.

Thus, the GMF may be in various states that are characterized by the presence or absence of some variations and the distribution of their intensities.

#### 2.4.1 Parameters and indices of the GMF

In order to describe the behavior of the variable GMF component they use various local and global indices of geomagnetic activity. Also to determine the indices the *GMF parameters* are of importance, because they define the magnitude and direction of the GMF vector at a point of observation. We note the following parameters:

**H** — the horizontal component of the GMF vector,

**Z** — the vertical component of the GMF vector,

$I$  — the magnetic inclination, i.e., the angle between **H** and the GMF vector at a given point,

$D$  — the declination, i.e., the angle between the **H** vector and the direction of the geographic meridian at a given point, from north to south.

Various indices of geomagnetic activity are found from the behavior of the temporal variation of these quantities. The meaning of some of the commonest indices is explained below.

- *C*-index. Determined during 24h. Takes on values 0, 1, or 2 depending on whether the day was quiet, perturbed, or strongly perturbed in terms of magnetic

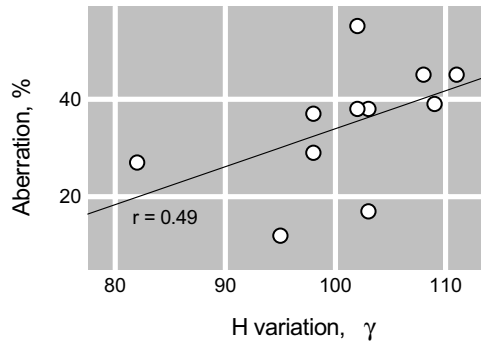


**Figure 2.29.** Correlation diagram. Variation of the GMF horizontal component and the change in the chromosome aberration frequency in rat liver cells. Processed data of Fig. 34 (Dubrov, 1978).

activity.<sup>17</sup>

- $u$ -index. Determined as a difference of mean values of  $\mathbf{H}$  modulus during the current and previous day.
- $K$ -index. Estimated every 3 h as the mean perturbation in a ten-point scale.
- $C_i$  —  $C$ -index averaged over several major observatories scattered all over the globe.
- $K_p$  — special-purpose averaging of  $K$ -indices from various observatories. The sum of  $K_p$ -indices over a day reflects the mean perturbation intensity of the solar wind.
- $A_p$  — the daily mean amplitude of GMF strength oscillations in the middle latitudes.
- $AE$  — a measure of geomagnetic activity in high latitudes; and  $D_{st}$ , in low latitudes. Determined during various time intervals.

There are also many other indices that reflect various frequency-temporal, space, and power characteristics of an intricate process of GMF variation (Akasofu and Chapman, 1972; Stern, 1996).

#### 2.4.2 Characteristic experimental data

The temporal correlation of various indices of geomagnetic activity with a wide variety of biological characteristics and processes was observed. Such correlations set in at the cellular level or even at the level of chemical reactions *in vitro*, e.g.,

<sup>17</sup>There exist many criteria for such an estimate, but their exact description is of no consequence for our treatment.

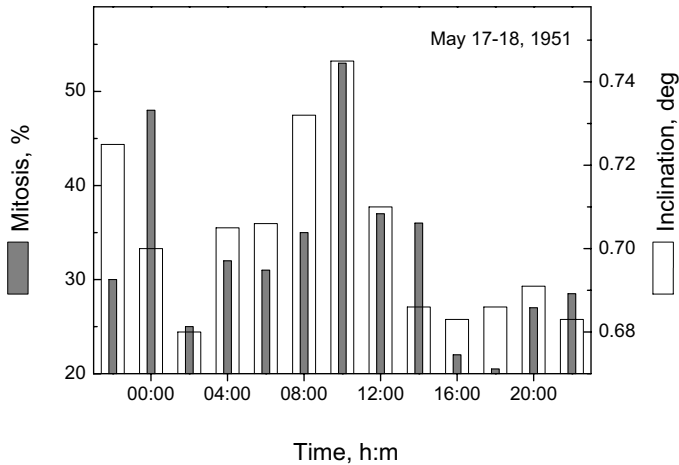


**Figure 2.30.** The daily rhythm behavior of cancer cell mitoses and the variation of geomagnetic field inclination, according to Fig. 32 in the monograph (Dubrov, 1978).

in the Piccardi reaction. It is difficult, therefore, to find a process in the biosphere that would not correlate with some parameters of the helio-geosphere.

In many frequency ranges under about 0.1 Hz a correlation of GMF variations with some biological processes has been found. The pioneering works were those by Chizhevskii and Piccardi. Some of their papers (e.g., Piccardi, 1962; Chizhevskii, 1976) have laid a dramatic foundation for the further development of heliobiology. It has taken nearly half a century for investigations into helio-geobiocorrelations to be promoted from the status of a “pseudo-science” to, at first, an exotic (Gnevyshev and Oll, 1971) and then to a common domain of scientific research (Shnoll, 1995a). It is quickly becoming one of the hottest fields now.

- A voluminous monograph by Dubrov (1978) addresses the studies of correlation of biospheric processes in objects ranging from plant and microorganism cells to higher animals, humans, and ecological systems, with variations of the geomagnetic field within a wide range of times scales, from hours to decades. The book contains more than 1200 references to original works of Russian and international researchers. Juxtaposing geophysical and biomedical data, the author has shown quite convincingly for the first time that the bio-GMF correlations are not an exotic phenomenon, but rather a common fact that warrants careful investigation. In what follows the correlations contained in that book are provided between geomagnetic correlations and some processes of vital activity, mutations, cancer, and so on.

Figure 2.29 shows regression analysis data for an approximately synchronous course of two processes. One of them is the variation of the density of chromosome

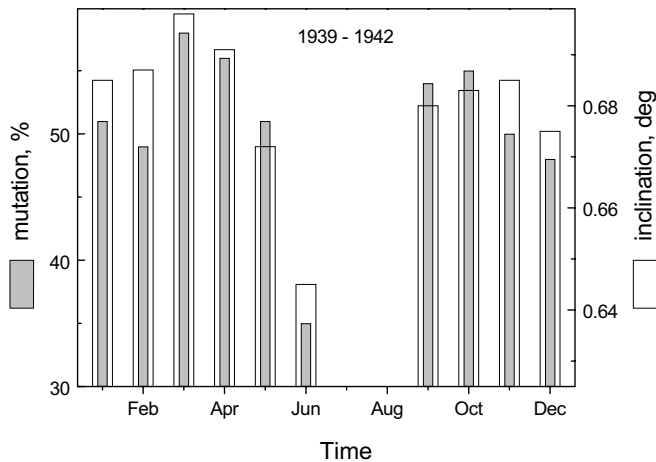


**Figure 2.31.** The behavior of the natural seasonal mutation process and the variation of the GMF parameter, according to Fig. 65 from the monograph (Dubrov, 1978).

structural defects in rat liver cells upon an injection of dipine, an antitumor preparation. The other process is the variation of the magnitude of the GMF horizontal component at the experiment site. Figure 2.30 provides the circadian rhythm of the mitosis of human carcinoma cells and the GMF inclination value within appropriate time spans. Figure 2.31 is a plot of the seasonal variation of chromosome inversions of the *ST* gene in *Drosophila* under natural conditions and the mean monthly variations of inclination.

Correlation diagrams for these graphs are given in Fig. 2.32 and Fig. 2.33. These graphs are seen to show correlation connections for various time scales, which is evidence for the hypothesis of the direct influence of GMF variations on the behavior of biological processes.

- In some plants, enhancements and retardations of their development was observed (Kamenir and Kirillov, 1995) when the Earth passed through sectors with positive and negative polarity of the interplanetary MF, respectively. It was shown (Alexandrov, 1995) that the activity biorhythms in aquatic organisms vary with the regional MF. The bioluminescence of *Photobacterium* bacteria changes markedly during magnetic storms (Berzhanskaya *et al.*, 1995), so that changes occur a day or two before the onset of a storm and last for two or three days after the storm has ebb.
- Gurfinkell *et al.* (1995) conducted regular measurements of capillary blood flow in 80 heart ischemia cases. On the day of a magnetic storm 60-70% patients showed impaired capillary blood flows. At the same time, only 20-30% of patients responded

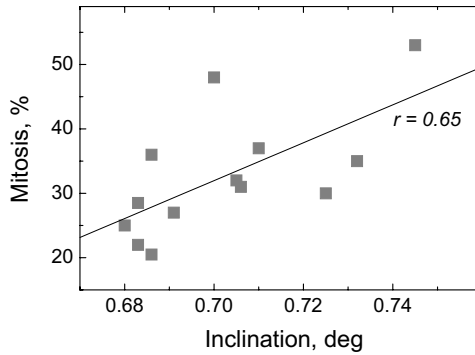


**Figure 2.32.** Correlation diagram of the biological and geomagnetic processes in Fig. 2.30.

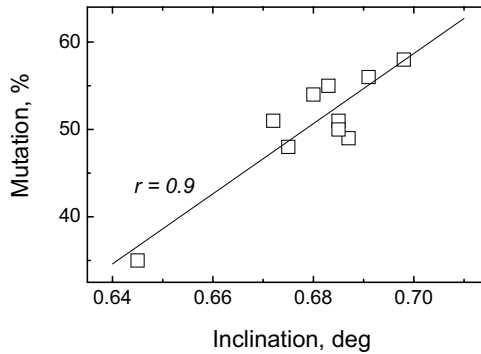


**Figure 2.33.** Correlation diagram of biological and geomagnetic processes in Fig. 2.31.

to changes in the atmospheric pressure.

- Oraevskii *et al.* (1995) found that even short-term variations of the interplanetary MF polarity within 24 h correlate with serious medical maladies. Shown in Fig. 2.34 is the regression analysis of their data. There is a significant correlation between the number of emergency calls in connection with myocardium infarction (on days with anomalously large or anomalously small number of calls) and the index of interplanetary MF variations. The index was approximately equal to the daily integral  $B_z$ , i.e., to the  $z$ -component of the interplanetary MF. It was worked out as a sum of hourly values of

$$B_s = \begin{cases} 0, & B_z \geq 0 \\ -B_z, & B_z < 0 \end{cases}$$

during the 24-h interval shifted 6 h back in relation to the 24 h under consideration.

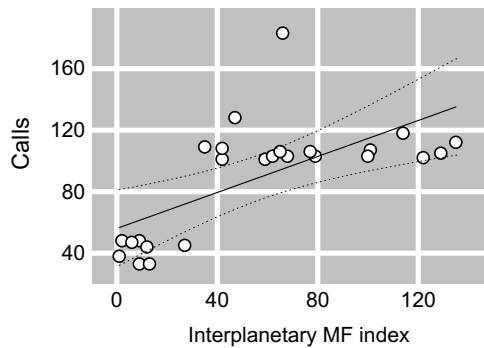


**Figure 2.34.** Correlation diagram: the abscissa axis is the interplanetary MF index, the ordinate axis is the daily number of emergency calls in connection with myocardium infarction; data of Oraevskii *et al.* (1995) processed, the confidence interval at a level of 0.95.

The authors obtained a similar statistics for emergency calls in connection with insult, hypertonic crisis, bronchial asthma, epilepsy, and various injuries.

- Villoresi *et al.* (1995) conducted a thorough statistical analysis of the relation of the incidence of acute cardiovascular pathologies in the years 1979–1981 with the GMF variations. The authors showed that strong planetary-scale geomagnetic storms are related to the growth in the number of myocardium infarction cases by 13% to within a statistical confidence of  $9\sigma$ , and the number of brain insults, by 7% with a statistical confidence of  $4.5\sigma$ . It was found that such pathologies as myocardium infarction, stenocardia, and cardiac rhythm violations correlate in a similar manner with the onset of geomagnetic storms (Gurfinkell *et al.*, 1998). Figure 2.35 provides those findings.

According to observational evidence gleaned over nine years (Zillberman, 1992) a correlation was revealed of geomagnetic activity,  $A_p$ -index, with a density of true predictions in mass-number lotteries,  $R = -0.125$  for significance 99.74%. The density correlated with  $A_p$  precisely on the day of issue and did not correlate with that index on previous or later days.

Also, correlations were found of the geomagnetic perturbations with the decrease in morphine analgesic effect in mice (Ossenkopp *et al.*, 1983); of the index of short-period oscillations of the  $H$ -component of the GMF with the brain functional status (Belisheva *et al.*, 1995); of a change in the direction of the interplanetary MF with leucocyte and hemoglobin content in mouse blood (Ryabyh and Mansurova, 1992); of the daily sum of  $K$ -indices with the suicide frequency (Ashkaliev *et al.*, 1995); of the  $A_p$ -index with the criminal activity in Moscow (Chibrikin *et al.*, 1995b); of the  $A_p$ -index with the amount of cash circulating in Russia (Chibrikin *et al.*, 1995a); of the occurrences of magnetic storms with the probability of air crashes (Sizov *et al.*, 1997).

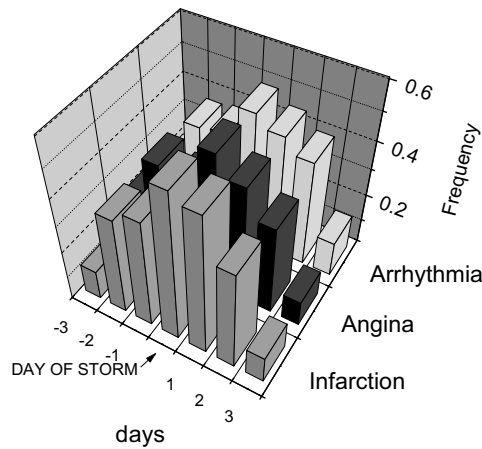


**Figure 2.35.** Relative incidence of cardiovascular pathologies before, during, and after magnetic storms, according to Gurfinkell *et al.* (1998).

For more information on a variety of biospheric processes that correlate with the geomagnetic activity see some special issues of the *Biophysics* journal (Pushchino, 1992, 1995, 1998), and collections of works (Gnevyshev and Oll, 1971, 1982; Krasnogorskaya, 1984, 1992).

### 2.4.3 Physical aspects of bio-GMF correlations

The mechanisms responsible for a correlation of the behavior of biological processes with GMF variations are unclear as yet. There are several points of view on the possible nature of that phenomenon.

#### 2.4.3.1 Direct action of a magnetic field

The commonest view is that GMF variations affect biological or biochemical *in vivo* processes (Vladimirskii, 1971; Dubrov, 1978; Zillberman, 1992; Temuriyants *et al.*, 1992b; Gurfinkell *et al.*, 1995; Breus *et al.*, 1995; Alexandrov, 1995). Specifically, this gives rise to the question (Vladimirskii, 1995) of whether heliobiology could be referred to as a part of electromagnetic biology.

Experimental evidence for the idea consists of both “pros” and “cons”. Works by Opalinskaya and Agulova (1984) on the action of man-made variable MFs larger than GMF fluctuations suggest that the idea is well grounded. At the same time, not all the data provided by the group are confirmed by independent studies (Piruzyan and Kuznetsov, 1983).

Agadzhanian and Vlasova (1992) modeled short-period GMF pulsations at frequencies of 0.05–5 Hz and intensities of about 100 nT. They found that such MFs activated spontaneous rhythmic activity in the nerve cells of the mouse cerebellum.

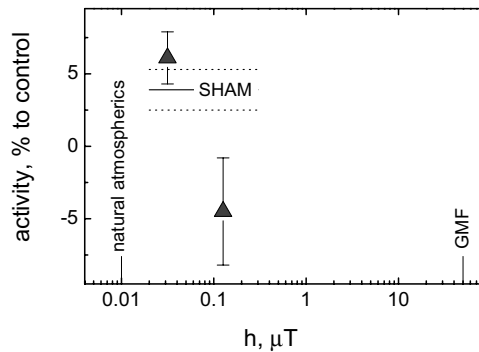


**Figure 2.36.** Proliferative activity of glioma cells in an EMF that simulates natural atmospherics as a function of the pulse amplitude, according to Ruhenstroth-Bauer *et al.* (1994).

Artificial magnetic pulsations that imitate the level and temporal behavior of local magnetospheric pulsations stimulated the growth of some grassy plants (Kashulin and Pershakov, 1995). At the same time, stronger field variations caused no biological response, which supports the hypothesis for biosystems being directly affected by GMF variations.

Tyasto *et al.* (1995) report that during weekends and holidays they observed a 40-50% reduction in magnetic fluctuations of a technogenic origin in the frequency range of  $\sim 10^{-3}$ – $10^{-1}$  Hz and, concurrently, a 70% reduction of myocardium infarction cases. The authors believe that this suggests that magnetic fluctuations may play the role of a trigger mechanism for acute disorders in humans with cardiovascular maladies.

Ruhenstroth-Bauer *et al.* (1994) addressed the proliferative activity of N6-gliome cells *in vitro* exposed to an EMF that imitated naturally occurring atmospherics — short, weak quickly decaying EMF pulses. The often observed MF shape of an atmospheric, that of a wave packet of length  $\sim 400 \mu\text{s}$ , frequency  $\sim 10$  kHz, band 5–20 kHz, and amplitude  $\sim 0.01 \mu\text{T}$ , was digitized and stored. They generated then, using a computer, a series of such pulses separated by a random interval of 50–150 ms, amplified them, and fed them to single-turn Helmholtz coils. The DC MF level, it seems, corresponded to a local GMF. Exposure to a field produced using that scheme changes the proliferative activity, Fig. 2.36, measured from radioactivity per unit of DNA with  $^3\text{H}$ -thymidine. Biological activity is thus inherent in combined MFs with a noise-like variable component. Here too for relatively small amplitudes the dependence is non-monotonous in nature. These findings also support the hypothesis that GMF perturbations affect the biosphere directly.

There is no clear understanding as yet of the possible biophysical mechanisms for the direct action of so small MF disturbances. Biophysical mechanisms for fields similar to the Earth's seem to be clearer — those fields are three or four orders of

magnitude larger, but even for them appropriate mechanisms should be regarded as suppositions that need further study.

#### 2.4.3.2 The radon hypothesis

An alternative view on the nature of bio-GMF correlations involves the dependence or correlation of radon density in the lower atmosphere and the electromagnetic activity on the Earth's surface (Shemii-Zade, 1992).

Radon isotopes, mostly  $^{222}\text{Rn}$ , are constantly emanated by the ground via a chain of alpha-decays of small amounts of  $^{238}\text{U}$ ,  $^{235}\text{U}$ , and  $^{232}\text{Th}$  naturally occurring in the lithosphere. Radon is a chemically neutral heavy atomic gas with a half-life of 1600 years. The natural radiation level in the biosphere is partly due to radon decay and its short-lived derivatives  $^{218,216,214}\text{Po}$ ,  $^{214}\text{Bi}$ , and  $^{214,212}\text{Pb}$ . The radiation level is subject to strong changes, by tens of times, owing to mechanical processes in the lithosphere and the "locking" of radon in the ground by aquifers.

The marked correlation of radiation near the ground with the geomagnetic activity enabled Shemii-Zade (1992) to come up with a mechanism for bio-GMF correlation. The author hypothesized that the flares of geomagnetic perturbations cause a magnetostrictional deformation of minerals and rocks that include ferromagnetic compounds. That increases radon diffusion from the ground and its density in the lower atmosphere. Through breathing and metabolism radon finds its way into living systems, causing various biological effects as it accumulates. Note that so far no experiments with artificial MFs are known that would confirm the strictional mechanism in the lithosphere for MF perturbations as small as geomagnetic storms.

This issue is being discussed not only in connection with geomagnetic perturbations. It has been established that radon is a risk factor for lung cancer. Radon decay products, specifically the unstable polonium, are transferred by particles of various aerosols, which are always available in the air. Since they carry an electric charge, they are drawn into areas with a heightened electric field strength.

Henshaw *et al.* (1996) used an alpha counter to measure radioactive aerosol density near household electric cables and found it to be higher several fold. The authors looked at cases where in dwellings and production premises there is a power-frequency electric field from a nearby transmission line and enquired whether that exposure might cause radon products to settle on the surface of lungs and lead then to cancer cases. Despite the small volume of experimental evidence, insufficient statistics, lack of special-purpose epidemiological, and even biological studies, the authors believe to have found the missing link in the physical mechanism for the connection of weak electromagnetic fields with cancer risk. According to their hypothesis, which causes some dispute and is not shared by all, electromagnetic fields act on living matter in an indirect manner, via the growth of radon product density.

At the same time, for computer terminals with their much higher electric fields of up to 30–50 kV/m at a distance of 10 cm, it was found (Akimenko and Voznesenskii, 1997) that the fields do not affect the density of daughter radon decay products. In both exposed and control samples it was about  $91.5 \pm 2.5 \text{ Bq/m}^3$ .

### 2.4.3.3 Common synchronizing factor

Lastly, a third view of the physical nature of bio-GMF correlations takes account of the following circumstance. It is well known that the intensity of nearly all biological and biochemical *in vivo* processes undergoes to some degree or other some cyclic oscillations. Most of such biological rhythms — an obvious example being the circadian rhythm — occur somewhat in sympathy with geophysical and even space-physical processes (Piccardi, 1962; Chizhevskii, 1976; Dubrov, 1978; Shnoll, 1995a; Klochek *et al.*, 1995). Infradian rhythms (nearly 3.5, 7, 27 days) are a corollary of the periodic activity and rotation of the Sun. The same rhythms are to be found in many biological systems (Breus *et al.*, 1995), including unicellular ones.

The Earth's rotation and revolution around the Sun, and the Moon's motion jointly drive some biological rhythms and cause variations of some GMF variables. For instance, found in the power spectrum of geomagnetic aa-index variations are groups of spectral peaks near 27, 14, 9, and 7 days. On the one hand, these rhythms are conditioned by variations of solar wind parameters; on the other hand, they appear in biospheric processes. Therefore, a correlation of the temporal behavior of bioprocesses and the GMF does not necessarily imply any cause-effect relations, a fact that has repeatedly been stressed in the literature. It is not to be excluded that GMF variations cause no biological response. They may be a corollary of a yet unknown true reason of a common synchronizing natural factor.

Environment parameters often vary in sympathy with one another, since they are to a large degree dictated by solar universal rhythms (Vladimirskii *et al.*, 1995). Electromagnetic perturbations are accompanied by elevated infrasound noises and microseisms, by a drop in the intensity of galactic space rays, and by a rise in the atmosphere radioactivity. Vladimirskii *et al.* note that those background developments do not make it any easier to answer the question of which physical factor underlies the biorhythms.

Shnoll (1995b) reported that the mean amplitude of fluctuations of processes of various nature changes markedly already 1–2 days prior to the Earth's crossing the boundaries of interplanetary MF sectors. That rather suggests the presence of an unknown influencing factor, perhaps connected with some processes on the Sun. It was assumed (Akimov *et al.*, 1995) that this factor is the fields engendered by the torsion of space bodies. This factor was found (Klochek *et al.*, 1995) to feature a high penetrability, and to correlate with biological and geomagnetic activities and with solar RF fluxes in the meter–centimeter ranges. That also corroborates the hypotheses that the bio-GMF correlation has a non-magnetic nature.

The issue of the influence of weak low-frequency electric fields on living organisms against the background of a DC MF is still not clearly understood. A concise overview of relevant work was performed by Binhi and Goldman (2000). The vertical electric component of geomagnetic pulsations is known to attain 10 V/m and be rigidly correlated ( $r \sim 0.8$ ) with variations of the meridian projection of the horizontal GMF component (Chetaev and Yudovich, 1970). Therefore, it is not to be

excluded that biological effects are due not to geomagnetic variations themselves, but to the geoelectric fields that are synchronous with the former.

There may well exist several mechanisms of similar significance that are responsible for the correlation in question. Their competition is dependent on many nearly unaccountable factors, so that correlation values are not too large and the results are not properly reproducible. At the same time the very variety and spectrum of manifestations of bio-GMF correlations is indicative of their non-random nature.

## 2.5 SPIN EFFECTS IN MAGNETOBIOLOGY

Evidence for the manifestation of spin degrees of freedom in magnetobiological experiments is fairly scarce. There are no assays that have been reproduced by various research groups. This situation may well be due to traditionally large intensities of MFs used to observe spin effects. In such experiments the signal-to-noise ratio largely grows with the MF. Another reason behind the lack of progress with the idea on spin effects in magnetobiology is the smallness of the energy of electron magnetic spin moment, let alone that of nuclear magnetic moments, in an MF similar to the geomagnetic one. It is as low as  $10^{-7} \kappa T$ ; therefore many believe that physically an MBE through spin magnetic resonance mechanism is impossible.

At first sight, it looks highly unlikely that atomic nuclear spins of molecules in a living tissue can influence life processes. After all, nuclear spins interact with the ambient environment via interaction of magnetic spin moment with internal inhomogeneous electric and magnetic fields. These magnetic interactions are proportional to the nuclear magnetic moment, which is two orders of magnitude smaller than that of the electron. Nevertheless nuclear spins are somehow involved in biochemical reactions. A circumstantial testimony of that is the fact that various substrates of biological systems, such as cells and tissues, feature different carbon isotope compositions (Jacobson *et al.*, 1970).

It was reported (Ivlev, 1985) that the pyruvate decarboxylizing reaction involved separation of  $^{12}\text{C}$  and  $^{13}\text{C}$  carbon isotopes, the mechanism for isotope inhomogeneity in amino acids being not quite clear. This reaction affects the carbon isotope composition of carbon dioxide exhaled by man and animals. This composition undergoes daily variations (Lacroix *et al.*, 1973) and reflects hormone-metabolic status (Ivlev *et al.*, 1994). The carbon isotope ratio in exhaled air may change within minutes of the administration of some preparations. This is convenient for express diagnostics. In laser orthomolecular medical diagnostics (Stepanov *et al.*, 2000), the  $^{13}\text{C}/^{12}\text{C}$  ratio is thought to give a clue to the presence of some disorders of the digestive system.

The two isotopes differ in mass by 8%, while  $^{13}\text{C}$ , unlike  $^{12}\text{C}$ , has a spin; i.e., it possesses a different dimension. It is quite possible that it is the spin of  $^{13}\text{C}$ , rather than the mass difference, that is a factor responsible for isotope separation in relevant biochemical reactions. Especially attractive in that respect is observation of an isotope effect for relatively heavy ions, such as Ca, Zn, and Cu, with a mass difference of only 1–2%.

It appears that MBEs are really unlikely if they occur through a spin resonance mechanism in its conventional sense, i.e., as a resonance change in the EMF energy absorption rate by a relaxing spin system. Also unlikely are MBE mechanisms concerned with energy accumulation due to a spin magnetic moment. One can and must, however, dispute the thesis that magnetic interactions of electron and nuclear spins have nothing to do with magnetobiology. The role of spins, including nuclear ones, as go-betweens in the transfer of information signals of an MF is not yet understood (Binhi, 1995b).

It is believed that underlying the mechanism for the biological action of low-frequency MFs is a magnetosensitive process of a recombination of free radicals that occur in a biological tissue. That process is influenced by the state of electron spins of radicals that enter into the reaction. The state of spins, in turn, is determined by an MF. However, there is no reliable experimental evidence to date to support such a mechanism for magnetoreception. It is primarily because it does not possess frequency selectivity and is only sensitive to the magnitude of an MF. The fact of magnetoreception in itself thus does not suggest that there must be a contribution of spins — there are also other explanations for an MBE that are not necessarily concerned with spins. Therefore, the following is an overview of experiments where spins manifest themselves in frequency-selective biological responses to an EMF, with effective frequencies in the regions of spin resonance. Those assays, if they are not to be taken to be artifacts, point to direct involvement of spin processes in magnetoreception.

- Jafary-Asl *et al.* (1983) performed one of the early works to juxtapose biological effects with spin magnetic resonance conditions. They studied yeast cells using dielectrophoresis, i.e., a method relying on a shift of cells owing to their polarization in an inhomogeneous electric field. Pre-processed *S. cerevisiae* cells were placed in an electrochemical cell and viewed under microscope. When a field was applied, the cells would begin to move towards the electrodes to form on them some chains along field lines. The electric field was turned off 3 min later, and the mean chain length was measured. The assays were conducted in a controlled DC MF  $B(50-500)$  and a variable electric field  $f(200-5 \cdot 10^4)$ , such that the potential difference across the electrodes was 40 V. Since the authors provided no information on cell design, it is hard to estimate the value of the electric field and its gradient. There were also no data on the mutual orientation of the electric and magnetic fields.

Shown in Fig. 2.37 is an experimental curve produced by the processing of five frequency spectra obtained in 50-, 100-, 150-, 300-, and 500- $\mu$ T MFs. The plot displays a clear dip in the region of 4.26 kHz/G. Also shown is the variation of the probability amplitude of a spin state of a Zeeman duplet, computed from the NMR mechanism for the proton for  $b_p/B = 0.1$ .

Since the experiment used a variable electric, rather than a magnetic, field, the results of Fig. 2.37 are just a circumstantial indication of the possible role of nuclear spins in those experiments.

The work also contained spectra of the complex permittivity  $\epsilon(f) = \epsilon'(f) + i\epsilon''(f)$

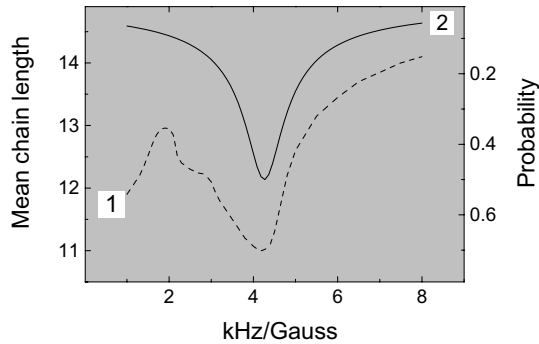


**Figure 2.37.** Comparison of experimental evidence (Jafary-Asl *et al.*, 1983) for dielectrophoresis of yeast cells in a weak MF with a  $^1\text{H}$  NMR curve.

in the range of  $f(90-10^5)$ , and in the region of frequencies that correspond to a spin resonance of an electron in an MF  $50\ \mu\text{T}$  for a cell culture with a density of  $1.9 \cdot 10^6\ \text{ml}^{-1}$ . At some fixed frequency values they observed narrow,  $\sim 1\ \text{Hz}$ , flares of 3–15%. Provided below are (i) frequencies (Hz) found in experiment, (ii) nuclei that, according to the authors, correspond to them, and (iii) NMR frequencies of those nuclei in a field of  $50\ \mu\text{T}$ :

2130	$^1\text{H}$	2128.2
861	$^{31}\text{P}$	862.6
563	$^{23}\text{Na}$	563.4
208	$^{35}\text{Cl}$	208.8
99	$^{39}\text{K}$	99.4

To within the experiment accuracy ( $\sim 1\ \text{Hz}$ ) there is a nearly complete agreement. Also shown is the growth of dielectric losses at a frequency of electron spin resonance  $\sim 2.79\ \text{MHz/G}$ .

That work also describes studies of other cells under NMR conditions. Earth bacteria cultures were exposed to an MF at an NMR of  $^1\text{H}$

$$B(25 \cdot 10^3)B_p(85)f(1.064 \cdot 10^6) .$$

In the experiment, cell concentration doubled during a 10-h exposure in comparison with controls, while the size of the smallest cells reduced by half. It was possible to stop the enzyme reaction of lysozyme with its substrate under near-NMR conditions for  $^1\text{H}$

$$B(2 \cdot 10^5)f(7 \cdot 10^6-10^7) .$$

Similar data were supplied by Shaya and Smith (1977). It was concluded by Jafary-Asl *et al.* (1983) that their data point to the ability of  $^1\text{H}$  NMR conditions to encourage the DNA replication process.

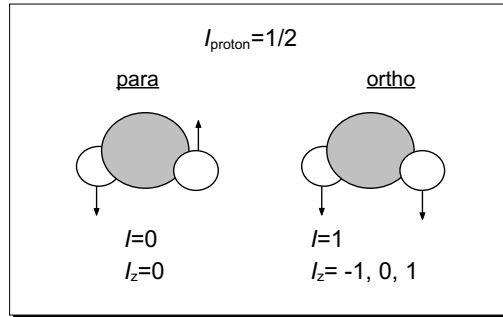


**Figure 2.38.** Para- and ortho-states of water molecules. Ortho-states feature wave functions that are symmetrical in spin transmutations.

- Aarholt *et al.* (1988) report that in a proton magnetic resonance (perpendicular fields) the mean lifetime of a generation of *E. coli* cells decreases. The authors also reported that a 55-MHz EMF with a bandwidth of 50 Hz caused eye pupil cataracts in animals *in vitro*, if the frequency modulation corresponded to an NMR at  $^1\text{H}$ , i.e., at 2.13 kHz in a geomagnetic field of  $50 \mu\text{T}$ .

- Works by Konyukhov and Tikhonov (1995), Konyukhov *et al.* (1995), and Belov *et al.* (1996) contain circumstantial evidence that proton nuclear spins can contribute to the primary reception of an MF by biosystems. The authors also report that they managed to reveal the *existence* of liquid water with metastable deviations from the equilibrium ratio 3:1 of the amounts of water ortho- and para-molecules  $\text{H}_2\text{O}$ . In a singlet para-state the molecular spin  $I = 0$  is formed by oppositely directed proton spins and has the only projection  $I_z = 0$  on an arbitrary quantization axis, Fig. 2.38.

For ortho-states, proton spins are unidirectional, and the molecular spin  $I = 1$  has three possible components  $I_z = -1, 0, 1$ , and in a magnetic field it forms a triplet. In a strong external MF the energy of its interaction with proton magnetic moments,  $\mu H$ , is larger than the energy of magnetic dipole-dipole interaction  $\sim \mu^2/r^3$ . That occurs in the field

$$H > \frac{\mu}{r^3} \sim 10 \text{ G} .$$

Proton spins will then behave as good as independently of one another. In a weak MF, a combination of proton spins make up a molecular spin that interacts with the MF as a whole.

The adsorption of water molecules from a gaseous phase is sensitive to the rotational state of water molecules, and therefore it reveals the molecular spin state. In a specially weak  $^1\text{H}$  NMR MF

$$B(150)B_p(5)f(\sim 6384)$$

that provides quantum transitions between the states  $I_z = 0$  and  $I_z = \pm 1$ , it was possible to record a growth in the adsorption rate of water ortho-molecules (Konyukhov and Tikhonov, 1995) and then to obtain, on that basis, liquid water with a non-equilibrium content of ortho- and para-molecules. The authors dubbed it spin-modified water. It was found, using submillimeter spectroscopy, that the lifetime of spin-modified water is 45 min at room temperature and 4.5 months at liquid nitrogen temperature.

Mechanisms responsible for such long lifetimes of nuclear spin degrees of freedom in liquid water are yet unclear. It may well be that it is connected with the details of proton exchange in liquid water in an MF (Binhi, 1996, 1998b). However, the very fact of the existence of such states at room temperature points to their possible significance in biology.

- An MBE observed by Blackman *et al.* (1988) under the conditions  $B(38)b(?)e(?)f(405)$  was associated with the NMR of carbon  $^{13}\text{C}$ , whose frequency in a given MF is 406.9 Hz.
- Direct changes of parameters of a biosystem in a weak MF at the  $^1\text{H}$  NMR frequency were observed by Lednev *et al.* (1996b). They found that the MBE variation in neoblast cells of regenerating planaria with frequency had a resonance form, Fig. 4.33. However, the MBE spectrum was measured with magnetic fields aligned in parallel

$$B(42.74 \pm 0.01)b(78.6 \pm 0.8)f(1808-1830/\sim 3) .$$

With such an alignment there is no NMR. It is indicative of another physical mechanism for MBEs that is concerned with the spin. One such mechanism is discussed in Binhi (1997a,b) and in this book in some detail.

- Ossenkopp *et al.* (1985) observed the variation of the morphine anesthetic effect in mice exposed to an MF following the protocol of the standard NMR tomograph. It is unclear yet whether that effect was concerned with excitation of the spin subsystem, or rather the driving force was the strong DC MF of the tomograph as such. In any case, these factors point to possible unpredictable consequences of the common procedure of NMR scanning of humans.

## 2.6 EFFECTS OF LOW-FREQUENCY ELECTRIC FIELDS

Biological action of an electric field reduces primarily to the action of ion currents it induces in intra- and intercellular plasma. A redistribution of ions results in local changes of electropotentials on the surface of macromolecules and cellular membranes. This in turn is accompanied by a change in biochemical reaction rates.

It is well known that relatively intensive and short pulses of electric current encourage penetration of large molecules of DNA or protein type into biological cells. For instance, anticarcinogenic effectiveness of bleomycin is hampered by the fact that a bleomycin molecule is unable to get through a cell membrane. Current

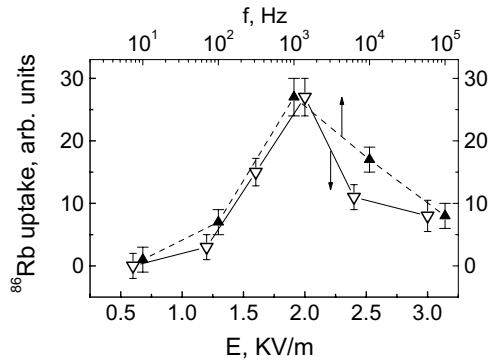


**Figure 2.39.** Frequency–amplitude dependences of the rubidium tracer uptake in erythrocyte suspension on exposure to an AC electric field.

pulses improve the membrane permeability and bring about corresponding biological effects. The fact that relatively strong DC and AC electric fields can affect things raises no doubt, although in that case as well mechanisms for such an action are not always clear (Mir *et al.*, 1995).

- Fibroblast cells on human skin were exposed (Whitson *et al.*, 1986) to the action of a 100-kV/m, 60-Hz electric field to find no changes in cell growth and DNA repair rate. Also, no changes were observed in the behavior of cancer cells upon exposure to electric fields, in contrast to the case of radiation combined with an MF (Phillips *et al.*, 1986b). A summary of works on biological effects of 5–105 kV/m electric fields is given in Stern and Laties (1998).
- Serpersu and Tsong (1983) have established that an AC electric field affects the work of (Na,K)AOFase on membranes of human erythrocytes. They placed some erythrocyte suspension enriched in  $^{86}\text{Rb}$  rubidium isotope between electrodes and measured the uptake of a radioactive tracer by erythrocytes on a 1-h exposure. It appeared that the passage rate of rubidium ions, which because of their similar size sort of substitute for potassium in the workings of a membrane pump, varies in an extremal manner both with the frequency and with the field amplitude. The same exposure did not influence the passage of Na ions, as measured from the  $^{22}\text{Na}$  tracer. The findings given in Fig. 2.39 show a relatively wide “resonance” in frequency with a center at around 1 kHz. The authors note that this corresponds to the frequency of natural conformational changes in proteins. A decline in the effect with the field amplitude was explained by a field-induced change in protein geometry, which leads to a violation in its normal functioning.

### 2.6.1 Weak electric fields

It has been found that in a number of cases biological effects are caused by weak electric fields induced by low-frequency MFs. Correlation between the level of

an induced electric field and a biological effect was observed, for instance, by Schimmelpfeng and Dertinger (1997). Proliferation of HL-60 cells was studied in a sinusoidal 2.8-mT, 50-Hz MF. A homogeneous MF affected the cells only where the induced electric field exceeded the threshold level of 4–8 mV/m.

An overview of experiments that had demonstrated the effectiveness of electrostimulation of cell metabolism was compiled by Berg (1993). Changes were observed in biopolymer synthesis, enzyme activity, membrane transport, proliferation, and morphological structures. These changes occurred, in particular, under the action of low-frequency variable MFs of about 0.1–10 mT, which engender in a biological medium electric fields of the above level. In certain cases in a given range some frequency and amplitude windows of stimulation effectiveness (Lei and Berg, 1998) were found. It is hard to analyze experiments on the stimulation of an MF in the millitesla range in the absence of detailed amplitude–frequency spectra, because mechanisms of various nature, e.g., spin and electrochemical ones, can contribute to the formation of an ultimate response. Therefore, to study the biological effects of an electric field it is preferable to employ electric, rather than magnetic fields. Although here too it is unclear, in the absence of detailed studies, what is responsible for the final biological response: an electric field as such or an electric current (electrochemical processes).

In some cases the intensity of the current induced by an electric field is small. At the same time the electric field itself can have a value comparable, in terms of the atomic effects it produces, with a weak magnetic field, see Sections 1.4 and 4.6. The biological action of an electric field can then be viewed in the same context as an MBE. The similarity of biological effects of low-frequency MFs and electric fields and the correlation of their effective parameters were discussed by Blank and Goodman (1997). The problem here is that it is unclear beforehand with what situation they handle in an experiment where they use relatively small non-thermal electric fields: with the action of an electrochemical current or with the action of the field itself. Therefore, the choice of experiments considered below is to a certain degree subjective.

- Bawin and Adey (1976) found on exposure to a low-frequency electric field some frequency and amplitude windows in the efflux rate from chicken brain tissue of  $^{45}\text{Ca}$  ions, Fig. 2.40. A maximum effect was observed in the region of 16 Hz and 10–60 V/m. Shown are field strengths between plates of the capacitor, where tissue samples were placed. The electric field within the tissue decreases owing to the fact that ambient molecules are polarized dielectrically, and that charge carriers, in this case ions, are redistributed.

Interestingly, the opposite effect of calcium efflux rate growth was observed by Bawin *et al.* (1975) upon exposure to a modulated EMF of high frequency, 147 MHz. An effectiveness window near a frequency of 16 Hz was registered at frequency modulation scanning in the low-frequency range.

- McLeod *et al.* (1987b) studied  $^3\text{H}$ -proline incorporation into a newly synthesized collagen in the collagen matrix of the bull fibroblast cell carrier. They found

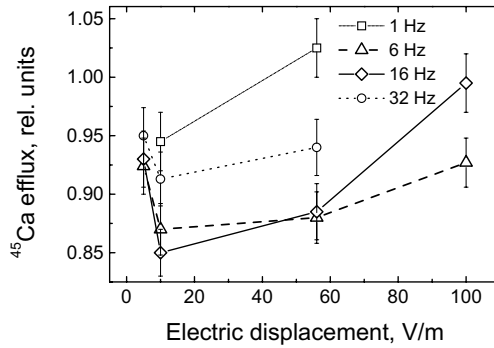


**Figure 2.40.** Frequency and amplitude windows when an electric field affects the efflux of calcium ions pre-introduced into brain tissue, according to Bawin and Adey (1976).

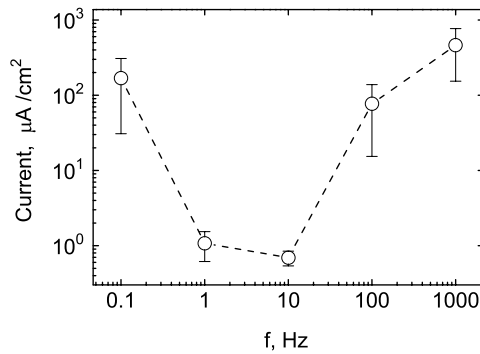


**Figure 2.41.** The threshold density amplitude of the current that reduces the protein synthesis rate in fibroblasts in an electric field, according to McLeod *et al.* (1987b).

that a weak,  $0.1\text{--}100\ \mu\text{A}/\text{cm}^2$ , low-frequency electric current, switched on for 12 h, retarded proline incorporation beginning with some threshold level, the value of that threshold being dependent on the field frequency, Fig. 2.41. A maximum 30% response was attained at a frequency of 10 Hz and a current density amplitude of  $0.7\ \mu\text{A}/\text{cm}^2$ . Since the specific resistance of the tissue was about  $65\ \text{ohm cm}$ , the authors concluded that AC electric fields of about  $4.5\ \text{mV}/\text{m}$  are able to cause a biological reaction. They also observed a reduction in the reaction threshold for long cells aligned along the field. Note that a field induced by a 50-Hz,  $100\text{-}\mu\text{T}$  AC MF in a sample 1 cm in size on the solenoid axis is an order of magnitude smaller ( $\sim 0.2\ \text{mV}/\text{m}$ ).

- Blackman *et al.* (1988) studied the efflux of calcium ions from chicken brain tissue *in vitro* in a wide frequency range for a combined action of weak magnetic and electric fields. The experiment formula is

$$b(0.085-0.1)e_p(20 \text{ V/m})f(1-510/15)B_p(< 38)B(?) .$$

They used double controls: sham-controls and controls outside of the exposure device. What is noteworthy here is the fact that the amplitude of an AC MF (tens of nanoteslas) is relatively small, which corresponds to the level of some geomagnetic variations. For 16 out of 38 tested frequencies a statistically significant MBE was found,  $P < 0.05$ . Also found were MBE frequency windows. A large frequency step, 15 Hz, is insufficient to warrant any conclusions about the potential target for an MF. It is not to be excluded that in various ranges work various primary biophysical mechanisms. One important observation, however, consisted in that virtually over all the frequency spectrum the MBE had the same sign; that is, the calcium efflux increased when an EMF was switched on.

- Fitzsimmons *et al.* (1989) addressed the proliferation of chicken bone tissue cells in a weak low-frequency electric field as  $^3\text{H}$ -thymidine was incorporated into the cells. They also measured the mitogenic activity of exposed culture on another, unexposed one. A plate with a cell culture was placed between a capacitor's plates, in the absence of conductive coupling. The AC field between the plates, in the absence of a dish, was 10 V/2.3 cm. The experiment formula

$$e(430 \text{ V/m})B(?)f(8-24/4)n(6)$$

made it possible to establish the presence of an effectiveness frequency window, Fig. 2.42. In terms of an ion interference mechanism, in a variable electric field, Section 4.6, the effective frequencies are the same as in the case of a uniaxial MF: the cyclotron frequency and its (sub)harmonics. If we take a local MF, of which there was no mention in the paper, to be 20  $\mu\text{T}$ , then the frequency maximum 16 Hz will correspond to a Larmor frequency of calcium ions.

- The activity of ion-activated membrane enzyme Na,K-ATPase was investigated by Blank and Soo (1990). The suspension contained substrate and enzyme. To platinum electrodes separated by 5 cm they applied a sinusoidal voltage with an amplitude from 1 to 1000 mV for 15 min. Correspondingly, an electric displacement for the smallest voltage was about 20 mV/m, the current amplitude in the circuit being about 70  $\mu\text{A}/\text{cm}^2$ . Frequency windows were found for effectiveness with a maximum effect at 100 Hz, Fig. 2.43. These dependences can hardly be referred to as spectral ones owing to the log scale of frequency variation. However, the frequency selectivity of the effect is obvious. The value of the MF was not controlled. The authors assumed that the processes of Na and K ion binding by an enzyme were involved in electroreception.
- Amplitude dependences were observed by Blank *et al.* (1992) when they addressed biological transcription in low-frequency electric fields. They studied the

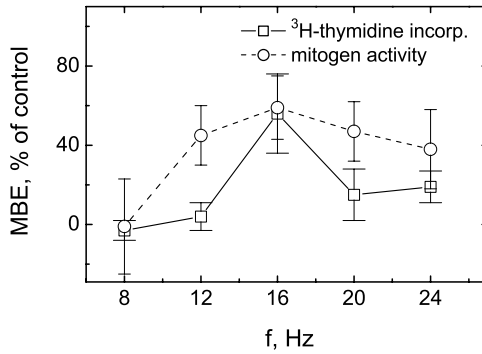


**Figure 2.42.** Response of embryonic chick calvaria cells to a variable electric field. Proliferation and mitogenic activity depending on the field frequency, according to Fitzsimmons *et al.* (1989).

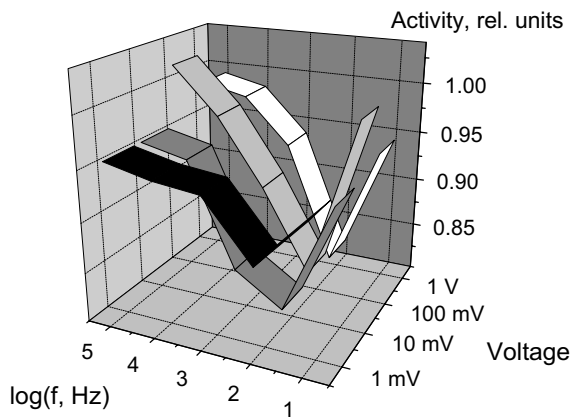


**Figure 2.43.** Frequency windows of relative activity of Na,K-ATPase enzyme for various amplitudes of the voltage across the electrodes, according to Blank and Soo (1990).

behavior of HL-60 cell culture on passing a current of frequency 60 Hz and amplitude density 0.1–100  $\mu\text{A}/\text{cm}^2$ . A maximum statistically significant 40% response was observed on a 20-min exposure to a current of 1  $\mu\text{A}/\text{cm}^2$ . At 0.1 and 100  $\mu\text{A}/\text{cm}^2$  the effects were 9 and 5%, respectively; at 10  $\mu\text{A}/\text{cm}^2$ , the effect did not differ from controls. The authors note that their findings do not support the hypothesis that the effect is proportional to the electric field. The data suggest that there is an effectiveness window in the amplitude of an internal electric field near 10 mV/m, which approximately corresponds to a current density of 1  $\mu\text{A}/\text{cm}^2$  in a biological

tissue.

- Liburdy (1992) designed a special dish with concentric sections, which was placed in a solenoid. The sections enabled a passage through a cell culture (rat thymocytes) of a 60-Hz AC electric current equal to the one that was induced by a 60-Hz, 22-mT MF in a solenoid. In both cases, the electric field in the cell had the same geometry and was 62–170 mV/m. Correspondingly, the current density for the observed electrical conductivity  $\sigma = 1.685 \text{ S/m}$  was  $\sim 10\text{--}30 \mu\text{A/cm}^2$ .

The field value correlated with the value of the effect, i.e., with the intracellular calcium density, measured spectrophotometrically in real time. In these assays the AC electric field with any exposure form increased, in 10–15 min, the calcium density by 20–30% as compared with controls. Thereby, the AC MF per se seemed to be immaterial. Using various biochemical techniques, the author also established the probable target for the action of a field, namely the calcium membrane channel.

It was maintained in the paper that the GMF component parallel to the solenoid axis was  $20.5 \mu\text{T}$ , which generally speaking does not exclude ion interference mechanisms for the action of an electric field.

- Nazar *et al.* (1996) found a frequency selectivity in the action of a sine electric field on the specific activity of the enolase enzyme in a *E. coli* cell culture. The cells were exposed to an electric field of amplitude 65.4 V/m. The frequency interval was 10–72 Hz. The effect, i.e., the difference of exposed and control activities divided by the control value, is shown in Fig. 2.44. It is seen that as the electric field frequency was varied, the effect changed not only its value but also its sign. Local MF parameters, it seems, were not controlled. The picture obtained is characteristic for MBE frequency spectra in low-frequency EMFs, although the authors only determined the statistical confidence of the effect at a frequency of 60 Hz. The mean frequency step and data dispersion were relatively large; therefore no reliable conclusions could be made. However, it is interesting to note a similarity of the data in Fig. 2.44 and the MBE frequency spectrum, also for *E. coli*, from Alipov and Belyaev (1996), see also Fig. 4.32. Such a similarity also points to a similar physical nature of the above biological effects of electric and magnetic fields.

- Cho *et al.* (1996) studied, using a fluorescent video-microscope, the reorganization of cytoskeleton threads as an electric current was passed through a cell culture of *Hep3B* human hepatoma. The electric field parameters varied within a frequency range of 0–60 Hz, the zero frequency corresponding to the passage of a DC current, and field amplitudes of 0–1 kV/m. The amplitudes were worked out from the measured current and conductivity of the cell medium. Only some cells responded when a field was switched on. Figures 2.45 and 2.46 give the results — the relative number of sensitive cells that responded when a field was on for 15 min. The non-resonance form of the spectrum suggests that underlying the effect is a reaction to a DC field with a characteristic time of 0.1 s, oppositely directed fields producing opposite effects. In such a case, the actions of positive and negative half-waves of a sine signal with a frequency of  $> 10 \text{ Hz}$  largely compensate for each other.

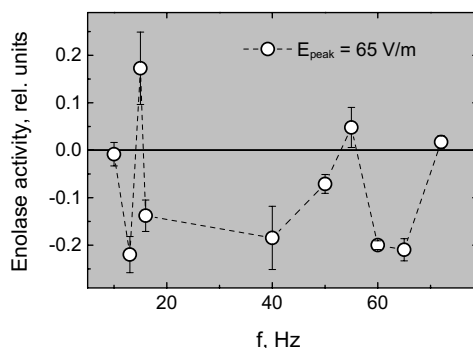


**Figure 2.44.** The relative activity of enolase in *E. coli* at various electric field frequencies, according to Nazar *et al.* (1996).

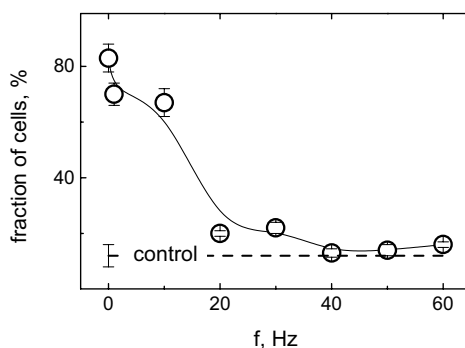


**Figure 2.45.** The relative number of human hepatoma cells that respond by restructuring their cytoskeleton to a 500 V/m EF depending on the frequency. According to Cho *et al.* (1996).

It is seen that an effect occurs already in a weak electric field (about 1 V/m), and it does not possess an amplitude selectivity. Underlying such effects, which are characterized by the absence of frequency–amplitude windows, could be activation-type mechanisms as described in Section 3.4.

- The glycolysis rate in mouse brain exposed to an electric field of 50–1500 V/m was measured by Huang *et al.* (1997). A cell culture in a flat dish was located between capacitor planes separated by 1 cm. When the negative electrode was at the top, the glycolysis rate was about 20% larger at 1000 V/m. A polarity change reversed the effect sign, but its magnitude was much smaller, about 4%. It is of interest that the effect magnitude varied with the field voltage in a non-trivial

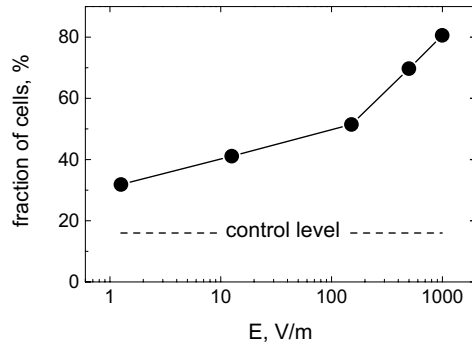


**Figure 2.46.** The relative number of human hepatoma cells that respond by restructuring their cytoskeleton to a 1-Hz EF depending on the amplitude. According to Cho *et al.* (1996).

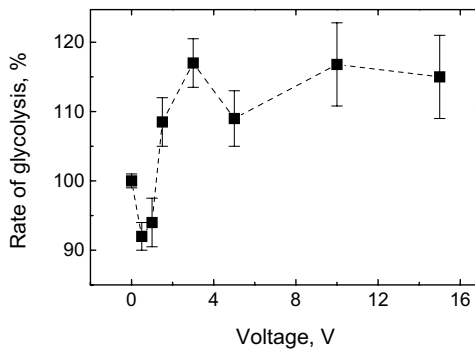


**Figure 2.47.** The glycolysis rate in mouse brain upon a 30-min exposure to an electric field of a given value, in percent to controls at  $U = 0$  V, according to Huang *et al.* (1997).

manner, Fig. 2.47.

Considering that the cell culture with a permittivity of  $> 50$  and the dish bottom with a permittivity of  $\sim 5$  took up 1 mm each (the cell size was about 0.01 mm), the authors worked out that the cells were subjected to a field of  $\sim 30$  mV/m, when a voltage of 15 V was applied. Even such a relatively small electric field is able to cause a biological effect with a complicated voltage dependence. The authors believe that a static electric field can affect the orientation of an electrically charged protein of  $\text{Na}^+, \text{K}^+$ -ATPase in a cellular membrane, and hence it can affect the extracellular  $\text{K}^+$  density. The asymmetry of the response upon field polarity changes can be caused by cells being primarily oriented either in a gravitational or in an uncontrolled local magnetic field.

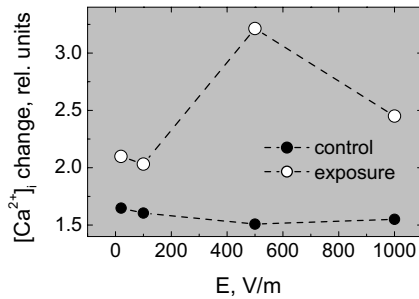


**Figure 2.48.** Intracellular calcium density in an osteoblast culture in mice upon exposure to a 10-Hz EF of various amplitudes. According to Tang *et al.* (1998).

- Sontag (1998) used plane electrodes inside or outside to apply to a medium with HL-60 cells a low-frequency electric field with an amplitude range of 1–4000 V/m and a frequency range of 0.1–100 Hz. After a 15-min exposure to such fields, measurements of the intracellular content of free calcium ions using a fluorescent spectrometer yielded no results. The GMF component normal to an electric field was 12  $\mu\text{T}$ ; no reference was made to the other component. Effective exposure to a current of 250  $\mu\text{A}/\text{cm}^2$  at a frequency of 4 kHz in an amplitude window that was about 200  $\mu\text{A}/\text{cm}^2$  wide was found later (Sontag, 2000) in measurements of interleukin release from cells. Here they used 0–125 Hz low-frequency modulation of the current.

- Tang *et al.* (1998) studied the proliferation of osteoblast cells in mice. Cells subjected to a 10-Hz, 20-V/m electric field for 20 min would grow 60% faster than controls. Also measured using the fluorescent method was the intracellular calcium density, while exposing the cells to rectangular electric field pulses by the scheme

$$e(20-1000 \text{ V/m})f(1-1000) .$$

Frequency and amplitude windows were also found. A maximum effect was found in the range 5–15 Hz. The amplitude spectrum is shown in Fig. 2.48; it has a maximum effect at 500 V/m.

## 2.6.2 Frequency–amplitude windows

We can identify in the above experiments two groups by the manner in which an electric field is applied. In the first case, a system under study is placed between a capacitor's plates, without any direct electric contact. In the second case, a current is passed using electrodes introduced into the biological medium. In both cases effectiveness windows for parameters of an electric field are observed.

Data for the first group are summarized in Table 2.2. In all experiments there are only several experimental points, which are hard to associate with any smooth

**Table 2.2.** Experiments with an externally applied EF

Medium	$f$ , Hz	$E$ , V/m	Effect
Brain tissue enriched in $^{45}\text{Ca}$	3–24	10–60	–15 % Ca discharge (Bawin and Adey, 1976)
Bone cell culture	12–20	430	+50 % cell proliferation (Fitzsimmons <i>et al.</i> , 1989)
<i>E. coli</i> cell culture	10–70	65	–20 % special activity of enolase (Nazar <i>et al.</i> , 1996)
Osteoblastic cells in mice	5–15	500	> 50 % proliferation and concentration $[\text{Ca}^{2+}]_i$ (Tang <i>et al.</i> , 1998)

curve. However, a general conclusion is possible that effective electric fields approximately feature the following intervals: 10–100 Hz in frequency, and 10–100 V/m in amplitude.

In the second group of experiments, the observable was the current passed through a physiological medium containing cells to be studied. In that case, the internal electric field can be worked out knowing the medium conductivity. The findings are summarized in Table 2.3. It follows from the table that the expected effectiveness ranges in such experiments are 10–100 Hz and 1–10  $\mu\text{A}/\text{cm}^2$ .

Expected frequency effectiveness windows of 10–100 Hz are the same for both groups of experiments. Larmor and cyclotron frequencies are fundamental for any EMF biological reception mechanism involving ions. These frequencies fall precisely into the interval for most of the biologically important ions exposed to an MF similar to the geomagnetic field.

A note on amplitude windows is in order. In the first group of experiments the mean electric field within a medium falls off approximately by two orders of magnitude as compared with the external field owing to the polarization of water with  $\varepsilon \sim 80$ . The effective dielectric permittivity of the medium can grow further several fold because of the special properties of a double electric layer surrounding the charged surface of the cellular membrane (Chew, 1984). This means that effective internal electric fields in a medium are at least about 100–1000 mV/m and are perhaps yet smaller.

In the second group of experiments, the internal EF can be found from the relationship  $E = j/\sigma$ , where  $j$  is the current density in a medium and  $\sigma$  is the medium conductivity. For biological tissues  $\sigma \approx 1 \text{ S/m}$ . It follows that the effective field range corresponds to the interval 5–500 mV/m. There is thus an approximate coincidence also of amplitude windows in both groups. A question emerges as to whether the above windows are physically equivalent when an EF is applied to

**Table 2.3.** Experiments involving the passage of a current

Medium	$f$ , Hz	$J$ , $\mu\text{A}/\text{cm}^2$	Effect
Fibroblasts in collagen medium	1–10	$> 1$	–30 % DNA synthesis (McLeod <i>et al.</i> , 1987b)
Substrate-enzyme suspension	20–1000	$> 70$	–15 % Na,K-ATPase activity (Blank and Soo, 1990)
HL-60 cell culture	60	0.3–3	+30 % transcription level (Blank <i>et al.</i> , 1992)
Rat thymocytes	60	20	+25 % $[\text{Ca}^{2+}]_i$ density (Liburdy, 1992)
Fibroblasts in collagen medium	10–100	5–7	+60 % DNA synthesis (Goldman and Pollack, 1996)
HL-60 cell culture	0–100 (mod)	200–400	+100 % interleukin release (Sontag, 2000)

a medium in various ways. In any case, there are no grounds to maintain that the physical mechanisms underpinning the biological effects in the two groups are different. It is shown in Sections 4.6 and 4.9.6 that quantum interference of ions is capable of accounting for the biological effectiveness of weak EFs, irrespective of the way it was transported to a microlevel.

Some other experiments on DNA–RNA synthesis, enzyme activity, cell proliferation, and calcium transport, which reveal window spectra of effective electromagnetic exposure, are provided in a concise overview by Berg (1995). They also point to the existence of an optimal frequency–amplitude regime in a frequency range of 10–100 Hz and field amplitudes of 10–100 mV/m.

## 2.7 BIOLOGICAL EFFECTS OF HYPERWEAK FIELDS

A body of experimental evidence is gradually taking shape that testifies to biological activity of hyperweak MFs,  $\lesssim 1 \mu\text{T}$ . There are no data so far on the dependence of these effects on the level of a DC MF at experiment site. The mean intensity of an AC MF in those observations being much lower than the possible level of a DC field, it makes sense to class such experiments in a separate group. Mechanisms for biological effectiveness of hyperweak fields seem to be different from those for the action of fields at the geomagnetic level.

Earlier experimental evidence for the biological detection of hyperweak variable signals, both magnetic, up to 1 nT, and electric, up to 0.1 mV/m, are given by Presman (1970). Sensitivity of sea sharks and rays to fields of up to  $0.5 \mu\text{V}/\text{m}$  was discussed by Bastian (1994).

Changes in peroxidase activity in leukocytes of peripheral blood in rabbits upon a 3-h exposure to hyperweak MFs of 8 Hz were observed by Vladimirkii *et al.* (1971). In those experiments MF strengths were 0.02, 0.2, 1, and 2 nT. At all of those field values they observed changes in cytochemical activity of neutrophils as compared with controls. The changes varied from about  $9 \pm 2\%$  at 0.02 nT to  $72 \pm 23\%$  at 2 nT. The authors believe that this could bear witness to living systems being directly affected by geomagnetic storms.

Keeton *et al.* (1974) reported that natural GMF fluctuations ( $\sim 100$  nT) influence orientation in pigeons.

Delgado *et al.* (1982) studied changes in morphological parameters of chicken embryo growth upon a 48-h exposure to pulsed MFs. The body of evidence is insufficient to construct amplitude or frequency spectra, however a statistically significant effectiveness of regimes  $0.12 \mu\text{T}$  100 Hz and 1000 Hz is shown.

Rea *et al.* (1991) reported that 16 humans they had studied showed a sufficient sensitivity to an EMF to sense the switching on of an MF. Volunteers were exposed to an inhomogeneous MF, which varied from  $2.9 \mu\text{T}$  in the region of their feet to  $0.35 \mu\text{T}$  near their knees, and to 70 nT near their heads.

The influence of a 0.05–5 Hz, 100-nT sine-wave field on the pulsed activity of neurons in a mouse cerebellum section was observed by Agadzhanian and Vlasova (1992). The assays were conducted in a chamber shielded from external magnetic interferences.

Jacobson (1994) used variable MFs as small as 5 to 25 pT to treat epilepsy and Parkinson disease cases. A sinusoidal field of 2–7 Hz was applied to the brain so that to affect the epiphysis. MF stimulation was correlated with melatonin production.

Kato *et al.* (1994) determined the action of a circularly polarized 50-Hz,  $1\text{-}\mu\text{T}$  MF on the level of nocturnal melatonin density in mouse blood. Controls were animals placed in a similar exposure chamber with a residual field of  $< 0.02 \mu\text{T}$ . By the end of a 6-week exposure in both chambers melatonin density was in controls  $81.3 \pm 4.0$  pg/ml, and in exposed groups  $64.7 \pm 4.2$  pg/ml. That difference vanished when measurements were made a week after the exposure. Obviously, division into control and exposed groups here is fairly conditional, since exposure in fields of such a low intensity is in itself not indifferent to animals. In any case, however, the studies have demonstrated the effectiveness of fields at a level of  $1 \mu\text{T}$ .

Works by Novikov (1996) and Fesenko *et al.* (1997) are devoted to investigations into the molecular polycondensation reaction of some amino acids in solutions exposed to a variable MF of about 20 nT parallel to a local DC MF of about the geomagnetic field. The MF had a frequency of several hertz, which corresponded to cyclotron frequencies of amino acid molecules. Unfortunately, the authors did not report how they determined cyclotron frequencies of amino acid molecules. That is important since the electric charge of those molecules in solution is dependent on its acidity. At the same time, the very fact of MF being effective at such a low level was shown quite convincingly. There is no evidence so far on the confirmation of those assays in independent laboratories.

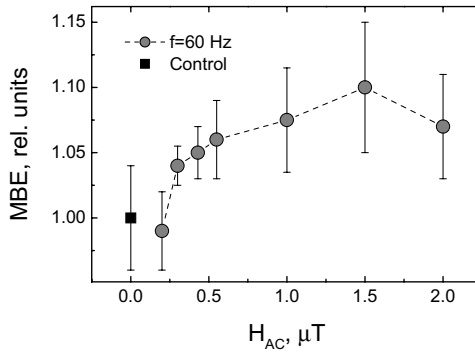


**Figure 2.49.** The activity of membrane ion pump in a hyperweak variable MF, according to Blank and Soo (1996).

Blank and Soo (1996) determined the sensitivity limit for the activity of Na,K-ATPase enzyme in a medium with microsomes in relation to power–frequency MFs. The sensitivity level was 200–300 nT, Fig. 2.49.

West *et al.* (1996) found that when a JB6 cell culture of mouse epidermis was exposed for several days to a 60-Hz, 1- $\mu T$  MF against the background of a static laboratory MF, the number of cells grew by a factor of 1.2–2.4 as compared with controls.

Akerstedt *et al.* (1997) studied the effect of nocturnal exposure to a 50-Hz, 1- $\mu T$  MF on various physiological characteristics of human sleep (with 18 volunteers). They found that such an MF drastically curtailed the so-called slow sleep phase.

Harland and Liburdy (1997) found that a 60-Hz, 1.7- $\mu T$  (and even 0.28  $\mu T$ ) MF

$$b(1.7)b_{\text{stray}}(< 0.06)B(< 0.3)B_p(< 0.3)f(60)$$

suppresses the inhibitory action of melatonin and tamoxifen. Melatonin at a physiological concentration  $10^{-9}$  M and tamoxifen at a pharmacological concentration  $10^{-7}$  M were used to inhibit the growth of MCF-7 cancer cells in humans. The evidence was of importance since it pointed to a potential hazard of even very weak fields, and so the research was reproduced in another laboratory by other workers, see Blackman *et al.* (2001). In both cases, the results appeared to be the same, with inhibitory effects declining in a statistically significant manner by tens of percent.

Some experimental works were performed by various groups using the Tecno AO device, Tecnosphere, France, reg. PCT/FR93/00546 (Hyland *et al.*, 1999). When the device is located close to an object under study (chicken embryos, human volunteers), the harmful influence of videomonitors and mobile phones is more or less compensated for (Youbicier-Simo *et al.*, 1998). The device is essentially a metal vessel filled with an aqueous solution. The nature of the active agent is still unknown.

The most obvious approach is to link it to the hyperweak magnetic field reemitted by the aqueous solution.

In some works, biological effects of *microwaves* of very small intensity were observed:  $10^{-2} \mu\text{W}/\text{cm}^2$  (Aarholt *et al.*, 1988),  $5 \cdot 10^{-6} \mu\text{W}/\text{cm}^2$  (Grundler and Kaiser, 1992), and  $10^{-12} \mu\text{W}/\text{cm}^2$  (Belyaev *et al.*, 1996).

Kuznetsov *et al.* (1997) exposed a *S. cerevisiae* yeast culture to the action of 7.1-mm microwaves within a wide range of powers. There was a response that consisted in the emergence in a synchronous cell culture of a proliferation process, such that the temporal dependence of the density looked like a step function. Such a response occurred some time  $t$  after the beginning of the exposure, and that time depended on the microwave power. The measured dependence was close to a linear one (from power logarithm) within  $t = 5$  min at  $1 \text{ mW}/\text{cm}^2$  and  $t = 240$  min at  $10^{-12} \mu\text{W}/\text{cm}^2$ . It is interesting to note that the value  $10^{-10}$ – $10^{-11} \mu\text{W}/\text{cm}^2$  corresponds to a sensitivity threshold of sight and hearing receptors.

The physical nature of biological effects of weak variable MFs (about the geomagnetic one) remains unclear. Therefore, experimental data on biological reception of MFs that are 3–10 orders of magnitude weaker look, of course, quite challenging. The body of that evidence is not large so far, but knowledge is being gleaned.

# 3

---

## THEORETICAL MODELS OF MBE

With such quantitative scantiness we must resign ourselves to the fact that our Pegasus is piebald, that not everything about a bad writer is bad, and not all about a good one good.

V. Nabokov, *The Gift*

How can a weak, under 1 G, low-frequency magnetic field cause a biological response? The question has no straightforward answer. The magnetobiological effect is conditioned by processes occurring at different levels of the organization of a living system, from physical ones to complicated adaptational biological ones (Kholodov and Lebedeva, 1992). Workers in various fields come up with their own answers. Human health workers single out, in humans, organs and general physiological processes that are sensitive to magnetic fields. Biologists attempt to reveal cellular and subcellular structures that form biological responses to the action of a field. Biochemists search for targets — links of biochemical reactions — whose rates are dependent on the parameters of an MF. (Bio)physicists try to isolate magnetosensitive processes in the interaction of a magnetic field with relatively simple molecular structures. It is at that level that occur involved spectral or “window” conditions of the correlation of biophysical processes with biotropic parameters of an MF.

This chapter takes a critical look at the hypotheses and models (including some author’s work) of the biological reception of *weak* magnetic fields. A review of possible mechanisms of the magnetoreception of strong MFs, from fractions of Tesla and beyond, has been made by Piruzyan and Kuznetsov (1983).

### 3.1 THEORETICAL STUDIES IN MAGNETORECEPTION

It would perhaps be a good idea to begin an overview of magnetoreception theory with the identification of groups of similar accounts of magnetobiological effects. Such groups do exist, and they lead to some conditional classifications of models in magnetobiology. So, Polk (1991), Adey (1993), and Berg and Zhang (1993) came up with their MBE classification. The fact that such classifications are in existence and that they are ambiguous and date quickly attests to the difficulties in the accounting for magnetobiological effects, to their paradoxical nature, and to the

dearth of knowledge of the nature of the biological activity of weak electromagnetic fields.

The above reviews could be complemented with those of groups of physical processes and ideas (Binhi, 1999a, 2001) that are assumed to underlie magnetoreception. In so doing, we will have to class them as phenomenological, macroscopic, and microscopic. Phenomenological descriptions are not concerned with the nature of an event; they only offer mathematical toolkits to handle external manifestations of an object. In contrast, macro- and microscopic accounts are attempts at gaining insights into the physical nature of an object; they establish limitations on the validity of specific phenomenological models. They differ in the scale of objects under consideration.

There is also a group of theoretical treatments that could be described using the following general terms. The thesis that *A does exist* as a physical event lends itself to a relatively easy proof. Suffice it to provide an experimental support of its existence under *any* feasible conditions. In contrast, the opposite thesis that *A as a physical event does not exist* is more difficult to prove. To this end, the validity of the thesis will have to be proven under *all* feasible conditions. More often than not, all the feasible conditions are impossible to identify. It is exactly the case with the biological reception of weak MFs. Substantiating the thesis is a matter of practical scientific work. Within the framework of positivistic conceptions, the whole body of experimental evidence has falsified the thesis that there is no MBE. There is no denying the existence of the phenomenon either experimentally or logically. In the latter case, if we set out to identify the conditions, i.e., the possible mechanisms of the action of an MF, we will never exhaust the possibilities. There will always remain a possibility that we have overlooked some special cases. Nevertheless, despite the intrinsic logical inconsistency of any attempts to theoretically refute the very existence of MBE, such attempts do occur. Some works (e.g., Adair, 1991, 1992), and also *Bioelectromagnetics*, **19**, 136, **19**,181, 1998, contain physical models of the hypothetical processes underlying the MBE that are proposed in the literature. However, since they are refuting in nature, the models contain no productive element and are devoid of any predictive power. The substance of those works cannot be tested; therefore we will overlook those models in our reasoning.

### 3.1.1 Classification of MBE models

In a way, the classification bellow is conventional, and the selection of specific works included into a group is fairly arbitrary — it is not always possible to unambiguously refer a work to this or that group. This author does not claim to provide a complete treatment, and does not maintain that the models considered are better or worse than other members of a group. At the same time, such a division appears to be handy, enabling one to consider not some specific ideas, mechanisms, and models, but rather their *types*. The classification does not cover the mechanisms of the biological action of strong MFs. A review of concepts, such as diamagnetic orientation, liquid-crystal effects, the redistribution of molecules in an inhomogeneous MF, and

magnetohydrodynamic effects, is available, for instance, in Kuznetsov and Vanag (1987); a review of relevant experiments is available in the book by Simon (1992). In what follows we will only focus on *a priori* probable origins of the MBE — the biological effects of weak MFs.

### 3.1.1.1 Phenomenological models

— Complicated behavior of the solutions to chemical-kinetics-type equations (Grundler *et al.*, 1992; Kaiser, 1996; Galvanovskis and Sandblom, 1998).

— Stochastic resonance as an amplifying mechanism in magnetobiology and other random processes (Makeev, 1993; Kruglikov and Dertinger, 1994; Bezrukov and Vodyanov, 1997a).

— Magnetosensitive phase transitions in biophysical systems viewed as liquid crystals (Simonov *et al.*, 1986) or ordered membrane proteins (Thompson *et al.*, 2000).

— “Radiotechnical” models, in which biological microstructures and tissues are presented as equivalent electric circuits (Jungerman and Rosenblum, 1980; Pilla *et al.*, 1994; Astumian *et al.*, 1995; Barnes, 1998).

### 3.1.1.2 Macroscopic models

— Biomagnetite in a magnetic field and ferromagnetic contamination (Kirschvink *et al.*, 1985; Kobayashi *et al.*, 1995).

— Joule heat and eddy currents induced by variable MFs (Chiabrera *et al.*, 1984, 1985; Polk, 1986).

— Superconductivity at the level of cellular structures (Cope, 1973, 1981; Achimowicz *et al.*, 1979; Achimowicz, 1982; Costato *et al.*, 1996) and alpha-spiral protein molecules (Davydov, 1994).

— Magnetohydrodynamics, see the overview Kuznetsov and Vanag (1987).

— Ion macroclusters, charged vortices in cytoplasm (Novikov and Karnaukhov, 1997).

### 3.1.1.3 Microscopic models

— The motion of charged and spin particles in a magnetic field, including resonance effects (Chiabrera *et al.*, 1985; Liboff *et al.*, 1987a; Lednev, 1991; Binhi, 1995b); oscillatory effects (Chiabrera *et al.*, 1991; Belyaev *et al.*, 1994; Lednev, 1996; Zhadin, 1996); interference effects (Binhi, 1997b, 1998a, 1999b, 2000); free-radical reactions (Buchachenko *et al.*, 1978; Steiner and Ulrich, 1989; Brocklehurst and McLauchlan, 1996); and collective excitations of manyparticle systems (Fröhlich, 1968b; Davydov, 1984b; Wu, 1996).

— Biologically active metastable states of liquid water that are sensitive to variations of an MF (Kislovsky, 1971; Binhi, 1992; Fesenko *et al.*, 1995; Binhi, 1998b).

— Biological effects of fields that are assumed to be connected with an MF and with a modified geometry of space (Akimov *et al.*, 1997; Shipov, 1998).

These papers vary strongly in the depth of treatment. Only some of them have been brought up to the level of mathematical models featuring some predictive potential. A theoretical account seems to be of any value only when it admits a numerical correlation with experimental data. It is important here to be able to compare, not numbers, but functions. That is, the theory must be able to compute

the amount of the effect depending on MF parameters. That is why mechanisms that do not meet this requirement — and there are many of them — are not considered in some detail, but are just mentioned. It makes no sense to criticize such mechanisms, because it is impossible in principle to compare theory with experiment, a major yardstick of the validity of any scientific judgment.

The MBE macromodels form a more or less independent group. By contrast, phenomenological models need a microscopic substantiation. So, the models that are built around some special solutions to chemical-kinetics equations need a clarification as to what chemical reaction has its rate dependent on the MF and in what manner. When considering a stochastic resonance one should be specific as to what physical object is involved. Models with magnetosensitive phase transitions require that objects interacting with an MF be specified. In the general case, such objects are microparticles that have a charge or a spin. Anyway, all the non-macroscopic mechanisms rely on some special dynamics of particles in an MF. Dynamics, both classical and quantum, is sort of underlying any theoretical treatment of the MBE, especially where the MBE is paradoxical in nature.

The body of evidence on the dynamics of particles in a magnetic field to account for the MBE is fairly large. Virtually all of the mechanisms proposed have been realized as models. It would therefore be advisable to classify models within that group by their dynamics type, whether classical or quantum, and by the type of the quantity that varies as the particles interact with an MF. Such a classification is quite objective, and thus convenient to compare the model types.

Before we embark on this classification, we will note the nontrivial similarities and differences in the behavior of single- and multiparticle systems. Virtually all the objects one encounters in physics are multiparticle systems. However, it is often possible to isolate more or less independent particles whose motion is determined by the combined action of all the other particles. These latter sort of produce an effective potential for the motion of an isolated particle. In that case, single-particle models are capable of featuring the main properties of the isolated system. Such is, for instance, the atomic model in which each of the electrons can be satisfactorily described by the joint potential of the nucleus and the cloud of the remaining electrons. Another example is the rotation of a molecule in gaseous phase. Single-particle models properly describe many physical systems. They are singularly convenient and graphic, although not always correct.

However the motion of several particles is, as a rule, analytically intractable. The motion is too involved. In certain cases, where the interparticle coupling causes structures that are more or less symmetrical at equilibrium to be formed, it is possible to determine the generalized coordinates of a multiparticle system, their number being proportional to the number of the particles. The system's motion can then be represented as a superposition of independent motions along those coordinates. The vibrational spectra of symmetrical molecules, for instance, can be studied analytically using group theory, if the number of atoms is about ten or less.

As the particles grow in number and if they interact fairly strongly, there occur *collective* cooperative motions of particles, the so-called collective excitations or

**Table 3.1.** MBE models with particle-magnetic field interaction

Variable	Dynamics	
	Classical	Quantum
coordinate	<b>Lorentz force</b> particle deviation (Antonchenko <i>et al.</i> , 1991), oscillation polarization (Edmonds, 1993)	<b>Interference of quantum states</b> (Binhi, 1997b,c, 1998a, 1999b; Binhi and Goldman, 2000; Binhi, 2000; Binhi <i>et al.</i> , 2001)
momentum, angular momentum, energy	<b>Energy pumping</b> cyclotron resonance (Liboff, 1985; Zhadin and Fesenko, 1990), parametric resonance (Chiabrera <i>et al.</i> , 1985; Zhadin, 1996)	<b>Quantum transitions</b> at Zeeman and Stark sublevels (Chiabrera <i>et al.</i> , 1991), parametric resonance (Lednev, 1991; Blanchard and Blackman, 1994)
spin	—	<b>Spin dynamics</b> spin resonance (Binhi, 1996), rad- ical (Vanag and Kuznetsov, 1988) and exchange reactions (Binhi, 1992, 1995b, 1998b), spin-dependent quan- tum interference (Binhi, 1997b)

dynamic oscillation modes. Normally, that situation is described in the so-called continuum approximation, where instead of the particle coordinates their continuously varying density is introduced. Mathematically, the dynamics of such modes is equivalent with single-particle systems and is, therefore, more convenient and graphic. In the classic case, the dynamic variable is the amplitude of the collective excitation; in the quantum case, it is the number of excitation quanta. Interaction with an MF may result in the pumping of excitation energy, which could be a mechanism responsible for the MBE. Original works considered collective excitations, the vibrations of biological membranes, and the waves of rectilinear and torsional shifts in biopolymer molecules (Bohr *et al.*, 1997). The natural frequencies of such collective excitations, however, fall into the microwave range. There is no evidence for the collective excitations of biophysical structures in the range of 1–100 Hz that is of interest to us, so we will confine ourselves to a summary of single-particle models for the MBE mechanisms, for which natural frequencies on the order of  $\sim qH/Mc$  have been found. For particles such as biologically significant ions with mass  $M$  and charge  $q$  in a field  $H$  that is similar to the geomagnetic one, these frequencies fall within the specified range. A summary of models by dynamics groups and variables affected by an MF is given in Table 3.1.

### 3.1.2 Overview of MBE mechanisms

We will consider in some detail the magnetoreception mechanisms that are especially popular in the literature. It is assumed that they can form the foundation for the MBE.

Historically, one of the early ideas in magnetobiology is concerned with the so-called biogenic magnetite (of biomineralization) in a magnetic field. The systems of some animals and microorganisms develop in a natural way some microscopic crystals, usually of magnetite, which can be magnetized. When exposed to an external magnetic field, the crystals are subjected to a torque and exert a pressure on the surrounding tissues, which causes a biological reaction. This mechanism, which is studied consistently by Kirschvink *et al.* (1992), seems to take place. Magnetite crystals have been found in the brain of some birds, which are known to possess a striking capability to take their bearings in the geomagnetic field, and also in some insects and bacteria.

The explanation of the biological action of a low-frequency MF on cells *in vitro* in terms of ferromagnetic contaminants (Kobayashi *et al.*, 1995) is a development of the idea of biogenic magnetite. The magnetic contaminants are present not only in the ambient dust, but also in plastics and glasses, and in laboratory chemical preparations and water. The average size of such particles is about  $10^{-5}$  cm; they are ferro- and ferrimagnetic in nature, i.e., they feature spontaneous magnetization. The authors have shown that routine laboratory procedures of pouring and rinsing enrich cellular cultures with magnetic particles so that they can outnumber the cells manifold. The energy of a magnetic particle is around three orders of magnitude higher than  $\kappa T$ . The authors believe that such a particle, when adsorbed on the cellular surface, may transfer its energy to the neighboring cellular structures, e.g., to mechanically activated ion channels.

These magnetoreception mechanisms are in a class by themselves, and they do not account for the major issue of magnetobiology. After all, unicellular organisms that do not contain magnetite are also able to react to an MF, and depending on the field parameters in many cases the reaction may be complicated non-linear and multipeak in nature. The main task of magnetobiology is exactly to account for that phenomenon, which is a paradox in terms of classical physics.

Sometimes the biological activity of weak MFs is explained using the representation of biological matter or biophysical structures as equivalent distributed electric circuits. In any case, this approach, being a phenomenological one, gives no answers to the issues of magnetobiology. Even the descriptive potential of such an approach is dubious. So, in *Biophysics*, **38**(2), 372, 1993, one finds an explanation of the influence of a DC MF on the propagation of the action potential along a nerve fiber. Ion channels of biological membranes were represented as oscillatory circuits with electric solenoids. These microsolenoids produce MFs, when their channels are open, and thus interact with one another and with an external MF. Underlying that representation were, for one thing, the experimental measurements of the natural inductance and capacitance of biomembrane areas and, for the other, the

assumption that an ion in an ion channel moves along a spiral. It was shown in Binhi (1995c), however, that (1) the equivalent inductance only reflects the inertia of the ion channels on changing the voltage; (2) the propagation of an ion along the channel is hardly classical in nature; and (3) the ions in the channel move one after another, and the MF caused by that motion does not correspond by far to the MF caused by the charges moving simultaneously in all the solenoid sections. It is clear that any explanation drawing on the model of ion channels–solenoids is just an illusion of explanation.

The hypothesis has been tested many times that a driving force behind the irradiation of biological system by a low-frequency MF is the eddy currents induced by an AC MF in biological tissues. The current can bring about the heating of the tissue, see Section 1.4.1. Polk has shown that eddy currents can also cause electrochemical EMF effects owing to a redistribution of charges. The current varies with the strength of the induced electric field, which is proportional to the product of the amplitude and frequency of the MF. If the hypothesis holds true, then in experiment the MBE should correlate with the variations of that quantity. There are indeed experimental data pointing out that such a correlation occurs as the strength of the AC MF grows (Lerchl *et al.*, 1990; Schimmelpfeng and Dertinger, 1997), but with relatively weak MFs (like the geomagnetic one), no correlation has been revealed (Juutilainen, 1986; Liboff *et al.*, 1987b; Ross, 1990; Blackman *et al.*, 1993; Jenrow *et al.*, 1995; Prato *et al.*, 1995). Specifically, it was shown in Ross (1990) that within a certain frequency range the MBE remained unchanged as the value of the induced currents was changed nearly 40 times. This attests to the existence of primary MBE mechanisms that are not connected with the eddy currents.

It is often maintained that the action of weak physico-chemical factors on biological systems is an information action. This suggests that a biosystem is in a state close to the conditions of an unstable dynamic equilibrium. The system is believed to need some pushing for it to transfer to another state due to some external resources. Put another way, the so-called biological amplification of a weak MF signal will occur. To arrive at a phenomenological description of the process they use the equation of chemical kinetics. Under certain conditions, their solutions feature a bifurcation, i.e., when exposed to a weak excitation they may pass into a qualitatively different dynamic condition. Kaiser (1996) discussed that concept in the electromagnetobiological context.

There is one important question. Thermal fluctuations have energy scales that are ten orders of magnitude larger than the energy of the quantum of an MF, but they do not destroy the MBE. Why? The answer is generally linked to the idea of the coherent action of an external factor against an incoherent thermal noise background. It is then possible to drive some high-Q oscillator (time coherence) to a state, where its energy will be sufficient to make an initiating push, or to drive synchronously a system of oscillators (spatial coherence) for it to yield a quantum of collective excitation (Fröhlich, 1968a; Popp, 1979). Another answer is that it is not energy but some other oscillator variables, such as oscillation polarization, that

acquire in an MF some properties that are of consequence for the biophysical systems involved. For example, Zhadin and Fesenko (1990) and also Edmonds (1993) discussed the application of the Larmor theorem to an ion bound in the calmodulin microcavity. The discussions relied heavily on the fact that the ion oscillation direction was of critical importance for the protein form, which in turn causes the enzyme activity to change. In terms of classical dynamics, the variation of the oscillation direction in AC MFs of different configurations was studied. In the context of effects to be expected, the Larmor frequency was found to be effective with perpendicular MFs. No answer was found to the question as to why the parallel configuration of the AC and DC fields can change the enzyme activity, but precisely that configuration was found earlier to be the most effective in many experiments.

The oscillators here were various microscopic-level objects, molecular groups, biological membranes, and whole organelles. It is noteworthy that neither the oscillator idea nor the collective excitation idea has led so far to some predictive mechanisms. Wu (1996) has shown that for a biological response to emerge there must be a threshold exposure time and a threshold amplitude of microwave radiation.

A further idea of overcoming a thermal factor appeals to the so-called stochastic resonance. This resonance is basically an amplification of a small signal against a background caused by energy redistribution in the signal-plus-noise spectrum. What is essential is that noise here is no hindrance but a useful asset of a system. Under stochastic resonance, relatively weak biological signals can bring about noticeable changes in the behavior of a dynamic system against the background of a wide variety of relatively strong perturbations. It is shown in Wiesenfeld and Moss (1995) that the response of mechanoreceptor cells in crayfish to an acoustic stimulus in the form of a subthreshold signal superimposed upon a Gaussian noise could be described in terms of a stochastic resonance. The phenomenon was used in Makeev (1993) and Kruglikov and Dertinger (1994) to handle the "kT problem", but real gains, around one hundred, when the signal declines in quality and coherence (McNamara and Wiesenfeld, 1989), are not enough by far to account for the biological activity of weak low-frequency MFs.

The rate of free-radical reactions varies with the strength of the DC MF (Buchachenko *et al.*, 1978). The probability for a product to be produced from two radicals that have a spin angular momentum is dependent on their total momentum, i.e., on the relative spin aligning. A DC MF affects the probability of a favorable orientation and is, thereby, able to shift the biochemical balance. At the same time, the mechanism shows no frequency selectivity. The lifetime of a radical couple before the reaction or dissociation, i.e., the time when the radical couple is sensitive to an MF, is about  $10^{-9}$  s. The couple sees a low-frequency MF as a DC field, and no resonances emerge. Therefore, to give an explanation of the multipeak dependences of the MBE on the MF variables Grundler *et al.* (1992) and Kaiser (1996) made an assumption that the magnetosensitive free-radical reaction is a part of the system described by a set of non-linear equations of chemical kinetics with bifurcations. The problems of this model group are concerned with the primary process of the action of a DC MF on the radical reaction rate. There are some physico-chemical

factors that limit the MF sensitivity of the rate to within 1%/mT, which is not enough to account for the bioeffects of weak AC MFs with an amplitude of about  $50 \mu\text{ T}$  and below.

Sometimes weak MFs feature resonance-type effects, with their natural frequencies being close to cyclotron frequencies of the ions  $\text{Ca}^{2+}$ ,  $\text{Na}^+$ , and others. Liboff (1985) assumed that it is the cyclotron resonance that underlies the phenomena observed. Various authors propounded the concept of such a resonance in magnetobiology, but it seems to have received no recognition due to the difficulties of correct physical justification. At the same time, these experiments have demonstrated the significant role played in magnetobiology by ions, especially by  $\text{Ca}^{2+}$ . It is to be noted that the coincidence of natural frequencies with cyclotron frequencies is no conclusive indication in favor of the cyclotron resonance concept in biology. For instance, *any* MBE theoretical model based on the electric-charge dynamics will be in terms of characteristic frequencies  $\Omega_c = qH/Mc$ . There is no other combination of the charge and MF variables that would have frequency dimensions.

To circumvent the hurdles of the cyclotron resonance concept assumptions were made of charged macrostructures in biological plasma, or vortices formed by ion clusters (Karnaukhov, 1994). Such targets for weak MFs are chosen because they have fairly large energies, which are comparable with  $\kappa\mathcal{I}$ . Then even a weak MF can change markedly the energy of an object that carries, for instance, a large macrocharge. To be sure, that requires a strictly defined condition: the center of mass of the object must have an angular momentum (Binhi, 1995b). It is fairly unlikely that such a motion is possible. Moreover, for a comparison of the energy of a vortex with  $\kappa\mathcal{I}$  to have a meaning, it requires a mechanism to deliver the energy of a *macroscopic* vortex to an individual degree of freedom, i.e., to a *microscopic* object, but to imagine such a mechanism would be fairly difficult. Also unclear is the nature of the molecular forces needed to support the existence and stability of such an ion cluster.

Some magnetobiological effects of a modulated MF display effectiveness bands in the frequency and amplitude of the MF. The spectra of the variations of the MBE with the MF parameters yield much information on the primary magnetoreception mechanisms. The spectra have been described using the mechanisms of the transformation of the MF signal in the context of microdynamics, classical and quantum models of the coupling of some ions by proteins (Chiabrera and Bianco, 1987; Chiabrera *et al.*, 1991; Lednev, 1991; Zhadin, 1996). The biological activity of a protein is conditioned by the presence of a respective ion in a bound state. It was also assumed that some magnetobiological effects are determined by the intensity of the transitions in the ion quantum levels, which in turn is affected by an MF. However, the parallel static and low-frequency MFs only act upon the phases of wave functions, so that they cause no transitions in Zeeman sublevels and do not change the intensities of transitions due to other factors. The population of each state remains the same irrespective of the MF variables. Nevertheless, it was found (Lednev, 1991) that some MBE have amplitude spectra similar to those in the parametric resonance effect in atomic spectroscopy (Alexandrov *et al.*, 1991),

a science that studies quantum transitions. That all has generated a number of publications (Blanchard and Blackman, 1994; Lednev, 1996; Zhadin, 1996), which, however, have failed to provide any additional support for that similarity. The authors refer to the mechanisms under discussion as ion parametric resonance.

The author has brought in the well-known phenomenon of the quantum state interference to gain an insight into the physical nature of the magnetoreception found in Binhi (1997b,c). As an MF is varied in magnitude with the orientation being unchanged, it only changes the phases of the wave functions of a charged particle. It is the interference that relates the variations in the wave function phases with the physical observables. The interference of quantum states is observed in physical measurements either for free particles, including heavy ones such as atoms, or for bound particles. In the latter case, the interference of particle states is only observed from the characteristics of the re-emitted electromagnetic field. This reduces the particles whose interference could be observed to atomic electrons. We made an original assumption that the interference of states of heavy bound particles, ions, can also be observed, using circumstantial nonphysical measurements on natural active biophysical structures. The assumption is in good agreement with experiment (Binhi, 1997b, 1998a, 1999b). The interference of bound ions can be regarded as a previously unknown physical effect, which is in principle only to be registered by biochemical or biological means. The phenomenon of interference of quantum states, which is well known in atomic spectroscopy, is concerned with coherent quantum transitions in the atom and is independent of the inner structure of the electron wave function. At the same time, it is this inner structure of the ion wave function that defines the effect of the ion interference in the protein cavity subject to a variable MF in the absence of quantum transitions. Currently, the ion interference mechanism predicts, see Chapter 4, the following multipeak biological effects:

- strength/orientation-modulated MF
- magnetic vacuum
- DC MF with natural rotations of ion–protein complexes taken into account
- pulsed MFs against the background of a parallel DC MF
- MF in the range of NMR frequencies with spin degrees of freedom of ion isotopes taken into account
- AC–DC MFs with the interference of the states of a molecular group with a fixed rotation axis (interfering molecular gyroscope) taken into account
- weak variable electric fields
- shifts of spectral peaks of the MBE under the rotation of biological specimens.

The biological effects accountable in terms of the interference mechanism have been observed in various experiments. The formulas yield the variation of the probability of the dissociation of the ion–protein complex with the MF characteristics, the frequency of the variable components, the values and mutual orientation of the DC, and variable components. The spectra characteristics and the positions of the peaks are dependent on the masses, charges, and magnetic moments of the ions

involved. Most studies have revealed that the relevant ions are those of calcium, magnesium, zinc, and hydrogen, and sometimes of potassium.

Many authors connect the biological action of an MF with changes in water states (Kislovsky, 1971; Binhi, 1992; Fesenko *et al.*, 1995; Konyukhov *et al.*, 1995). The states change owing to an action of external fields on the water and the change is passed on further to the biological level as the water gets involved in various metabolic reactions. It is not clear so far what in the liquid water can be a target for the action of an MF. It was assumed (Kislovsky, 1971) that some calcium ions in the water form hexaaquacomplexes  $[\text{Ca}(\text{H}_2\text{O})_6]^{2+}$  with octahedral coordination of water molecules, in relation to oxygen atoms. The complexes in turn form closed pentagon dodecahedrons with cavities, whose size (4.9–5.2 Å) is about the size of the complexes. That sort of provides a relative stability of the structures. An MF shifts an equilibrium so that more free calcium gets bound into complexes to influence the biological signalization. Fesenko *et al.* (1995) used the results of the studies of low-frequency spectra of water electric conductivity to look into stable water-molecular associates that possess a memory of electromagnetic exposure.

Stable structural changes in the water were observed in Lobyshev *et al.* (1995) based on the luminescence spectra. The changes were associated with the presence in the water of all sorts of defects with specific centers of irradiation.

Changes in the biological activity of the water under the action of a DC MF were found in Rai *et al.* (1994) and Pandey *et al.* (1996). The radiation of a household TV set also changed the biological activity of the water (Akimov *et al.*, 1998). When a physiological solution was preliminarily exposed for several minutes to a DC MF of several microteslas and nerve cells were then kept in it, the cells' physiological parameters changed (Ayrapetyan *et al.*, 1994). In Binhi (1992) nuclear spins of protons in the water were considered as primary targets of an MF, and the metastability was associated with orbital current states of protons in the hexagonal water-molecule rings and deviations from normal stoichiometric composition of the water. The existence of such states is testable in relatively simple experiments (Binhi, 1998b). Memory effects of the water exposed to an MF were observed in Sinitsyn *et al.* (1998) from radio-frequency spectra. They were associated with oscillations of hexagonal water-molecular ring associates. There is no consensus yet as to the nature of the memory carriers in the liquid water and their interaction with an MF.

There is an evidence, both experimental and theoretical, that warrants the hypothesis that there exist long-range fields of the changed space geometry. The scientific endeavor to geometrize physical fields is with us since the last century. The common element of novel theories, specifically of the theory by Shipov (1998), is fields, which are related with the well-known geometric property of space–time by the property of torsion. Mathematically, they are tensor fields that describe the curvature of space and the Ricci torsion, rather than the Cartan torsion, as in standard gravitational field theories. The well-known fundamental fields and their equations emerge here as some limiting cases. We will note that the theory has difficulties (e.g., Rubakov, 2000).

The presumptive fields do not change the energy of quantum systems with which they interact; they can only act on the phases of wave functions. In the process, a charged particle, such as a bound ion in the protein cavity, might react to such a field in a resonance-type manner. Therefore, one possible explanation of biological sensitivity to very weak EM fields might be concerned with the specific changes in space geometry they engender (Akimov *et al.*, 1997). It should be emphasized that this idea is for today just a hypothesis.

### 3.2 FUNDAMENTAL LIMIT OF SUSCEPTIBILITY TO EMF

The ever growing body of magnetobiological evidence indicates that an MF of less than  $10\ \mu\text{T}$  can also affect biological processes. These data, shown schematically in Fig. 3.1, are of great interest. They agree with neither of the assumed primary mechanisms of the biological action of an MF. This leads to the question of physical constraints that stem from the possible fundamental nature of the bioeffects of very weak fields.

The areas denoted by numerals in the figure are the ranges of the variables of the following fields: 1, low-frequency EMFs used in most magnetobiological experiments; 2, the EMF of magnetic storms, which are known to correlate in time with exacerbations of cardiovascular disorders; 3, background EMFs that are engendered by a wide variety of household electric appliances, TV, and computer screens; 4, an MF that causes changes in solutions of some amino acids (Novikov and Zhadin, 1994; Fesenko *et al.*, 1997); 5, MFs supposedly reemitted by the protective device Tecno AO, Tecnosphere, France, patent reg. PCT/FR93/00546, which sort of make up at the biological level for the radiation of video monitors and cellular phones (Youbicier-Simo *et al.*, 1998); 6, an EMF below the QED limit, which causes the biological reaction in a cell culture *E. coli* (Belyaev *et al.*, 1996); 7, the sensitivity limit of the human eye to an EMF within the optical range; and 8, MFs used in the treatment of some diseases (Jacobson, 1991).

The picture also shows theoretical limits concerned with various mechanisms and descriptions of the EMF bioeffects. The upper inclined line divides, approximately, the areas of thermal and nonthermal effects, the lower inclined line, the quantum-electrodynamic (QED) limit. It is natural to describe the EMF in quantum terms below that line. The stepped line — one of the well-known thresholds of safe values of the EMF — is given following the version of the American Conference of Industrial Hygiene (ACGIH) (Nakagawa, 1997). The  $kT$ - and thermal limits are well known. On the left of the dashed vertical line that separates the “paradoxical area” a quantum of EMF energy is many orders of magnitude smaller than the characteristic energy of the chemical transformations  $\sim kT$ . Many physicists who do not specialize in magnetobiology believe that such fields are unable to cause any biological reactions. Now such a view appears to be quite superficial, since there is a large body of experimental data that refute it. It is seen that virtually all electromagnetobiology falls into “paradoxical area”.

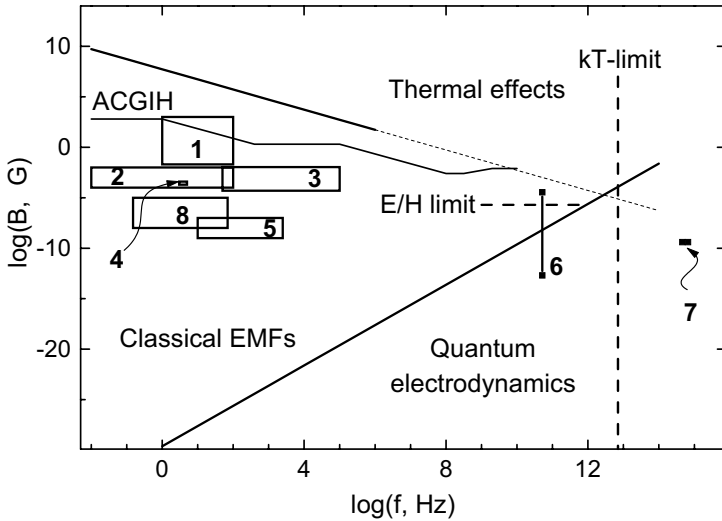


**Figure 3.1.** Shown are various limits and fields of biological effects of an EMF as a function of two variables, the EMF frequency  $f$  and the classical amplitude of its magnetic induction  $B$ . Explanation is given in the text.

The thermal limit has been repeatedly derived in fundamental and standardization works concerned with safe levels of EMF radiation, see also Section 1.4.1.

The dashed horizontal line in the range of relatively high frequencies is defined in relation to the idealization of plane waves. Below that line one can ignore the influence of the electric component of a plane wave on the dynamics of a bound particle, see Section 1.4.3.

A couple of comments are in order about the quantum-electrodynamical limit. Interactions of EMF and matter can be classed by description types, either classical or quantum, both of the field and of the matter. Most of proposed primary mechanisms use the classical description of matter particles that interact with a classical EMF, a wave field. The mechanisms that describe EMF bioeffects on the basis of the quantum description of ion particles in a classical EMF rely on a semi-classical approximation. The validity of the classical description of the EMF is conditioned by quantum electrodynamics: the population of the quantum states of the EMF oscillators must be large enough as compared with unity. This suggests the relationship that relates the frequency and the classical amplitude of the magnetic EMF component:  $H > \sqrt{\hbar c}(2\pi/c)^2 f^2$ . The lower line in the figure depicts this limit. As is seen for the low-frequency effects, unlike the superweak microwave radiation, it is possible to apply the classical description of the EMF using the Maxwell equations. In certain cases, however, we can also speak about low-frequency EMF

quanta. A semiclassical approximation could be sufficient to describe bioeffects of low-frequency MFs, but the presence of EMF bioeffects in area 6 does not rule out involvement of QED mechanisms of magnetoreception.

The quanta of the EMF seem to be related with the natural fundamental limit of the sensitivity to a low-frequency field. As with any receptor of physical nature, the natural limitation on the electromagnetic sensitivity of biosystems has to be predetermined by the general laws of quantum mechanics. All the physical limitations, as proposed to date, are based on *a priori* assumed primary mechanisms of reception, rather than on elementary physical principles. It is, therefore, of interest to obtain some estimations of the limiting sensitivity, however approximate, proceeding from the general laws of physics.

It is worth noting, first of all, that the formulation of the issue of the minimum amplitude of a variable MF registered by a receptor is not correct. The most general description of the interaction of a field and an idealized atom is in terms of the quantized EMF and the quantized oscillator. A low-frequency EMF quantum, which has been initially delocalized in an indefinitely large volume, is absorbed by an atom-like microscopic system as the field wave function is being reduced. This increases the number of excitation quanta of the atom by one. The QED limit shown in Fig. 3.1 determines approximately the boundary of the MF value, where the notion of the amplitude of a classical field is no longer valid. In the quantum description, this boundary corresponds to several excitation quanta of field oscillators.

In the general case, the receptor sensitivity can be characterized by an energy flux  $p$ , i.e., the number  $N$  of quanta  $\hbar\Omega$ , absorbed by a system during the time  $t$  of its coherent interaction with the field:

$$p = N\hbar\Omega/T .$$

However, in the range where the classical description holds well that quantity displays no unique relation to the field amplitude  $H$ , thus indicating that that notion is not applicable as a limiting sensitivity. The constraints on the value of  $p$  follows from the fundamental relation of quantum mechanics between the variations of a quantum system energy  $e$  and the time  $\tau$  required for that variation to be registered

$$e\tau > \hbar .$$

Given  $N$  registered quanta, the relation can be written as  $\tau > 1/N\Omega$ , since  $e \sim N\hbar\Omega$ . However, in any case the variation registration time cannot exceed the time of the coherent interaction of a field with an atomic system.

For a low-frequency EMF, the time of coherent interaction is basically the lifetime of the quantum state  $T$  defined by the details of the interaction with the thermostat. This gives the inequality  $T > \tau > 1/N\Omega$ , i.e.,  $T > 1/N\Omega$ , which, when substituted into the expression for  $p$ , gives a simple estimate for the limiting sensitivity

$$p > \hbar/T^2 . \tag{3.2.1}$$

The limiting sensitivity to a low-frequency EMF is thus determined by the lifetime of a quantum state of the receptor target. For instance, the spin states of protons

of liquid water “live” for several seconds. The appropriate limiting sensitivity of  $p \sim 10^{-19}$  W is close to the sensitivity limit of physical measuring instruments at ambient temperature. It is to be recalled that the limit (3.2.1) follows from the fundamental principles alone. The sensitivity of devices, including biophysical targets, is also dependent on the probability of their absorbing EMF quanta, and it seems to be markedly less and the limiting sensitivity accordingly markedly greater than (3.2.1).

It is of principle, however, that the probability for EMF quanta to be absorbed is now determined by the specific target structure. The primary principles of physics impose virtually no limitations on the limiting sensitivity. The microscopic structure of a bioreceptor and the time of its coherent interaction with an EMF control the level of sensitivity in any special case. It is important that the time of coherent interaction may be sufficiently large if the state of the living system is far from a thermal equilibrium.

### 3.2.1 Noise limits of susceptibility of biostructures to EMF

One of the phenomenological approaches to the definition of the limiting sensitivity of biosystems to an EMF postulates that an EMF biological detector of whatever nature can be regarded as an equivalent, in a way, electric circuit or a radiotechnical structure that consists of resistors and capacitors. That is convenient since the proper electric noise can then be estimated using the Nyquist formula. It is further maintained that the assumed biodetector, which does not possess any prior information on the signal being detected, is only able to record a signal that is no less than its intrinsic noise. It follows that the estimation of the sensitivity of a biological system boils down to the estimation of the level of the intrinsic noise of a detector.

In the simplest case, a biodetector has assigned to it a complex impedance  $Z(\omega)$  with an active resistance  $R = \Re(Z)$ . The spectral density of the random electromotive force (e.m.f.) will then be

$$(\epsilon^2)_\omega = 2\kappa\mathcal{T}R.$$

In this case, the validity conditions for the Nyquist formula are assumed to be met:  $\hbar\omega \ll \kappa\mathcal{T}$ ,  $\lambda \ll c/\omega$ , where  $\lambda$  is the size of the detector. It is believed that biological tissues and biophysical structures possess no internal inductive impedances. Sometimes measurements yield an inductive component due to current retardation caused by electro-chemical processes (Binhi, 1995c). The reactive impedance component is, therefore, determined by the capacitive reactance, which is inversely proportional to the frequency  $\Im(Z) = 1/\omega C$ . The effective frequency range of the detector will then be  $\Delta\omega \sim 2\pi/RC$ . The Nyquist formula gives to that range the average squared noise e.m.f. of the detector  $\epsilon^2 = 4\pi\kappa\mathcal{T}/C$ .

A hypothesis has been repeatedly voiced that the molecular target for an EMF is ion channels of biological membranes. Membranes formed by phospholipids have

a thickness of about  $d \approx 5 \cdot 10^{-7}$  cm and a permittivity of about  $\varepsilon \approx 10$ . Since the capacitance of the membrane section with a radius of about that of the ion channel  $r \approx 10^{-7}$  cm is  $C \sim \varepsilon r^2/4d$ , the noise e.m.f. divided by the membrane thickness, i.e., the noise electric field in the ion channel, will be

$$E_{\text{noise}} \sim \frac{1}{r} \sqrt{\pi \kappa T / d} \sim 3 \cdot 10^{-3} \text{ CGS units} \sim 100 \text{ V/m} .$$

It is to be recalled that a field induced by a 50-Hz, 100- $\mu$ T AC MF in a specimen of size 1 cm near the solenoid axis has an order of magnitude of 0.1 mV/m. It has also been found that biosystems exhibit some response to currents in tissues induced by fields 3–5 mV/m, and so, constraints imposed by noises do not enable a single channel to act as a receptor of weak electric fields within the framework of “radiotechnical” representation.

Formally, the inverse proportionality of  $E_{\text{noise}}$  to the size  $r$  of the membrane area warrants an assumption that a detector with a relatively larger size could be much more sensitive. There are some indications that such treatments could be linked with the estimation of the sensitivity of a hypothetical detector of a weak electric field as a large ensemble of single channels or as an isolated cell, see Astumian *et al.* (1995).

This topic is approached from another angle by Jungerman and Rosenblum (1980), who supposed that the fact that Lamelibranchia find their bearings in the geomagnetic field is conditioned by an e.m.f. induced in large (the order of the transverse dimension of a fish) circuits by changes in the magnetic flux through the circuit. Electroreceptors in fishes are highly sensitive (Brawn and Iliinsky, 1984) and could be responsible for the magnetoreception in connection with electroconductive circuits.

According to sources (Jungerman and Rosenblum, 1980), electroreceptors in rays have a resistance of  $10^5$  ohm. Suppose that the characteristic frequency associated with the ray motion, just as the effective frequency range of the electroreceptor, is about  $\omega = 10$  Hz, and the area of the conductive circuit is  $S = 10 \text{ cm}^2$ . Then, by equating the mean noise and the e.m.f.  $S\omega V/c$  induced by circuit tilts we can easily derive the relationship for the threshold sensitivity to an MF

$$B = \frac{c}{S} \sqrt{\frac{2\kappa T R}{\omega}} \sim 10 \mu\text{T} .$$

The figure is not at variance with the hypothesis that relates the magnetoreception in those fishes with the magnetic induction and electroreceptors. It also agrees with the experimental data of Kalmijn (1982).

Despite the apparently general nature of the estimations they are only applicable to mechanisms concerned with the currents flowing through a detector caused by the additional deterministic e.m.f. of a signal. If the signal modulated, for instance, only the internal resistance of a detector, there would be no detection. Also conflicting with this scheme are mechanisms in which the signal causes the chemical reaction rate to be changed: that process has no electric analogue. Also, the mechanisms

that provide amplitude windows in the MF effectiveness cannot be considered in terms of this treatment: linear electric circuits, even the most complicated ones, because of their linearity, possess selective properties only in relation to frequencies of signals, and not to their amplitudes. On the other hand, if *ad hoc* additional non-linear elements were introduced into equivalent electric structures, it would be impossible to apply the Nyquist formula. The fluctuation–dissipation theorem that underlies the Nyquist formula is limited to systems with a linear response.

We note that the very possibility of representing a biosystem as an electric circuit needs a justification. Pilla *et al.* (1994) assumed that a biological tissue can be described by a linear one-dimensional circuit of electrically connected single cells, each of which has an equivalent electric circuit of resistors. Such a circuit will, under certain conditions, overcome the noise limit beginning with fields of around 1 mV/m, but, for one thing, the reduction of a biological tissue to a one-dimensional circuit does not carry much weight. On the other hand, effects of weak electric fields are also observed at the level of cellular systems where cells are not in direct contact. There is no evidence so far that the calculated limiting sensitivity in this representation would agree not with the number but with experimental *curves*. Barnes (1998) suggested that neurons, the pyramidal cells from the cortex of the brain, be viewed as some sort of radiotechnical phased array antennas with amplifiers and filters. Such arrays would be responsible for the detection of coherent signals induced by low-frequency external fields in neuron dendrites against the background of thermal noise. However, no way of testing the hypothesis has been proposed yet. There is thus much room for the search for alternative non-linear mechanisms of bioreception of weak MFs that are not concerned with electric currents.

If we restrict ourselves to the bioeffects of an MF at the level of the geomagnetic field, then the most important in terms of fundamental physics would be two problems of equally paradoxical nature: (1) the mechanism or process of the transformation of an MF signal into a biochemical response with an energy scale  $\kappa T$  that is ten orders of magnitude larger than the MF energy quantum and (2) the question as to why thermal fluctuations of the same scale  $\kappa T$  do not destroy the above transformation process. At first glance, the paradox of the second issue is more apparent, as the “obvious” answer to the first one is to accumulate the energy of the MF signal or to amplify it. Appropriately, most effort was devoted to the second issue, the transformation mechanism being chosen almost arbitrarily. However, it is the transformation mechanism that conditions the presence of “windowed” multippeak spectra observed in experiment, and it is the transformation mechanism that is responsible for the predictive power of a model. That is why so far we have had no predictive model that would solve both problems. At the same time, some predictive models (Binhi, 1997b, 1998a; Binhi and Goldman, 2000; Binhi, 2000; Binhi *et al.*, 2001) that take care of the first problem have made their appearance. That is a significant phase that is characteristic of the state of the art in magnetobiological theoretical studies. With the models becoming more predictive, we can now work out such an important ecological factor as the bioeffects of weak MFs.

Let us now take a closer look at some of the commonest MBE mechanisms. Critique of such works, however unrewarding, seems to be a necessary exercise.

First of all, we note that there is some terminological confusion. Speaking of “cyclotron resonance in magnetobiology” authors often imply several models by Liboff, which are different in nature. These models are remembered nearly always, when they find an MBE at a cyclotron frequency  $\Omega_c$  of an MF. In so doing, they normally overlook the fact that such a combination of ion constants has to do not only with cyclotron resonance but also with a number of other effects. On the other hand, in the literature “parametric resonance in magnetobiology” is concerned not with a concrete name, but rather with the specific features of mathematical equations, so that it is concerned with a multitude of models, both classical and quantum, with and without potential forces, etc. However, we still will retain that terminology, if only because of the literature tradition, and we do believe that the reader is going to have no difficulty identifying each of the following models in terms of the objective classification proposed above. To begin with, we will consider the phenomenological models, and then we will pass on to macroscopic ones. We will then go on to look at the most promising MBE mechanisms, i.e., microscopic ones.

### 3.3 CHEMICAL-KINETICS MODELS

The equations of chemical kinetics are written for concentrations  $C_i(\mathbf{x}, t)$  of substances that enter into a reaction

$$\frac{\partial}{\partial t} C_i = d_i \nabla^2 C_i + \sum_i a_i C_i + \sum_{ik} b_{ik} C_i C_k + \dots, \quad (3.3.1)$$

where  $\nabla^2$  is the Laplacian,  $d_i$  are the diffusion coefficients for molecules or other objects of a given kind, and  $a, b, \dots$  are the coefficients determined by reaction rates, and hence by external parameters. In the general case, the coefficients may also depend on coordinates, thus representing sources and drains of reagents.

Even when we ignore the spatial distribution of reagents, the above relations, especially for biochemical systems, are complicated non-linear sets of differential equations. Such sets often offer a wide variety of solutions, oscillatory ones included, depending on the variable values and the initial conditions. The phase snapshot of such sets can include several areas of “attraction” of a dynamic point. When it gets into one such area, a system undergoes in it oscillatory movements, i.e., it resides in a dynamic equilibrium, or it seeks a stable static equilibrium. If not exposed to some external controlling actions on their parameters or variables, such systems, dubbed polystable ones, are unable to transfer into other stability regions. If a system is in a stable area close to an unstable one, i.e., it lies between the stability areas, then even minute controlling or noise perturbations are capable of “switching” a system over from one dynamic condition to another. The situation is known as bifurcation.

Provided that  $\partial C_i / \partial t = 0$ , i.e., under stationary conditions, some solutions (3.3.1) are so-called dissipative structures. Those are inhomogeneous distributions

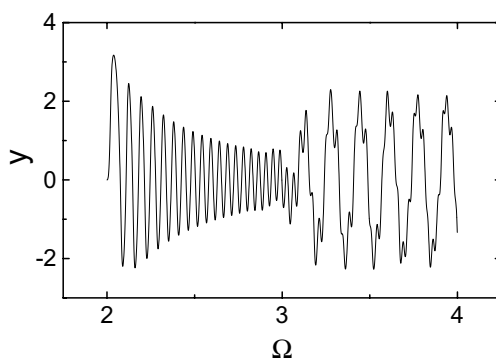


**Figure 3.2.** The bifurcation in the change of the stability of the Van der Pole oscillator with the frequency of the exciting force.

of reagent densities that occur when there are energy or mass flows through systems, which in this case are open systems. The existence of dissipative structures, some sort of patterns or spatial structures, is also controlled by a combination of parameters and can undergo some bifurcations as parameters are varied.

By way of example, Fig. 3.2 depicts the variation of the coordinates of the Van der Pole oscillator excited by an external harmonic force

$$y'' - (1 - y^2)y' + y = 10 \sin(\Omega t)$$

with the excitation frequency, which was varying smoothly in time. It is seen that there emerge qualitatively different dynamic conditions with a two-frequency spectrum at a certain value of the frequency.

At present a wide variety of applications are known for the above and similar equations describing different processes, not necessarily chemical ones. Their overview is available, for example, in the book by Prigogine (1980).

When dealing with magnetobiology, most authors rely on the assumption that an EMF is able to cause a change in the rate of one or several biochemical reactions that constitute a system under study. It is also shown that the system *can* exist in a region close to an unstable condition and that normally studied are various dynamic conditions of chemical processes, which emerge as some parameters or other are changed slightly. If the nature of the dynamic conditions turns out to be close to those observed in experiment, then that strongly suggests that the experimental system is indeed in a nonstable equilibrium, and that an EMF acts exactly on the link in the chain of biochemical transformations that has been subjected to a variation.

It is clear that the physical or biophysical processes of the primary reception of an MF fall out of the scheme. The relationship between the reaction rate, for instance, and the MF value is normally postulated as a linear dependence. It is

then possible to correlate with experiment both frequency and amplitude spectra of the response of a dynamic system to an excitation of a constant that is potentially sensitive to an EMF, but the importance of such a correlation would be questionable. The primary reception process is not prohibited to feature some frequency or amplitude selectivity. Because of that, it is unlikely to obtain a good agreement of the responses to an EMF in experiment and in models using the chemical-kinetics equations. Even when such a correspondence is available, it is fairly difficult to interpret. There are works that put forward “through” models where the primary reception process with its characteristics is built into a kinetic scheme. Grundler *et al.* (1992) and Kaiser (1996) have considered a group of such mechanisms based on the assumptions as to the properties of the primary process.

Also considered is the interaction of an MF with spatial structures in motion, such as autowaves in excitable media, e.g., spiral waves (Winfrey, 1994), which are also solutions to some special cases of Eq. (3.3.1).

Plyusnina *et al.* (1994) used the equations of chemical kinetics with special solutions to describe premembrane processes in an EMF. The model by Eichwald and Kaiser (1995) relies on experiments concerned with the influence of low-frequency fields on the cells of the immune system, specifically on T-lymphocytes. That work considers the possibility for an external field to affect the process of signal transduction between activated receptors on the cellular membrane and G-proteins. It was shown that depending on the specific combination of intracellular biochemical and external physical factors there may occur absolutely different response forms.

The number and diversity of models of that class are great. The scheme of the search for an MF target drawing on responses of non-linear systems has been realized quite consistently by Kaiser (1996) and Galvanovskis and Sandblom (1998). The latter is a study of the spectrum of intracellular oscillations of the concentration of  $\text{Ca}^{2+}$  ions caused by an external stimulus under periodic modulation of the rate of one of the intracellular reactions involving calcium. The  $\text{Ca}^{2+}$  oscillations were modeled using the set of conventional non-linear differential equations proposed in Goldbeter *et al.* (1990). It was shown that a system's response expressed as a total spectral power of the oscillations is complicated in nature and is dependent on the frequency and amplitude of the modulating signal. The frequency windows of the effect emerged in the characteristic natural frequency of oscillations ( $\sim 0.01$  Hz) and smaller windows at its harmonics. An amplitude window was also noted. The authors varied all the system parameters in order to determine the most sensitive area in the system of reactions. The reaction appeared to be the reaction of the liberation of calcium within the cell from a state bound in intracellular proteins.

We will stress the value of the chemical-kinetics models. In the process of the development and comparison of the models with experiment the most sensitive points of biochemical systems may be sought. That simplifies the search for primary mechanisms, since the potential circle of reactions sensitive to an EMF becomes more definite.

### 3.4 MODELS OF BIOLOGICAL EFFECTS OF WEAK ELECTRIC FIELDS

One of the possible scenarios of the action of a low-frequency MF on a biological system is for the MF to induce in a tissue a variable electric field. That field, in turn, causes eddy currents and electrochemical phenomena. The frequency- and amplitude-selective action of external weak variable EFs is a problem in its own right. The appropriate mechanisms are described using the chemical-kinetics equations, where some reactions are characterized by a relatively large change in the electric dipole moment, and the constants of these reactions are assumed to be dependent on the EF strength.

Normally, when assessing the action of a weak EF on a cell one proceeds from the additional potential on the surface of the cell in the EF. The models consider spherical or cylindrical dielectrics placed in an external field. It is known that the EF potential  $\mathbf{E}$  in a spherical system that coincides with the center of a dielectric sphere has the form (Landau and Lifshitz, 1960)

$$\varphi = -\mathbf{E}\mathbf{r}(1 - A/r^3) ,$$

where the constant  $A$  is found from the conditions on the boundary of the sphere. On a spherical or cylindrical surface of radius  $R$ , see Appendix 6.4,

$$\varphi_{\text{sphere}} = -\mathbf{E}\mathbf{R} \left( \frac{3\varepsilon}{2\varepsilon + \varepsilon^i} \right) , \quad \varphi_{\text{cyl}} = -\mathbf{E}\mathbf{R} \left( \frac{2\varepsilon}{\varepsilon + \varepsilon^i} \right) , \quad (3.4.1)$$

where  $\varepsilon$  and  $\varepsilon^i$  are the permittivity of the medium and of the object being modeled. Since usually  $\varepsilon \sim 80$  and  $\varepsilon^i \sim 3$ , the additional potential on the sphere is given by

$$\varphi \approx -1.5 ER \cos \theta , \quad (3.4.2)$$

which is often used in the literature, see, for instance, Weaver and Astumian (1990); the accurate data on dielectric parameters of biological cells and tissues are available in the review (Markx and Davey, 1999). In addition, the two-layer cell membrane carries a large charge, negative on the inner membrane, which creates the trans-membrane potential difference  $U_m \sim 70$  mV. It is caused by the action of membrane pump-enzymes, which push ions against their density gradient. The additional potential difference on the cell surface at points that are opposite in relation to the field direction follows from (3.4.2) and is  $3ER$ . The conductivity of the intracellular plasma is large as compared with the membrane conductivity; it is therefore assumed that the potential difference is composed only of the contributions from the opposite membrane areas. Thus the additional EF inside the membrane induced by an external field is larger than the external one by a factor of  $R/2d$ .<sup>18</sup> On the one side of the cell the transmembrane potential grows; on the

---

<sup>18</sup>This statement occurs quite often in papers on the action of an EF on biological cells, e.g., *Bioelectromagnetics*, **21**(4), 325, 2000. It is based on erroneously ignoring the thermal effects and dielectric properties of the intracellular medium. The conductivity of the cytoplasm is conditioned

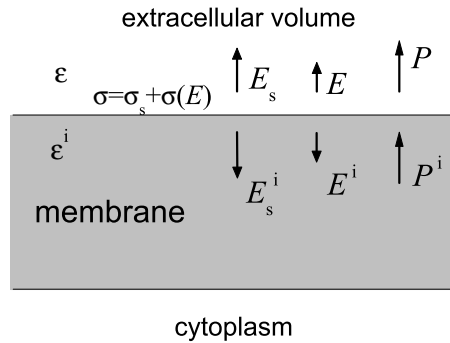


**Figure 3.3.** The fields and polarizations on the external membrane surface. The surface density of charges is formed by external and polarization charges.

other, it decreases. It can easily be worked out that the relative change for a cell of the size  $R \sim 10 \mu\text{m}$  in the field  $1 \text{ V/m}$  will be

$$\frac{3ER}{2U_m} \sim 10^{-4} . \quad (3.4.3)$$

The smallness of that quantity is also a problem in electromagnetobiology. What is not clear is how such small changes can affect membrane processes.

In actual fact, the situation is even more dramatic, since there are biological reception data for fields of about  $1 \text{ mV/m}$ . Besides, the very formula (3.4.2) is hardly valid for the evaluation of the potential changes in a void structure, since it was derived for a solid dielectric. We do not want to complicate matters by spherical symmetry, which in this case yields only the insignificant coefficient of around unity. The cell can be better modeled by a rectangular box filled with cytoplasm whose dielectric properties are similar to those of intercellular solution. On the surface of the membrane box there are external charges due to pump-proteins and also charges due to the polarization by an external electric field  $E$ . The surface density of charges induced by the field is equal to the difference of polarizations of the medium on the internal and external sides of the membrane (Landau and Lifshitz, 1960), see Fig. 3.3,

$$\sigma(E) = P^i - P .$$

Since we consider the polarization effects in a linear approximation, the polarization density of charges can be found by supposing that there are no external charges.

---

by free ions, i.e., by well-localized charge carriers. The energy of thermal scale is greater than the energy of displacement of the charge  $q$  by the cell length in an external EF not stronger than  $1 \text{ kV/m}$ :  $\kappa T \gg q\varphi$ . The thermal diffusion of free ions, therefore, prevents ion redistribution and effective field screening within the cell. It follows that the potential drops mainly due to the dielectric polarization of cytoplasm, whose conductivity can be ignored.

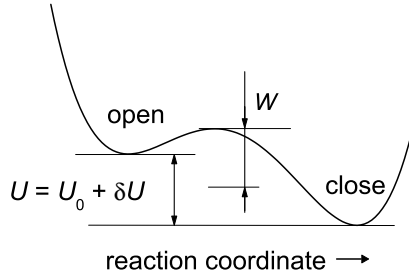


**Figure 3.4.** The dependence of the free energy of the protein channel on the generalized coordinate. Both open and closed states are stable.

In that case, on the boundary of the dielectric holds the relationship  $\varepsilon E = \varepsilon^i E^i$ . Using also the equality  $4\pi P = (\varepsilon - 1)E$  on either side of the membrane gives

$$4\pi\sigma(E) = \varepsilon^i E^i - E^i - \varepsilon E + E = (1 - \varepsilon/\varepsilon^i)E .$$

The surface charge density is related to the transmembrane potential by the relationship of the flat capacitor

$$U_m(E) = 4\pi[\sigma_s + \sigma(E)]d/\varepsilon^i ,$$

where  $d \sim 5$  nm is the biomembrane thickness. We then find the change  $\delta U_m(E)$  of the transmembrane potential in relation to its value in the absence of the field  $U_m(0) = U_m$ ,

$$\frac{\delta U_m(E)}{U_m} = \left(1 - \frac{\varepsilon}{\varepsilon^i}\right) \frac{dE}{\varepsilon^i U_m} \sim 10^{-6} ;$$

i.e., it is another two orders of magnitude smaller than (3.4.3).

- The relationship (3.4.2) was used, for example, by Astumian *et al.* (1995). They proposed a hypothetical mechanism to illustrate the action of a variable electric field on a biological cell. That mechanism possesses neither frequency nor amplitude selectivity. Anyway, we will consider the idea itself, which will help us to clarify the prospects of its use.

The membrane channels of the cell can be either in an open state or in a closed state, Fig.3.4. Such a point of view is supported by the experimental observations of the discrete variation of the conductivity of singular protein channels. In a thermodynamic equilibrium, at Boltzmann distribution, the ratio of the channel probabilities in open and closed states is

$$p \equiv p_{\text{open}}/p_{\text{close}} = \exp(U/\kappa T) . \quad (3.4.4)$$

If the external electric field causes the potential difference to vary according to

$$U = U_0 + \delta U ,$$

then the probability ratio can be represented as a series in the powers of the small parameter  $x = \delta U/U_0$ . In terms of the notation  $\beta = U_0/\kappa\mathcal{I}$ , we have

$$p(x) = e^\beta e^{\beta x} = p(0) + p'(0)x + p''x^2/2 + \dots .$$

The variation of  $p$  with time on average seems to be associated only with a term that is quadratic in  $x$ :

$$\delta p = \frac{1}{2}\beta^2 e^{\beta\overline{x^2}} .$$

The supposition consisted in that the deviation of  $p$  from an equilibrium value can result in a growth of the rate of the transfer by protein of oxidant molecules inside a cell and in an accumulation due to that of damages of DNA for a sufficiently long time.

The quantity  $U_0$  in Fig. 3.4 corresponds to the transmembrane potential of a cell with a transferable charge of several units. Then  $\delta U$  will be the change of the potential in an external electric field. As was shown above, the amplitude of the relative change of the transmembrane potential in a field 1 V/m has the order of magnitude  $10^{-6}$ . Therefore, the time average of the square  $\overline{x^2}$  is

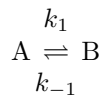
$$\overline{x^2} \sim \frac{1}{2}10^{-12} ,$$

where  $x \sim \cos \Omega t$ . On the other hand, the quantity  $\beta$  for physiological temperatures is about eight. This gives an estimate of the permanent component in the variation of  $p$  in a variable field

$$\delta p \sim 10^{-6} - 10^{-8} .$$

The smallness of that quantity questions the application of this idea. According to the authors of the idea, the specified level of the variable field could lead to a biological effect, but several idealizations in the course of the calculations markedly reduce the value of such a conclusion. The mechanism predicts a quadratic dependence of the effect with the amplitude of an electric field.

- The mechanism of the action of an EF on biological systems and cells that feature a frequency selectivity was put forward in a number of works, whose overview is given in Tsong (1992). The concept of the mechanism is as follows: if conformational states A and B of a molecule have a dipole electric moment, then the chemical equilibrium of these forms



can be shifted in an external electric field  $E$  by a van't Hoff-type equation

$$[\partial \ln K / \partial E]_{P,V,T} = \Delta M / RT, \quad (3.4.5)$$

where  $K = k_1/k_{-1}$  is an equilibrium constant,  $\Delta M$  is the difference of mole electric dipole momenta of states A and B, and  $R$  is the gas constant. This has been applied to conformational states, both active and inactive, of the enzyme of ATP-ase type, which catalyzes the reaction of the membrane transport of the substrate within the cell. The frequency selectivity is a postulate and a corollary of the correspondence of the frequency of the external field and rates of reagent relaxation. The model features no amplitude selectivity, although the review of ATP-ase reaction experiments in a strong EF of  $\sim 0.5\text{--}5\text{ kV/m}$  contained in that work attests to the presence of a maximum in the region of  $2\text{ kV/m}$ . A qualitative result obtained by computer simulation for certain combinations of some parameters that describe enzyme transport indicates that an EF can cause the pumping of the substrate through the membrane that is on average constant in time. No theoretical estimates of the magnitudes of effective fields are given. Such an estimate follows from Eq. (3.4.5), normalized to one molecule,

$$K/K_0 = \exp\left(\frac{\delta D E}{\kappa T}\right),$$

where  $\delta D$  is the difference of molecular dipole momenta at states A and B. This quantity is sometimes associated with the traveling of several elementary charges through a distance of about the membrane thickness  $d$ , i.e.,  $\delta D \sim 10ed$ . For physiological temperatures and a field  $E \sim 1\text{ kV/m}$ , we obtain  $\delta K/K_0 \sim 10^{-3}$ . This suggests that we should recognize, perhaps, the promise of that model to account for biological effects of strong electric fields. One weakness here is the inadequate predictive power of the model and the complexity of its experimental verification. Specifically, the authors did not predict the dependences of the effect on some other variations of the electromagnetic environment.

- In Tsong (1992) a further mechanism is proposed to account for the biological reception of weak (about  $\mu\text{V/m}$ ) variable EFs. The mechanism assumed that the height of the barrier  $W$  that separates active and inactive states of the membrane protein-enzyme in the Michaelis–Menten-type reaction, see Fig. 3.4, changes in sympathy with the electric field. The frequency selectivity is here postulated, and its nature is associated with the high-Q oscillations of a charged group of atoms within the protein induced by an external field. Those oscillations cause the barrier height to be modulated. It is clear that the name of the game here is not the change in the state probabilities, but rather the change of the rate of the transition between those states. According to the theory of absolute reaction rates, the rate constant for the direct and return reactions can be written as

$$k_{\pm 1} = k_0 \exp\left(-\frac{W \pm U/2}{\kappa T}\right).$$

Since the transition rate constants have a non-linear exponential dependence on the barrier height, we get a non-zero time-averaged input due to the external variable

EF. This expression is quite analogous with (3.4.4), thus suggesting that the relative change of the reaction rate has the same order of magnitude as the relative change of the equilibrium constant, i.e., also very small. The mechanism possesses no amplitude selectivity. Additionally, the quantitative estimates were based on some model assumptions. Physically, the main assumption was dubious — an external EF can be amplified by a plasma membrane so that the change of the field induced within the membrane is larger than the initial external EF by a factor of  $R_{\text{cell}}/d_{\text{membr}}$ . The use of that mechanism in the process of biological reception of weak electric fields is still questionable, since no special-purpose experiments to test the mechanism have been conducted.

- Markin *et al.* (1992) proposed the model of “electroconformational coupling”, which predicts not only the frequency window, but also the amplitude one. The model proceeds from the supposition that both the state of an ion in a membrane protein-transporter and the state of the transporter itself — open whether inside or outside — are dictated by an electric field and are thermally activated processes. The interaction of these processes causes an amplitude window to emerge. A frequency window is caused by relaxation processes, just as in Tsong (1992). An amplitude window was found in the region of 2 kV/m for (Na, K)-ATP-ase of the human erythrocytes. That is too much for the model to be applied to account for frequency- and amplitude-selective biological reception of weak electric fields, e.g., those induced in biological tissue by low-frequency MFs.

- Weaver and Astumian (1990) worked out the limiting sensitivity of a cellular system to an electric field, assuming that the EF reception is caused by some process similar to the mechanisms considered above. Such a process is determined by the transmembrane potential difference. Therefore, according to the authors, the limiting sensitivity could correspond to the noise fluctuations of the transmembrane potential difference. To evaluate those fluctuations use was made of the Nyquist formula (e.g., Lifshitz and Pitaevsky, 1978). As to the legitimacy of the usage of that formula a word is in order. The formula follows from the fluctuation–dissipation theorem for generalized susceptibilities of *linear* systems, which specifically can be the electric resistance. The current in a circuit, which is a reaction to an external electric field, is related to the field strength in a linear manner, but the main electric characteristic of the plasma membrane is its significant non-linearity. It is this property that is responsible for the emergence of a transmembrane potential, which is at the core of the processes of nervous excitability. It is to be admitted that in this case the general physical laws of linear responses were used beyond their applicability ranges. At any rate, such a dramatic idealization calls for some justification.

Other electrochemical mechanisms of the cellular reception of electric fields that are based on electrophoresis, electro-osmosis, and receptor and channel redistribution on the surface of cellular membranes are reviewed by Robinson (1985).

### 3.5 STOCHASTIC RESONANCE IN MAGNETOBIOLOGY

It is now beyond doubt that theoretical MBE models must include thermal excitations. Nevertheless, no models are in existence so far in which a consistent consideration of the influence of the thermostat would not destroy the desired effect of a weak MF. Thermal excitations of a medium behave as random forces acting on a supposed MF target, and more often than not those are charged particles. Search is going on for subtle details in the behavior of dynamic systems exposed to random forces that might be responsible for conservation and transformation of a weak MF signal to the level of a biochemical response. Actually, those works deal with the very essence of the so-called “kT problem”.

It is fairly easy to identify several areas of research in this domain where thermal noise would be considered explicitly as a stationary random process of some spectrum or other. It seems quite obvious that applications of the methods of equilibrium thermodynamics or statistical physics cannot yield appropriate results. Current studies focus mainly on dynamic systems with quasichaotic behavior.

#### 3.5.1 Stochastic resonance

Benzi *et al.* (1981) suggested that a phenomenon that consists in a relatively significant redistribution of the power spectrum of a dynamic variable of a non-linear multistable system under the action of a weak deterministic component against the background of additive noise under certain resonance-type conditions be referred to as a stochastic resonance (SR). Just like atomic parametric resonance, so a stochastic resonance is no resonance in the sense that it does not increase the response as the frequency of a controlling signal is fine-tuned to the system’s natural frequency. The analogy lies in the fact that the output signal-to-noise ratio appears to be largest as the noise level in an output signal is adjusted to some definite value.

Stochastic resonance is known to occur in systems described by first-order differential equations. For a mechanical system, that corresponds to overdamped motion, i.e., one without inertia forces. In that case, the equations contain no accelerations, and the rates of coordinate variations vary with the forces applied. For one particle, the equation becomes

$$\dot{x} = -\frac{\partial}{\partial x}U(x, t) + \sqrt{D}\xi(t) , \quad (3.5.1)$$

where  $\xi$  is a random process, which is normally taken to be  $\delta$ -correlated, with a zero mathematical expectation, and  $D$  is the dispersion of the random force on a particle. The case is well studied where the potential function  $U(x, t)$  corresponds to the motion of a particle in a double-well potential under a regular harmonic force:

$$U(x, t) = U_0 (-2x^2 + x^4) - U_1 x \cos(\Omega t) .$$

The constant part of the potential is depicted in Fig. 3.5. From (3.5.1) we get

$$\dot{x} = 4U_0x(1 - x^2) + U_1 \cos(\Omega t) + \sqrt{D}\xi(t) . \quad (3.5.2)$$

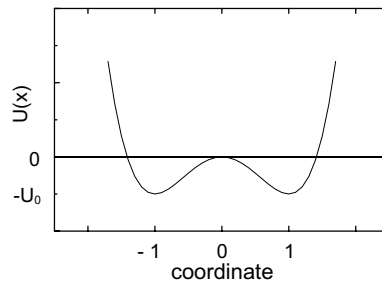


**Figure 3.5.** A simple double-well potential, which makes a dynamic system bistable.

Computer simulation of Eq. (3.5.2) for illustration purposes is not difficult. We have performed our own calculations. The equation had the following parameters:  $U_0 = 1$ ,  $U_1 = 1$ ,  $\Omega = 0.1$ . The random process  $\xi(t)$  was modeled by a sequence of normally distributed virtually uncorrelated numbers with a zero mathematical expectation and unity dispersion. The coordinates of a particle were calculated using the Runge–Kutta method at 8192 points with a time step  $\Delta t = 0.1$ . Appropriate spectra were obtained by fast Fourier transform. The amplitude of the spectral density  $S$  of the signal was obtained by averaging the height of the spectral peak at a frequency of  $\Omega = 0.1$  over six spectrum realizations. The realizations were derived by repeated computations with different input points for the random number generator.

Figure 3.6 shows the variation of the signal-to-noise ratio with the spectral noise density  $D$ . It has a local maximum at a certain noise density and is in agreement with well-known results. For instance, McNamara and Wiesenfeld (1989) carried out more detail computations: the local maximum appeared to be several times higher. Such a behavior of the curve could be easily understood, Fig. 3.7.

When a deterministic periodic force is fixed at a level that is insufficient for a particle to overcome a barrier, the particle will stay at all times within one of the potential wells, if the noise level is small, Fig. 3.7 (upper left). The amplitude of the displacement of a particle will on average be constant. As the noise intensity  $D$  goes down, the signal-to-noise ratio will obviously grow with  $D^{-1}$ , as is shown on the left part of the curve in Fig. 3.6.

As the noise intensity is increased, a particle can sometimes leap from well to well when it is shifted to the barrier by a deterministic force, and some random noise pulses appear to be sufficiently large and also oriented in the direction of the barrier, Fig. 3.7 (upper right). This gives rise to a correlation between the deterministic periodic force and random transitions of the particle from well to well. The amplitude of such displacements is seen to be much larger than that of displacements within one well. This increases the signal-correlated component in the displacement spectrum.

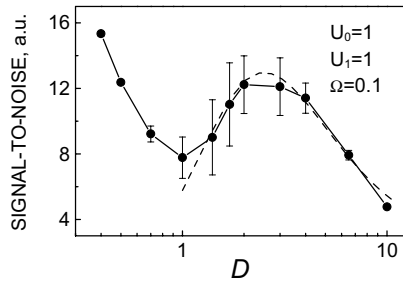


**Figure 3.6.** Signal-to-noise ratio in the spectrum of a displaced particle under a harmonic force at various noise levels. A computer simulation of the dynamics (3.5.2).

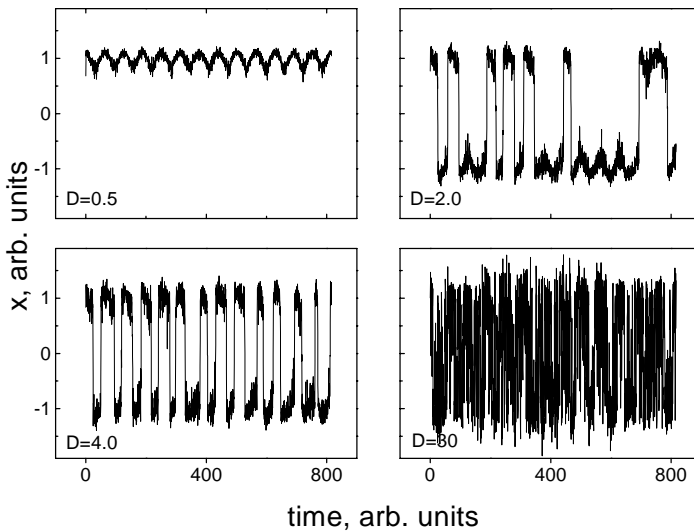


**Figure 3.7.** Displacements of a coordinate of an overdamped particle in a double-well potential under the action of a harmonic force and a random force of various levels  $D$ .

This component on average reaches a maximum at a certain (resonance) noise level, when virtually any half-cycle of the action of a regular force gives rise to a transfer of a particle from well to well, Fig. 3.7 (lower left).

Further growth of noise does not lead anymore to a noticeable increase in the mean displacement amplitude; therefore the signal-to-noise ratio again becomes inversely proportional with noise  $\propto D^{-1}$ , Fig. 3.7 (lower right). This corresponds to the right-hand side of the dependence in Fig. 3.6.

It appeared that a stochastic resonance is a more general phenomenon than is illustrated by a bistable system. Specifically, it is also observed in one well when the combined action of signal and noise, which upsets the equilibrium and exceeds some threshold, triggers some other process. One example is the firing of a neuron by the combined action of signal and mediator density fluctuation.

The middle section of the curve in Fig. 3.6, which corresponds to a situation where noise growth at the input improves the signal-to-noise ratio at a system's output, is a subject of heated debate. Stochastic resonance has been observed in artificial systems with noise, such as Schmitt trigger circuits, ring bistable lasers, and superconductive quantum interferometers, as summarized in the work by Wiesenfeld and Moss (1995). Also discussed is whether it is possible to describe some natural phenomena, specifically, biological ones, using the laws of stochastic resonance. The discussions focus on the ability of weak biological signals to bring about marked changes in the behavior of a dynamic system against the background of a wide variety of relatively intense perturbing factors — in a stochastic resonance. It was reported (Wiesenfeld and Moss, 1995) that the reaction of mechanoreceptor cells in crayfish to an acoustic stimulus in the form of a subthreshold signal against Gaussian noise obeyed a dependence similar to that in Fig. 3.6.

### 3.5.2 Possible role of stochastic resonance in MBE: “Gain”

It is believed that all sensor biosystems are threshold devices to a certain degree. Therefore, the assumption that magnetoreception of organisms is caused by, or employs, the stochastic resonance mechanism is quite justified. The effectiveness of detection of weak MF signals can be improved through the action of noise factors.

Theoretical considerations of various stochastic resonance models yields an approximate relation for the variation of signal-to-noise ratio  $R$  with the noise level  $D$  around a maximum

$$R \propto \left(\frac{U_1}{D}\right)^2 \exp\left(-2\frac{U_0}{D}\right). \quad (3.5.3)$$

The relationship is derived assuming that the output signal is only generated when a particle jumps from well to well or only on reaching some threshold. It follows that the formula gives an approximate description of the fast growth and further decline of  $R$ , dashed line in Fig. 3.6. It does not describe the rise on the left of the figure, which is of no consequence for applications. That is quite enough for analysis.

We would like to know to what extent the signal-to-noise ratio can increase with noise  $D$ . At fixed  $U_0$ ,  $U_1$ , according to (3.5.3),  $R$  has a maximum

$$R_{\max} = \left(\frac{U_1}{U_0}\right)^2 e^{-2}.$$

That maximum is attained for the *optimal* noise level

$$D = U_0 . \quad (3.5.4)$$

As  $D$  decreases, the signal-to-noise ratio drops theoretically to 0:

$$R_{\min} = \lim_{D \rightarrow 0} R = 0 .$$

It would seem that we can get an arbitrarily large “gain” of the signal  $K = R_{\max}/R_{\min}$  due to noise, but that is not the case for the following reasons.

For small noise  $D$ , the probability of well-to-well transitions  $W$  becomes exponentially small. It is exactly this that yields arbitrarily small values of  $R$ . At the same time, to observe such rare transitions requires exponentially large times. That is why small values of  $D$  are of no practical significance. A reasonable estimate of real gain  $K$  can be obtained from the relation for the mean time of the first crossing of a barrier (Cramer, 1946)

$$\tau = W_{-1} = \exp\left(\frac{2U_0}{D}\right) , \quad (3.5.5)$$

where  $\tau$  is dimensionless and expressed in units of system relaxation time scale. The quantities  $U_0$ ,  $D$ , and  $U_1$ , as was already assumed in writing Eq. (3.5.2), are dimensionless as well.

We suppose that a biological receptor senses a subthreshold signal at a certain optimal noise level  $D' = U_0$  during the time  $t(D')$ . Let, for instance, it be such that  $N$  intersections are needed for the receptor to respond after the appearance of a signal

$$t(D') = N\tau(D') .$$

At a lower noise level  $D''$ , under ideal conditions, it would take the receptor more time  $t(D'') = N\tau(D'')$  to sense a signal. We should consider that the physiological or biochemical readiness of the receptor to sense the signal is only retained during some characteristic time  $T$ . If  $T < t(D'')$ , it will be impossible in experiment to detect a signal at a given noise level. Accordingly, there will be no estimating the signal-to-noise ratio as well. The receptor “lifetime”  $T$  will thus determine the lower noise boundary in experiment, when the signal-to-noise ratio still has some meaning. To arrive at some estimates we will assume that the receptor lifetime  $T$  is  $n$  orders of magnitudes longer than the time of its optimal reaction  $t(D')$ , i.e., for  $D' = U_0$ . It follows immediately that

$$\frac{\tau(D'')}{\tau(D')} = 10^n . \quad (3.5.6)$$

Using (3.5.3) and (3.5.5), we can write the relation for the maximum gain

$$K = \frac{R(D')}{R(D'')} = \left(\frac{\ln \tau(D')}{\ln \tau(D'')}\right)^2 \frac{\tau(D'')}{\tau(D')} .$$

Considering (3.5.6) and  $\tau(D') = \tau(U_0) = e^2$ , we will write the last equality as

$$K = \left( \frac{\ln \tau(D')}{\ln \tau(D') + n \ln 10} \right)^2 10^n = \frac{10^n}{(1 + 1.15n)^2}. \quad (3.5.7)$$

It follows that if, for example, the lifetime of a receptor is longer than the time of its reaction to  $n = 1, 2, 3$ , or is about 4 orders of magnitude, then the largest gain will be about  $K \approx 2, 9, 50$ , and 320, respectively. In decibels<sup>19</sup> these quantities are 3, 9.5, 17, and 25.

We note that during the receptor lifetime all the biochemical conditions that support the reaction are maintained. Homeostasis in the organism, i.e., a status where all of its functions, composition, etc., remain relatively unchanged, only occurs as a *dynamic* equilibrium. Therefore, it is safe to say that whereas some receptors are destroyed by metabolic processes or discontinue their operations, other just emerge. Considering that for most receptors the reaction time is a fraction of a second, the quantity  $n$  that is not higher than  $n = 3-4$  looks quite plausible; in such a case, the receptor lifetime would be a matter of minutes.

Experiments, however, yield slightly smaller gains. Signal-to-noise vs noise dependences derived from the results of pertinent experiments and numerical models of stochastic resonance show the following (data are given in McNamara and Wiesenfeld (1989) and Wiesenfeld and Moss (1995); they summarize the results of several studies). In a ring laser the gain was 11 dB; in an experiment with mechanoreceptor in crayfish, 6 dB; in computer models of the double-well potential, 4 dB, of the neuron, 7 dB, of SQUID,<sup>20</sup> 12 dB; of the trigger, 10 dB. In our own two-well model we obtain a gain of 1.5, i.e., about 2 dB, Fig. 3.6. This implies that in most studies performed so far the noise caused the signal-to-noise ratio to increase on average only by an order of magnitude. To reveal larger gains under the action of noise requires a possibility of putting the noise down and increasing observation times. That possibility is not always available in real experiments.

### 3.5.3 Constraints on the value of detectable signal

After amplification, the signal-to-noise ratio must clearly be no less than unity, approximately. Otherwise, we should look for another system with another level of organization, which would ensure that the signal be isolated from noise.

There are some constraints imposed on the value of a deterministic signal  $U_1$  to be “amplified”. On the one hand, the signal has to be not very large. Otherwise, the signal, irrespective of noise, will be large enough for a particle to get through a barrier. This occurs when the potential at the maximum signal

$$U(x) = U_0(-2x^2 + x^4) - U_1x$$

has only one extremum, a minimum. That is, the equation  $U'_x = 0$  only has one solution. Hence it easily follows that the upper boundary of the amplified signal is  $U_1 = 8U_0/3\sqrt{3}$ .

<sup>19</sup>A decibel, dB, is one tenth of the decimal logarithm of the ratio of two quantities.

<sup>20</sup>SQUID — superconductive quantum interference device.

On the other hand, for a weak signal to be detected against a noise background requires that it be “accumulated” during some time. In numerical simulations, for instance, that implies averaging over many, say  $m$ , realizations of output signal spectra, when the noise wing of the spectrum irons out and the  $\delta$ -like peak of the signal in the spectrum becomes apparent. The same occurs when the time span of an observation of a random (ergodic) system is increased by a factor of  $m$ . As was mentioned above, in experiment or in a biosystem, that time  $T$  is limited for some considerations. That imposes some constraints on the value of the weakest detectable signal.

The following considerations lead to rough estimates of a barely detectable signal, which are still sufficient for our purposes. In the presence of a signal, the Cramer’s time becomes<sup>21</sup>

$$\tau \propto \exp [2(U_0 + U_1 \cos \Omega t)/D] .$$

Changes in the Cramer’s time, i.e., the difference  $\Delta\tau$  of quantities  $\tau(U_0) \sim \exp[2U_0/D]$  and  $\tau(U_0 + U_1) \sim \exp[2(U_0 + U_1)/D]$ , make a signal detectable. That difference is only made apparent when a system passes from well to well. For the difference, i.e., a signal, to be apparent, it should be reproduced a sufficient number of times, say, in  $n$  transitions, and  $n\Delta\tau$  should correspond to the characteristic scale of the process, i.e.,  $n[\tau(U_0 + U_1) - \tau(U_0)] = \tau(U_0)$ . Hence

$$n \frac{d\tau(U_0)}{dU_0} U_1 = \tau(U_0) , \quad \text{that is, } U_1 = \frac{D}{2n} .$$

For a weak signal to be detected requires a sufficient number  $n$  of transitions to be accumulated, but it is limited by the receptor lifetime  $n\tau(U_0) < T$ . This yields a boundary for detectable signals in the optimal noise range  $D = U_0$ ,  $U_1 \sim U_0\tau(U_0)/2T$ . Detectable signals thus fall into the range

$$\frac{D\tau(D)}{T} \lesssim U_1 \lesssim D . \quad (3.5.8)$$

In terms of the concepts of bioreceptor lifetime laid down above, for a signal to be just detectable, it could be  $(10^{-1}-10^{-4})D$ . Recall that corresponding to the signal levels  $U_1 \sim D \sim U_0$  is the maximum signal-to-noise ratio.

### 3.5.3.1 SR and microparticles

A further limiting factor is noteworthy. A stochastic resonance is observed in dynamic systems described by first-order differential equations. That means that a particle that is a supposed target for an MF is overdamped; i.e., the forces of “viscous friction” must be larger by far than inertia forces. For a microparticle such friction occurs on the same degrees of freedom of the ambient environment as does

---

<sup>21</sup>That holds true if a signal varies rather slowly and does not disturb the transition statistics (adiabatic approximation), i.e., if the frequency  $\Omega$  is smaller than the inverse relaxation time of a system.

thermal noise. It is not consistent, however, to repeatedly take into consideration one and the same factor, i.e., the random displacement of particles that interact with a target, both as phenomenological damping and as a perturbing force. A change over to quantum dynamics will then offer no new possibilities for a microparticle. The particle Hamiltonian includes inertia forces — terms that include operators of double differentiation with respect to coordinates. Introducing damping needed for a stochastic resonance to occur is fraught with the same difficulties as in classical dynamics. Even for spin degrees of freedom, whose Hamiltonians contain no differentiation with respect to spatial coordinates at all, the situation does not change. The dynamic equations in that case are first-order equations, but they are written for a complex function and are in a way counterparts of second-order equations for a real function. Thus here damping for the stochastic resonance model will have to be introduced as well, but the forces that cause spin relaxation will again look like thermal perturbations.

A way out could be to assert that a random external force has the same physical nature as a signal; i.e., it is electromagnetic. However, we have already seen that input signal and noise should be similar, so that the resonance mechanism would work for a unity signal-to-noise ratio. The problem of the biological detecting of a weak electromagnetic signal would then boil down to the problem of detecting a weak sum of electromagnetic signal and noise, which would definitely give us no clues. The difficulty of applying the stochastic resonance mechanism to a microparticle consists in that there are no sufficient grounds for writing appropriate equations.

It follows that the idea of stochastic resonance as applied to a microparticle, a potential target for an MF, appears to be unlikely for the following reasons:

- the “gain” of a signal at stochastic resonance is far from  $10^{10}$ , a value required to account for MBEs in the low-frequency range,
- the amplitude of magnetic signals is far from the expected level of noise perturbations of a particle; a stochastic resonance could, however, manifest itself only when such a correspondence is available,
- it is difficult to justify the writing of corresponding dynamic equations for a microparticle.

### 3.5.4 SR in chemical reactions

Bezrukov and Vodyanoy (1997b) have shown that a stochastic resonance can also occur in physico-chemical and other systems controlled by thermal transitions through an activation barrier. The reaction rate for such systems, which is proportional to the Boltzmann factor, is approximately described by the empirical Arrhenius equation

$$k \sim a \exp(-U/\kappa T) ,$$

where  $a$  is a constant and  $U$  is the so-called activation energy. The theory of activation complex (e.g., Glasstone *et al.*, 1941) has shown that  $U$  is mainly the height of

a potential barrier that separates the states of reagents from those of reaction products. In a number of cases, the barrier height depends on an external parameter. For instance, when a transition through a barrier is accompanied by a displacement of the effective charge  $q$ , the barrier height is dependent on the strength of the electric field  $E$ . The reaction rate will then be written as

$$k = k_0 \exp(dE/\kappa T) , \quad (3.5.9)$$

where  $k_0$  is the reaction rate in the absence of the field  $E$  and  $d$  is the dipole moment of the transition. The rates  $k$  have the meaning of time-averaged quantities measured in experiment. For microtimes, a chemical reaction is a sequence of separate random events, elementary acts of a chemical reaction. Such a sequence is described by the Poisson flux. In the case under consideration the statistical parameter of the flux, which is its density, is modulated by an external field. In Bezrukov and Vodyanoy (1997b) the flux spectrum was studied for the case where an external field was an additive mix of noise and weak low-frequency signal:

$$E(t) = E_N(t) + E_S \sin(2\pi f_S t) , \quad E_S \ll E_N .$$

In the absence of a control field  $E$ , the spectral density is close to the uniform density of white noise. The length of the unity event pulse  $\tau$  predetermines the upper boundary  $f_c$  of that spectrum. In the presence of a control field, the spectrum displays a low-frequency discrete component that varies with  $\delta(f - f_S)$ . The authors introduce a signal-to-noise ratio  $R$  as the ratio of the amplitude of a discrete component to the intensity of the continuous spectrum in a certain narrow frequency interval  $\Delta f$  of the discriminator near  $f_S$ . The signal-to-noise ratio appears to be dependent on noise dispersion in the control field  $D = \langle E_N^2(t) \rangle$ , where the brackets imply averaging over the ensemble. The calculated relative quantity  $R$  will be

$$R(D)/R(0) = \left[ \exp(-D/2) + \frac{k_0}{f_c} \frac{D}{2} \sum_1^{\infty} \frac{D^{n-1}}{n! n} \right]^{-1} . \quad (3.5.10)$$

Here  $R(0) = E_S^2 k_0 / 4 \Delta f$  is the initial signal-to-noise ratio. The variation of the ratio  $k_0/f_c = 10^{-2}$  is plotted in Fig. 3.8; it shows that signal-to-noise ratio is amplified by a factor of 4 as the noise intensity is increased from 1 to 2.

The very fact of such a behavior of a non-dynamic system is of interest. However, any attempts to apply the formulas to real chemical systems are difficult. After an amplification the absolute value of  $R$  is thought to be close to unity. It can be easily found that under these conditions we have

$$E_S^2 f_c / \Delta f \approx 100 ;$$

i.e., by narrowing down the frequency range of the discriminator we can have  $R = 1$  at the output for an arbitrarily small input signal  $E_S$  at the input. Physically, that result is doubtful, since range narrowing is bound to increase the time to signal

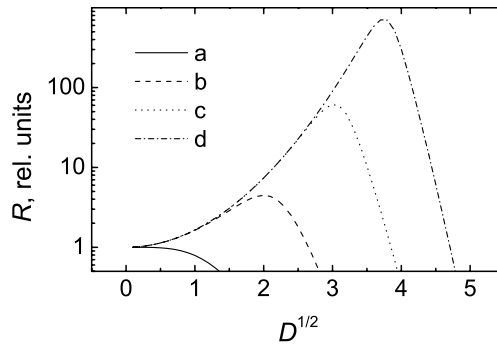


**Figure 3.8.** Variation of signal-to-noise ratio with noise intensity at  $k_0/f_c = 1$  (a),  $10^{-2}$  (b),  $10^{-5}$  (c), and  $10^{-8}$  (d).

detection, but the times of life and workable state of biological receptors are limited. It is also seen in Fig. 3.8 that the gain  $R$  can be arbitrarily large for fairly short ( $f_c = 1/2\pi\tau$ ) pulses or pulses with a low repetition rate ( $k_0$ ). That result is non-physical as well. Difficulties associated with the model seem to be concerned with an excessive mathematical idealization in describing a physical system.

To work out the Fourier spectrum of the flux of reaction unit acts calls for a wide variety of realizations both for a random Poisson process at  $E = 0$  and for the noise process in the controlling voltage. Owing to those abstractions a discrete spectrum component makes its appearance at the frequency of an input signal. A representation of the output signal as a  $\delta$ -component of the spectral density is quite graphical mathematically, but quite inadequate under real-life conditions. Any real-life system, living and man-made alike, has to detect an output signal using only one realization, which is limited in time at that. The Fourier integral for a process of a finite length  $\theta$ , however, contains no discrete components. A peak at the signal frequency acquires some broadening. That fact to a large degree invalidates the reasoning about gain at stochastic resonance.

The stochastic resonance per se is no detector or discriminator. After a SR has occurred in a biological detector a discrimination system is required, which can “make a decision” as to whether a signal is present in noise. For the discriminator, the signal-to-noise ratio is not the only parameter of significance. Another, no less important, parameter to define the quality of a signal is its coherence. A coherent signal in an additive mix with noise can be found using phase detection, i.e., accumulation of phased realizations: the signal power will then vary with the observation time  $T$ , and the noise power only with  $\sqrt{T}$ . A moment comes when the signal-to-noise ratio becomes larger than 1, and the discriminator works.

Signal-to-noise gain under SR is achieved due to the broadening of a signal spectral line. That is easily seen in Fig. 3.9. The signal power in the range  $\Delta f$ , i.e.,

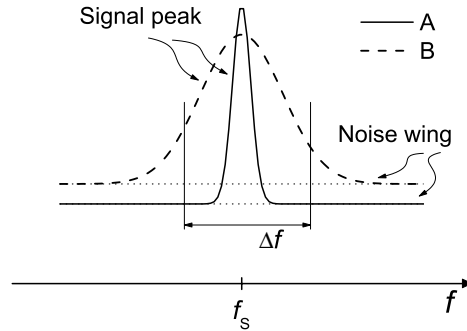


**Figure 3.9.** The spectral density of signal and noise outside of SR - A; and under SR - B.

the area between the signal curve and the noise wing, grows faster with noise under SR than the power of the noise itself. The broadening of the signal component in the spectrum mix implies that the signal is not coherent anymore. Information about the signal phase is lost during the autocorrelation time  $\tau_a$ ; therefore the signal accumulation time decreases. The discriminator has to make its decision drawing on less information; hence the probability of correct detection drops and the probability of false firing without signal goes up. Thus, this strongly suggests that as noise under SR grows, despite the fact that the signal-to-noise ratio improves, the probability of true detection of a signal falls off monotonously. This agrees with common sense: an added noise does not improve the reliability of signal detection.

Equation (3.5.9) is a graphic indication of the fact that a control field must be sufficiently large for any changes to become noticeable:

$$dE \sim \kappa T .$$

With simple chemical reactions in most cases a charge about the electron charge  $e$  travels a distance of several angstroms. The dipole moment of the transfer will therefore be about  $d \sim 10$  D, and so the electric field that markedly changes the barrier height has to be about  $10^8$  V/m. In other words, the idea of SR holds no promise as applied to simple chemical processes. According to sources, in some proteins controlling the transport of ions through ion channels, an effective charge of about  $10e$  is transported across a distance of the membrane thickness  $\sim 5$  nm, see Section 3.4. Since the required electric field is comparable with the field within the biomembrane, a SR could occur in principle, but no reliable experimental evidence is available so far. However, even if an SR does appear, it was shown above that it is not necessarily concerned with an improvement in the signal detection situation.

We have considered some general constraints on the applicability of the SR idea in magnetobiology. About ten publications are available that suggest and consider various biophysical systems under SR. We will only cite some of them without much

detail, since the difficulties and the range of validity of SR in those works have not been resolved.

- The possible role of stochastic resonance in MBEs was discussed by Makeev (1993), Kruglikov and Dertinger (1994), and Bezrukov and Vodyanoy (1997a) as applied to the conductivity of potential-dependent ion channels.
- The stochastic resonance as applied to oscillatory  $\text{Ca}^{2+}$  biochemical processes near biological membranes was studied by Kaiser (1996); the biochemical model of calcium oscillations was developed earlier in Goldbeter *et al.* (1990) and Eichwald and Kaiser (1995). In the set of chemical-kinetics equations a link that can be dependent on an MF was found. At the same time, the primary mechanism for the action of an MF on the rate of that reaction has not been considered. Also, no calculations of the dependence of observables on MF variables have been conducted.
- Semm and Beason (1990) report that amplitude modulation of the geomagnetic field by a 0.5-Hz sine signal with an amplitude of  $2.5 \mu\text{T}$  causes spike activity of a ganglion nerve cell to fire simultaneously with MF maxima. The authors assumed that biomagnetite crystals contribute to the formation of a cell response. In such a case, the stochastic resonance mechanism is quite suitable for accounting for the effect. Thermal fluctuations of a crystal bring about spikes at random moments of time, and the superposition of a weak harmonious signal synchronizes the appearance of spikes.

The idea of stochastic resonance somewhat improves the situation with possible explanations for MBEs, but not to the extent sufficient for the problem to be solved. It is possible that the idea that a variable MF signal has to be “amplified” because of its energy quantum being small as compared with  $\kappa\mathcal{T}$  is no good in principle as an account for the primary MBE mechanism. Moreover, even if a stochastic resonance does occur in one system or another, that gives rise to a further question. Does nature here employ an SR for its natural purposes, or rather is the phenomenon no more than just an epiphenomenon?

### 3.6 MACROSCOPIC MODELS

#### 3.6.1 Orientational effects

All the substances feature magnetic properties to some degree or other. Diamagnetics and paramagnetics are magnetizeable; i.e., they acquire a magnetic moment in an external MF. Ferromagnetic materials possess spontaneous magnetism. In both cases, the magnetic moment  $\boldsymbol{\mu}$  of a magnetized particle in an external MF  $\mathbf{H}$  produces a torque

$$m = \frac{d}{d\varphi}(-\boldsymbol{\mu} \mathbf{H}) \quad \mathbf{m} = \boldsymbol{\mu} \times \mathbf{H} ,$$

which tends to bring the particle into a state with the lowest energy. That is stopped by the random forces of thermal excitations of a medium. Under certain conditions,

where magnetic forces on a rotational degree of freedom impart to it an energy of about the mean energy of thermal fluctuations per degree of freedom  $\kappa T/2$ , the orientation of such particles in the medium will no longer be chaotic. A sense of predominant orientation appears, which in principle could produce a biological response, if the particles being oriented would somehow be included into the metabolic system of an organism.

### 3.6.1.1 Orientation of diamagnetic molecules

Minimal magnetic properties are inherent in diamagnetics. Their acquired magnetic moment points mainly counter the MF. Classed with diamagnetics are substances that do not possess any other, stronger forms of magnetism — either spin paramagnetism or ferro- or ferrimagnetism. Virtually all the substances that make up living tissues, specifically, molecules of water, fats, proteins, and hydrocarbons, are diamagnetic in their principal state.

Diamagnetism stems from the quantum properties of molecules. The electron clouds that surround the nucleus of an atom or a molecule are some circular areas of higher electric conductivity. When the MF flux through such areas grows, an electric current is induced in them, which produces an oppositely directed MF that reduces the external flux.

The very existence of diamagnetism, that common phenomenon, often suggests the question of whether it can underlie at least some of the magnetobiological effects.

Let us consider a charge  $q$  of mass  $M$  in a “box” of size  $a$ . The energy of a moment in an external field is  $\varepsilon = -\boldsymbol{\mu} \cdot \mathbf{H}$ . A simplifying assumption is that the moment induced by the external field is parallel with it. Then the magnetic moment in an  $n$ th state could be found  $\mu_n = -\partial\varepsilon_n/\partial H$ . The induced magnetic moment of the atom is not quantified and can be arbitrarily small. It is the magnetic moment of a closed system that is quantified. In this case, the system consists of an atom and a source of an external MF.

We arrive at the thermal-equilibrium value of the magnetic moment by averaging with the Boltzmann distribution  $f_n$ :  $\mu = \sum_n f_n \mu_n$ . However, the electrons at room temperature are most probably at a ground state. We will take this into consideration. Moreover, the electrons often fill up the inner shells, and the valence bonds are formed by electron couples with zero total spin. To illustrate diamagnetism, it is thus sufficient to have the model of a particle at a ground state (zero orbital momentum) with zero spin. That state is not subject to Zeeman splitting in a magnetic field.

A measure of diamagnetism is the proportionality factor between the induced magnetic moment  $\mathbf{I}$  of a unit volume of matter, in our case  $I \approx \mu/a^3$ , with the external field, i.e., the magnetic susceptibility

$$\chi = \frac{\partial I}{\partial H} = -\frac{1}{a^3} \frac{\partial^2 \varepsilon}{\partial H^2}. \quad (3.6.1)$$

It is possible to estimate the value if we know the Hamiltonian of a system, e.g., (4.1.1), where the Zeeman term must be omitted. The correction to the energy of

the ground state in terms of perturbation theory will then be

$$\varepsilon = \langle \psi | \frac{q^2}{8Mc^2} (\mathbf{H} \times \mathbf{r})^2 | \psi \rangle = \frac{q^2 H^2}{8Mc^2} \langle \psi | (x^2 + y^2) | \psi \rangle, \quad (3.6.2)$$

where the DC MF is aligned with the  $z$  axis. In that expression  $q$  and  $M$  are, of course, the charge and mass of an electron. For axially symmetric atoms  $\langle \psi | x^2 | \psi \rangle = \langle \psi | y^2 | \psi \rangle = \langle \psi | r^2 | \psi \rangle / 3$ . In a real atom, in the general case, many electrons occupy their states within the same volume. The expression has to be summed up over all the electrons. It is clear, however, that the greatest contribution is made by valence electrons with the largest mean orbit size; in our model that is the box size. If we denote the mean squared radius of the atom in the  $xy$  plane as  $\langle \psi | r^2 | \psi \rangle = \langle r^2 \rangle$ , we obtain by substituting the Langevin formula for the diamagnetic susceptibility

$$\chi = -\frac{q^2}{6aMc^2} \langle (r/a)^2 \rangle.$$

The quantity in brackets is clearly around unity. On the other hand, the atomic size  $a$  is about the Bohr radius  $a \sim \hbar^2/Mq^2$ . It follows that the diamagnetic susceptibility will approximately be

$$\chi \sim \alpha^2/6 \sim 10^{-5},$$

where  $\alpha = q^2/c\hbar = 137^{-1}$  is the fine structure constant.

The additional energy acquired by a molecule in a magnetic field thus varies with the diamagnetic susceptibility. Molecular electron shells do not show spherical symmetry. This manifests itself as some anisotropy of diamagnetic susceptibility, i.e., its dependence on the mutual alignment of molecule and MF. The energy correction is always positive, as follows from (3.6.1),

$$\varepsilon = -\chi a^3 H^2/2 \sim \langle r^2 \rangle.$$

It is minimal for molecules with electron shells aligned with the field. At a thermodynamic equilibrium there are more such aligned molecules, which amounts to the appearance of an aligning torque when an MF appears or changes. The probability density for a diamagnetic molecule at an angle  $\varphi$  to the MF varies with the Boltzmann factor

$$\beta = \exp(\chi(\varphi) a^3 H^2/2\kappa T) \sim \exp(-\varepsilon(\varphi)/\kappa T),$$

which for low-atomic molecules is very nearly unity. This implies that the molecules are oriented in all directions with equal probability.

However, the energy of a polymer-type molecular structure made up of similarly aligned anisotropic molecules grows with the polymer size in proportionality to the number  $N$  of the molecules. Thus the degree of the alignment of such rigid structures that possess the same number of rotational degrees of freedom is given by the factor

$$\beta^N \sim 1 + N\varepsilon/\kappa T.$$

Therefore, for fairly large and rigid stacks,  $N \sim 10^5$ – $10^{10}$ , the diamagnetic alignment becomes significant.

Kuznetsov and Vanag (1987) have considered a wide variety of forms of ordered molecular structures of similarly aligned anisotropic molecules to come to the conclusion that fields stronger than 1–10 T could produce a marked alignment, and hence a biological response. To be sure, the mechanism for the orientation of diamagnetic molecules and their complexes cannot account for the biological effects of weak MFs.

In a weak MF, the paramagnetic susceptibility of radicals, i.e., molecules with uncoupled valence electron, is small as well (Ashcroft and Mermin, 1976),

$$\chi \sim \mu_{\text{B}}^2 / a^3 kT < 10^{-3} ,$$

where  $\mu_{\text{B}}$  is the Bohr magneton. Such molecules form no ordered complexes. Therefore, their spin paramagnetism, which is three orders of magnitude stronger than diamagnetism, supplies no physical justification for the magnetoreception of weak MFs. Dorfman (1971) addressed the pulling of diamagnetic and paramagnetic molecules into the area of a stronger field in nonhomogeneous MFs, and found that the effect could have some biological consequences in fields of around 0.1–1 T.

It is common knowledge that in some aromatic substances a residual magnetization can occur that is associated with the fact that  $\pi$ -electrons of the molecular rings of aromatic substances produce circular currents that are able to catch a magnetic flux like that in the Meissner effect in superconductive rings. Such substances, upon special treatment, behave like paramagnetic substances (Pohl and Pollock, 1986), and in the crystalline form they display a constant magnetic moment of around  $10^{-4} \mu_{\text{B}}$  per molecule (Tolstoi and Spartakov, 1990). A minute effect, it can hardly be of use in magnetoreception mechanisms.

### 3.6.1.2 Biomagnetite in a magnetic field

There is one group of macroscopic models, or rather one idea, that is being addressed by many authors. It relies on the presence in a multicellular living organism of crystals of a ferromagnetic compound, known as magnetite. In a DC MF such a crystal is exposed to a significant rotational moment, which is many orders of magnitude larger than that in diamagnetic substances. It can therefore exert some pressure on a near-by receptor (Pasechnik, 1985; Kirschvink *et al.*, 1992). In all probability, such a mechanism does exist. Magnetite crystals have been found in the brain of some birds, which are known to feature a striking ability to take their bearings in the geomagnetic field (Walcott *et al.*, 1979; Kirschvink *et al.*, 1985; Beason and Brennan, 1986; Wiltschko *et al.*, 1986). Such crystals are also found in some insects (Gould *et al.*, 1978, 1980) and bacteria (Blakemore, 1975; Frankel *et al.*, 1979).

At the same time, such a magnetoreception mechanism is in a class by itself, and is no answer to the main problem of magnetobiology. After all, unicellular organisms that contain no magnetite are also able to sense an MF. The main task of magnetobiology is exactly to account for that phenomenon, which is a paradox in terms of classical physics.

- Kobayashi *et al.* (1995) suggested a mechanism to account for the biological action of low-frequency MFs on cells *in vitro* in the presence of ferromagnetic contaminants. Magnetic contaminants are available not only in the ambient dust, but they are also adsorbed by the surfaces of laboratory equipment; they enter into the composition of plastics and glasses, laboratory chemical preparations, and water. Their mean particle size is about  $10^{-5}$  cm, and they consist of ferro- and ferrimagnetic substances; that is, they display spontaneous magnetization. The saturation magnetic induction varies within  $4\pi J_s = 500\text{--}7000$  G.

The authors have shown that routine laboratory procedures of pouring and rinsing enrich cellular cultures *in vitro* with magnetic particles, these latter outnumbering the cells dozens of times. The magnetic particle energy  $V$  in a magnetic field of  $H = 0.5$  G will be about  $\varepsilon_p = 4\pi J_s V H \sim 10^{-11}$  erg; i.e., it is larger than  $\kappa\mathcal{T}$  by three orders of magnitude. The authors believe that such a particle, when adsorbed on the cellular surface, can transfer its energy to neighboring cellular structures, e.g., to mechanically activated ion channels.

The problem is concerned with the fact that the magnetic particle energy being much larger than  $\kappa\mathcal{T}$  provides no explanation for the effect. That energy should be somehow transferred to the molecular level. A transfer of kinetic energy is impossible because the particle and the molecule have different sizes and masses. For a molecule with thermal velocity  $v_m$  the particle is a kind of wall that travels at  $v_p \sim \sqrt{2\varepsilon/M_p}$ . It can be easily found that upon a collision the molecular velocity cannot increase by more than  $2v_p$ . The relative increase in the molecular energy will be no more than  $4v_p/v_m$ . Substituting the velocities estimated from the respective energies and the masses of the magnetic particle and the molecule gives

$$\frac{\Delta\varepsilon}{\varepsilon} \sim 100 \sqrt{\frac{M_m}{M_p}} \ll 1 .$$

This suggests that even if we can talk about some mechanism that makes use of the energy of the magnetic moment of a magnetic particle, it will be rather realized through the pressure exerted by the particle on the surrounding tissue, i.e., through a transfer of potential energy. The energy will then be transferred to a large number of molecules, so that each will receive an energy that is small in comparison with  $\kappa\mathcal{T}$ . Here we will need detailed calculations.

The mechanism holds well to explain the reception of a DC FM, but for variable fields it is dubious. The natural frequencies of the oscillations of a magnetic particle introduced into an elastic tissue lie much higher than the low-frequency range. Therefore, it would hardly be possible to explain low-frequency efficiency windows, let alone amplitude ones, using that mechanism.

- Edmonds (1996) addressed the possibility of utilizing the magnetic properties of suspensions of nematic liquid crystals and magnetite microcrystals in the magnetic compass orientation of birds. In an idealized model situation, a nematic suspension with filamentary magnetite microcrystals was placed between glass plates with specially treated surfaces, which resulted in a certain anisotropy of the liquid

crystal director vector. In this case, the polarization of the radiation that passed through the stack varied with the applied MF. The torque on the microcrystals was transferred to the nematic molecules and changed the director sense. The relative intensity of the radiation passed through two crossed polarizers was measured. Between the polarizers a system with a liquid-crystal substance was placed. The MF dependence of the intensity was a curve with saturation, the maximum slope being about  $3\%/\mu\text{T}$ . Given is an estimate of the magnetic moment alignment for a  $5\text{-}\mu\text{m}$  drop that contains magnetite microcrystals in a liquid matrix with a volume concentration of  $10^{-3}$ . The alignment is significant even in a field of  $0.15\ \mu\text{T}$ , which could form the foundation for the mechanism of the optomagnetic aligning capability in animals.

In search for uses for such a mechanism, the question of whether birds' eyes contain structures with extended dye molecules of  $\beta$ -carotene type that absorb light radiation at a certain orientation to the electric field vector and magnetite microcrystals that are responsible for the orientation of dye molecules in a magnetic field was discussed.

This mechanism relies on the interaction of magnetic microcrystals with nematic molecules. Liquid-crystal molecules per se display general magnetic properties of diamagnetic type. The anisotropy of the induced magnetic moment causes the director to turn in a magnetic field. However, this effect is fairly small to account for any MBEs. Known are only optomagnetic sensors of strong MFs, on the order of tens of tesla, constructed using that principle.

### 3.6.2 Eddy currents

One of the MBE mechanisms establishes that the driving force in the exposure of biological systems to a low-frequency MF is electric eddy currents induced by a variable MF in biological tissues.

The current is, on the whole, proportional with the strength  $\mathbf{E}$  of the electric field related to the MF  $\mathbf{B}$  by one of the Maxwell equations

$$\text{rot}\mathbf{E} = -\frac{1}{c} \frac{\partial\mathbf{B}}{\partial t} .$$

For a sinusoidal MF with frequency  $\Omega$  and amplitude  $b$ , the electric field amplitude varies with the product  $\Omega b$ . If the hypothesis is true, then observed MBEs should correlate with changes in that quantity. However, no correlations have been found for the case of relatively weak fields (around the geomagnetic field).

Juutilainen (1986) reports the absence of a dependence of the MBE on  $\partial\mathbf{B}/\partial t$ . Liboff *et al.* (1987b) cited four independent works on different biological systems within various ranges of the variable MF, where the eddy current hypothesis had been checked and not supported. Specifically, Liboff *et al.* (1984) studied the action of variable MFs on the growth of the DNA synthesis rate in human fibroblasts within the range of  $b(1.6\text{--}400)f(15\text{--}4000)$ . However, the effect, which on average was no

more than 50%, was independent of the product  $bf$ , which was varied within four orders of magnitude.

Statistically meaningful  $\sim 6\%$  variation of the fibroblast cell proliferation rate, as measured by Ross (1990), remained virtually unchanged under various magnetic conditions that correspond to the cyclotron configuration of calcium ions:  $B(131)b(131)f(100)$ , as well as  $B(98)b(98)f(75)$  and  $B(21)b(21)f(16)$ . The product  $fb$  is seen to change nearly 40 times, with the effect remaining the same.

Blackman *et al.* (1993) have shown that a 50-Hz MF with an amplitude of 0–42  $\mu\text{T}$  against the background of a DC field similar to the geomagnetic one makes up for the action of matter that induces a double neurite outgrowth in certain animal cells. Such changes, beginning with an amplitude of 6  $\mu\text{T}$  and stabilized at a new level of about 10  $\mu\text{T}$ , emerged. Therefore, to clarify the role of an induced electric field, an amplitude of 8  $\mu\text{T}$  was taken, which corresponds to the maximum sensitivity of a system to MF changes. Petri dishes with concentric sections of various diameters containing cells were placed in a homogeneous MF coaxially with a vertical solenoid. With that configuration the electric fields in various sections differed markedly and their amplitude was varied from 3 to 65  $\mu\text{V/m}$ , whereas the MF was the same. Measurements yielded the same quenching level in various sections, which pointed to the fact that the induced electric fields were insignificant.

The recent results of Jenrow *et al.* (1995) have also shown that there is no correlation of MBEs with induced currents.

Very strong evidence against the eddy current hypothesis was supplied by Prato *et al.* (1997), where the parameters  $B_{\text{DC}}$ ,  $B_{\text{AC}}$ , and  $f$  grew concurrently at first twofold and then fourfold. In the process, the product  $fB_{\text{AC}}$  increased up to 16 times, but the statistically certain MBE level remained constant, Fig. 4.41.

It is to be noted that as the amplitude or frequency of a variable MF grows, a moment is still reached, when induced fields and currents become of biological significance, provided that a small biological system is not placed at the geometric center of an exposure system, see Section 1.4.1. Experimental evidence that, as the variable MF strength grows, there emerges a correlation of biological response with the product  $fB_{\text{AC}}$  is available in Schimmelpfeng and Dertinger (1997). Greene *et al.* (1991) specially studied the transcription rate of the HL-60 leukemia cells in Petri dishes with concentrically divided sections placed on the axis of a solenoid with a variable MF of 60 Hz. Figure 3.10 shows the kinetics of inclusion of a radioactive marker  $^3\text{H}$  introduced into a cellular culture with uridine into RNA molecules being synthesized. The cells were 0.2 and 2 cm away from the axis and were exposed, in addition to an MF, to the action of an induced electric field. It is seen that the cells responded to the variations of the electric, rather than magnetic, field.

Eddy currents can produce a biological response either due to tissue heating by Joule heat, Section 1.4.1, or due to electrochemical effects by the action of induced electric currents on charge carriers in the tissue — ions or charged molecular groups in various biophysical structure. Polk (1986) discussed a possible mechanism for the action of a low-frequency MF on the distribution and dynamics of ions on the surface of cellular membranes. He used the classical dynamics of charges in a

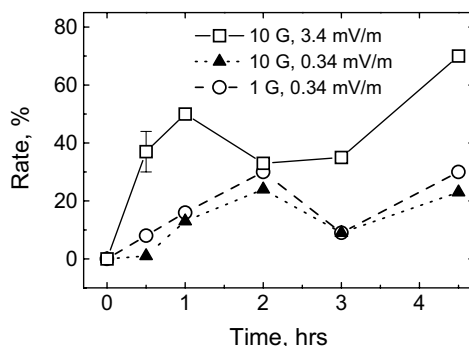


**Figure 3.10.** The kinetics of the transcription of HL-60 leukemia cells in various electric and MFs with a frequency of 60 Hz, according to Greene *et al.* (1991).

magnetic field in the presence of thermal diffusion and phenomenological damping, and the equations of the electrodynamics of continua for the current density  $\mathbf{j}$

$$\nabla \mathbf{j} = -\frac{\partial}{\partial t} \rho, \quad \mathbf{j} = u\rho \mathbf{E} - \frac{u}{q} \kappa T \nabla \rho.$$

The first equation is the continuity equation; it relates the current density to the density  $\rho$  of free charges  $q$  of mobility  $u$ . The second equation shows that the current is determined by the electric field  $\mathbf{E}$  and the diffusion thermal dissipation of inhomogeneities of charge density distribution. From this we can find the perturbations in the distribution caused by the electric eddy fields.

It was shown that induced currents on the membrane surface would under certain conditions exceed the thermal level. Specifically, the movement of ions must be constrained to a thin, around  $10 \text{ \AA}$ , layer on the cellular surface, and the cells themselves must form macroscopic  $> 3 \text{ cm}$ , closed chains. A threshold level was found for the product  $fB \sim 1 \text{ T/s}$  when exposed to a sine MF. This, for instance, corresponds to the amplitude  $B \sim 100 \text{ \mu T}$  at frequency  $f = 1 \text{ kHz}$ . Although this estimate relies on a possible electrochemical mechanism, its value is close to the thermal effect threshold, see Section 1.4.1. We note that the condition of macroscopic cellular chains imposes a significant constraint on the applicability of that model. For instance, it cannot be used to account for MBEs in cellular cultures in homogeneous solutions *in vitro*.

There are also other electrochemical mechanisms for biological effects of an MF. Chiabrera *et al.* (1984) discussed the possibility of an action of induced electric fields on the transportation of ions and molecules through biological membranes.

### 3.6.3 Superconductivity at the cellular level

The idea of a superconductive state in a biological matter is attractive in that it enables the problem of electromagnetobiology to be reduced to the substantiation of superconductivity in a biological tissue. In actual fact, if such a superconductive state does exist, its characteristics beyond doubt change even in hyper-weak MFs. It is exactly the properties of the superconductive state and its inter-phase boundaries (Josephson junctions (Josephson, 1962), see Addendum 6.7) that are used by supersensitive detectors of an MF — quantum interference devices (SQUIDS). The “kT problem” as well requires no explanation — after all we here deal with superconductivity at normal physiological temperatures, i.e., with high-temperature superconductivity. In the literature, there are many speculations on that topic (Achimowicz *et al.*, 1979; Cope, 1981; Achimowicz, 1982; Miller, 1991; Costato *et al.*, 1996).

Fröhlich was one of the first to point to the biological cell as a possible receptor of EM waves (Fröhlich, 1968a,b). That follows from the Bose-condensation mechanism he proposed for some modes of collective excitations in systems of interacting molecular dipoles in a living cell, within the millimeter (mm) range. Ever since search is under way for other mechanisms at the cellular level that would be able to account for biological reception of weak MFs in the low-frequency range as well. For instance, in Costato *et al.* (1996) the possibility of the presence of superconductivity in living cells and the appearance of Josephson effects at junctions of such superconductive areas are discussed. It is maintained that properties similar to the dynamics of the Josephson junctions are observed for single cytoskeleton cells and for two neighboring cells. It follows that an EMF can affect intercellular communication.

Electron bisolitons, which transfer a double elementary charge and travel along alpha-spiral protein molecules without damping, were given a theoretical treatment by Davydov (1994). No way to experimentally test the existence of bisolitons in living organisms was proposed.

A manifesto of sorts of cellular superconductivity is a review by Miller (1991). It contains an extensive bibliography on the subject. At the same time, there are no sufficient theoretical grounds so far for the emergence of a superconductive phase in cellular structures. Also absent are productive predictive models for such a state. It should be noted that no high-temperature (300 K) superconductivity as a physical effect has been found as yet. Therefore, the idea of the emergence of a high-temperature superconductive state in biological tissues raises some doubts.

Attempts are known to support that idea experimentally. They rely on the fact that indicators of a superconductive state are an abnormally high conductivity of the medium, and hence abnormal diamagnetism, and the quantization of the magnetic flux through an area constrained by a superconductive contour. This causes the current through the contour, other parameters being fixed, to assume only a series of discrete values. Under some, fairly rigid, conditions, specifically where the contour contains a section with disrupted superconductivity — a Josephson junction

— one can observe current oscillations and an electromagnetic emission at a characteristic frequency as the e.m.f. in the contour grows. Miller (1991) pointed to some experimental works that treat magnetic measurements of biological and organic media as the presence of molecular or subcellular superconductivity domains.

We also note the experiments of Ahmed *et al.* (1975), which measured the diamagnetic susceptibility of weak solutions of lysozyme enzyme in a static MF of 40–200 mT. Variation of susceptibility with the MF, temperature, and enzyme concentration behaved in an involved multipeak manner. A susceptibility maximum was observed in the region of 60 mT, such that the susceptibility per molecule exceeded normal values by a factor of more than one thousand. The authors came up with an explanation in terms of superconductive domains with superconductivity disrupted in a stronger MF.

Del Giudice *et al.* (1989) assumed that the properties of Josephson junctions are inherent in the biological membrane that separates two new cells as the initial cell undergoes a mitosis process. The authors assumed that Josephson-type phenomena could occur not only at superconductor junctions, but also in a more general case — at the boundaries between the phases of a correlated state. The role of electron pairs will then be played by quasi-particles — correlation carriers, e.g., bosons of coherent excitations of molecular dipoles in the Fröhlich model, see Addendum 6.6. We will put aside those esoteric ideas and consider experiments described in Del Giudice *et al.* (1989). According to the authors, they support the existence of superconductivity or similar macroquantum states in a biological tissue.

They measured the current in a circuit including an electrochemical cell unit with cellular culture *S. cerevisiae* in a de-ionized solution of sucrose immediately before, during, and after mitosis. The cells in the unit between electrode needles formed chains after the fashion of pearl threads, which was observed under microscope. Also measured was the voltage across the unit. Using a current generator with an internal resistance of 12 Mohm, the current in the circuit was increased bit by bit and voltage jumps across the unit were observed. This means that the voltage–current characteristic was stepwise in nature. That effect was not observed with sterilized cells. In general, such a dependence is characteristic of the current in a superconductive contour with a Josephson contact, since the magnetic flux through the contour only assumes values that are multiples of the magnetic flux quantum. The jumps occur when the superconductive current component reaches a critical value and destroys specific quantum phenomena in the region of the contact.

It was of importance for the observation that the synchronized cell suspension displayed current and voltage jumps only in cytokines, the final stage of mitosis, when a wall between two daughter cells was being formed. Moreover, the voltage jumps were varied in the range of 0.3–3 from a mean value, which is rather due to a scatter of cell sizes. If we consider this wide scatter of jump values and the fact that dividing cells formed threads between the electrodes, we will get another explanation of the observed results, which does not rely on the idea of biological superconductivity. When a cell splits to form two cells, the electric resistance jumps, and so does the voltage across the electrodes with the result that the current in the

circuit drops. The small current drop is well seen in the curve (Del Giudice *et al.*, 1989), thus suggesting that the internal resistance of the current generation is similar to the unit resistance. It is noteworthy that the voltage jumps were influenced by the value of an external MF. The mean values of the jumps  $\Delta V$  were 1580, 470, and 15 nV, the field  $H$  taking up values 400 mT, 50, and  $\sim 1 \mu\text{T}$ , respectively. The last value of  $1 \mu\text{T}$  was not measured, but it was characteristic of the MF inside mumetallic magnetic screens, a place where the appropriate measurements were made. That series forms a near-logarithmic dependence  $\Delta V(H)$ , a curious fact, but such a behavior does not fit properly with the idea of superconductivity.

In that work, they also observed electromagnetic emission of cells in the cytokines phase. The emission was also observed by other authors, Hoelzel and Lamprecht (1994) and Berg (1995), under similar conditions. The emission of yeast cells at around 7 MHz displayed a spectral maximum of width  $\sim 5$  KHz. The measurements were performed in a magnetically screened chamber, when the above experiments with voltage jumps yielded a value of about 15 nV. The authors assumed that the emission is caused by quantum transitions of a system to a neighboring current state. One justification was the following coincidence. The calculated frequency of the emission by a Josephson junction fed by a 15-nV voltage source is  $eV/\pi\hbar \approx 7.3$  MHz, which agrees with the experimentally observed values, but that justification is hard to accept. Even if we assume for a minute that in both cases — the voltage jumps and the radiation — there occurs a Josephson effect, then we get a significant contradiction. In the first case, that would be a stationary effect; in the second, a non-stationary Josephson effect. The voltages under these conditions have different physical meanings. Therefore, one cannot use voltages obtained for some conditions to compute effects under other conditions.

It should be emphasized that dividing cells could emit due to current impulses on the membrane surface caused by a redistribution of surface charges as a cell membrane splits in two. The impulse length can be easily estimated from the formula for the mean square of the ion diffusion displacement  $\langle r^2 \rangle \sim 6Dt$ , where  $D$  is the diffusion coefficient, see p. 281. Substituting the characteristic size of the charge redistribution area  $0.1\text{--}1 \mu\text{m}$  and considering that the ion diffusion on the cellular surface, the so-called lateral diffusion, is a couple of orders of magnitude faster than the volume diffusion (Eremenko *et al.*, 1981) gives a rough estimate of the impulse length of  $0.01\text{--}1 \mu\text{s}$ . Such impulses produce an electromagnetic field in the range of  $1\text{--}100$  MHz. This range characterizes the estimation inaccuracy, rather than the radiation spectrum width. In the final analysis, the spectrum width is determined by the scatter of physical parameters of cells, primarily by the scatter of their sizes.

The experiment under consideration and the Josephson effects seem to display only external similarity, rather than uniformity of causes. Biological superconductivity still remains one of marginal hypotheses in magnetobiology. Being still of interest, it has no reliable theoretical and experimental substantiation.

### 3.6.4 Magnetohydrodynamics

There are treatments of magnetohydrodynamic effects occurring as blood or other bioplasm flowing through vessels is exposed to an MF, see review (Kuznetsov and Vanag, 1987). Studied was, for instance, the additional pressure on vessel walls under a Lorentz force acting on free charges in the blood. Those treatments, however, generally overlooked the fact that macroscopic pressure effects are provided for by appropriate microprocesses. If in that case no explanation is forthcoming for marked changes in the state of a single microparticle in an MF, then any positive statements on macroscopic corollaries look feeble. Such statements must contain derivation mistakes — mathematical, physical, and, most often, logical and conceptual ones, i.e., those relying on concepts beyond the validity area.

Magnetic hydrodynamics looks into the interplay of electromagnetic fields and moving liquid or gaseous media with a relatively high conductivity, such as in metals. When a medium moves in a magnetic field, it has currents engendered in it. These latter, for one thing, are subject to an external MF; for the other, they are themselves a source of additional MFs. To estimate the degree of the influence of an MF on the liquid flow they normally use the Hartmann number, the density ratio of magnetic and viscous forces (Landau and Lifshitz, 1960)

$$G = \frac{rH}{c} \sqrt{\frac{\sigma}{\eta}},$$

where  $r$  is the characteristic distance,  $\sigma$  is the electric conductivity of a medium, and  $\eta$  is the viscosity coefficient. Hartmann investigated the flow of a viscous incompressible liquid between two planes in a perpendicular MF  $H$  to show that if  $G \ll 1$ , then magnetic effects will be small. Conversely, if  $G \gg 1$ , then the viscous properties of the liquid can be ignored. For example, the movement of blood with a conductivity of  $\sim 1 \text{ S/m} = 9 \cdot 10^9 \text{ CGS units}$  and a viscosity of  $0.01 \text{ g/cm}\cdot\text{s}$  along a vessel about  $10^{-2} \text{ cm}$  in diameter in a magnetic field  $\sim 1 \text{ G}$  is characterized by a Hartmann number of  $G \sim 10^{-6}$ . Consequently, magnetohydrodynamic effects in magnetobiology do not warrant any studies.

To evaluate contributions of other possible effects we will pass over to a reference system moving in a magnetic field  $H$  with the liquid at a velocity  $v$ . In such a system an electric field that is around  $E \sim vH/c$  emerges. Generally speaking, the electric field could align molecules with a dipole moment, e.g., water molecules with the moment  $d = 1.855 \text{ D}$ . However, the additional energy  $dE$  acquired by a water molecule in this EF for an MF of  $1 \text{ G}$  and a velocity of  $1 \text{ cm/s}$  is 14 orders of magnitude smaller than the disordered thermal scale  $\kappa\mathcal{T}$ . That makes useless any discussion of biological consequences of dipole aligning. Another scenario looks at the pulling of oppositely charged ions in opposite directions. The work needed to move a charge  $e$  a macroscopic distance  $r$  in a field  $E$  is  $erE$ , whereas the diffusion processes that hinder that movement have the same energy scale  $\kappa\mathcal{T}$ . This suggests that for changes in ion concentration on volume walls to be observed requires five or six more orders of magnitude, even for  $r \sim 1\text{--}10 \text{ cm}$ .

### 3.6.5 Macroscopic charged objects

Macroscopic objects as targets for weak MFs are chosen because of their sufficiently large own energy comparable with  $\kappa\mathcal{T}$ . This takes care of the problem. In fact, even a weak MF is capable of significantly changing the energy of an object that carries, for instance, a large electric charge (Karnaukhov, 1994), or moves at a high velocity relative to other objects. True, this requires that the object travel under strictly defined conditions. A change in the object energy in an MF is associated with some biochemical processes. However, in *all* works of that class known to this author the existence of such objects was *postulated*. They have not been observed in any other experiments not concerned with magnetobiology. Therefore, that postulate can hardly be justified. Models can be thought to be of value, where an insignificant assumption, or even an idealization, yields some consequences of significance. In our case, however, the “weight” of a postulate is comparable with that of the problem itself. Postulating the existence of such objects — macroscopic charged ion vortices (Karnaukhov, 1994), etc. — amounts to postulating the absence of the issue of magnetobiology per se.

Novikov and Karnaukhov (1997) explained MBEs and the action of a combined MF at a cyclotron frequency on amino acid solutions. Instead of individual ions in a solution they considered their clusters with a macroscopically large number  $N$  of ions. The mean value of random forces with which the thermostat acts on the cluster at sufficiently large  $N$  becomes smaller than the mean value of the force produced by an MF, i.e., the Lorentz force. The authors believe that this sort of removes the problem. Without criticizing the quality of their reasoning we will only bring out the following bottlenecks of the idea.

Firstly, the nature of interior forces that are responsible for the existence of a cluster is unclear. Secondly, according to this work, a cluster is a system with mass  $NM$  and charge  $Nq$ , whose dynamics in an MF is controlled by the motion of the center of mass; otherwise the notion of the cyclotron frequency for a cluster would become meaningless. The thermal energy of the motion of the center of mass is then the same as with an individual ion, since both an ion and a cluster are, in that respect, identical with a point particle with three degrees of freedom. It is common knowledge that thermal energy is distributed uniformly between the degrees of freedom, not between individual particles of a system.

At the same time, the contribution of an MF to the cluster energy does not grow with its charge in proportion to  $N$ , as it might seem due to the growth of the Lorentz force. This author (Binhi, 1995b) estimated the instantaneous power of transformation of the energy of a variable MF into the energy of the momentum of a classical particle (Eq. (20) in the article). In terms of conventions adopted here, the formula has the form <sup>22</sup>

$$G \leq \omega_1 \Omega L ,$$

---

<sup>22</sup>For a quantum particle in an MF, energy splitting is  $\varepsilon_m \propto m\hbar\omega_0 = m\hbar qH/2Mc$ . In an AC MF we have  $dH \sim H\Omega dt$ , hence the power  $d\varepsilon/dt \propto \omega_1 \Omega m\hbar$ . Here  $m\hbar$  is an angular momentum of the  $m$  state.

where  $\omega_1 = qH_{AC}/2Mc$  is the Larmor frequency related to the amplitude of a variable MF, and  $L$  is the angular momentum. It is worth noting that the Larmor frequency of an individual ion equals that of an ion cluster; the same is valid concerning the cyclotron frequency. Therefore, it is of interest to evaluate the angular momenta  $L$  of the ion and the cluster. The question boils down to the following: whether there exist some mechanisms or constructions in a living tissue or a solution, which are able to provide a non-zero angular momentum of a particle during a time of about  $\Omega^{-1}$ ? It can be assumed that for an ion such a construction is the macromolecule cavity. When an ion gets into the cavity for some time it retains an initial angular momentum, and so it can exchange energy with an MF. A cluster being a macroscopic system, it would be hard to make whatever assumptions. The only reasonable estimate in this case is  $L = 0$ , since nothing can cause the cluster center of mass that undergoes numerous thermalizing collisions to move in a circle or an arch. There are also no reasons for a toroidal cluster to have an angular momentum, but assumptions of such a cluster form are also available in the literature. It is, thus, hard to agree that ion clusters will somehow clarify the magnetobiological issue.

Generally speaking, when exposed to an MF ions in a solution acquire an angular momentum, although an extremely small one. It can readily be found from the equation

$$\frac{d\mathbf{L}}{dt} = \mathbf{K} = \mathbf{r} \times \frac{q}{c} \mathbf{v} \times \mathbf{H} ,$$

where  $\mathbf{L}$  is the angular momentum,  $\mathbf{K}$  is the torque, and  $\mathbf{r}$  is the radius vector of a particle. Clearly, the derivative  $dL/dt$  is bounded from above by  $rqvH/c$ . Since an ion undergoes thermalizing collisions with ambient media particles, the angular momentum between collisions is

$$L \sim \tau r q v H / c \sim \tau^2 q v^2 H / c ,$$

where  $r \sim 10^{-8}$  cm is the length, and  $\tau$  is the time of the mean free path. Since the squared velocity of a particle in a solution is about  $\kappa T / M$ , then for  $\tau \sim 10^{-10}$  s,  $\Omega_c \sim 100$  Hz

$$L \sim \kappa T \Omega_c \tau^2 \ll \hbar .$$

That is, the angular momentum of a free ion is much smaller than the quantum uncertainty for the momentum. To prove that, we will find the diamagnetic contribution concerned with the emergence of that momentum. The gyromagnetic ratio for the orbital motion is  $\gamma = q/2Mc$ , and so the magnetic moment for a volume unit equals  $I = \gamma L / r^3$ , and the diamagnetic susceptibility  $\chi = \partial I / \partial H$  will be

$$\chi \sim \frac{q}{Mc} \kappa T \frac{\partial \Omega_c}{\partial H} \frac{\tau^2}{r^3} \sim \frac{q^2}{Mc^2 r} \sim 10^{-9} .$$

There is no need to average over particles since that quantity is extremely small, namely several orders of magnitude smaller than the atomic diamagnetic susceptibility, see Section 3.6.1.1.

### 3.7 CYCLOTRON RESONANCE IN MAGNETOBIOLOGY

In a number of cases biological effects of weak MFs have a resonance nature; it was initially established in Liboff (1985) and Liboff *et al.* (1987b) that the effective frequencies are close to cyclotron frequencies of  $\text{Ca}^{2+}$  and  $\text{Na}^+$  ions, and so on. This suggested that the phenomena observed rely on a cyclotron resonance. The idea of cyclotron resonance in magnetobiology is credited to A. Liboff of Oakland University, USA. Various authors elaborated the topic of such a resonance in magnetobiology, but it failed to receive any recognition because it was impossible to supply a correct physical substantiation. At the same time, these experiments demonstrated the significant role of ions, especially  $\text{Ca}^{2+}$ , in magnetobiology. Nearly 12% of works on electromagnetobiology contain discussions on the role of ions, and 9% on the role of calcium.

#### 3.7.1 Cyclotron resonance

For a classical charged particle in an electromagnetic field

$$\mathbf{E} = -\text{grad}A_0 - \frac{1}{c} \frac{\partial \mathbf{A}}{\partial t}, \quad \mathbf{H} = \text{rot} \mathbf{A}, \quad (3.7.1)$$

equations of motion are (e.g., Landau and Lifshitz, 1976a)

$$M \frac{d\mathbf{v}}{dt} = q\mathbf{E} + \frac{q}{c} \mathbf{v} \times \mathbf{H}, \quad (3.7.2)$$

where the right part is the Lorentz force. Considering that the kinetic energy of a particle is  $\varepsilon = Mv^2/2$ , we can easily find from (3.7.2) the energy variation rate  $d\varepsilon/dt$

$$\frac{d}{dt} \varepsilon = q\mathbf{v} \mathbf{E}. \quad (3.7.3)$$

Let a particle move in a plane perpendicular to a direction  $\mathbf{H} \parallel z$ , and the field  $\mathbf{E}$  be aligned along the  $x$  axis. Also let the EF  $E_x \sim \cos \Omega t$  be so small that the orbit of the motion of a particle varies little during the time  $\sim \Omega^{-1}$ , so that the particle can be viewed as free. From (3.7.2) it follows that the particle moves in a circle with cyclotron frequency  $\Omega_c = qH/Mc$ . The  $x$  component of its velocity will then, up to a phase, vary as  $\cos \Omega_c t$ . Correspondingly, we find from (3.7.3)

$$\frac{d}{dt} \varepsilon \sim \cos \Omega t \cos \Omega_c t = \frac{1}{2} \cos(\Omega - \Omega_c)t + \frac{1}{2} \cos(\Omega + \Omega_c)t.$$

The energy change is mainly dictated by the first term with the small frequency  $\beta = \Omega - \Omega_c$ . Let that change be measured during the time span from  $t - T$  to  $t + T$ . Divided by the time span it is equal to

$$\varepsilon_T = \frac{1}{2T} \int_{t-T}^{t+T} \cos \beta \tau d\tau \sim \frac{\sin \beta T}{\beta T} \cos \beta t. \quad (3.7.4)$$

The energy change can be both positive and negative, depending on the random moment of observation  $t$ . Therefore, the intensity of the particle energy variation

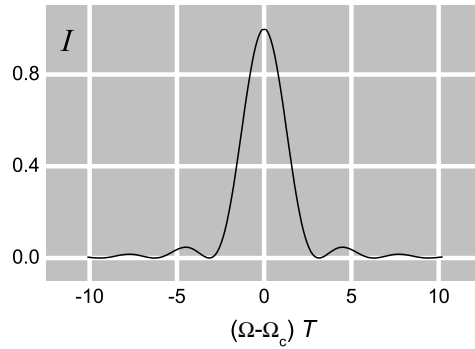


**Figure 3.11.** The energy exchange intensity between an EM field and a charged particle at a cyclotron resonance measured during the time interval  $[-T, T]$ .

can conveniently be characterized by the mathematical expectation of the squared quantity (3.7.4), i.e.,

$$I = \overline{\varepsilon_T^2} \sim \left( \frac{\sin \beta T}{\beta T} \right)^2,$$

where the overbar implies the averaging of an ergodic process over the time interval  $\gg T$ .

That function is plotted in Fig. 3.11. It is seen that the particle energy variation rate is largest at a *cyclotron resonance* when frequencies  $\Omega$  and  $\Omega_c$  coincide. The supposition that an ion cyclotron resonance also occurs at odd harmonics of cyclotron frequency and does not occur at even harmonics (Smith *et al.*, 1995) is not quite justified. For instance, under certain conditions in metals the time interval between successive collisions of electrons with dissipating centers is on average larger than the FM period. When the MF vector is strictly parallel with the metal surface, electrons only spend a small part of the motion period near the metal surface, where they are exposed to an external variable electric field. Conditions then emerge for a resonance at all the multiple frequencies. Similar conditions are realized in *cyclotrons*, accelerators of charged particles. In a biological medium or in biophysical structures, there is no way for an external EF to act on ions through a small section of their orbits, if only because there are no orbits as such. Therefore, resonances at multiple frequencies are impossible. Generally speaking, with circular EFs induced by a variable MF, a resonance is possible at a cyclotron frequency or its subharmonics. However, that is not a cyclotron resonance, but rather a parametric one. It will be considered later in the book.

The idea of cyclotron resonance has been employed many times to explain biological effects of low-frequency MFs. Being quite graphic, the idea enjoys support of many researchers, mostly biologists. The main argument of its advocates is that MBEs appear mostly at frequencies formally predicted by the cyclotron resonance

formula  $\Omega_c = qH/Mc$  for biologically significant ions of Ca, Mg, etc. A effective frequency shift that varies with  $H$  (Liboff *et al.*, 1987b) was observed, along with a shift in accordance with ion isotope mass (Liboff *et al.*, 1987a).

The main argument of the opponents of that concept (e.g., Sandweiss, 1990; Adair, 1991) boils down to the following. In a living matter ions occur in a water solution at a temperature of about 300 K. They feature a thermal energy of about  $\kappa\mathcal{T}$ . A particle in a magnetic field moves in a circle, whose radius can be easily worked out from the fact that the thermal energy is equal to the energy of motion:

$$R = \frac{1}{\Omega_c} \sqrt{\frac{\kappa\mathcal{T}}{M}} .$$

In an MF similar to the Earth's field, for a calcium ion this yields more than 1 m. It is clear then that this value does not match an ion cyclotron resonance, say, in a biological cell of size that is six orders or magnitude smaller.

What is more, an ion in a solution is hydrated; i.e., it carries on it a shell of water molecules. Its effective charge is then several times smaller. It then makes no sense to correlate the external field frequency with the cyclotron frequency of an ion without a shell.

There are also other considerations that lead to the same conclusion. An ion particle in a cytoplasm or intercellular medium undergoes numerous thermalizing collisions with neighboring molecules, the particle moving about in a diffusion manner. Of course, that motion, which is correlated in phase with an external MF, is limited by the free path time, i.e., by the time between two consecutive collisions with media molecules. In a water solution that time  $T$  is  $10^{-11}$  s. In Sandweiss (1990) that estimate for calcium follows from the formula

$$T = \frac{1}{n\sigma v} ,$$

where  $v = \sqrt{2\varepsilon/M}$  is the thermal velocity of an ion,  $n \approx 4 \cdot 10^{28} \text{ m}^{-3}$  is the atom density in a biological medium,  $\sigma \approx \pi a_0^2 = 8 \cdot 10^{-21} \text{ m}^2$  is the collision cross-section, and  $a_0$  is the Bohr radius.

Clearly, the "resonance bandwidth"  $\sim 1/T$  (see below) is many orders of magnitude larger than the cyclotron resonance frequency. This also suggests that the cyclotron resonance concept does not hold good for an ion in a solution.

### 3.7.2 Cyclotron resonance in ion channels

To circumvent the difficulties, it was suggested that an ion cyclotron resonance occurs within ion channels of biological membranes, where the orbit radius could not be large. Ion channels that pierce the membranes are formed by spiraling proteins. They are responsible for the life-supporting exchange of ions and some molecules with the cytoplasm and the extracellular medium. The most complete treatment of the model is given by McLeod *et al.* (1992b). That work maintains that the motion

of an ion within a channel occurs largely without random thermalizing collisions. Then it is phased in for a sufficiently long time with an external MF, and can thus be described by an equation of classical dynamics for a particle under a Lorentz force.

The work also postulated that (1) an ion begins its motion from a channel's mouth from rest, and (2) a channel of cylindrical symmetry has two contractions: at the middle and at the end of the channel. As it sets out from the mouth, the ion is spiraling under the action of a transmembrane potential difference and a variable MF. The idea underlying the model is the ability of an ion to acquire under special conditions an extremely small energy near the contractions. Therefore, the cyclotron orbit diameter is smaller than that of the contractions, so that the ion finds its way through the channel's bottlenecks. The structure of the protein that forms the channel in that model acts as a filter or a gate for a variety of spiral paths for ions. The filter efficiency is determined by the parameters of an external low-frequency MF. That enables theoretical ion paths in the channel to be correlated with the conditions in magnetobiological experiments.

It is common knowledge that the equation of motion for a charged particle in a medium with energy dissipation under an electromagnetic field and an external force has the vector form<sup>23</sup>

$$\frac{d\mathbf{U}}{dt} = \frac{q}{m} \mathbf{E} + \frac{q}{m} \mathbf{U} \times \mathbf{B} - \frac{1}{\tau} \mathbf{U} + \frac{1}{m} \mathbf{F} . \quad (3.7.5)$$

Cylindrical coordinates  $P_r, P_\varphi, P_z$  of an arbitrary vector  $\mathbf{P}$  will be (Korn and Korn, 1961)

$$P_r = P_x \cos \varphi + P_y \sin \varphi , \quad P_\varphi = -P_x \sin \varphi + P_y \cos \varphi , \quad P_z = P_z .$$

Using these rules, we easily find the physical coordinates of the velocity vector  $\mathbf{U}$

$$U_r = \frac{dr}{dt} , \quad U_\varphi = r \frac{d\varphi}{dt} , \quad U_z = U_z \quad (3.7.6)$$

and the acceleration vector  $\frac{d}{dt} \mathbf{U}$

$$\begin{aligned} \left( \frac{d}{dt} \mathbf{U} \right)_r &= \frac{d^2 r}{dt^2} - r \left( \frac{d\varphi}{dt} \right)^2 = \frac{dU_r}{dt} - U_\varphi \frac{d\varphi}{dt} , \\ \left( \frac{d}{dt} \mathbf{U} \right)_\varphi &= r \frac{d^2 \varphi}{dt^2} + 2 \frac{dr}{dt} \frac{d\varphi}{dt} = \frac{dU_\varphi}{dt} + \frac{1}{r} U_r U_\varphi , \\ \left( \frac{d}{dt} \mathbf{U} \right)_z &= \frac{dU_z}{dt} \end{aligned} \quad (3.7.7)$$

in a cylindrical coordinate system. Substituting (3.7.6) and (3.7.7) into (3.7.5) gives the following equations of motion

---

<sup>23</sup>MKS unit system.

$$\begin{aligned}
\frac{dU_r}{dt} - U_\varphi \frac{d\varphi}{dt} &= \frac{q}{m} E_r + \frac{q}{m} U_\varphi B_z - \frac{U_r}{\tau} + \frac{F_r}{m}, \\
\frac{dU_\varphi}{dt} + \frac{1}{r} U_r U_\varphi &= \frac{q}{m} E_\varphi - \frac{q}{m} U_r B_z - \frac{U_\varphi}{\tau} + \frac{F_\varphi}{m}, \\
\frac{dU_z}{dt} &= \frac{q}{m} E_z - \frac{U_z}{\tau} + \frac{F_z}{m},
\end{aligned} \tag{3.7.8}$$

where, as in McLeod *et al.* (1992b), it was assumed that the MF is aligned along the  $z$  axis, which coincides with the channel axis, i.e.,  $B_x = B_y = 0$ .

The equations used by McLeod *et al.* (1992b) differ from (3.7.8) and contain some inaccuracies. Further, the dissipative term  $-\mathbf{U}/\tau$  in the equation of motion (3.7.5) implies that there occur numerous chaotic collisions of a macroscopic particle under consideration with a host of microparticles, which are molecules of the liquid medium. At the same time, the walls only confine an ion in a channel, so that each collision will markedly change its momentum. That means that the physical conditions under which the use of the phenomenological dissipative term is valid are ignored.

The most fundamental challenge of the model is concerned with rigid initial conditions for an ion. The ion has to have a near-zero initial velocity, so that cyclotron radii of motion would be smaller than the transverse size of an ion channel. At a channel radius of about  $R \sim 10 \text{ \AA}$ , the velocity that can be estimated from a formula for cyclotron motion in a magnetic field similar to the Earth's field,  $\sim 50 \mu\text{T}$ , must be at least

$$U \leq R \frac{q}{M} B \sim 10^{-7} \text{ m/s}$$

for a potassium ion, and 40-fold larger for a hydrogen ion. Can ions move so slowly at the channel entrance? The mean thermal velocity of a potassium ion at  $\mathcal{T} = 300 \text{ K}$  will be

$$U \sim \sqrt{\frac{\kappa \mathcal{T}}{M}} \approx 10^2 \text{ m/s}.$$

Even if an ion is placed within a channel of length  $L \sim 50 \text{ \AA}$ , the uncertainty, according to the Heisenberg relation, will be more than

$$\Delta U \geq \frac{\hbar}{ML} \sim 0.3 \text{ m/s}.$$

Correspondingly, the ion velocity will not be smaller, a fact that is at variance with the assumption underpinning the model.

The idea underlying the model is attractive, but removing the mathematical inaccuracies does not save it. The equation of the Lorentz force is hardly applicable to describe the ions that are constrained by the ion channel. Such ions are rather waves than particles, although their mass is relatively large, see p. 215.

### 3.7.3 Ion cyclotron resonance

In the literature there is one broad treatment of the subject of cyclotron resonance. It is known as ‘‘ion cyclotron resonance’’ (ICR). ICR appeals, for one thing, to the

fact that ions contribute to magnetoreception, and, for the other, to the fact that the effective frequencies coincide with the frequencies of the cyclotron series. In this broad sense, the idea of cyclotron resonance is obviously correct and useful, since it proceeds from more or less reliable experimental evidence. In that case, ICR is also a prototype of more advanced models still to be constructed, which will meet all the criteria of scientific methodology. It is important that the broad treatment of the cyclotron resonance leaves much room for specific realizations of that concept. One interesting suggestion is that an ion is exposed to internal or endogenous electric fields (Liboff, 1997). These are always present in an organism owing to a wide variety of biochemical processes involving charge transport. Liboff assumes that such fields can have complicated frequency spectra; specifically, they can excite ions at characteristic frequencies of the cyclotron series. That makes it possible to interpret the biological effects of weak DC MFs. In a modified MF, cyclotron frequencies change, and so does the picture of their “superposition” on the frequency spectrum of endogenous electric fields. This changes the conditions under which ions undergo excitations. There is no testing the hypothesis so far, since to this end spectra of endogenous fields will have to be measured concurrently with an MBE.

### 3.7.4 On the bandwidth of a resonance-like response

It is seen in Fig. 3.11 that there is some resonance width caused by the fact that the measurement time  $T$  is limited. Such a broadening also occurs in the absence of damping factors. The peak, or maximum, width is about  $\Delta\Omega = 2\pi/T$ . In the ideal case of infinite measurement time  $T = \infty$ , the width becomes zero, as the case should be for the ideal oscillator without damping.

The damping, or relaxation, is often taken into consideration *phenomenologically* by including into a particle’s equation of motion an additional friction force, which is proportional with the velocity, e.g., the term  $-\mathbf{U}/\tau$  on the right-hand side of (3.7.5). That yields an additional factor of the broadening of the resonance curve.

It is impossible to know beforehand which of the two broadening factors will prevail. In magnetobiological experiments the measurement time  $T$  is not totally controlled by the researcher, so that it cannot be made arbitrarily long. The time-limiting capability is passed over to a biological system under study, or rather to those biochemical processes that are involved in the interaction with a particle, the primary target for an MF. The measurement time  $T$  here should be taken to be the characteristic communication time during which a biophysical or biochemical system “enables” the primary oscillator, an MF receptor, to accumulate the MF energy or, more generally, to stay at a state that is in phase with the MF. We can talk here about the time of the coherent interaction of the particle with the MF.

The characteristic time of the development of biochemical processes, from split seconds to minutes, seems to be able to substantially affect the width of observed frequency responses in the low-frequency range, when the order of magnitude of the

observed frequencies is comparable with the characteristic frequency  $T^{-1}$ . This circumstance is often overlooked. For instance, in Liboff *et al.* (1987b), Lednev (1991), Blanchard and Blackman (1994), and Lednev (1996) the resonance width is only discussed in connection with the damping factor, or the oscillator attenuation.

For sufficiently large measurement times, the shape of a resonance curve or the variation of the power of forced oscillations, i.e., the squared amplitude of oscillations  $y$ , with the frequency  $\Omega$  of an external force, has the form

$$y^2 \sim (\Omega^2 + a\Omega + b)^{-1} ,$$

where  $a$   $b$  are coefficients. A similar Lorentz form is displayed by the amplitude of resonance transitions in a quantum system, see Fig.4.19. In Blackman *et al.* (1999) an attempt was made to show that the contour of the frequency dependence of an MBE experimental peak in Fig.2.25 (for five fixed frequency values) has the form of a Gaussian distribution. The authors believe that this shape should emerge in the MBE spectral peak, since the latter is the collective response of an ensemble of individual resonating systems with a random spread of parameters. We note, however, that the five points located more or less symmetrically about the maximum, as in Fig.2.25, could also be approximated by several other functions, including the Lorentz form and the interferential motif  $(\sin x/x)^2$ .

This author doesn't know of works where the width of MBE experimental spectral peaks would be given a treatment different than the damping of classical oscillators or resonance quantum transitions. For a Zeeman multiplet there are no resonance transitions induced by uniaxial MFs, and then, since there is no resonance, the very idea of resonance width becomes void. At the same time, the broadening of spectral peaks due to the limited time of coherent interaction, or the communication time, has a general nature and manifests itself irrespective of the physical nature of the spectra.

### 3.8 PARAMETRIC RESONANCE IN MAGNETOBIOLOGY

#### 3.8.1 Parametric resonance of a free particle in an MF

The binding of ions or macromolecules with their receptors in terms of the classical dynamics of a particle in an MF was studied by Chiabrera *et al.* (1985). In a DC MF, the motion of a free particle is finite, and there is no time-averaged displacement of the particle. Studied was the case of the parallel orientation of a DC and an AC MF

$$H = H_{DC} + H_{AC} \cos(\Omega t) .$$

It was shown that if the frequency of an AC MF is the  $n$ th subharmonic of the cyclotron frequency of a particle, then the MF is responsible for a constant component in the particle's displacement. The authors believe that this affects the probability for a ligand to be found with a receptor. The displacement has been obtained as a combination of the Bessel functions of order  $n$ ,  $n + 1$ , and  $n - 1$ . It is

noteworthy that if  $n = 1$ , i.e., if the field frequency equals the cyclotron frequency, then the first *zero* of the response function emerges at a definite DC-to-AC field amplitude ratio  $H_{AC}/H_{DC} \sim 1.85$ , with a maximum at  $H_{AC}/H_{DC} \sim 0.9$ . Applying that model to the  $\text{Ca}^{2+}$  ion enabled the model to be correlated with Blackman's data on MBEs obtained at various frequencies and at various  $H_{AC}/H_{DC}$  ratios. That seems to have been the first ever, although fairly imperfect, model of magnetosensitive binding of ions.

We will provide the derivation of a relationship for the velocity, rather than for the ion displacement, in the notation of that book, and using a procedure that is in a way somewhat simpler than that in Chiabrera *et al.* (1985). That work considered the motion of an ion in the  $x$ - $y$  plane in a magnetic field  $\mathbf{H} \perp z$ , in the limiting case of very small damping. We will write the equations of motion for a particle under the Lorentz force in coordinate form, where  $x$  and  $y$  below are *velocity* components,

$$\dot{x} = f + gy, \quad \dot{y} = -gx, \quad f = qE(t)/M, \quad g = qH(t)/Mc, \quad (3.8.1)$$

where an electric field is along the  $x$  axis. Mathematically, (3.8.1) is the Hill set of equations, and its special solutions are a parametric resonance.

An implicit assumption in Chiabrera *et al.* (1985) was that the area of motion for a particle is small in comparison with the size of the source of a homogeneous MF. Only in that case can one suppose that the induced electric field on the particle is independent of the particle coordinates (see Section 1.4.1), a fact that is reflected in the form of Eq. (3.8.1). With no loss of generality, the field  $\mathbf{E}$  can be viewed as directed along the  $x$  axis and having the strength

$$E = \frac{R}{c} \frac{dH}{dt}.$$

Here  $R$  is the constant that characterizes the size of the MF source, the scalar field potential being assumed to be zero.

The solution (3.8.1) can be easily found by the method of the variation of constants. We will write the equations in matrix form

$$\dot{\mathbf{u}} = \mathbf{A}\mathbf{u} + \mathbf{B}, \quad \mathbf{u} = \begin{pmatrix} x \\ y \end{pmatrix}, \quad \mathbf{A} = \begin{pmatrix} 0 & g \\ -g & 0 \end{pmatrix}, \quad \mathbf{B} = \begin{pmatrix} f \\ 0 \end{pmatrix}. \quad (3.8.2)$$

There are two linearly independent solutions of the appropriate homogeneous ( $B = 0$ ) equation:

$$\mathbf{u}_1 = \begin{pmatrix} \sin w \\ \cos w \end{pmatrix}, \quad \mathbf{u}_2 = \begin{pmatrix} \cos w \\ -\sin w \end{pmatrix}, \quad w = \int g dt.$$

The solution (3.8.2) will be found in the form  $\mathbf{u} = c_1\mathbf{u}_1 + c_2\mathbf{u}_2$ . Substituting the solution into that equation gives for the coefficients  $c$

$$\dot{c}_1 \sin w + \dot{c}_2 \cos w = f, \quad \dot{c}_1 \cos w - \dot{c}_2 \sin w = 0,$$

which has the obvious solution  $\dot{c}_1 = f \sin w$ ,  $\dot{c}_2 = f \cos w$  or

$$c_1 = \int f \sin w dt, \quad c_2 = \int f \cos w dt. \quad (3.8.3)$$

It follows from the form of  $\mathbf{u}$  that the velocity components can be written as

$$x = c_1 \sin w + c_2 \cos w, \quad y = c_1 \cos w - c_2 \sin w.$$

We will then find that the squared velocity modulus is  $v^2 = x^2 + y^2 = c_1^2 + c_2^2$ . That could be written as the sum of squared real and imaginary parts of the complex coefficient

$$v^2 = \Re^2\{c\} + \Im^2\{c\}, \quad c = \int f e^{iw} dt. \quad (3.8.4)$$

Integrating  $g$ , we get

$$w = \int g dt = 2\omega_0 t + 2\omega_1 \sin(\Omega t)/\Omega,$$

where  $\omega_0$  and  $\omega_1$  are the Larmor frequencies, associated with the fields  $H_{DC}$  and  $H_{AC}$ , respectively. Hence, substituting into (3.8.4), introducing the notation  $z_0 = 2\omega_0/\Omega$ ,  $z_1 = 2\omega_1/\Omega$ , and using the relationship

$$e^{iz \sin \tau} = \sum_n J_n(z) e^{in\tau},$$

we find, having calculated  $f = -2\Omega\omega_1 R \sin(\Omega t)$ , after fairly simple transformations, the coefficient  $c$  in the form

$$c = -2\omega_1 R \sum_n J_n(z_1) \int \sin \tau e^{i(z_0+n)\tau} d\tau. \quad (3.8.5)$$

The integral is derived by repeated integration by parts. It will be

$$\frac{i\alpha \sin \tau - \cos \tau}{1 - \alpha^2} e^{i\alpha\tau}, \quad \alpha = z_0 + n.$$

We will ignore both the the initial conditions and the fact that the system observation time is finite, since we only desire to illustrate the general nature of the response. The expression for the integral suggests that under resonance conditions,  $\alpha = \pm 1$ , the coefficient  $c$  and the particle velocity grow indefinitely. It is seen that the terms of the sum in (3.8.5) decline quickly with  $n$  due to the integral properties. In our estimates we will confine ourselves to two terms that make the most contribution; their numbers  $n$  can be worked out from  $z_0 + n = \pm 1$ . Then the real and imaginary parts of the coefficient  $c$  will be

$$\Re\{c\} = -\omega_1 R J_n(z_1) \sin^2 \tau, \quad \Im\{c\} = \omega_1 R J_n(z_1) (\sin \tau \cos \tau - \tau), \quad \tau = \Omega t.$$

Hence the squared velocity averaged over a large time interval becomes

$$\langle v^2 \rangle = \omega_1^2 R^2 J_n^2(z_1) \langle \sin^4 \tau + \sin^2 \tau \cos^2 \tau + \tau^2 - 2\tau \sin \tau \cos \tau \rangle.$$

The input of the first two terms is 1/2, and that of the last term is zero. The input of the term  $\tau^2$  reflects the unlimited growth of velocity under resonance conditions  $z_0 + n = \pm 1$  in the absence of damping.

A part of the mean square velocity is of interest that varies in a non-trivial manner with the MF amplitude. We will agree to call that part magnetodependent. It is

$$\langle v^2 \rangle \approx \frac{1}{2} \omega_1^2 R^2 J_n^2(z_1) .$$

With a DC MF fixed, the frequency of (parametric) resonance, given by  $z_0 + n = \pm 1$ , is equal for two above-mentioned terms (3.8.5)  $\Omega = -2\omega_0/(1+n)$  and  $\Omega = 2\omega_0/(1-n)$ . If the MF frequency  $\Omega$  is selected so that its modulus equals that of the Larmor frequency, then the appropriate values of  $n$  will be 1 and  $-1$ , and the values of the argument  $z$  will be  $-2\omega_1/\omega_0$  and  $2\omega_1/\omega_0$ . However, since for real arguments and integer  $n$  the Bessel functions satisfy the equalities  $J_n^2(-z) = J_n^2(z)$  and  $J_{-n}^2(z) = J_n^2(z)$ , then both terms will make equal inputs to the mean square velocity. Since  $\omega_1/\omega_0 = H_{AC}/H_{DC}$ , then

$$\langle v^2 \rangle \sim \omega_1^2 R^2 J_1^2 \left( 2 \frac{H_{AC}}{H_{DC}} \right) . \quad (3.8.6)$$

This formula is a fairly good illustration of the variation of the velocity with MF parameters. The fact that this function more or less fits experimental data in Fig. 2.11 seems to be a coincidence. The magnetodependent part of the squared velocity does not exceed  $\omega_1^2 R^2$ . Consequently, the change in the energy, or rather its part that depends in a multipeak manner on the AC MF amplitude, does not exceed  $d\varepsilon \sim MVdV$ , where  $V$  is the particle velocity, and  $dV = \omega_1 R$  is the change of the velocity in the induced electric field. If we assume that the ion was at first moving with a thermal velocity, then the relative change in its energy is easily seen to be limited by  $d\varepsilon/\kappa T \sim 10\%$ . That might be of interest, if it were not for the fact that at thermal velocity the area of the ion motion of about the cyclotron radius in the geomagnetic field is much higher than not only the size of a biological cell, but also the reasonable size  $R$  of an MF source. That makes the above treatment invalid due to the initial form of the equations irrespective of the size of a biological system. Moreover, interaction with ambient molecules leads not to processes that could be described by phenomenological damping, but rather to the Brownian motion of ions. To all intents and purposes, that leaves no hope that the response to an MF signal in any dynamic parameter of the ion will accumulate.

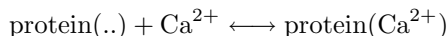
In order to circumvent that difficulty, Chiabrera and Bianco (1987) proposed that the motion (flat) of a charged particle, such as an ion, hormone, or antigen, be considered at a binding site, where, according to the authors, the intensity of thermalizing collisions with water molecules is small because these latter are forced out of the binding area by hydrophobic forces. However, the residence or "flight" time for a free particle in such an area is small, and so the mechanism under consideration has no time to develop properly. After all, for the averaged velocity and displacement to have a meaning, it is necessary for the averaging time to cover at least several periods of cyclotron motion. At ion thermal velocities such a motion scale will in any case be much larger than the binding site size. The metastable motion of an ion with small non-thermal energy could occur within some molecular

cavity protecting from thermal perturbations, but then no equations of free motion will be applicable.

The work (Chiabrera *et al.*, 1985) was not without its positive influence. It showed for the first time that some parameters of the motion of a charge, specifically of a  $\text{Ca}^{2+}$  ion, in a combined MF are, in a complicated manner, e.g., via Bessel functions, dependent on the *ratio of the amplitude of an AC MF and the magnitude of a DC MF*. Clearly, the model is no good for real motions of ions in biological structures. This notwithstanding, the presence in the model of amplitude and frequency efficiency windows for an MF, which are a good match to the experimentally observed windows, suggested that the search for MBE mechanisms associated with ion dynamics holds promise. Later, Lednev (1991) drew attention that such involved dependences on the parameter  $H_{\text{AC}}/H_{\text{DC}}$  emerge when optical radiation is dispersed by an atomic system exposed to an MF. That occurs owing to transitions in quantum states of a bound atomic electron. For ions confined within the binding cavities of some proteins, Lednev assumed that their dynamics could also follow some parametric resonance patterns in an atomic system. That idea is considered in Section 3.8.3.

Since the model (Chiabrera *et al.*, 1985) uses the equations of classical dynamics to describe the microscopic motion of an ion, it is unable to describe some effects observed in experiments. The model predicts response maxima at a cyclotron frequency and its subharmonics, and does not predict peaks at harmonics and subharmonics of those harmonics. Such predictions are shown in Chapter 4, to yield a mechanism of ion interference.

Lednev (1991) assumed that an MF causes a parametric resonance of a  $\text{Ca}^{2+}$  ion bound with some proteins (calmodulin, proteinkinase C, etc.). Therefore, an MF shifts an equilibrium of the reaction



and causes the response observed. In a model that described the influence of an MF on a bound  $\text{Ca}^{2+}$ , the author used the analogy with the phenomenon of paramagnetic resonance known in atomic physics. When one modulates an MF with a frequency  $\Omega$  close to the time-averaged frequency difference  $\Delta\omega$  of Zeeman sublevels of the particle, the intensity of spontaneous luminescence excited by a wide-band electromagnetic radiation, generally of optical range, also appears to be modulated with a frequency  $\Omega$ . The modulation depth attains a maximum at  $\Omega = \Delta\omega/n$ ,  $n = 1, 2, \dots$

The author postulated that the magnitude of the biological effect in an MF is approximately described by the relation for the radiation intensity or the probability of spontaneous radiative transitions in a particle ensemble. Underlying that postulate was the fact that in certain magnetobiological experiments the effect plotted as a function of the AC MF amplitude could be well approximated by the parametric resonance formulas of atomic spectroscopy.

Liboff guessed the connection of experimental frequency spectra with cyclotron frequencies of ions and attempted, therefore, to draw on cyclotron resonance the-

ory to account for the MBE. Likewise, Lednev divined the association of observed amplitude spectra with the Bessel-type dependences in atomic parametric resonance and tried to draw on that theory to account for the experimental evidence. Later on various forms of the idea were discussed by various authors in the literature (Adair, 1992; Blanchard and Blackman, 1994; Blackman *et al.*, 1994; Engström, 1996; Zhadin, 1996), but no consensus has been reached so far (Lednev *et al.*, 1997; Blackman *et al.*, 1997). This seems to be due to the fact that the authors, except for Zhadin (1996), relied in their reasoning on an oversimplified illustration of the parametric resonance theory in atomic spectroscopy, sort of overlooking the physical content of the effect. To perceive the essence of the differences it would perhaps make sense to lay down the theory of parametric resonance in atomic spectroscopy in more detail.

### 3.8.2 Parametric resonance in atomic spectroscopy

Let us consider the so-called parametric resonance in atomic spectroscopy (Alexandrov *et al.*, 1991), abiding, where appropriate, by the terminology and notation of that monograph. We will arrive at the main properties of that effect using the simple example of a three-level atomic system in the field of an exciting electromagnetic irradiation, normally of optical range, in a combined low-frequency MF.

Common idealizations consist in that (1) the exciting irradiation is constant in time and has a constant spectral density within a fairly wide frequency band, the spectral components being  $\delta$ -correlated; (2) the absorption and spontaneous emission of an electromagnetic wave are independent processes; (3) the perturbation introduced by the wave is small, so that the population of the ground level can be taken to be constant, and that of the excited levels to be relatively small; (4) the excited level splits in a magnetic field  $H(t)$  into a Zeeman doublet, Fig. 3.12; and (5) the Raman scattering is small.

Let an electron state in an atom be a superposition of eigenstates  $|k\rangle$  of the Hamiltonian  $\mathcal{H}_0$

$$\Psi = \sum_k c_k(t) |k\rangle .$$

The intensity of spontaneous emission from levels 1 and 2 to level 0 is determined by populations of the states,  $|c_k|^2$ , and also by other elements of the density matrix

$$\sigma_{nk} = c_n^* c_k .$$

Since the amplitude of the electric field of the emitted wave, in the transition from a ground state  $|n\rangle$  to a state  $|0\rangle$ , is proportional to the matrix element

$$E_{0n} \propto \langle 0 | \mathbf{d} \mathbf{e} | n \rangle ,$$

where  $\mathbf{d}$  is the operator of the electric dipole moment of an atomic electron and  $\mathbf{e}$  is the polarization vector of the emitted wave, then the amplitude of the superposition of the waves emitted from levels 1 and 2 is

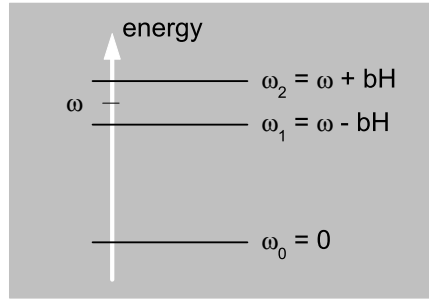


**Figure 3.12.** The diagram of the energy levels of an idealized quantum system.

$$E \propto \sum_n c_0^* c_n \langle 0 | \mathbf{d} \mathbf{e} | n \rangle ,$$

and the intensity of the wave  $I = E^* E$  is

$$I \propto c_0^* c_0 \sum_{nk} \sigma_{nk} G_{nk} , \quad (3.8.7)$$

where  $G_{nk} = \langle 0 | \mathbf{d} \mathbf{e} | n \rangle \langle 0 | \mathbf{d} \mathbf{e} | k \rangle^*$  is the so-called observation matrix. We note that in addition to terms that vary with the population of levels 1 and 2, i.e.,  $\sigma_{11}$  and  $\sigma_{22}$ , which determine the invariable part of the radiation intensity, this expression includes the cross-terms  $\sigma_{12}$ ,  $\sigma_{21}$ , concerned with the interference of waves emitted from levels 1 and 2. Those terms make a contribution to the intensity that is governed by magnetic conditions.

Let an atomic system be subjected to a field of a wide-band electromagnetic radiation, and the perturbation operator look like

$$\mathcal{V} = \mathbf{d} \mathbf{E}(t) , \quad \mathbf{E}(t) = \mathbf{e} \int E_\omega \exp(-i\omega t - i\varphi_\omega) d\omega + \text{c.c.} \quad (3.8.8)$$

Here  $E_\omega$  and  $\varphi_\omega$  are the amplitude and phase of spectral components, and  $\mathbf{e}$  is the polarization vector for the external radiation.

The dynamic equation for the density matrix, known as the Liouville quantum equation,  $i\hbar \dot{\hat{\sigma}} = [\mathcal{H}_0 \hat{\sigma}]$  written in matrix form in the  $|n\rangle$  representation is

$$i\hbar \dot{\sigma}_{nk} = \sum_m [(\mathcal{H}_0)_{nm} \sigma_{mk} - \sigma_{nm} (\mathcal{H}_0)_{mk}] .$$

Considering the equality  $\mathcal{H}_0 |n\rangle = \hbar\omega_n |n\rangle$ , which can also be written as  $(\mathcal{H}_0)_{nm} = \hbar\omega_n \delta_{nm}$ , this leads to the equation for the density matrix elements with coefficients  $\omega_{nk} = \omega_n - \omega_k$ :

$$\dot{\sigma}_{nk} = -i\omega_{nk} \sigma_{nk} .$$

In terms of perturbation  $\mathcal{V}$  and phenomenological damping introduced by the additional term  $-\Gamma_{nk} \sigma_{nk}$ , the equation becomes

$$\dot{\sigma}_{nk} = -(\Gamma_{nk} + i\omega_{nk})\sigma_{nk} - \frac{i}{\hbar} \sum_m (\mathcal{V}_{nm}\sigma_{mk} - \sigma_{nm}\mathcal{V}_{mk}) . \quad (3.8.9)$$

We will at first consider elements with  $n = 0$ ,  $k \neq 0$ . Since in the spectrum  $\mathcal{V}$  contains no low-frequency components, the elements  $\mathcal{V}_{nk}$  are only non-zero for the transitions between ground and excited states. Then

$$\dot{\sigma}_{0k} = -(\Gamma_{0k} + i\omega_{0k})\sigma_{0k} - \frac{i}{\hbar} \sum_{m=1}^2 \mathcal{V}_{0m}\sigma_{mk} + \frac{i}{\hbar}\sigma_{00}\mathcal{V}_{0k} .$$

Due to postulate (3) we can ignore the term  $\sim \sum_{m=1}^2 \mathcal{V}_{0m}\sigma_{mk}$ , and take  $\sigma_{00}$  to be a constant. We have

$$\dot{\sigma}_{0k} = -(\Gamma_{0k} + i\omega_{0k})\sigma_{0k} - \frac{i}{\hbar}\sigma_{00}\mathcal{V}_{0k} .$$

A solution to the equation  $\dot{\sigma} = f\sigma + g(t)$ , where

$$f = -(\Gamma_{0k} + i\omega_{0k}) , \quad g(t) = -\frac{i}{\hbar}\sigma_{00}\mathcal{V}_{0k} , \quad (3.8.10)$$

has the form

$$\sigma = e^{ft} \left( C + \int e^{-ft} g dt \right) . \quad (3.8.11)$$

We will simplify the situation by setting the initial conditions so that  $C = 0$ . Since in (3.8.10)

$$\mathcal{V}_{0k} = v_{0k} \int E_\omega \exp(-i\omega t - i\varphi_\omega) d\omega + \text{c.c.} , \quad v_{0k} \equiv (\mathbf{de})_{0k} , \quad (3.8.12)$$

then the integral in the solution will be

$$\frac{-i}{\hbar}\sigma_{00} \int \exp(\Gamma_{0k}t + i\omega_{0k}t) \left[ v_{0k} \int E_\omega \exp(-i\omega t - i\varphi_\omega) d\omega + \text{c.c.} \right] dt .$$

It contains the exponential functions  $\exp[i(\omega_{0k} - \omega)t]$  and  $\exp[i(\omega_{0k} + \omega)t]$ . The fast-oscillating term is insignificant; therefore taking the time integral gives

$$\int e^{-ft} g(t) dt = \frac{i}{\hbar}\sigma_{00}v_{0k} \int E_\omega \frac{\exp\{[\Gamma_{0k} + i(\omega_{0k} - \omega)]t - i\varphi_\omega\}}{\Gamma_{0k} + i(\omega_{0k} - \omega)} d\omega ,$$

which on substituting into (3.8.11) yields

$$\sigma_{0k} = \frac{i}{\hbar}\sigma_{00}v_{0k}E \int \frac{\exp(-i\omega t - i\varphi_\omega)}{\Gamma_{0k} + i(\omega_{0k} - \omega)} d\omega . \quad (3.8.13)$$

Hence we have

$$\sigma_{n0} = \sigma_{0n}^* = \frac{-i}{\hbar}\sigma_{00}v_{0n}^*E \int \frac{\exp(i\omega t + i\varphi_\omega)}{\Gamma_{0n} - i(\omega_{0n} - \omega)} d\omega . \quad (3.8.14)$$

We assume in (3.8.13) and (3.8.14) that the spectral density  $E_\omega = E$  is constant in the range of interest to us.

We now consider the elements of the density matrix for excited states  $n \neq 0$ ,  $k \neq 0$ . In that case, what remains of the sum over  $m$  (3.8.9) is the only term  $m = 0$ , since the remaining terms contain multipliers  $\mathcal{V}_{mn} = 0$ :

$$\dot{\sigma}_{nk} = -(\Gamma_{nk} + i\omega_{nk})\sigma_{nk} - \frac{i}{\hbar}(\mathcal{V}_{n0}\sigma_{0k} - \sigma_{n0}\mathcal{V}_{0k}) . \quad (3.8.15)$$

We introduce the notation

$$b^\pm \equiv \int \exp[\pm i(\omega t + \varphi_\omega)] d\omega , \quad c_{0k}^\pm \equiv \int \frac{\exp[\pm i(\omega t + \varphi_\omega)]}{\Gamma_{0k} \mp i(\omega_{0k} - \omega)} d\omega .$$

In terms of that notation, we will rewrite (3.8.12), (3.8.13), and (3.8.14) in the form

$$\begin{aligned} \mathcal{V}_{0k} &= E v_{0k} b^- + E v_{0k}^* b^+ , & \mathcal{V}_{n0} &= \mathcal{V}_{0n}^* = E v_{0n}^* b^+ + E v_{0n} b^- \\ \sigma_{0k} &= \frac{i}{\hbar} \sigma_{00} E v_{0k} c_{0k}^- , & \sigma_{n0} &= -\frac{i}{\hbar} \sigma_{00} E v_{0n}^* c_{0n}^+ . \end{aligned}$$

We can now write the perturbation in Eq. (3.8.15)

$$-\frac{i}{\hbar}(\mathcal{V}_{n0}\sigma_{0k} - \sigma_{n0}\mathcal{V}_{0k}) = \frac{E^2\sigma_{00}}{\hbar^2} [2\Re(v_{0n}v_{0k}b^-c_{0k}^-) + v_{0n}^*v_{0k}(b^+c_{0k}^- + b^-c_{0n}^+)] .$$

The term  $\Re(\dots)$  contains a fast-oscillating factor, which we will omit. The expression in the brackets in the second term is

$$\begin{aligned} &\iint \left[ \frac{\exp[i(\omega't + \varphi_{\omega'})] \exp[-i(\omega t + \varphi_\omega)]}{\Gamma_{0k} + i(\omega_{0k} - \omega)} \right. \\ &\quad \left. + \frac{\exp[-i(\omega't + \varphi_{\omega'})] \exp[i(\omega t + \varphi_\omega)]}{\Gamma_{0n} - i(\omega_{0n} - \omega)} \right] d\omega' d\omega . \end{aligned}$$

Since  $\varphi_\omega$  is a  $\delta$ -correlated random function of frequency, i.e.,  $\overline{\varphi_{\omega'}\varphi_\omega} \sim \delta(\omega' - \omega)$ , the last integral reduces to

$$\int \left[ \frac{1}{\Gamma_{0k} + i(\omega_{0k} - \omega)} + \frac{1}{\Gamma_{0n} - i(\omega_{0n} - \omega)} \right] d\omega .$$

Integration<sup>24</sup> of each of the terms using  $\int_{-\infty}^{\infty} (1+x^2)^{-1} dx = \pi$  gives  $\pi$ . Therefore, the perturbation in (3.8.15), caused by the pumping matrix, is equal to

$$\frac{2\pi E^2\sigma_{00}}{\hbar^2} v_{0n}^* v_{0k} \equiv F_{nk} , \quad (3.8.16)$$

and is here independent of time. Thus the equation for the cross terms of the density matrix looks like

---

<sup>24</sup>Since the integration is within the limits  $(-\infty, \infty)$ , then, for instance, the first integral is independent of  $\omega_{0k}$ . It can be reduced to a sum of terms  $\Gamma \int (\Gamma^2 + \omega^2)^{-1} d\omega$  and  $i \int (\Gamma^2 + \omega^2)^{-1} \omega d\omega$ , where the second term contains under the integral a product of odd and even functions, and hence is zero.

$$\dot{\sigma}_{nk} = -(\Gamma_{nk} + i\omega_{nk})\sigma_{nk} + F_{nk} . \quad (3.8.17)$$

Suppose now that the modulation of a DC MF is on, so that the frequency of the Zeeman transition  $\omega_{nk}$ , a parameter in (3.8.17), becomes a periodic function of time with an external modulating field frequency  $H_{AC} \cos(\Omega t)$ :

$$\omega_{nk} = 2bH(t) = \omega_{nk}^0 (1 + h' \cos(\Omega t)) , \quad \omega_{nk}^0 = 2bH_{DC} , \quad h' = \frac{H_{AC}}{H_{DC}} .$$

In this case as well, the derivation of Eq. (3.8.17) remains valid due to the inequality  $\Omega \ll \omega_{0n}$ . All the quantities in (3.8.17) have identical indices; therefore it is convenient to discard them. Now the equation becomes

$$\dot{\sigma} = -\{\Gamma + i\omega^0 [1 + h' \cos(\Omega t)]\} \sigma + F . \quad (3.8.18)$$

Its solution has the form

$$\sigma = e^{\int g dt} \left( C + F \int e^{-\int g dt} dt \right) , \quad g = -\Gamma - i\omega^0 [1 + h' \cos(\Omega t)] . \quad (3.8.19)$$

We introduce the notation

$$x = \Gamma + i\omega^0 , \quad z = h' \frac{\omega^0}{\Omega} \quad (3.8.20)$$

and take the integral in the exponent:

$$\int g dt = -xt - iz \sin(\Omega t) .$$

Substitution into (3.8.19) at  $C = 0$  and accounting for  $\exp[iz \sin(\Omega t)] = \sum_n J_n(z) \exp(in\Omega t)$  leads, after some straightforward transformations, to

$$\sigma = F \sum_{nm} J_n(z) J_m(z) \frac{\exp[i(n-m)\Omega t]}{x + in\Omega} . \quad (3.8.21)$$

The radiation intensity (3.8.7), related to the cross terms of the density matrix, varies with

$$\tilde{I} \propto \sigma_{12} G_{12} + \sigma_{21} G_{21} = 2\Re(\sigma_{12} G_{12}) . \quad (3.8.22)$$

Assuming  $G_{12} \equiv G \exp(i\gamma)$ , using the formula

$$\Re \left( \frac{z_1}{z_2} \right) = \frac{\Re(z_1)}{\Re(z_2)} \cos(\arg z_1 - \arg z_2)$$

and substituting (3.8.21) into (3.8.22), we can easily obtain the relation

$$\tilde{I} \propto GF \sum_{nm} J_n(z) J_m(z) \frac{\cos \left[ (n-m)\Omega t - \arctan \left( \frac{\omega^0 + n\Omega}{\Gamma} \right) + \gamma \right]}{\left[ \Gamma^2 + (\omega^0 + n\Omega)^2 \right]^{\frac{1}{2}}} .$$

This quantity seems to have maxima<sup>25</sup> at subharmonics of the unperturbed transition frequency

$$\Omega_{\max} = -\omega^0/n, \quad (3.8.23)$$

proportional to the electron cyclotron frequency in a magnetic field  $H_{\text{DC}}$ .

On average, over a fairly large time interval  $T \gg \Omega^{-1}$ , all the time-dependent series terms, i.e. the terms with  $n \neq m$ , vanish. The remaining terms produce, at the frequency of the main maximum  $\Omega = -\omega^0$ , an input

$$\bar{I} \propto GF \sum_n J_n^2(h') \frac{\cos \left[ \gamma - \arctan \left( \frac{\omega^0(1-n)}{\Gamma} \right) \right]}{\left[ \Gamma^2 + \omega^{02}(1-n)^2 \right]^{\frac{1}{2}}}. \quad (3.8.24)$$

This series converges quickly; therefore the dependence of the relative MF amplitude  $h'$  is mainly determined, as is seen from the denominator in (3.8.24), by the term  $n = 1$ :

$$\bar{I} \propto J_1^2(h'). \quad (3.8.25)$$

This expression attains the first maximum at  $h' \approx 1.8$ .

We note that at the first subharmonic frequency  $\Omega = -\omega^0/2$  the denominator in (3.8.24) is

$$\left[ \Gamma^2 + \omega^{02} \left( 1 - \frac{n}{2} \right)^2 \right]^{\frac{1}{2}}.$$

Hence the amplitude dependence, subject to (3.8.20), will look like

$$\bar{I} \propto J_2^2(2h') \quad (3.8.26)$$

with a maximum in the region of  $h' \approx 1.5$ .

The relations (3.8.23) and (3.8.25) have attracted some attention as possible explanations of the primary mechanism of some MBEs. Similar dependences have been observed in experiments with biological systems subjected to weak combined parallel MFs. The works (Lednev, 1991; Blanchard and Blackman, 1994) are attempts to illustrate these relations using some oversimplified reasoning, which is erroneous.

The form of the dependence of  $\bar{I}$  on the frequency at around maxima, i.e., the shape of the spectral peaks, is determined mainly by the Lorentz factor

$$\left[ \Gamma^2 + (\omega^0 + n\Omega)^2 \right]^{-\frac{1}{2}}. \quad (3.8.27)$$

It can be easily found that the peak width is about  $\Gamma$ . On the other hand, the spectral peak at frequency  $-\omega^0$  will be resolved, if its width is at least smaller

---

<sup>25</sup>In what follows if the index max is attached to some symbol that is a frequency or an MF, this means the presence of a maximal effect at that frequency or at the indicated value of the MF. For other physical quantities the max index will imply, as usual, their maximal values.

than  $|\omega^0|$ , i.e., if  $\Gamma < \omega^0$ . As is seen from (3.8.9), the quantity  $\Gamma^{-1}$  has a physical meaning that is close to the lifetime of excited states  $\tau$  of the Zeeman doublet. This imposes some constraints on the lifetime of excited states, which makes it possible to observe the effect, i.e., the variations in the intensity of scattered light

$$\tau > 1/\omega^0 . \quad (3.8.28)$$

The concept of parametric resonance in atomic spectroscopy, however, is associated precisely with the modulation of the scattered light intensity, rather than with the modulation magnitude, which has a maximum at the Zeeman frequency splitting. The methods of the registration of harmonic signal amplitude in physical measurements are well developed; therefore the constraint (3.8.28) does not hinder the observation of the modulation fact, although the modulation depth in itself can be fairly small, for instance  $10^{-3}$ . This notwithstanding, some measures are taken to properly prepare an atomic ensemble in the form of rarefied gas in a strong MF. The gas being rarefied increases the lifetime of states, and a strong MF increases the splitting frequency of the Zeeman doublet, so that relation (3.8.28) is close to being met. If an experiment is only capable of observing the mean intensity, when modulation oscillations are ironed out, then constraint (3.8.28) prevails.

The amplitude of forced oscillations of the density matrix elements grows at certain frequencies  $\Omega$ . Mathematically, that is, by definition, a parametric resonance. Physically, the usage of the term “parametric resonance” in this case is rather a convention, and the correct meaning of the effect, as noted in Alexandrov *et al.* (1991), is concerned with the parametric modulation of scattered radiation. In relation to processes in quantum systems the term “resonance” is only applied where the frequencies of an external radiation and of a quantum transition coincide. In the process, transition probabilities jump sharply, which manifests itself as an increase in the intensity of energy exchange of an atomic system with an electromagnetic field, i.e., of the intensity of absorption and emission of electromagnetic waves.

In the case under discussion of the wideband electromagnetic radiation that affects an atomic system, all the optical transitions appear to be saturated. It is this circumstance that is reflected by fact that the pumping matrix elements are constant. On the other hand, the integral intensity of spontaneous emission in all direction is constant as well. The modulation of the intensity of re-emitted waves shows up when an atomic system is observed at an angle that is defined by the observation matrix. The reason the intensity changes is the interference of waves emitted from Zeeman sublevels of the system. As the emission intensity is reduced in one direction, it is increased in another direction, so that the total power of scattered radiation is constant.

Thus, with parametrically modulated intensity of scattered radiation, the intensity of the energy exchange of an atomic system with an electromagnetic field is permanent, so that a resonance can only be referred to in some conventional meaning. The picture remains the same, if we look at another, non-electromagnetic factor of perturbation in a system. For instance, thermal collisions of an atom with the environment reduce to a series of  $\delta$ -like perturbations within a high accuracy. Since

these perturbations feature a continuous wideband spectrum within the frequency range under consideration, then all the relationships are derived in a similarly manner. In this case we should talk about the constancy of the energy exchange with the environment rather than with the electromagnetic field.

### 3.8.3 Ion parametric resonance

If we know what atomic parametric resonance is about, we can easily see to what extent its use in magnetobiological models is justified.

Consider at first the attempt of Blanchard and Blackman (1994) to refine the formula proposed in Lednev (1991) for the amplitude spectrum, relying on the same analogy with a spectroscopic parametric resonance. Re-emitting atomic electrons exposed to a variable MF and to optical radiation were identified with ions contained in protein capsules and excited by thermal oscillations of capsule walls.

The authors believe that a uniaxial MF brings about a change in the populations of ionic quantum states. As has been pointed out above, the mean radiation intensity in an atomic parametric resonance only changes in definite directions. The integral radiation intensity is constant, and so are the populations of the emitting Zeeman levels. The populations are in a dynamic equilibrium. Let us consider the population  $\sigma_{nn}$  of some excited levels, see (3.8.17). Since the frequency difference is  $\omega_{nn} = 0$ , the equation reduces to

$$\dot{\sigma}_{nn} = -\Gamma_{nn}\sigma_{nn} + F_{nn} ; \quad (3.8.29)$$

i.e., it contains no time-dependent parameters at all. The equilibrium constant value of populations  $\sigma_{nn}(\infty) = F_{nn}/\Gamma_{nn}$  is determined by the balance of pumping and relaxation factors and is independent of the MF.

The above argument “covers” those models built by analogy with atomic parametric resonance that relate the bioeffect intensity to the variation of the populations of quantum ion states in a variable MF. The authors attempt to retain the apparent positive assets of the analogy, which consist in the similarity of the amplitude spectra, and assume the connection of the bioeffect with another physical factor, the mean intensity of ion spontaneous electromagnetic emission. So, an account of the biological action of a low-frequency EMF boils down to the assertion that radio-frequency EMFs possess such an action.<sup>26</sup> However, its mechanisms are also unclear as yet.

Further, the authors (Blanchard and Blackman, 1994) go on to expand the list of potentially meaningful ions to include atoms that form covalent bonds with protein structures: V, Mn, Cu, Ni, Co, and others. The exercise itself makes sense, but when determining cyclotron frequencies the authors assume the charges of those atoms to be equal to their valences, which is not exactly the case. For atoms that form ion bonds, the charge is a well-defined quantity. We can only determine in terms of electron charges the effective charge of covalently bound atoms, which, due to strong redistribution of the electron density, is markedly different from valence.

---

<sup>26</sup>The frequency of ion dipole transitions in a capsule is about  $10^{10}$  Hz.

The important positive meaning of the works (Blanchard and Blackman, 1994; Blackman *et al.*, 1994) consists in that they pay attention to the presence of a body of experimental evidence, where the dependence of the bioeffect on the ratio  $h' = H_{AC}/H_{DC}$  at a maximum in the frequency  $\Omega$  variation corresponds to the function  $J_n(2nh')$ , rather than to  $J_n(nh')$ , as is the case in Lednev (1991).

The assumption that the intensity of a bioeffect when exposed to an MF can be approximated by a formula for the radiation intensity or probability of spontaneous radiative transitions of a particle ensemble was criticized in Adair (1992) and Engström (1996). The authors of these works made an attempt to prove, without drawing on parametric resonance theory, that thermal perturbations make the proposed mechanism unworkable at room temperature 300 K. In so doing, they seem to have relied on the fact that the mechanism was workable in the absence of thermal perturbations, i.e., at zero temperature, but, as we have seen, the mechanism does not work irrespective of the temperature factor. The “con” arguments laid down in those works are based on the same illustrative concepts of atomic parametric resonance, as are the “pro” arguments of the inventors of the model itself, and so they are unsuitable as well.

Adair (1992) has long been exploiting the idea that any magnetobiological effects, see Adair (1991), are impossible because those effects do not have any strict scientific explanation. To prove the invalidity of explanations available in the literature, use is made of the well-known and naive, as applied to living systems, concepts of equilibrium thermodynamics: for an effect to be observed, the energy of the perturbation caused by an MF per degree of freedom must be around  $\kappa T$ , but since that is impossible, any accounts of MBEs are doomed. Such a reasoning, however naive, seems to many to be quite convincing.

Obviously, those criticisms of the model of ion parametric resonance in magnetobiology led Lednev (1996) to come up with another account for MBE amplitude spectra. The novel explanation appeals to the peculiarities of the motion of a *classical*, rather than quantum, particle in a magnetic field, although the author retained the name “parametric resonance”. Mathematically, that holds well, but that work has nothing to do with parametric resonance as put forward earlier on in Lednev (1991), and so it will be considered in another section.

### 3.9 OSCILLATORY MODELS

Coming under this heading are both classical and quantum models in which particles move around within some space under some forces that are, as a rule, functions of oscillatory potential.

#### 3.9.1 Quantum oscillator

The two related works by Chiabrera *et al.* (1991) seem to have been the first attempt at a consistent description of ion binding under the action of collinear MFs in terms of quantum mechanics. They *formally* calculated the probability of

a transition between states  $\Psi_0$  and  $\Psi$ , the wave functions of an ion without and within an MF, respectively. The probability of such a transition and the amount of magnetic bioeffect, according to the first work, are interrelated. However, that idea is at variance with the fact that an MF, when it only acts on the phase of state  $\Psi_0$ , produces no quantum transitions. The probability of the state remains constant irrespective of the MF parameters.

In fact, the angular part of the eigenfunctions of the central potential is described in terms of spherical functions  $\sim \exp(im\varphi)$ . On the other hand, the operator of the interaction of a uniaxial MF with the orbital magnetic moment of an ion varies with  $\partial/\partial\varphi$ . Therefore, the matrix elements of the operator in states with a different magnetic quantum number contain the factor

$$\langle e^{im\varphi} | \frac{\partial}{\partial\varphi} | e^{im'\varphi} \rangle \sim \delta_{mm'} ,$$

such an operator just shifts levels depending on the magnetic number  $m$  (Zeeman splitting). If we consider states with different orbital numbers  $l$ , then the parity selection rules only allow transitions with  $l$  changing by unity. However, such states possess unlike parities; the matrix elements of the scalar interaction operators in unlike parity states are zero (Landau and Lifshitz, 1977).

The idea underlying that model is a quantum oscillator in a magnetic field. A uniaxial MF does not “mix” oscillator states; therefore the oscillation amplitude does not change.

The second article assumes that the biological effects of an MF are related to the probability for an ion to reside within an imaginary sphere that bounds the central area of the binding cavity in proteins. At the same time, no closed relations for that probability have been obtained. It is to be noted that this idea is close to that of the interference of ion quantum states in a protein cavity, which forms the core of the book. One difference is that the interference mechanism accounts here for the redistribution of the ion probability density over the angular, rather than radial, variable. It is important since the angular redistribution as compared with the radial one practically does not require energy.

### 3.9.2 Phase shifts of oscillations in an MF

Belyaev *et al.* (1994) and Matronchik *et al.* (1996a) proposed a mechanism to account for the actions of a DC and low-frequency combined MF on living cells. The mechanism relies on two main postulates: (A) a target for an MF in prokaryote cells is a nucleotide that acts as a nucleus that can be represented as a three-dimensional harmonic oscillator within the EHF range; and (B) the specific electric charge of the nucleotide varies as

$$q(t) = q_0(1 + \cos\omega_q t) .$$

To begin with, the authors look at the equation for the Lorentz force in a uniaxial MF — it coincides, up to notation, with (3.7.5) — to arrive at its approximate solution. They go on to consider the behavior of the phase of high-frequency oscillations

as the MF varies. The authors believe that if a change  $\Delta B$  in the DC MF causes a change  $\pi$ ,  $3\pi$ , ... in the phase, i.e., the phase changes up to antiphase, then such a change produces maximal bioeffects. This suggests the expression for a series of quantities

$$\Delta B \propto \frac{\omega_q}{q_0} ,$$

which yield extreme and zero effects. It is thus possible to reach a *qualitative* agreement with experiment for the same group of researchers, where cells were placed for 15 min in a space with a changed field.

Let us take a closer look at the model's postulates. A nucleoid of bacterial cells is formed by the so-called bacterial chromosome, a single ring-shaped DNA molecule that forms a compact "nucleus" about  $10^3$  Å in size. The DNA folded thread has a multitude of degrees of freedom and resides in the cell cytoplasm while changing its shape. Would it be permissible to regard the flexible thread as a point mass with 2–3 degrees of freedom?

Also unclear is the nature of the forces that are responsible for the oscillatory potential for the center of mass of a nucleoid that behaves like a high-quality EHF resonator. We can readily work out the rigidity  $c$  of the oscillator "spring" by substituting the solution  $x = \exp(i\Omega t)$  into the pendulum equation  $M\ddot{x} + cx = 0$ . The molecular mass of the nucleoid of *E. coli* being  $M \sim 10^9$  amu, the rigidity of the "spring" of an oscillator with a frequency of  $\Omega \sim 2\pi \cdot 50$  GHz would be

$$\Omega^2 M \approx 10^5 \text{ kg/s}^2 . \quad (3.9.1)$$

That is a very rigid spring, and is two orders of magnitude more rigid than the covalent hydrogen–oxygen bond. If we nevertheless admit, as a working hypothesis, that a nucleoid is a mass with three degrees of freedom on a spring with rigidity (3.9.1), then the thermal amplitude  $X$  of oscillations of the center of mass would, according to the relationship  $\Omega^2 M X^2 \sim \kappa T$ , be

$$X \sim 10^{-14} \text{ Å} .$$

This is too small a quantity even for microscales; hence postulate (A) is hardly acceptable. Apropos of postulate (B) we note that it is obligatory for the model, since the final expression for the fields  $\Delta B$ , which produced an extreme MBE, contains some parameters  $\omega_q$  and  $q_0$  of the postulate. At the same time, it is not properly substantiated. It is unclear why the charge of a large macromolecule as a whole can change in such a regular and dramatic manner.

Lastly, the very connection of the bioeffect with the variation of the phase of high-frequency oscillations is not indisputable. In essence, the authors implicitly assume that an oscillating nucleoid remembers the phase state of high-frequency oscillations and retains that information during the exposure time  $T_e$  in a changed MF, which in experiment is several minutes. Such a time coherence can only be realized for an unrealistically large oscillator quality:

$$Q \sim \Omega T_e \approx 10^{13} .$$

This is indicative of the dubious nature of the supposition.

The model has an advantage in that it displays a sophisticated correlation of oscillator phase oscillations with an MF. The idea is of value because it provides some insights into possible magnetoreception mechanisms. It does not attract any resonance energy transformations, which in any case, when activated by MFs, will be beyond comparison with the thermal scale  $\kappa\mathcal{T}$ .

### 3.9.3 Parametric resonance of a classical oscillator

The recent work by Lednev (1996) is an attempt to elaborate on the parametric resonance concept in a direction that is not concerned with parametric resonance in atomic spectroscopy.

The author views an ion as a classical particle and considers the polarization of ion oscillations in proteins. According to that view, which relies heavily on the main assumption of work (Edmonds, 1993), the variation of the activity of calcium-binding proteins in an AC MF is due to the variation of the degree of polarization of ion oscillations at a binding site within a protein. That idea, although quite attractive, was not without drawbacks, however, when realized as a specific mathematical model.

First, it was shown in Binhi (1995c) that the motion of ions in microscopic volumes, e.g., in an ion channel or a protein binding site, can hardly be described in classical, as in Lednev (1996) and Edmonds (1993), rather than in quantum terms. Second, there exists the following mathematical inaccuracy. The content of formula (17) in the original paper (Lednev, 1996)

$$p = \left( \overline{A_X^2} - \overline{A_Y^2} \right) / \left( \overline{A_X^2} + \overline{A_Y^2} \right) , \quad (3.9.2)$$

subject to formulas (12) and (13) from that article for squared oscillation amplitudes

$$A_X^2 = 2A^2 \left\{ \left[ \cos^2 \alpha (\sin \Omega t - \sin \Omega t_0) \right] \cos^2 \Omega_L (t - t_0) \right. \\ \left. + \left[ \sin^2 \alpha (\sin \Omega t - \sin \Omega t_0) \right] \sin^2 \Omega_L (t - t_0) \right\}$$

and the notation in that paper

$$\alpha = \Omega_L / \Omega , \quad \Omega_L = qB_{AC} / 2m ,$$

reduced to the functional dependence for the sought degree of polarization

$$p = p(\Omega, B_{AC}) ,$$

where  $\Omega$  is the frequency of the variable component of an MF with amplitude  $B_{AC}$ . We note that here  $p$  is independent of the magnitude of the DC MF  $B_{DC}$ . Further,

according to the author, transforming formula (3.9.2) and averaging over time, he arrived at the following expression for the polarization of ion oscillations:

$$p = J_0^2(2\alpha) \frac{1}{1 + \Omega_c^2 \tau^2} + \sum_{n=1}^{\infty} J_n^2(2\alpha) \left[ \frac{1}{1 + (n\Omega - \Omega_c)^2 \tau^2} + \frac{1}{1 + (n\Omega + \Omega_c)^2 \tau^2} \right]. \quad (3.9.3)$$

The author maintains that this formula is identical with the formula, known from the literature, for the polarization of radiation reemitted by an atomic ensemble. However, formula (3.9.3), in terms of the author's notation  $\Omega_c = qB_{DC}/m$ , reduces then to a function of another type

$$p = p(\Omega, B_{AC}, B_{DC}).$$

There is no accounting for the appearance in the function  $p$  of a new argument, the DC field  $B_{DC}$ , as a result of averaging — that would be a mathematical revelation. Formula (3.9.3) does not follow from (3.9.2).

Further, the author interprets relationship (3.9.3) and compares it with experiment. As follows from the above, however, such an explanation of magnetobiological effects is in no way concerned with the initial premises of the oscillatory model under discussion. In actual fact, the author returns to the invalid analogy with the ensemble of coherently emitting atoms in a magnetic field, since he notes that the well-known formula (3.9.3) describes the degree of polarization of atomic emission.

- Zhadin (1996) addressed the classical oscillatory dynamics of the molecular system of ligands of a binding protein cavity and a bound ion under thermal perturbations. The problem has been repeatedly posed previously. Chiabrera *et al.* (1985) and Chiabrera and Bianco (1987) obtained for the mean ion velocity some analytical expressions that show extremes at some selected frequencies and amplitudes, although no good agreement with experiment was attained. Muehsam and Pilla (1994) numerically integrated the dynamics of the ion oscillator in a binding cavity, but they did not consider the frequency and amplitude spectra.

The results obtained (Zhadin, 1996) are basically two verbal statements. One of them is that it is unlikely to get a parametric ion resonance, viewed in its orthodox sense, as a growth of the particle energy when the MF, a parameter in an appropriate equation, is modulated. One productive and in a sense opposite statement was that at MF frequencies of Larmor or cyclotron type a redistribution of the thermal oscillation energy for the ion-environment medium might emerge and that the ion thermal energy might increase by several degrees.

To prove that, the author of that work at first writes the equations for the Lorentz force in Cartesian coordinates. The following is one of the equations for the  $x$  coordinate:

$$\frac{d^2x}{dt^2} + \gamma \frac{dx}{dt} + \omega_0^2 x - 2\Omega_L(1 + \beta \cos \Omega t) \frac{dy}{dt} + \beta y \Omega_L \Omega \sin \Omega t = \sum_k C_{kx} \cos(\omega_k t + \delta_{kx}).$$

The first and third terms here correspond to a conventional harmonic oscillator with a natural frequency  $\omega_0$ , the second to damping, the fourth and fifth to the forces engendered by an AC MF, and the right-hand side to the Fourier expansion of random forces engendered by the neighboring particles. The writing of the equation is questionable.

(1) One and the same dynamic factor, namely the interaction of an ion with thermal oscillations of ligands, is included in the equation twice: as a phenomenological damping, which varies with the coordinate variation rate, and as external forces on the right-hand side of the equation. Note that the phenomenological damping is basically the averaged action of the external forces; therefore the coefficient  $\gamma$  depends on the correlation function of external forces, as in the Langevin equation. This dependence is absent here.

(2) Phenomenological damping, as an averaging of microscopic forces, is normally introduced for macroscopic bodies, such that their infinitesimal interval of motion includes a sufficiently large number of collisions with the environment. That is scarcely applied to an ion in a binding cavity.

(3) A random external force is represented here by a Fourier series, rather than by a Fourier integral. At the same time, there are no grounds to regard the random force as a (quasi)periodic function.

(4) The fifth term of the equation, according to the author, is the force of an eddy electric field that is a result of the time variation of an MF. One well-defined quantity in a variable MF is the rotor of the electric field:

$$\text{rot}\mathbf{E} = -\frac{1}{c} \frac{\partial \mathbf{H}}{\partial t} .$$

It is impossible to derive from that equality an expression for  $\mathbf{E}$  without taking into account some additional conditions. To work out the force that acts on a charge in a variable homogeneous MF, i.e., the electric force engendered by such a field, it would be necessary to integrate the forces due to all the elementary sources of given MFs that are somehow arranged around the charge. In this case the author implicitly used the condition that the origin of the coordinate system of an ion coincides with the origin of the axially symmetric coordinate system of MF sources. It is easily seen now that this condition will be met at best only for a single ion of some ensemble, rather than for all the ions of the ensemble. Therefore, the above form of the expression for the eddy electric force is not general enough for further analysis. We note that that is quite a common mistake. It is done by advocates and opponents of the biological magnetoreception alike. So, a recognized “authority” among the critics of the MBE, Adair, in his Note in *Bioelectromagnetics* **19**, 136, 1998, undertook to substantiate the impossibility of the action of a weak low-frequency MF on a DNA in a cell. He used the formula  $E = -(r/2c)\partial B/\partial t$  to estimate the *maximal* electric field in a cell of size  $r$ , induced by an MF  $B$ . It is easily seen, however, see Section 1.4.1, that it is an estimate of the field difference on the cell edges, rather than the magnitude of the electric field.

Further, after a transition to a non-inertial, non-uniformly rotating reference frame the Coriolis force is lost. Another point is that the statement that in a rotating reference frame an ion is not subject to MFs is wrong. It relies on the Larmor theorem. According to the theorem, the behavior of a system of like charges  $q$  with mass  $M$ , which undergo a finite motion in a centrally symmetrical electric field and a weak homogeneous MF  $\mathbf{H}$ , amounts to the behavior of that system of charges in the same electric field in a reference frame that rotates uniformly at angular velocity  $\boldsymbol{\Omega} = q\mathbf{H}/2Mc$ . The theorem holds well where the potential energy of the system of charges in the special case of one ion is invariant to rotations of the reference frame (Landau and Lifshitz, 1976a). Clearly, this necessary condition was not met when allowing for the additional forces present in the equation as phenomenological damping or external forces. Moreover, the Larmor theorem is valid for a DC MF. There is no evidence as to whether it could be extended to include variable MFs.

The transformed equation was then reduced to the inhomogeneous Mathieu equation with a variable right-hand side, but the inference as to the nature of its solutions was made based on the well-known solutions to the homogeneous Mathieu equation, and that, at least, is questionable.

A multitude of such omissions and unjustified approximations significantly reduces the value of the result obtained. Also, there is no way to use or test it, since no functional dependences on the MF variables have been derived.

Some comments on the conceptual aspects of the above treatment are in order. There is a pendulum that is parametrically excited by a very weak signal in the presence of a more powerful additive random force. An assumption is proposed that at a resonance frequency the pendulum energy may grow markedly. However, even in the absence of noise and damping, under optimal conditions, the ion energy could vary noticeably only after several months of coherent swinging of such a pendulum, see Section 3.10. Consequently, this all could only refer to the case where an MF controls the process of energy exchange between an ion and the source of a random force. However, no mechanism that would act against the natural trend for thermal energy to be equally distributed over all the degrees of freedom was proposed.

Also unconvincing are computer simulation results provided in one of the later works on the subject. In the time interval of interest, which is several seconds, the noise factor is close to a  $\delta$ -correlated random process with a spectrum near characteristic EHF frequencies of ion bonding. That factor was modeled by a signal that differs from the real one in three positions, which are the most significant ones at that. First, the assumption that the signal is deterministic excludes averaging over random variables of the noise signal; such an averaging would be quite unfavorable for modeling results; second, the signal is harmonic, which also excludes the unfavorable time averaging; third, the frequency of that signal was reduced nine orders of magnitude against the real one and chosen to be comparable with the Larmor frequency. As a result, within the time interval of computer calculations the relative phases were retained for both signals — “noise” and the MF. It is only natural that under such conditions some occurrences of parametric resonance were observed.

However, the main drawback of principle of that and similar models is that they “do not work” even in the absence of noise factors; therefore, they are incapable of making any productive testable assumptions.

### 3.9.4 Models of the enzyme reaction

Several proposals concerning mechanisms of the influence of an EMF on enzyme reactions are known. All of them, however, provide relatively high frequencies of supposedly effective EMFs.

- Zubkus and Stamenkovich (1989) considered the action of an EMF on biochemical reactions catalyzed by transferases, i.e., reactions in which an atom or a group of particles are transferred from a substrate to a product. It was assumed that the reaction rate could vary in an AC electric field owing to the variation of the diffusion rate and the probability of tunneling through a barrier along the reaction coordinate. The effective EMF frequencies in such mechanisms are close to natural frequencies of oscillations of a particle being transported on a bond being disrupted. For instance, that would be  $\Omega \sim 10^{13}\text{--}10^{14}\text{ s}^{-1}$  for a proton on a hydrogen bond. There are no estimates of effective amplitudes of an external field.
- Belousov *et al.* (1993) addressed a possible scenario of the variation of the rate of an enzyme reaction in an EMF at physiological temperatures. They used the electron-oscillatory model of an enzyme reaction, in which adiabatic potentials have the form of oscillatory wells along the generalized coordinate of the reaction. An external EMF influences the probability of nonradiative dissociation of a product–enzyme complex. The influence of microwave fields on the reduction of the activation energy of the complex was considered. That model predicts the appearance of a trigger effect in the dependence of the reaction on the intensity of an external field. At the same time, no estimates of effective fields are available. It is still unclear whether such models include windows of effective variables. The model thus seems to be invalid for low-frequency MFs, since the mechanism of the “hooking” of a field to a quantum system is represented by the energy of the dipole moment of a complex in the electric field component of an EMF.

### 3.10 MAGNETIC RESPONSE OF SPIN PARTICLES

Underlying any mechanism of EMF biological action is the interaction of field with matter, i.e., with atomic nuclei and electrons. A fundamental description of the interaction of an EMF with matter particles with spin  $\frac{1}{2}$  is concerned with representation of the latter as a spinor Dirac field. On atomic scale, it gives a quantum-mechanical description of electrons and a phenomenologically correct description of protons.

The Lagrangian of the interaction of an EMF with a spinor field stems from the requirement that a theory be invariant to the local phase transformation of a spinor field and have the form  $L(x) = eA_\mu(x)j^\mu(x)$ , where  $e$  is the electron charge,

$A_\mu = (A_0, \mathbf{A})$  is the 4-potential of an EMF, and  $j^\mu$  is the current of the particle field. In terms of the Hamiltonian semiclassical formalism, such a Lagrangian leads to the momentum operator  $\mathbf{P}$  being replaced by  $\mathbf{P} - e\mathbf{A}/c$ . The velocity of particles constituting a biological system is much lower than the velocity of light, and so relativistic effects can only yield minor corrections to relatively slow dynamics. Therefore, in the Dirac equation for the wave function of a particle in an EMF the nonrelativistic approximation is used. Up to the terms  $\sim c^{-2}$ , it yields the equation  $i\hbar\partial\Psi/\partial t = \mathcal{H}\Psi(\mathbf{r}, s)$  with the Hamiltonian

$$\mathcal{H} = \mathcal{H}(\mathbf{P}, U) + \mathcal{H}(\mathbf{P}, \mathbf{A}) + \mathcal{H}(\mathbf{S}, \mathbf{A}) + \mathcal{H}(\mathbf{S}, \mathbf{P}, A_0) ,$$

where  $\mathbf{r}, s$  are variables in the space of coordinates and spins.  $\mathbf{P}, \mathbf{S}$  are the momentum and spin operators, respectively.  $\mathcal{H}(\mathbf{P}, U)$  describes the dynamics of the orbital  $\mathbf{r}$  degrees of freedom for some fixed potential  $U(\mathbf{r})$ .  $\mathcal{H}(\mathbf{P}, \mathbf{A})$  accounts for the variation of that dynamics under an EMF.  $\mathcal{H}(\mathbf{S}, \mathbf{A})$  defines the dynamics of the particle spin in an EMF; lastly,  $\mathcal{H}(\mathbf{S}, \mathbf{P}, A_0)$  describes the interaction of spin and orbital degrees of freedom.

Even at this stage there are some mechanisms of the action of an EMF on orbital degrees of freedom. It is these degrees that determine the progress of biochemical processes and control indirectly the behavior of biological systems. Clearly, a biological reaction to the action of a variable MF is, in the final analysis, conditioned by the absorption of the MF energy, however small it might be, and by its transformation, possibly via spin degrees, into the energy of orbital degrees of freedom. The interaction of an MF with possible collective excitations in biophysical systems relies on the interaction of an MF with individual particles. Therefore, the processes of energy or signal transformation in one-particle dynamics form the foundation for MBE mechanisms. Signal transformation is only reduced to two possibilities. The first one is concerned with the terms  $\mathcal{H}(\mathbf{P}, U)$ ,  $\mathcal{H}(\mathbf{P}, \mathbf{A})$  and has a classical analogy in the motion of a point particle in some potential under the Lorentz force  $\mathbf{F} = e\mathbf{E} + e[\mathbf{v}\mathbf{H}]/c$ , where  $\mathbf{E}, \mathbf{H}$  are the electric and MFs. In the process, the MF energy transforms either directly into the energy of the particle orbital motion or into a redistribution of the probability density for a particle. In the latter case, the redistribution energy of an interference pattern is connected with a change in the number of EMF quanta, which requires, generally speaking, that we transcend the limits of the Hamiltonian semiclassical description.

The second, purely quantum, possibility is associated with the terms  $\mathcal{H}(\mathbf{S}, \mathbf{A})$  and  $\mathcal{H}(\mathbf{S}, \mathbf{P}, A_0)$ . It is believed that the MF energy is at first transformed into the energy of spin degrees of freedom, and then into the energy of orbital motion either following the "spin exclusion" or due to the spin-orbit interaction. The spin dynamics manifests itself in interaction with orbital degrees of freedom. Therefore, the relatively small interaction  $\mathcal{H}(\mathbf{S}, \mathbf{P}, A_0)$  could be significant.

Any studies of quantum effects in a magnetic field are normally begun with the writing of the magnetic Hamiltonian

$$\mathcal{H} = -\mathbf{M}\mathbf{H}(t),$$

where the operator of the magnetic moment  $\mathbf{M}$  depends on the type of a system under study. For instance, in some approximation, for a one-electron atomic system it looks like

$$\mathbf{M} = \mu_B(\mathbf{L} + 2\mathbf{S}) + \gamma\hbar\mathbf{I}, \quad (3.10.1)$$

where  $\mathbf{L}$ ,  $\mathbf{S}$  are the operators of the orbital and spin electron momentum,  $\mathbf{I}$  is the atomic nuclear spin operator,  $\gamma = \mu/I\hbar$  is the gyromagnetic ratio of the nucleus spin, and  $\mu$  is the magnetic moment of the nucleus.

In most problems, where electron–nucleus interaction is not important, the nuclear spin is ignored, since the nuclear magneton is more than three orders of magnitude smaller than the Bohr magneton. We will be interested in the motion of an ion as a whole particle in some effective potential. The simplest idealization here will be the adiabatic approximation that is valid when a system has fast and slow variables. The slow motion can then be described “adiabatically”, i.e., in the time-averaged or effective potential, which the fast variables produce. In this case, slow and fast dynamics refer to the motion of nuclei and electrons. The internal paired electrons of an ion make up an “elastic” atomic shell, which defines the ion effective radius, and the external valence electrons that bind the ion with ligands create the effective potential, such that an ion moves in it as a whole. Experiments on atomic interference in atomic beams support the validity of the adiabatic approximation in such cases.

To study the quantum dynamics of an ion in a magnetic field as an individual particle in an effective potential, we will have to write the magnetic moment operator proceeding from the “primary principles”. It appears that in that case the energy of the orbital motion of an ion as a whole is comparable with the energy of the ion spin. The ion spin, because of valence electrons being paired, is equivalent with the ion nuclear spin.

The issue thus emerges of the study of the dynamics of charged particles with spin in MFs. That issue has been repeatedly studied in much detail in applications to various domains of physics (e.g., Landau and Lifshitz, 1976a). As applied to biomagnetic reception models, the problem has features that make their estimation worthwhile.

The Hamiltonian of a particle with spin  $\frac{1}{2}$  in an external MF, allowing for spin–orbit coupling, has the form (e.g., Fermi, 1960; Akhiezer and Berestetskii, 1965; White, 1970)

$$\mathcal{H} = \frac{(\mathbf{P} - \frac{q}{c}\mathbf{A})^2}{2M} + qA_0 - 2\mu\mathbf{S}\mathbf{H} + \frac{2\mu^2}{q\hbar}\mathbf{S}(\nabla A_0 \times \mathbf{P}), \quad (3.10.2)$$

where  $\mu$ ,  $M$  are the magnetic moment and mass of the particle, respectively;  $\mathbf{A}$  and  $A_0$  are the vector and scalar potentials of the electromagnetic field;  $\mathbf{H} = \text{rot}\mathbf{A}$  is the MF;  $\mathbf{S}$  is the spin operator; and  $\mathbf{P} = -i\hbar\nabla$  is the momentum operator in an electromagnetic field. In a homogeneous MF,  $\mathbf{A} = \mathbf{H} \times \mathbf{r}/2$ , and in a centrally symmetric potential of electrostatic nature the Hamiltonian (3.10.2) can also be written as

$$\mathcal{H} = \frac{\mathbf{P}^2}{2M} + U(r) - (b\hbar\mathbf{L} + \gamma\hbar\mathbf{S}) \mathbf{H} + \frac{2\mu^2}{q\hbar} \mathbf{S}(\nabla A_0 \times \mathbf{P}), \quad (3.10.3)$$

where  $b = q/2Mc$  is the ion “charge-to-mass” ratio, and the expression in parentheses is the operator of the effective magnetic moment of an ion, which includes the energies of the orbital and spin magnetic momenta. Their inputs are comparable: the magnitude of the ratio  $\gamma/b = 2\gamma Mc/q$  is always more than one. Therefore, generally speaking, spin effects in ion dynamics should play quite a significant role. The dimensionless coefficient  $\gamma Mc/q$ , equal to the ratio of the NMR and cyclotron frequencies of an ion, appears in relationships quite often. In the book, a special name “ion–isotope constant” is introduced for it:

$$\Gamma = \frac{\Omega_N}{\Omega_c} = \frac{\gamma Mc}{q}.$$

Its numerical values for different ions and different isotopes of their nuclei are given in Table 6.1.

It is seen from Eq. (3.10.3) that the energy of a particle’s magnetic moments in an MF varies with  $b\hbar H$  for the angular momentum and  $\gamma\hbar H$  for spin. In a variable MF  $H \sin(\Omega t)$  we can readily find the instantaneous rate of transformation of the MF energy into the energy of, say, a spin:  $d\varepsilon/dt \sim \gamma\hbar H\Omega$ . That is a relatively small quantity. It would take a decade for an ion to accumulate an energy of about  $\kappa\mathcal{T}$  in a  $\sim 100\text{-}\mu\text{T}$ ,  $\sim 100\text{-Hz}$  MF for such a transformation rate.

In reality, the situation is even more hopeless. A homogeneous MF causes no quantum transitions; therefore the time-averaged energy of a particle does not change. Quantum transitions in an AC MF occur: (1) when spin–orbit interaction is taken into consideration (Binhi, 1995b), (2) when the orbit is not flat (Binhi, 1990b), and (3) when the MF is not homogeneous. However, contributions of these effects to the energy transformation rate is yet several orders of magnitude smaller.

Such low-energy changes of a particle, concerned with both spin and orbital magnetic momenta, indicate that utilization of the energy of an MF in MBEs, as it accumulates at some degrees of freedom, is unlikely. Therefore, it is advisable to search for alternative mechanisms, which would use not energetic, but some other, signal, properties of an MF.

### 3.10.1 Weak and strong MF approximations

Although quite small in some of its manifestations, spin–orbit interaction plays an important role in the dynamics of particles in weak MFs. In the absence of an MF, spin–orbit interaction, however small, implies that, in a central potential, there exists the conservable total momentum  $\mathbf{J}$  of a system composed of an orbital and spin momenta:  $\mathbf{J} = \mathbf{L} + \mathbf{S}$ . That follows from the fact that in a central potential the particle Hamiltonian, in addition to the spin–orbit interaction under consideration, which in this case varies with the product  $\mathbf{L}\mathbf{S}$ , contains a term that only depends on the radius  $r$  and a term that varies with the squared angular momentum,  $\sim \mathbf{L}^2$ .

The product  $\mathcal{L}\mathcal{S}$  clearly commutes with all the parts of the Hamiltonian. By virtue of the operator identity

$$\mathcal{J}^2 = \mathcal{L}^2 + \mathcal{S}^2 + 2\mathcal{L}\mathcal{S} ,$$

commuting with the Hamiltonian is also the operator of the squared total momentum  $\mathcal{J}^2$ , which precisely implies that the appropriate physical quantity is conserved. Also conserved is the component of the total momentum along any axis that is described by the operator  $\mathcal{J}_z$ . The wave functions of the system can be taken to be eigenfunctions for all the above operators and, correspondingly, indexed by quantum numbers, such as the radial  $n$ , the total momentum  $j$ , and its component  $m$ , and also the orbital momentum  $l$ , i.e., the functions  $|njlm\rangle$ .

A homogeneous MF reduces the spherical symmetry of a system to an axial one. In the Hamiltonian appear additional terms of the Zeeman interaction of orbital and spin magnetic moments with an MF. Now the operator of spin-orbit interaction does not commute with the Hamiltonian; therefore, a system's total momentum is not conserved, and so  $j$  is not a good quantum number.

If an MF is sufficiently large, we can ignore spin-orbit interaction. The spin and orbital magnetic momenta will then interact with the MF separately, the orbital momentum magnitude is conserved, and so do the components of the two momenta, the appropriate eigenfunctions being the functions  $|nlm_l m_s\rangle$ , specified by the azimuthal  $l$  and magnetic quantum numbers  $m_l$  and  $m_s$ . The splitting of energy levels in a relatively strong MF, which is indexed by the same numbers, is called the Paschen-Back effect. The position of the levels is slightly modified by spin-orbit interaction, which is regarded as a perturbation.

In a relatively weak MF, in contrast, we can take a perturbation to be the Zeeman energy, and we can work out the splitting as the diagonal elements of a perturbation in the shells of unperturbed functions of the total momentum and its component. Such a splitting, which is indexed by the quantum number  $j$ , is called the abnormal Zeeman effect. The normal Zeeman effect is defined as splitting in an arbitrary MF of levels of a spinless particle.

It is clear that for particles with spin a criterion of the applicability of wave functions of some symmetry or other boils down to the possibility of ignoring spin-orbit interaction as compared with the Zeeman one. For the comparison, of the two Zeeman energies we must take the smaller one. The ratio of the splittings due to spin and orbital magnetic moments is  $\hbar\Omega_N/\hbar\omega_0 = 2\Gamma$ . Since the magnitude of the ion-isotope constant  $\Gamma$  is always larger than 1, see Table 6.1, the smaller one is the energy of the orbital momentum, whose magnitude is  $\hbar\omega_0$ . Spin-orbit interaction has the form, see (3.10.2),

$$\mathcal{H}_{\text{so}} = \frac{2\mu^2}{q\hbar} \mathcal{S} (\nabla A_0 \times \mathcal{P}) .$$

In a central field  $\nabla A_0 = (\mathbf{r}/r)\partial A_0/\partial r$ . We can, therefore, write

$$\mathcal{H}_{\text{so}} = \frac{2\mu^2}{qr} \frac{\partial A_0}{\partial r} \mathcal{S}\mathcal{L} ,$$

where  $\mathcal{L} = -i\mathbf{r} \times \nabla$  is the dimensionless operator of the orbital angular momentum. The energy scale, i.e., the constant of spin-orbit interaction, follows after the quantum-mechanical averaging of the operator  $\mathcal{H}_{\text{so}}$  regarded as a perturbation. Using the above operator identity, we will estimate the order of magnitude of

$$\frac{2\mu^2}{q} \left\langle \frac{1}{r} \frac{\partial A_0}{\partial r} \right\rangle.$$

The potential  $A_0$  of an ion in the cavity is not quite defined yet. Apparently, one reasonable estimate of the mean quantity in the last expression will be  $q/a^3$ , where  $a$  is the radius of the cavity potential. We thus arrive at the energy scale for spin-orbit interaction in the form  $2\mu^2/a^3$ . To determine a critical MF, such that it divides areas of various approximations, we will equate the energy scales for spin-orbit and orbit momenta:  $2\mu^2/a^3 = \hbar\omega_0 = \hbar q H_{\text{th}}/2Mc$ . Now, using the definition of the ion-isotope constant  $\Gamma = \mu Mc/\hbar Sq$ , we find the critical field:

$$H_{\text{th}} \sim 4\mu S\Gamma/a^3. \quad (3.10.4)$$

We can readily work out, using Table 6.1, that for ions in the table, which have a nuclear spin, the critical field varies in the range of 5–500 mT for cavities with an effective potential of radius 0.7 Å. For an electron in a well of radius 1 Å, from the relationship  $2\mu_{\text{B}}^2/a^3 \sim \hbar e H_{\text{th}}/2m_e c$ , we could find the critical field in the region of 2 T, which is in full conformity with the well-known data of atomic spectroscopy. That is, of course, just a rough estimate because we do not know the exact form of the ion potential in a cavity. It is clear, nevertheless, that the geomagnetic field, which is somehow present in most magnetobiological experiments falls rather in the interval of weak (in the above sense) fields. It thus makes sense to investigate approximations of both strong and weak fields, when an external MF interacts with the total magnetic moment of an ion.

### 3.11 FREE RADICAL REACTIONS

The conditions under which reactions involving radical pairs (RP) occur are well studied; there are a multitude of works devoted to radical reactions in a magnetic field. Good introductions to the topic are popular reviews by Buchachenko *et al.* (1978), Salikhov *et al.* (1984), and Steiner and Ulrich (1989). The processes of magnetosensitive recombination of radical pairs may form a foundation for biological effectiveness of weak MFs. That is a common and attractive idea, primarily because these processes are virtually independent of the ambient temperature. Therefore, there is no “kT problem” here. Frequency and amplitude windows of MF variables with such a primary mechanism of magnetoreception are associated with the non-linear equations of chemical kinetics. The radical reaction is a sensitive link in a complicated biochemical system described by non-linear equations (Grundler *et al.*, 1992). At the same time such a mechanism imposes some theoretical constraints on the magnitude of MBEs. It is possible that biological effects of an MF, both DC and AC, of a relatively large intensity  $> 1$  mT follow precisely that mechanism.

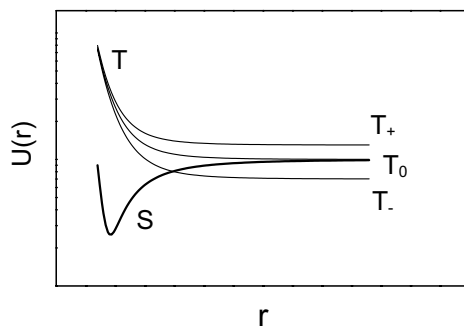
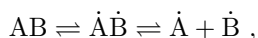


**Figure 3.13.** The energy of Coulomb interaction of an RP, allowing for the energy of exchange interaction with singlet  $S$  and triplet  $T_+$ ,  $T_0$ ,  $T_-$  states of the electrons of the pair.

### 3.11.1 Geminate recombination

Some organic molecules seem to consist of two relatively strong and large parts, A and B, connected by a single covalent bond. The latter can be broken by thermal perturbations:  $AB \rightleftharpoons A + B$ . The parts are large and the medium is viscous, and so the parts are incapable of quickly separating to a large distance and appear to be as if confined to a “cage”. Here we thus have a special state of the reagents, such that it can be identified neither with the product AB nor with reagents A and B. The products of the decomposition of the AB molecule behave as radicals  $\dot{A}$  and  $\dot{B}$ , molecules with an unpaired valence electron. The reaction is, therefore, represented as



where the interim state  $\dot{A}\dot{B}$  is a radical pair with unpaired electrons in a cage.

The spin state of an RP with spins  $\frac{1}{2}$  is described by singlet–triplet states with the following notation borrowed from RP chemistry:  $S$  is a singlet state with zero total spin, and  $T$  is the triplet state with unity total spin. In the latter case, spin one can have components along a selected axis equal to 1, 0, or  $-1$ . These states are designated as  $T_+$ ,  $T_0$ , and  $T_-$ , respectively. Of significance here is the exchange interaction of the electrons of a pair, which depends not only on the spin state of an RP, but also on the separation between the radicals, Fig. 3.13. The figure depicts the RP terms in a relatively strong MF, when the spin and orbital magnetic momenta interact with the MF individually.

It is obvious that a stable state (recombination product) of an RP only occurs in a singlet state. There is no detailed description of the process of the formation of AB from  $\dot{A}\dot{B}$  as yet. Therefore, they use a phenomenological description: they assume that the product AB formation rate is mainly proportional to the probability (or population, or intensiveness) of an RP singlet state. As the product forms, the

relative share of RP in the singlet state (chemical polarization of electrons — CPE) is reduced. Since an MF in principle affects the evolution of the RP spin state, i.e., it causes singlet–triplet transitions, the field is capable of changing the equilibrium relationship of free radicals  $\dot{A}$ ,  $\dot{B}$  and AB molecules. It is supposed that this could be one of the MBE mechanisms.

To describe RP dynamics we will need an RP magnetic Hamiltonian, which specifically contains Hamiltonians of the magnetic momenta of each radical. The magnetic moment operator  $\mathbf{M} = (\mu/S)\mathbf{S}$  for the electron and the respective Hamiltonian have the form

$$\mathbf{M} = 2\mu_B\mathbf{S}, \quad \mathcal{H} = -\mathbf{H}\mathbf{M} = -2\mu_B\mathbf{H}\mathbf{S}.$$

However, in a weak MF the magnetic moment operator, see Section 3.10.1, should be written as  $\mathbf{M} = \mathcal{G}\mathbf{J}$ , where  $\mathbf{J}$  is the total momentum operator. In a homogeneous MF  $H_z$  the magnetic Hamiltonian has the form  $\mathcal{H} = \mathcal{G}\mathcal{J}_zH_z$ , and it defines level splitting, see Addendum 6.2, which is a multiple of

$$\Delta\varepsilon = -b\hbar gH_z, \quad (3.11.1)$$

where  $b = e/2m_e c$ , and  $g$  is the g-factor (6.2.2). The active electron of a radical is subject to the action of an effective molecular field (in the solid-state theory they use the term “crystal field”). That gives rise to chaotic precession of the electron orbital momentum, so that its mean value is zero. The orbital angular momentum is then said to be “frozen”:  $\langle \mathbf{L} \rangle = 0$ . That means that the magnetic Hamiltonian only contains the spin operator:  $\mathcal{H} = \alpha\mathcal{S}_zH_z$ . That Hamiltonian will obviously split the electron level according to

$$\Delta\varepsilon = \alpha H_z.$$

Comparing this expression with (3.11.1) gives  $\alpha = -b\hbar g = -\mu_B g$ . Therefore, formally, the electron magnetic Hamilton becomes

$$\mathcal{H} = -\mu_B g H_z \mathcal{S}_z. \quad (3.11.2)$$

In the ideal situation of the complete freezing of the orbital momentum, substituting into (6.2.2) values of the electron quantum numbers  $i = \frac{1}{2}$ ,  $l = 0$  (formally, as  $\langle \mathbf{L} \rangle = 0$ ),  $j = \frac{1}{2}$ ,  $\Gamma = 1$ , we find  $g = 2$ . In reality, the motion of an electron in a molecular field is not completely chaotic. There remains some measure of order stemming from the special nature of the molecular field of a given kind of molecule. In that case, electron orbital motion produces some additional MF. It should be taken into consideration in spin dynamics (Slichter, 1980). In a fixed external MF the effect manifests itself as a minor deviation of the g-factor from the ideal value 2. That paves the way to identifying molecular radicals by their electron spin resonance (ESR) spectra.

Let us consider a simple model of a molecule that in a singlet spin state splits under thermal excitation into a pair of neutral radicals. The simplest idealization is that of the so-called exponential model. It postulates the Poisson flux of radicals

leaving a cage. Correspondingly, the lifetime of radicals in the cage is a random quantity distributed by the exponential law

$$f(t) = \frac{1}{\tau_c} e^{-t/\tau_c}, \quad (3.11.3)$$

where  $\tau_c$  is the mean lifetime of an RP in a cage, an important variable of the model. The lifetime  $\tau_c$  is about  $\tau_c \sim R^2/D$ , where the cage size for neutral radicals is  $R \sim 10 \text{ \AA}$ , and the diffusion coefficient for non-viscous solvents, such as water,  $D \sim 10^{-5} \text{ cm}^2/\text{s}$ . That is,  $\tau_c \sim 10^{-9} \text{ s}$ .

Initially, an RP is in a singlet state. In that state, radicals recombine at some rate  $K$ . External and internal MFs give rise to singlet–triplet transitions. Since the spin selection rule only allows for recombination from an  $S$ -state, generally speaking, this reduces the recombination rate. It is clear that if the rate of  $S$ – $T$  transitions is small, the spin state of an RP fails to change during its lifetime. In that case, the recombination rate will be  $K$  and, clearly, independent of the MF. In the opposite case of intensive  $S$ – $T$  transitions any correlation between RP spins is quickly destroyed. The recombination rate will then be independent of the MF as well and will only be defined by the mean weight of the  $S$ -state for a random selection of radical spin states, i.e.,  $K/4$ . Thus, there is an MF interval normally from units to hundreds of millitesla, when the statistical weight of the  $S$ -state changes markedly during a time of about  $\tau_c$ , thus causing the recombination rate to depend on the MF. The position of that MF interval is, clearly, proportional with  $1/\tau_s$  and also dependent on the nature of magnetic interactions inside the cage. These interactions define the mechanism type for  $S$ – $T$  transitions. There are several such types.

### 3.11.1.1 Relaxation mechanism

The spin state of an RP after its formation varies due to relaxation of each spin down to its equilibrium state. In general, a superposition of  $S$ - and  $T$ -states changes their relative weights, which suggests the presence of  $S$ – $T$  transitions. The relaxation time of neutral radical spins in liquids with viscosity similar to that of water  $\sim 1 \text{ sP}$  is equal to  $10^{-7}$ – $10^{-6} \text{ s}$ ; i.e., it is much larger than  $\tau_c$ . Therefore, that mechanism becomes of value, for instance, in the cellular recombination of oppositely charged ion radicals, for which  $\tau_c$ , due to mutual attraction, can be much larger than  $10^{-9} \text{ s}$ .

### 3.11.1.2 $\Delta g$ mechanism

After radicals have been formed, their spins precess, see Addendum 6.3, in a magnetic field, the latter being a superposition of (1) an external MF and (2) a field of magnetic moments of the radicals' nuclei. Suppose now that the latter MF is zero, i.e., all the nuclei of radicals are even and do not possess a magnetic moment. The precession will then go on in an external MF with a Larmor frequency. It will be proportional to the Zeeman splitting and, in the general case, will be different for each radical due to different  $g$ -factors:

$$\omega_1 = \frac{1}{\hbar} \mu_B g_1 H_z, \quad \omega_2 = \frac{1}{\hbar} \mu_B g_2 H_z.$$

The relative rate of de-phasing, i.e., the difference of these frequencies, will be

$$\frac{1}{\hbar} \mu_B \Delta g H_z .$$

An MF exerts its influence via the  $\Delta g$  mechanism where it is large enough for RP de-phasing during an RP lifetime to become noticeable, say, one radian. The order of effective MFs at  $\Delta g \sim 10^{-3}$  will then be

$$H \sim \frac{\hbar}{\mu_B \Delta g \tau_c} \sim 10^5 \text{ Oe} .$$

These fields are too large to provide a reliable account for the MBEs that occur at fields under 1 Oe.

### 3.11.1.3 Resonance excitation

If RP spins have different precession frequencies, then, by choosing the frequency of an external AC field, one can tune to a magnetic resonance of one of the spins. Its state will then begin to oscillate with a Rabi frequency,  $\gamma H_{AC} = 2\mu_B H_{AC}/\hbar$ , executing thereby  $S$ - $T$  transitions of an RP spin state. De-phasing of about one occurs in fields  $H_{AC} \sim \hbar/2\mu_B \tau_s \sim 100 \text{ Oe}$ . Clearly, this mechanism of the mixing of singlet-triplet states as well has nothing to do with the magnetobiological effects discussed in this book.

### 3.11.1.4 HFI mechanism

Hyperfine interaction (HFI), i.e., interaction of electrons with nuclear spins, yields more optimistic estimates. For example, when one of the radicals has nuclei with a magnetic moment, radical spins precess in markedly different MFs. Even if the difference of g-factors is insignificant, RP terms do mix or  $S$ - $T$  transitions do occur. Let an external MF be zero. Approximately, de-phasing is determined by the precession of the magnetic moment of only one electron of a pair in the field of a nuclear magnetic moment,  $\sim 100 \text{ Oe}$ . During the RP lifetime the phase progression will then be  $\mu_B g H \tau_s / \hbar \sim 1$ , i.e., a quantity large enough to be observable. The question is whether an additional external MF of about the geomagnetic field is capable of changing noticeably the rate of  $S$ - $T$  transitions.

The relatively simple model — the influence of an external MF on the recombination of an RP with one magnetic nucleus with spin  $\frac{1}{2}$  by the HFI mechanism — has been addressed many times (Buchachenko *et al.*, 1978). In addition to the Zeeman energy of spins (3.11.2), the Hamiltonian of the model includes the exchange interaction

$$\mathcal{H}_{\text{exch}} = -\hbar J(r) (1/2 + 2\mathbf{S}^1 \mathbf{S}^2)$$

with a constant  $J(r)$ , and hyperfine interaction, in which, due to fast chaotic rotations of radicals in a cage, normally only its isotropic part is retained

$$\mathcal{H}_{\text{hf}} = \hbar A \mathbf{S} \mathbf{I} .$$

The spin Hamiltonian of an RP in an external MF  $H \parallel z$  looks like

$$\mathcal{H} = \mathcal{H}_0 + \hbar A \mathbf{S}^1 \mathbf{I} , \quad \mathcal{H}_0 = -\mu_B g H (\mathcal{S}_z^1 + \mathcal{S}_z^2) - \hbar J(r)(1/2 + 2\mathbf{S}^1 \mathbf{S}^2) , \quad (3.11.4)$$

where g-factors are, for simplicity, assumed to be equal for all the radicals, and the Zeeman energy of the nuclear magnetic moment is ignored. It is common knowledge that the eigenfunctions of the Hamiltonian  $\mathcal{H}_0$  are singlet–triplet states, which, in terms of one-particle spin states  $\psi_\alpha$ , which are eigenfunctions of the operator  $\mathcal{S}_z$ , are given by

$$\nu_m = \begin{cases} \psi_2^1 \psi_2^2 & m = -1 \\ \frac{1}{\sqrt{2}} (\psi_1^1 \psi_2^2 + \psi_2^1 \psi_1^2) & m = 0 \\ \psi_1^1 \psi_1^2 & m = 1 \\ \frac{1}{\sqrt{2}} (\psi_1^1 \psi_2^2 - \psi_2^1 \psi_1^2) & m = 2 . \end{cases} \quad (3.11.5)$$

Here the first three basis vectors form a symmetric (in particle permutations) triplet  $T_-, T_0, T_+$ ; the last vector is an antisymmetric state or singlet  $S$ . The variation range of the index  $m = -1, 0, 1, 2$  was chosen so that for triplet states it would coincide with the magnetic quantum number — the  $z$  component of the total spin  $\mathbf{S}^1 + \mathbf{S}^2$ . We will denote the nuclear spin state as  $\chi_\alpha$ , so that a basis for the investigation of the dynamic equation with the Hamiltonian (3.11.4) will be the functions

$$\xi_{m\alpha} = \nu_m \chi_\alpha .$$

Then the arbitrary RP state can be represented as a superposition

$$\Psi = \sum_{m\alpha} c_{m\alpha} \xi_{m\alpha} .$$

The Latin indices assume the values -1, 0, 1, 2 (2 for the singlet state), and the Greek indices, 1 and 2 (the up and down spin states). The density matrix, whose diagonal elements are populations of electron singlet–triplet terms, is defined as

$$\sigma_{nm} = \sum_{\alpha\beta} c_{n\alpha}^* c_{m\beta} . \quad (3.11.6)$$

It is found by solving the equation of motion for the density matrix

$$i\hbar \dot{\sigma}_{nm} = \sum_k [\mathcal{H}_{nk} \sigma_{km} - \sigma_{nk} \mathcal{H}_{km}] .$$

In certain cases it is assumed that the radicals of a pair have a fixed separation. Further, the population of the singlet state  $\sigma_{22}(t)$  is found. The recombination rate  $p$  is assumed to be proportional to the time-averaged population of the singlet state. Since RP lifetimes in a cage are distributed by (3.11.3), the averaging is carried out using the exponential distribution

$$p \sim \frac{1}{\tau_c} \int_0^\infty e^{-t/\tau_c} \sigma_{22}(t) dt .$$

In more realistic cases, considered along with spin dynamics is the spatial motion of radicals in a cage, their repeated contacts due to diffusion. The density matrix then

depends not only on spin variables, but also on the separation between radicals  $r$ . Accordingly, the dynamic equation changes as well. The spin effects of RP recombination, subject to the molecular motion of radicals, were considered in much detail in the monograph by Buchachenko *et al.* (1978).

Analytical studies of RP dynamics, even ignoring the molecular motion, are hindered by the fact that calculations use three-part spin functions. We will not provide here solutions for specific models. We will rather make use of approximate estimates and known results of the numerical analysis of equations.

It follows from (3.11.4) that any significant change in spin dynamics can only be expected where the Zeeman and HFI energies have similar scales, i.e.,  $\mu_B g H \sim \hbar A$ . The HFI constant has an order of magnitude  $A \sim 10^8$ – $10^9$  Hz, whence we find the appropriate MF scale:

$$H \sim \frac{\hbar A}{\mu_B g} \sim 0.5\text{--}5 \text{ mT} .$$

The numerical calculations (see reviews Steiner and Ulrich, 1989; Buchachenko *et al.*, 1978) indicate that in most cases maximal changes of the recombination rate in specified fields are no more than 1 %, the characteristic RP lifetime being  $\sim 10^{-9}$  s. Making quite an approximate assumption of the field-effect variation being linear in the range under consideration, we find that in the geomagnetic field  $\sim 0.05$  mT the effect will not exceed 0.1 %. Experimental curves for radical reaction rates in a magnetic field (Grissom, 1995) substantiate that estimation. In a model with one magnetic nucleus, Brocklehurst and McLauchlan (1996) obtained, using numerical methods  $\sim 10$  %, the change as recalculated to the geomagnetic field, but they used  $\tau_c \sim 2 \cdot 10^{-7}$  s. For common values  $\sim 10^{-9}$  s here too we have 0.1 %. Obviously, this quantity should be regarded as fairly justified for estimations of possible biological effects in a magnetic field similar to the geomagnetic one. Such insignificant changes in the reaction rate suggest that a further “biochemical” amplification is needed. Grundler *et al.* (1992) and Kaiser (1996) considered the free radical reaction as an element of a system described by a set of non-linear equations of chemical kinetics with bifurcations. Even minor variations of the reaction rate could then cause significant, even qualitative, changes in the behavior of a biological system.

### 3.11.2 Representative experiments

There are indirect experiments supporting the idea of radical pairs in magnetobiology. In Lai and Singh (1997b) they measured the mobility of brain cell DNA in rats and found a statistically meaningful 30 % change of that variable after a 2-h exposure of the animals to 2.45-GHz, 2-mW/cm<sup>2</sup> microwaves, in pulsed 2- $\mu$ s, 500-Hz mode. It is significant that an injection of melatonin and other scavengers of free radicals blocked the emergence of a biological effect of the microwaves.

In contrast, other evidence points against the idea. In Taoka *et al.* (1997) they measured the rate of some enzyme reactions *in vitro* associated with a co-enzyme B<sub>12</sub>. The cobalt–carbon coupling of the co-enzyme can generate a spin-correlated radical pair. However, no meaningful MF dependence in the range of 50–250 mT for

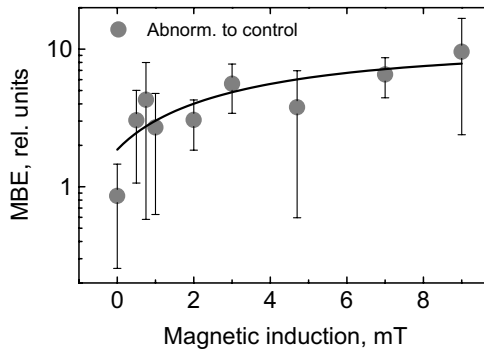


**Figure 3.14.** The relative number of deviations from the normal development of fly larvae exposed for 30 min to a DC MF, according to Ho *et al.* (1992).

the two enzyme reactions studied has been found. The authors conclude that the action of an MF on physiological processes is hardly associated with given enzymes.

- Ho *et al.* (1992) addressed the deviations from normal development of *Drosophila* larvae caused by their 30-min exposure to a DC MF. Studied were more than 10 various parameters characterizing the morphological process occurring during the first 24 h of the development of embryos. Figure 3.14 shows the deviation index vs MF curve. The range of DC MFs, beginning with 1 mT, where significant changes were observed, points to possible mechanisms of the influence of an MF on free radical reactions.

- Galvanovskis *et al.* (1999) measured, using a fluorescent microscope, the spectral density of the power of the oscillations of the calcium ion concentration in T-cells of human leukemia in the spectral interval 0–10 mHz. The magnetic layout of the experiment

$$B(36)b(0-566)B_p(14)f(50)b_{\text{background } 50 \text{ Hz}}(< 0.2)$$

enabled one to evaluate the variation of the parameter being measured with the AC MF amplitude. Figure 3.15 displays the field amplitude dependence of the MBE computed as the difference of control and experimental values in relation to the control one. The scale of MFs that cause changes, about 1 mT, and the gently sloping curve are characteristic of magnetosensitive radical reactions. Unfortunately, data on frequency selectivity of the effect observed were not provided.

- Lai and Carino (1999) studied cholinergic activity of rat brain tissues, those of the frontal cortex and hippocampus. To this end, they used a 60-Hz MF of various intensities and exposure durations. The authors assumed that a statistically trustworthy effect is only caused by combinations of variables, such that the product of the field intensity by the exposure time is sufficiently high, Fig. 3.16. The body of evidence is too small to warrant any reliable conclusions. For instance, we can

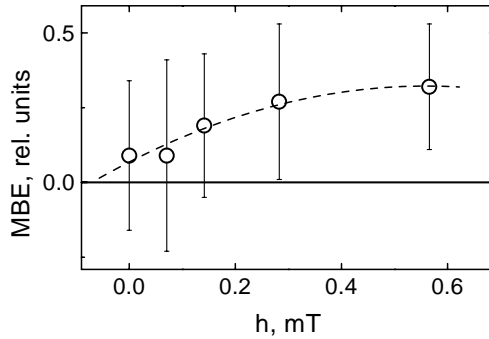


**Figure 3.15.** The relative magnitude of the spectral density of intracellular Ca oscillations in an AC MF, according to Galvanovskis *et al.* (1999).

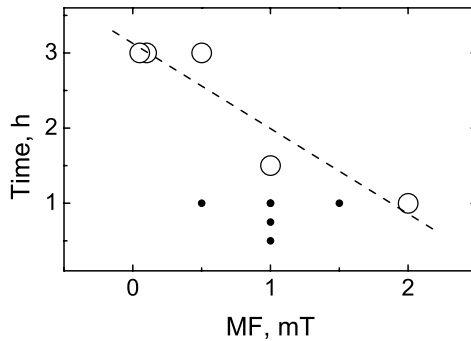


**Figure 3.16.** The MF intensity and the exposure time, which cause an MBE  $p < 0.05$  in brain tissue (O), and do not cause any effect (●), according to Lai and Carino (1999).

also assume that here too there were different physical mechanisms: an interference mechanism in the region of relatively weak MFs, and a spin-prohibition one, for relatively large MFs.

• Li *et al.* (1999) undertook to find out whether a 50-Hz MF can be a promoter of carcinogenic action of 12-O-tetradecanoilforbol-13-acetate (TPA). The characteristic of intercellular communication processes was measured using the method of die injection with a count of tinted cells. Figure 3.17 shows that in these experiments an MF produced changes in a biological system, qualitatively similar to that of a carcinogenic preparation. The action of the preparation itself was amplified when exposed to an MF. The interval of effective MFs was, just as above, in the region of 1 mT.

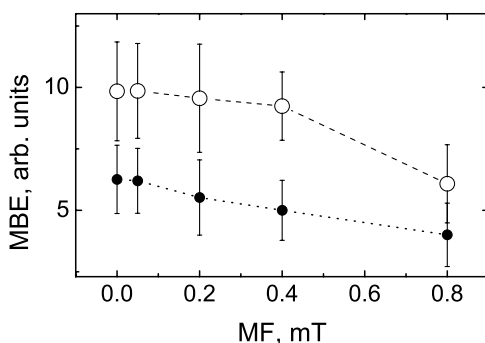


**Figure 3.17.** The index of intercellular communication processes in a culture of cells of Chinese hamster lung at various intensities of an AC MF, with (●) and without (O) a carcinogenic TPA preparation, according to Li *et al.* (1999).

Characteristic of all the above experiments, which measure biological effects of DC and AC MFs, is the fact that the effect grows monotonously with MF intensity in the interval from fractions to several milliteslas. The RP mechanism of magnetoreception is not to be excluded here. However, so far no special studies that give a reliable proof of the involvement of RP-based reactions in biological magnetoreception are known. The geminate recombination rate is governed by many variables: medium viscosity, structure and size of radicals, their  $g$ -factors, spins and isotopic composition of core nuclei, and size and characteristics of an external MF. Different combinations of possible values of these parameters form a wide variety of physico-chemical modes of radical reactions. This hinders the identification of RPs as possible targets for a weak MF. Such investigations could, on the surface of it, rely heavily on the absence of frequency selectivity as an effect, but the involved metabolic system can feature its own natural frequencies. This does not enable a proper judgment of primary magnetoreception mechanisms to be formed. By stepping up the frequency, we can sooner or later surpass the limits of a low-frequency interval of a bound chemico-kinetic system, but thermal and electrochemical effects here are quite likely. Amplitude spectra bear virtually no information, since they are well-defined neither for RP reactions nor for a metabolic system, and are conditioned by a host of factors beyond our control. It is quite probable that the only possibility for RP reactions to be identified as targets for a magnetic field is to replace potentially responsible magnetic nuclei by their non-magnetic isotopes.

### 3.12 “KT PROBLEM” IN MAGNETOBIOLOGY

So far there is no physically acceptable understanding of how weak low-frequency MFs cause living systems to respond. Paradoxically as it is, such fields are able to change the rate of biochemical reactions, the effect being like a resonance at that.

The physical nature of that phenomenon is yet unclear, and that is one of the most important issues of magnetobiology, if not the main one.

Many physicists, those who do not deal with that problem directly, ask themselves a question that has already become a rhetorical one. That question, although imperfect in form, is important in essence. An individual act of chemical transformation of molecules requires an initiating pulse with an energy of about  $\kappa\mathcal{T}$ , i.e., of thermal scale. How then can an energy quantum of a low-frequency MF, whose energy is 10 orders of magnitude smaller, influence that process? Another form of the question appeals to the fact that a chemical transformation act with a characteristic energy  $\kappa\mathcal{T}$  is localized in a microscopic volume. The same energy, about  $\kappa\mathcal{T}$ , of a weak MF  $H$  in its classical presentation, e.g., of the geomagnetic one, is contained in a volume  $V$  that is 12 orders of magnitude larger (corresponding to the volume of a biological cell). That can be readily found from an expression for the energy density of an MF:

$$\kappa\mathcal{T} \sim \frac{1}{8\pi} \int H^2 dV.$$

How is the energy to be collected from all over the macroscopic volume and transferred to a microlevel? It is widely believed that these questions allegedly solve the problem by suggesting that no MBE is possible. At the same time, there also exist counterarguments to that viewpoint.

Firstly, some non-thermally activated reactions are known, e.g., enzyme ones, of the “key–lock” type.

Secondly, the very notion of the EMF quantum in a low-frequency range has a limited meaning. For a given MF intensity an adequate physical description of an EMF is only given by the Maxwell equations of classical electrodynamics (see 1.4.2).

Thirdly, we cannot apply to living systems the notions of equilibrium thermodynamics, specifically the thermal scale  $\kappa\mathcal{T}$ . In a thermodynamically equilibrium system the energy  $\kappa\mathcal{T}$  is the mean energy of thermal motion per one dynamic variable or, put another way, per one degree of freedom. In a non-equilibrium system, in the general case, there are no objects that could be characterized by  $\kappa\mathcal{T}$ . On the one hand, the thermodynamic factor  $\kappa\mathcal{T}$  must be taken into consideration. On the other hand, it is clear that we here deal with an interim interval where, as shown in Romanovsky *et al.* (1984), the laws of mechanics and principles of thermodynamics “lose their productive nature, i.e., their ability to describe phenomena and predict them.”

Fourthly, the two forms of the above questions — which juxtapose to  $\kappa\mathcal{T}$ , in one case, the field quantum; in the other, the field energy density — bring out just individual aspects — the frequency one, in the former case, and the amplitude one, in the latter case — of the unified, integral nature of an EMF. That points to the logical inadequacy of the issue.

It is quite probable that there are other counterarguments as well. What is important, however, is that these have not yet led, for decades to date, to the

construction of a workable physical mechanism of magnetoreception.

The issue under discussion contains, in fact, two equally paradoxical issues, and the problem of biological action of low-frequency MFs has two apparent aspects: (1) what is the *mechanism of transformation* of a weak low-frequency MF signal into variations at the level of a  $\kappa\mathcal{T}$ -scale (bio)chemical process; and (2) what is the *mechanism of stability*, i.e., how do such minor actions manage not to get lost against the background of  $\kappa\mathcal{T}$ -scale thermal perturbations of the medium? The “kT problem”, formulated in such a form, allows a detailed physical analysis.

The second question is only productive if the transformation mechanism is known or proposed. An answer to the first question alone, the one on transformation mechanism, does not solve the problem, although it is an integral part of the solution. At the same time, there is no way of solving the problem, it seems, without analyzing it, i.e., without solving it by parts. So far there are no models, i.e., sets of equations, that jointly consider the magnetic and thermal factors and that have solutions that are adequate to experiment.

Against the background of practical completeness of dynamic and statistic theories, the presence of a problem that cannot be solved for decades appears to be rather strange and challenging. Therefore, many researchers, in the absence of a unified theoretical treatment, believe that the very existence of electromagnetobiology is an artifact. The proposed transformation mechanisms often raise objections because they fail to solve the latter of the above questions; i.e., they do not solve the problem as a whole.

As mentioned above, when accounting for the paradoxical action of weak EMFs against the background of thermal noise, they often lean on the coherency of an EMF and on the possibility for its energy to be accumulated by oscillators.

For an EHF electromagnetic field, where the quantum energy is just two or three orders of magnitude lower than  $\kappa\mathcal{T}$ , the energy accumulation idea is sufficiently workable. True, it is no good for explanations of the biological effects of EHF fields of super-low intensity found by Aarholt *et al.* (1988), Grundler *et al.* (1992), and Belyaev *et al.* (1993, 1996). The EM radiation flux here seems to be extremely small, but the effect is observed anyway. The effect remains when the radiation power is attenuated from normal to superlow, within  $10^{-3}$ – $10^{-18}$  W/cm<sup>2</sup>, Fig. 3.1. The effect seems to be controlled by one and the same mechanism, which is not associated with energy accumulation, since in the case of superweak radiation there is simply nothing to be accumulated. That seems to be a special aspect of a more general nature, which will await its solution for a long time.

For the low-frequency MF range, the accumulation idea is hopeless. It takes years to pump  $\kappa\mathcal{T}$ -level MF energy, say, into an ion oscillator, even under ideal conditions, specifically under those of an infinite-quality oscillator.

Thus, the fact that coherent action of an MF differs from incoherent noise is in itself insufficient, and it does not contribute to our understanding of the mechanisms of the action of weak MFs. It would perhaps make sense to somehow take into consideration the qualitative distinctions of an MF from thermal actions, and its special nature as a physical entity. As far back as 1970, Presman stressed that it is

necessary to take into consideration signal, rather than energetic, properties of an EMF, to account for its biological action.

One specific feature of an MF shows itself primarily in the way an MF appears in dynamics equations. The quantities that account for the action of an MF and thermal noise exert a qualitatively different action of the behavior of dynamic variables. It is only natural, therefore, to make that circumstance responsible for the quantitative energetic incompatibility of initiating moments of disparate nature, namely magnetic and thermal, which produce responses of similar proportions. That is, an answer to that question should be sought for at the level of the primary process of magnetoreception, described by the dynamic equations of microparticles in a magnetic field. It is clear that the ideas of non-equilibrium, instability, etc., become of secondary importance and are rather a necessary link in the ensuing long chain from the primary (biophysical) act of MF reception to the experimentally observed biological response.

A further question, which is generally not raised when discussing the informational nature of weak electromagnetic fields, is where and in what form is the information that comes from an MF at the earliest stage stored? Only provided we get a productive answer could we recognize that an MF contains some information. It appears that the only way to store information on an MF is to transform it into a microparticle state in a suitable biophysical system, if such storage is not at variance with some other principles, of course. There is no alternative to that statement so far.

This reasoning, if viewed from whatever quarter, thus suggests that it is necessary to look into the dynamics of microparticles in a magnetic field. This topic seems to have been well studied long ago. It appears, nevertheless, that the quantum dynamics of sufficiently heavy particles, such as ions, in combination with the non-linear behavior of biophysical systems results in a series of peculiarities. These could be successfully utilized to account for the biological action of weak low-frequency MFs.

According to quantum physics, a measurement of the energy of a quantum system to within  $\Delta\varepsilon$  cannot be performed faster than during the time  $\hbar/\Delta\varepsilon$ . Specifically, any observation of the consequences of the absorption by a quantum system of a photon with energy  $\varepsilon = \hbar\Omega$  takes at least  $1/\Omega$ . The low-frequency interval of fields used in more or less reproducible magnetobiological experiments begins with about 10 Hz. Thus the conditions needed for measurements must be sustained for no less than 0.1 s. Specifically, the lifetimes of states of a quantum system that absorbs a photon must have the same order of magnitude or larger.

Such long-lived states at  $T \sim 300$  K can appear to be unlikely. However, if experiment shows that an MF of that frequency range still causes some effects, then the assumption that there are long-lived modes looks quite justified, and there is nothing exotic about it. For instance, the states of spins of protons of liquid water at room temperature "live" about 3 s. Moreover, lifetime also grows with temperature, quite unexpectedly. That is a corollary of the specific features of the interaction of spins of water protons with thermal perturbations.

Spin relaxation is controlled by the relativistic spin-orbit interaction that is proportional to the gradient of a microscopic electric field. Since the diffusion mobility of a proton is relatively large and grows with temperature, the microrelief of an electric field for a proton will to a large degree be averaged, or ironed out. Therefore, a proton “sees” the electric field as a fairly homogeneous field and almost does not interact with it. The above refers to spin-lattice relaxation. The spin-spin relaxation is caused by magnetic dipole-dipole interaction of protons with one another. The mean MF on a proton caused by magnetic moments of other protons is relatively small and spin-spin relaxation is hindered as well. That does not imply that the proton spin states do not show up at all. As it will be shown in appropriate sections, if we take into account the states of nuclear spins of protons and ions, we will arrive at magnetobiologically important inferences.

The relatively large lifetime of spin states is conditioned by the details of the interaction of spins with thermal oscillations of the lattice. Likewise, the metastability of certain spatial or, as they say, orbital degrees of freedom can stem from the *specific features* of their interaction with thermal oscillations.

It is well known that energy transport along protein  $\alpha$ -spiral polymer molecules can be attributed to the soliton transfer of oscillation energy of atoms C=O in peptide groups of monomers of a protein chain (Davydov, 1984b), see Addendum 6.5. Some indirect experimental evidence for the existence of solitons in proteins was obtained from the absorption spectrum of crystalline acetanilide, whose hydrogen-bonded chains are similar to those of peptide groups in  $\alpha$ -spiral proteins (Careri *et al.*, 1984). The concept of the Davydov soliton is employed in biophysics because of its possible stability at physiological temperatures  $\sim 300$  K. Davydov (1987) gave an analytical treatment of the thermal effects to prove that at physiological temperatures the soliton does exist. Kadantsev *et al.* (1988), and also Cruseiro *et al.* (1988), conducted a numerical investigation into soliton dynamics in terms of quantum thermal oscillations and found that thermal oscillations make for the formation of a soliton. In contrast, Lomdahl and Kerr (1985), and also Lawrence *et al.* (1986), showed that numerical simulation in terms of thermal oscillations using the “classical” Langevin equation reveals the instability of a Davydov soliton around physiological temperatures. The question of the stability of the Davydov soliton in protein macromolecules with thermal oscillations still awaits its answer. At the same time, it is clear that the existence of long-lived excitations of orbital degrees of freedom at room temperature is, at least, not forbidden (e.g., Zolotaryuk *et al.*, 1991).

When dealing with the “kT problem”, we should remember that the very concept of  $kT$  comes from statistical physics. It only makes sense for systems that do not stray too far from statistical equilibrium. In fact, in such systems the quantum  $\hbar\Omega$  does not noticeably change the statistically mean energy per one degree of freedom of a dynamic system. However, in systems out of equilibrium, e.g., in systems that have a weak connection with the thermostat, where the thermalization process is relatively slow, the field quantum causes a relatively large change in the energy of some degrees of freedom. It is common knowledge that the metabolism of living sys-

tems is a combination of primarily non-equilibrium processes. The birth and decomposition of biophysical structures that occur within time intervals shorter than the thermalization time for the degrees of freedom of these structures are a good example of systems that are far from equilibrium, where even small field quanta are not forbidden to manifest themselves via the variables of structure decomposition. In other words, if the lifetime (thermalization) of some degrees of freedom that interact with field quanta is longer than the characteristic lifetime for the system itself, then such degrees of freedom occur when there is no temperature as such, and the comparison of changes of their energies with  $\kappa T$  on quanta absorption makes no sense anymore.

The mechanism of the interference of quantum states of an ion in an idealized protein cavity, first proposed by this author in Binhi (1997b,c), reduces to the following:

An ion finds its way to a protein cavity via relatively narrow "gates" and stays there in a superposition of quantum states, of the eigenfunctions of the Hamiltonian. The probability density of the ion contains an interference contribution that makes its distribution within the cavity inhomogeneous. In a DC MF the distribution pattern rotates about the MF direction as an integer with a cyclotron frequency. It appears that by superimposing an additional AC MF with special parameters we can sort of stop the pattern rotation. After a long period of stopping or very slow rotation comes an abrupt turning. The pattern sort of freezes. In such a state the rate of ion tunneling from the protein as a non-linear function of the probability density of the ion near the gate changes markedly. We arrive at expressions that relate the "magnetic" part of the probability of the dissociation of an ion-protein complex with MF parameters. The expression predicts multipeak spectra in the MF frequency and amplitude.

In that mechanism the metastability of angular modes of ion oscillations, or rather the metastability of the phase difference of Zeeman sublevels, is postulated. We note that postulated here is not some new entity, but some property of a known object. A substantiation of that are the formulas derived for a number of magnetobiological effects, which, for one thing, possess a predictive capability, and for the other, stay in good, and sometimes even striking, agreement with the experimental evidence due to various authors. That is to say, the methodological requirements of science are met. The good agreement suggests that the interference mechanism of the transformation of an MF signal to a biochemical response is quite real, and that it would make sense to look into why it is workable under thermal perturbations of the walls of a protein capsule.

Section 5.4 addresses the molecular gyroscopic degree of freedom, which seems to possess a relatively long lifetime. In combination with interference effects, such a model enables MBEs to be interpreted even without drawing on serious postulates, and it thus claims to provide a solution to the "kT problem".

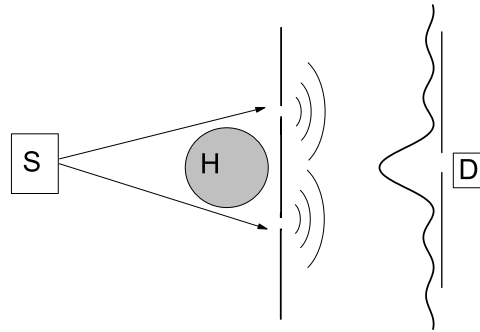


**Figure 3.18.** Interference of charged particles in an AC MF: S, a particle source; H, an MF perpendicular to the plane of the picture; D, a particle detector.

### 3.12.1 Why interference?

We would now like to illustrate the interference MBE mechanism using the following thought experiment on microparticle wave interference. Charged particles from a source can pass through two slits, thus forming an interference pattern on the screen, Fig. 3.18. An AC MF  $H(t) = H \sin \Omega t$  induces a circular electric field that shifts the phases of the wave function in the opposite direction. As a result, the interference pattern will oscillate relative to a position corresponding to  $H = 0$ , at the frequency of the MF.

A characteristic natural frequency here is, clearly, a combination of the parameters of the particle and the MF, such that it possesses a requisite physical dimensionality, i.e.,  $\Omega_c = qH/Mc$ . Therefore, as the MF is varied, the particles will arrive at the target with a phase difference about  $\varphi \sim (q/Mc) \int H(t) dt$  or

$$\varphi \sim \frac{\Omega_c}{\Omega} \sin \Omega t .$$

It is easily seen that the interference pattern will be either stationary, as is the case with high frequencies of an external MF, or completely smeared out, as is the case with low frequencies. Obviously, the most remarkable changes will occur in the frequency range corresponding to the cyclotron frequency of particles, although, of course, any cyclotron resonance is out of the question.

It follows from the last relationship that the amplitude of the oscillations of the interference pattern will vary with both frequency and amplitude of an MF. If they are chosen so that at the extreme positions of the pattern the counter location will coincide with interference maxima, the counter will register the maximal particle flux. In the general case, the dependence of the readings on any MF variable will have several extrema.

Concerning this interference scheme, one might as well pose the question: why does a weak MF with an energy quantum many orders smaller than the characteristic energy of the processes in the particle counter cause, nevertheless, a significant change in the particle flux intensity? An answer is apparent from Fig. 3.18 and is, clearly, no paradox. Interference patterns based on phase shifts rely on what is basically the classical behavior of an electromagnetic field. In the quantum picture, just as is suggested by the form of the above question, corresponding to interference phenomena are multiquantum processes. It follows that the "kT problem" in its initial formulation, which involves a single-quantum process, is formulated incorrectly.

The condition for interference to be observed presupposes a similarity of the characteristic length  $R$  of the problem and the de Broglie wavelength of particles  $\lambda_B = 2\pi\hbar/p$ . It follows that the MF-dependent ion interference could be observed microscopically: the de Broglie wavelength for biologically important ions at physiological temperatures is a fraction of an angstrom. The cavities of some ion-binding proteins are arranged so that they realize this scheme at the microlevel.

# 4

---

## INTERFERENCE OF BOUND IONS

No decision is final, since decisions branch out  
to give rise to others.

J.L. Borges. *Ficciones/The Babylon Lottery*

Interference, or mutual reinforcing and neutralizing of waves, is common to wave systems of different natures: elastic, electromagnetic, etc., for which the superposition principle holds. According to the superposition principle, the complex amplitude of the resulting wave  $A = \sum_i A_i$  equals the sum of amplitudes  $A_i$  of component waves. If the observable is a non-linear function of amplitude, e.g., intensity, which varies with the squared amplitude modulus, then the distribution of that observable will display an interference. The intensity of the resulting wave at any point

$$|A|^2 = \sum_i |A_i|^2 + \sum_{i \neq j} A_i^* A_j$$

is seen to differ from the sum of the intensities of the component waves, which is exactly what constitutes reinforcing and neutralizing of waves.

According to the L. de Broglie hypothesis (1924) on the universal nature of the corpuscular-wave dualism, wave properties are inherent in any matter particles, and not only in photons, quanta of electromagnetic field. The characteristic wavelength  $\lambda_B$  that corresponds to a particle with a momentum  $p$  will be  $\lambda_B = 2\pi\hbar/p$ . An obvious criterion for interference to be observed is that the de Broglie wavelength should be comparable with the scale  $r$  of an observation system. That is a significant constraint; among other things it does not enable interference of macroscopic particles to be observed. At the same time, interference of electrons, atoms, and even molecules is well known.

A treatment of the nature of de Broglie waves, as proposed by M. Born, is relying on a quantum-mechanical description of particles using the wave function or the complex probability amplitude  $\psi$ . The quantum state of a particle is in the general case described by a superposition of its possible states

$$\Psi(\mathbf{x}) = \sum_i a_i \psi_i(\mathbf{x}) ,$$

where  $a_i$  are complex coefficients, and  $\mathbf{x}$  is a set of variables. The probability density for a particle to be detected at point  $\mathbf{x}_0$ , according to Born's concept, is

$$|\Psi(\mathbf{x}_0)|^2 = \Psi^*(\mathbf{x}_0)\Psi(\mathbf{x}_0) = \sum_i |a_i|^2 |\psi_i(\mathbf{x}_0)|^2 + \sum_{i \neq j} a_i^* a_j \psi_i^*(\mathbf{x}_0) \psi_j(\mathbf{x}_0),$$

which also contains an interference (second) term.

The main way to observe interference is to create conditions for diffraction (scattering) of free particles by regular structures with a period similar to a particle's de Broglie wave.

Diffraction of optical-range photons is observed using optical diffraction gratings with a period of  $\sim 10^{-4}$  cm. The energy of X-ray photons is several orders of magnitude larger, and here gratings that are formed by the regular structure of matter, mainly crystalline matter, are suitable.

They observe interference of particles with a rest mass. Electron diffraction on a rough surface is the underpinning idea of various electron microscopes. Energies of heavier particles, such as protons, neutrons, and light atoms, can be so selected or made up that their de Broglie waves would fall into the range  $1 \text{ \AA} = 10^{-8}$  cm. In such a case, particle scattering by regular structures of that scale, i.e., crystalline bodies, produces diffraction maxima of particle flux in certain directions, which can be derived from constructive interference conditions. In the process, information on the microscopic spatial structure of scattering crystals is transformed into the angular distribution of maxima, which is easily recorded in macrolevel experiments. Interference occurs here in a flux of free particles that probe into the microstructure of matter.

Interference of waves or quantum states of helium atoms in diffraction at a grating formed by a standing EM wave, i.e., by photons, was investigated in Pfau *et al.* (1994).

Also possible is the interference of bound particles. The Heisenberg uncertainty principle (1927) has it that for a particle localized in a microscopic area of size  $r$  the mean momentum will be no less than  $\sim \hbar/r$ , and respectively the de Broglie wavelength will be  $\lambda_B \lesssim 2\pi r$ . Then, by the interference observability criterion, an observation is only possible if a measurement of a particle state is localized in the same area  $r$ . Interference of bound electrons is observed. It is known as interference of quantum atomic states, see, e.g., the monograph by Alexandrov *et al.* (1991), although in essence the nature of the interference of free particles is quantum as well. Interfering electron states in an atom are probed using optical electromagnetic radiation whose wavelength is four orders of magnitude larger than atomic distances. That EMF range corresponds to the energy of quantum transitions between interfering states, which is fractions of electronvolts, and it is therefore most suitable. Emissive transitions induced by an optical field, in the simplest case from two neighboring levels to some lower level, are accompanied by an emission of electromagnetic waves with close frequencies. It is the interference of those waves that produces the observed modulation of emission intensity with differential frequency.

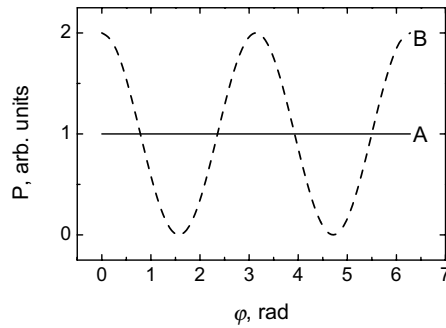


**Figure 4.1.** The angular distribution of probability density: A, state  $m = 1$ ; B, superposition of states  $m = \pm 1$ .

In that respect, it is not quite correct to talk specifically of interference of atomic states, although the term has long been accepted in the literature.

Scattered light that includes modulated re-emitted waves carries information on the intra-atomic state of electrons, thus yielding deeper insights into matter structure.

There have been no reports of interference of bound ions. That is concerned with some details of the observation of interference of atomic states.

It makes sense to talk also of interference of atomic states in the precise sense of the term, without specific reference to the interference of re-emitted probing light. In a more general aspect, one can talk about interference of bound states of atomic type. We will explain that using the following example.

Suppose there is some instrument that enables one to measure probability density distribution for a particle bound in an arbitrary central potential where it resides. Let now the measurand be the angular distribution of density  $p(\varphi)$ . If the particle is in a  $p$ -state, the orbital and magnetic quantum numbers will be  $l = 1$ ,  $m = 0, \pm 1$ , respectively. The angular mode of the wave function in a state  $m = 1$  is<sup>27</sup>  $e^{i\varphi}$ ; therefore the density angular distribution is uniform,  $p(\varphi) = |e^{i\varphi}|^2 = 1$ , Fig. 4.1-A. The same holds true for a particle in a state  $m = -1$ . If a superposition of states  $m = 1$  and  $m = -1$  occurs, then the probability density will depend on the angle in a non-trivial manner, e.g.,

$$p(\varphi) = \left| \frac{1}{\sqrt{2}}e^{i\varphi} + \frac{1}{\sqrt{2}}e^{-i\varphi} \right|^2 = 2 \cos^2 \varphi .$$

That is, the particle stays primarily in certain angular sectors of its residence area, near the values  $\varphi = 0$  and  $\varphi = \pi$ , Fig. 4.1-B. Polarization then occurs, or rather the aligning of the particle state along some axis.

<sup>27</sup>Here we omit insignificant normalization coefficients.

A particle's wave functions also have phase factors that depend on a state's energy and time  $e^{-i\epsilon t/\hbar}$ . For states  $m = \pm 1$  energies are the same, and the availability of additional phase factors does not change the situation. Changes occur in a magnetic field  $\mathbf{H}$ . One should then take into consideration the Zeeman splitting of initially degenerated states  $m = \pm 1$ , whose energies are now  $\epsilon_{\pm} = \epsilon \pm \Delta\epsilon$ . For the probability density we then get

$$p(\varphi) = \left| \frac{1}{\sqrt{2}} e^{i\varphi} e^{-i\epsilon_+ t/\hbar} + \frac{1}{\sqrt{2}} e^{-i\varphi} e^{-i\epsilon_- t/\hbar} \right|^2 = 2 \cos^2 \left( \varphi - \frac{\Delta\epsilon}{\hbar} t \right) .$$

In a coordinate system rotating about the axis  $z \parallel \mathbf{H}$  with an angular velocity  $-\Delta\epsilon/\hbar$ , the angular distribution is clearly stationary. Therefore, in the laboratory system the sectors of the preferred residence of a particle rotate with an angular velocity  $\Omega = \Delta\epsilon/\hbar$ . Also if the measuring instrument has an inertia that does not allow it to record any changes faster than those occurring during the time  $\Omega^{-1}$ , then it is impossible to measure angular distribution. The instrument will record a uniform distribution. It appears, however, that by superimposing on a system an additional variable MF of a certain frequency and amplitude, one can effectively discontinue the rotation of the sectors, see Section 4.1.1. Now it becomes again possible to register the sector structure of a wave function.

Thus, an MF has several regimes that enable the interference of bound quantum states to be observed. Those are zero MF (a magnetic vacuum) and a number of combinations of a DC and AC MFs with certain parameters. These latter, as will be seen later, are dependent on the level of the DC MF and the properties of a bound particle.

What instrument or method would be suitable to register sector structure of the wave function of a bound particle in an MF? With electron states in atomic spectroscopy, one can judge of the polarization of an atomic state from the state of the polarization of a re-emitted electromagnetic field. Is it possible to register polarization outside of radiation probes? One possible way would be to locally reduce the potential in a small angular space of the total solid angle. Let a particle be contained within an impenetrable sphere with a hole, so that the particle potential at the hole is reduced to some finite value. The particle overcomes the potential barrier through tunneling. Since the probability of a tunnel transition depends on the probability density for the particle to be near the hole, the decomposition of a bound state, i.e., the exit of the particle beyond an area of its metastable residence, could be an indicator of some special MF conditions that cause the emergence of a sector structure.

One interesting version of such a scheme is associated with the recently discovered and intensively studied class of structural organization of carbon atoms, namely with fullerenes (Kroto *et al.*, 1985; Ball, 1993; Taylor and Walton, 1993). The molecular formula of those compounds is  $N_{60}$ ,  $C_{70}$ , etc. Their distinctive characteristic is that a fulleren molecule has the shape of a spherical envelop, or rather of a high-order polyhedron. The fulleren cavity can also contain "extraneous" atoms, which with time leave the cavity due to quantum diffusion. A concise overview of

such fullerenes (they call them endofullerenes) as  $\text{Ca}@C_{60}$ ,  $\text{Y}@C_{82}$ ,  $\text{La}@C_{82}$  and others is given in Bethune *et al.* (1993). It would be reasonable to suppose the presence of weak MF effects, i.e., the influence of an MF on the decay rate of a metastable bound state of endofullerenes. The inner cavity of fullerenes containing a  $^3\text{He}$  atom was probed (Saunders *et al.*, 1994) using NMR spectroscopy. However, there is no evidence for the influence of variable MFs on processes involving endofullerenes yet.

A further possible way to independently observe the effect is through the use of tunnel microscopy. Tunnel microscopes have long been employed to study two-dimensional electron states that occur on the surface of copper, silver, gold, etc., see, e.g., (Andryushechkin *et al.*, 1998). The images show clearly some patterns of surface electron density engendered by interference of electron waves, the incident one and the one scattered by surface defects (Crommie *et al.*, 1993b). For surface defects here adsorbate molecules, which can be organized, using the microscope scanning needle, are proposed as an electron container of arbitrary shape (Zettle, 1993).

So Crommie *et al.* (1993a) managed to put on an atomically even copper surface 48 iron atoms arranged as a closed circumference. Within the circumference, there emerged characteristic density waves like those produced by a stone thrown on the water. Electrons, when captured in a suitable container, appear to be in a metastable state. A superposition of angular modes of such bound states in a properly selected MF would produce an interference redistribution of electron density. A naturally occurring idea would be to try and reveal it using the same microscope. Those who thrive on generalizations would see in it a prototype of nanoscopic memory cells controlled by a magnetic field for the computers of the future.

Suitable cavities are also available in some crystalline electrider-type salts, in which a cation is coupled by ionic bonds with crown-ethers (Wagner *et al.*, 1994).

Interesting objects for possible observations of dissociation interference effects are crystals, polycrystals, and solutions of a trimethylsilyl-derivative of a silicate anion. The molecule of that matter  $[(\text{CH}_3)_3\text{Si}]_8\text{Si}_8\text{O}_{20}$  differs in that it has at its center a near-cubical cavity made up of 20 oxygen atoms. The oxygen atoms sit at the apexes and centers of cube edges deformed into a sphere. Such a cavity, as shown in Sasamori *et al.* (1994), is capable of retaining hydrogen atoms, without forming chemical bonds with them. Exposure of methyl groups to  $\gamma$ -rays of radioactive  $^{60}\text{Co}$  knocks out some ( $4.3 \cdot 10^{-5}$ ) hydrogen atoms, which appear to be within the cavities. Atomic hydrogen is identified by the g-factor and superfine splitting of the ESR doublet. It is to be noted that ESR spectra of atomic hydrogen can be observed for years if samples are not heated above  $150^\circ\text{C}$ . Experiments with such a substance are especially convenient since the tunneling of hydrogen from the cavities is directly related to the ESR signal intensity.

Of special interest are cavities of protein macromolecules that bind some ions. Protein activity, including that in relation to other enzymes, is dependent on the availability of an ion in a bound state. Then biological effects occur, when an MF affects the decay probability for a bound state, or rather the dissociation probability

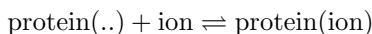
of the respective ion-protein complex. Interestingly, that hypothesis is supported by magnetobiological observations (Binhi, 1997b, 1998a, 1999b, 2000; Binhi *et al.*, 2001).

For many biologically significant ions, the de Broglie wavelength, even at  $T = 300\text{ K}$  is only three–six times smaller than their ion radii and is close to the size of the effective potential of a binding cavity. For instance, the ion–ligand separation at a calcium-binding site in troponin C protein is  $2.4\text{ \AA}$  (Satyshur *et al.*, 1988). That site also binds magnesium ions. Radii of the binding ions  $\text{Ca}^{2+}$  and  $\text{Mg}^{2+}$  are  $1.74$  and  $1.36\text{ \AA}$ , respectively. Consequently, the effective potential radius is  $0.7\text{--}1\text{ \AA}$ . At the same time, their de Broglie wavelengths  $\lambda = 2\pi\hbar/p$  are  $0.28$  and  $0.36\text{ \AA}$  for the mean thermal momentum  $p = \sqrt{2MkT}$ . Therefore, on atomic scale, ions display properties that cannot be reduced to the behavior of classical particles. It takes quantum mechanics to describe ion states within protein cavities.

#### 4.1 DISSOCIATION OF ION-PROTEIN COMPLEXES IN A MAGNETIC FIELD

This section deals with a physically consistent model that accounts for one mechanism for the behavior of biological systems exposed to weak low-frequency magnetic fields. It relies on changes in probability density for an ion within a protein exposed to a magnitude-modulated magnetic field. Dissociation probability for an ion-protein complex is significantly dependent on the details of a magnetic field, which is a corollary of interference of angular modes of quantum states of an ion within a protein cavity. Using that model, frequency–amplitude dependences are derived for ion-binding probability, or rather for the dissociation probability of an ion-protein complex.

A reaction of protein binding of ions



occurs as follows. A protein sort of captures an ion into a cavity formed by ligands. This changes the biological activity of the protein. Since an MF can shift an equilibrium of that reaction, in the final analysis an activity change manifests itself through an observed biological response.

An ion finds its way into a binding cavity through the “gate”, Fig. 4.2. It appears to be trapped in the cavity, since the gate potential barrier is fairly high. According to the findings of biochemical kinetics, a relaxation time for an equilibrium of that reaction is about  $0.1\text{ s}$ , see p. 230. The following model rests on the assumption that the probability for an ion to exit is not indifferent to the quantum state of an ion in the cavity. We will believe that the probability of ion exit or dissociation of an ion-protein complex varies in a non-linear manner with the ion probability density near the gate. Owing to interference of ion quantum states, an MF causes a redistribution of the ion cloud, which affects the reaction equilibrium constant.

The structure of some calcium-binding proteins is known with an accuracy sufficient to get an insight into the internal geometry of ion-binding cavities. Some

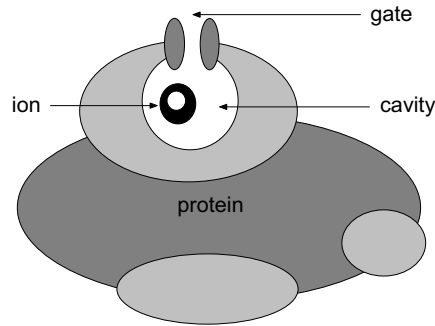


**Figure 4.2.** An ion finds its way into a binding cavity through the gate formed by interstices of oxygen-binding ligands.

results of diffractometric analysis of the structure of troponin C are reported in Satyshur *et al.* (1988). High resolutions of nearly  $2 \text{ \AA}$  were obtained using a synchrotron emission source. Troponin C binds four  $\text{Ca}^{2+}$  ions by two cavities with a high affinity to calcium, which also bind  $\text{Mg}^{2+}$  ions, and by two other cavities with a low affinity. Calcium binding with troponin C leads to a significant conformational restructuring of a protein, which in the final analysis is transferred to the level of observed biochemical or biological responses. Coordination of calcium ions in the cavity approaches seven. The structure of high-affinity cavities is shown in Fig. 4.3. Ligands are arranged in a nearly octahedral manner, interligand spacing being  $R \approx 2.4 \text{ \AA}$ . Ion radii of calcium and oxygen atoms in ligands are  $1.74$  and  $0.136 \text{ \AA}$ . Similar findings were reported in Babu *et al.* (1988) for the binding cavity of calmodulin protein.

As is seen in Fig. 4.3, the motion area size for a calcium ion is fairly small. That makes the calcium ion potential within a cavity fairly close to a spherically symmetrical or central potential. To arrive at an approximate numerical estimate, we will assume that ions form rigid spheres of appropriate radii, and that ligands are fixed in their idealized octahedral positions, and that the shift of a central ion is only limited by contacts of ion spheres. Suppose, for instance, that an ion shifts in a horizontal plane. The smallest shift is in the direction of a ligand, the largest between ligands. A dependence of the maximally possible shift  $x$  on the polar angle follows from geometrical considerations

$$x(\varphi) = r \cos \varphi - \sqrt{(r_{\text{ca}} + r_{\text{ox}})^2 - r^2 \sin^2 \varphi}, \quad 0 \leq \varphi \leq \pi/4,$$

where  $r$  is the distance from the cavity center to the ligand center, and  $r_{\text{ca}}$  and  $r_{\text{ox}}$  are ion radii for calcium and oxygen atoms, respectively. From that function one can isolate a constant component, which is concerned with the central potential, and also an angle-dependent part, which represents an additional potential function with a low-order symmetry. Omitting computations, we will only indicate here that

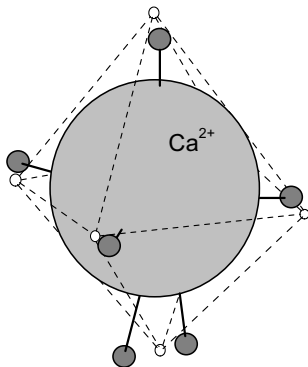


**Figure 4.3.** Octahedral coordination of an ion in a binding protein cavity; proportions are retained of ion radii for a particle and ligands, and cavity size. According to Babu *et al.* (1988) and Satyshur *et al.* (1988).

for given sizes of ions and cavities, the potential function is largely (approximately 80 %) a central-symmetrical potential of radius  $0.7 \text{ \AA}$ , which is only slightly smaller than the electron Bohr radius. Therefore, in this mathematical model we will assume an ion to be a point charge in an effective potential of radius about  $0.7 \text{ \AA}$ .

#### 4.1.1 Model

We will take an idealized view of an ion as a particle with charge  $q$  and mass  $M$  that in the general case has its own angular momentum  $I$ , in  $\hbar$  units, and nuclear magnetic moment  $\mu$ . An ion resides in a spherically symmetrical potential  $U(r)$  created by the walls of a protein binding site. The ion gets into the site through a relatively narrow gate, whose opening is determined by the value of the probability density for an ion to be found near the gate.

The Hamiltonian for a free particle in an MF can be found in many books, e.g., in Slichter (1980) and Landau and Lifshitz (1977). Up to terms  $\propto c^{-1}$  it can be written as

$$\mathcal{H} = \frac{(\mathbf{P} - \frac{q}{c}\mathbf{A})^2}{2M} + qA_0 - \gamma\hbar\mathbf{I}\mathbf{H}.$$

Here  $\mathbf{P} = -i\hbar\nabla$  is the momentum operator;  $\mathbf{A}$ ,  $A_0$  are the vector and scalar potentials of an electromagnetic field, respectively;  $\mathbf{H} = \nabla \times \mathbf{A}$  is the MF strength;  $\hbar$  is the Planck constant; and  $\gamma = \mu/I\hbar$  is the gyromagnetic ratio. Let us chose the potentials of an external homogeneous field in the form  $\mathbf{A} = \mathbf{H} \times \mathbf{r}/2$ ,  $A_0 = 0$ . Then for a spherically symmetric potential  $U$  we write

$$\mathcal{H} = \frac{\mathbf{P}^2}{2M} + U - (\hbar b\mathbf{L} + \hbar\gamma\mathbf{I})\mathbf{H} + \frac{q^2}{8Mc^2}(\mathbf{H} \times \mathbf{r})^2. \quad (4.1.1)$$

Here  $\mathcal{L} = -i\mathbf{r} \times \nabla$ ,  $\mathcal{I}$  are operators of the angular momentum and spin, and  $b = q/2Mc$  is the parameter of an ion. We have taken into consideration that

$$\mathbf{A}\nabla = \nabla\mathbf{A} = \frac{1}{2}\nabla(\mathbf{H} \times \mathbf{r}) = -\frac{1}{2}\mathbf{H}(\nabla \times \mathbf{r}), \quad i\frac{q\hbar}{Mc}\mathbf{A}\nabla = -\frac{q\hbar}{2Mc}\mathbf{H}\mathcal{L}.$$

We here ignore the contribution of  $\propto \mathbf{A}^2$  (see the estimate (5.4.14)), i.e., the last term in the Hamiltonian that determines the small diamagnetic susceptibility of a system. Then the Hamiltonian (4.1.1) will include the kinetic, potential, and Zeeman (orbital and spin) energies. For ions with a nuclear spin, the coefficients in (4.1.1) meet the inequality  $\gamma > b$ . Therefore, we cannot ignore the spin effects, and so they are considered in Sections 3.10 and 4.8. We here put  $I = 0$ . If the MF varies only in magnitude, but not in direction, i.e.,

$$H_x = H_y = 0, \quad H_z = H_{\text{DC}} + H_{\text{AC}} \cos(\Omega t), \quad (4.1.2)$$

then the potential  $U(r)$  retains the  $z$  component of the angular momentum. The appropriate operator is replaced by its eigenvalues  $l_z = m$  and the Hamiltonian takes on the form

$$\mathcal{H} = \mathcal{H}_0 - \eta_m H_z, \quad \mathcal{H}_0 = \frac{\mathbf{p}^2}{2M} + U, \quad \eta_m = m\hbar b. \quad (4.1.3)$$

In the absence of an MF the wave functions of an ion, eigenfunctions  $\mathcal{H}_0$ , up to normalization have the form (Landau and Lifshitz, 1977)

$$\psi_{klm} = R_{kl}(r)P_l^{|m|}(\theta) \exp(im\varphi), \quad (4.1.4)$$

where  $R_{kl}$  are radial functions that depend on the form of  $U(r)$ .  $P_l^m(\theta)$  are associated Legendre functions;  $k, l, m$  are the radial, orbital (or azimuthal), and magnetic quantum numbers; and  $r, \theta, \varphi$  are the spherical coordinates. The operator  $-\eta_m H_z$ , which reduces to a multiplication operation, clearly does not affect the functions (4.1.4) and therefore only changes the instantaneous values of the energies of these states (Zeeman splitting). There are no quantum transitions between the states of an ion exposed to a field (4.1.2), and so there are no resonance conditions for transitions. What can depend on the variables of an MF in that case?

We will write the solution of the Schrödinger equation with a Hamiltonian (4.1.3)

$$\Psi = \sum_{klm} a_{klm} R_{kl}(r) P_l^{|m|}(\theta) \exp \left[ im\varphi - \frac{i}{\hbar} \varepsilon_{kl} t + \frac{i}{\hbar} \eta_m \int H_z dt \right], \quad (4.1.5)$$

where  $\varepsilon_{kl}$  are unperturbed energies of states  $\psi_{klm}$ , and the coefficients  $a_{klm}$  specify the initial conditions.

To arrive at quantities that could be compared with experimental evidence, in what follows one will have to average over an ensemble of independent particles. Therefore, one should have specified in (4.1.5) random phases of angular modes  $\exp(im\varphi)$  defined on an ensemble. Considering that statistical distributions of those

phases are uniform in the interval  $[0, 2\pi)$ , the mathematical expectation of appropriate harmonic processes can be sought in an ergodic approximation, as a limit of averaging over an infinite time interval. We will adopt that averaging formula, as it is simpler to treat. No random phases are written, and all the formulas obtained by averaging over an infinite time interval should be treated as formulas for an average over a particle ensemble.

Let us now find the probability density for an ion to be near a gate, i.e., for some value of  $\varphi = \varphi_0$ ,

$$\begin{aligned} p(\varphi_0, t) &= \langle \Psi(\varphi_0, t) | \Psi(\varphi_0, t) \rangle_{r, \theta} \\ &= \sum_{mm'} a_{mm'} \exp \left[ i\Delta m \varphi_0 + i\Delta m b \int H_z dt \right], \end{aligned} \quad (4.1.6)$$

where  $\Delta m$  is the difference of quantum numbers  $m' - m$ . The coefficients

$$a_{mm'} = \sum_{k, k', l, l'} a_{klm}^* a_{k'l'm'} \exp \left[ \frac{i}{\hbar} (\varepsilon_{kl} - \varepsilon_{k'l'}) t \right] \langle R_{kl} | R_{k'l'} \rangle \langle P_l^{m'} | P_{l'}^{m'} \rangle \quad (4.1.7)$$

are density matrix elements in the representation of eigenfunctions of operator  $l_z$ . They consist of constants ( $k = k', l = l'$ ) and fast-oscillating terms. In fact, for an ion  $\text{Ca}^{2+}$  in a trap of size  $R \sim 0.7 \text{ \AA}$  in the ground and excited states the frequency of these oscillations is about  $\hbar/MR^2$ , i.e., about  $10^{11}$  Hz. This size corresponds to the Ca-binding cavity of troponin C (Satyshur *et al.*, 1988). Calmodulin, a low-molecular regulatory protein, which is abundant in living tissues, has binding cavities of similar size (Babu *et al.*, 1988). Sizes for various cavities of other proteins are given in Williams *et al.* (1994). Since in what follows averaging will be done over the time interval  $T \gg 10^{-10}$  s, the elements  $a_{mm'}$  can be considered constant. Transforming (4.1.6), subject to (4.1.2), we find<sup>28</sup>

$$\begin{aligned} p(\varphi_0, t) &= \sum_{mm'} a_{mm'} \exp \left[ i\Delta m \left( \varphi_0 + \omega_0 t + \frac{\omega_1}{\Omega} \sin(\Omega t) \right) \right], \\ \omega_0 &= bH_{\text{DC}}, \quad \omega_1 = bH_{\text{AC}}, \quad b = q/2Mc. \end{aligned} \quad (4.1.8)$$

The frequency  $\omega_0 = qH_{\text{DC}}/2Mc$  is called the Larmor frequency. Note that the quantity in parentheses in (4.1.8) is proportional to the phase difference of interfering angular modes.

It can be shown that averaging over time we get  $\bar{p} = \text{Const}$ . At first we write  $p$  averaged over a finite time interval  $[-T, T]$ , which we will need later

$$\begin{aligned} p_T &\equiv \frac{1}{2T} \int_{t-T}^{t+T} p(\varphi_0, t') dt' \\ &= \frac{1}{2\Omega T} \sum_{mm'} a_{mm'} \exp(i\Delta m \varphi_0) \int_{\Omega(t-T)}^{\Omega(t+T)} \exp(i\alpha z \tau) \exp(iz \sin \tau) d\tau, \end{aligned} \quad (4.1.9)$$

---

<sup>28</sup>To go over to the MKS system one should put  $b = q/2M$ .

where we have introduced the designations

$$z = \Delta m \frac{\omega_1}{\Omega}, \quad \alpha z = \Delta m \frac{\omega_0}{\Omega}, \quad \alpha = \frac{\omega_0}{\omega_1} = \frac{H_{DC}}{H_{AC}}. \quad (4.1.10)$$

Since

$$\exp(iz \sin \tau) = \sum_{n=-\infty}^{\infty} J_n(z) \exp(in\tau), \quad (4.1.11)$$

then the integral in (4.1.9) can be taken easily. It is

$$2 \sum_n J_n(z) \frac{\sin[(\alpha z + n)\Omega T]}{\alpha z + n} \exp[i(\alpha z + n)\Omega T].$$

After its substitution, (4.1.9) becomes

$$p_T = \sum_{mm';n} a_{mm'} \exp[i\Delta m \varphi_0 + i(\alpha z + n)\Omega T] \frac{\sin[(\alpha z + n)\Omega T]}{(\alpha z + n)\Omega T} J_n(z). \quad (4.1.12)$$

In the general case, where  $\alpha z + n \neq 0$

$$\bar{p} = \lim_{T \rightarrow \infty} p_T = \sum_m a_{mm}, \quad (4.1.13)$$

since all the terms of the sum (4.1.12) with  $m' \neq m$  tend to 0. That expression is independent of MF, and so we arrive at a trivial result that cannot be correlated with patterns observed in experiment.

In a special case, the frequency of an external MF can be so selected that the condition  $\alpha z + n = 0$  will be met:

$$\Omega = -\frac{\Delta m}{n} \omega_0.$$

The condition will be met for several terms of the sum, for which  $m, m', n$  are such that  $\Delta m/n$  has the same value. These terms produce a time-independent contribution to  $p_T$

$$\sum_{mm';n} a_{mm'} \exp[i\Delta m \varphi_0] J_n(z).$$

That is, under these conditions, substituting  $z = -n/\alpha$ , we get

$$\bar{p} \sim \text{Const}_1 + \text{Const}_2 \sum_n J_n\left(-n \frac{H_{AC}}{H_{DC}}\right). \quad (4.1.14)$$

It might seem that the sought behavior of the model system has been found. At certain frequencies of an external field, defined by

$$\Omega_p = \frac{\Delta m}{n} \omega_0, \quad (4.1.15)$$

a situation occurs where the probability for an ion to reside within some angular position  $\varphi_0$  is non-trivially dependent on the value of the DC MF and on the

amplitude of a variable MF by (4.1.14). An explanation could be forthcoming from experiments where MBEs are observed under similar magnetic conditions. Nevertheless, such an explanation is not correct, since the equality  $\alpha z + n = 0$  cannot be realized physically in experiment. Any infinitesimal deviation from it yields the result  $\bar{p} = \text{Const}$ , different from (4.1.14). The probability density  $\bar{p}$ , taken to be a function of the MF frequency  $\Omega$ , is not continuous at points (4.1.15)

$$\lim_{\Omega \rightarrow \Omega_p} \bar{p}(\Omega) \neq \bar{p}(\Omega_p) .$$

Experiment yields another, smooth, dependence of an MBE on frequency. Such a disagreement could be treated as a broadening of the resonance curve caused by damping. However, in a given case, as mentioned above, there is no resonance, and so the notion of resonance width is void. This incorrectness is also caused by the fact that the expression for (4.1.14), which is comparable with an MBE, is dependent on the angle  $\varphi_0$ , which is clearly no parameter of the model. It is over that angle that the averaging should be done, but that also yields a trivial result  $\bar{p} = \text{Const}$ , which is also at variance with experiment.

One solution is to take into consideration the non-linear nature of the relation for the probability density  $p(\varphi_0, t)$  with an intermediate quantity, namely the probability for an ion to leave the binding cavity. In the final analysis, it is a change in this probability that causes an MBE.

Let the probability  $P$  of a biochemical reaction itself, namely of the dissociation of an ion-protein complex, be *non-linearly* dependent on the probability  $p$  for a particle to be found near the gate. We will only take into account the linear and quadratic expansion terms<sup>29</sup>

$$P(p) = P(\bar{p}) + P'_p \tilde{p} + \frac{1}{2} P''_{pp} \tilde{p}^2 + \dots , \tag{4.1.16}$$

where  $\tilde{p} = p - \bar{p}$ . Averaging over time yields  $\bar{P} = c_1 + c_2 \overline{\tilde{p}^2}$ , where  $c_{1,2}$  are constants. Of interest here is the quantity  $\overline{\tilde{p}^2}$ , which determines the dependence of  $\bar{P}$  on MF parameters. Further, the notation  $\mathbf{P}$  refers precisely to that quantity. In our estimates we will rely on the fact that relatively fast oscillations of density  $\tilde{p}$  cause no non-linear response in a protein, for it has no time to respond by changing its conformation to a state that could be tagged, for instance, as “gate open”. Therefore, it would be natural to at first average  $\tilde{p}$  over some time interval  $T$  of about the response time, and then work out the squared mean of the quantity derived

$$\mathbf{P} \sim \overline{(\tilde{p}_T)^2} . \tag{4.1.17}$$

Physically, the time  $T$  is the measurement time or the time taken for changes in probability density to accumulate, the time during which a protein “allows” a particle to stay in a state that is correlated in phase with an MF. If the time is

---

<sup>29</sup>Contribution of further terms is considered separately in Section 4.2.

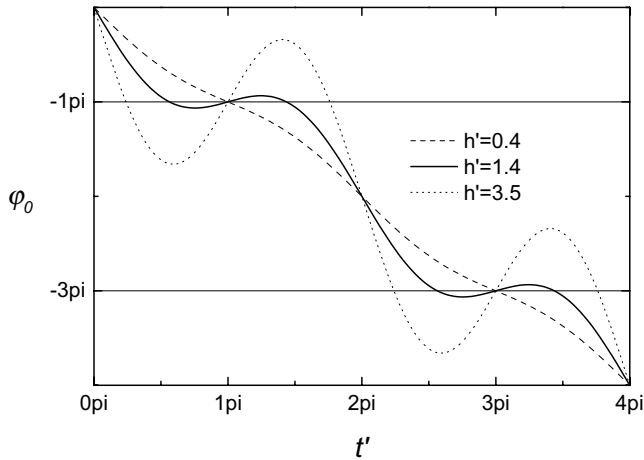


**Figure 4.4.** A shift of a probability density maximum for an ion depending on time  $t'$  at frequency  $\Omega' = \frac{1}{2}$  and various values of relative amplitude  $h'$ .

long, then the protein will only take notice of changes that will have accumulated during that time span. For changes accumulated during  $\sim T$  to be noticeable, there should be a slow component in the process of changing the probability density. That is, the frequency of an external field must be sufficiently close to the frequency of an interference maximum. It is thus clear beforehand that the time  $T$  is a model parameter connected with the frequency width of a biological response.

We will illustrate this by a simple example. Consider the behavior of function  $p(\varphi_0, t)$  with  $a_{mm'} = 1$ . We will introduce the dimensionless variables  $t' = \omega_0 t$ ,  $h' = H_{AC}/H_{DC}$ ,  $\Omega' = \Omega/2\omega_0$ ; then from (4.1.8) we find

$$p(\varphi_0, t') = \sum_{mm'} \cos \left[ \Delta m \left( \varphi_0 + t' + \frac{1}{2} \frac{h'}{\Omega'} \sin(2\Omega' t') \right) \right].$$

In order to explain the general nature of the behavior of probability density we will consider interference of angular states with magnetic quantum numbers differing by 1 at frequency  $\Omega' = \frac{1}{2}$ . That frequency, as it will become clear from what follows, corresponds to a maximum of interference angular modes. Up to an inessential factor, the probability density is equal to

$$p_{\Delta m=1}(\varphi_0, t') = \cos(\varphi_0 + t' + h' \sin t').$$

This is the part of probability density that depends on MF; it can take on negative values. The angular position of a probability density maximum is then given by the equation

$$\varphi_0(t', h') = -t' - h' \sin t' .$$

That function for various values of amplitude of a field  $h'$  is given in Fig. 4.4. It is clearly seen that at some value of  $h'$  a probability density maximum remains nearly stationary for a relatively long time. That is due to the fact that during that time the phase difference of interfering modes remains almost unchanged. Then the maximum quickly shifts to an equivalent position; i.e., it turns through a full angle. This sort of “freezes” the phase difference, and the maximum density “hangs” in some angular position. In the general case, where the field frequency does not correspond exactly to frequencies of maxima interference, that fast turn is slightly different from  $2\pi$ . Therefore, a sector that corresponds to a maximum is rotating slowly. It is this that makes an average over a large time interval to be equal to  $\bar{p} = \text{Const}$ . However, if a protein’s response time to a thickening of a probability cloud is smaller than the period of that slow rotation, then the protein will have time to respond. Such an averaging over an ensemble or over an infinite time interval should be conducted after one has taken into consideration the protein’s response to a density thickening. At the same time, it is expedient to perform immediately a sliding averaging in order to smooth out the relatively fast oscillations.

Considering that, safe for physically unrealizable cases,  $\bar{p} = \sum_m a_{mm}$ , one can apply to  $\tilde{p}$  and  $\tilde{p}_T$  the formulas (4.1.8) and (4.1.12), respectively, where in the summation over  $m, m'$  we put  $m \neq m'$

$$\tilde{p}_T = \sum_{m \neq m'; n} a_{mm'} \exp [i\Delta m \varphi_0 + i(\alpha z + n)\Omega t] \frac{\sin[(\alpha z + n)\Omega T]}{(\alpha z + n)\Omega T} J_n(z). \quad (4.1.18)$$

To derive P, one should square (4.1.18) and average over the time interval  $\gg T$ . Clearly, contributing to the expression for P will only be those terms of  $\tilde{p}_T \cdot \tilde{p}_T$ , which are products of complex conjugate terms (4.1.18). They contain no oscillating dependence on time; therefore in a final averaging their contribution does not vanish. Put another way, here the squared sum (4.1.18) reduces to the sum of some squared terms. Therefore,

$$P = \sum_{m \neq m'; n} |a_{mm'}|^2 \left( \frac{\sin[(\alpha z + n)\Omega T]}{(\alpha z + n)\Omega T} \right)^2 J_n^2(z). \quad (4.1.19)$$

We see that a dependence on  $\varphi_0$  vanished, as expected. In fact, the angular position of the gate in relation to a spherically symmetrical potential should play no role. Substituting the designations (4.1.8) and (4.1.10), we will write the final expression for the dissociation probability of an ion-protein complex ( $2\pi f = \Omega$ )

$$P(f, H_{DC}, H_{AC}) = \sum_{m \neq m'; n} |a_{mm'}|^2 \quad (4.1.20)$$

$$\times \left( \frac{\sin[b(m' - m)H_{DC}T + 2\pi n f T]}{b(m' - m)H_{DC}T + 2\pi n f T} \right)^2 J_n^2 \left[ (m' - m) \frac{b}{2\pi f} H_{AC} \right].$$

The effect described by (4.1.20) is no resonance; i.e., it does not involve a resonance pumping of oscillator energy from some modes to others. That is basically

an effect of interference of quantum states of an ion within a protein capsule. For certain MF parameters, interference results in a thickening of the probability cloud for an ion to be found in a certain angular position. The thickening is shifting slowly and, when it passes the gate, it triggers a protein response to a change in the gate size.

#### 4.1.2 Ion states in a protein cavity

The most frequently heard objection to the Hamiltonian writing (4.1.1) is that it fails to take into account a deviation from the spherical symmetry of the potential of a binding cavity and the absence of terms describing the interaction of an ion with thermal oscillations of binding ligands.

It was pointed out above that, considering the size of an ion in a cavity, its potential primarily consists of a centrally symmetrical part. In a further approximation, the potential of an ion can be represented as a sum

$$U(\mathbf{r}) = U(r) + \zeta u(\theta, \varphi), \quad \zeta \ll 1.$$

In that approximation the small octahedral contribution  $u(\theta, \varphi)$  can be viewed as a permanent perturbation of the Hamiltonian. Then each Zeeman sublevel of an ion would appear to be split once more in accordance with a irreducible representation of the symmetry group of an octahedron. In terms of the model at hand, that would lead to an appearance of a new quantum number to identify sublevels with the same values of magnetic quantum numbers, and to a need to average over that number as well. That new splitting is much stronger than magnetic splitting. Therefore, changing that quantum number does not influence the interference of close states with different magnetic quantum numbers. To be sure, calculated spectra would change, but only in some minor details.

Magneto-dependent interference also exists in the opposite approximation where we can ignore a central potential and only consider a low-symmetrical potential. Such an approximation is known as that of a crystalline field. It leads to the so-called freezing of the orbital momentum. An atom's angular momentum in a low-symmetrical field moves between several preferred directions determined by the symmetry of a potential, so that the time-averaged angular moment is zero. Relative phases of wave functions also take on a series of preferred values. An additional MF makes some of them more probable and brings about an interference. In that case, however, the MF-dependent interference part of probability density of an ion is small in comparison with its permanent part, sought as the completely averaged density, but in a central potential these parts have the same order of magnitude. Therefore, the presence of a central potential in the Hamiltonian is needed for significant interference effects, and the presence of a small low-symmetrical potential is immaterial. We note that  $U(r)$  enters only into the factors  $a_{mm'}$  in (4.1.20). Therefore, neither peak positions in a frequency spectrum nor those in the amplitude spectrum are dependent on the exact form of the central potential. For instance, it

could have a maximum at the center of a cavity, whereby equilibrium positions of an ion are shifted to ligands. There are good reasons to regard such a potential as a more realistic model than a potential with a minimum at the center.

A further question is concerned with the presence of a gate: whether it significantly distorts the central potential of an ion? The ion gate in a binding cavity is a convention meant to simplify the visualization of binding and decay processes. An ion may tunnel between any three neighboring ligands in an octahedron. An ion gate is a local dip in the potential function at respective places. Quantum-mechanically, ion leakage from a cavity occurs quite rarely, with a characteristic time of 0.1 s, which is why that potential reduction is quite small. Therefore, we can believe with a high accuracy that the gate does not perturb the ion potential. Leakage probability is only determined by exponentially small “tails” of the wave function of an ion between ligands.

It seems that the most important question is that of the thermal fluctuations of ligands. We consider at first a simple one-dimensional model of a spring linked with a fluctuating foundation. At time  $t = 0$ , a particle with a mass is fixed to the loose end of the spring. Gradually, the particle develops some random oscillations. The time  $T$  for a dynamic equilibrium to set up depends on the rigidity of a spring. If a spring is soft, that time can be very large. A dynamic state of a mass within time interval  $< T$  is normally referred to as a metastable state. This means that the state is far from thermodynamic equilibrium, but is approaching it. At a metastable state, even a force that is minor in comparison with fluctuation scales can exert a noticeable action on a particle. Consider now a three-dimensional system, a mass in potential  $U(\mathbf{r})$ . Normally, the dynamics of such a system is described in so-called normal coordinates that possess some special properties. Excitation of one normal coordinate exerts no influence on the dynamics along other normal coordinates. It is clear now that the process of the establishing of a dynamic, or thermal, equilibrium can have different rates for different normal coordinates. For example, a normal variable A is in equilibrium with a force that causes it to fluctuate, whereas a variable B is in a metastable state; i.e., it is not thermalized and thus easily controlled. Here we deal with the only classical particle that is thermalized along one normal variable and at the same time not thermalized along another normal variable. It can be said that thermal relaxation rate depends on the type of relationship between a particle and a random force.

The spectrum of relaxation times in gases, liquids, and solids is extremely wide. Normally, at room temperature, characteristic for the Cartesian coordinates of free particles, atoms, and ions in a liquid are picosecond relaxation times. A relaxation time scale can be microseconds for electron spins, seconds for nuclear spins, and a wide variety of special times for so-called collective variables in multiparticle ordered systems, e.g., in crystals. Biological membranes and other macromolecules as well are systems in which collective excitations are possible. Often they are described in terms of QM equations, thus demonstrating their fundamental quantum properties.

In quantum mechanics, normal modes of quantum oscillations (Hamiltonian eigenfunctions) play a role of normal variables. For bound particles, normal modes

are generally a discrete series of functions, numbered by successive quantum numbers. The wave function of a particle in a central potential has radial, azimuthal, and polar modes, so that a wave function is factored out into three eigenfunctions. An external force excites various modes in accordance with quantum selection rules. For instance, pulses of a homogeneous, and even relatively strong, electric field shift an ion, more or less, as in collisions. However, they cause no transitions between Zeeman levels of polar modes due to parity selection rules, whereas interstate transitions of radial and azimuthal quantum numbers may take place.

Returning to the general objection that a weak MF,  $\hbar\Omega_c \ll \kappa\mathcal{I}$ , is unable to control thermally excited ion dynamics, we note the following. That would be the case if an ion, before it escapes, would be completely thermalized; i.e., it would stay within a cavity during a sufficiently long time. That is not so, however. An ion gets into a cavity at some moment, thereby triggering thermalization processes. Only two modes of ion dynamics, the radial and azimuthal ones, take part in fast thermalization, since the modes are not subject to unfavorable selection rules. Soon thereafter, the ion finds itself in a thermalized state over radial and azimuthal modes and in a metastable state relative to the polar mode  $\exp(im\varphi)$  with a level in an MF split into Zeeman sublevels. That is exactly the state that is described by the Hamiltonian (4.1.1) for an interval smaller than the relaxation time. In that state there is no need to introduce into the Hamiltonian a thermal interaction term, since it does not influence angular polar modes. The action of that term on other modes gives rise to a distribution over their quantum numbers and is described by appropriate averaging. The relaxation time  $\tau_L$  of the *phase difference* of polar modes, considering the unusual geometry of the system, if fairly large, lies conceivably in the region of hundredths of a second. That is enough for interference mechanisms to manifest themselves. To be sure, the idealization  $\tau_L > \Omega^{-1}$  assumed in the model should be considered in exactly that manner, just as an idealization. It is substantiated by a good agreement between theoretical and experimental curves. At the same time, reasons behind the workability of that idealization should be supported theoretically.

A further important question occurs in relation to small magnetic numbers, usually  $m < 3-4$ , which are taken care of in theory, in order to attain a good agreement with experimental data. When an ion gets into a cavity, at an initial time moment there is no reason for it to be in a state described by a separate eigenfunction of the Hamiltonian. It is in a superposition of various eigenfunctions. Mathematically, the dissociation effect is dictated mainly by small magnetic numbers irrespective of their actual energy distribution among the angular modes and modes of other quantum numbers. Larger  $m$  means a fine-grained interference picture or a fine-grained distribution of ion probability density. Such a distribution, however, causes no changes in dissociation. Formally, Eq. (4.1.20) gives some insights into what occurs at large  $m$ . The dissociation effect is more pronounced when modes with large  $m$  have smaller populations.

Initial distribution over magnetic numbers depends on the many parameters of a binding protein and is hardly predictable. It is beyond doubt, however, that thermal

perturbations of a potential cannot excite states with large quantum numbers. Ion vibrations have the characteristic energy

$$n^2 \frac{\hbar^2}{MR^2},$$

where  $n$  is the sum of radial and azimuthal quantum numbers. Since, for instance, for a calcium ion in a potential of radius  $0.7 \text{ \AA}$  the energy  $\hbar^2/MR^2$  is only two orders of magnitude smaller than  $\kappa\mathcal{T}$ , under thermodynamic equilibrium only states with quantum numbers not larger than several units, where the magnetic quantum number is not higher in magnitude than the azimuthal number, are populated.

In such a cavity an electron would be in the ground state, and thermal excitations on the order of  $\kappa\mathcal{T}$  would not excite other states. Correspondingly, no interference would be possible. In a large cavity, ions would be characterized by excitation of states with large quantum numbers, and interference would have a fine-grained structure to be unobservable. It is surprising that masses of ions and sizes of binding cavities have values that make for the similarity of inhomogeneities of an interference pattern and ion gate size. It is this that enables interference to be observed.

### 4.1.3 Width of spectral peaks

The dependence of dissociation probability (4.1.20) on the amplitude of the variable MF component is contained in the argument of Bessel functions. The frequency dependence is contained in two factors. However, it can be maintained that maxima of  $P$  are defined mainly by zeros of the denominator in (4.1.20), i.e., by the equation  $\alpha z + n = 0$ . The solution to the equation yields the following relationship for frequencies  $\Omega_{\max}$  that are close to the frequencies of the maxima  $P^{30}$

$$\Omega_{\max} = \frac{\Delta m}{2n} \Omega_c, \quad n = 1, 2, \dots, \quad (4.1.21)$$

where  $\Omega_c = qH_{DC}/Mc$  is the cyclotron frequency of an ion. The number of maxima and their intensity are thus dependent on the relative value of density matrix elements  $a_{mm'}$  for levels with various values of magnetic quantum numbers  $m$ .

It is possible to estimate the width of maxima  $\Delta f$ ,  $f = \Omega/2\pi$ , taking account of the fact that the width of function  $\sin^2 x/x^2$  is about  $\pi$ , i.e., the value of  $x = \pi$  determines the peak width. Considering that  $x = (\alpha z + n)\Omega T$ , and using the obvious relation  $[(\alpha z + n)\Omega T]'_f \Delta f = \pi$ , we find  $\Delta f = 1/2nT$ . For example, for a peak at  $\Omega_{\max} = \Omega_c$ , by virtue of (4.1.21), the terms of the sum (4.1.20) with  $\Delta m = 2n$  are suitable. The smallest of these term  $n = 1$  makes the main contribution to the maximum width, so that for that peak we have  $\Delta f = 1/2T$ . Numerical calculations confirm that this estimate is fairly correct, despite the fact that the second factor of  $P$ ,  $J_n^2$ , also depends on  $f$  and can influence the peak width.

---

<sup>30</sup>Further, in the expression for spectrum frequencies, we will omit the minus sign, which is concerned with the choice of the phase for a sinusoidal MF.

In the literature they discuss the probability for various ions to simultaneously contribute to the response of a biological system exposed to an MF with some fixed parameters. That can occur if the subharmonics and harmonics of various ions differ from one another by less than the peak width in the response. In the process, the resulting spectral curve will, in the general case, have a maximum at a frequency that does not coincide with characteristic frequencies of any ion. The regular method of separating the inputs then consists in simultaneously and proportionately increasing all the three parameters of an MF,  $H_{DC}$ ,  $H_{AC}$ ,  $f$ . Let, for instance, at fixed values of  $H_{DC}^{(0)}$ ,  $H_{AC}^{(0)}$ ,  $f^{(0)}$  an MBE maximum be observed. Most often we have  $H_{AC}^{(0)} = 1.8H_{DC}^{(0)}$ ,  $f^{(0)} = qH_{DC}^{(0)}/2\pi Mc$ . Let, also, the coefficient of proportional increase be  $k$ , i.e.,

$$H_{DC} = kH_{DC}^{(0)}, \quad H_{AC} = kH_{AC}^{(0)}, \quad f = kf^{(0)}.$$

In terms of the ion interference model, the MBE level of each ion will then be independent of  $k$ . At the same time, the relative extremum width for some ion

$$\frac{\Delta f}{f_{\max}} \sim k^{-1}$$

is inversely proportional to  $k$ . Thus, *the resolution of interference spectral peaks for various ions improves with strengths and frequency of an MF*. Figure 4.5 plotted according to McLeod *et al.* (1987a) illustrates this. In all the cases, the DC field strength was chosen so that cyclotron frequencies would equal those indicated in the figure.

We note also that the model is constructed in the idealization of the small angular size of the gate, as compared with  $\Omega T$ . Account of the finite size would result in some additional broadening of spectral peaks. However, as it will become clear from a comparison of theoretical predictions with experiment, that approximation is well met.

Using the wave function of the form (4.1.5), we will compute the energy of the system

$$\varepsilon(t) = \langle \Psi | \mathcal{H} | \Psi \rangle = \varepsilon_0 - H_z(t) \sum_{klm} |a_{klm}|^2 \eta_m,$$

where  $\varepsilon_0$  is the system energy in the absence of an MF,  $\eta_m$  is defined by (4.1.3), and the basis functions are orthogonal in all their indices. Since  $\eta_m = -\eta_{-m}$ , then, if, for instance, states  $\pm m$  have the same weights, the energy  $\varepsilon$  is strictly constant. If the energy of a quantum system is constant, then how can an MF signal be transferred through that system? That contradiction is concerned with the use of a semiclassical approximation, when a quantized or Schrödinger field of matter interacts with a classical electromagnetic field. If quantum electrodynamics is used, where an EMF is quantized, then states with different phases would answer EMF states with different numbers of photons. That is, a particle would exchange its energy with the field, and there would be no contradiction. For the purpose of this work, where only the state of a particle is of interest, a semiclassical approximation would be sufficient.

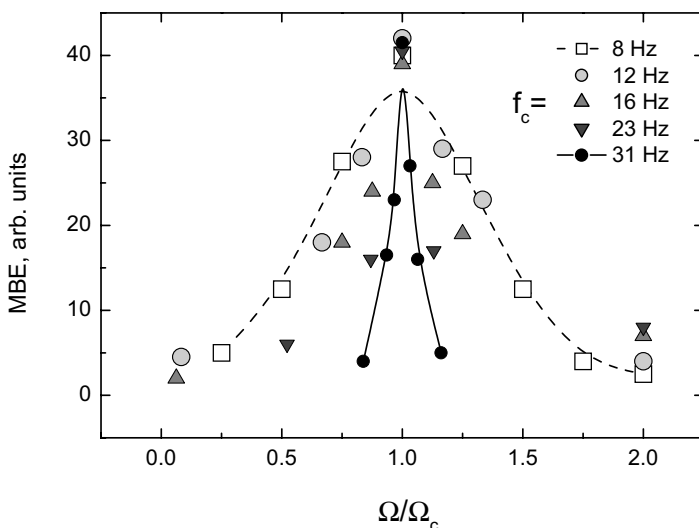


**Figure 4.5.** Mobility of diatomic algae exposed to a low-frequency AC MF whose frequency is in the vicinity of specified cyclotron frequencies for the calcium ion. The root-mean-square deviation near 3–5 %, adapted from the data of McLeod *et al.* (1987a).

#### 4.1.4 Dissociation probability in dimensionless variables

To derive a formula for ion interference in a convenient form with dimensionless arguments, we will denote

$$h' = \frac{H_{AC}}{H_{DC}}, \quad \Omega' = \frac{\Omega}{\Omega_c} = \frac{f}{f_c} = f'; \tag{4.1.22}$$

i.e., we will introduce dimensionless parameters, the amplitude of an MF variable component  $h'$  and its frequency  $\Omega'$  or  $f'$ , measured in  $H_{DC}$  and  $\Omega_c$  (or  $f_c$ ), respectively. In the new notation

$$\alpha = h'^{-1}, \quad z = \frac{\Delta m}{2} \frac{h'}{f'}, \quad \alpha z = \frac{\Delta m}{2} \frac{1}{f'}.$$

Then formula (4.1.19) becomes

$$P = \sum_{mm'n} |a_{mm'n}|^2 \frac{\sin^2 A}{A^2} J_n^2 \left( \frac{\Delta m}{2} \frac{h'}{f'} \right), \quad A = \left( \frac{1}{2} \Delta m + n f' \right) \Xi. \tag{4.1.23}$$

Here

$$\Xi = \Omega_c T \tag{4.1.24}$$

is the only quantity in (4.1.23) that depends on the properties of an ion and a protein binding center. It is interesting that the parameters of an ion,  $\Omega_c(H_{DC})$ ,

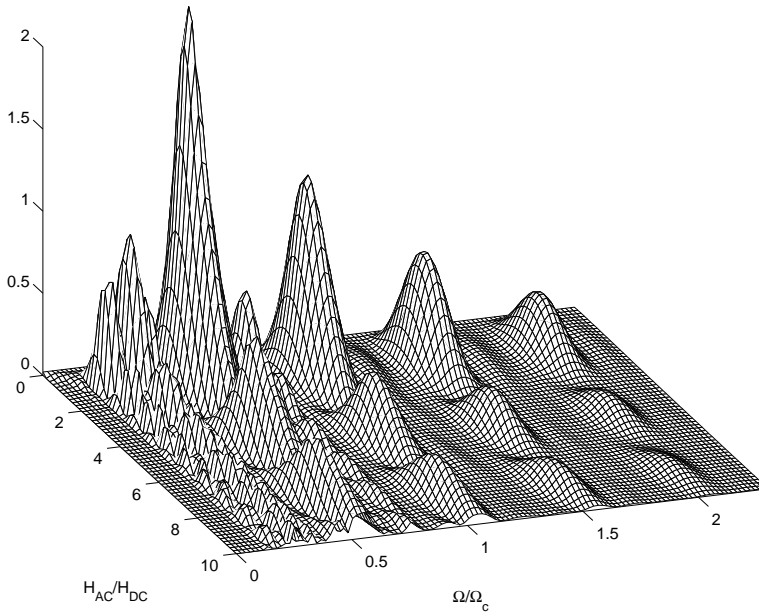


**Figure 4.6.** General form of surface  $P(h', f')$ , computed by (4.1.23). The main interference maximum is at  $f' = \frac{1}{2}$ ,  $h' = 1.8$ .

and protein,  $T$ , enter into the formula as a dimensionless product that characterizes the entire ion-protein complex. For  $^{40}\text{Ca}^{2+}$  ion in an MF  $H_{\text{DC}} = 45 \mu\text{T}$ , at complex dissociation time  $T = 0.1 \text{ s}$  (Forsen and Lindman, 1981) we get

$$\Xi \approx 22 . \quad (4.1.25)$$

We can expect that the value of that quantity for other ions and complexes will not stray too far from (4.1.25), since for lighter ions it is natural to assume a shorter dissociation time and, conversely, for heavier ones longer times.

The rate of calcium binding with binding centers was obtained for several calcium-binding proteins using methods of  $^{43}\text{Ca}$  NMR spectroscopy (Forsen and Lindman, 1981) and biochemistry (Mamar-Bachi and Cox, 1987). For two strongly binding centers the rate constant was  $\sim 1\text{--}10 \text{ Hz}$ , for two weakly binding ones more than  $200 \text{ Hz}$ .

Note that peak positions on (4.1.23) in the dimensionless variable  $f'$

$$f'_{\text{max}} = \frac{\Delta m}{2n} \quad (4.1.26)$$

are fixed, which is fairly convenient. Dependent on  $\Xi$  is only the relative width of maxima in frequency

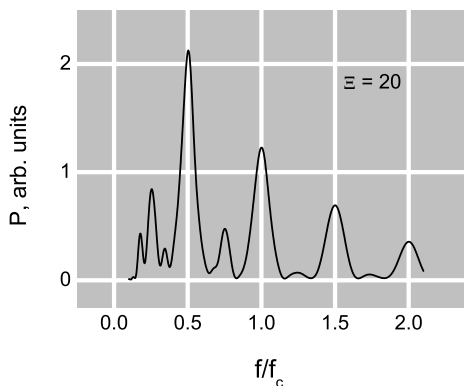


**Figure 4.7.** Dissociation probability as a function of the frequency of the variable MF  $f'$  component at the optimal amplitude  $h' = 1.8$ . The value  $\Xi = 20$  corresponds to the Ca-calmodulin complex.

$$\left[ \left( \frac{\Delta m}{2} + n f' \right) \Xi \right]_{f'}' \approx \pi \quad \Longrightarrow \quad \Delta f' = \frac{\pi}{n \Xi} . \quad (4.1.27)$$

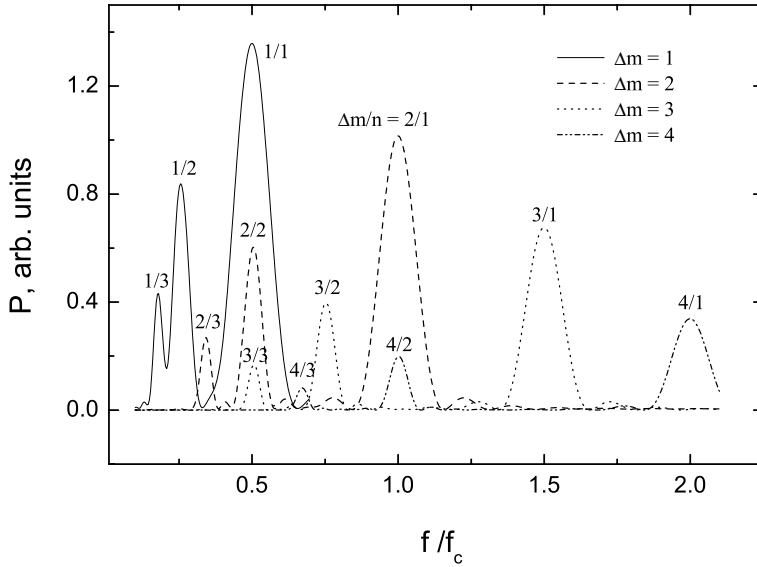
Hence the relative peak width is inversely proportional to a DC MF. Trillo *et al.* (1996) and Blackman *et al.* (1999) used a reduced MF of about  $3 \mu\text{T}$  and observed a distinct relatively wide MBE maximum, presumably on protons. It was much harder to reveal such an MBE in the geomagnetic field, see Lednev *et al.* (1996b), due to the fact that the position of a relatively narrow “resonance” floated in accordance with GMF daily variations.

Figure 4.6 illustrates the formula (4.1.23). Depicted in it is the surface  $P(h', f')$ , computed by the scheme

$$h'(0; 10) f'(0; 2.3) \Xi(21.68) m(-2; 2) n(-3; 3) a_{mm'}(1.0) .$$

Series of peaks or maxima at various specified values of  $f'$  are generally made up of contributions of several terms of the sum (4.1.23) with different sets of numbers  $\Delta m$ ,  $n$ . Such a series of maxima  $f' = \frac{1}{2}$  is composed of contributions of terms with  $\Delta m$  and  $n$  that meet the equality  $\Delta m/n = -1$ , i.e., of several terms  $-1/1$ ,  $-2/2$ , etc. All maxima of a series along the amplitude axis,  $f'$  being fixed, are formed jointly by all the sum terms contributing to the series. Peaks of the series for a fixed amplitude  $h'$  are formed by various groups of the sum terms. Figure 4.7 shows such a series at  $h' = 1.8$ . Next Fig. 4.8 provides a deciphering of maxima that seems to be valid for any MF amplitude.

Since elements  $a_{mm'}$  are dependent on the initial conditions for an ion to enter a binding site, some of them may appear to be much smaller than others. As a result, terms with appropriate  $m$ ,  $m'$  and  $\Delta m$  are “cut out” and some maxima



**Figure 4.8.** Contributions of interference angular modes to the complex dissociation probability. The fraction at each peak indicated which terms of the sum (4.1.23) contributed to its formation: the numerator,  $\Delta m$ ; the denominator,  $n$ , the order of an appropriate Bessel function.

of the frequency series vanish. This comment is significant for accounting for some experimental evidence.

#### 4.1.4.1 Fixed frequency of a field

Sometimes, out of the three characteristics of an external MF,  $H_{AC}$ ,  $H_{DC}$ ,  $\Omega$ , they fix the frequency of the field, rather than its static value. It is then convenient to introduce other dimensionless variables. We define the “Larmor MF”  $H_0$  for a given ion and a fixed frequency  $\Omega$  as

$$\Omega = bH_0 .$$

That implies that the Larmor frequency of an ion in a field  $H_0$  equals the frequency of an external field. We also introduce new dimensionless parameters in the form

$$H' = H_{DC}/H_0 , \quad h' = H_{AC}/H_0 , \quad T' = T\Omega .$$

The formula for dissociation probability then becomes

$$P = \sum_{mm'n} |a_{mm'}|^2 \frac{\sin^2 A}{A^2} J_n^2(\Delta m h') , \quad A = (\Delta m H' + n)T' .$$

For rotating ion–protein complexes, see Section 4.5,  $A = [\Delta m(H' + \Lambda') + n]T'$ ,  $\Lambda' = \Lambda/\Omega$  — the relative angular velocity of rotation.

Later in this book we will use only previously defined dimensionless parameters of the field.

## 4.2 NON-LINEAR REACTION OF A PROTEIN

When we considered the non-linear dependence of the probability  $P$  of a biochemical reaction on the probability density  $p$  of finding an ion in some angular position, we took into consideration both the linear (its contribution vanishes) and quadratic terms of the expansion (4.1.16). This gives rise to the question of how general are the results derived in the form (4.1.19), whether they depend in a significant manner on the non-linearity form, i.e., on whether further terms are included.

### 4.2.1 Estimate of contribution of cubic non-linearity

As in (4.1.17), respective effects can be obtained from an analysis of the expression

$$P_3 \sim \overline{(\tilde{p}_T)^3}, \quad (4.2.1)$$

where

$$\tilde{p}_T = \sum_{m \neq m'; n} a_{mm'} \exp [i\Delta m\varphi_0 + i(\alpha z + n)\Omega t] \frac{\sin[(\alpha z + n)\Omega T]}{(\alpha z + n)\Omega T} J_n(z)$$

is the expression (4.1.18) for the sliding mean of  $\tilde{p} = p - \bar{p}$  provided here for convenience.

In the general case the terms of the triple product

$$(\tilde{p}_T)^3 \quad (4.2.2)$$

depend on the angle  $\varphi_0$ . To derive a result that agrees with experiment one has to average over the angle  $\varphi_0 \in [0, 2\pi)$ , which will clearly yield zero. However, some terms do not depend on  $\varphi_0$ . Those terms must be selected among those that are also independent of time. Then, when averaging over a long time span, by (4.1.18), their contribution to  $P_3$  does not vanish.

In order to tell summation indices and other expressions that could be referred to different factors in the product we will supply them with an upper index in parentheses, i.e., for example,

$$(\tilde{p}_T)^3 = \prod_i T^{(i)}[\tilde{p}].$$

It is seen from the expression for  $\tilde{p}_T$  that one must select the terms of the sum

$$\prod_i T^{(i)}[\tilde{p}] = \prod_i \sum_{(mm'n)^{(i)}} \dots$$

with  $\Delta^{(i)}m$  and  $n^{(i)}$ , which satisfy the relations

$$\sum_i \Delta^{(i)}m = 0, \quad \sum_i (\alpha z + n)^{(i)} = 0. \quad (4.2.3)$$

Moreover, all the three factors

$$\frac{\sin[(\alpha z + n)^{(i)}\Omega T]}{(\alpha z + n)^{(i)}\Omega T}$$

in (4.2.2) must yield maxima for similar values of  $\Omega$ , since otherwise the contribution of each term will be small, i.e.,  $(\alpha z + n)^{(i)} = 0$ , or

$$\Omega_k = -\frac{\Delta^{(i)}m}{n^{(i)}}\omega_0 = \text{Const},$$

for all  $i$ . Therefore, Const is a constant that is independent of  $i$ . Transforming it gives

$$\Delta^{(i)}m = kn^{(i)}, \quad (4.2.4)$$

where  $k$  is an integer identical for all  $i$ . Hence we immediately get

$$\sum_i n^{(i)} = 0. \quad (4.2.5)$$

Note that the terms of the product (4.2.2), where at least one of  $n^{(i)}$  is zero, do not produce any contribution, since then the relation

$$\frac{\sin(\alpha z \Omega T)^{(i)}}{(\alpha z \Omega T)^{(i)}}$$

yields a spike only at  $\alpha z = 0$ , i.e.,  $\Delta m = 0$ , but that value of  $\Delta m$  does not enter into the expression for  $\tilde{p}_T^{(i)}$ .

The terms of the product (4.2.2) at extremum points with frequencies  $\Omega_k$  contain factors of the form

$$\prod_i J_{n^{(i)}}(-n^{(i)}/\alpha).$$

Since the magnitudes of the Bessel functions are not larger than unity, then it is possible to isolate among other terms in (4.2.2) a group of "weightier" terms, in which two of the three  $n^{(i)}$  coincide. We denote these quantities by  $n$ , and the remaining ones by  $n'$ , that latter being, by (4.2.5), equal to  $-2n$ . The quantities  $\Delta^{(i)}m$  that, by virtue of (4.2.4), correspond to them will be denoted as  $\Delta m$  and  $\Delta m' = -2m$ . We can thus write the expression for  $P_3$  at points  $\Omega_k$  of the extrema

$$P_3(\Omega, \alpha)|_{\Omega=\Omega_k} \approx \sum_{n \neq 0} |a_{(kn)}|^2 a_{(-2kn)} J_n^2(-n/\alpha) J_{-2n}(2n/\alpha).$$

Here the quantities  $a_{mm'}$  and summation over  $m, m'$  are replaced by one-index quantities  $a_{\Delta m}$  and by summation over  $\Delta m$ , since the expression  $P$  is only dependent on  $\Delta m = m' - m$ . The writing  $a_{(kn)}$  should be taken to mean  $a_{\Delta m}$ ,  $\Delta m = kn$ .

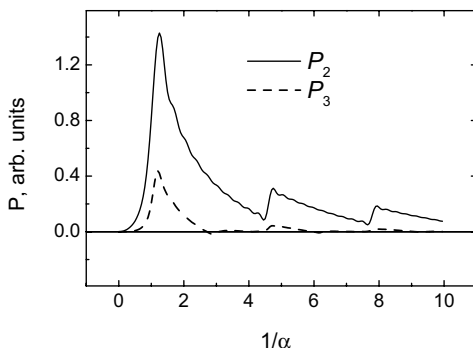


**Figure 4.9.** Contribution to MBE amplitude spectra of quadratic,  $P_2$ , and cubic,  $P_3$ , non-linearity in the response to a probability density change for an ion.

In the latter expression the summation over  $\Delta m$  falls out, since we only consider  $P_3$  at extremal points, where the relation (4.2.4) for indices holds.

An expression was derived earlier for  $P$  (4.1.19) with the quadratic expansion term (4.1.16). We now denote that quantity by  $P_2$  and find its values at extremal points. From (4.1.19) we get

$$P_2(\Omega, \alpha)|_{\Omega=\Omega_k} \approx \sum_{n \neq 0} |a_{(kn)}|^2 J_n^2(-n/\alpha).$$

Since  $J_{-n}^2 = [(-1)^n J_n]^2 = J_n^2$  and  $J_{-2n} = (-1)^{2n} J_{2n} = J_{2n}$ , then indices designating the order of Bessel functions can be written in their absolute values.

To approximately estimate  $P_3$  in comparison with  $P_2$ , we will take all the factors that define the initial conditions for an ion in a macromolecule cavity to be equal to, i.e.,  $a \equiv 1$ . The graphs of the functions

$$P_2(\alpha) = \sum_{n \neq 0} J_{|n|}^2(-n/\alpha), \quad P_3(\alpha) = \sum_{n \neq 0} J_{|n|}^2(-n/\alpha) J_{|2n|}(2n/\alpha) \quad (4.2.6)$$

are shown in Fig. 4.9, in dependence on the relative MF amplitude  $\alpha^{-1} = h' = H_{AC}/H_{DC}$ ,  $|n| = 1, \dots, 10$ . It is seen that the cubic non-linearity in general introduces only minor corrections to those dependences, which are described by quadratic non-linearity.

#### 4.2.2 Contribution of fourth-order non-linearity

Another case arises when we take into account fourth-order non-linearity

$$P_4 \sim \overline{(\tilde{p}_T)^4}.$$

A reasoning similar to that in the analysis of the contribution of cubic non-linearity leads then to Eq. (4.2.5), in which summation is over four values of index ( $i$ ). It is

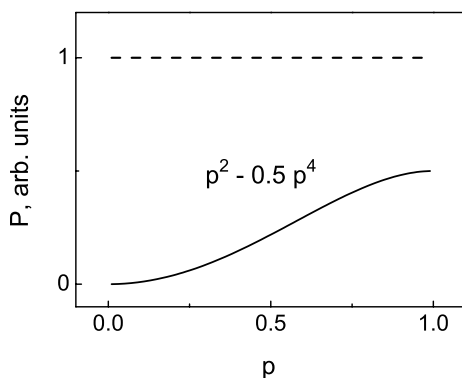


**Figure 4.10.** The general view of the dependence of the protein reaction probability on the probability density of an ion: at large  $p$  the fourth-order non-linearity with the minus sign comes to the fore.

obvious that this equation can be met by properly selecting equal-magnitude values of  $n$  for all ( $i$ ), which is out of the question for a sum of three  $n^{(i)}$ . That is, two of  $n^{(i)}$  have  $n$ , whereas the other two have  $-n$ . It is easily seen that the sum of such terms, which are major contributors to  $P_4$ , is simply equal to squared  $P_2$ , i.e.,

$$P_4 \approx P_2^2. \quad (4.2.7)$$

It is clear that if  $P_2$  is sufficiently high, then  $P_4$  cannot be ignored. It is also important that the sign of the factor in the fourth-order term in (4.1.16) can be negative, with the result that the contribution of  $P_4$  under certain conditions could compensate for  $P_2$ . Actually, the probability  $P(p)$  is limited from the top by unity, therefore fourth-order non-linearity must show up at sufficiently large values of  $p$ , Fig. 4.10. For the averaged probability of a biochemical reaction we will have then to write, instead of (4.1.17), the expression

$$P \sim P_2 + c_4 P_2^2. \quad (4.2.8)$$

The factor  $c_4$  is negative since the growth rate of function  $P(p)$  must fall off with  $p$ . The value of  $c_4$  depends on the form of  $P(p)$ ; i.e., it is determined by (i) the specific structure of a macromolecule and a binding cavity in it, (ii) the nature of the connection of the macromolecule's biochemical properties with the state of an ion and the state of the ambient environment, etc. Because of a sea of factors that influence the behavior of  $P(p)$ , it is impossible to theoretically calculate the factor  $c_4$  in (4.2.8). Some indication of the best value of the coefficient can be obtained proceeding from agreement with experiment in each specific case.

Figure 4.11 shows the frequency and amplitude spectra computed using (4.2.8) at  $c_4 = -3.0$ ,  $\Delta m = 2$ ,  $|n| = 1, \dots, 4$ . It is seen that as the relative MF amplitude

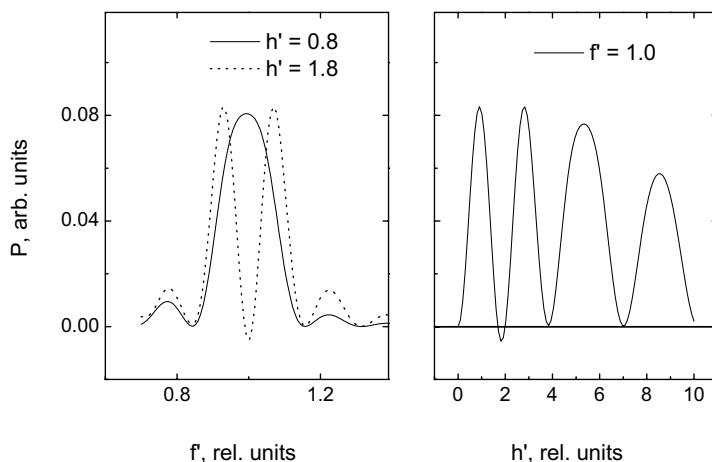


**Figure 4.11.** MBE maximum reversal at a cyclotron frequency with the growth of the field amplitude due to fourth-order non-linearity; right — the amplitude spectrum at frequency  $\Omega_c$ .

increases from 0.8 to 1.8 there occurs a reversal of the upper section of a maximum at a cyclotron frequency, so that the effect at that frequency vanishes or can become opposite in sign. In the process, a doublet emerges with frequencies close to cyclotron ones. It will be recalled that the quantity  $P$  has the meaning of an MF-dependent part of the probability of a biochemical reaction; therefore negative values are admissible.

A similar behavior, namely a reversal of a frequency spectrum maximum near a cyclotron frequency for  $^{45}\text{Ca}$  ions in a field  $H_{\text{DC}} = 0.21$  G with the growth of the relative MF amplitude from 1.4 to 10.1, was observed by Liboff *et al.* (1987a), but no good agreement in amplitude values has been reached yet. The amplitude spectrum gets complicated as well owing to a reversal of the main amplitude maximum at  $h' = 1.8$ .

### 4.2.3 Dissociation as a Poisson process

Earlier, in deriving (4.1.19), we used sliding averaging for oscillations of ion probability density. The averaging time interval corresponded to the characteristic time  $T$  of non-linear protein reaction. We had to substantiate that step, as it is not that apparent. Therefore, it is a good idea also to consider another, physically transparent, way of deriving behavior patterns described by (4.1.19), although it is not that general in nature.

Unlike the hypothesis of non-linear protein reaction (4.1.16), a starting point here is the fact that the dissociation process has a structure of a Poisson random

process, defined on a statistical ensemble of protein molecules. The probability for a dissociation not to occur within the time interval  $[t - T, t + T]$  is (Korn and Korn, 1961)  $\exp(-2T\lambda)$ , where  $\lambda$  has the meaning of the mean density of dissociation events per time unit. We will assume that the quantity  $\lambda$  is proportional to probability density of an ion near the gate, i.e.,

$$\lambda = \frac{cp(t)}{2T},$$

where  $T$  is the time scale, and  $c$  is some proportionality coefficient. Considering the time dependence of probability density, we will write the dissociation probability in the form

$$\exp\left(-\int_{t-T}^{t+T} \lambda dt\right).$$

Therefore the dissociation probability during time  $[t - T, t + T]$  has the form

$$P(t) = 1 - \exp\left(-\frac{c}{2T} \int_{t-T}^{t+T} p(\varphi_0, t') dt'\right). \quad (4.2.9)$$

Using the definition (4.1.9), we write (4.2.9) as

$$P(t) = 1 - \exp(-cp_T) = cp_T - \frac{1}{2}c^2p_T^2 + \dots \quad (4.2.10)$$

Relationship (4.2.10) defines dissociation probability during a time interval  $2T$  for an ion-protein complex formed at time  $t - T$ . For  $i$ th complex, the time  $t = t_i$  represents a uniformly distributed continuous random quantity on an ensemble of molecules. To derive the dissociation probability that is concerned with experimental observations, we will have to average (4.2.10) over a random parameter  $t$ . In this case, the mathematical expectation coincides with the time average. Thus,

$$P = E[P(t)] = \overline{P(t)} = c\overline{p_T} - \frac{c^2}{2}\overline{p_T^2} + \dots \quad (4.2.11)$$

It follows from (4.1.12) that in physically meaningful cases where  $\alpha z + n \neq 0$ , we have  $\overline{p_T} = 0$ . Therefore, (4.2.11) coincides up to a coefficient with (4.1.17) and leads to the same formula (4.1.19).

Note that in such a derivation of the formula no assumption of non-linear protein reaction to a thickening of probability density was used. It was supposed instead that the dissociation process is a Poisson flux. By virtue of expansion (4.2.10), that assumption yields, however, the same sign of contributions to  $P$  of second- and fourth-order non-linearities. Therefore, reversals of a maximum to a minimum, or rather to a doublet, are impossible. That minor departure is important when observing MBE reversals in experiment. It is clear that what is preferred here is the idea of a protein that actively responds to ion states, rather than that of a passive lifeless system that can only provide for a Poisson flux of dissociations.

### 4.3 INTERFERENCE IN PULSED MAGNETIC FIELDS

In magnetobiology many experiments with pulsed MFs are known. Pulsed fields of a variety of configurations are widely employed in medicine to expedite the curing of bone fractures and growth of bone tissues (Congress EMBM, 1997; Bassett, 1984). At the same time mechanisms for their action remain largely unclear, and reproducibility levels of assays in various laboratories are insufficient. In what follows we will consider pulsed MFs of relatively simple shape, which apply to a large proportion of practically used fields. It appears that ion interference in such fields features a number of interesting distinguishing details (Binhi, 1998a). In some cases they correspond to known experiments fairly well.

#### 4.3.1 Parallel pulsed and DC magnetic fields

It has earlier been shown that the growth of the probability  $P$  of dissociation of an ion-protein complex involves “freezing” of the phase difference of angular modes of the wave function of an ion, Fig. 4.4. The idea behind the mechanism of the action of a pulsed series of an MF is that the progression of the phase difference of angular modes during a time  $t$ , which is concerned with the term  $\omega_0 t$ , i.e., with the presence of a DC MF, must be made up for by a change in phase difference due to pulses of an AC MF  $h(t)$ , see (4.1.6), (4.1.8)

$$p(\varphi_0, t) = \sum_{mm'} a_{mm'} \exp \left[ i \Delta m \left( \varphi_0 + \omega_0 t + b \int_0^t h(t) dt \right) \right]. \quad (4.3.1)$$

We will now write the pulsed MF in the form of  $\delta$ -pulses of intensity  $\xi$ , which follow with frequency  $f$ ,

$$h(t) = \xi \sum_{k=-\infty}^{\infty} \delta(t - f^{-1}k).$$

Such a consequence approximates, for instance, rectangular pulses, Fig. 4.12 with period  $f^{-1}$  and product  $\tau h = \xi$ .

Phase difference progression due to a DC field  $\Delta m \omega_0 t$  will be compensated for, if during that time pulses change their phase difference to  $2\pi r - \Delta m \omega_0 t$ ,  $r = 0, \pm 1, \dots$ . One pulse occurs during a time  $f^{-1}$ . As follows from (4.3.1), a pulse turns the phases by  $\Delta m b \xi$ . Equating the phase shifts yields the relationship  $\Delta m b \xi = 2\pi r - \Delta m \omega_0 f^{-1}$ . It relates the parameters of MF pulses to the value of a local DC field and ion parameters through the coefficient  $b = q/2Mc$ , to arrive at the maximum  $P$ :

$$\xi = \frac{1}{b} \frac{2\pi r}{\Delta m} - \frac{H_{DC}}{f}. \quad (4.3.2)$$

The negative values of  $\xi$  imply opposite directions of DC and pulsed fields. At  $r = 0$ , the rule (4.3.2) means that a DC MF can be compensated for by a DC component of the pulsed sequence; i.e., there emerges a kind of magnetic vacuum. Intensities

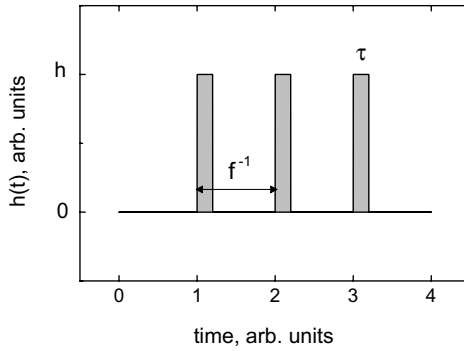


**Figure 4.12.** Sequence of rectangular MF pulses with specified parameters. The pulse intensity is  $\xi = \tau h$ .

with smaller magnitudes, although they can be a formal solution to (4.3.2), yield no noticeable interference effects. In any case, effective intensities of a pulsed sequence are limited by the condition

$$|\xi f / H_{\text{DC}}| > 1 .$$

Intensive pulses are capable of turning the phase through an additional angle of  $2\pi r$ , which is of no consequence for constructive interference, but let us look at this in more detail. We take an integral of MF pulses

$$\int_0^t \xi \sum_{k=-\infty}^{\infty} \delta(t - f^{-1}k) dt = \xi \sum_k \Theta(ft - k) ,$$

where  $\Theta$  is a unit or theta-function

$$\Theta(x) = \begin{cases} 0, & x \leq 0 \\ 1, & x > 0 . \end{cases}$$

Substituting into  $p(\varphi_0, t)$  gives

$$p(\varphi_0, t) = \sum_{mm'} a_{mm'} \exp \left[ i \Delta m \left( \varphi_0 + \omega_0 t + b \xi \sum_k \Theta(ft - k) \right) \right] .$$

Hence it is seen that if

$$\Delta m b \xi = 2\pi l , \quad l = 0, \pm 1, \dots ,$$

then  $p(\varphi_0, t)$  coincides with (4.1.8) at  $H_{\text{AC}} = 0$ , i.e., with the case of interference in a DC MF, where the only maximum P occurs at  $H_{\text{DC}} \rightarrow 0$ . Naturally, pulses that rotate the phases through  $2\pi l$  do not change the behavior of a system.

Consider the average over the time interval  $2T = (t, t + nf^{-1})$

$$p_T = \frac{1}{nf^{-1}} \int_t^{t+nf^{-1}} p(\varphi_0, t') dt' = \frac{1}{n} \sum_{mm'} a_{mm'} \exp(i\Delta m \varphi_0) \quad (4.3.3)$$

$$\times \int_\tau^{\tau+n} \exp \left[ i x \tau' + i y \sum_k \Theta(\tau' - k) \right] d\tau' ,$$

where we denote

$$x = \Delta m \frac{\omega_0}{f} , \quad y = \Delta m b \xi , \quad \tau = ft .$$

Introducing the auxiliary variable  $t = \tau' - \tau$ , we write the integral (4.3.3) in the form

$$I = \exp(ix\tau) I' , \quad I' = \int_0^n \exp \left[ i x t + i y \sum_k \Theta(t + \tau - k) \right] dt .$$

Note that

$$\sum_k \Theta(t + \tau - k) = 1 + \sum_k \Theta(t + (\tau - 1) - k) ,$$

i.e., shifts of a unit ladder, which leads to the right and upwards, by a step back and by a step upwards, are equivalent. Then we get

$$\sum_k \Theta(t + \tau - k) = \tau + \sum_k \Theta(t - k) .$$

Then

$$I' = \exp(iy\tau) I'' , \quad I'' = \int_0^n \exp \left[ i x t + i y \sum_k \Theta(t - k) \right] dt .$$

Further

$$\sum_k \Theta(t - k)|_{t \in (-1, 0)} = \sum_k \Theta(t - k)|_{t \in (0, 1)} - 1 .$$

Denoting the left part of the last equality by  $\zeta$ , we transform the integral  $I''$ :

$$I'' = \int_0^1 \exp(ixt) \exp[iy(\zeta + 1)] dt + \int_1^2 \exp(ixt) \exp[iy(\zeta + 2)] dt$$

$$+ \dots + \int_{n-1}^n \exp(ixt) \exp[iy(\zeta + n)] dt$$

$$= \exp(iy\zeta) \sum_{l=1}^n \exp(iyl) \int_{l-1}^l \exp(ixt) dt . \quad (4.3.4)$$

Since

$$\int_{l-1}^l \exp(ixt) dt = \frac{2}{x} \exp \left[ i x \left( l - \frac{1}{2} \right) \right] \sin \frac{x}{2} ,$$

then back substitutions into  $I''$ ,  $I'$ ,  $I$  give

$$I = \exp \left[ i(x+y)\tau + iy\zeta - i\frac{x}{2} \right] \frac{\sin(x/2)}{x/2} S, \quad S = \sum_{l=1}^n \exp[i(x+y)l]. \quad (4.3.5)$$

Substitution into (4.3.3) gives

$$p_T = \frac{1}{n} \sum_{mm'} a_{mm'} \exp \left[ i\Delta m\varphi_0 + i(x+y)\tau + iy\zeta - i\frac{x}{2} \right] \frac{\sin(x/2)}{x/2} S.$$

Computing  $P = \overline{p_T \cdot p_T}$ , we note, as before, that only complex conjugate terms  $p_T$  make a contribution that does not vanish on time averaging. Considering that  $x \propto \Delta m$ ,  $y \propto \Delta m$ , we get

$$P = \frac{1}{n^2} \sum_{mm'} |a_{mm'}|^2 \left( \frac{\sin(x/2)}{x/2} \right)^2 S^* S.$$

A maximum  $P$  is now achieved at such  $x, y$  that the value of  $S^* S$  is equal to its maximal value, i.e., at  $x + y = 2\pi r$ ,  $r = 0, \pm 1, \dots$ . Substituting the values of  $x, y$ , we get the maximal effect rule when exposed to a pulsed MF with pulse intensity  $\xi$  and frequency  $f$ . It coincides, as expected, with (4.3.2). That simple rule for the observation of an MBE in pulsed fields yields another non-trivial prediction of the theory of interference of bound ions. At  $r = 0$ , the condition of a maximum of  $\xi f = -H_{DC}$  implies that the constant component of a pulse sequence compensates for DC MF.

To estimate  $S^* S$  we go over from summation over  $l$  to integration

$$S = \sum_{l=1}^n \exp[i(x+y)l] \rightarrow \int_0^{2Tf} \exp[i(x+y)v] dv.$$

However, in the process we lose a very important property  $S(x+y) = S(x+y+2\pi r)$ ,  $r = 0, \pm 1, \dots$ . To retain it, we write  $S$  in the form

$$S = \sum_{l=1}^n \exp[i(x+y+2\pi r)l].$$

Now, passing over to integration, we get the estimate  $S^* S$

$$\sum_{r=-\infty}^{\infty} \left| \int_0^{2Tf} \exp[i(x+y+2\pi r)v] dv \right|^2 = 4 \sum_r \frac{\sin^2[(x+y+2\pi r)Tf]}{(x+y+2\pi r)^2}.$$

Thus, finally, the formula for  $P$  becomes

$$P = \sum_{mm'r} |a_{mm'r}|^2 \left( \frac{\sin(x/2)}{x/2} \right)^2 \left( \frac{\sin[(x+y+2\pi r)Tf]}{[(x+y+2\pi r)Tf]} \right)^2. \quad (4.3.6)$$

Figure 4.13 demonstrates the dependence of  $P$  for calcium and magnesium ions ( $f_c = 76.6$  and  $126.3$  Hz in a field of  $100 \mu\text{T}$ , respectively) on the pulse length  $\tau$

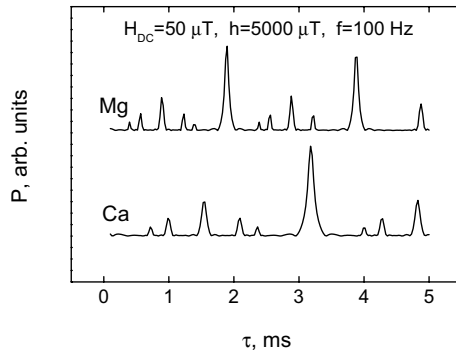


**Figure 4.13.** Dissociation probability for ion–protein complexes of calcium and magnesium in a pulsed magnetic field as a function of the pulse width.

with the pulse amplitude fixed and calculated by the formula (4.3.6) following the scheme

$$H(50)f(100)h(5000)T(0.07)m(-2; 2)r(-6; 6) .$$

The common peak  $r = 0$  is not seen here, since the DC component of the pulsed MF has the same sign as the DC field, and their mutual compensation is impossible.

No special-purpose experiments targeted at revealing such dependences of MBEs on MF pulse parameters are known. There are some reports on uses of optimal parameters, selected empirically, which do not contradict the conclusions of this section.

The pulse intensity  $\xi$  can be realized in a variety of way. However, unlike wide and low pulses, high and narrow pulses of the same intensity  $h\tau$  induce noticeable eddy currents. That increases the probability of biological effects of non-interference nature, namely of thermal or electrochemical ones.

### 4.3.2 Interpretation of some experiments with pulsed fields

Biological action of pulsed MFs is often accounted for by electric currents induced in biological tissues (Goodman *et al.*, 1983; Lerchl *et al.*, 1990; Goodman *et al.*, 1993b). That mechanism predicts that bioeffects within some range vary, just like induced currents, proportionally with the time derivative of the MF. One should expect at least a good correlation between the level of an induced electric field and bioeffects it causes. Such a correlation was observed, for instance, by Schimmelpfeng and Dertinger (1997). They studied the proliferation of cells in a sinusoidal 2.8-mT, 50-Hz MF. HL-60 human cells only grew in those regions of a homogeneous MF where the level of an induced electric field was higher than 4–8 mV/m. At the same time, many researchers note a disagreement of such predictions with results observed in relatively low-frequency variable MFs (Juutilainen,

1986; Liboff *et al.*, 1987a; Ross, 1990; Blackman *et al.*, 1993; Jenrow *et al.*, 1995; Prato *et al.*, 1996). For instance, Ross (1990) used various MFs that met definite “cyclotron” conditions  $\pi f/b = H_{DC} = H_{AC}$  for calcium. The product  $fH_{AC}$ , i.e., the level of an induced electric field, was successively stepped up until it became larger by a factor of 40, but the statistically significant biological effect remained unchanged. That points to the existence of other mechanisms for the biological action of weak MFs.

This section suggests an explanation for biological effectiveness precisely of weak pulsed MFs, insufficient to cause electrochemical or thermal effects. Therefore, it is expedient to identify an interval of MF parameters that suit the interference mechanism at hand.

Many rules and standards are known that establish limiting values of safe exposure levels for AC MFs. Limiting population exposure levels established by the CENELEC 50166-1 standard boil down to a certain simple rule. The frequency  $f$  in the interval 1–1000 Hz at amplitude  $h$  of a sinusoidal MF must obey the relationship

$$hf < k_C = 3 \times 10^4 \mu\text{T/S} . \quad (4.3.7)$$

That quantity is just a convention, since an induced eddy electric field is dependent on the details of the structure of MF sources. The level (4.3.7) can also be taken to mean a properly averaged quantity. It is assumed that smaller exposures do not cause any normal electrochemical or thermal effects. Nevertheless, such exposures can cause biological resonance-like effects (Liboff *et al.*, 1987a; Berg and Zhang, 1993; Prato *et al.*, 1995; Alipov and Belyaev, 1996). Therefore, it is natural to use the specified limit in relation to an interference mechanism in order to define conditions for its occurrence.

Along with other physical constraints, that limit leads to some inequalities that define static MFs, in which one can observe complicated (from two extrema) MBE spectra in pulsed MFs.

The factor  $\sin(x/2)/(x/2)$  in (4.3.6) implies that  $x = \omega_0 f^{-1} \Delta m$  must be fairly small. That means that an angular shift of an interference pattern during the time  $f^{-1}$  must be smaller than the angular size of the gate  $\sim \pi/2$ . An MF pulse must return the pattern to its initial condition to within the gate size. That is,  $f^{-1} < \pi/2 \Delta m \omega_0$  (a formal solution to Eq. (4.3.2) at  $\xi = 0$  makes no sense, as is clearly seen beforehand). At the same time, the pulse duration can be written in the form  $\tau < 0.5 f^{-1}$ . Combining the latter inequalities, we write

$$f^{-1} = \frac{\alpha\pi}{2\omega_0} , \quad \alpha < 1 \quad \text{and} \quad \tau = \frac{\beta\pi}{4\omega_0} , \quad \beta < 1 . \quad (4.3.8)$$

Relationship (4.3.7) holds well for a sinusoidal MF  $H(t) = h \sin(2\pi ft)$  that induces an electric field  $E(t) \propto hf \cos(2\pi ft)$ . Thermal and electrochemical effects vary with the time-averaged squared electric field, i.e.,  $\overline{E^2(t)} \propto h^2 f^2/2$ . Let the power level of  $W$  limit that quantity, which amounts to meeting the relationship (4.3.7):

$$h^2 f^2/2 < W \quad \rightarrow \quad hf < \sqrt{2W} = k_C . \quad (4.3.9)$$

Consider now a pulsed MF acting on a biological system. We will write it as a Fourier series  $H(t) = a_0/2 + \sum_{n=1}^N a_n \cos(2\pi nft)$ . The frequency spectrum of the pulsed MF must be limited; otherwise the power of an induced electric field becomes infinite. Therefore, we suppose that MF pulses have a leveled-out shape and duration  $\tau$ , the frequency of the maximal harmonic  $N$  in the expansion being  $\sim \tau^{-1}$ , i.e.,  $N \sim 1/\tau f$ . We now find  $\overline{E^2(t)}$ . After some transformations and the substitution of the coefficients of the Fourier expansion  $a_n = 2h \sin(\pi n\tau f)/\pi n$ , we obtain

$$\overline{E^2(t)} \propto f^2 \sum_{n=1}^N a_n^2 n^2 \overline{\sin^2(2\pi nft)} = fh^2/\pi^2\tau.$$

Substitution of  $W$  from (4.3.9) into  $\overline{E^2(t)} < W$  gives the relationship  $h\sqrt{f/\tau} < k_C\pi/\sqrt{2}$ , or

$$h_{\max} < k_C\pi\sqrt{\tau/2f}. \quad (4.3.10)$$

It is a replacement for the limit (4.3.7) for pulsed MFs. Rule (4.3.2) defines  $\xi$  for a series of P peaks or extrema. The difference  $\xi = h\tau$  of the zeroth ( $r = 0$ ) and first ( $r = 1$ ) peaks is equal to  $2\pi/b$ . That means that  $\Delta h = 2\pi/b\tau$ , if we change the value of pulse  $h$  and would like to observe two peaks on the  $h$ -dependence of an MBE. Since in all the cases we must have  $\Delta h < h_{\max}$ , we have, combining with (4.3.10),  $\Delta h < k_C\pi\sqrt{\tau/2f}$ .

Substituting relations for  $\Delta h$ , (4.3.8), and  $\omega_0 = bH_{\text{DC}}$ , we arrive at the inequality

$$H_{\text{DC}} < (\alpha\beta^3)^{1/4} \sqrt{\frac{\pi^2 k_C}{32b}}. \quad (4.3.11)$$

The last constraint consists in that the angular shift of an interference pattern during the reaction time  $T$  for a protein in the absence of pulsed MFs must be larger than the angular size of a gate  $\sim \pi/2$ . Otherwise, there would be nothing to compensate for with field pulses. That leads to another inequality  $\omega_0 T > \pi/2$ . For the best selection  $\alpha = \beta = 1$ , which corresponds to pulses in meander form, we obtain inequalities that define the interval of DC MFs that are suitable for observations of complicated spectra of ion interference

$$\frac{\pi}{2bT} < H_{\text{DC}} < \sqrt{\frac{\pi^2 k_C}{32b}}. \quad (4.3.12)$$

Optimal parameters of a pulsed MF are selected from a specified level of a DC MF. To begin with, we find the frequency  $\omega_0 = bH_{\text{DC}}$ , then  $f > 2\omega_0/\pi$ , then  $\tau < f^{-1}/2$ , and finally  $h < \pi k_C\sqrt{\tau/2f}$ . Then, we have to fine-tune the found parameters in accordance with rule (4.3.2).

Inequality (4.3.12) suggests that not all the ions that are characterized by a charge-to-mass ratio or by a parameter  $b = q/2Mc$  can display multipeak spectra in a pulsed field. Shown in Fig. 4.14 are  $b$ -dependences of the left and right limits in (4.3.12) for a DC MF. Also shown are values of  $b$  for various ions. It is seen that in DC fields at the geomagnetic level in the middle latitudes 40–50  $\mu\text{T}$ , K, Na, Ca, Mg,

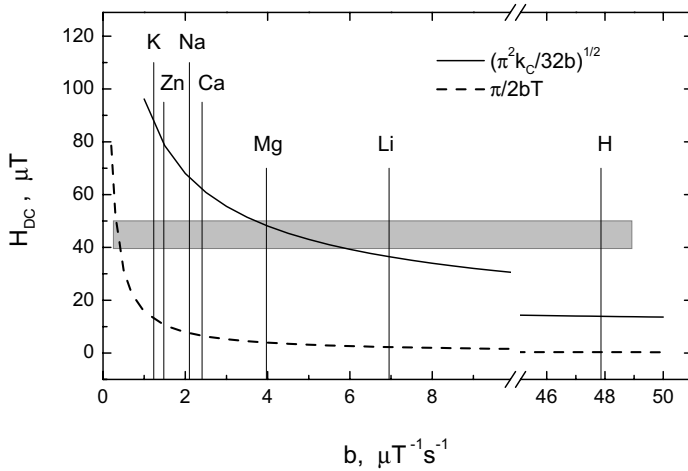


**Figure 4.14.** Upper and lower limits (4.3.12) of a DC MF for multippeak ion interference spectra in pulsed MFs to be measured, as a function of the charge-to-mass ratio  $b = q/2Mc$ .

and Zn ions are suitable for the mechanism under consideration, and that Li and H light ions lie outside of the interval and require lower DC MFs. An interference mechanism could also be observed at fields larger than in (4.3.12), if it were not for the growing probability of bioeffects of another physical nature.

Rule (4.3.2) is not met if the product of pulse intensity  $h\tau$  and frequency of pulse occurrence  $f$  is smaller than the DC MF  $H_{DC}$ . In that case, the interference mechanism, in the specific scheme provided here, cannot account for biological effects of a pulsed field. Such effects for very weak pulsed MFs were observed, e.g., by Berman *et al.* (1990) and Farrell *et al.* (1997). In both works  $h\tau f \approx 0.05 \mu\text{T}$ .

- Takahashi *et al.* (1986) observed, in a similarly weak pulsed MF, complicated dependences simultaneously on three parameters: frequency, magnitude, and duration of pulses, which is characteristic of ion interference. They also studied the rate of DNA synthesis in a V79 cell culture of Chinese hamster upon incorporation of  $^3\text{H}$ -thymidine into a special preparation. The experiment scheme was  $h(2; 400)f(5; 300)\tau(6; 125 \mu\text{s})H(?)H_p(?)$ . A multippeak dependence of the effect on pulse intensity is shown in Fig. 4.15. The frequency spectrum had two maxima in the region of 10–15 and 100 Hz. The characteristic value of the mean MF produced by pulses  $\tau hf$  is close to  $0.1 \mu\text{T}$ , which is much smaller than the geomagnetic field. Therefore, it is impossible to connect that effect with the model under consideration. However, the multippeak nature of the curve points to the interference nature of the effect. Since the spectrum of this pulsed sequence attained 40 kHz, it is quite likely that the interference picture here was conditioned by sufficiently large electric

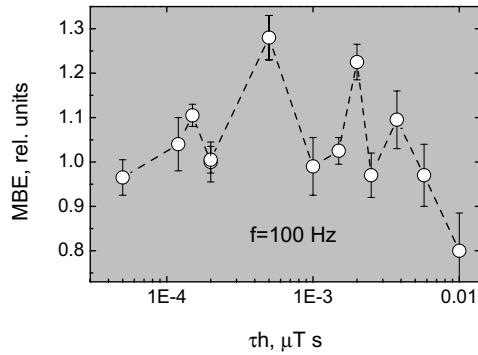


**Figure 4.15.** DNA synthesis rate vs MF pulse intensity, according to Takahashi *et al.* (1986).

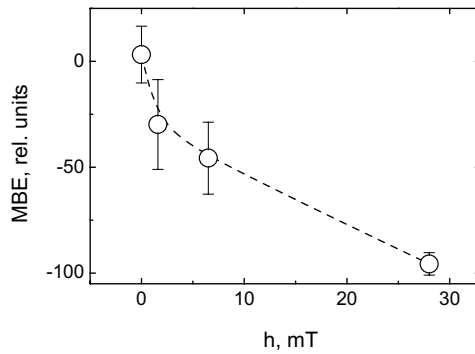


**Figure 4.16.** Capture of radioactive calcium tracer in rat thymocytes vs pulse height of 3-Hz MF meander, according to Walleczek and Budinger (1992).

fields induced in a medium.

- Bersani *et al.* (1997) studied a redistribution of transmembrane proteins induced by a pulsed MF on the surface of cells in a DC MF  $196 \mu\text{T}$ . They reported a significant effect for triangular-shaped pulses at 50 Hz, so that  $h\tau f \sim 850 \mu\text{T}$ . That is a relatively large quantity in comparison with a DC field. The pulse shape is far from  $\delta$ -bursts, and the fundamental harmonic of the signal is close to the standard limit (4.3.7). It is fairly hard, therefore, to comment on those results in terms of ion interference. At the same time there are no apparent contradictions as well.
- Walleczek and Budinger (1992) studied the capture of a  $^{45}\text{Ca}^{2+}$  tracer induced by concanavalin A added to a suspension of rat thymocyte cells. That parameter changed on a 30-min exposure to a pulsed MF, so that changes were only observed

at a definite concentration of concanavalin (physiological window). Under such conditions, the effect also depended on the pulsed MF intensity. The MF signal was square, single-pole, with frequency  $f = 3\text{ Hz}$  and 50% pulse-to-period duration ratio ( $\tau = 0.5/f$ ). The pulse height changed in the interval  $h = 0\text{--}28\text{ mT}$ . Figure 4.16 illustrates the dependence of the effect on the pulse height.

In those experiments the AC MF was more than 30 times stronger than the geomagnetic static field. This makes the effect unexplainable in terms of the ion interference mechanism, which requires that a static field  $H_{\text{DC}}$  and the product  $f\tau h$  for a pulsed MF have similar orders of magnitudes.

On the other hand, all the values of the MF, except for the largest one, used in that experiment were lower than the threshold level for thermal effects of induced eddy currents, see (4.3.10).

The primary physical process that provides for the “hooking” of an MF at a biological system seems to be concerned with an action of an MF on the rate of reactions involving free radicals. That is suggested both by the range of effective MFs with a suitable intensity and the monotonous dependence of the effect on the MF intensity. Unfortunately, the authors report nothing of the frequency selectivity of the effect observed, which could shed some light on the nature of a given MBE.

- Goodman *et al.* (1983) established that some parameters of RNA synthesis in salivary gland cells exceeded the control level by a factor of 11–13 on exposure to low-frequency (15 and 72 Hz) pulsed MFs. Within this range, the biological effect varied widely; however, the work contained neither sufficiently detailed descriptions of pulses nor the value of a local static MF.

RNA and mRNA synthesis increased two- and threefold as compared with controls in the cells of the T-lymphoblastic line, which were obtained by nearly rectangular 72-Hz MF pulses, according to Phillips and McChesney (1991). Again, the MFs involved were described inadequately for theoretical analysis.

A pulsed 75-Hz MF induced a two- to fivefold increase in intensity of DNA synthesis in human osteoblast cells, as shown by Sollazzo *et al.* (1996); the MF was also described inadequately. However, it met the standard  $hf < k_C$ ; i.e., it fell in the effectiveness range for interference mechanism.

Comparison of theory with most known experiments is hindered by the dearth of information on the MF employed. For instance, only one-third of the 27 reports (Congress EMBM, 1997) concerned with biological and biomedical applications of pulsed MFs contained an accurate description of the pulses. No reports are extant where pulsed MFs with finely varied parameters were used. Not a single report provides information on the value of the local DC MF.

A comparison of predictions of the interference mechanism with two experimental works (Aarholt *et al.*, 1982; Smith *et al.*, 1991) containing a fairly complete description of the MF involved is given in Section 4.9.

The formula for the frequency spectrum of dissociation in a sinusoidal MF (along a static field) predicts a fairly uniform series of effective frequencies:  $\Omega_c$ , and its harmonics and subharmonics. In contrast, relation (4.3.6) predicts values that would

be impossible to identify *a priori* with some obvious frequencies. Therefore, the rule (4.3.2) gives a simple way to test: *a biological effect, within a certain interval, must remain unchanged where pulse values and durations vary so that their product remains constant.* The same must take place where pulse frequencies vary with the applied DC MF. We stress that the rule (4.3.2) is rigidly connected with the dissociation mechanism due to interference of ion quantum states. Therefore, when the rule is met, unequivocal conclusions as to the physical nature of effects observed are possible. Qualitative predictions have it that biological effects of pulsed MFs should be observed against the background of DC fields for those ions, for which such effects are observed in a parallel sinusoidal and DC MF or in a magnetic vacuum.

### 4.3.3 Amplitude spectra for pulsed modulations of an MF

Consider the behavior of the amplitude spectra of dissociation in a sinusoidal MF modulated by pulses that switch on/off the field, see Fig. 2.17. We write the MF as follows

$$H(t) = H_{\text{DC}}[1 + h' \cos(\Omega t)M(t)] ,$$

where  $M(t)$  is a modulating function. We again proceed from the writing of the ion probability density at some value of angular coordinate

$$p(\varphi_0, t) = \sum_{mm'} a_{mm'} \exp \left[ i\Delta m \left( \varphi_0 + \omega_0 t + \omega_1 \int \cos(\Omega t)M(t)dt \right) \right] .$$

We represent the function  $f(t) = \cos(\Omega t)M(t)$  in the form of a Fourier series, and take the period  $\lambda$  of the modulating function to be a multiple of the period  $2\pi/\Omega$  of the sinusoidal MF. As a result of that constraint, which is not very strong physically,  $f(t)$  becomes  $\lambda$ -periodical. Assuming also  $M(t)$  to be an even function and denoting  $\omega = 2\pi/\lambda$ , we write

$$f(t) = \sum_{k=1}^{\infty} a_k \cos(k\omega t) , \quad a_k = \frac{2}{\lambda} \int_{-\lambda/2}^{\lambda/2} f(t') \cos(k\omega t') dt' . \quad (4.3.13)$$

then the integral in the expression for  $p$  can easily be taken, so that we can write the equalities

$$\begin{aligned} & \exp \left[ i\Delta m \left( \varphi_0 + \omega_0 t + \frac{\omega_1}{\omega} \sum_{k=1}^{\infty} a_k \frac{\sin(k\omega t)}{k} \right) \right] \\ &= \exp[i\Delta m(\varphi_0 + \omega_0 t)] \prod_{k=1}^{\infty} \exp \left[ i\Delta m \omega_1 a_k \frac{\sin(k\omega t)}{k\omega} \right] . \end{aligned}$$

Using the following notation and equality

$$z_k = \Delta m \frac{\omega_1}{k\omega} a_k , \quad \exp[(iz_k \sin(k\omega t)] = \sum_n J_n(z_k) \exp(ink\omega t) ,$$

we rewrite the infinite product in the last expression in the form

$$\prod_{k=1}^{\infty} e^{iz_k \sin(k\omega t)} = \sum_{n'} J_{n'}(z_1) e^{in'1\omega t} \sum_{n''} J_{n''}(z_2) e^{in''2\omega t} \dots$$

It can also be written differently

$$\sum_{n'n''n'''\dots} J_{n'}(z_1) J_{n''}(z_2) J_{n'''}(z_3) \dots \times e^{i\omega t(1n'+2n''+3n'''+\dots)} \quad (4.3.14)$$

Clearly, in the general case, the infinite product of Bessel functions is zero, since  $|J_n| \leq 1$ . One of the main contributions to (4.3.14) will produce terms with  $n' \neq 0$ ,  $n'' = n''' = \dots = 0$ . It will only occur when the quantities  $z_2, z_3, \dots$  are close to zero, then  $J_0(z_k) \approx 1$ .

We will show that such an infinite product has a finite non-zero value. We now find the coefficients  $a_k$  for the above Fourier series. As indicated above, the period of the modulating function is chosen to be a multiple of the period of a sinusoidal MF  $2\pi/\Omega$ . The time interval of MF switching  $\tau$  can also be conveniently expressed in these units. We then write the definitions

$$\lambda = s 2\pi/\Omega, \quad \tau = r 2\pi/\Omega,$$

where  $s$  is a positive integer, and  $0 \leq r \leq s$  is a real number. Then computing the coefficients in (4.3.13) yields

$$a_k = \frac{2}{\lambda\Omega} \left[ \frac{\sin(k/s - 1)r\pi}{(k/s - 1)} + \frac{\sin(k/s + 1)r\pi}{(k/s + 1)} \right]. \quad (4.3.15)$$

For large values of  $k$  we can write

$$a_k \leq \frac{2}{\lambda\Omega} \left[ \frac{1}{(k/s - 1)} + \frac{1}{(k/s + 1)} \right] \approx \frac{4s}{\lambda\Omega k}.$$

Therefore, beginning with a certain number  $k = K$ , we have the inequality

$$z_k = \Delta m \frac{\omega_1}{k\omega} a_k < \Delta m \frac{\omega_1}{k\omega} \frac{4s}{\lambda\Omega k} < \frac{1}{k}.$$

Since at  $z_k \rightarrow 0$

$$J_0(z_k) = 1 - z_k^2/2 + o(z_k^3) > 1 - 1/k^2,$$

then the infinite product of Bessel functions under discussion has a finite value:

$$\prod_{k=K}^{\infty} J_0(z_k) > \prod_{k=2}^{\infty} J_0(z_k) > \prod_{k=2}^{\infty} (1 - 1/k^2) = \frac{1}{2}.$$

Returning to (4.3.14) and retaining in it the specified main contribution, we write the probability density for an ion in the form

$$\begin{aligned}
 p(\varphi_0, t) &= \sum_{mm'} a_{mm'} e^{i\Delta m \varphi_0} e^{i\Delta m \omega_0 t} \sum_{n'} J_{n'}(z_1) e^{i\omega n' t} \\
 &= \sum_{mm'n} a_{mm'} e^{i\Delta m \varphi_0} J_n(z_1) e^{i\alpha t} ,
 \end{aligned}$$

where

$$\alpha = \Delta m \omega_0 + \omega n .$$

Sliding averaging here reduces to the averaging of the last exponential function:

$$T[e^{i\alpha t}] = e^{i\alpha t} \sin(\alpha T) / \alpha T .$$

The average over time  $t$  of the square  $T^2[p(\varphi_0, t)]$  is a sum of products of complex conjugate terms. The dissociation probability of an ion–protein complex is equal to

$$P = \sum_{mm'n} |a_{mm'}|^2 \frac{\sin^2(\alpha T)}{(\alpha T)^2} J_n^2(z_1) . \quad (4.3.16)$$

The condition for maxima  $P$ ,  $\alpha = 0$ , after substitution of  $\alpha$ , gives the spectrum of effective frequencies of the modulating pulse sequence

$$\omega_{\max} = \frac{\Delta m}{n} \omega_0 = \frac{\Delta m}{2n} \Omega_c .$$

It is seen that the fundamental frequency of the MF spectrum must obey the same condition as the MF frequency for an exposure to a non-modulated sinusoidal MF (4.1.21). In the limit we get the earlier expression for the spectrum of effective frequencies, when the parameters of a modulating signal are such that the MF becomes sinusoidal.

The dependence of a modulating function on the parameters is also determined by the argument  $z_1$  of the Bessel function in (4.3.16), which on substitution of  $a_1$  from (4.3.15) becomes

$$z_1 = \frac{\Delta m h'}{2\pi f'} \left[ \frac{\sin(1 - 1/s)r\pi}{(1 - 1/s)} + \frac{\sin(1 + 1/s)r\pi}{(1 + 1/s)} \right] .$$

Here it was taken into consideration that  $\omega\lambda = 2\pi$  and  $\omega_1/\Omega = h'\Omega_c/2\Omega = h'/2f'$ , where, as before,  $h' = H_{AC}/H_{DC}$ ,  $f' = \Omega/\Omega_c = f/f_c$  are the relative amplitude and frequency of a sinusoidal MF. In the case of a purely sinusoidal MF we shall put  $\tau = \lambda = 2\pi/\Omega$  or  $r = s = 1$ . Then

$$z_1 = \frac{\Delta m h'}{2\pi f'} \lim_{\beta \rightarrow 0} \frac{\sin \beta \pi}{\beta} = \frac{\Delta m h'}{2f'} .$$

Thus, in the limiting case of non-modulated sinusoidal MFs, formula (4.3.16) reduces to formula (4.1.23), obtained specially for that case.

Formula (4.3.16) is a multipeak dependence on the variables of a modulating signal. For instance, the dependence of  $P$  on the MF switching interval  $r$  has a

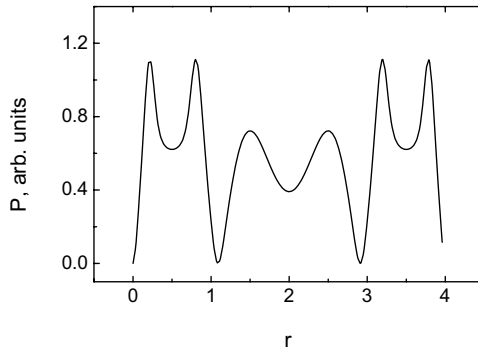


**Figure 4.17.** A typical dependence of dissociation probability on the switching interval length for a sinusoidal MF under pulsed modulation.

form shown in Fig. 4.17. The plots in it have been calculated with the following parameters:  $h' = 11$  (where a purely sinusoidal signal yields a near-zero effect),  $f' = 1$ ,  $\Xi = 6$  (corresponds to the reaction time  $T = 0.1$  s of a protein with calcium at  $H_{DC} = 0.1$  G),  $s = 4$  (one period of the modulating function is equal to four periods of the sinusoidal signal). A characteristic feature of such dependences is their being symmetrical relative to point  $r = s/2$ . That gives a possibility of convenient experimental tests.

Considered above was the case where non-zero products of Bessel functions in (4.3.14) were primarily determined by the first factor in the expansion (4.3.13). That holds well where the period  $\lambda$  and interval  $\tau$  of the modulating function are close in magnitude to the period of a sinusoidal signal. Another situation is possible where the period is  $\lambda \gg 2\pi/\Omega$ , i.e.,  $s \gg 1$ . In that case, only the factor  $a_{k=s}$  will be the largest and main contributor. As follows from (4.3.15), it equals  $a_{k=s} \approx (2/\lambda\Omega)r\pi = r/s$ . The remaining  $a_k$ , along with  $z_k$ , are close to 0. Then the main input to (4.3.14) comes from products with indices  $n' = 0$ ,  $n'' = 0 \dots$ ,  $n^{(s)} \neq 0$ ,  $n^{(s+1)} = 0, \dots$ . Derivation of formulas for  $P$  then repeats the previous procedure, the only departure being that instead of  $z_1$  one should substitute  $z_s$ , and instead of  $\omega$ , one should substitute  $s\omega$ . For the index  $n^{(s)}$ , over which summation is carried out, we retain the symbol  $n$ . Then

$$P = \sum_{mm'n} |a_{mm'}|^2 \frac{\sin^2(\alpha T)}{(\alpha T)^2} J_n^2(z_s), \quad \alpha = \Delta m \omega_0 + sn\omega, \quad z_s = \Delta m \frac{\omega_1 r}{s\omega s}. \quad (4.3.17)$$

The last definitions for  $\alpha$  and  $z_s$  can also be written in the form

$$\alpha = \Delta m \omega_0 + n\Omega, \quad z_s = \frac{\Delta m h' r}{2f' s}.$$

The first of these defines the frequency spectrum ( $\alpha = 0$ ), which, as with a purely sinusoidal signal, is

$$\Omega_{\max} = \frac{\Delta m}{2n} \Omega_c .$$

The second definition, an argument of Bessel functions, depends on the modulating function parameters  $r, s$ . At  $r = s$  (purely sine MF), we have (4.1.23) again. Similarly, we can derive formulas for combined MFs with harmonic modulation.

Litovitz *et al.* (1997b) used pulse-modulated MFs to observe changes of enzyme activity. The period of a modulating function was 1 s at  $f = 60$  Hz,  $H_{AC} \sim H_{DC} \sim 0.1$  G. In that case, we have  $s \sim 60$ ,  $h' \sim 1$ . We can assume that the frequency  $f$  was close to one of the effective frequencies spectrum (4.3.17), i.e., the condition  $\Delta m/f \sim 2n$  was met. A dependence on the pause  $l = s - r$  between MF switching intervals, as predicted by formula (4.3.17), could then have a form close to

$$J_n^2(nr/s) = J_n^2[n(1 - l/s)] .$$

That dependence shows a decline of  $P$  with the pause, which could account for a falloff of enzyme activity under these conditions, see Fig. 2.17.

Note that the ion interference mechanism is non-linear in the sense that the sum of magnetic signals  $a + b$ , such that each one causes a reaction  $A$  and  $B$ , does not cause a reaction  $A + B$ . Specifically, when exposed to a pulsed MF, the reaction does not reduce to a sum of reactions to each of the harmonics of a signal. Therefore, predictions of any “resonance” model, in particular, the parametric resonance model for ions, which of necessity involved only one subharmonic, namely one whose frequency coincides with the Larmor frequency of Zeeman splitting, is markedly different from predictions of the ion interference model, which considers the complete pulse shape and predicts the emergence of response maxima as a function of pulse intensity even when none of the signal harmonics coincides with a Larmor frequency. It is thus possible to establish whether it is resonance transitions in a Zeeman multiplet or interference phenomena that underlie the effect observed in experiment.

#### 4.4 TILTED CONFIGURATION OF MAGNETIC FIELDS

Tilted orientations of AC and DC components of an MF in experiment are used quite often, because perhaps they are simple to realize. To produce a variable field it is sufficient to have a solenoid, vertical or horizontal. The role of a DC MF is normally played by the geomagnetic field. The GMF vector in the northern hemisphere is pointed down at an angle to the horizontal.

At the same time, with such an orientation it is fairly difficult to explain the experimental findings. Complications begin right with attempts to consider results in terms of some model representations. Consider, for instance, a physical phenomenon or a mechanism whose model only takes account of a uniaxial MF. Then the question emerges of how to select the main axis. With which MF component pair are we to associate the observed effect, Fig. 4.18? Should we take into consideration the component of the AC MF  $\mathbf{B}_{AC}$  along the DC direction or, in contrast, the component of the DC field  $\mathbf{B}_{DC}$  along the AC field direction? These versions

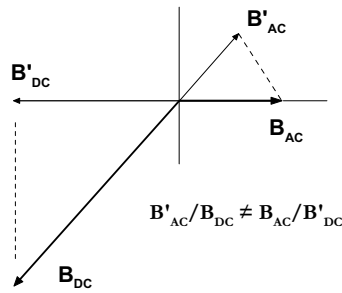


**Figure 4.18.** Corresponding to different choices of parallel components of the AC and DC MFs are their different ratios — an important parameter of the theory.

give different ratios of uniaxial components, but it is exactly that ratio that is a parameter of promising theoretical mechanisms.

Blackman *et al.* (1990) discussed that question, although, physically, its formulation is incorrect. The observed effect has to be associated not with two parameters,  $\mathbf{B}_{AC}$  and  $\mathbf{B}_{DC}$ , but rather with three: the values of the fields and the angle between them. The questions of what is the phenomenon real mechanism and to what extent that mechanism allows an idealized description using only two parameters lies outside the framework of our preliminary analysis. That is often overlooked, in favor of calculating, for instance, the cyclotron frequency of an ion by considering only one DC field component, the one that is parallel with the AC MF vector (Ružič and Jerman, 1998). This only makes sense when the primary MF target features an anisotropy, i.e., utilizes some other vector as a reference vector, and all the individual molecular targets of a biological system are constructed in one direction. To be sure, the AC MF vector cannot be that reference vector, since both AC and DC magnetic fields have the same physical nature. A suitable situation may occur in the stem of some plants aligned along the gravity vector. Can ions concerned with some primary target of an MF distinguish between components of a DC MF, i.e., can they “know” of their presence? That is an experimental issue; today such data are not known. Therefore, the best prior choice is accounting for the complete MF vector.

In experiment the effectiveness of both parallel and perpendicular MF orientations is observed. The effectiveness of either orientation was observed in the same biological system (Garcia-Sancho *et al.*, 1994). This suggests that it is advisable to simultaneously consider both possibilities for one model. For an ion interference mechanism, that implies that the dissociation probability of a complex is a function of four quantities, the AC and DC components of an MF, the angle between them, and the frequency of variable components. In terms of idealizations used in Section 4.1 such a problem can be solved.

Choice of the quantization  $z$  axis is immaterial. The observables, formed by

quantum-mechanical averaging  $\langle |..| \rangle$  are independent of that. There is a complete analogy with the choice of a coordinate system in classical physics. Eigenfunctions of an ion in a DC MF generally depend on the angle between the  $z$  axis and the direction of the DC field. It is more convenient still, as usual, to align the  $z$  axis along the DC component of an MF and do without an angle dependence of these functions. The vector of an oscillating AC MF is then decomposed into components along and perpendicular to the DC field. We will separately consider the action of perpendicular components, and then clarify when a joint action is possible with the parallel component, which cannot be reduced to a simple sum of effects.

#### 4.4.1 Interference in perpendicular fields

For a perpendicular orientation of DC and AC fields, an MBE is normally associated with magnetic-resonance type mechanisms, since it is precisely for such resonances that perpendicular components appear to be of importance. A DC MF splits a particle's quantum levels into Zeeman sublevels, and an AC field engenders transitions in sublevels (a uniaxial field causes no transitions). A particle goes over from a sublevel to a lower one, liberating in the process some energy that is utilized supposedly in the course of a biochemical reaction. Since it is clear *a priori* that this energy is many orders of magnitude smaller than  $\kappa\mathcal{T}$ , the treatment is normally confined to the hypothesis that a biochemical reaction is in some unknown manner concerned with those transitions. Beyond that there is no progress: no formulas have been obtained so far that relate a biological effect with the variables of a magnetic field. This reasoning at best yields a model predicting transition frequencies proportional to a DC field, i.e., cyclotron frequencies for some assumed ions. According to that mechanism, the dependence of an effect on the amplitude of an AC field is monotonous in nature. Allowance for relaxation processes leads to a saturation of quantum transitions with the AC field amplitude. It is impossible to obtain a decrease in the transition probability with amplitude, and that disagrees with a body of evidence for multippeak dependences of an MBE on the amplitude of an AC field.

According to ion interference mechanism, we will associate an MBE in perpendicular fields not with the fact that an ion passes into some state of quantum spectrum, but with the fact that such transitions change the angular distribution of its probability density. We will assume that the levels are Zeeman ones, and transitions between them are caused by a perpendicular MF with frequency  $\Omega$  that is close to a resonance one. Let the wave function of a system be derived in the form

$$\sum_{\{i\}} c_{\{i\}}(t) \psi_{\{i\}} \exp(-i\varepsilon_{\{i\}}t/\hbar) , \quad (4.4.1)$$

where  $\psi_{\{i\}}$  are reference functions (4.1.4), and  $\{i\}$  is a set of quantum numbers  $k, l, m$ . The equation for coefficients then assumes the well-known form

$$i\hbar\dot{c}_{\{i\}} = \sum_{\{i'\}} c_{\{i'\}} \langle \psi_{\{i\}} | \mathcal{V}(t) | \psi_{\{i'\}} \rangle \exp[-i(\omega_{\{i'\}} - \omega_{\{i\}})t] . \quad (4.4.2)$$

It is clear that the only time-dependent coefficients here are those of Zeeman levels within each series with fixed values of radial and azimuthal quantum numbers  $k, l$ . A low-frequency field cannot induce transitions that entail changes in those numbers. Therefore, quantum numbers  $k, l$  are here parameters of the solution, and they can be omitted until we need to perform an averaging over states with different  $k, l$ . To identify possible effects it is sufficient to derive results for a three-level system. Suppose that numbers  $m$  of resonating states have values  $m = -1, 0, 1$

$$i\hbar\dot{c}_m = \sum_{m'} c_{m'} \langle \psi_{\{i\}} | \mathcal{V}(t) | \psi_{\{i'\}} \rangle \exp(i\omega_{mm'}t) . \quad (4.4.3)$$

We now substitute an interaction operator, concerned with an AC MF, in the form

$$\mathcal{V}(t) = \mathcal{F}e^{-i\Omega t} + \mathcal{G}e^{i\Omega t} , \quad (4.4.4)$$

where  $\mathcal{F} = \mathcal{G}^+$  are Hermitian conjugate time-independent operators.

The operator of interaction of the orbital magnetic moment of an ion with an MF has the form, see (4.1.1)

$$-\frac{q\hbar}{2Mc} \mathbf{L} \mathbf{H} , \quad \mathbf{L} = -i\mathbf{r} \times \nabla .$$

In the so-called precessing MF containing a component rotating in the  $z = 0$  plane

$$H_x = H_{AC} \cos \Omega t , \quad H_y = H_{AC} \sin \Omega t , \quad H_z = H_{DC} ,$$

the interaction operator is equal to

$$\mathcal{V}_0 + \mathcal{V}(t) .$$

In the notation adopted earlier, these operators are

$$\mathcal{V}_0 = i\hbar\omega_0 \frac{\partial}{\partial \varphi} , \quad \mathcal{V}(t) = -\hbar\omega_1 (\mathcal{L}_x \cos \Omega t + \mathcal{L}_y \sin \Omega t) .$$

Operator  $\mathcal{V}_0$  splits levels degenerated in the absence of an MF into Zeeman multiplets. The time-dependent operator  $\mathcal{V}(t)$  causes transitions in multiplet levels. That operator can conveniently be written in the following form, see Appendix 6.1,

$$\mathcal{V}(t) = -\frac{\hbar\omega_1}{2} (\mathcal{L}_+ e^{-i\Omega t} + \mathcal{L}_- e^{i\Omega t}) . \quad (4.4.5)$$

The case of a linearly polarized AC MF oscillating along one axis, perpendicular to  $z$ , reduces to a sum of operators (4.4.5) with opposite signs of their respective frequencies  $\Omega$ . Comparing (4.4.5) and (4.4.4), we note that the operator  $\mathcal{F}$  equals

$$\mathcal{F} = -\frac{\hbar\omega_1}{2}\mathcal{L}_+ = -\frac{\hbar\omega_1}{2}e^{i\varphi}\left(\frac{\partial}{\partial\theta} + i\cot\theta\frac{\partial}{\partial\varphi}\right). \quad (4.4.6)$$

We find its matrix elements. The wave functions of the central potential

$$\psi_{klm} = R_{kl}(r)Y_{lm}(\theta, \varphi) \quad (4.4.7)$$

are products of radial functions and orthonormal spherical functions, which are eigenfunctions for the operators of squared angular momentum  $\mathcal{L}^2$  and its component along  $\mathcal{L}_z$ . Since the operator  $\mathcal{F}$  only acts on the variables  $\theta, \varphi$ , its matrix elements can be found in the functions  $Y_{lm}(\theta, \varphi)$ , if we assume the radial functions to be normalized to unity,  $\langle R_{..}|R_{..}\rangle = 1$ . The matrix elements of the operator  $\mathcal{L}_+$  are found, for instance, in Landau and Lifshitz (1977). They are non-zero for transitions that increase  $m$  by one and leave  $l$  unchanged. Therefore, the matrix elements  $\mathcal{F}$  can be written as

$$\mathcal{F}_{m,m-1} = -\frac{\hbar\omega_1}{2}\langle Y_{lm}|\mathcal{L}_+|Y_{l,m-1}\rangle = -\frac{\hbar\omega_1}{2}\sqrt{(l+m)(l-m+1)}. \quad (4.4.8)$$

Note that

$$\mathcal{F}_{10} = \mathcal{F}_{0,-1} = -\frac{\hbar\omega_1}{2}\sqrt{l(l+1)}.$$

After some simple transformations, by virtue of  $\mathcal{G}_{nm} = \mathcal{F}_{mn}^*$ ,  $\omega_{mn} = \omega_{m+1,n+1}$ , we obtain from (4.4.3), (4.4.4) the equations

$$\begin{aligned} i\hbar\dot{c}_1 &= \mathcal{F}_{10}e^{-i\epsilon t}c_0, \\ i\hbar\dot{c}_0 &= \mathcal{F}_{10}(e^{-i\epsilon t}c_{-1} + e^{i\epsilon t}c_1), \\ i\hbar\dot{c}_{-1} &= \mathcal{F}_{10}e^{i\epsilon t}c_0, \end{aligned}$$

where

$$\epsilon = \omega_{01} + \Omega. \quad (4.4.9)$$

Substitution

$$x = \exp(i\epsilon t)n_1, \quad y = \exp(-i\epsilon t)c_{-1}, \quad z = c_0$$

gives equations that could be written in matrix form as

$$\dot{\mathbf{u}} = \mathbf{A}\mathbf{u}, \quad \mathbf{u} = \begin{pmatrix} x \\ y \\ z \end{pmatrix}, \quad \mathbf{A} = \begin{pmatrix} a & 0 & -v \\ 0 & -a & -v \\ -v & -v & 0 \end{pmatrix}, \quad a = i\epsilon, \quad v = i\mathcal{F}_{10}/\hbar. \quad (4.4.10)$$

The equation has an exact solution, although it is not necessary. The resonance curve for forced quantum oscillations is well known, Fig. 4.19. The population of states  $\beta$ , with the initial state  $\alpha$ , varies in a two-level system as

$$\left(1 + \frac{\epsilon^2}{4|v|^2}\right)^{-1} \sin^2\left(t\sqrt{\frac{\epsilon^2}{4} + |v|^2}\right). \quad (4.4.11)$$

It is seen that the variation amplitude attains a maximum under resonance, i.e., when  $\epsilon = 0$ .

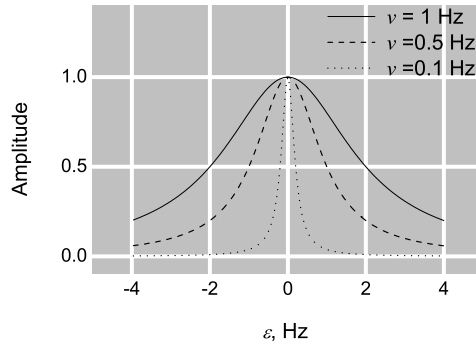


**Figure 4.19.** The variation of oscillation amplitude for the population of quantum states with detuning  $\epsilon$  for various intensities of the “driving force”.

For a multilevel system of equidistant levels a resonance comes about simultaneously in each pair of neighboring levels. Depending on the initial conditions, initially unpopulated upper levels gradually get populated, and this corresponds to the pumping of energy in forced classical oscillations. The population oscillation amplitude for each level, averaged over a sufficiently large time interval is maximal at resonance, although oscillations are not strictly periodical (for an infinite number of levels).

Therefore, we will confine ourselves to the case of exact resonance  $\epsilon = 0$ , see (4.4.9). Then  $a$  in matrix  $A$  will be zero. Equations  $\det(A - \lambda I) = 0$  and  $A\mathbf{u}_i = \lambda_i \mathbf{u}_i, i = 0, 1, 2$  yield eigenvalues  $\lambda$  for matrix  $A$

$$\lambda_0 = 0, \quad \lambda_{1,2} = \pm v\sqrt{2} \quad (4.4.12)$$

and normalized eigenvectors

$$\mathbf{u}_0 = \frac{1}{\sqrt{2}} \begin{pmatrix} -1 \\ 1 \\ 0 \end{pmatrix}, \quad \mathbf{u}_1 = \frac{1}{\sqrt{2}} \begin{pmatrix} -1/\sqrt{2} \\ -1/\sqrt{2} \\ 1 \end{pmatrix}, \quad \mathbf{u}_2 = \frac{1}{\sqrt{2}} \begin{pmatrix} 1/\sqrt{2} \\ 1/\sqrt{2} \\ 1 \end{pmatrix}.$$

The general solution to (4.4.10) is a combination of these vectors of the form

$$\mathbf{u} = \sum_{i=0}^2 d_i \mathbf{u}_i e^{\lambda_i t}.$$

Back substitutions yield the coefficients  $c_i$  ( $\epsilon = 0$ )

$$\begin{aligned}
 c_1 &= \frac{1}{\sqrt{2}} \left( -d_0 - \frac{d_1}{\sqrt{2}} e^{\lambda_1 t} + \frac{d_2}{\sqrt{2}} e^{\lambda_2 t} \right), \\
 c_0 &= \frac{1}{\sqrt{2}} (d_1 e^{\lambda_1 t} + d_2 e^{\lambda_2 t}), \\
 c_{-1} &= \frac{1}{\sqrt{2}} \left( d_0 - \frac{d_1}{\sqrt{2}} e^{\lambda_1 t} + \frac{d_2}{\sqrt{2}} e^{\lambda_2 t} \right).
 \end{aligned} \tag{4.4.13}$$

We assume that at  $t = 0$  a system was in a state  $m = 0$ , i.e.,  $|c_0(0)|^2 = 1$ ,  $|c_1(0)|^2 = |c_{-1}(0)|^2 = 0$ . Hence we find the coefficients meeting those conditions. In particular,  $d_0 = 0$ ,  $d_1 = d_2 = 1/\sqrt{2}$ . Substituting these into expressions for  $c_i$  and considering that

$$\lambda_{1,2} = \pm i\lambda, \quad \lambda = \frac{\mathcal{F}_{10}}{\hbar} \sqrt{2}, \tag{4.4.14}$$

we get

$$c_0 = \cos \lambda t, \quad c_{1,-1} = \frac{-i}{\sqrt{2}} \sin \lambda t. \tag{4.4.15}$$

The populations of states  $m = 0$ ,  $m = \pm 1$  then oscillate respectively as  $\cos^2 \lambda t$  and  $\frac{1}{2} \sin^2 \lambda t$ .

The form of the wave function (4.4.1) here implies that the probability density at point  $\varphi_0$  is

$$\begin{aligned}
 p(\varphi_0, t) &= \langle \Psi(\varphi_0, t) | \Psi(\varphi_0, t) \rangle_{r,\theta} \\
 &= \sum_{\{i\}\{i'\}} c_{\{i\}}^*(t) c_{\{i'\}}(t) \langle \psi_{\{i\}} | \psi_{\{i'\}} \rangle_{r,\theta} \exp[-i(\varepsilon_{\{i'\}} - \varepsilon_{\{i\}})t/\hbar].
 \end{aligned} \tag{4.4.16}$$

The group of indices  $\{i\}$  consists of radial  $k$ , azimuthal  $l$ , and magnetic  $m$  quantum numbers,

$$\psi_{\{i\}} = R_{kl}(r) Y_{lm}(\theta, \varphi) \propto R_{kl}(r) P_l^{|m|}(\theta) \exp(im\varphi),$$

see (4.1.4). The terms of the sum (4.4.16) with  $k \neq k'$  and  $l \neq l'$  oscillate fast; therefore we ignore their contribution. Here we will need a formula for spherical functions

$$Y_{lm} = \Theta_{lm}(\theta) \frac{1}{\sqrt{2\pi}} \exp(im\varphi). \tag{4.4.17}$$

Functions  $\Theta_{lm}(\theta)$  are normalized by the condition

$$\langle \Theta_{lm} | \Theta_{lm} \rangle = \int_0^\pi |\Theta_{lm}|^2 \sin \theta d\theta = 1.$$

They have the form (Landau and Lifshitz, 1977)

$$\Theta_{lm} = (-1)^{(m+|m|)/2} i^l \left[ \frac{2l+1}{2} \frac{(l-|m|)!}{(l+|m|)!} \right]^{1/2} P_l^{|m|}(\cos \theta), \quad |m| \leq l, \tag{4.4.18}$$

where

$$P_l^m(x) = (1-x^2)^{m/2} \frac{d^m}{dx^m} P_l(x), \quad x = \cos \theta, \quad m \geq 0$$

are associated Legendre functions, and

$$P_l(x) = \frac{1}{2^l l!} \frac{d^l}{dx^l} (x^2 - 1)^l$$

are Legendre polynomials.

The radial functions being normalized, the probability density is

$$p(\varphi_0, t) = \sum_{kl} p_l(\varphi_0, t) , \quad (4.4.19)$$

$$p_l(\varphi_0, t) = \sum_{mm'} c_{lm}^*(t) c_{lm'}(t) \langle \Theta_{lm} | \Theta_{lm'} \rangle \exp[i\varphi_0 \Delta m - i(\varepsilon_{m'} - \varepsilon_m)t/\hbar] .$$

Summation over  $k$  reduces to an insignificant constant coefficient and is later omitted. Functions  $\Theta_{lm}(\theta)$  are not generally orthogonal for various  $m$ . We denote

$$a_{mm'} = \langle \Theta_{lm} | \Theta_{lm'} \rangle , \quad c_{mm'} = c_{lm}^* c_{lm'} , \quad (4.4.20)$$

and take account (see (4.1.3)) of the fact that

$$\varepsilon_m = -\eta_m H_z = -\frac{q\hbar}{2Mc} m H_{DC} = -\hbar\omega_0 m . \quad (4.4.21)$$

The probability density then takes on a convenient form

$$p_l(\varphi_0, t) = \sum_{mm'} a_{mm'} c_{mm'}(t) \exp[i\Delta m(\varphi_0 + \omega_0 t)] . \quad (4.4.22)$$

It will be recalled that density (4.4.22) refers to a particle in a superposition of states of a Zeeman multiplet with a definite azimuthal number.

There are two inputs to the density (4.4.22), an interference one and a non-interference one. The latter,  $m = m'$ , clearly, reduces to a constant ( $a_{mm} = 1$ )

$$p = \sum_m a_{mm} c_{mm}(t) = \sum_m c_{mm}(t) = \text{Const} ,$$

since the sum of probabilities of multiplet states is taken to be unchanged.

We write the interference contribution as follows, introducing for convenience the notation  $\nu = \varphi_0 + \omega_0 t$ , and considering that  $a_{m, m\pm 1} = \langle \Theta_{lm} | \Theta_{l, m\pm 1} \rangle = 0$ ,  $a_{-1, 1} = -1$ :

$$p_l(\varphi_0, t) = a_{-1, 1} (c_{-1, 1} e^{2i\nu} + \text{e.n.}) . \quad (4.4.23)$$

Substituting quantities from (4.4.15), we find up to a coefficient

$$p_l(\varphi_0, t) = \sin^2 \lambda t \cos(2\nu) \propto (1 - \cos 2\lambda t) \cos 2(\varphi_0 + \omega_0 t) . \quad (4.4.24)$$

We then proceed as in Section 4.1. At first we find the sliding average for the probability density over interval  $[-T, T]$ . Then we average the squared quantity obtained. The result will be a magneto-dependent part of dissociation probability

for an ion–protein complex in perpendicular DC and AC MFs. We can show that sliding averaging yields the estimate

$$\begin{aligned} T[p_l(\varphi_0, t)] &= \frac{1}{2} \int_{t-T}^{t+T} p_l(\varphi_0, t') dt' \\ &\approx \cos 2(\varphi_0 + \omega_0 t) \frac{\sin 2\omega_0 T}{2\omega_0 T} - \frac{1}{2} \cos 2\varphi_0 \cos 2\kappa t \frac{\sin 2\kappa T}{2\kappa T}, \end{aligned}$$

where  $\kappa = \lambda \pm \omega_0$ . The square of that quantity reduces to the square of its two terms, since the main contribution, depending on magnetic conditions, is produced by either of the terms. Averaging  $T^2[p_l(\varphi_0, t)]$ , we will take account of the relationships

$$\overline{\cos^2 \kappa t} = \frac{1}{2}, \quad \overline{\cos^2 2\varphi_0} = \frac{1}{2},$$

where the averaging is respectively over an infinite time interval and over a uniformly distributed random quantity  $\varphi_0 \in [0, 2\pi)$ . Finally, we get

$$P \sim \frac{\sin^2 2\omega_0 T}{(2\omega_0 T)^2} + \frac{1}{8} \frac{\sin^2 2\kappa T}{(2\kappa T)^2}, \quad \kappa = \lambda \pm \omega_0. \quad (4.4.25)$$

Thus, in perpendicular fields there also exists an effect of magneto-sensitive dissociation due to interference of quantum states of an ion. The first term (4.4.25) describes the growth of dissociation probability in a zero DC field, i.e., at  $\omega_0 \rightarrow 0$ . Interestingly, this also occurs in the absence of an AC MF, in contrast to ion interference in parallel fields.

The second term (4.4.25) is associated with the action of an AC MF, which is perpendicular to a DC one. Unlike interference in parallel fields, the factor  $\sin x/x$  now defines the amplitude spectrum, rather than the frequency one. Selection rules, which follow from the form of the operator of interaction of a perpendicular AC MF with an ion, allow only transitions with  $\Delta m = \pm 1$ . Therefore, the frequency spectrum, as follows from (4.4.9), (4.4.21) will then include only one maximum at

$$\Omega_{\text{peak}} = -\omega_0, \quad (4.4.26)$$

whose form follows from the relationship (4.4.11).

The amplitude of the dissociation spectrum is derived from  $\kappa = \lambda \pm \omega_0 = 0$ ,  $\lambda = \sqrt{2}\mathcal{F}_{10}/\hbar$  or

$$\mathcal{F}_{10} = \pm \hbar \omega_0 / \sqrt{2}. \quad (4.4.27)$$

Using (4.4.8), after some simple transformations we obtain a formula for the magnitude of the relative amplitude of an AC MF, for which a maximal response is possible:

$$h' = \frac{H_{\text{AC}}}{H_{\text{DC}}} = \frac{\omega_1}{\omega_0} = \sqrt{\frac{2}{l(l+1)}}. \quad (4.4.28)$$

In particular, at resonance interference levels  $l = 1$  we get

$$h'_{\text{peak}} = 1 ,$$

which strongly differs from the value  $h' = 1.8$  for the location of the first spectral amplitude peak in parallel MFs, Fig. 4.28. Moreover,  $h' = 1$  is no minimal value for observations of resonance interference in perpendicular fields. As a matter of fact, interference in Zeeman levels of groups  $l = 2, 3, 4, 5, \dots$  occurs independently, and appropriate amplitudes of maximally effective MFs are 0.58, 0.41, 0.32, 0.26, etc. The relative contribution of those groups to the total effect is determined by populations of  $l$ -states. In this connection, we note the following.

The above dependences are valid for a three-level system,  $l = 1$ . When Zeeman multiplets with further azimuthal numbers  $l$  are populated, resonance transitions occur simultaneously for all the neighboring level pairs, even if initially only levels  $m = 0, \pm 1$  are populated, since all the levels are equidistant. With time, the population of levels  $m = 0, \pm 1$ , which define resonance interference, will fall off due to transitions to higher angular modes. Generally speaking, this reduces the relative amplitude of interference maxima of states  $l > 1$ . Therefore, observation of the interference of bound ions in perpendicular fields is dependent, to a larger degree than in parallel ones, on the realization of peculiar initial conditions where only a small number of Zeeman sublevels appear to be populated.

It is important that resonance interference is only displayed by a multiplet for which the condition of an effective amplitude of an MF is met, and interference effects emerge independently for each multiplet. Then, by (4.4.25), (4.4.19), (4.4.14), (4.4.8), we can write

$$P \sim \sum_l a_l \frac{\sin^2 2\kappa_l T}{(2\kappa_l T)^2} , \quad (4.4.29)$$

$$2\kappa_l T = \left( \frac{\mathcal{F}_{10}}{\hbar} \sqrt{2} + \omega_0 \right) 2T = \left( 1 - h' \sqrt{\frac{l(l+1)}{2}} \right) \Xi .$$

An amplitude spectrum, computed using that formula, for decreasing relative interference amplitudes and increasing  $l$  according to  $a_l \sim 2^{-l}$ , is shown in Fig. 4.20.

In a more general case, where in a linear combination (4.4.13) factors  $d$  are arbitrary (but still obeying the normalization condition  $\sum_i d_i^* d_i = 1$ ), we should write another expression for  $c_{-1,1}$ , see (4.4.23),

$$c_{-1,1} = D_0 + iD_1 \sin(\lambda t + \chi_1) + iD_2 \sin(\lambda t + \chi_2) + D_3 \cos(2\lambda t + \chi_3) , \quad (4.4.30)$$

where

$$\begin{aligned} D_0 &= -d_0^* d_0 / 2 + (d_1^* d_1 + d_2^* d_2) / 4 , \\ D_1 &= -\sqrt{2} |d_0 d_1^*| / 2 , & \chi_1 &= -\arg\{d_0 d_1^*\} , \\ D_2 &= -\sqrt{2} |d_0 d_2^*| / 2 , & \chi_2 &= \arg\{d_0 d_2^*\} , \\ D_3 &= -|d_1^* d_2| / 2 , & \chi_3 &= -\arg\{d_1^* d_2\} . \end{aligned}$$

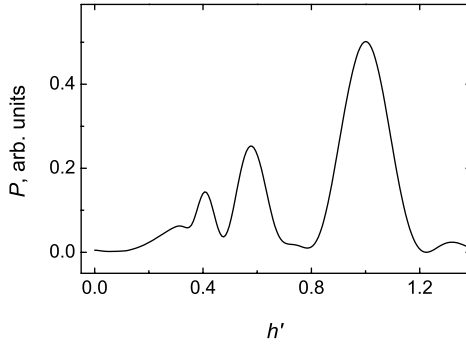


**Figure 4.20.** Amplitude dissociation spectrum in perpendicular MFs. The peak width is determined by parameters  $\Xi = \Omega_c T$ ; calculations are done for  $\text{Ca}^{2+}$  at  $H_{\text{DC}} = 45 \mu\text{T}$ ,  $T = 0.07 \text{ s}$ .

It can be shown that phase shifts  $\chi_i$  are immaterial for the computation of P. As compared with (4.4.24), after substitution of  $c_{-1,1}$  in (4.4.23), we see here a new term  $p_l(\varphi_0, t)$ , which is proportional to

$$\propto \sin(\lambda t) \sin 2(\varphi_0 + \omega_0 t) .$$

As a result, in P there appears an additional term

$$\propto \frac{\sin^2(2\sigma T)}{(2\sigma T)^2} , \quad \sigma = \lambda/2 \pm \omega_0 ,$$

which gives interference peaks at  $\sigma = 0$ . In addition to (4.4.28), we then have an additional relationship for possible effective amplitudes

$$h' = 2\sqrt{\frac{2}{l(l+1)}} .$$

It follows that in the general case the amplitude interference spectrum in a perpendicular MF is a superposition of the spectrum in Fig. 4.20 and of a similar spectrum extended by a factor of 2 along the  $h'$  axis. Therefore, unlike interference in parallel fields, not only the relative height, but also the positions of spectral superposition maxima is dependent on initial conditions for an ion in a capsule. The initial conditions being *a priori* uncertain, one should expect a complicated and poorly reproducible amplitude spectrum within the range  $h' \sim 0.2\text{--}2.2$ .

We note that the amplitude spectra just considered are valid for a circularly polarized or rotated AC MF. For linear polarization, only one circular component is effective; it has an amplitude that is one-half of the amplitude of a linearly polarized field.

- Garcia-Sancho *et al.* (1994) observed a 16% MBE in mutually perpendicular magnetic fields

$$b(141)B_p(41)f(14.5)n(8)C(100 \pm 34.2)MBE(116 \pm 6.7)P(< 0.001) .$$

Here C is a control level, MBE is a level of the effect in an MF, and P is the probability to err by declining the zero hypothesis. The relative amplitude, allowing for effectiveness of one circular component, was  $h' = 1.72$ . The utilized frequency, in a given DC MF, is close to a Larmor frequency of ions of calcium, 15.7 Hz, and sodium, 13.7 Hz. Although a  $^{42}\text{K}$  tracer uptake was observed, it can be assumed that the process was controlled by some Ca-binding protein.

- Blackman *et al.* (1996) measured, by the technique described in Section 2.3, the relative number of nerve cells with neurite outgrowths, which appear after an exposure of a cell culture to a perpendicular MF. The formula of the experiment

$$b(18.7-48.6)B_p(36.6)B(< 0.28)f(45)$$

enabled the interval of the MBE amplitude spectrum to be determined. These data, reduced to the dimensionless variable  $H_{AC}/H_{DC}$ , together with the above-mentioned two components of the theoretical amplitude spectrum, adapted to the case of a linear, as in the experiment, polarization of an MF, are given in Fig. 4.21. Considering that the relative weights of the components are uncertain and that the broadening of spectral peaks is quite probable, we can think of the agreement between theory and experiment as quite satisfactory. The frequency 45 Hz used in experiment is close to the Larmor frequency for lithium ions in a given DC field, 40.5 Hz. Unfortunately, in Blackman *et al.* (1996) no MBE frequency spectrum is available. The interference mechanism predicts a fairly large frequency width of the peak P under these conditions, which could quite easily be established in experiment. The peak form is determined by an envelope (4.4.11),  $(1 + \epsilon^2/4|v|^2)^{-1}$ . It is seen that the peak's half-height width is  $4|v|$  or  $4|\mathcal{F}_{10}|/\hbar$ . Since (4.4.27) gives  $|\mathcal{F}_{10}| = \hbar\omega_0/\sqrt{2}$  at effective amplitudes, then the peak frequency width will be  $\Delta f = \sqrt{2}\Omega_c$  or  $\Delta f' = \sqrt{2}$ .

- Sienkiewicz *et al.* (1998) studied, using a special-purpose technique, the learning of mice when exposed to perpendicular MFs of various intensities by the formula

$$b(0, 7.5, 75, 750, 7500)B_p(40)f(50) .$$

After learning and exposure the mice made mistakes. On each of the successive 10 days the mice were tested for mistakes. This author performed his own analysis of the data. On the first and tenth days after exposure there was no difference between exposed and control mice. For analysis, data were taken from the second to the ninth days, and the respective results were averaged. The measured quantity was the relative level of mistakes  $L$  in % for all experimental lines, both control and after various exposures. The relative number of mistakes  $(L_{\text{contr}} - L_{\text{exp}})/L_{\text{contr}}$  was computed and represented as a function of the AC MF intensity. These data are

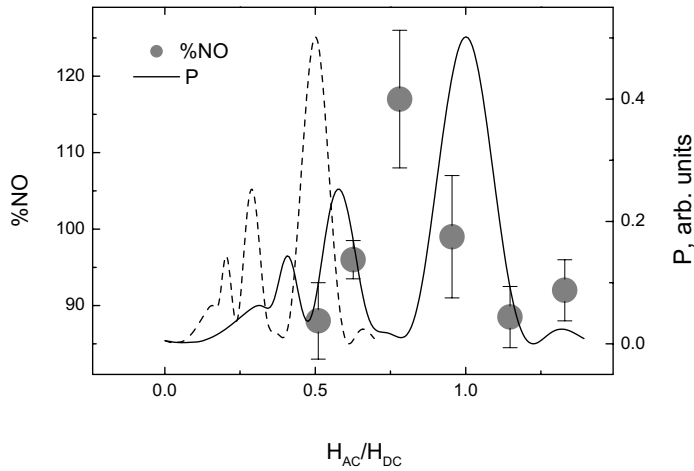


**Figure 4.21.** Components of the amplitude spectrum of ion–protein dissociation and data (Blackman *et al.*, 1996) on MBE in PC–12 cells in mutually perpendicular DC and linearly polarized AC magnetic fields.

given in Fig. 4.22 together with a typical theoretical curve for perpendicular fields. It is seen that in the region of large amplitudes there is a total disagreement, since theory predicts a decline in interference effect. It is quite probably concerned with an input of other mechanisms as well, since even the field intensity of  $750\ \mu\text{T}$  at a given frequency exceeds the assumed limits of safe exposures. We note that the frequency  $f = 50\ \text{Hz}$  in a  $40\text{-}\mu\text{T}$  DC MF is close to the Larmor frequency of  ${}^7\text{Li}$  ions, which is  $43.7\ \text{Hz}$ , and that of  ${}^6\text{Li}$  is  $51\ \text{Hz}$ .

We note one feature: *the relative peak width at interference in perpendicular MFs is relatively large and dependent neither on the type of an ion involved in magnetoreception nor on the constants of its protein binding.*

#### 4.4.2 Interference for tilted field orientations

Tilted orientation of a DC and an AC MF, as stated above, reduces to a simultaneous action of parallel and perpendicular components of a variable field. Two situations are possible.

##### 4.4.2.1 MF frequency is different from the Larmor frequency

An MF with a frequency distinct from  $\omega_0$  can markedly increase the dissociation probability of an ion–protein complex for a parallel orientation, Fig. 4.8. At the same time, with a perpendicular orientation, the MF frequency differs from that of Zeeman transitions ( $\omega_0$ ); therefore, no resonance interference occurs. That means

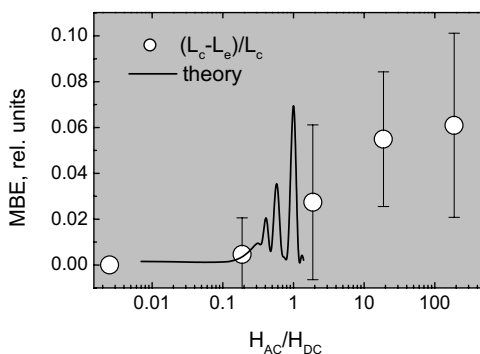


**Figure 4.22.** Adapted experimental evidence (Sienkiewicz *et al.*, 1998) for MBE in mice exposed to perpendicular MFs of various intensity. The line depicts a typical theoretical dependence.

that a response to an MF can only be formed following the mechanism for interference in parallel fields. The availability of a component of an MF perpendicular to a DC field does not influence the formation of a response to parallel components. It is important that this conclusion, allowing for a large resonance width, holds well where the separation of an excitation frequency from the Larmor frequency is fairly large,  $\sim \Omega_c$ . Otherwise, we have a situation close to the following one.

#### 4.4.2.2 MF frequency equals a magnetic resonance frequency

In this case, there occur transitions that change populations of quantum states. The formation of responses is not an independent process. It would be logical to expect, by virtue of the structure of dynamic equations with coefficients of the type (4.4.2), that a simultaneous action of parallel and perpendicular components would disturb the specific conditions of interference according to each mechanism. As a result, the probability of magneto-sensitive dissociation will not grow, even if the variables of the parallel or perpendicular components of an AC MF correspond to the conditions for response maxima found above.

That general statement does not exclude the possibility of burst interference for some unique combinations of fields, frequencies, and angles. It is hardly expedient, however, to perform their calculations and experimental tests, since that would not improve our knowledge of the phenomenon. Strictly parallel or perpendicular combinations of fields would be self-sufficient from the point of view of studies of interference effects concerned with dissociation.

## 4.5 ROTATION OF AN ION-PROTEIN COMPLEX IN A MAGNETIC FIELD

Many biochemical reactions occur not on the surface of cell membranes and structures that are related with them, but in the cytoplasm, or they are attached to

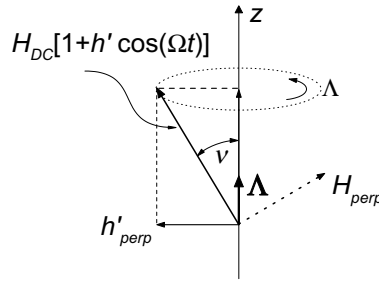


**Figure 4.23.** Components of a uniaxial MF in a rotating coordinate system.

organelles gyrating in the process of their vital activity. For instance, the hairs of the flagella motor of some cells of *E. coli* rotate at about 300 rps, and so the bacterium body rotates in the opposite direction at a frequency of several rounds per second. Also rotating in the process are ATPase enzyme, some enzymes attached to DNA-RNA in the process of nucleosynthesis, etc.; appropriate references are available in Binhi *et al.* (2001). In that case, as proposed in Binhi (1997d), it is advantageous to take into account rotations of macromolecules containing binding cavities, both individual molecular rotations and macroscopic rotations together with a biological system.

#### 4.5.1 Molecular rotation in AC-DC MF: Amplitude spectrum

Let an ion be connected with a protein gyrating with angular velocity  $\Lambda$ . In the general case, the gyration direction does not coincide with that of an MF. We orient the  $z$  axis along the gyration axis and pass over to a reference frame rotating with the protein, Fig. 4.23.

In that coordinate system, a DC MF is  $H_{DC} \cos \nu$ , and an AC MF that is uniaxial to it reduces to  $H_{AC} \cos \nu \cos(\Omega t)$ , so that the relative amplitude  $h'$  retains its previous value irrespective of the angle  $\nu$  between the direction of gyration and the MF. This implies that only a cyclotron frequency will change with an angle  $\nu$ ,  $\Omega_c = qH_{DC} \cos \nu / Mc$ , so that some MF frequency  $\Omega$ , effective in the case of  $\nu = 0$ , becomes ineffective with increasing  $\nu$ .

Estimates of the range of  $\nu$ , within which a given frequency  $\Omega$  is still effective, are based on the relationship for the relative peak width P:  $\Delta f' = \pi/n\Xi$ , see (4.1.27). A relative decrease in cyclotron frequency because of the misalignment of the axes must be less than a peak half-width:

$$1 - \cos \nu < \pi/2n\Xi .$$

This defines the limiting angle  $\nu \approx 23^\circ$  for a Ca-protein complex ( $\Xi \approx 20$  at  $H_{DC} = 40 \mu\text{T}$ ). From that we can readily find that the relative number of arbitrarily gyrating ion-protein molecules, which could form a given spectral peak in the

response, is equal to  $1 - \cos \nu$ . That number is about 5-10%, and it grows with decreasing  $H_{DC}$ .

In a gyrating reference frame, there emerges a perpendicular rotating MF component. This component causes resonance transitions in a wide,  $\sim \Omega_c$ , frequency range with the center at a Larmor frequency, provided the relative amplitude components  $h'_{\text{perp}}$  are about unity, see Section 4.4.

Such transitions destroy constructive interference that yields pronounced peaks P, or rather under such conditions it does not occur. Therefore, only those molecules that rotate about the MF axis respond when exposed to an MF. The relative number of potentially responding molecules must also be estimated from that relationship. It appears to be stronger. At amplitude  $h'_{\text{perp}} \approx 0.1$ , the response to a perpendicular AC MF becomes much narrower in frequency and causes no effects, except for the relatively rare situation where the angular velocity  $\Lambda_k$  equals a Larmor frequency. It follows from Fig. 4.23 that the quantity  $h'_{\text{perp}} \sim 0.1$  defines  $\nu \approx 6^\circ$  and a smaller, but still significant, number  $\sim 1\%$  of responding ion-protein molecules.

If there is an additional DC MF  $H_{\text{perp}}$  perpendicular to the initial field,  $H_{DC}(1+h' \cos \Omega t)$ , there are also changes in the rotating coordinate system. The MF  $H_{\text{perp}} \cos \nu$  is added to  $h'_{\text{perp}}$ , obviously without any consequences. The small quantity  $H_{\text{perp}} \sin \nu$  is added to the uniaxial field:  $H_{DC} \cos \nu(1 + h' \cos \Omega t) + H_{\text{perp}} \sin \nu$ , thus defining the effective cyclotron frequency  $\tilde{\Omega}_c$ , which is equal to

$$\tilde{\Omega}_c = \Omega_c \left( \cos \nu + \frac{H_{\text{perp}}}{H_{DC}} \sin \nu \right).$$

It follows that a perpendicular component in a fixed coordinate system,  $H_{\text{perp}}$ , can exceed the DC component of a uniaxial MF several fold without marked changes in the position, and hence in the magnitude, of the effect in rotating complexes. That phenomenon is absolutely out of the question for stationary complexes, since they do not possess a “tool”, like the rotation axis, in order to register the difference between MF components. Fixed complexes respond to the magnitude of the static MF  $(H_{DC}^2 + H_{\text{perp}}^2)^{1/2}$ , and not to its components.

A special-purpose experimental study (Belyaev *et al.*, 1994) of a narrow spectral MBE peak on a *E. coli* cell culture in a combined MF  $H(43.6)H_p(0; 147)h(30)f(9)$ , in the presence of a variable perpendicular component 0–147  $\mu\text{T}$ , revealed no changes. Apparently, rotating ion-protein complexes are involved in magnetoreception under given conditions.

In general, frequency spectral peaks broaden asymmetrically (red shift) because molecular rotation axes are oriented randomly. However, we will not complicate formulas by averaging over the angle  $\nu$ , since that would not lead to qualitatively new effects. Making account of the more or less significant part of arbitrarily rotating molecules that contribute to P-response at a given effective frequency, we will consider the case of  $\nu = 0$ , i.e., of molecules rotating about the same axis as the MF.

In that case, the coordinates of the initial reference frame  $r, \theta, \varphi$  and those of the rotating system  $r', \theta', \varphi'$  are connected by a simple relationship:  $r = r'$ ,

$\theta = \theta'$ ,  $\varphi = \varphi' + \Lambda t$ . That transformation does not change the operators that enter into the Hamiltonian (4.1.1), since derivatives with respect to the polar angle are equal in both systems:  $\partial/\partial\varphi = \partial/\partial\varphi'$ . Therefore, all the relations, except for those containing  $\varphi$ , remain valid in a rotating system as well. A transition in a rotating system thus occurs simply through a substitution of  $\varphi + \Lambda t$  for  $\varphi$ .

This suggests that the angular coordinate of the gate of a protein that rotates with an angular velocity belonging to the discrete series  $\Lambda_k$  will be

$$\varphi_0 + \Lambda_k t .$$

Clearly, the probability density for an ion in a rotating protein can be obtained from (4.1.8) by a substitution of  $\omega_0 \rightarrow \omega_0 + \Lambda_k$ . Therefore, the dissociation probability is derived from (4.1.23) by that substitution

$$P = \sum_{mm'nk} |a_{mm'}|^2 |c_k|^2 \frac{\sin^2 A}{A^2} J_n^2 \left( \frac{\Delta m}{2} \frac{h'}{f'} \right) , \quad (4.5.1)$$

$$A = \left[ \Delta m \left( \frac{\omega_0 + \Lambda_k}{\Omega_c} \right) + n f' \right] \Xi ,$$

where  $|c_k|^2$  are statistical weights of rotating states. The case of different ion-protein complexes with quantized rotations in a DC MF is considered by Binhi *et al.* (2001).

In order to show changes in the amplitude spectrum  $P$  in a uniaxial MF it is sufficient to consider them for any one velocity  $\Lambda$ . Locations of frequency spectral peaks  $P$  are given by equation  $A = 0$ , which leads to the relationships

$$f'_{\max} = -\Delta m(1 + 2\Lambda')/2n ,$$

where  $\Lambda' = \Lambda/\Omega_c$  is the relative velocity of molecular rotation. It is important that relative frequencies of maxima  $P$  are dependent on angular velocities.

The main contribution to sum (4.5.1), up to 80–90%, comes from terms with  $n = \pm 1$ . By virtue of  $J_1^2(x) = J_{-1}^2(x)$ , the case taken for our analysis is of no consequence, and so we will take  $n = 1$ . Correspondingly, the input will be maximal at

$$f'_{\max} = -\Delta m(1 + 2\Lambda')/2 , \quad (4.5.2)$$

and any of these terms has the form

$$J_1^2 \left( \frac{h'}{1 + 2\Lambda'} \right) , \quad (4.5.3)$$

which follows from Eq. (4.5.1). We will now identify the conditions under which an amplitude spectrum has a functional motif  $J_1^2(\alpha h')$ , where  $\alpha$  is some factor (not to be confused with  $\alpha$  in (4.1.10)). That makes sense, since experimental spectra that can be approximated by function  $J_1^2(2h')$  are known. The value  $\alpha = -2$  is also suitable, by  $J_1^2(-x) = J_1^2(x)$ . From (4.5.2) and (4.5.3), we can easily find that  $\alpha$  is

related to, or defines, the relative frequency of complex rotation and the frequency of an MF, at which the amplitude spectrum will have the specified shape  $J_1^2(\alpha h')$ :

$$\Lambda' = - (1 \mp \alpha^{-1}) / 2, \quad f' = \Omega' = \mp \Delta m / 2\alpha. \quad (4.5.4)$$

In the general case, the shape of an amplitude spectrum of a rotating complex is controlled by the type of a bound ion, and so the coefficient in the argument of the Bessel function can take on various values. Thus, the first maximum in the response can occur even at values of  $h'$  lower than 1.8. It is seen that locations of spectral MF amplitude peaks vary widely depending on the complex's rotation speed.

In the special case where the natural angular velocity of a complex corresponds to an ion's parameters and the DC field, and the field frequency is  $f' = \frac{1}{2}$ , i.e.,

$$\Lambda' = -\frac{1}{2} \pm \frac{1}{4}, \quad f' = 1 + 2\Lambda' = \pm \frac{1}{2}, \quad (4.5.5)$$

then the amplitude spectrum has the specified shape  $J_1^2(2h')$ , with a maximum at  $h' \approx 0.9$ . It is interesting that magnetic conditions used in Blackman *et al.* (1994, 1995b), where such a spectrum was observed, meet these rules nearly completely, if we assume that lithium- or magnesium-protein rotating complexes are involved in magnetoreception. A detailed analysis of the agreement between experimental data and theoretical predictions for rotating complexes is given in Section 4.9, see also a work by Binhi (2000).

Note that the specified amplitude spectrum is no consequence of a shift of peaks of the conventional spectrum  $J_n^2(h')$  to lower amplitudes at molecular rotation. That spectrum vanishes gradually as a whole on deviations of the angular velocity or frequency MF from their optimal values.

It is of interest that Eqs. (4.5.4) predict conditions for a system to be sensitive to a hyperweak MF. For sufficiently large values of  $\alpha \gg 1$  the first maximum of the response emerges in a variable field with amplitude  $\sim H_{DC}/\alpha$ . By (4.5.4), the frequency of a field also must be small,  $f \sim f_c/\alpha$ , and a DC MF must be selected so that the Larmor frequency would coincide with the natural frequency of rotation of a complex. That corresponds precisely to the realization of magnetic vacuum conditions for rotating complexes. A sensitivity-limiting factor here is the lifetime of angular modes of quantum states  $\tau_L$ : the workability of a mechanism is limited from below by MF frequencies of about  $1/\tau_L$ .

There is some experimental evidence for biological sensitivity to hyperweak MFs, but unfortunately no amplitude spectra have been measured, whereby no comparative analysis is possible. Also unknown from experiments not concerned with magnetobiology are long-lived,  $> 10$  s, quantum states at room temperature. We note that states of an ion in a protein cavity, whose lifetime in this book is postulated to be no shorter than 0.1s, are hypothetical. Their nature is also unknown, but their introduction is justified by a high level of agreement between calculated and experimental data. It is thus important that molecular constructions like a gyroscope, see Section 5.4, could ensure lifetimes required for hyperweak MFs to be registered.

#### 4.5.2 Macroscopic rotation in a uniaxial MF: Spectral shifts

Rotation of ion-protein complexes, which changes frequency locations of spectral peaks in accordance with (4.5.2), can also be viewed as a macroscopic rotation. The latter implies rotation together with the entire biological system of a sample placed, for instance, on a rotating platform. The notation  $\Theta$  is used for the angular velocity of macroscopic rotation; the notation  $\Lambda$  is retained for microscopic molecular rotation. Macroscopic rotation at an arbitrarily large angle to the direction of a uniaxial MF will destroy constructive interference for the same reasons as in the case of molecular rotations. Therefore, we assume as before that the macroscopic rotation is coaxial with MF. In this section, without loss of generality, we also assume that there are no molecular rotations, i.e.,  $\Lambda = 0$ ,

$$f'_{\max} = -\Delta m(1 + 2\Theta')/2n ,$$

where  $\Theta' = \Theta/\Omega_c$ . At a given  $\Theta'$ , a peak shift is  $\Delta m\Theta'/n$ . A shift will be resolved, if its magnitude is larger than the peak half-width. The argument in the factor  $\sin^2 A/A^2$  in (4.5.1), i.e.,

$$A = \left[ \Delta m \left( \frac{1}{2} + \Theta' \right) + nf' \right] \Xi ,$$

defines peak widths. Considering that  $A \sim \pi$  corresponds to the width of function  $\sin^2 A/A^2$  at its half-height and using the relationship  $\Delta f' \partial A / \partial f' \sim \pi$ , we can find the peak width  $\Delta f' \sim \pi/n\Xi$  (4.1.27). Therefore, for a shift to be resolved the inequality  $\Delta m\Theta' > \pi/2\Xi$  must be satisfied. The most pronounced peak comes from interference quantum angular modes with a difference of magnetic quantum numbers  $\Delta m = 2$ , and in any case it is  $\Delta m \geq 1$ . We then get a simple relation that defines the minimal velocity of macroscopic rotation for observation of a shift of spectral peaks:  $\Theta' > \pi/2\Xi$ . For magnitudes, the relation becomes

$$\Theta > \pi/2T . \quad (4.5.6)$$

As stated above, good agreement of experimental and computed frequency spectra for calcium and magnesium ions occurs at  $T = 0.05-0.1$  s. A shift will then be guaranteed if the rotation speed  $\Theta/2\pi$  is only 1.5-2 rps or higher. Figure 4.24 demonstrates the results of computations of  $\mathbf{P}$  with an angular velocity of  $\Theta = 0.1\Omega_s$ . Where the peaks will shift, to higher or lower frequencies, is dictated by the direction of rotation in relation to an MF.

*The effect of the shift of MBE spectral extrema as a biosystem rotates* is one of the essential and testable predictions of the interference mechanism for bound ions (Binhi, 1997d).

#### 4.5.3 A decline in the magnetic vacuum effect

Let an ion-protein complex be in a state with a discrete series of molecular rotations  $\Lambda_k = k\Lambda$ . That enables us to describe both the quantum top (gyroscope) and

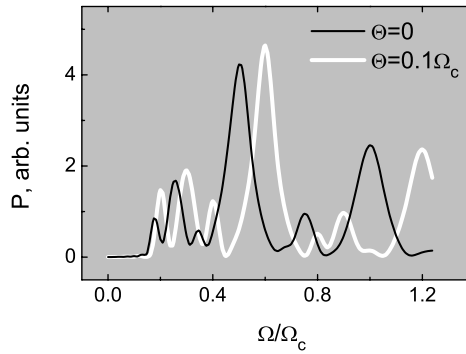


**Figure 4.24.** A shift of frequency maxima of dissociation probability  $P$  when an ion–protein complex rotates in a uniaxial MF with an angular frequency of  $\Theta' = 0.1$ .

the classical rotator in the following situation. Various molecules of an ion–protein complex can be fastened both to relatively fixed ( $k = 0$ ) carriers of biological membrane type, and to rotating DNA-type ones. Then the sign of an angular velocity component along the MF direction defines the value of  $k = \pm 1$ . Provided that  $H_{AC} = 0$ , all the Bessel functions, save for  $J_0(0) = 1$ , fall out of the sum (4.5.1). We end up with the only value of  $n = 0$  in (4.5.1). The formula of dissociation in a DC MF then becomes

$$P = \sum_{mm'} |a_{mm'}|^2 |c_k|^2 \frac{\sin^2 A}{A^2}, \quad A = \Delta m (\omega_0 + \Lambda_k + \Theta) T. \quad (4.5.7)$$

We note that the factor  $\sin^2 A/A^2$  now defines the dependence of  $P$  on the MF magnitude, rather than on the field frequency. The formula predicts the maximal effect at  $A = 0$ , or at  $\omega_0 = -\Lambda_k - \Theta$ , which gives an expression for DC MFs that provide the maximal dissociation probability,

$$(H_{DC})_{\max} = -\frac{1}{b}(k\Lambda + \Theta), \quad (4.5.8)$$

where  $b = q/2Mc$  varies with the ion charge-to-mass ratio. For ion–proteins, which do not rotate in themselves ( $k = 0$ ), there is the only maximum  $P$  at field strength  $H_{DC} = -\Theta/b$ . If also there is no macroscopic rotation, then the given peak will appear at  $H_{DC} = 0$ , which is associated with the so-called biological effect of a magnetic vacuum. In addition to that maximum, additional peaks may appear due to the rotation of the complex in accordance with (4.5.8). Such extrema are considered in a work by Binhi *et al.* (2001) in relation to the multippeak dependence of an MBE on a DC MF in *E. coli* cells in the range of 0–110  $\mu\text{T}$  (Belyaev *et al.*, 1994).

Here we study fixed complexes, for which  $k = 0$ . If a DC MF is sufficiently small, all the ion types that could interfere in a constructive way under other conditions,

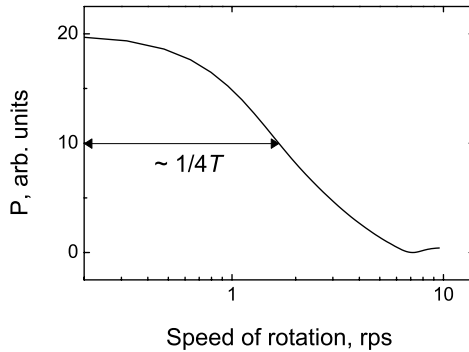


**Figure 4.25.** Decline in the magnetic vacuum effect with the rotation speed for a Ca-protein complex, formula (4.5.7),  $k = 0$ .

which are specific for each type of ion, display such an interference simultaneously. That is one of the possible reasons for biological effects of a magnetic vacuum, because a maximum  $P$  at  $H_{DC} = 0$  is independent of ion variables.

Observation of complicated dependences of an MBE in an MF is often conditioned by a lucky concurrence of circumstances: one has to guess the type of ions involved in magnetoreception and select agreed MF parameters. In contrast, biological effects of a magnetic vacuum were observed for many biological systems, see, for instance, (Dubrov, 1978; Chew and Brown, 1989; Kato *et al.*, 1989; Kashulin and Pershakov, 1995; Lednev *et al.*, 1996b; Belyaev *et al.*, 1997). This is circumstantial evidence for the involvement of many types of ions in the magnetic vacuum effect.

Moreover, rotation in a zero MF acts on all ions of these types, and not only on ions of the above 1% of rotating complexes, because there is no specified MF direction. Obviously, the effect must then be especially significant. Macroscopic rotation in a magnetic vacuum is a common method for testing predictions of MBE interference mechanisms. In a weak MF, the location of a peak connected with a fixed complex is given by

$$(H_{DC})_{\max} = -\Theta/b . \quad (4.5.9)$$

The location is dependent on the angular velocity. It is easily seen that a shift will be resolved under the same condition (4.5.6). That is, for calcium- and magnesium-protein complexes 1.5–2 rps. *The effect of MBE extrema shift in a DC MF for a rotating biosystem* implies a decline in the effect at  $H_{DC} = 0$ , Fig. 4.25.

In the absence of an MF,  $P$  is determined by the argument  $A = \Delta m \Theta T$ . When there is no rotation, the argument is  $A = \Delta m \omega_0 T$ . It follows that equal effects occur at  $\omega_0 = \Theta$  or

$$H_{DC} = \Theta/b .$$

The last relationship is close in shape to (4.5.9), but it has another physical meaning. *A DC MF and macroscopic rotation have identical actions on fixed ion-protein complexes*, where they act individually. This can be established in relation to the control level of an effect common for both variables, i.e., to the effect at  $H_{DC} = 0$ ,  $\Theta = 0$ .

It follows that amplitude dissociation spectra of ion-protein complexes with their own molecular rotation differ from spectra for relatively fixed complexes. They are close in shape to  $J_1^2(\alpha h')$ , where coefficient  $\alpha$  is determined by rotation speed.

It is possible that in living organisms we have a wide variety of conditions for the functioning of metalloproteins including their rotating states. The first extremum was observed by Blackman *et al.* (1994) in the amplitude spectrum at  $h' \approx 0.9$ , and not at  $h' \approx 1.8$ , as is predicted by a model for fixed molecules. That caused a discussion (Liboff *et al.*, 1995), where the authors made assumptions as to mistakes and artifacts in their opponents' works. We note that differing amplitude spectra were obtained on different biological models; therefore, it is good thinking to suppose that in Blackman *et al.* (1994) they measured an MBE connected with dissociation of rotating complexes. The amplitude spectrum in Prato *et al.* (1995) also has a clearcut first maximum at  $h' \approx 0.5$ , Fig. 4.39. The first maximum at frequency  $\Omega_c$  of the  $H^+$  ion was observed (Trillo *et al.*, 1996) for  $h' \approx 0.6-0.7$ , and in Lednev *et al.* (1997), at  $h' \approx 1.4$ . In Blackman *et al.* (1999) an amplitude spectrum (Trillo *et al.*, 1996) was confirmed, see Fig. 2.24 and Fig. 2.25. Groups of proton-binding sites seem to be located at macromolecules that possess a natural rotation or a forced rotation, as is the case with DNA-RNA synthesis processes. Then amplitude spectra (Trillo *et al.*, 1996; Blackman *et al.*, 1999) can be approximated by functions of ion interference, see Section 4.9.

A component of a DC field perpendicular to an AC MF, for tilted fields, does not influence the location and magnitude of frequency maxima  $P$  on rotating complexes. That agrees with observations (McLeod *et al.*, 1987a; Belyaev *et al.*, 1994). At the same time, fixed complexes are sensitive to the magnitude of a DC MF, and hence to each of its components.

Experimental spectra are often so complicated that explaining them is difficult without a purposeful test of predictions in terms of a model of some specific MBE mechanism. An experiment with biological samples stationed on a slowly rotating platform exposed to a DC or uniaxial AC MF can support or disprove theoretical predictions. Rotation in a uniaxial MF predicts a frequency shift of MBE. Rotation in a DC field predicts a drop in the magnetic vacuum effect, irrespective of the type of ions involved in magnetoreception, or a shift of MBE peaks with the field magnitude, if complexes also exhibit their own molecular rotation. The rotation of biological samples in itself, because of centripetal accelerations, is able to cause a biological reaction, and therefore requires special control.

Underpinning the predictions of the ion interference mechanism for rotating complexes are two assumptions: (1) a sufficiently large lifetime  $> T$  of ion quantum states, or rather only of angular modes of those states, and (2) the presence of

preferred locations in a binding cavity, such that the exit of an ion is a non-linear function of ion probability density. In order for interference effects to be observed, at least these assumptions must work and they must work simultaneously. Therefore, it is unlikely that such predictions could be obtained within the framework of some other theory. This implies that if there were tests and confirmations of the equivalence of a static MF and a macroscopic rotation in relation to a system placed initially in a magnetic vacuum, that would be direct proof of the involvement of ions in magnetoreception. That is important, since such a proof would identify the domain of search for possible solutions of the “kT problem”. Now we would search for an answer to the question of why a model of long-lived states described by eigenfunctions of a central potential gives such a good approximation to true ion states in a binding cavity perturbed by thermal fluctuations. That question, unlike that of the “kT problem”, has no signs of being a paradox.

## 4.6 INFLUENCE OF AN ELECTRIC FIELD ON INTERFERENCE OF IONS

Low-frequency electric fields (EFs), like low-frequency MFs, cause no noticeable redistribution of populations due to transitions changing radial or azimuthal quantum numbers. Respective transition frequencies are about 10 orders of magnitude higher than the frequency range under consideration. It follows that, as in the previous section, it makes sense to consider processes in terms of individual Zeeman multiplets.

As stated in Section 1.4.3, relatively weak electric fields,  $\sim 10\text{--}100\text{ V/m}$ , are able, due to the quadratic Stark effect, to change markedly the energies of levels. The changes have the same order of magnitude as the Zeeman splitting. Clearly, that cannot influence interference effects in a uniaxial MF, but it can destroy resonance interference in perpendicular fields, since it changes the frequency of transitions.

### 4.6.1 Interference of ions in a variable electric field

The fact is that an inhomogeneous AC EF causes both phase shifts and transitions in Zeeman sublevels, producing under some conditions an interference effect.

Among all the indices  $i$  that number wave functions of the central potential  $\psi_i$ ,  $i = \{klm\}$  we will identify a group  $p$ , concerned with functions of some degenerate level with an  $\varepsilon_p$ , and a group  $q$  of indices of all the remaining functions. In a homogeneous EF, degeneration is partly removed, and wave functions for each sublevel of group  $p$  can be written as (Alexandrov *et al.*, 1991)

$$\psi_p'' = \psi_p + \sum_q \frac{\mathcal{V}_{qp}}{\varepsilon_p - \varepsilon_q} \psi_q .$$

Since indices  $p, q$  are different at least in one index of their radial and azimuthal numbers, correction to wave functions are very small, about  $\mathcal{V}_{qp}/(\varepsilon_p - \varepsilon_q) \ll 1$ . Clearly, interference effects, which depend on the electric field, will have the same

order of smallness, and so they are of no interest. Another situation occurs in an inhomogeneous EF.

We now work out the matrix elements of the operator of interaction of an electric field  $\mathbf{E}$  with the dipole moment of a particle  $\mathbf{d} = q\mathbf{r}$

$$\mathcal{V} = -q\mathbf{r}\mathbf{E} .$$

We note at once that all the states of an individual Zeeman multiplet have the same parity  $(-1)^l$ ; i.e., they either change or do not change the sign upon a coordinate inversion. In a homogeneous EF the matrix elements of operator  $\mathcal{V}$  are proportional to the matrix elements of vector  $\mathbf{r}$  in states with like parity and are therefore equal to 0 (Landau and Lifshitz, 1977). Non-zero elements may emerge either due to interactions with a quadrupole moment or in a inhomogeneous EF. In the latter case, a field can be represented by a Taylor series near point  $\mathbf{r} = 0$

$$\mathbf{E}(\mathbf{r}) = \mathbf{E}(0) + (\mathbf{r}\nabla)\mathbf{E}(0) + \dots$$

The part of  $\mathcal{V}$  that creates a non-zero contribution to the matrix elements is

$$\mathcal{V} \approx -q\mathbf{r}(\mathbf{r}\nabla)\mathbf{E}(0) = -q \sum_{ik} x_i x_k \frac{\partial}{\partial x_i} E_k , \quad (4.6.1)$$

where  $x_i$  are Cartesian coordinates. Each component of that quantity is a true scalar. Operator  $\mathcal{V}$  is also a scalar; therefore its matrix elements in the states of a Zeeman multiplet are, generally speaking, non-zero. Consider effects concerned with the presence of components  $(E_z)'_z$  of the tensor  $\partial E_k / \partial x_i$ . As will become clear later in the book, it is this component that brings about dissociation-type effects in a parallel MF, i.e., effects concerned with phase modulation of angular modes. We will not consider other components: they lead to resonance transitions in a multiplet only at a Larmor frequency, and so they are of less general nature.

Recall that Cartesian coordinates in a spherical coordinate system are

$$x = r \sin \theta \cos \varphi , \quad y = r \sin \theta \sin \varphi , \quad z = r \cos \theta .$$

In the first case, the component  $\mathcal{V}$ , which is proportional to  $z^2$ , does not affect the variable  $\varphi$ . Its matrix in states of a Zeeman multiplet is diagonal, since only transitions with a conservation of magnetic quantum numbers are allowed. Let the  $z$  component of the gradient of field  $E_z$ , which for convenience will be denoted as  $E'$ , oscillate in time. Then

$$\mathcal{V} = V \cos \Omega t , \quad V = -qE'z^2 = -qE'r^2 \cos^2 \theta .$$

We can immediately write an equation for the coefficients of the sought wave function of an ion in a DC MF and in a variable gradient electric field, which is coaxial

with the former. In the symbols of (4.4.3), using for the Zeeman Hamiltonian the expression  $\mathcal{H}_Z = -m\hbar\omega_0$ , we find

$$i\hbar\dot{c}_m = c_m (V_{mm} + \mathcal{H}_{Zmm}) ;$$

hence the solution is

$$c_m = a_m \exp \left( i\omega_0 m t - i\nu_m \frac{1}{\Omega} \sin \Omega t \right) , \quad \nu_m = V_{mm}/\hbar .$$

Here  $a_m = c_m(0)$ , and indices  $k, l$  are omitted for short. Therefore, the wave function has the form, see (4.4.1),

$$\Psi_{klm} = \sum_{klm} a_{klm} R_{kl} Y_{lm} \exp \left( im\varphi - \frac{i}{\hbar} \varepsilon_{kl} t + i\omega_0 m t - i\nu_m \frac{1}{\Omega} \sin \Omega t \right) .$$

The probability density for an ion near a gate is, see (4.1.6),

$$p(\varphi_0, t) = \sum_{mm'} a_{mm'} \exp \left[ i\Delta m \left( \varphi_0 + \omega_0 t + \frac{\omega_1}{\Omega} \sin(\Omega t) \right) \right] ,$$

$$\omega_1 = \frac{\nu_m - \nu_{m'}}{\Delta m} , \quad (4.6.2)$$

where  $\Delta m = m' - m$ . That expression is basically the equality (4.1.8) for density in a parallel MF with the following refinement. In (4.6.2), the frequency  $\omega_1$  has another meaning, one concerned with the amplitude of changes in the EF-magnitude gradient. Therefore, the formula for dissociation probability is here identical with (4.1.19). What remains is to substitute the new value of  $\omega_1$  into (4.1.10). It is seen from (4.1.10) that undergoing changes in the dissociation probability formula is only the argument of the Bessel functions  $z = \Delta m \omega_1 / \Omega = (\nu_m - \nu_{m'}) / \Omega$ , which defines the amplitude spectrum. It follows that the frequency dissociation spectrum is still determined by the ion cyclotron frequency, its harmonics, and their subharmonics. The relative weights of spectral maxima are related with factors  $a_{mm'}$  via the initial conditions for an ion in a capsule.

We will also provide formulas that pertain to the case where, in addition to a variable component, the EF gradient also has a DC component. Then

$$V = V(1 + \gamma \cos \Omega t) , \quad V = -qE'z^2 = -qE'r^2 \cos^2 \theta ,$$

where  $\gamma$  is the relative amplitude of  $E'$  changes. The solution of the equation for coefficients

$$c_m = a_m \exp \left( i\omega_0 m t - i\nu_m t - i\nu_m \frac{\gamma}{\Omega} \sin \Omega t \right) , \quad \nu_m = V_{mm}/\hbar ,$$

gives the wave function

$$\Psi_{klm} = \sum_{klm} a_{klm} R_{kl} Y_{lm} \exp \left( im\varphi - \frac{i}{\hbar} \varepsilon_{kl} t + i\omega_0 m t - i\nu_m t - i\nu_m \frac{\gamma}{\Omega} \sin \Omega t \right) .$$

The probability density for an ion

$$p(\varphi_0, t) = \sum_{mm'} a_{mm'} \exp \left[ i\Delta m \left( \varphi_0 + \omega_2 t + \frac{\omega_1}{\Omega} \sin(\Omega t) \right) \right],$$

$$\omega_2 = \omega_0 + \frac{\nu_m - \nu_{m'}}{\Delta m}, \quad \omega_1 = \gamma \frac{\nu_m - \nu_{m'}}{\Delta m}, \quad (4.6.3)$$

is again the equality (4.1.8) for density in a parallel MFs with the following refinement. In (4.6.3), the frequency  $\omega_1$  has another meaning. Again, instead of  $\omega_0$  we have  $\omega_2$ . Therefore, the formula for dissociation probability will again be identical to (4.1.19), provided that we substitute values of  $\omega_1$  and  $\omega_2$  into (4.1.10). Hence we can easily find, by omitting computations, that relatively small constant gradients, i.e., for  $\gamma > 1$ , cause a shift in peak positions on the frequency spectrum. These constant gradients being unpredictable, they need to be averaged, thus leading to a broadening of calculated spectral maxima. We again return for convenience to the case of purely AC EF gradients.

We study an amplitude dissociation spectrum in a gradient EF magnitude field. We find quantities  $\nu_m$  in the argument  $z$ :

$$\nu_m = \frac{1}{\hbar} V_{mm} = \frac{-qE'_z}{\hbar} \langle R_{kl}(r) | r^2 | R_{kl} \rangle_r \langle Y_{lm}(\theta, \varphi) | \cos^2 \theta | Y_{lm} \rangle_{\theta, \varphi}. \quad (4.6.4)$$

The integral  $\rho = \langle R_{kl} | r^2 | R_{kl} \rangle_r$  depends on the specific shape of a central potential. Since it is unknown, we can only estimate it. The radial functions of a particle in a "box" of radius  $R$  are normalized by the condition

$$\int_0^R |R(r)|^2 r^2 dr = 1.$$

Marginal values of  $\rho$  occur where the wave function is mainly concentrated around the center, or, in contrast, near a surface of radius  $R$ . Their estimates are 0 and  $R^2$ , respectively. We will take  $\rho = R^2/2$ .

Taking the integral  $y_{lm} = \langle Y_{lm} | \cos^2 \theta | Y_{lm} \rangle_{\theta, \varphi}$  reduces to applying the recurrent relation (Korn and Korn, 1961), which holds for  $|m| < l$ ,

$$\cos \theta Y_{lm} = Y_{l+1, m} \sqrt{\frac{(l-m+1)(l+m+1)}{(2l+3)(2l+1)}} + Y_{l-1, m} \sqrt{\frac{(l+m)(l-m)}{(2l-1)(2l+1)}}.$$

The spherical functions being orthonormal, we find

$$y_{lm} = 2 \sqrt{\frac{(l-m)(l+m)(l-m+1)(l+m+1)}{(2l-1)(2l+1)(2l+3)(2l+1)}}.$$

We will separately consider the case of  $l = m$ . The spherical functions, defined by (4.4.17) and (4.4.18), contain associated Legendre functions  $P_l^m$ , which at  $m = l$  are equal to

$$P_l^l(x) = (2l - 1)! (1 - x^2)^{l/2}, \quad x = \cos \theta.$$

Here the modified factorial  $!$  means omission of even terms in an appropriate product. We then find  $Y_{ll}$  and

$$y_{ll} = \frac{(2l + 1)[(2l - 1)!]^2}{2(2l)!} \int_{-1}^1 (1 - x^2)^l x^2 dx.$$

The value of the last integral is given in Dwight (1961):

$$\text{Int} = \Gamma(l + 1)\Gamma\left(\frac{3}{2}\right) / \Gamma\left(l + \frac{5}{2}\right).$$

Using the properties of the gamma-function

$$\Gamma(l + 1) = l!, \quad \Gamma\left(\frac{3}{2}\right) = \sqrt{\pi}/2, \quad \Gamma\left(n + \frac{1}{2}\right) = \frac{(2n - 1)!}{2^{n-1}(n - 1)!} \sqrt{\pi}/2,$$

we get  $y_{ll} = 1/(2l + 3)$ . With Kronecker symbols, the general expression for numbers  $y_{lm}$  assumes the form

$$\begin{aligned} y_{lm} &= \langle Y_{lm} | \cos^2 \theta | Y_{lm} \rangle_{\theta, \varphi} \\ &= \frac{1}{2l + 3} \delta_{lm} + 2 \sqrt{\frac{(l - m)(l + m)(l - m + 1)(l + m + 1)}{(2l - 1)(2l + 1)(2l + 3)(2l + 1)}} (1 - \delta_{lm}). \end{aligned}$$

It can be shown that the asymptotic behavior of that function at  $l \rightarrow \infty$  is

$$y_{lm} = [1 - (m/l)^2] / 2. \tag{4.6.5}$$

For small  $l$ , beginning with unity, the error of that formula for differences is 10-15 %, which is quite sufficient for our estimates. The difference of  $y_{lm}$  for various values of  $m$ , which we are going to need now, will, obviously, be

$$y_{lm} - y_{lm'} = \frac{m'^2 - m^2}{2l^2}.$$

Returning to (4.6.4), we write it as

$$\nu_m = \frac{-qE'\rho}{\hbar} y_{lm},$$

and the argument of the Bessel functions becomes

$$z = (\nu_m - \nu_{m'}) / \Omega = \frac{m^2 - m'^2}{2l^2} \frac{qE'\rho}{\hbar\Omega}. \tag{4.6.6}$$

Unlike the case of a parallel MF, the argument contains a difference of squared magnetic quantum numbers, rather than  $\Delta m$ . This suggests that angular modes, which only differ in the sign of  $m$ , do not interfere. As a matter of fact, an electric

field is known not to remove degeneration in the sign of  $m$ , and so the behavior of phases of those modes in an electric field is identical.

The quantity  $\rho_{kl}$  and statistical weights of states with various  $l$  being unpredictable, we can only estimate the lower boundary of effective values of  $E'$ . The fine structure of the amplitude spectrum of the motif  $J_n(z)$  will inevitably be smeared out in averaging over several variables that have a statistical meaning, including the magnitude and direction of the gradient of an EF. Clearly, to estimate the threshold values of  $E'$  we will have to put  $l = 1$  and, appropriately,  $m^2 - m'^2 = 1$ . As before, we will use for  $\rho_{kl}$  the estimate  $\sim R^2/2$ . Substituting the frequency of an external field  $\Omega$  in a relative form  $\Omega = f'qH_{\text{DC}}/Mc$ , we will write the argument in the form

$$z = \frac{E' McR^2}{4\hbar f' H_{\text{DC}}}.$$

It was shown in Section 4.1 that in the dissociation response to an MF the first maximum emerged at  $z = 1.8$  and frequency  $f' = \frac{1}{2}$ . Substituting these values we estimate

$$E' \sim \frac{\hbar H_{\text{DC}}}{McR^2} = \frac{\hbar \Omega_c}{qR^2} \sim 0.2 \text{ CGS units } (\text{cm}^{-3/2} \text{g}^{1/2} \text{s}^{-1}). \quad (4.6.7)$$

It would be of interest to compare this level of field gradients, which is needed for interference effects to make their appearance, with those macro- and microscopic gradients that occur in a real cellular medium.

In what follows, for convenience, we will talk about the EF gradient in a wider sense, taking it to mean, of course, some averaging over the components of tensor  $\partial E_i/\partial x_k$ , which could characterize the value of EF inhomogeneities.

Microscopically, in a biological medium, a magnetic field is virtually identical to an external MF. In contrast, an electric field, induced by an external field, has inhomogeneities owing to a difference in the polarizability of various biological subsystems, such as inter- and intracellular plasma, organelles, and membranes. In a tissue, an EF weakens due to the polarization of tissue surface layers, and it acquires, in addition, an inhomogeneous spatial structure. The microscopic inhomogeneity of an electric field is also determined by the presence in the medium of charged particles and dipoles.

## 4.6.2 Electric gradients in a biological tissue

### 4.6.2.1 Gradients due to inhomogeneous polarization

The most likely location of primary EMF reception processes is thought to be the surface of cellular membranes (Adey, 1993). In Addendum 6.4 it is shown that, in continuum approximation, EF gradients on the surface of biological cells are close to  $E/R_c$ , where  $R_c$  is the cell size. Substituting that value into (4.6.7) and using the variables of the  $\text{Ca}^{2+}$  ion in the Earth's MF and the cell size  $\sim 10^{-3}$  cm, we estimate the threshold EF value that causes an effect.

$$E_{\text{th}} \sim \frac{\hbar\Omega_c}{qR} \frac{R_c}{R} \sim 25 \text{ V/m} . \quad (4.6.8)$$

Thus, gradients (4.6.7) emerge on the surface of cells in the presence within a medium of an electric field (4.6.8). These gradients have a macroscopic, about the cell size, scale of inhomogeneities.

In a cellular medium there are also other sources of gradient fields. First, these are free ions present in a physiological medium due to electrolytic dissociation of various inorganic salts. Generally, these are sodium chloride NaCl, sodium bicarbonate NaHCO<sub>3</sub> and phosphate NaH<sub>2</sub>PO<sub>4</sub>, potassium KCl and calcium CaCl<sub>2</sub> chlorides, and magnesium sulfate MgSO<sub>4</sub>. Especially abundant,  $\sim 0.1 \text{ M}$  (mol/l), are chloride and sodium ions, which make the main contribution to the electric conductivity of a tissue. Second, in a biological medium there are molecular and subcellular structures that have an electric dipole moment, which also are sources of electric gradients. Superimposing an external AC EF produces in the dynamics of ions and dipoles a component that is coherent with an external field. As a consequence, there also emerge variable microscopic gradients of the field. Let us now make some estimates.

#### 4.6.2.2 Free ions in an electrolyte

The motion of ions in an electrolyte can be easily imagined by comparing the following characteristic dimensions:

- mean interion separation,
- ion drift amplitude in a variable electric field,
- diffusion shift of an ion during an EF oscillation period,
- characteristic size of a possible area of ion residence.

The mean interion separation at a given density  $c$  [M] is

$$\bar{r} = 10 (N_A c)^{-1/3} \text{ [cm]} .$$

For above density 0.1 M that will give 2.5 nm.

In electrochemistry the mobility of ions  $u$  is determined as a proportionality coefficient between drift velocity  $v$  and macroscopic EF strength in a solution  $E$ , i.e.,  $v = uE$ . In a field  $E = E_0 \cos \Omega t$ , the drift shift will clearly be  $(uE_0/\Omega) \sin \Omega t$ . The mobility of ions in biological tissues is close to  $10^{-7} \text{ m}^2/\text{V}\cdot\text{s}$ . In the Gauss system, that gives  $u \sim 0.3 \text{ cm}^3/2 \cdot \text{g}^{-1/2}$ . In an EF of  $\sim 1 \text{ V/m}$  and frequency  $\Omega \sim 100 \text{ Hz}$ , the ion shift amplitude will be

$$r = uE_0/\Omega \sim 1 \text{ nm} .$$

At the same time, diffusion shift during time  $t = 2\pi/\Omega$ , which is given by  $\langle r^2 \rangle \sim 6Dt$ , is several orders of magnitude higher. If we use the Einstein relation for the diffusion coefficient  $D \sim \kappa T u/q$ , see for instance (Landau and Lifshitz, 1976b), we can easily find that

$$r_d \sim 2\pi \sqrt{\frac{\kappa T u}{q\Omega}} \sim 30 \text{ } \mu\text{m} .$$

That implies that conductivity ions still move about in a random manner. From the point of view of the supposed EMF receptor, of molecular or even of cellular size  $\sim 1 \mu\text{m}$ , regular drift shifts are imperceptible against the background of more intensive random processes. Hence we specifically find that a redistribution of ion density exposed to such an external AC field is too small for it to exert a noticeable action on the workings of a biophysical system. Being fairly insignificant, the regular EF component and its gradients for moving free ions do not need to be estimated.

#### 4.6.2.3 Dynamics of macromolecular dipoles

For relatively massive particles the random component in the dynamics of particles in a solution is drastically reduced. It is well known that some molecules in biological tissues, including large subcellular structures and even some cell types, are electrically polarized or they feature a significant dipole moment, from units to thousands D (Rapoport, 1968; Porschke and Grell, 1995). For example, dipole moment of ATP monomer is  $430 \pm 50 \text{ D}$ , or  $1.4 \cdot 10^{-27} \text{ C m}$ .

The rotational dynamics of a massive dipole  $\mathbf{d}$  in a viscous medium in an electric field  $\mathbf{E}$  is described by the equation

$$I\ddot{\varphi} - \gamma\dot{\varphi} = Ed\sin(\varphi - \varphi_0) , \quad (4.6.9)$$

where  $\varphi$  is the angle between  $\mathbf{E}$  and the dipole axis,  $I$  is the inertia moment, and  $\gamma$  is the damping factor. The right part of the equation is the torque  $dU/d\varphi$  on the dipole produced by the electric field, since the energy of a dipole is  $U = -\mathbf{dE} = -Ed \cos \varphi$ .

An external EF causes rotational oscillations of a dipole, which lead to the appearance of a variable component in the gradient of an electric field magnitude around the dipole. That component can produce an interference effect of the dissociation of an ion subjected to the gradient. For an interference to occur it is necessary that gradient oscillations would be a more or less regular process with an autocorrelation time longer than the characteristic time  $\tau \sim 0.1 \text{ s}$  of the dissociation of an ion-protein complex. However, owing to rotational diffusion, not all dipoles will create around them gradient oscillations that are sufficiently coherent in time. Clearly, rotational diffusion must have a characteristic time larger than  $\tau$ ; then within time intervals  $< \tau$  the dynamics of a dipole will be sufficiently regular to bring about an interference. This imposes a limitation on the dipole size.

For rough estimates of the quantities involved it is convenient to simplify a dipole to a sphere of radius  $R$ . Then, in a medium with viscosity coefficient  $\eta$ , the characteristic time of the diffusion turn by  $2\pi$  will approximately be  $\eta R^3/\kappa T$ , see (Landau and Lifshitz, 1976b). We find that for dynamics to be sufficiently coherent, the dipole size should exceed

$$R \sim \sqrt[3]{\tau \kappa T / \eta} \sim 0.6 \mu\text{m} , \quad (4.6.10)$$

where estimates rely on physiological temperatures and water viscosity  $\eta \sim 10^{-3} \text{ Pa}\cdot\text{s}$ , or  $10^{-2} \text{ g/cm}\cdot\text{s}$  in the Gauss system. We will assume that such dipoles occur in biological media. In particular, those can be biological cells per se, which possess a dipole moment, either natural or induced.

Having written Eq. (4.6.9) for the dimensionless independent variable  $\Omega t \rightarrow t$ , we can easily establish that dipoles of that size are overdamped, since a coefficient at  $\dot{\varphi}$  is much larger than that at  $\ddot{\varphi}$ . Their ratio is

$$\gamma/I\Omega \sim 10^6 .$$

In that estimate, use was made of formulas  $\gamma \sim 4\pi\eta R^3$  (Landau and Lifshitz, 1976b),  $I = 2MR^2/5$ , and  $M = \rho 4\pi R^3/3$ , where  $\rho$  is the mean density of dipole matter.

Hence in a variable field with amplitude  $E_0$ , the equation has the form

$$\dot{\varphi} = -\frac{E_0 d}{\gamma \Omega} \sin t \sin(\varphi - \varphi_0) .$$

In the ranges of given quantities of interest to us, coefficient  $E_0 d/\gamma \Omega$  is much smaller than unity. Therefore, the derivative  $\dot{\varphi}$  is also small, and so the quantity  $\sin(\varphi - \varphi_0)$  is virtually unchanged and is determined by the initial orientation of the dipole  $\varphi_0$ . This suggests an estimate of the oscillation amplitude  $\delta_\varphi$  for the variable  $\varphi$

$$\delta_\varphi \sim E_0 d/\gamma \Omega . \tag{4.6.11}$$

Knowing the amplitude of field-induced rotation, we can also determine the variation amplitude for the gradient of an electric field of the dipole. The dipole field is given by

$$\mathbf{E}(\mathbf{r}) = \frac{3(\mathbf{nd})\mathbf{n} - \mathbf{d}}{r^3} , \tag{4.6.12}$$

where  $\mathbf{n}$  is the unit vector along the direction of vector  $\mathbf{r}$  from the dipole to a point where the field is to be determined. One approximate characteristic of inhomogeneity of a vector field at point  $\mathbf{r}$  could be the field divergence  $\nabla \mathbf{E}$ , which sums up diagonal elements of tensor  $\partial E_i/\partial x_k$ . Using the differential relationships

$$\nabla(r^n) = nr^{n-2}\mathbf{r} , \quad \nabla(\mathbf{rd}) = \mathbf{d} , \quad \nabla(f\mathbf{r}) = 3f + (\nabla f)\mathbf{r} ,$$

where  $\mathbf{d}$  is a vector, and  $f$  is an arbitrary scalar function, we work out

$$\nabla \mathbf{E} = 12\mathbf{nd}/r^4 = 12d \cos \varphi /r^4 .$$

Here the angle  $\varphi$  is the angle between the dipole axis and the direction at a point where the field inhomogeneity is determined. The angle derivative  $\nabla \mathbf{E}$  is about  $12d/r^4$ , and hence, when the dipole axis oscillates, the sought amplitude  $g$  of field inhomogeneity changes will be

$$g \sim \frac{1}{\varepsilon}(12d/r^4)\delta_\varphi \sim \frac{12E_0 d^2}{\varepsilon r^4 \gamma \Omega} ,$$

where the relationship (4.6.11) is used, and the screening effect of a polarizable medium with a dielectric permittivity  $\varepsilon$  taken into consideration.

Near the dipole  $r \sim R$ . Moreover, we can assume that the dipole moment varies with the dipole size  $d \sim 2Rq$ , where  $q$  is an equivalent charge at dipole poles. Then, substituting also  $\gamma \sim 4\pi\eta R^3$ , we arrive at an estimate of the amplitude of EF gradients

$$g \sim \frac{4E_0q^2}{\varepsilon\eta\Omega R^5} \sim 0.02 \text{ CGS units } (\text{cm}^{-3/2}\text{g}^{1/2}\text{s}^{-1}). \quad (4.6.13)$$

We used here the specified size of the dipole (4.6.10), an electric field of 25 V/m or  $25 \cdot 0.333 \cdot 10^{-4}$  CGS units and dielectric permittivity of water  $\varepsilon \sim 80$ . This estimate is an order of magnitude smaller than the value required for interference (4.6.7). With the quadratic dependence of dipole poles on equivalent charges, which may markedly exceed the elementary charge, such a coincidence could be recognized as satisfactory. At the same time, strong dependence on dipole size requires that the point of gradient reception would be not too far separated from a dipole. If we deal with a cell suspension, then its density must be sufficiently large, for the separation between cells to be about the cell size. Targets on the surface of one of the cells could then assume gradients created by a neighboring cell. It can easily be worked out that the density of such a suspension must not be lower than  $10^{10} \text{ cm}^{-3}$ . If, nevertheless, dipoles are subcellular macromolecules, this lifts any limitations on the suspension density.

A low-frequency,  $f \sim 10 \text{ Hz}$ , EF of 10–100 V/m makes an approximately similar input to the variable component of EF inhomogeneity in a medium both due to inhomogeneous dielectric polarization in continuum approximation and due to modulation of the rotational dynamics of macroscopic dipoles. In both cases, inhomogeneities have a macroscopic scale, on the order of  $1 \mu\text{m}$ , and its value is obviously insufficient for interference effects.

### 4.6.3 Gradients due to electron polarization of ligands

Finally, there are EF gradients engendered by induced dipole moments of neighboring binding ligands. They emerge due to a shift of electron shells relative to the core of ligands in an external EF. We will roughly estimate the field inhomogeneity regarding the binding cavity of ligands as an induced dipole of size  $2R$ , where  $R$  is the radial size of the cavity. The dipole moment is  $d \sim \alpha E$ , where  $\alpha$  is the electron polarizability of ligand atoms, which is about  $10^{-24} \text{ cm}^3$ . On the other hand, the effective electric charge  $Q$  at dipole poles is related to its dipole moment by  $Q \sim d/2R$ . It can be easily found using Coulomb law, that the EF gradient at the center between poles on the dipole axis is

$$g \sim 4Q/R^3 = 2\alpha E/R^4.$$

Having equated the quantity to (4.6.7), we find the field amplitude in a medium that is needed for interference effects caused by the electron polarizability of ligands (Binhi and Goldman, 2000):

$$E_{\text{th}} \sim \frac{\hbar\Omega_c R^2}{2q\alpha}. \quad (4.6.14)$$

Its order of magnitude is  $4 \cdot 10^{-8}$  CGS units or 1 mV/m. The estimate is obtained using fairly strong idealizations. Specifically, gradient magnitudes vary markedly over the cavity volume. Even if we take account of this, the estimate is sufficient to explain some experimental evidence where amplitude windows for the biological action of weak variable EFs appear for larger field strengths. It will be recalled that the estimate (4.6.14) relates to an internal electric field averaged over a physically small volume of a biological medium. The estimate gives the lower limit of effective EFs. This implies that the expected dependence on the magnitude of an internal electric field has the form

$$J_1^2(1.8E/E^*) , \quad (4.6.15)$$

where  $E^* > E_{\text{th}}$ . As was said above, any estimate of the magnitude of  $E^*$  is complicated owing to the fact that there are many variables of biological nature, on which it is dependent.

One prediction of the interference mechanism is that *resonance interference in perpendicular MFs can be destroyed by switching on an electric field* in parallel to a DC MF. In fact, some MF biological effects are connected with the Zeeman splitting of energy levels of a binding particle in the geomagnetic or other DC MF. This follows from observations of biological effectiveness of a magnetic vacuum. Then static EFs of about 10–100 V/m must also influence the above effects, as they result in a similar splitting of levels. This means that it is expedient to conduct magnetobiological experiments in a Faraday cage or when controlling a DC EF. We note that for a local DC EF to be measured requires special-purpose devices, e.g., a rotating dipole.

Relation (4.6.14) shows that the lower limit of an EF  $E_{\text{th}}$  and hence the characteristic field  $E^*$  in (4.6.15) are proportional to the cyclotron frequency  $\Omega_c$  or the magnitude of a DC MF  $H_{\text{DC}}$ . Connected with that is a further prediction. *The position of a maximum on the dependence of the MBE on the amplitude of a variable EF shifts with the level of a DC MF.* That prediction holds for a relatively wide frequency spectrum. Otherwise, the effect will decline at a fixed frequency  $\Omega$  with the static MF owing to a deviation of the characteristic frequency  $\Omega_c$  from  $\Omega$ .

It is of interest to suppose that biological effects appear when the mutual orientation of the MF and the EF changes. As is shown in Section 4.5, in a DC MF, an MBE can follow the ion interference mechanism in the presence of rotating ion–protein complexes. Such an effect is also clearly dependent on the presence of a DC EF, its magnitude, and its orientation. It is well known that the Earth's EF, connected with its electric potential, is subject to strong local changes depending on the states of the atmosphere. For instance, the quasi-static EF vector of scale kV/m may even acquire an opposite direction if a cloud appears above the site (Benninghoff and Benninghoff, 1982). Thus a weather change is accompanied by a long-term change of the EF magnitude and its mutual orientation with an MF. That is not without consequence for rotating ion–protein complexes and, generally speaking, may involve finite biological reactions. According to Gurfinkell *et al.* (1998), among cardiovascular disorder cases there are twice as many of those who

respond to MF variations than of those who respond to variations of local atmospheric pressure. It is not to be excluded that pressure variations also affect indirectly, via variations of a local EF that correlate with them.

#### 4.7 INTERFERENCE AGAINST THE BACKGROUND OF A MAGNETIC NOISE

The interference mechanism is non-linear in the sense that a response to a signal A+A is not equal to the sum of responses to each individual signal. The ion interference mechanism also has another feature that enables it to be distinguished from other non-linear mechanisms. In the ion interference mechanism the dissociation probability of an ion-protein complex P is mathematically a non-linear functional of the MF signal. That implies that even if there is a way to transform such a functional into an explicit function of parameters of possible signals, then the form of such a function depends, generally speaking, on the signal shape. Suppose, for instance, that some deterministic MF signal leads to constructive interference described by some functional dependence. A superposition of an additional MF will then change the shape of that dependence.

In that sense, a noise MF has an interesting distinction. A changed dependence on MF parameters will then become a product of two functions. One of them is a dependence on MF parameters without noise. The other one, in contrast, is only dependent on the variables of the magnetic noise and represents a modulating coefficient smaller than unity. The action of magnetic noise thus reduces to suppression of an MBE.

For convenience let us consider interference in parallel MFs. It is shown in Section 4.1 that the probability density of an ion at some angular position  $\varphi_0$  is determined by the sum of terms of the form

$$p = \exp \left[ i \Delta m (\varphi_0 + \omega_0 t + b \int h dt) \right] .$$

In this section this summation is of no significance, and so we omit it without loss of the generality of our conclusions. Let an AC MF  $h$  be composed of a deterministic signal  $h_1$  and noise

$$h = h_1(t) + \sigma \eta(t) ,$$

where  $\eta(t)$  is a centralized, i.e., with a zero mean, random process with unit dispersion, and  $\sigma$  is a root-mean-square deviation, i.e., a square root of the dispersion  $\sigma^2$  of noise signal  $\sigma \eta(t)$ , with the dimensionality of MF. Then we will write the probability density as

$$p = p' \exp \left[ i \epsilon \int \eta(t) dt \right] , \quad \epsilon = \Delta m b \sigma .$$

Here  $p'$  is a part of the density  $p$  that depends on the variables of a deterministic signal.

We will take the random process  $\eta$  to be ergodic. Then its statistical characteristics, specifically, the mean values of functions of  $\eta$ , may be obtained just from its single realization, by averaging over time. We will suppose that we have an interval of such a realization. Let the interval length  $\theta$  be longer than all the time scales inherent in a real physical system being modeled. A realization  $\eta(t)$  of a random process  $\eta$  can then be constructed by reiterating such an interval and, being a periodic function, it can be represented by a Fourier series

$$\eta(t) = \sum_k d_k \exp(i\omega_k t) = \sum_k c_k \cos(\omega_k t + \phi_k) , \quad c_k = |d_k| , \quad \omega_k = \frac{2\pi}{\theta} k . \quad (4.7.1)$$

The longer the interval  $\theta$ , the closer the random real spectral amplitudes  $c_k$  and phases  $\phi_k$  will be to deterministic values defined by the spectral density  $G(\omega)$  of the process  $\eta$ .

We recall that the spectral density of a centralized stationary, i.e., with permanent statistical properties, random process  $\eta$  is the quantity

$$G(\omega) = \frac{1}{2\pi} \int_{-\infty}^{\infty} \overline{\eta(t)\eta(t+\tau)} e^{-i\omega\tau} d\tau ,$$

where the overscribed bar stands for time averaging. A specific realization  $\eta(t)$  of a random process  $\eta$  can be represented by the Fourier integral

$$\eta(t) = \int_{-\infty}^{\infty} \eta_\omega e^{-i\omega t} d\omega . \quad (4.7.2)$$

Spectral amplitudes  $\eta_\omega$  are random functions on an ensemble of realizations, and they obey the relation

$$\overline{\eta_\omega^* \eta_\omega} = G(\omega) \delta(\omega) . \quad (4.7.3)$$

For a more detailed introduction to the applied theory of random processes see, e.g., Akhmanov *et al.* (1981). Assuming the realization  $\eta(t)$  to be periodic with a large period  $\theta$ , we get a discrete spectrum with a dense series of frequencies  $\omega_k$ . The spectral expansion will then have the form of a series, rather than that of a Fourier integral, which is convenient for further analysis.

Substituting the cosine expansion (4.7.1) into  $p$  we write

$$p = p' \exp \left[ i\epsilon \sum_k \frac{c_k}{\omega_k} \sin(\omega_k t + \phi_k) \right] = p' \prod_k \exp \left[ i \frac{\epsilon c_k}{\omega_k} \sin(\omega_k t + \phi_k) \right] .$$

Using (4.1.11), we then get

$$p = p' \prod_k \sum_n J_n(a_k \epsilon) \exp [in(\omega_k t + \phi_k)] , \quad a_k = c_k / \omega_k .$$

That expression reduces to a sum of products of a large number of Bessel functions, including products of Bessel functions of the same order. Since  $|J_n| \leq 1$ , the only

contribution that does not vanish in the limit  $\epsilon \rightarrow 0$  is the product of zero-order Bessel functions.<sup>31</sup> Hence,

$$p \approx p' \prod_k J_0(a_k \epsilon) .$$

In addition to  $p'$ , that expression includes a coefficient that is independent of time and is only determined by variables concerned with magnetic noise. Therefore, in the dissociation probability  $P = \overline{p_T} \cdot \overline{p_T}$  that coefficient appears as a modulating factor  $y$ :

$$y = \prod_k J_0^2(a_k \epsilon) . \quad (4.7.4)$$

That coefficient is unity at  $\epsilon = 0$ , i.e., in the absence of noise, and tends to 0 with  $\epsilon$ . That is, as noise intensity increases, interference effects vanish. To determine the nature of that dependence, we will find the first terms of the expansion of  $y$  in the small parameter  $a_k \epsilon$ . We note that in the argument of the Bessel functions not only  $\epsilon$ , which varies with the noise signal amplitude, but also  $a_k = c_k / \omega_k$  are small. They are the smaller, the denser the frequency series of the noise spectrum. For small  $x$ , it is convenient to represent  $J_0(x)$  as an exponential function with a series in its exponent:

$$J_0(x) = \exp(ax^2 + bx^3 + \dots) . \quad (4.7.5)$$

It begins with a quadratic term, since  $J_0'(0) = 0$ . From the expansions

$$\exp(x) = \sum_{n=0}^{\infty} \frac{x^n}{n!} , \quad J_0(x) = \sum_{n=0}^{\infty} (-1)^n \frac{(x/2)^{2n}}{(n!)^2}$$

we can determine the coefficients in (4.7.5),  $a = -\frac{1}{4}$ ,  $b = 0$ . The remaining terms of the expansion are minor, and we will not derive them. Then

$$y = \prod_k [\exp(-a_k^2 \epsilon^2 / 4)]^2 = \exp \left[ -\frac{\epsilon^2}{2} \sum_k \frac{c_k^2}{\omega_k^2} \right] .$$

We now replace the dense discrete spectrum of frequencies  $\omega_k$  with a smooth function  $G(\omega)$ . The spectral amplitudes of the discrete series  $c_k$  (4.7.1) will then become functions  $\eta_\omega$  (4.7.2), which obey the relationship (4.7.3). In actual fact, we will have to write  $c_k^2 \rightarrow G(\omega) d\omega$ . Substituting  $\epsilon$ , we can also arrive at

$$y = \exp \left[ -\frac{\sigma^2 b^2 \Delta^2 m}{2} \int \frac{G(\omega)}{\omega^2} d\omega \right] . \quad (4.7.6)$$

This suggests that as the magnetic noise intensity, i.e., dispersion  $\sigma^2$ , grows, interference effects abate. We note that the integral in (4.7.6) converges, since the spectrum  $G(\omega)$  is bounded from below, at least, by the frequency  $\theta^{-1}$ . Spectrum  $G(\omega)$  enters

---

<sup>31</sup>A more rigorous treatment involving terms up to  $o(\epsilon^2)$  supports that deduction.

into  $y$  through the integral, thus suggesting relatively weak dependence of  $y$  on details of the spectrum shape.

Let, for instance, the magnetic noise spectrum be uniform within an interval  $\nu_1, \nu_2$ . Then  $G(\omega) = (\nu_2 - \nu_1)^{-1}$ , and the integral in (4.7.6) can be easily seen to be equal to  $1/\nu_1\nu_2$ . The value of that integral differs by 20–30% for a good, i.e., ensuring the integral convergence, Gaussian spectrum that is centered at point  $(\nu_1 + \nu_2)/2$ . For a uniform spectrum the dependence of the modulating factor on noise intensity becomes

$$y = \exp \left[ -\sigma^2 \frac{b^2 \Delta^2 m}{2\nu_1\nu_2} \right].$$

The noise intensity at which the interference effect begins to decline is given by  $y = \exp(-1/2)$ . From this we can readily find the characteristic value of the root-mean-square amplitude:  $\sigma = \sqrt{\nu_1\nu_2}/b\Delta m$ . The largest contribution to dissociation probability comes from the difference of magnetic quantum numbers  $\Delta m = 1, 2$ . Since the cyclotron frequency varies with the DC MF,  $\Omega_c = 2bH_{DC}$ , it is convenient to describe the threshold amplitude by the relationship

$$\frac{\sigma}{H_{DC}} \approx \frac{\sqrt{\nu_1\nu_2}}{\Omega_c}, \tag{4.7.7}$$

i.e., *the relative amplitude of magnetic noise that suppresses ion interference varies with the relative value of the geometric mean of the frequencies at the boundaries of the noise spectrum*. It is important that noise would manifest itself mathematically as a modulating factor, which is independent of a specific interference mechanism.

#### 4.7.1 Agreement with experimental evidence

It appears that it is the suppression of an MBE by a magnetic noise that has been repeatedly observed by the Litovitz group in experiments with a concurrent exposure to deterministic EMF signals of various forms and a magnetic noise. Mullins *et al.* (1993) have shown that a growth of activity of ornithine-decarboxylase exposed to a 60-Hz MF in L929 cells of rodents is suppressed by a low-frequency magnetic noise. Litovitz *et al.* (1994a) and Litovitz *et al.* (1994b) observed a reduction, under the action of low-frequency magnetic noise, of the level of deviations from the normal development of chicken embryos caused by a low-frequency sinusoidal MF. Lin and Goodman (1995) confirmed those findings for an MBE with a permanently heightened level of transcription of *c-myc* protooncogene in HL-60 cells exposed to a 60-Hz sinusoidal MF. A superposition of a magnetic noise with a frequency band 30–100 Hz and a root-mean-square amplitude of  $6.7 \mu\text{T}$  suppressed the MBE. Litovitz *et al.* (1997a) measured the activity of ornithine-decarboxylase in L929 cells exposed to an amplitude-modulated microwave radiation, such as the emission of a mobile phone with modulation, and also to a homogeneous low-frequency MF. In all the cases the radiation increased the activity of the enzyme. An additional simultaneous exposure to a low-band

magnetic noise of 30–100 Hz with effective amplitude 2–5  $\mu\text{T}$  produced an effect. A further study on this topic was conducted by Raskmark and Kwee (1996). The MBE consisted in an increase in the growth rate of human epithelium cells exposed to a sinusoidal MF of frequency 50 Hz. Simultaneous superposition of a noise with a band of 40–60 Hz and a root-mean-square amplitude of up to 50  $\mu\text{T}$  also reduced the MBE level.

It makes sense to introduce the dimensionless quantities

$$\sigma' = \sigma b_{\text{H}} / \sqrt{2\nu_1\nu_2}, \quad b' = b/b_{\text{H}},$$

where  $b_{\text{H}} = e/2m_{\text{p}}c$  is the charge-to-mass ratio for the hydrogen ion. In this notation, the formula for the suppression coefficient is especially simple

$$y = \exp(-\sigma'^2 b'^2). \quad (4.7.8)$$

We note that all the variables of the magnetic noise are contained in its relative amplitude  $\sigma'$ . That is rather convenient since it enables one to compare various experimental data with the only theoretical curve, in terms of the hypothesis of the involvement of some ion species in MBEs. Our choice corresponds to hydrogen ions,  $b = b_{\text{H}} = 47.8 \text{ s}^{-1} \mu\text{T}^{-1}$ .

The findings of the above experiments were normalized as follows. The maximum MBE for each experiment was taken to be unity, and the control level was taken to be zero.

Shown in Fig. 4.26 are the results of experiments (Litovitz *et al.*, 1994a,b; Lin and Goodman, 1995; Raskmark and Kwee, 1996; Litovitz *et al.*, 1997b) and a theoretical curve computed by (4.7.8) for hydrogen ions. It is seen that theoretical conclusions are in a satisfactory agreement with experiment. In this case the theoretical curve is just an estimate. Therefore, it is hardly possible in these experiments to identify ions from the agreement of experiment and theory, although it would be possible under special-purpose magnetic conditions. Rule (4.7.6) gives a specific dependence on the spectral parameters of magnetic noise, and it is another way of an experimental check of the fundamental ideas of the theory.

The data of Raskmark and Kwee (1996) better agree with the hypothesis of the involvement in magnetoreception of lithium ions  $b_{\text{Li}} = 6.87 \text{ s}^{-1} \mu\text{T}^{-1}$ . Lithium ions, just as ions of hydrogen, calcium, magnesium, and zinc, were discussed as possible targets for an MF by Thomas *et al.* (1986) and Smith (1988). Multippeak MBE spectra for neurons, measured by Blackman *et al.* (1994) and Blackman *et al.* (1995a), were explained by this author (Binhi, 2000) assuming that lithium ions form complexes with rotating proteins.

It remains for us to find maximum values of  $\sigma$  for which formula (4.7.8) is still valid. Clearly, returning to (4.7.5), we should write  $x = \epsilon c_k / \omega_k \ll 1$ . For a spectrum homogeneous within  $[\nu_1, \nu_2]$ , we have  $c_k^2 = c^2 = 1/K$ , where  $K$  is the maximal number of the discrete series of frequencies, because  $\sum_k c_k^2 = 1$ . It is obvious that the number equals the ratio of the upper spectrum boundary and the small frequency  $\theta^{-1}$ , determined by the periodicity interval length for noise

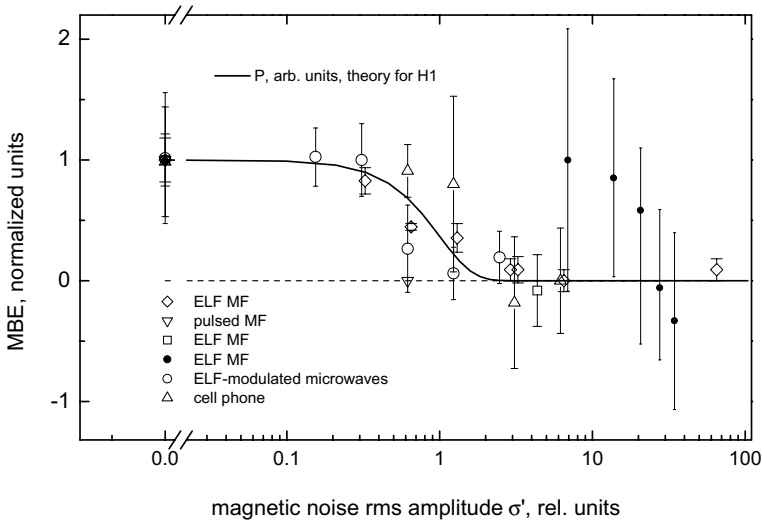


**Figure 4.26.** The dependence of various MBEs on the level of magnetic noise and the typical theoretical curve of the decay of dissociation probability, on the assumption that hydrogen ions participate as primary targets for an MF,  $\diamond$  (Litovitz *et al.*, 1994a),  $\nabla$  (Litovitz *et al.*, 1994b),  $\square$  (Lin and Goodman, 1995),  $\bullet$  (Raskmark and Kwee, 1996),  $\circ, \triangle$  (Litovitz *et al.*, 1997a).

realization  $K = \nu_2\theta$ . Thus,  $c \sim \sqrt{1/\nu_2\theta}$ . On the other hand, in order to arrive at a valid estimate, we must take the smallest of the frequencies  $\omega_k$ , i.e.,  $\nu_1$ . Then  $\epsilon \ll \omega_k/c_k \sim \nu_1\sqrt{\nu_2\theta}$ . In relative units, that constraint becomes

$$\frac{\sigma_{\max}}{H_{\text{DC}}} \ll \frac{\nu_1}{\Omega_c} \sqrt{\nu_2\theta} .$$

If the recurring intervals in the realization of the noise signal have a length of not less than  $\theta = 10$  s, which is absolutely attainable in experiment, by substituting the quantities  $\nu_1$  and  $\nu_2$  employed above, we will arrive on average at  $\sigma \ll H_{\text{DC}}$ . In that range, the theoretical curve yields a fairly good approximation to the expression (4.7.4). The periodicity interval length  $\theta$  can, of course, be enlarged. This will also increase the validity interval for formulas (4.7.8). In actual fact, that implies that at large  $\sigma$  for small values of  $y$  to be measured more observation time is required. When measuring MBE suppression by noise for more than 10 min, i.e., when  $\theta > 600$  s, constraints on the permissible value of magnetic noise correspond to the level of a DC MF.

Generally speaking, in magnetobiological experiments data scatter is generally so large that it makes any mathematically rigorous estimates hardly needed. Comparison of the qualitative behavior of curves yields here more reliable information than a comparison of accurately measured and accurately calculated values.

#### 4.8 NUCLEAR SPINS IN ION INTERFERENCE MECHANISMS

The energy of the nuclear magnetic moment of an ion  $\sim \mu H$  in an MF  $H$  is somewhat larger than the energy scale of the orbital magnetic moment  $\sim \hbar\Omega_c$ . Spin effects are, therefore, important for the action of weak MFs on the dynamics of bound ions. Spin-conditioned interference of states of a bound ion shifts the interference spectrum to higher frequencies. It is possible to observe that effect if the lifetime of nuclear spin states of an ion is sufficiently long, namely longer than the characteristic interference time scale defined by the frequency of an external field:  $\tau_N > \Omega^{-1}$ . In this section we use that idealization, but its validity is to be established experimentally from a good agreement of calculated and measured spectra. Since an ion in a binding cavity oscillates with a microwave frequency, gradients of an electric field induced by thermal oscillations of capsule walls and “visible” by spins are averaged. Correspondingly, also hindered is the relaxation of spin states. For instance, the large mobility of protons of liquid water also enables them to “see” only the averaged gradient of a microscopic electric field magnitude and results in an abnormally large lifetime of spin states of protons  $\sim 3$  s. Thus this suggests that the spin states of ions in binding cavities are long-lived states.

As seen in Section 3.10.1, the dynamics of bound ions with a nuclear spin is dependent on which approximation is used, that of a strong or weak MF. A transitional region is equal or larger than the geomagnetic field, so that it is not known *a priori* which approximation is closer to reality.

In a relatively strong MF, spin dynamics develops independently of the orbital one. The dynamic equation has the form of the Pauli equation

$$i\hbar \frac{\partial \Phi}{\partial t} = \left[ \frac{(\mathbf{P} - \frac{q}{c}\mathbf{A})^2}{2M} - \gamma\hbar\mathbf{I}\mathbf{H} + U \right] \Phi ,$$

which allows separation of variables in the solution

$$\Phi = \Psi(r, \theta, \varphi)\Sigma(\sigma) ,$$

where  $\Psi$  and  $\Sigma = \sum_i a_i \nu_i$  are functions of spatial and spin variables. Interference presupposes the presence of an interference term in probability density of an ion near a gate. Probability density, the squared magnitude of a scalar field  $\Phi$ , at some angular position is

$$p = \langle \Phi | \Phi \rangle_{r, \theta, \sigma} = \langle \Psi | \Psi \rangle_{r, \theta} \sum_{ik} \langle a_i \nu_i | a_k \nu_k \rangle = \langle \Psi | \Psi \rangle_{r, \theta} \sum_i a_i^* a_i . \quad (4.8.1)$$

Since spin functions are orthogonal, i.e.,  $\langle \nu_i | \nu_k \rangle = \delta_{ik}$ , the density equals the sum of densities caused by each spin component.

It was shown earlier (4.1.6) that the quantity  $\langle \Psi | \Psi \rangle_{r, \theta}$  contains terms related to interference of angular modes with different values of magnetic quantum numbers  $m$ . At the same time, density (4.8.1) contains no terms that vary with the product of amplitudes of different spin modes  $a_i^* a_k$ . In that sense, it can be said that spatial

modes of a wave function that correspond to various values of the spin variable do not interfere. That implies that there are no spin-conditioned interference effects in the strong field approximation.

#### 4.8.1 Spin-dependent effects in the weak field approximation

In relatively weak MFs spin-orbit interaction of an ion with spin in a central potential is significant:

$$\mathcal{H} = \frac{\mathbf{P}^2}{2M} + U(r) - (b\hbar\mathbf{L} + \gamma\hbar\mathbf{I}) \mathbf{H} + \mathcal{H}_{\text{so}} . \quad (4.8.2)$$

Magnetic interactions are weaker than spin-orbit ones, and the magnetic Hamiltonian

$$\mathcal{H}_{\text{M}} = -\mathbf{MH} = -\hbar(b\mathbf{L} + \gamma\mathbf{I})\mathbf{H}$$

can be viewed as a perturbation for an unperturbed Hamiltonian

$$\mathcal{H}_0 = \frac{\mathbf{P}^2}{2M} + U(r) + \mathcal{H}_{\text{so}} .$$

The solution to the Schrödinger equation with a given Hamiltonian can no longer be reduced to the product of orbital and spin functions. It is formed by a superposition of eigenfunctions  $|lijm\rangle$  of the operation of total angular momentum  $\mathbf{J}$  and its component  $\mathcal{J}_z$ . Each of these functions is a linear combination composed of products of eigenfunctions of the angular momentum, i.e., of the spherical functions  $Y_{lm_l}(\theta, \varphi)$  and the spin functions  $\nu_{im_i}$ . Here  $j, m$  are quantum numbers of the total angular momentum and its component along an identified axis,  $l, m_l$  are numbers of the orbital momentum and its component, and  $i, m_i$  are the same for spin momentum. Index  $i$ , which is the spin value, is fixed for each ion type. The location of the index in the formula makes it different from an imaginary quantity  $\sqrt{-1}$ . Eigenfunctions  $\mathcal{H}_0$  are equal (e.g., Davydov, 1973; Landau and Lifshitz, 1977)

$$|lijm\rangle = \sum_{m_l m_i} C_{lm_i im_i}^{jm} Y_{lm_l} \nu_{im_i} , \quad (4.8.3)$$

where Klebsch-Gordan coefficients meet the orthogonality conditions

$$\begin{aligned} \sum_{jm} C_{lm_i im_i}^{jm} C_{lm'_i im'_i}^{jm} &= \delta_{m_l m'_l} \delta_{m_i m'_i} \\ \sum_{m_l m_i} C_{lm_i im_i}^{jm} C_{lm_i im_i}^{j'm'} &= \delta_{jj'} \delta_{mm'} \\ C_{lm_i im_i}^{jm} &= 0 \text{ if } m \neq m_l + m_i . \end{aligned} \quad (4.8.4)$$

Hence we can find that functions  $|lijm\rangle$  are also orthogonal, specifically,  $\langle lijm | lij'm' \rangle = \delta_{mm'}$ . That does not mean however that the interference term in the

density  $p(\varphi_0, t)$  is absent. To work out the probability density for an ion at point  $\varphi = \varphi_0$ , we will write the state of an ion with eigenfunctions  $|lijm\rangle$  in a form that takes account of the angle dependence of functions and omit for a moment the time dependence, see (4.4.17):

$$\psi_{lijm} = \frac{1}{\sqrt{2\pi}} \sum_{m_l m_i} C_{lm_l m_i}^{jm} \Theta_{lm_l}(\theta) \exp(im_l \varphi) \nu_{im_i} . \quad (4.8.5)$$

Here also we omitted the radial part of wave functions, which is immaterial for this section. The state of an ion after it has entered a capsule is, generally speaking, a superposition of functions  $\psi_{lijm}$  with different weights for each possible set of indices. Therefore, the density for an ion will contain products with differing sets. We can identify three cases. The first one is where sets of indices coincide. Such products make contributions to the constant component of the density. That is the sum of statistical weights for each state. The second case is where sets of indices differ in their orbital  $l$  or total  $j$  moment. These contributions to the density oscillate with a microwave frequency and play no role in the dynamics averaged over a fairly large time interval of about  $1/\Omega_c$ . The third case is where the sets differ only in their values of magnetic quantum numbers  $m$  of the component of the total moment. Such products produce marked low-frequency oscillations of ion density.

In order not to complicate formulas, we will not, in this section, write out statistical weights of various states, thus suggesting that the dependences derived shall be averaged appropriately.

The ion probability density due to interference of states with quantum numbers  $m$  and  $m'$  is

$$\begin{aligned} p(\varphi_0, t) &= \langle \psi_{lijm'} | \psi_{lijm} \rangle \theta \\ &= \frac{1}{2\pi} \sum_{m_l m_i m'_l m'_i} C_{lm_l m_i}^{jm} C_{lm'_l m'_i}^{jm'} \langle \Theta_{lm'_l} | \Theta_{lm_l} \rangle e^{i\varphi_0(m_l - m'_l)} \langle \nu_{im'_i} | \nu_{im_i} \rangle . \end{aligned}$$

The scalar product of spin functions dictates the condition  $m'_i = m_i$ . The Klebsch-Gordan coefficients  $C_{lm_l m_i}^{jm}$  are distinct from 0 at  $m = m_l + m_i$ ; i.e., the summation in the last expression is actually over one index  $m_i$ , since the others are defined by  $m'_i = m_i$ ,  $m_l = m - m_i$ ,  $m'_l = m' - m_i$ . We will now take into consideration the factors dictating the time dependence of wave functions. Then we can write

$$\begin{aligned} p(\varphi_0, t) &= \frac{1}{2\pi} e^{-i(\varepsilon_{lijm} - \varepsilon_{lijm'})t/\hbar} \\ &\times e^{i\varphi_0(m - m')} \sum_{m_i} C_{l(m-m_i)m_i}^{jm} C_{l(m'-m_i)m_i}^{jm'} \langle \Theta_{l(m'-m_i)} | \Theta_{l(m-m_i)} \rangle . \end{aligned} \quad (4.8.6)$$

The contribution of perturbation  $\mathcal{H}_M$ , which is diagonal in the shells  $|lijm\rangle$ , reduces only to a change in the level energy for these states. It is known that the difference of energy levels in an abnormal Zeeman effect is

$$\varepsilon_{lijm} - \varepsilon_{lijm'} = -(m - m')g\hbar H_z ,$$

where  $g$  is the Landé factor for an ion with nuclear spin. In Addendum 6.2, the Landé factor is defined for some important biological ions. If an MF  $H_z$  is a function of time, and the perturbation operator matrix is diagonal, just as in the case at hand, then the product  $H_z t$  will have to be replaced by the integral  $\int H_z dt$ . Hence the probability density becomes

$$p(\varphi_0, t) = c_{lijmm'} \exp \left[ i\Delta m \left( \varphi_0 + gb \int H_z dt \right) \right], \quad (4.8.7)$$

where the factor  $1/2\pi$  enters into the coefficient  $c_{lijmm'}$ , which represents the sum in the previous expression. In actual fact, density (4.8.7) coincides with expression (4.1.6) derived earlier, except for the fact that instead of coefficient  $b$  we have  $gb$ . Thus, for the dissociation probability we can use the previous formula (4.1.19), where appropriate substitutions have to be made. In the coefficients  $\alpha z = \Delta m \omega_0/\Omega$  and  $z = \Delta m \omega_1/\Omega$  we will have to employ new values for the Larmor frequency  $\omega_0 = gbH_{DC}$  and for the frequency associated with the variable field  $\omega_1 = gbH_{AC}$ . It is convenient to retain the previous meaning of the notation for the Larmor frequencies; therefore, anywhere in formulas we will make substitutions  $\omega \rightarrow g\omega$ . We will arrive at the result for a contribution to the dissociation probability of modes  $|lijm\rangle$  and  $|lijm'\rangle$  due to interference,

$$\sum_n \frac{\sin^2 A}{A^2} J_n^2 \left( \frac{\Delta m gh'}{2 f'} \right), \quad A = \left( \frac{\Delta m}{2} g + n f' \right) \Xi, \quad (4.8.8)$$

where all of these designations retain the meanings assumed in the book.

It is seen that changes, in comparison with ions without spin, occur both in frequency and in amplitude spectrum. Effective frequencies follow from the equality  $A = 0$ :

$$f' = -g \frac{\Delta m}{2n}. \quad (4.8.9)$$

Since the Landé factor  $g$  is dependent on quantum numbers  $l$  and  $j$ , the frequency dissociation spectrum is given by a superposition of spectra (4.8.8) determined by these numbers. The statistical weights of appropriate states take shape when an ion enters a cavity, and they are governed by a multitude of uncontrolled factors. Therefore, generally speaking, positions of peaks are also dependent on the “biophysical state” of a protein. One exception is the case of light ions, where the width of peaks is small, and they almost do not overlap. It is then natural to expect that spectral peaks will appear for each permitted set of quantum numbers.

It will be recalled that for specified orbital  $l$  and spin  $i$  moments the total moment  $j$  may take on values  $|l - i| \leq j \leq l + i$ , and its possible components will be numbers  $m = \pm j, \pm(j - 1), \dots$ . Let us take a closer look at states with spin  $\frac{1}{2}$ .

At  $l = 0$ , the remaining quantum numbers are equal:  $m_l = 0, j = \frac{1}{2}, m = m_l + m_i = m_i = \pm \frac{1}{2}$ . Substituting these values into (4.8.5), we will find functions that, due to spin brackets, appear to be orthogonal in  $m$ . It follows that they make no contribution to interference effects. These functions in general cannot produce

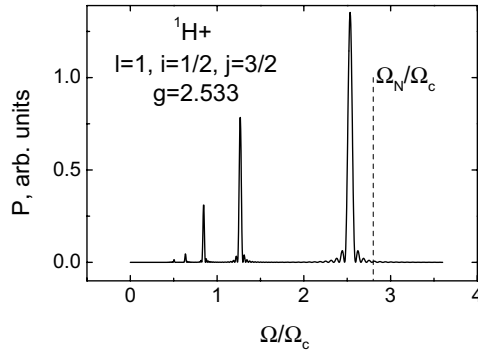


**Figure 4.27.** Dissociation spectrum for a hydrogen complex in a weak MF,  $h' = 1.8$ : the frequency of the main maximum is smaller than the NMR frequency.

interferential nodes and antinodes in an angular variable, since they are independent of angles.

At  $l = 1$ , the component is  $m_l = 0, \pm 1$ , and the possible values of the total momentum will be numbers  $j = \frac{1}{2}$  and  $j = \frac{3}{2}$ . In the first case, the component of the total momentum takes on values  $\pm \frac{1}{2}$ . The numbers  $m$  and  $m'$  in (4.8.6) can differ only by one. However, then the brackets  $\langle \Theta_{l(m'-m_i)} | \Theta_{l(m-m_i)} \rangle$  are equal to 0, since they are distinct from 0 only for even values of the difference of magnetic numbers. Hence these states too make no contribution to interference.

States with  $l = 1, j = \frac{3}{2}$  provide non-zero values for the coefficient  $c_{lijmm'}$  in (4.8.7) and result in interference. Numbers  $m, m'$  can assume values  $\pm \frac{3}{2}, \pm \frac{1}{2}$ , then all the non-zero brackets are identical:  $\langle \Theta | \Theta \rangle = -1$ . Using the relation between the Klebsch–Gordan coefficients and Wigner  $3j$ -symbols

$$C_{j_1 m_1 j_2 m_2}^{j m} = (-1)^{j_1 - j_2 + m} \sqrt{2j + 1} \begin{pmatrix} j_1 & j_2 & j \\ m_1 & m_2 & -m \end{pmatrix},$$

and the formula for  $3j$ -symbols in the special case (Landau and Lifshitz, 1977),

$$\begin{pmatrix} j_1 & j_2 & j_1 + j_2 \\ m_1 & m_2 & -m_1 - m_2 \end{pmatrix} = (-1)^{j_1 - j_2 + m_1 + m_2} \times \left[ \frac{(2j_1)!(2j_2)!(j_1 + j_2 + m_1 + m_2)!(j_1 + j_2 - m_1 - m_2)!}{(2j_1 + 2j_2 + 1)!(j_1 + m_1)!(j_1 - m_1)!(j_2 + m_2)!(j_2 - m_2)!} \right]^{1/2},$$

we can work out  $C_{1 -1 1/2 -1/2}^{3/2 -3/2} = 1$ , and so on. Exact values of coefficients  $c$ , which can be found otherwise, are of no consequence.

#### 4.8.1.1 Hydrogen

For states with moments  $l = 1, j = \frac{3}{2}$ , the Landé factor for a hydrogen ion, as follows from the Addendum 6.2, is equal to 2.533. Shown in Fig.4.27 is the dissociation

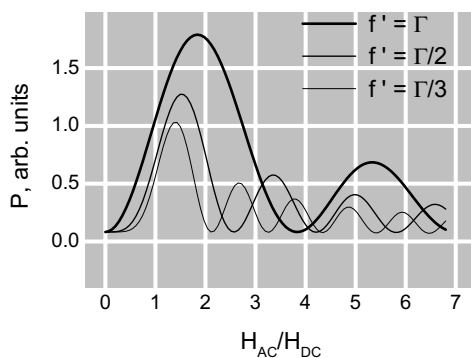


**Figure 4.28.** Amplitude dissociation spectra for a hydrogen complex in a weak MF for different frequencies.

spectrum for a hydrogen ion. It is seen that the frequency of the main spectral dissociation peak is not equal to the proton NMR frequency. Amplitude spectra, as before, depend on which frequency they are fixed at, Fig. 4.28. In calculating the spectra use was made of equal weights for all permissible combinations of  $\Delta m$ ,  $\Xi = 50$ .

#### 4.8.1.2 Potassium

States with  $l = 0$ , as stated above, do not interfere. At  $l = 1$ , among the possible values of the total momentum of a particle with spin  $\frac{3}{2}$  will be numbers  $\frac{1}{2}$ ,  $\frac{3}{2}$ , and  $\frac{5}{2}$ . States with  $j = \frac{1}{2}$  shall be ignored for precisely the same reasons as were provided for a particle with spin  $\frac{1}{2}$ . The case of  $j = \frac{3}{2}$  is also considered above. We will only have, when computing the spectrum, to substitute the value of g-factor for potassium,  $g_{|j=3/2} = 7.681$ . The case of  $j = \frac{5}{2}$  gives new terms when summing (4.8.8) over  $m, m'$ , where  $\Delta m = 4$ , and the g-factor is  $g_{|j=5/2} = 6.466$ . Calculations of the frequency spectra for these states are given in Fig. 4.29.

It is seen that main maxima occur at relative frequencies equal to the Landé factor. We note that in terms of the mechanism under consideration there is no effect at the NMR frequency for an ion.

Likewise, we can work out spectra for other values of the angular momentum. We then conclude that probable *effective frequencies of dissociation of complexes with magnetic ions, in units  $\Omega_c$ , coincide with the values of the Landé factor* for states, beginning with  $l = 1$ ,  $j = \frac{3}{2}$ .

Accounting for ions' nuclear spins in interference effects opens up promising possibilities for identification of MF targets. Since for magnetic, i.e., possessing a spin, ions the position of frequency spectral peaks is dependent not on the “charge-to-mass” ratio, but on a more specific ion–isotope constant  $\Gamma$ , identification becomes more reliable. Moreover, interference at magnetic ions gives a qualitatively different behavior in transitions from relatively weak MFs to stronger ones, when spin–orbit

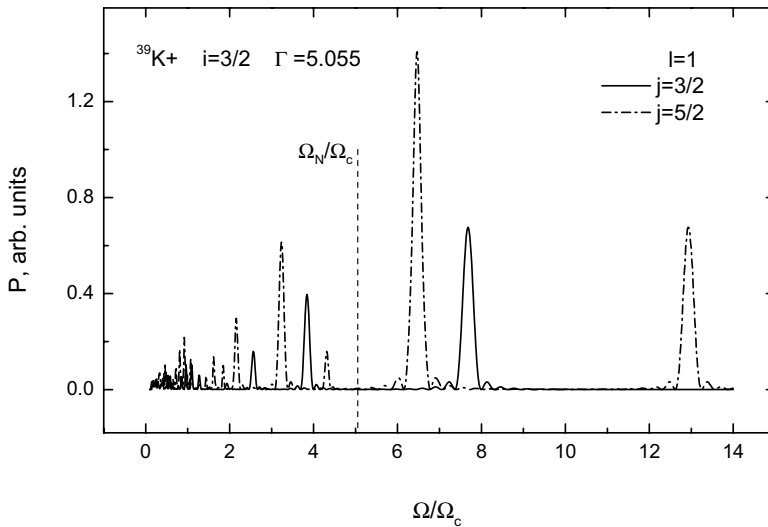


**Figure 4.29.** Dissociation spectra for a potassium–protein complex in a uniaxial MF,  $h' = 1.8$ ,  $\Xi = 10$ .

interaction becomes insignificant.

#### 4.8.2 Spin patterns in a uniaxial MF

Let us consider another (non-interference) model that takes into consideration the spin of ions. Suppose that the probability of some biochemical process depends on the spin states of an ion. That could be, for example, a biochemical reaction involving a proton transfer. Spin states to be discussed later are close in essence to polarized spin states, i.e., states with a chosen sense of the spin “vector”, see Addendum 6.3. For convenience, we will adopt an interpretation of quantum mechanics in which the uncertainty of non-commuting observables is referred to the measurement procedure; i.e., we can talk about a vector whose components cannot be measured at the same time. We recall that the predictions of quantum mechanics concerning the observables do not depend on an interpretation employed (e.g., Sudbery, 1986). The fact that there are more than 10 various interpretations of quantum mechanics is just a reflection of attempts to arrange and account for its postulates in a more appropriate manner.

Formulas for the MF dependence of process probability look like those that are obtained in considering the interference of angular orbital modes of an ion. Both cases are identical, which is seen for a DC MF. In the previous model, the magnetic moment of an ion’s orbital motion precessed, which implied that interference

antinodes of ion probability density rotate. Now an ion's spin magnetic moment precesses. Precession frequencies, of course, vary:  $\Omega_c/2$ , for the precession of the orbital magnetic moment, and  $\Omega_N$ , for the precession of the spin magnetic moment.

As before, a superposition of an additional parallel variable MF with definite parameters can sort of slow down the precession. The magnetic moment will then have preferred senses: one (polarization), two opposite ones (patterns), or several ones. Therefore a particle's spin also acquires preferred orientations. If a biochemical process occurs in some correspondence with spin selection rules, which is a postulate of a given model, then its rate will change.

For a proton in a uniaxial MF  $H_z = H_{DC} + H_{AC} \cos(\Omega t)$  the spin Hamiltonian is

$$\mathcal{H} = -\gamma\hbar\mathcal{I}_z H(t) ,$$

where  $\gamma$  is the gyromagnetic ratio for the proton. The Hamiltonian is diagonal in the matrix representation of the eigenfunctions  $\nu_1, \nu_2$  of the operator  $\mathcal{I}_z$ ; therefore, there are no quantum transitions in these states. The mean value of the spin component along the  $z$  axis is conserved. At the same time, other components of the spin "vector" undergo oscillations. We now find the spin component along the  $x$  axis, i.e.,  $\langle\mathcal{I}_x\rangle$ . We obtain the solution to the Pauli equation  $i\hbar\partial\Psi/\partial t = \mathcal{H}\Psi$  by substituting into it the expansion  $\Psi = \sum_k c_k\nu_k$  and using  $\mathcal{I}_z\nu_k = I_z\nu_k$ ,

$$c_k(t) = c_k(0) \exp\left(i\gamma I_k \int_0^t H_z dt\right) .$$

Here  $I_k$  are the eigenvalues of the spin component operator. Further, we write, taking account of the action of the Pauli matrix  $\sigma_1|\nu_m\rangle = |\nu_{\bar{m}}\rangle$ ,

$$\begin{aligned} \langle\mathcal{I}_x\rangle &= \left\langle \sum_k c_k\nu_k \left| \mathcal{I}_x \right| \sum_m c_m\nu_m \right\rangle = \frac{1}{2} \sum_{km} c_k^* c_m \langle\nu_k|\sigma_1|\nu_m\rangle \\ &= \frac{1}{2} \sum_{km} c_k^* c_m \delta_{k\bar{m}} = \frac{1}{2} (c_1^* c_2 + c_1 c_2^*) . \end{aligned}$$

Substituting the derived expansion coefficients and denoting

$$c_1^*(0)c_2(0) = c \exp(i\varrho) ,$$

we find

$$\langle\mathcal{I}_x\rangle = c \cos\left(\Omega_N t + h' \frac{\Omega_N}{\Omega} \sin(\Omega t) - \varrho\right) .$$

We will here omit  $c$  and  $\varrho$ , the parameters that define the orientation of a spin at the initial moment of time, which are insignificant for our further reasoning. It is clear that the average  $x$  component, and also the  $y$  component, can be written as the real  $\Re$  and imaginary  $\mathcal{I}m$  components:

$$\langle \mathcal{I}_x \rangle = \Re \exp \left[ i \left( \Omega_N t + h' \frac{\Omega_N}{\Omega} \sin(\Omega t) \right) \right] \quad (4.8.10)$$

$$\langle \mathcal{I}_y \rangle = \Im \exp \left[ i \left( \Omega_N t + h' \frac{\Omega_N}{\Omega} \sin(\Omega t) \right) \right] . \quad (4.8.11)$$

We now see that the spin “vector” rotates or precesses unsteadily. For certain MF parameters the field acquires some preferred orientations and scans them relatively quickly. The rate of a spin-dependent biochemical reaction is assumed to change if a spin for a relatively long time is oriented in some direction or its orientation changes while slowly passing through that direction. The probability for such a situation to occur is determined from any of its components (4.8.10), e.g., from the  $x$  component of a spin. We write, as before, the sliding average over the interval  $T$ :

$$\langle \mathcal{I}_x \rangle_T = \Re \left\{ \frac{1}{2\Omega T} \int_{\Omega(t-T)}^{\Omega(t+T)} \exp \left( i \frac{\Omega_N}{\Omega} \tau \right) \exp \left( i h' \frac{\Omega_N}{\Omega} \sin \tau \right) d\tau \right\} .$$

It is similar to (4.1.9) with a distinction that there is no summation over indices of magnetic quantum numbers, and the parameters assume the values

$$z = h' \frac{\Omega_N}{\Omega} , \quad \alpha z = \frac{\Omega_N}{\Omega} .$$

Therefore, using (4.1.12), we write

$$\langle \mathcal{I}_x \rangle_T = \Re \left\{ \sum_n \exp [i(\alpha z + n)\Omega T] A_n \right\} = \sum_n A_n \cos [(\alpha z + n)\Omega T] ,$$

where

$$A_n = \frac{\sin [(\alpha z + n)\Omega T]}{(\alpha z + n)\Omega T} J_n(z) .$$

Working out the mean square of the last expression, which by a postulate is related to the rate of a biochemical reaction, we find

$$\overline{\langle \mathcal{I}_x \rangle_T^2} = \sum_n A_n^2 \overline{\cos^2 [(\alpha z + n)\Omega T]} = \frac{1}{2} \sum_n A_n^2 .$$

Here we have taken into account the fact that the terms of the product  $\langle \mathcal{I}_x \rangle_T \cdot \langle \mathcal{I}_x \rangle_T$ , containing the factors, cosines with various arguments, i.e.,

$$\cos [(\alpha z + n)\Omega T] \cos [(\alpha z + n')\Omega T] , \quad n \neq n' ,$$

vanish on the final time averaging.

Thus, we must write the sought probability

$$P = \sum_n \left( \frac{\sin [(\alpha z + n)\Omega T]}{(\alpha z + n)\Omega T} \right)^2 J_n^2(z) .$$

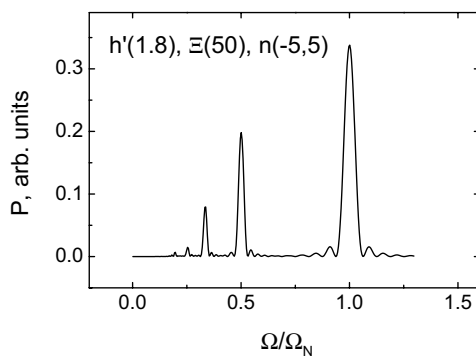


**Figure 4.30.** The frequency spectrum of the reaction with its probability dependent on the spin states of the proton. Calculations by formula (4.8.12).

In dimensionless variables  $h' = H_{AC}/H_{DC}$  and  $f' = \Omega/\Omega_N$ , since  $(\alpha z + n)\Omega T = (1 + f'n)\Xi$ , the formula becomes

$$P = \sum_n \left( \frac{\sin[(1 + f'n)\Xi]}{(1 + f'n)\Xi} \right)^2 J_n^2 \left( \frac{h'}{f'} \right), \quad \Xi = \Omega_N T. \quad (4.8.12)$$

The result of the calculation following the scheme

$$h'(1.8)f'(0-1.3)\Xi(50)n(-5-5)$$

is given in Fig. 4.30. The height of the spectral probability peaks falls off quickly with decreasing frequency due to the properties of the Bessel functions, and the shape of the curve is independent of the initial conditions. These latter define the relative value of the magneto-dependent part of the reaction probability, which is maximal for equally populated spin states.

The amplitude spectra are identical to those obtained earlier, Fig. 4.28. The frequency spectrum for a purely spin model

$$f'_{\max} = -\frac{1}{n} \quad (4.8.13)$$

differs from the dissociation spectrum for a hydrogen complex in the weak field approximation (4.8.9), since the location of the main peak coincides with the NMR frequency for the proton. That enables one to obtain experimental information on which of the two proposed MBE spin mechanisms is adequate to one specific situation or another.

## 4.9 COMPARISON OF THEORETICAL CALCULATIONS WITH EXPERIMENT

The path from a magnetic signal to a biological reaction is of necessity concerned with many factors at the biochemical and physiological level. Because of the sheer number of these factors and their uncertainty, there is no accounting for them. Transformation of electromagnetic energy into biological response can occur along several metabolic ways simultaneously (Berg and Zhang, 1993). Furthermore, biosystems can be sensitive even to such exotic factors as the temperature derivative of about 1 °C/h, which yield MBEs of the opposite sign (Blackman *et al.*, 1991).

The foregoing imposes some limitations on the way experiment and theory could be juxtaposed. Theory in magnetobiology is mainly aimed at accounting for primary biophysical mechanisms of magnetic reception, which is why its predictions are bound to be constrained by the level of physico-chemical processes. At the same time, predictions are nearly always compared only with biological data. As mentioned above, because of the many unaccountable factors, cause-effect situations are quite ambiguous here. It is no good idea, therefore, to juxtapose with calculations separate experimental points and even monotonous sections of curves. It would rather be more reasonable to juxtapose sections of dependences with extrema, although with some reservations.

If perturbations caused by an MF at the level of biophysical structures are small, then it is possible to employ a linear approximation for a multilevel non-linear system that relates these perturbations with the biological reaction being measured. If a biophysical response to an MF has several peaks, biological reactions on the MF will have several peaks as well. It is thus possible to compare the experimental evidence and theoretical predictions about *magnetic conditions* of the appearance of peaks, i.e., MF parameters that provide an extremal MBE.

In the general case it is possible to get a substantially non-linear response of a biological system to changes at the level of biophysical structures, where one extremum at the biophysical level corresponds to several extrema of the biological reaction *R*. Figure 4.31 shows how one maximum splits into two. Dependences like those in Fig. 4.31–b have been measured only rarely (Liboff *et al.*, 1987b); therefore, a linear approximation more often than not is quite justified.

Since a correct criterion of agreement of theory and experiment in magnetobiology is a coincidence of observed and computed *conditions* for reaction peaks to occur, all the forms of computer dependences obtained by shifting and scaling along the *y* axis are to be viewed as equivalent. Further, when comparing the findings it is assumed that such a transformation of theoretical curves or experimental data is conducted in order to arrive at the most perfect visual fit.

### 4.9.1 Frequency spectra

Alipov and Belyaev (1996) studied the biological response of *E. coli* K12 AB1157 cells to a combined MF by the scheme

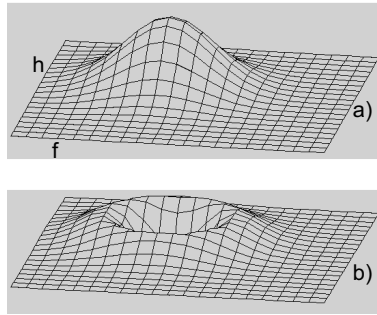


**Figure 4.31.** Non-linear transformation of an extremal dependence: (a) the dependence of the  $C$  enzyme density on MF frequency  $f$  and amplitude  $h$ ; (b) the dependence  $R(f, h)$  with a non-linear response to the enzyme density.

$$B(43 \pm 1)b(30)f(6-69)B_p(19 \pm 1) .$$

Maxima were found at frequencies of 8.9, 15.5, 29.4, and 62 Hz. There is also a small maximum at 44 Hz.

Calculations by (4.1.23) were performed for the  $^{40}\text{Ca}^{2+}$  ion and the above-mentioned values of fields  $H_{AC}$ ,  $H_{DC}$ . The perpendicular component, according to the findings of a special study (Belyaev *et al.*, 1994), was ignored. The period of sliding averaging approximately corresponded to the dissociation constant for the Ca-calmodulin complex:  $T = 0.1$  s. The cyclotron frequency was  $f_c = \Omega_c/2\pi = 32.9$  Hz. The best coincidence of relative peak heights in theory and experiment occurs at the following values of the density matrix elements:  $a_{mm'} = 1$  for  $\Delta m = 1, 2$ ,  $a_{mm'} = 0.5$  for  $\Delta m = 3$ , and  $a_{mm'} = 4$  for  $\Delta m = 4$ .

Computed curve and experimental evidence (Alipov and Belyaev, 1996) adapted to dimensionless frequency are provided in Fig. 4.32. We notice satisfactory agreement between theory and experiment for all maxima that straddle the cyclotron frequency  $f_c$ .

It is seen that the experimental peaks are slightly shifted to lower frequencies relative to theoretical values. Such a “red” shift of MBE maxima can be caused by a loss of some ion charge as a result of its binding. In fact, any chemical bond, including a relatively weak bond of ion type, presupposed a shift of an external electron cloud of a ligand in the direction of the ion — cation. As a result, the effective ion charge  $q$  decreases. Since the frequencies of MBE peaks vary with  $\Omega_c = qH/Mc$ , it implies their red shift.

As follows from Sections 4.4 and 4.5, the perpendicular component of a DC MF has no meaning for rotating complexes. If we assume that a given MBE was caused by a reaction of stationary complexes, then to determine cyclotron frequencies we will have to use the magnitude of the MF vector, which in this case is  $47 \mu\text{T}$ . The most suitable are ions of Mg,  $f_c = 59.3$  Hz, and Na,  $f_c = 31.4$  Hz. Calculations for Na are shown in Fig. 4.32. It is seen how difficult it is to identify ion targets.

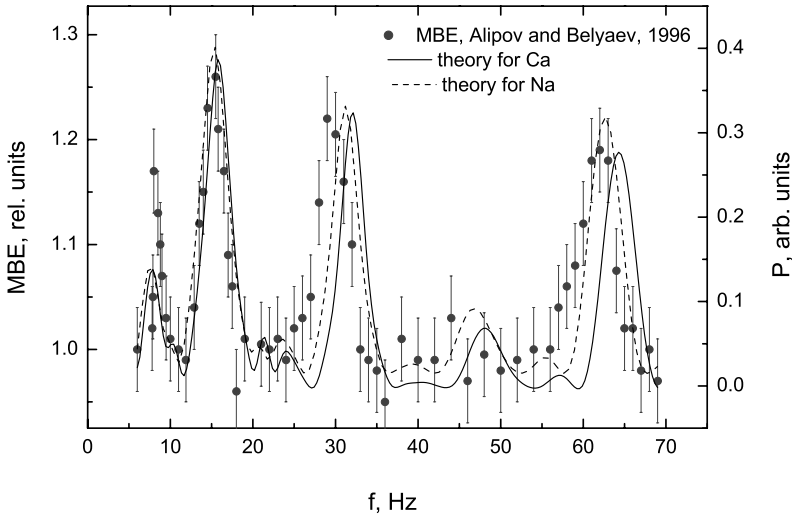


**Figure 4.32.** Interference spectra according to (4.1.23) for calcium and sodium ions and experimental data (Alipov and Belyaev, 1996) showing changes of suspension viscosity of *E. coli* cells in a combined MF.

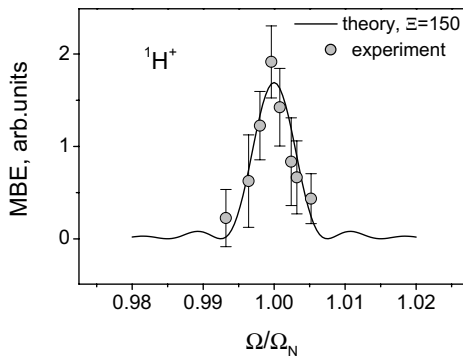


**Figure 4.33.** Comparison of calculated (formula (4.8.12)), and experimental (Lednev *et al.*, 1996b) frequency spectra of MBE near the NMR frequency of protons  $^1\text{H}$  in a uniaxial MF.

Perhaps, contributing to the formation of that spectrum are various ion species, and also rotating complexes.

- The frequency spectra for MBE on neoblast cells of regenerating planaria were

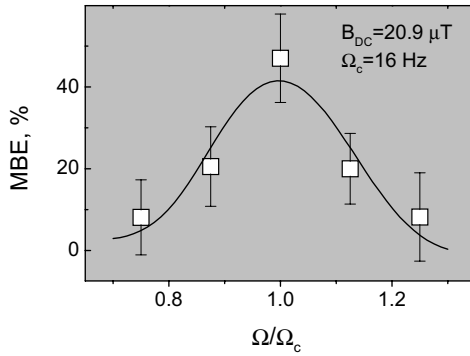


**Figure 4.34.** Experimental data for MBEs on planaria (Lednev *et al.*, 1996a) near the cyclotron frequency of  $^{40}\text{Ca}$  ions and a curve computed by the formula for ion interference.

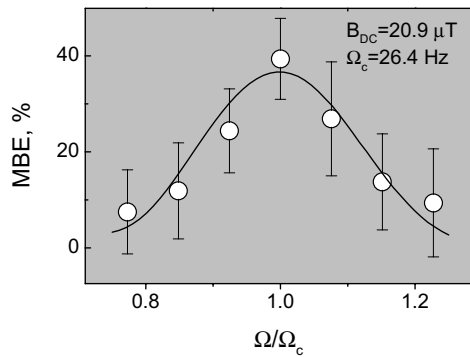


**Figure 4.35.** Experimental data (Lednev *et al.*, 1996a) and an appropriate theoretical curve near the cyclotron frequency for  $^{24}\text{Mg}$ .

studied at near-NMR frequencies of hydrogen atoms (Lednev *et al.*, 1996b) and in the range of cyclotron frequencies for  $^{40}\text{Ca}$  and  $^{24}\text{Mg}$  ions (Lednev *et al.*, 1996a). The following experimental scheme for hydrogen was employed:

$$B(42.74 \pm 0.01)b(78.6 \pm 0.8)f(1808-1830/\sim 3) .$$

The resonance-type frequency dependence with a 10-Hz-wide maximum at the NMR frequency for protons is shown in Fig. 4.33 in the form of several experimental points. The theoretical curve was computed by (4.8.12) at  $|n| \leq 3$ , and within experimental accuracy it coincides with the experimental evidence.

To measure spectra near cyclotron frequencies they used the schemes

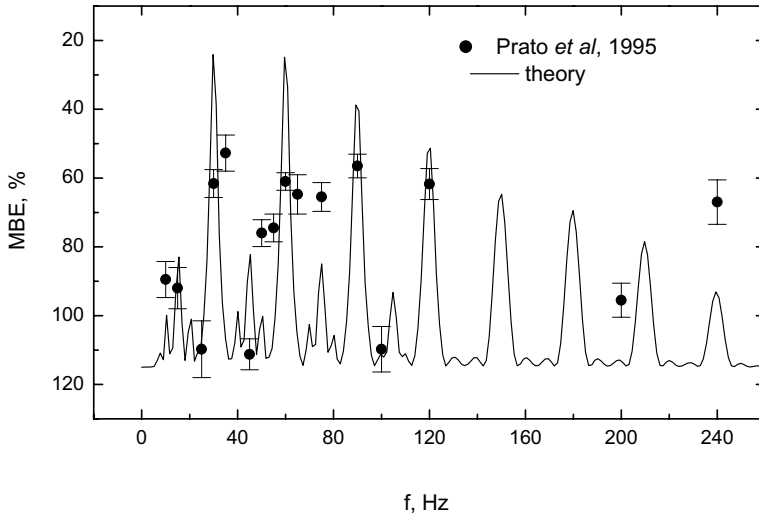


**Figure 4.36.** Matching of the calculated frequency spectrum for calcium ions and experimental findings (Prato *et al.*, 1995) for the MBE in land snails exposed to an MF  $H_{DC} = 78.1 \mu\text{T}$ ,  $H_{AC} = 141 \mu\text{T}$ .

$$B(20.9 \pm 0.1)b(38.4 \pm 0.1)f(12-20)T(11 \pm 0.5^\circ\text{C})$$

for calcium and

$$B(20.9 \pm 0.1)b(38.4 \pm 0.1)f(20.4-32.4)T(10.5 \pm 0.5^\circ\text{C})$$

for magnesium. Figures 4.34 and 4.35 display measurements of the mitotic index of cells and computations using the ion interference formula. The best fit is obtained when we take into account interference levels  $m = \pm 1$  and the bond parameter  $T = 0.09\text{s}$  for calcium, which agrees with the value  $T = 0.1\text{s}$  found by juxtaposing theoretical calculations with observations (Alipov and Belyaev, 1996). For magnesium the best value of the bond parameter was  $T = 0.06\text{s}$ .

• Prato *et al.* (1995) reduced the MBE frequency spectrum for land snails measured at  $B(78.1)b(141)f(10-240)$ . The spectrum has several extrema, and therefore it is suitable for correlations with theoretical calculations. The calculations were made for the  $^{40}\text{Ca}$  ion according to the scheme

$$h'(1.8)f'(0-4.3/0.02)\Xi(27)m(-4-4)n(-3-3)a(1) .$$

The data correlations results are shown in Fig. 4.36 and, by and large, they are in reasonable agreement. It is seen that the experimental data are not detailed enough for the spectrum peaks to be reliably identified.

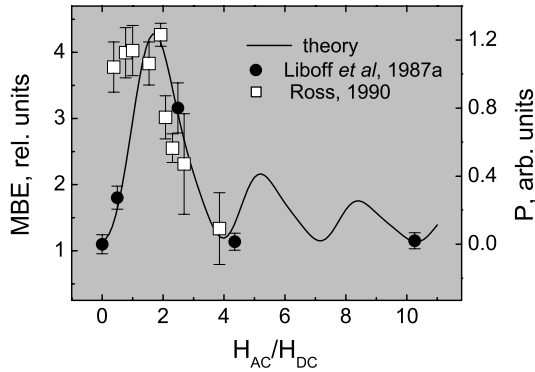


**Figure 4.37.** Comparison of the theoretical amplitude spectrum of interference with experimental findings (Liboff *et al.*, 1987a) on incorporation of calcium tracers into human lymphocytes.

#### 4.9.2 Amplitude spectra

Liboff *et al.* (1987a) studied the incorporation of  $^{45}\text{Ca}$  tracers into human lymphocytes exposed to combined parallel DC and AC MFs. The experiment scheme was chosen with due account of planned adjustment to the cyclotron frequency of that calcium isotope

$$B(21)b(0-220)f(14.3) .$$

The authors observed a marked growth of the MBE at  $b \approx 28 \mu\text{T}$ .

The theoretical curve was computed by formula (4.1.23) in a relative amplitude range of  $h' = 0-11$  at a cyclotron frequency  $f' = 1$ . All the matrix elements were taken to be unity. Account was also taken of interference of states with magnetic quantum numbers not larger than 2. Experimental data (Liboff *et al.*, 1987a) were represented as a dependence on a dimensionless relative amplitude and matched to the theoretical curve on the same graph, Fig. 4.37. It is seen that experimental points are in good agreement with the curve.

- Proliferation of fibroblast cells in a combined AC–DC field was studied by Ross (1990). He varied both the amplitude of an AC MF and the magnitude of a vertical DC MF component. The horizontal component of an external local MF was not controlled. Since assays were carried out in a five-layer steel incubator, it would be safe to assume the external field to be markedly reduced. Figure 4.37 is a plot of amplitude spectrum points for optimal scaling and shifting. The picture shows a more or less satisfactory agreement with the calculated curve.

Figure 4.38 displays a dependence on the magnitude of a DC MF, together with the calculated curve under the same magnetic conditions. It is seen that a treatment

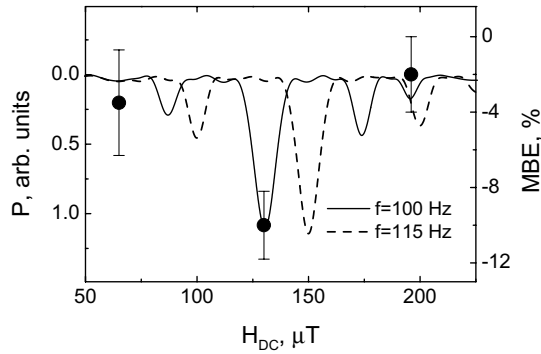


**Figure 4.38.** Proliferation of fibroblast cells as a function of the DC MF at amplitude  $250 \mu\text{T}$  and frequency 100 Hz of an AC MF, according to Ross (1990). Calculation for  $^{40}\text{Ca}$  ions under the same conditions.

using a frequency that is at variance with the experimental one does not supply a good fit anymore.

- Experiments of Prato *et al.* (1993) following the scheme

$$B(78)b(18-547)f(60)B_p(\pm 0.8)n(8-31)$$

were conducted for comparison with predictions by the formula proposed in Lednev (1991). No good agreement was achieved. These findings were later adapted by Blanchard *et al.* (1995), who compared the degree of fit for Lednev's and Blackman's calculations (Blanchard and Blackman, 1994). They indicated that neither formula is capable of predicting the dependence obtained.

Given in Fig. 4.39 are data (Prato *et al.*, 1993) and calculation results by the ion interference formula. We see here satisfactory agreement of theory and experiment. Later Prato *et al.* (1996) reported a reproduction of these results under the conditions

$$B(78.1)f(60)b(< 0.2, 141, 299, 414)n(\sim 25) .$$

These data also agree with theoretical calculations, although to a lesser degree, Fig. 4.40.

- The ion interference model predicts that an MBE is independent of a simultaneous proportional variation of  $H_{\text{DC}}$ ,  $H_{\text{AC}}$ , and  $f$ . It is clear that here the relative frequency  $f'$  and amplitude  $h'$  remain unchanged. It was found by Prato *et al.* (1997). The authors conducted experiments by the scheme

$$B(39k)b(70.5k)f(30k)n(\sim 33)k(1, 2, 4)$$

with an exposure of snails to a magnetic field in the dark and light. All in all, the trial included six experiments: three MF regimes and two illumination regimes. Six

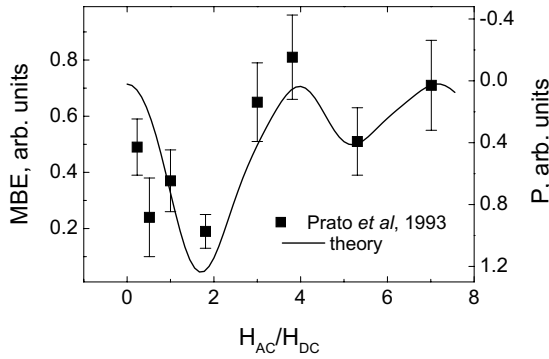


**Figure 4.39.** Comparison of experimental findings (Prato *et al.*, 1993) with calculations by the formula of the interference model.

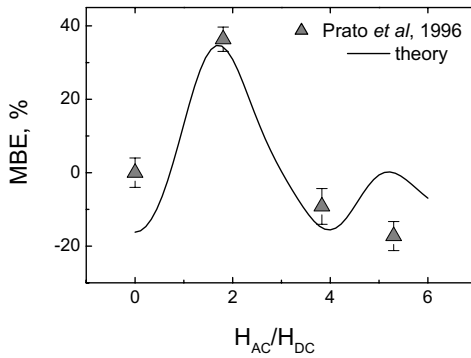


**Figure 4.40.** Experimental data (Prato *et al.*, 1996) on MBE for land snails at the  $^{40}\text{Ca}$  cyclotron frequency, and a theoretical curve.

controls where conducted at  $b(0 \pm 0.2)$ . The magnetic conditions corresponded to a cyclotron frequency of  $^{40}\text{Ca}$  ions. The results are represented in Fig. 4.41, and they agree with the model's predictions.

- When discussing the experimental data of Garcia-Sancho *et al.* (1994) on the influence of an MF on the uptake of a  $^{42}\text{K}$  radioactive tracer in Ehrlich cancer and human leukemia cells, it was pointed out that these are suitable for comparison with theoretical calculations. In fact, the utilized MF configuration corresponds to that considered in the basic interference model for bound ions. Although proteins, which are responsible for potassium binding, their structure and biochemical role are unclear; it made sense to compare model predictions with experimental evidence,

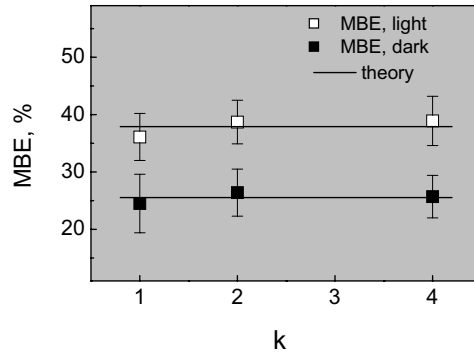


**Figure 4.41.** Unchanged MBEs for a simultaneous proportional, with a factor of  $k$ , change in MF variables. Experimental findings of Prato *et al.* (1997).

considering the possible generality of the molecular interference. To this end, the formula for dimensionless variables (4.1.23) was used, into which parameters of appropriate experiments were substituted. All the elements of the density matrix were assumed to be equal to unity. We recall that the elements control the relative height of various interference maxima. Since in this experiment they observed only a single extremum, the selection of the values of density matrix elements on the whole is immaterial. The comparison results are given in Fig. 4.42 where calculations follow the schemes

$$B(0.41)b(1.41)B_p(\sim 0)f(13.5-16.5/1)n(8-24)$$

$$B(0.41)b(0.71, 1.41, 2.82, 14.1)B_p(\sim 0)f(14.5, 15.5)n(8-24)$$

for frequency and amplitude spectra, respectively.

Here agreement of experiment and theory is fairly conventional in nature, especially in the case of comparison of amplitude dependences of the MBE. At the same time, there is no sign of acute contradiction, since the motif of the figures on the whole is the same. The number of experimental points is insufficient for any additional evidence to be derived. We note that Garcia-Sancho *et al.* (1994) also reported that they observed an effect for a perpendicular orientation of magnetic fields, which was discussed in Section 4.4.

- In addition to frequency spectra, Lednev *et al.* (1996b) measured the MBE amplitude spectrum. The experimental scheme  $B(20.87 \pm 0.01)b(0-80/\sim 20)f(889)$  was chosen so that to measure the amplitude dependence at  $\Omega_N$  for hydrogen atoms. The amplitude dependence had a maximum at a ratio of the amplitude of an AC field to the magnitude of a DC field of 1.8, Fig. 4.43. There is a good agreement with the theoretical curve calculated using the formula for the ion interference (4.8.12),  $|n| \leq 3$  for MF parameters that correspond to the experiment. A description of the experiment is available in the review section.

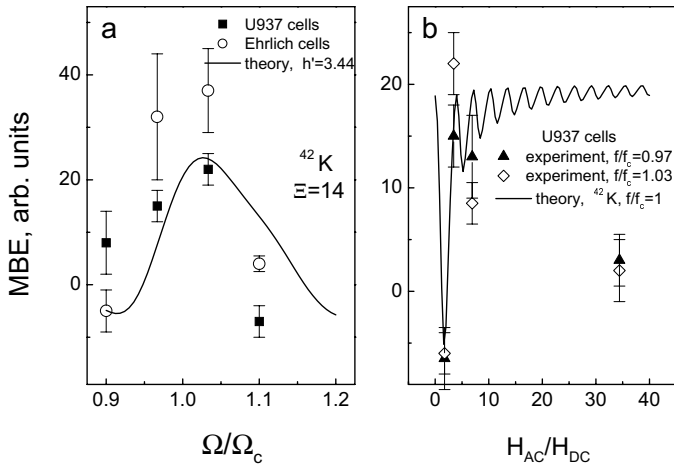


**Figure 4.42.** Comparison of data (Garcia-Sancho *et al.*, 1994) with calculations by the formula (4.1.23) for the  $^{42}\text{K}^+$  ion: a, frequency spectrum; b, amplitude spectrum of the interference of bound ions.

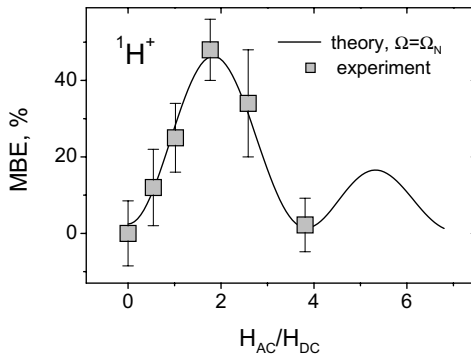


**Figure 4.43.** Theoretical amplitude of the spectrum by (4.8.12) and experimental spectrum (Lednev *et al.*, 1996b) at the proton NMR frequency.

Lednev *et al.* (1996a) also obtained amplitude spectra on planaria at cyclotron frequencies corresponding to ions of calcium

$$B(10.4 \pm 0.1)h'(0-3.6)f(8.0 \pm 0.1)$$

and magnesium

$$B(20.9 \pm 0.1)h'(0-3.8)f(26.4 \pm 0.1) .$$

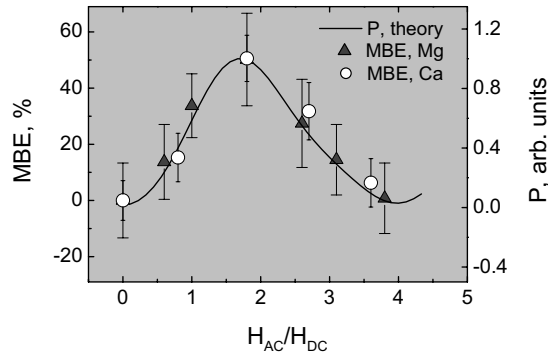


**Figure 4.44.** Comparison of MBE data (Lednev *et al.*, 1996a) in regenerating planaria at the cyclotron frequencies of  $^{40}\text{Ca}$  and  $^{24}\text{Mg}$ .

Shown in Fig. 4.44 are experimental points, and also a theoretical curve for the ion interference model. Here also we see convincing agreement.

#### 4.9.3 Spectra of rotating complexes

Theoretical analysis and experimental findings show that MBE amplitude spectra obtained using the ion interference mechanism are virtually independent of the type of ions involved in magnetoreception. This enabled data obtained on different biological systems to be compared with the same theoretical dependence. Within a 10% accuracy, that dependence is given by  $J_1^2(h')$ . At the same time, as was shown in Section 4.5, for rotating complexes the shape of amplitude spectra is dependent on the ion species. In the special case where the following relationships are obeyed,

$$\Lambda' = -\frac{1}{2} \pm \frac{1}{4}, \quad f' = \frac{1}{2}, \quad (4.9.1)$$

where  $\Lambda'$  is the relative rotation frequency, amplitude spectra are close to the specified function of a double argument,  $J_1^2(2h')$ . Experimental conditions in works by Blackman *et al.* (1994, 1995b), where such spectra were observed, meet these conditions nearly exactly if we assume the following.

Involved in magnetoreception are  $\text{Li}^+$  ions bound with proteins, rotating at 18 or 63 rps. Less acceptable are  $\text{Mg}^{2+}$  ions on proteins, rotating at 8.1 or 38.1 rps. These ions, just like lithium ions, were discussed also in the above works as possible targets for an AC–DC MF.

Interestingly, amplitudes of spectra of any other ions at any other rotation speeds were far from agreement with experiment. Spectra worked out by (4.5.1) are given in Fig. 4.45, together with adapted experimental data. In this figure we used the argument  $\alpha h'$ . Here  $\alpha$  is a coefficient, which makes it possible to employ the same curve  $J_1^2(\alpha h')$ , both for stationary and for rotating complexes. For these latter, the

**Table 4.1.** Quantities to compute spectra Fig. 4.45 for rotating complexes

Ion	$H, \mu\text{T}$	$f_c, \text{Hz}$	$f' = f/f_c$	$\Delta m$	$\Lambda'$	$f_{\text{rot}} = \Lambda/2\pi$	$\alpha$
H <sup>+</sup>	2.96	45.05	1	4	-0.25	11.25	-2
H <sup>+</sup>	2.96	45.05	-1	4	-0.75	-33.8	2
Li <sup>+</sup>	36.6	81	0.556	2	-0.222	18	-1.8
Li <sup>+</sup>	36.6	81	-0.556	2	-0.778	-63	1.8
Mg <sup>2+</sup>	36.6	46.2	0.975	3	-0.175	8.1	
Mg <sup>2+</sup>	36.6	46.2	-0.975	3	-0.825	-38.1	

MF frequency  $f = \Omega/2\pi$  equaled 45 Hz in all the cases as in experiments (Blackman *et al.*, 1994, 1995b; Trillo *et al.*, 1996; Blackman *et al.*, 1999). The angular velocity  $\Lambda' \equiv \Lambda/2\pi f_c$  for Li ions was calculated for the best visual fit of the curve to the experimental data, i.e.,  $\Lambda' = -(1 + \alpha^{-1})/2$  at  $\alpha = \pm 1.8$ . The sign of  $f'$  implies right or left rotation, in relation to the MF sense.

coefficient  $\alpha$  is specified, which imposes constraints on suitable ion types and the rotation speed for the complex.

We note that comparisons of predictions of ion interference in perpendicular MFs with experiments (Blackman *et al.*, 1996), see Section 4.4, also pointed to lithium ions as a likely target for an MF in MBEs on PC-12 nerve cells.

Trillo *et al.* (1996) and Blackman *et al.* (1999) conducted experiments on those cells, also shown in Fig. 4.45, in MFs tuned to a cyclotron frequency of the H<sup>+</sup> hydrogen ion. It is possible to approximate these data, if an MF excites interference states with magnetic quantum numbers that differ by four,  $\Delta m = 4$ . To have an agreement, the argument of the Bessel function  $J_1$  must be equal to  $\pm 2h'$ . On the other hand, the relative frequency  $f'$  is unity, as in experiment. This requires that  $\Delta m = \pm 4$ , see (4.5.4). We then obtain a relation, the same as in (4.9.1), for the angular velocity:  $\Lambda' = -\frac{1}{2} \pm \frac{1}{4}$ . All the parameters and main quantities needed to compute the spectra are given in Table 4.1.

The spectrum for the H<sup>+</sup> ion is worked out using (4.5.1) with the parameters taken from the table. The spectrum coincides with a similar spectrum for Li<sup>+</sup> ions. It displays good agreement with experiment, except for a narrow range at the peak center. A sharp drop in the MBE at the maximum center cannot be explained in terms of the mechanism under discussion. It was assumed in Blackman *et al.* (1999) that responsible for that could be different mechanisms or different H<sup>+</sup>-binding sites acting in opposite directions.

#### 4.9.4 Pulsed MFs

The influence of a pulsed sequence of MFs on the gene transcription rate was studied by Aarholt *et al.* (1982). They found a multipeak dependence of the rate on the size of rectangular MF pulses in the range of 200–660  $\mu\text{T}$  at a repetition

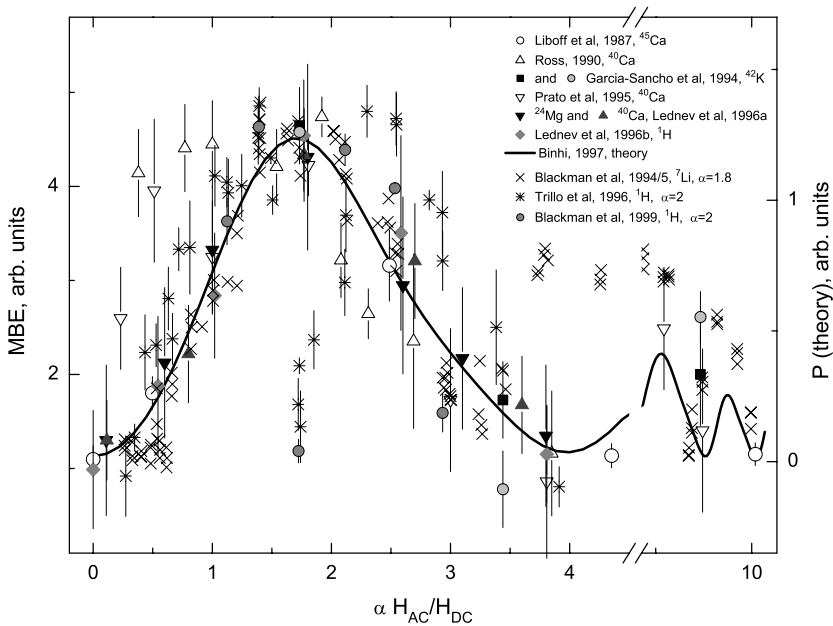


**Figure 4.45.** Experimental evidence (Liboff *et al.*, 1987a; Ross, 1990; Blackman *et al.*, 1994; Garcia-Sancho *et al.*, 1994; Blackman *et al.*, 1995b; Prato *et al.*, 1995; Lednev *et al.*, 1996a,b; Trillo *et al.*, 1996; Blackman *et al.*, 1999) for MBEs in a uniaxial MF, Ross (1990) noted a weak perpendicular component of a DC MF. The theoretical amplitude spectrum, solid line, was derived for fixed ion–protein complexes (factor  $\alpha = 1$  was not shown), and also for rotating complexes (a value of  $\alpha$  is shown).

rate of 50 Hz. The authors assumed that the transcription rate was influenced by a protein-suppressor that suppressed the synthesis; the activity of that protein was in turn controlled by a magnetic field.

That work contained no information on the magnitude and direction of the local DC MF and on the pulse duration. For comparison with calculations by the formula for interference in pulsed fields, a DC field was taken to be parallel to an AC one and equal to the mean geomagnetic field.

The interference mechanism for any one type of ion–protein complex predicts a change in one direction of the biological reaction for all the amplitude–frequency MF windows. At the same time, there is evidence for an oppositely directed action of an MF in various windows. A 16-Hz MF is reported (Dutta *et al.*, 1994) to boost the activity of enolase enzyme by 60%; a 60-Hz field reduced the activity by 25% against controls. Also observed (Garcia-Sancho *et al.*, 1994) were opposite effects of the uptake of  $^{42}\text{K}$  isotopes in some cancer cells on changes in the frequency or amplitude of the variable MF component. Such oppositely directed actions of an

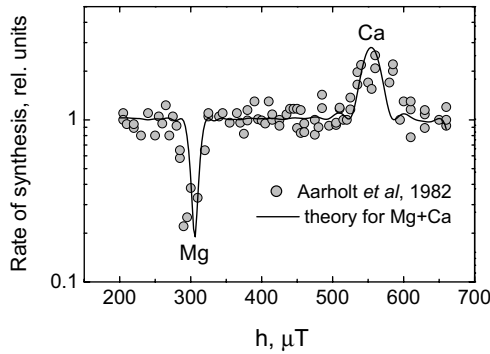


**Figure 4.46.** Comparison of data (Aarholt *et al.*, 1982) on gene transcription rate in *E. coli* exposed to a pulsed MF with calculation results. Given is the weighted sum of curves for magnesium and calcium ions.

MF were related to the fact that MF targets may be different ions, which cause opposite bioeffects (McLeod *et al.*, 1987a). Later the idea of the presence of effects that compete for the sign was shared by other authors.

The experimental evidence in Fig. 4.46 also points to two oppositely directed extrema in the action of an MF. This author assumed (Binhi, 1998a) that oppositely directed MBE extrema in pulsed MFs are also formed by responses of different ions, namely of calcium and magnesium, since they can compete for binding sites. Calculations followed the same scheme for both ion types

$$H(50)f(50)h(200-660)\tau(0.013)T(0.2)m(-1-1)r(-2-2)$$

by (4.3.6). For the best fit with the experimental curve, the sum of dependences for both ions was taken with weights  $-0.5$  for Mg and  $1.3$  for Ca. Figure 4.46 displays the result of a superposition of experimental points and theoretical curve.

- A change by 14% of the surface negative charge of U937 human cells,  $P = 0.03$ , in a pulsed MF was observed by Smith *et al.* (1991). The pulsed sequence consisted of pulse bursts occurring at a frequency of  $f = 25$  Hz. Each burst contained  $N = 22$  sawtooth pulses with a height of  $h = 630 \mu\text{T}$ , the leading front of  $\tau_1 = 200 \mu\text{s}$  and the trailing edge of  $\tau_2 = 20 \mu\text{s}$ . Under these conditions, an entire burst can be regarded as one pulse, since the interburst spacing was much larger than the burst duration. The “area” of such a composite pulse is  $\xi = Nh(\tau_1 + \tau_2)/2$ . No data on the DC MF magnitude were supplied; therefore agreement with theory could imply that the values of  $H_{\text{DC}}$  calculated by the maximum rule (4.3.2) are consistent

$$\xi = \frac{1}{b} \frac{2\pi r}{\Delta m} - \frac{H_{\text{DC}}}{f}.$$

It is easily seen that by selecting integer coefficients within relatively narrow intervals  $r \in [-1, 1]$ ,  $\Delta m \in [-1, 1]$ , one can find values of  $H_{\text{DC}}$  from the most likely range  $(-50, 50) \mu\text{T}$ , such that the rule (4.3.2) will be met exactly for ions of the series Ca, Mg, K, Na,  $b = 241, 394, 123, 210$ , respectively. So, for the main maximum  $r = 0$  we find for all ions that  $H_{\text{DC}} = -38.1 \mu\text{T}$ . We recall that the rule (4.3.2) at  $r = 0$  corresponds to the mutual compensation of a local DC field and a constant component of the sequence of pulses and therefore is independent of the type of ions. For maximum  $r = 1$ ,  $\Delta m = 1$ , we have  $H_{\text{DC}} = 36.7 \mu\text{T}$  for sodium ions and  $H_{\text{DC}} = 27.1 \mu\text{T}$  for calcium, etc. Thus, predictions of the interference mechanism for bound ions in pulsed MFs do not contradict the experimental evidence (Smith *et al.*, 1991).

- The data due to Mooney *et al.* (1986) also do not contradict the interference mechanism. They used phytohemagglutinin to encourage the blastogenic activity of mononuclear blood cells. It appeared that a 72-h exposure to 3-Hz MF pulses of  $h \sim 4.5 \text{ mT}$  and duration of  $\tau \sim 5 \text{ ms}$  reduced by 20% in a statistically meaningful manner the exit of traced thymidine. The parameters of a local MF were not specified, but the product  $f\tau h \sim 60 \mu\text{T}$  as a whole corresponded to the range of pulsed interference. At the same time, a maximal electric field induced by pulses was, according to the authors' estimates, nearly 23 mV/m. That does not exclude another MBE mechanism, which specifically utilizes interference in a low-frequency electric field, see Section 4.6.

#### 4.9.5 DC MFs and a magnetic vacuum

The experimental evidence of Lednev *et al.* (1996a) on the growth of proliferative activity in regenerating planaria with a decreasing DC MF down to the level of its daily geomagnetic variations together with calculated curves is represented in Fig. 4.47. It is only natural that if an MF is totally compensated for, all the ions participating in magnetosensitive processes of ion binding may respond to that compensation. In a zero MF Zeeman level splitting vanishes for all the particles at once. Contributions of various ions to an observable can then have unlike signs. It is complicated to separate the contributions. Some information on which ions determine the biological response in a near-zero MF can be derived from the width of a maximum on the MBE vs field dependence. Figure 4.47 provides curves calculated by (4.5.1),  $\Lambda = 0$ , for various ions, those of  $^{40}\text{Ca}$  and  $^1\text{H}$ .

The calculations relied on the value of the bond characteristic time  $T$  obtained from the best fit of theoretical frequency spectra and evidence from other experiments. For calcium  $T = 0.1 \text{ s}$  (Alipov and Belyaev, 1996); for hydrogen  $T = 0.036 \text{ s}$  (Lednev *et al.*, 1996b). Since, unlike calcium, hydrogen has a nuclear magnetic moment, two curves (1 and 2) were calculated for it: the first one with only spin dynamics taken into consideration. That made sense, since the appropriate value of  $T$  was obtained from comparison with an experiment where only spin effects were of consequence. The best agreement gives the assumption of hydrogen-dependent

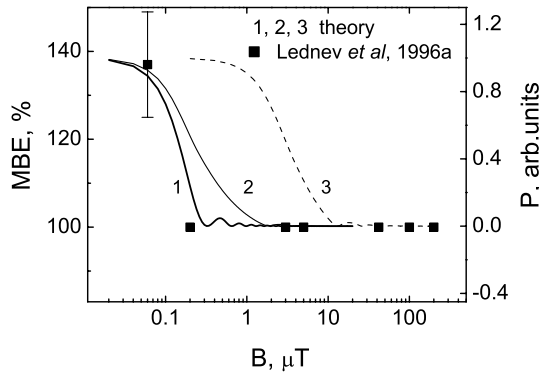


**Figure 4.47.** Theoretical curves in a DC MF for  $H^+$ , 1,2;  $Ca^{2+}$ , 3 and MBE according to Lednev *et al.* (1996a). Curve 1 was obtained considering only the spin dynamics of  $H^+$  ions.

processes in a zero MF. It was assumed in Lednev *et al.* (1996a) that contributions of other ions in regenerating planaria, those of calcium, magnesium, and potassium, exposed to a zero field are mutually compensated for. The role of orbital angular states of hydrogen requires a clarification on the basis of experimental data using MF frequencies that correspond to the cyclotron frequency of the proton.

- Data of Belyaev *et al.* (1994) on changes in the viscosity of suspension of lysed *E. coli* cells exposed to a DC MF together with calculation by (4.5.1) are represented in Fig. 4.48. Computations were carried out assuming that an experimental curve is a superposition of responses of various ions. Tested were various biologically important ions of Li, K, Na, Mg, Ca, and Zn. Binhi *et al.* (2001) showed that a satisfactory approximation can be achieved only for a unique superposition of contributions of ions of magnesium, calcium, and zinc at the same angular velocity of ion–protein complexes

$$P_{\text{sum}} = -P_{\text{Mg}} + P_{\text{Ca}} + P_{\text{Zn}} . \tag{4.9.2}$$

Contribution of each of these ions was required. In Fig. 4.48 they are shown separately. The reaction time  $T$  of complexes that correspond to those ions was chosen to be  $T = 0.1\text{ s}$ . Other calculation details are as follows:  $|m| < 3$ ,  $|k| < 5$ ,  $a = 1$ ,  $c_k^2 = 0.5^{|k|}$ . What is important is that the parameter of the angular velocity of ion–protein complexes for all ion–proteins was the same,  $\Lambda = 110\text{ s}^{-1}$ , which corresponds to a rotation speed of 18 rps. For those conditions, the only, unique combination of Mg, Ca, and Zn ions proving a satisfactory agreement was found. For other values of  $\Lambda$  there were no suitable combinations of ions.

If the types of ion–protein complexes and the direction of their action are fixed, i.e., magnesium action opposing that of calcium, and zinc acting in the same direction as calcium, there only remains one parameter,  $\Lambda$ , for fitting calculated

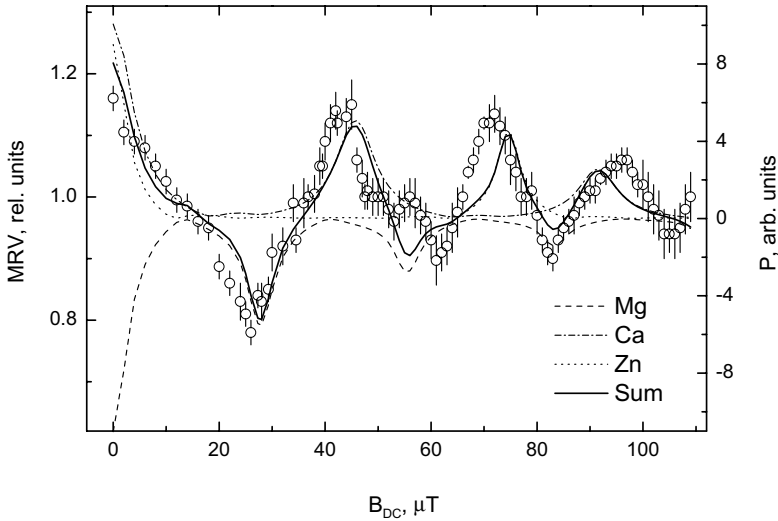


**Figure 4.48.** Approximation of MBE experimental data on *E. coli* cells in a DC MF by the formula for the interference of  $\text{Mg}^{2+}$ ,  $\text{Ca}^{2+}$ ,  $\text{Zn}^{2+}$  ions bound with a protein complex in a rotational state.

and observed positions of extrema. Physical mechanisms cannot predict the relative peak heights; they are rather determined by appropriate biochemical kinetics. Therefore, the relative weights (which appear to be the same) of contributions of ions and the width of their peaks, i.e., time  $T$ , were selected for the fitting of the entire curve only in order to stress the quality of agreement. It is interesting that the time of conformational reactions for calcium and magnesium coincided with quantities used earlier, and even some small details of the shape of measured peaks found their reflection in the calculations. We note that, mathematically, an approximation of a multippeak curve would require varying several parameters, one per extremum. It appears that good agreement of calculated and measured extrema achieved by the varying of only one parameter, the rotation speed of the complexes, is a corollary of the assumption that it is precisely rotating complexes that are involved in magnetoreception.

It was assumed in Binhi *et al.* (2001) that a probable common carrier of specified ion-protein complexes is DNA in the process of transcription. The rate of the process is about 40 nucleotides per second. It is accompanied by rotation of some proteins, specifically of RNA-polymerase, around the DNA (Cook *et al.*, 1992). It is well known that each RNA-polymerase molecule in *E. coli* cells binds two zinc atoms (Miller *et al.*, 1979). At those sites zinc ions can be replaced by magnesium and other two-valence ions (Panth *et al.*, 1991), thus changing the activity of a pro-

tein and the rate of the process. The DNA spiral period being 10 pairs of bases, the expected rotation speed is 4 rps, which is not at variance, as far as the order of magnitude is concerned, with the found rotation speed of 18 rps. Thus, the protein rotation speed in the transcription process can be one of the most important parameters of the process, which governs its reaction to an MF. We note the coincidence of that velocity with the possible rotation speed of Li-protein complexes in PC-12 cells, found above from a juxtaposition of amplitude spectra. A classical example of other biomolecular rotations are the flagellar mover and ATPase (Noji *et al.*, 1997).

#### 4.9.6 Spectra in an electric field

The scatter of experimental data on EF biological effects is much larger than in similar experiments with magnetic fields. This seems to be due to the fact that an EF has poorly predictable microscopic gradients that influence the position of spectral peaks. Unlike EFs, microscopic magnetic fields are only engendered by magnetic moments of atomic nuclei, but an area within a capsule is relatively far from a water medium with protons, emitting an MF, and the nuclei of ligands, such as  $^{16}\text{O}$ , are not magnetic.

Bellow is given a summary of results for two groups of experiments, depending on the way an EF is applied to a biological tissue; indicated are approximate windows for EF variables in which a statistically significant biological effect was observed.

In the first experimental group specimens were placed between the capacitor plates, without a direct electrical contact. Bawin and Adey (1976) measured the efflux rate of  $^{45}\text{Ca}$  ions from a chicken brain tissue pre-enriched in ions and subjected to an EF. They observed a 15% reduction in calcium efflux for EF parameters in the range of 3–24 Hz, 10–60 V/m. Fitzsimmons *et al.* (1989) reported that a bone cell culture increased the proliferation rate by 50% when exposed to a field of 12–20 Hz, 430 V/m. Nazar *et al.* (1996) observed a drop in the specific activity of enolase by 20% in a field of 10–70 Hz, 65 V/m. In all the experiments the response of a biological system was measured only for several values of the variables. It is hard, therefore, to connect the evidence with the behavior of some smooth curve. We can make a general conclusion, however, that in these experiments the activity window of an EF is roughly associated with a low-frequency range of 10–100 Hz and EF intensities of 10–100 V/m.

In the second group of experiments an EF in a medium was produced using electrodes immersed in the medium. Also measured was the current in the circuit, and the value of the EF could be worked out from the voltage drop across additional measuring electrodes. McLeod *et al.* (1987b) observed a 30% decrease in the rate of DNA synthesis in a collagen matrix with imbedded fibroblast cells exposed to an 1–10 Hz EF, the current density being  $> 1 \mu\text{A}/\text{cm}^2$ . Blank and Soo (1990) registered a 15% drop in the activity of Na,K-ATPase in a special-purpose enzyme suspension with a substrate for 20–1000 Hz,  $> 70 \mu\text{A}/\text{cm}^2$  fields. Blank *et al.* (1992) measured a 30% growth of the transcription rate in a HL-60 cell culture at 60 Hz,  $0.3\text{--}3 \mu\text{A}/\text{cm}^2$ . Goldman and Pollack (1996) and Cheng and Goldman (1998) also observed a 60%

change in the DNA synthesis rate in a collagen matrix with human fibroblasts in windows of 10–100 Hz,  $3\text{--}8\ \mu\text{A}/\text{cm}^2$ . It follows that in such experiments one can expect an EF effectiveness window in a range of 10–100 Hz,  $0.5\text{--}50\ \mu\text{A}/\text{cm}^2$ .

The expected frequency window of EF effectiveness at 10–100 Hz coincides for both groups of experiments. In relation to amplitude windows we note the following. In the first group of experiments, the mean EF within the medium is about one-hundredth of the external one, because of the dielectric polarization of water with  $\varepsilon \sim 80$ . Effective dielectric permittivity of a medium with cells can, as was shown by Chew (1984), grow several times more owing to the special properties of ions of a double electric layer that surrounds the charged surface of cell membranes. That is, an effective internal EF falls at least within the range of about 100–1000 mV/m or even lower. In the second group of experiments, an internal field can be worked out from the relation  $E = j/\sigma$ , where  $j$  is the current density in a medium, and  $\sigma$  is the electrical conductivity of the medium. For biological tissues, the order of magnitude of the conductivity is  $1\ (\text{ohm}\cdot\text{m})^{-1}$ . Hence the range of effective fields corresponds to the interval 5–500 mV/m.

Earlier data are extant on the sensitivity of fishes to very weak EFs of 50–500 Hz, 0.1–1 mV/m (Lissmann and Machin, 1963). In his concise overview Berg (1995) analyzed the variety of electric and magnetic conditions in relation to the biological processes of DNA–RNA synthesis, of enzyme activity, of calcium transport, and of cell proliferation. Conditions of electromagnetic stimulation were optimal mainly within a low-frequency range window for EF amplitudes of 10–100 mV/m.

Thus, also approximately coincident are amplitude windows for two groups of experiments. In any case, there are no grounds to maintain that the physical mechanisms responsible for biological effects in different groups are different. The above estimate of the internal EF,  $\sim 1\ \text{mV}/\text{m}$ , needed for ion interference caused by electron polarization of ligands to occur is consistent with experimental findings. It is not to be excluded that the ion interference mechanism underlies the observed windows of EF biological effectiveness. At the same time, for a conclusion to be reliable enough requires a large body of experimental evidence with detailed descriptions of dependences on EMF variables.

- Goldman and Pollack (1996) studied the proliferation of human fibroblast cells introduced into a collagen matrix with an AC current passed through the medium. Results including frequency and amplitude dependences for two measurables, viz. the rates of DNA synthesis and of the incorporation of thymidine traced with tritium, were analyzed in a work by Binhi and Goldman (2000). Experimental evidence was normalized to their control values and re-normalized to the unity values of maxima. They are shown in Fig. 4.49 and Fig. 4.50.

The findings were juxtaposed with theoretical conclusions contained in Section 4.6. As noted above, the locations of frequency peaks of interference in a variable gradient EF correspond mainly to Larmor and cyclotron frequencies. Static and relatively slowly varying gradients, which are due to the fact that ion systems are also close to other bound charges such as atomic groups with a dipole moment,

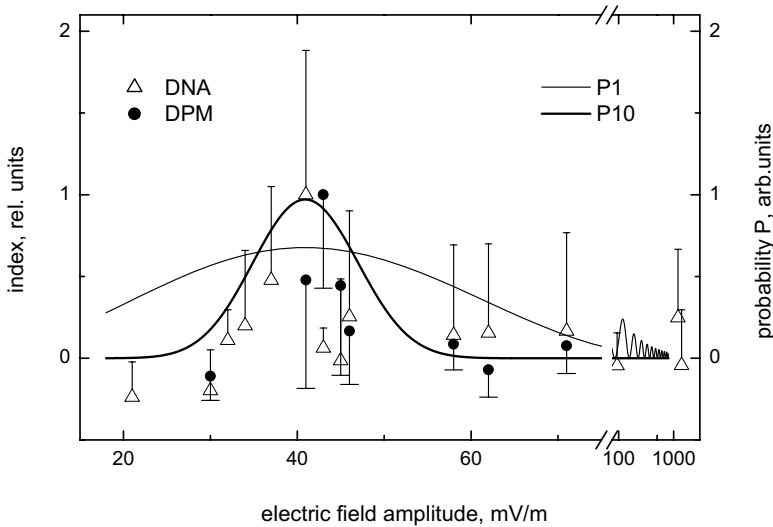


**Figure 4.49.** Amplitude dependences of human skin fibroblasts in an EF of 10 Hz from measurements:  $\triangle$ , of DNA synthesis;  $\bullet$ , of incorporation of  $^3\text{H}$ -thymidine. P1 is the dependence of the dissociation probability of an ion–protein monomer on the EF amplitude (4.6.15),  $E^* \sim 40 \text{ mV/m}$ ; P10, the same for an enzyme activated by 10 monomers.

shift spectral peaks to new locations depending on the values of those gradients. That suggests that it is necessary to average the theoretical dissociation probabilities over the possible values of static EF gradients. Such an averaging brings about a spreading of frequency peaks. Therefore, a relatively wide maximum of frequency dependences in Fig. 4.50 is explained by a wide distribution of quasistationary endogenous EF gradients near an ion target excited by exogenous variable gradients.

In contrast, experimental dependence on the amplitude is narrower than the theoretical dependence P1, Fig. 4.49. Binhi and Goldman (2000) note that a biochemical interpretation of this can be concerned with the availability of enzymes that include several similar subunits, or ion–protein monomers, each of which dissociates independently of others. For an enzyme to be activated, the state of all monomers must be the same within a characteristic time interval for a conformational transition of an enzyme to an active state. Clearly, the probability of enzyme activation by two monomers varies with the squared dissociation probability for a monomer; by three monomers, with the cubed probability. This narrows down the windows of field effectiveness parameters and drastically lowers the chances for an enzyme to be active with  $n$  monomers. However, if the enzyme molecule density is sufficiently large, the number of active molecules will be biologically significant.

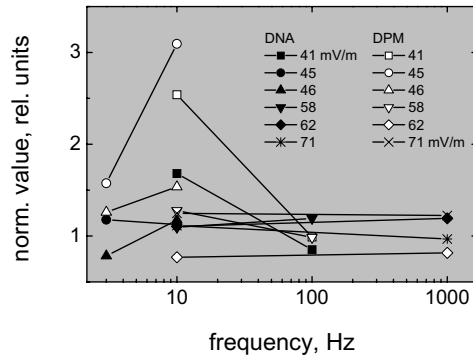


**Figure 4.50.** Normalized frequency dependences for fibroblasts in EFs of various amplitudes. Points for the same amplitude are connected by straight lines.

That idea is illustrated in Fig. 4.49 by curve P10. It is a result of raising the initial curve for the monomer to the tenth power and of subsequent appropriate scaling.

We note that a given mechanism is a “biochemical amplifier” of an external signal. Suppose, for instance, that the probability (per time unit) of natural dissociation of a monomer in the absence of constructive interference caused by some special combinations of excitation frequencies and amplitudes is  $P$ , and it grows just slightly when the excitation variables happen to be within an effectiveness window:  $P + P$ . We could associate with that case the signal-to-noise ratio  $P/P$ . The probability of natural activation of an enzyme with  $n$  monomers is  $W = P^n$ , since activation due to a wide variety of random factors, including noise electric fields and gradients, occurs independently for each monomer. In an effectiveness window it is  $W + w = (P + P)^n$ . In that case the signal-to-noise ratio, i.e.,  $w/W$ , as could be readily worked out in the approximation  $P \ll P$ , is

$$w/W \approx nP/P,$$

i.e., is  $n$  times better. That growth will be still more significant,  $\sim 2^n$ , if the probability  $P$  is comparable with the natural level  $P$ . We recall that these quantities are determined by the initial conditions for an ion in a binding cavity. In the initial excitation of states with small magnetic quantum numbers (by the way, only they can be excited by thermal perturbations of an ion in a binding cavity), the magneto-sensitive part of the dissociation probability is comparable with a permanent level.

- Beschkov and Peeva (1994) found a multipeak dependence of *Acetobacter suboxydans* cell proliferation on passing a DC electric current through a cell medium within a range of 0–100  $\mu\text{A}$ . Although we have not considered in much detail the theoretical dependence of the dissociation probability of ion–protein complexes on the DC electric field, a comment on a given experiment is possible from the viewpoint of

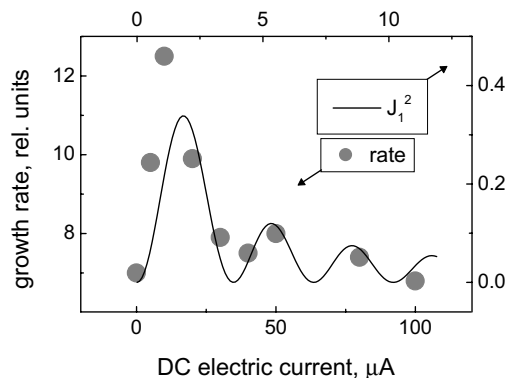


**Figure 4.51.** Dependence of cell growth rate on the magnitude of a DC current in the medium, according to Beschkov and Peeva (1994).

ion interference. It takes into consideration rotational states of many potential biophysical structures — targets for an electric field. In terms of rotating ion–protein complexes, an applied DC electric field is variable, and hence it causes variable EF gradients. Therefore, for rotating complexes the dependence of the effect on the value of an external DC field must be similar to the dependence on the amplitude of a variable field for relatively stationary complexes. The last one, as has been repeatedly shown above, has a motif of a squared first-order Bessel function. Figure 4.51 provides experimental data with a superimposed function  $J_1^2$ . Unlike exposure to a variable MF, the theoretical value along the abscissa axis, which has a meaning of the amplitude of variable EF gradients, is no measurable quantity. Therefore to juxtapose theory and experiment, we have to scale along both axes. This reduced the value of conclusions that follow from an agreement. However, in any case, the similarity of shapes of experimental and theoretical dependences is hardly an accident.

#### 4.10 HEURISTIC MBE PROBABILITY WITH VARIOUS IONS INVOLVED

Most of the biochemical transformations in an organism occur in the presence of enzymes, or biological catalyzers. Normally, in an enzyme they identify a center that contains a catalytically active group of non-protein nature, the so-called cofactor. Cofactors of many enzymes include ions of various metals, and also vitamins and their derivatives. The main reasons for high activity and specificity of enzymes are (1) the provision of correct orientation of reacting enzyme-substrate groups, (2) a competition of several catalytic groups of an active enzyme center, and (3) a strong departure of dielectric properties of a medium around an active center from appropriate values in a solution. These reasons account for an enhancement of the catalytic biochemical reaction by a factor of up to  $10^8$ – $10^{12}$ .

More than 3,000 enzymes are known. About one-third of them contain ions of complex-forming transition metals as cofactors. Many enzymes also have special intervals, where they interact with substances that control their catalytic activity. Such substances may also be metal ions and complex ions. Moreover, metal ions enter into the composition of non-enzyme proteins that perform important life-support functions. Thus, metal ions are often key triggers of some biochemical processes. Therefore, it is quite probable that they may take part in an MBE as targets for a magnetic field.

We will here cite some well-known examples (e.g., Volkenstein, 1983; Sybesma, 1989; Bergethon, 1998; Suckling *et al.*, 1998; Purich and Allison, 2000).  $K^+$  and  $Na^+$  ions provide for a naturally balanced acid–alkaline medium in the organism and excitation signal transfer processes along nerve cells. These ions are a working body of proteins, the so-called ion pumps, e.g., of  $Na,K$ -ATPase. The pumps produce an electric potential difference across a cell membrane by increasing the density of potassium in a cell, and of sodium in the extracellular medium.

Magnesium is a biological activator of enzyme groups, of kinases that are responsible for the transfer of phosphate groups from ATP molecules to various substrates.  $Mg^{2+}$  ions that are coordinationally connected with porphyrin ligands are the mainstay of the chlorophyll molecule, which takes part in photosynthesis in plants, algae, and some bacteria.

Calcium is very important for the workings of the organism.  $Ca^{2+}$  ions, by binding with some proteins, calmodulin, troponin C, etc., make these proteins to control the activity of many enzymes. Calcium ions contribute to many biological processes. In addition to enzyme activity, these are synaptic transfer, secretion, flagellar mobility, muscular contraction, proliferation, growth, and development.

Many enzymes contain  $Zn^{2+}$  ions: carboanhydrase, which decomposes carbon dioxide, carboxypeptidase A, which is involved in protein synthesis, phosphatase, etc. Zinc ions, as well as manganese and copper ions whose properties are close to zinc, encourage the transport of nutrients (oligopeptides) through the modulation of their affinity to binding sites of membrane carriers, which can be of physiological significance (Daniel and Adibi, 1995). A relation has been established between cancer occurrence with the amount of zinc in the organism and its relation with the workings of the endocrinal glands and the insulin system.

In metabolic processes,  $Mn^{2+}$  ions are in many respects similar to magnesium ions. Manganese is needed for the work of enzymes contributing to phosphorylation processes. It enters into the composition of pyruvate carboxylase and arginase, and stimulates the synthesis of vitamin C, cholesterol, and some liquid acids.

Molybdenum is a must for many biochemical reactions. It occurs in the coenzyme of the active center of nitrogenase, which catalyzes processes involving nitrogen. Aldehyde oxidase and xanthin oxidase, which are involved in purine exchange, also contain molybdenum. A molybdenum misbalance in the system causes some serious diseases. Plants contain molybdenum in nitratoreductase, which is important for nitrogen metabolism.

Iron enters into the composition of the porphyrin group and forms a heme

( $\text{Fe}^{2+}$  ion) or heme ( $\text{Fe}^{3+}$ ). In this form, iron occurs in hemo- and myoglobins and cytochromes, which are responsible for oxygen transport in the organism. A heme is available in catalase and peroxidase, which control the level of hydrogen peroxide in the blood. From one to several dozen  $\text{Fe}^{3+}$  ions, which hinder replication, are contained in a DNA molecule. Transferrin is a protein that transports iron in the organism.

Several dozen copper-containing proteins and enzymes are known: albumin, hepatocuprein ( $\text{Cu}^+$  and  $\text{Cu}^{2+}$  ions), cytochrome oxidase, albu-, cerebro-, and neurocupreins, thiosinase, and lysyl oxidase. In plants, copper is involved in the formation of chlorophyll.  $\text{Co}^{3+}$  ions belonging to the corrin group, which is similar to the porphyrin group, are contained in vitamin  $\text{B}_{12}$ , cobalamin. Also, cobalt  $\text{Co}^{2+}$  is an activator of carboanhydrase and carboxypeptidase. Chromium and nickel are relatively unimportant for biochemical processes. A dearth of chromium ions, however, may cause some diseases. Nickel activates trypsin, arginase, carboxylase, and other enzymes.

It is believed that cesium Cs and strontium Sr are necessary for the organism; however their physiological and biological roles are not yet clear. Rubidium ions  $\text{Rb}^+$  are used in experiments to replace potassium ions and to study biochemical processes that involve it. In the literature,  $\text{Li}^+$  ions were considered to be possible targets for an MF in mammal organisms. Classed with microelements are also vanadium and tin.

The abundance of inorganic ions in organisms is fairly high, on average one ion per several hundred water molecules. In such a “broth”, the interion spacing is not larger than 10–20 Å. The role of various ions in magnetobiological reception mechanisms has only recently become a subject of attention. Therefore, a prior *heuristic* analysis of possible contributions of ions to MBEs would make sense.

Ions that occur in living tissues, blood, cytoplasm, etc., vary widely in their ability to enter into various biochemical reactions. Some ions react easier with other molecules, and the rate of their metabolic turnover is higher. It would be natural to connect the effects of a weak MF precisely with such ions. The ability of chemical elements to enter into reversible reactions is mainly associated with their ionization potential, i.e., the energy needed to remove valence electrons. Also concerned with that quantity is the relative electronegativity of elements, i.e., their ability to attract the electrons of valence bonds. The most “mobile” are alkaline and alkaline-earth metals. Next come transition metals. Figure 4.52 provides data for the most biologically important elements.

It has been noted in the literature that harmonics and subharmonics of cyclotron frequencies of various ions are often very close to one another, which hinders the identification of their possible contribution to MBEs. It is natural, therefore, to construct an integral representation of spectral frequencies, at which, theoretically, a maximal MBE is possible.

A note is in order. Apparently, free ions in a solution are not targets for an MF. In that state, an ion possesses coordinates and a momentum, which in a weak MF vary quite insignificantly. Therefore, specifically, halogen ions in a solution, and

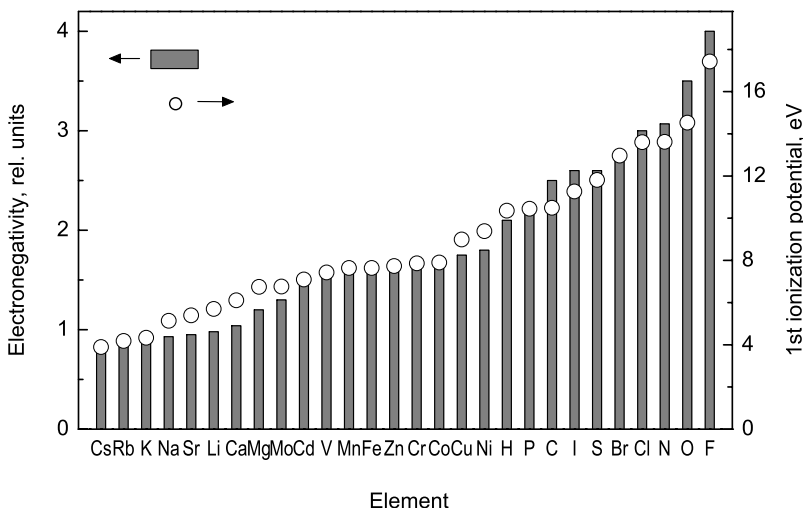


**Figure 4.52.** Electronegativity and the first ionization potential of some biologically significant elements.

also in fast covalent molecular bonds below, are not taken into consideration. Also, not considered are the elements Al, B, C, Si, N, P, O, S, which also form relatively strong covalent bonds.

Of more interest are bound ions, which play the role of a complex-former in the complex compound, a central cation surrounded by ligands. The coordination bond of a cation with ligands is markedly different for alkaline or alkaline-earth metals and for transition metals. With these former, by virtue of their small electronegativity, ligands form nearly ionic bonds. Electron clouds of bonds are concentrated at ligands, where normally elements with a larger relative electronegativity are present, such as O and N. In that case, the electric charge of a central ion (in electron charges) corresponds to or nearly equals its valence.

The situation is different with ions of transition elements, whose electronegativity is larger than that of alkaline and alkaline-earth metals. Now electron clouds are not markedly shifted to ligands, the binding is nearly covalent, and the charge of the central ion is shielded by covalent electrons. So,  $2+$  in the notation for  $\text{Fe}^{2+}$  in a heme does not correspond at all to its electric charge. This hinders the definition of cyclotron frequencies for nearly covalently bound ions of transition metals.

Hydrogen contributes to both covalent and hydrogen bonds, which dominate living media that are 90-95% water. Hydrogen bonds having specific properties, hydrogen atoms form  $\text{H}^+$ ,  $\text{OH}_3^+$  ions, etc., with a well-defined charge.

When considering a frequency spectrum of a cyclotron series, we will confine

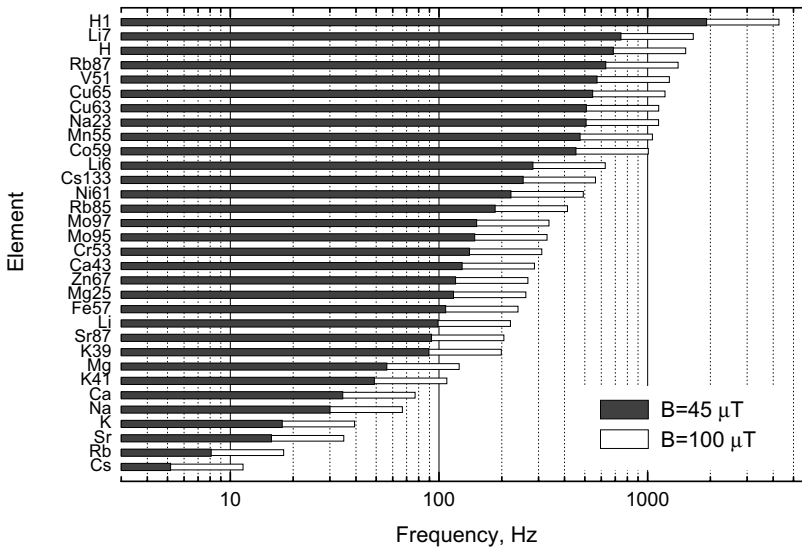
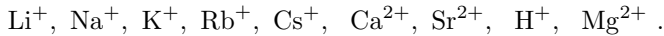
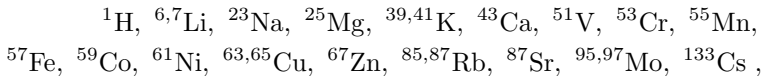


**Figure 4.53.** Cyclotron  $f_c = \Omega_c/2\pi$  and NMR  $f_N$  frequencies of ions and isotopes of vitally important elements. Corresponding to isotopes with their mass number specified is an NMR frequency.

ourselves to ions of alkaline and alkaline-earth metals, hydrogen, and also magnesium, which occupies an intermediate position in the series of electronegativities:



For spectral frequencies of an NMR series we will cite those isotopes with a nuclear spin that are significant for the life and whose natural abundance is larger than 1 %, and of  $^{43}\text{Ca}$ , because of the potential importance of that element. This list includes



see also Table 6.1. Cyclotron and NMR frequencies of specified elements in an MF of  $B_{\text{DC}} = 50 \mu\text{T}$  are represented in Fig. 4.53.

It is seen that cyclotron frequencies are mainly concentrated within the interval 10–100 Hz, and NMR frequencies, in the interval 100–1000 Hz. It is also apparent that these frequency intervals are filled unevenly. Figure 4.53 is not complete. Effective electric charges for ions of transition metals, as stated above, are unknown. Therefore, in the figure some values of  $f_c$  are absent. Since abundances of said isotopes are varied, the corresponding interference frequencies acquire some “weight”. Supplied for each interference frequency in Fig. 4.54 is the abundance of a given

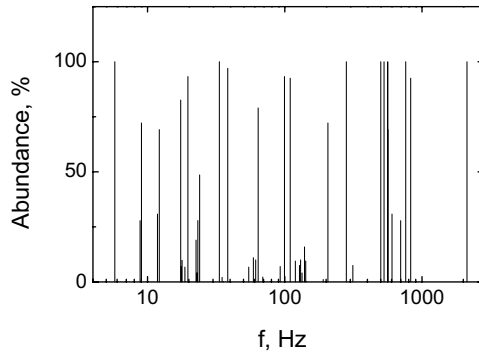


**Figure 4.54.** Spectrum of cyclotron and NMR frequencies and the abundance of appropriate elements.

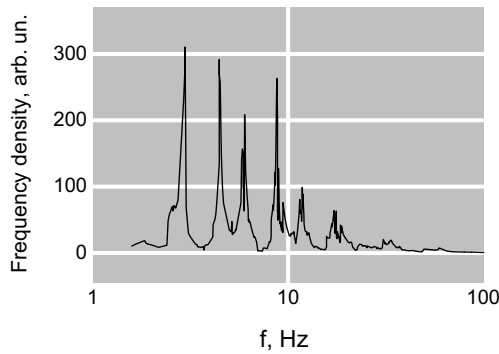


**Figure 4.55.** Density of interference frequencies of the cyclotron series,  $m = -2, \dots, 2$ ,  $n = 1, \dots, 4$  in the magnetic field  $B_{DC} = 50 \mu\text{T}$ .

isotope. It is seen that there are intervals on the frequency axis with a large total “weight” of respective spectral lines.

Cyclotron and NMR frequencies are defined here not because these physical mechanisms are involved in MBEs, but because bound ions respond at these frequencies and their harmonics and subharmonics. If we deal with the MBE interference mechanism, we will have to add to the above frequency series some satellites found by the formula for the spectrum of ion interference. Clearly, this gives rise to a fairly dense series of interference frequencies. We will confine ourselves to the spectrum of cyclotron series,  $f_{\max} = \Delta m f_c / 2n$ . We will estimate its density, considering that the relative “weights” of satellites are about

$$\frac{1}{\Delta m} J_n^2(n1.8),$$

provided *a priori* that all the matrix elements  $a_{\{i\}}$  are equal for an optimal ratio  $H_{AC}/H_{DC} \approx 1.8$ . We will evaluate the density as a ratio of the sum of the weights of interference frequencies that lie within a small interval to the width of that interval. A smoothed spectrum of interference frequencies thus constructed, with the natural abundance of elements taken into account, is given in Fig. 4.55.

This analysis does not cover, of course, complicated ions, which can also play an important role in MBEs, and ions of some transition metals with a charge that is not known *a priori*.

The curve in Fig. 4.55 is fairly conventional in nature. At best, if we regard the MBE sign and magnitude in a randomly chosen biosystem as random quantities, then we could with a measure of caution view the curve, or rather the square root of that function, as a *heuristic* estimate of the probability density for an MBE to be revealed using the ion interference mechanism under appropriate magnetic conditions.

#### 4.11 LIMITATIONS ON APPLICABILITY OF THE ION INTERFERENCE MECHANISM

Experiments indicate that in the general case genetically different kinds of cells of one functional orientation respond differently to an MF. Cancer cells of different kinds were studied in Garcia-Sancho *et al.* (1994). For *E. coli* cells of two kinds differences were observed not only in magnitude, but also in the positions of frequency peaks on the MBE spectrum (Belyaev *et al.*, 1996). Experimental evidence for the action of an MF on the mobility of diatomic algae is also dependent on the biological line of these organisms (Smith *et al.*, 1987). Peak frequencies can also depend on the states of the cell population. So, *E. coli* cells of stationary and logarithmic phases of population development displayed MBEs of unlike signs, and the peak frequency was shifting by 3–4% (Alipov *et al.*, 1994).

The interference model for bound ions does not explain these differences “in numbers”. It can be supposed that this is conditioned by different target ions in cells, or even by different combinations of ions. Such a supposition, clearly, puts that question outside the scope of a discussion from the viewpoint of physics. The question of why ions responsible for MBEs in some cells are such and in other cells of the same function they are different is essentially a biological question.

In terms of the ion interference model a significant factor for the shape of spectra is the population distribution of states with various magnetic quantum numbers at the initial moment of time, when an ion gets into a metastable state within a molecular capsule. It is clear beforehand that initial conditions must depend on a host of factors, largely on the conformational state of a molecule. It defines the physical characteristics of the ion gate. Consequently, such conditions as temperature, pressure, density of substances, on which the conformation of molecules itself is dependent, are also capable of changing the MBE spectrum shape. We note that

the temperature dependence of the MBE was observed in Jafary-Asl *et al.* (1983) and Blackman *et al.* (1991). Concentration dependences of the MBE are numerous (e.g., Aarholt *et al.*, 1982; McLeod *et al.*, 1987a; Belyaev *et al.*, 1995). The importance of biological parameters for MBE observations was stressed in Grundler *et al.* (1992). Such dependences also appear outside of the interference model; it only gives their qualitative treatment.

The model cannot as yet explain why sometimes effective are very small amplitudes of a variable MF against the background of a moderate parallel DC field. An estimate of frequency–amplitude boundaries is shown in Fig. 5.18. The base model gives a maximal effect for fields, both AC and DC, on the same order of magnitude. In Ruhenstroth-Bauer *et al.* (1994), Kato *et al.* (1993, 1994), and Loscher *et al.* (1994) they observed an MBE in a variable MF of about  $0.1 \mu\text{T}$ , which is 500 times smaller than the GMF level. Berman *et al.* (1990) and Farrell *et al.* (1997) studied the biological effects of low-frequency pulsed fields for  $\tau fh < 0.05 \mu\text{T}$ . It seems that other mechanisms are at work here. In Novikov and Zhadin (1994) and Novikov (1994, 1996) the effect occurred at a relative MF amplitude of about  $10^{-3}$  and did not occur at  $10^{-1}$ . It is quite probable that this is due to the presence of an electric field and a current in an electrochemical cell employed in those works. We recall that the interference mechanism for rotating complexes predicts a sensitivity to hyperweak MF. However, that would require the presence of quantum states with a lifetime of more than 10 s at physiological temperatures. *A priori* that seems unlikely, although structures like the molecular gyroscope, see Section 5.4, could provide such lifetimes for a gyroscopic degree of freedom.

There are many assays with a fairly satisfactory agreement of computed and experimental data. This suggests that behind theoretical mental processes there are real physical processes of interference, which could underlie some magnetobiological effects. The interference nature of the action of an MF on the angular modes of quantum states of ions and molecules, where only their phases are changed, is behind the fact that the energy needed for a noticeable bioeffect is fairly small.

The ion interference mechanism now describes multipeak effects of (a) an MF modulated in magnitude and direction; (b) a magnetic vacuum; (c) a DC MF with natural quantized and classical regular rotations of ion–protein complexes taken into account; (d) a pulsed MF against the background of a parallel DC MF; (e) an MF modulated in magnitude in the NMR frequency interval; (f) low-frequency electric fields; (g) an amplitude-modulated microwave field; (h) interference states of rotating molecular groups; (i) a shift of spectral peaks of dissociation probability in rotating biological specimens; and (j) magnetic noise. Theoretical predictions for ion interference (see Subject Index) were formulated so that they admit experimental checks.

At the same time, the ion interference theory is in a way phenomenological (except for the molecular gyro). Perhaps, it should be identified at the moment as a semi-phenomenological model. On the one hand, this theory has to do with the microscopic dynamics of particles, but on the other hand, it is built on the postulate of large lifetimes of angular modes and does not consider physical processes that

make for the conservation of the component of angular momentum along the MF direction.

Metastability of angular modes could be explained by the details of interaction of an ion with cavity walls. Electrostatically, an ion at the cavity center is not stable. It shifts to be bound more with some ligand. The process of the shifting of an ion and the response tuning of ligands have the same time scales as the oscillatory dynamics of the ion. Therefore, the idealized equation of ion dynamics must take into consideration the self-action of the ion. When the probability density of an ion is higher, its potential begins to diminish owing to the tuning of ligands. In the dynamic equation that corresponds to an additional Hamiltonian term proportional to the squared modulus of the wave function, it is this term that describes the self-action. The wave function sort of deepens the potential well for itself, especially where its density is large. The derived equation, up to the energy of interaction with an MF, is the non-linear Schrödinger equation, a soliton solution to which is known for the one-dimensional case.

Soliton states of an ion in a protein cavity account for the stability of dynamics under thermal perturbations. The action of thermal perturbations could be viewed as a further additive random factor that depends on time and coordinates. At a certain threshold amplitude of the random potential a soliton-like excitation breaks down fairly quickly. It is well known, however, that, as the perturbation amplitude grows further, long-lived soliton-like excitations can again be engendered (e.g., Davydov, 1987; Kadantsev *et al.*, 1988; Cruseiro *et al.*, 1988; Zolotaryuk *et al.*, 1991).

If the binding ligands are located at nodes  $\mathbf{r}_a$ , then for states of an MF-exposed ion we can write the following Schrödinger-type equation that takes into consideration both magnetic and thermal factors:

$$i\hbar \frac{\partial}{\partial t} \Psi(\mathbf{r}, t) = \left( \frac{\mathbf{P}^2}{2M} - \frac{q\hbar}{2Mc} \mathbf{LH} + \sum_a U_a \right) \Psi - \alpha \hbar \sum_a f(\mathbf{r} - \mathbf{r}_a(t)) |\Psi|^2 \Psi.$$

Here  $\mathbf{L} = -i\mathbf{r} \times \nabla$ , as before, is the angular momentum operator,  $U_a$  is the potential of an ion in the field of the  $a$ th ligand, and  $\alpha$ ,  $f(\mathbf{r})$  are model parameters. The fluctuating coordinate of the  $a$ th ligand  $\mathbf{r}_a(t)$  corresponds to the thermal oscillations of a medium. The numerical solution of such equations is realized sometimes in the form of soliton-like perturbations that are stable within some range of parameters of thermalizing factors.

It is quite likely that the interference theory for bound ions will only be a small step in the right direction. More sophisticated models will answer the question as to why the idealization of long-lived angular states is in such a good agreement with experiment.

# 5

---

## PROSPECTS OF ELECTRO- AND MAGNETOBIOLOGY

It states that the operation of counting modifies quantities  
and changes them from indefinites into definites.

*J.L. Borges, Ficciones/Tlön, Uqbar, Orbis Tertius*

### 5.1 POSSIBLE ROLE OF LIQUID WATER IN MAGNETOBIOLOGY

It has been established that water is an active element rather than a passive medium of biochemical processes. Water is a substrate carrying information which sensibly affects processes in a water medium. The qualitative characteristics of such an information charge may be formed by external physical impacts. This circumstance along with the fact of long-term memory of water opens a certain avenue for new methods of control of chemical, biochemical, and biological processes.

Biological activity of water is understood as its ability to determine (within known limits) the activity parameters of biological objects immersed in or associated with it. Under normal conditions (room temperature, atmospheric pressure, gas transfer to and from the environment, a natural background of electromagnetic fields), water attains, within a time span from a day to a few months, a quasi-stationary state that remains subsequently unchanged on the average. A time-average state over a rather long span of quasi-equilibrium will be termed an equilibrium state. Deviations from the equilibrium state are due to fluctuations or regular deviations of physical water-affecting factors from their normal level. An equilibrium water does not possess a biological activity by definition and serves as a control specimen of the natural medium. It should be clear that various physical and chemical properties of water come to equilibrium at different rates.

Physical impacts that condition water to impart a specific biological activity to it include magnetic fields, freezing and thawing to produce thawed water, degassing, and other factors. Depending upon the type of conditioning, the biological activity may be associated with a substantially reduced content of dissolved gases after outgassing, or else due to retaining tiny ice-like clusters after thawing, etc. In all cases, biological activity of water occurs as a consequence of water residing in metastable (non-equilibrium) states, whatever the nature of these states.

Water has long been drawing attention of researchers as a probable universal intermediary in transmitting electromagnetic signals to the biological level. In this case, the biological effect of EM fields is related to changed states of conditioned water (Kislovsky, 1971; Devyatkov, 1978; Klassen, 1982; Binhi, 1991b, 1992; Ayrapetyan *et al.*, 1994; Singh *et al.*, 1994; Fesenko *et al.*, 1995; Konyukhov *et al.*, 1995; Devyatkov *et al.*, 1996; Katin, 1996; Goldsworthy *et al.*, 1999). Water changes its state when immersed in conditioning fields. This change of state is transmitted to the biological level because this water is involved in a variety of metabolic reactions. If this chain of events is correct, it is intriguing to learn whether water could be conditioned by weak fields and could store its magnetic prehistory. For EM field exposure, it is interesting to know the target of EM fields in conditioned water.

Nuclear spins of water protons were thought to be prime targets for magnetic fields (Binhi, 1992). The magnetic moments of nuclear spins interact with the external magnetic field; simultaneously, spins take part in the spin-orbit interaction with the states of spatial degrees of freedom. It was hypothesized that singular quantum states of protons are metastable and can affect the birth and death rates of structural associates in water (Binhi, 1991a), and the rate of biochemical processes. However, a method to test this hypothesis has not been identified.

### 5.1.1 Experimental evidence for water memory

Abundant experimental evidence proves that liquid water has a memory of its physical and chemical exposure.

One of the physical impacts that renders water biologically active occurs in multiple dilutions of a substance (a procedure used, e.g., in homeopathy). A sequential dilution of an initial solution with water reduces the concentration of the dissolved substance to a level where there is virtually no molecules of the substance in the solution. However, at this level, as well as upon subsequent dilution, the water retains specific biological activity of the substance in some experiments.

Water media obtained in this way may be termed imaginary solutions (IS) (Binhi, 1991b). Alternatively they are called "ultra-diluted solutions", but this term refers to the preparation procedure rather than the property of the solution and leaves space for speculating on the presence of molecules of effective substance in the final solution.

One of the first observations of IS's biological activity in a specific biological test was reported as far back as the late 19th century. Experimenters used imaginary solutions of homeopathic substances, namely, aconite root, arborvitae, gold, and table salt. Solutions were prepared in a chemist's shop by a regular homeopathic procedure introduced in medical practice by Ch. Hahnemann around two centuries ago.

The biological parameter tested was the time of human response to a visual stimulus. Preliminary training imprinted automatic response in human subjects whereby the response time became independent of operator's will and thus reflected

objectively his or her internal state. Subjects were made to smell the “aroma” of an imaginary solution.

Butlerov, a known Russian organic chemist, described these experiments in 1882 as follows:

Leger experiments proved that homeopathic substances remain active after dilution to hundredth and thousandth fractions of their initial tincture. Moreover, they proved that the effect of homeopathic formulations is enhanced by dilutions, a common lore among homeopaths. ... In the initial tinct, aconite suppressed excitability, whereas dilutions increased it to peak at the 15th dilution. Further dilutions first reduce the effect of aconite to some degree, then enhance it to another peak (lower than the first one) at the 150th dilution. ... The characteristic features of this effect were identical for a 100th diluted aconite from different chemist shops. It is remarkable that an increasing effect up to the 15th dilution was found also for arborvitae, salt, and gold. This fact was stated identically by various experimenters. But the more remarkable fact is that table salt reveals the main maximum of its effect at the 2000th dilution, whereas it has its first maximum, like other substances, at the 15th dilution. (Butlerov, 1882, p.9)

Interest in the biological activity of ISs has been increasing in recent decades. Water memory research was reviewed by Burlakova (1994) and Binhi (1991b).

Water and water systems have been traditional objects of study in many fields of science. Eisenberg and Kauzmann (1969), Franks (1982), and Antonchenko *et al.* (1991) considered physical and chemical properties of water, and presented a history of pertinent research. Privalov (1968), Watterson (1988), and Aksenov (1990) discussed the role of water in biological systems and processes. We confine our attention to papers devoted to water memory or metastability in connection with electromagnetic exposure. Below we give a few recent publications on the subject. A review of engineering applications of magnetically conditioned water, researched in the 1960s and 1970s, may be found in a book of Klassen (1973).

- Berezinsky *et al.* (1993) demonstrated that conditioning a liquid water by a few mW/cm<sup>2</sup> of microwave radiation at 51.5 GHz for 5 min changed its refractive index by  $\Delta n = 2.5 \cdot 10^{-4}$ . This variation is 10 times the change in the sample index achieved with an equivalent thermal power. The effect had a frequency selectivity. It was measured with a He–Ne laser interferometer. Evidently, structural changes in water revealed by the polarizability of electrons have a relaxation time of at least 5 minutes.
- Singh *et al.* (1994) reported that water conditioned by microwave radiation influences the production of blue-green algae (cyanobacteria).
- Fesenko *et al.* (1995) demonstrated that a water solution used in measurements of the activity of calcium-dependent potassium channels memorizes exposure to microwave radiation. The activity of channels were measured by the “patch-clamp” method where a microscopic area of a membrane with channels covers the tip of a mini-pipette submerged in a solution and forms a part of an electric circuit.

Changes in channel activity changed current in the circuit. Since there were only a few channels on the test area and each of them can be in an open or closed state, the current changed discretely. Data processing yielded the probability of a channel to be in an open state. In these experiments, either the solution–membrane–pipette system (Geletyuk *et al.*, 1995) or the solution alone were exposed to 0.1–2 mW of CW 42.25-GHz microwave radiation for 20–30 minutes. In the last case, the conditioned solution was moved to replace an identical unconditioned solution in the system to observe how channel activities changed within a few minutes. Changes were the same as in the case of direct system exposure.<sup>32</sup> The changed state of the solution persisted for as long as 20 min. The effect of microwaves on the state of ion channels was attributed, at least partially, to changed properties of solutions. It was speculated that these changes might be due to gas transfer at the surface of solutions, specifically to a change in dissolved oxygen induced by microwave irradiation.

Indeed, Kazachenko *et al.* (1999) found that microwave radiation at this frequency, power density around 5 mW/cm<sup>2</sup>, and the above time of exposure reduced the concentration of oxygen dissolved in water and weak brines approximately by 1–3%. The conditioned water acquired a new physicochemical state stable to mechanical agitation and thermal convection. The new state persisted for over 4 h. Aeration of the water by bubbling changed the concentration of molecular hydrogen, but this change decayed within 10–20 min. A frequency dependence of this phenomenon was noted along with the fact that this dependence exists only in the presence of impurities (ions). The authors concluded that microwave radiation can affect the macrostructure of water set by impurities.

Fesenko and Gluvstein (1995) used a different physical method to study changes in water caused by microwave radiation. They measured how voltage oscillations across a capacitor filled with water decayed after a pulse excitation of the circuit. A computer analysis of low-frequency oscillations revealed two pronounced peaks near 5 and 47 Hz. Exposure of the cell to a 36-GHz field for several minutes suppressed the 47-Hz peak. This state of water persisted for several minutes or hours (depending on the strength of the exposure field) after the microwave field was shut down. It is remarkable that exposure to a 50- $\mu$ W/cm<sup>2</sup> field had a far more pronounced effect on the system than a hundred times stronger field. The authors discussed stable water-molecular associates that have a memory of electromagnetic conditioning.

- Konyukhov and Tikhonov (1995) and Konyukhov *et al.* (1995) reported observations of liquid water with deviations of ortho- and para- H<sub>2</sub>O from the equilibrium ratio, see Section 2.5. Using adsorption of water molecules from the gas phase sensitive to rotational state of the molecules, one can obtain an ortho-fraction enriched water taking advantage of the ortho-water spin-state control in a resonance magnetic field. This spin-modified water decays to the equilibrium state for dozens of

---

<sup>32</sup>Experiments indicating identical effects of EM-conditioned solutions of salts and solutions of salts produced by dissolving salts in an EM-conditioned water were reported by Kislovsky (1971), as far back as 1934.

minutes at a room temperature and for months at the liquid nitrogen temperature. Concentrations of fraction spin states were measured by the intensity of the respective lines in the rotational spectrum of water molecules in the microwave range. The authors assumed existence of a biological activity of spin-modified water.

- Pandey *et al.* (1996) reported that water conditioned in a permanent magnet affected the oestrus period or cycle in mice and their weight growth rate during the experiment (28 days). New portions of mouse drinking water were daily placed on the surface of permanent magnets for 1 to 8 h. The state of oestrus was also determined daily by microscopic studies of vaginal smears. On the surface of magnets, the magnetic field strength was 0.3 T. The proportion of elongated cycles turned out to be statistically significant,  $p < 0.01$ ; it increased by 40–80%, depending on the time of exposure. The weight increment in mice fed with conditioned water was 10–20%, whereas the control group increment was at most 2%. Rai *et al.* (1996) found that water conditioned in a similar way changed the rate of photosynthesis in unicellular green algae several times. Neither of the experimenters controlled gas transport between the liquid samples and the environment.

- Lobyshev *et al.* (1995) found that distilled water exhibited weak luminescence in the near ultraviolet and optical ranges. Emission spectra excited by UV light revealed relatively wide lines at 360 and 410 nm. The intensity of luminescence depended on the storage time of the water, conditions of preparation, presence of controlled impurity, and EM and thermal conditioning (Lobyshev *et al.*, 1999). The relaxation time of the metastable state ranged from hours to months. It is interesting to note it was an oscillation rather than an exponential process. The authors emphasized that these results could not be explained by the luminescence of impurities in the distilled water; rather, this luminescence was a property of the water. They assumed that it was associated with various types of defects in the water and molecular clusters or associates with characteristic emission centers. They speculated that the latter might be protons from the dissociated water.

Water luminescence spectra were also measured by Novikov *et al.* (1999). The authors used an earlier evaluated resonance mode of magnetic conditioning  $b(4 \cdot 10^{-2})B(42)f(3.7)$ , effective with respect to a number of solutions of amino acids. They measured the luminescence of a solution of bovine serum albumin and other proteins as well as luminescence of water. In the last case, after a 2–4 h conditioning, the intensity of both short-wave and long-wave luminescent bands increased several times. Addition of a conditioned water produced a specific effect on the albumin, which is comparable with the effect achievable by a direct conditioning of the solution by an MF. A many-hour memory of the water is evident. The authors explain this effect by the presence of macroscopic water clusters that might possess biological activity.

- Devyatkov *et al.* (1996) and Katin (1996) demonstrated a difference in the physiological state of an operator after intake of water conditioned by a microwave field of a commercial medical instrument as compared to the state after intake of an

unconditioned control sample of water. In either case, the human state was tested by measuring the potentials of biologically active points. Katin (1996) used a water conditioned for 15 min, and the changed state persisted for 4–6 h.

- Khizhnyak and Ziskin (1996) observed convective vortices in water exposed to a  $\sim 49$ -GHz microwave field beginning with rather low power densities of  $1 \text{ nW/cm}^2$ . After 20–40 min of exposure, vortices disappeared and failed to reappear under these conditions for  $\sim 4$  h. The authors believe that this stagnation could have been caused by an induced state of water with changed viscosity, perhaps, due to gas exchange.

- Interesting experiments demonstrating an EM exposure memory in water were performed by Berden *et al.* (1997). They used electro-photography to study a corona discharge (Kirlian effect), that occurs near the surface of water droplets on a photographic paper in a 12.5-kV, 45-kHz field. Photographs of simultaneous discharge of two droplets were digitally processed for eight parameters of the discharge pattern. Different patterns suggested different states of two identical water drops. Droplets differed only in details of water sample preparation.

They took initially identical glass containers with identical samples of water to immerse in it for a few hours quartz test tubes with germinating fir seeds both living and dying, and with larvae and case-worms of mealworm. Thus, they obtained chemically identical samples of water that differed from one another in changes induced by extremely weak radiation of living organisms. Each pair of compared samples was subjected to 20–45 repeated measurements. The difference in the photographs of respective droplet discharges proved to be statistically significant. The authors assumed that these differences reflected metastable changes in the water structure caused by a very weak EM radiation of live organisms. Earlier Jerman *et al.* (1996) demonstrated that similar changes in water had a biological effect on the rate of fir seed germination.

- Belov *et al.* (1997) demonstrated that the magnitude of water permittivity fluctuations increased when the water was subjected to mechanical agitation such as stirring or decantation. Fluctuations were studied in  $\sim 1 \text{ mm}^3$  of water placed between the arms of a capacitor with insulated electrodes. The test alternator operated at a frequency of 160 MHz. Frequency fluctuations associated with dielectric permittivity fluctuations were recorded accurate to  $\sim 10^{-7}$  as frequency spectra. Changed fluctuation spectra of the form  $1/f^{-\alpha}$ ,  $\alpha = 1.3\text{--}2.0$  were found to decay to the initial state over more than an hour. It was hypothesized that the metastable fluctuation spectra are associated with changes in the structure of hydrogen bonds.

- Shirahata *et al.* (1997) demonstrated that, compared to the water taken from the anode, the so-called reduced water taken at the cathode of an electrolysis unit is characterized by a higher pH, lower dissolved oxygen, higher dissolved molecular hydrogen, and higher negative redox potential. In biochemical tests, such a water exhibited an activity specific of superoxide dismutase enzyme. The water retained its activity during a month and even after such procedures as freezing-thawing,

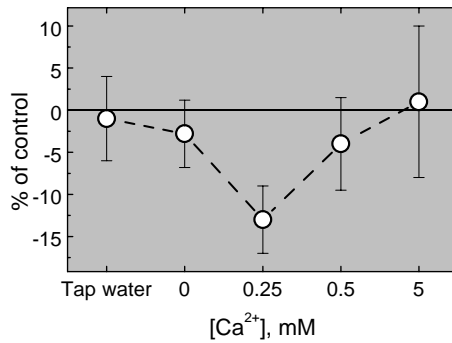


**Figure 5.1.** Biological activity of a magnetically conditioned water solution at different concentration of calcium ions, after (Ružič and Jerman, 1998).

degassing, intense shaking, boiling, filtering, and autoclaving in a closed vessel. Autoclaving in an open container or else in a closed vessel with an atomic hydrogen scavenger eliminated the activity. It was assumed that the activity of reduced water with respect to free radicals was associated with its high stable content of atomic hydrogen.

- Ružič and Jerman (1998) compared the effects of low-frequency magnetic fields and samples of water or water solutions conditioned in such fields on the germination of spruce seeds *Picea abies*. The magnetic field configuration was

$$b(105 \pm 7)B(22 \pm 3)B_p(40 \pm 5)f(50)b_{\text{stray}, 50\text{Hz}}(< 0.2)t(12\text{ h}) .$$

Water was conditioned right before the experiment. Seeds were soaked in this water and the number of germinated seeds was counted on the fifth day. Control samples were soaked in non-exposed water. In the alternative experiment, seeds were exposed to this magnetic field after being soaked in non-conditioned water for 12 h a day, while an identical control compartment with non-exposed seeds was simultaneously monitored.

Experiments revealed a biological activity of conditioned water that had an effect similar to that due to direct exposure. Both versions produced a 7–13% inhibition of growth by the fifth day and had no effect at the final germination state on the seventh day. Five experiments with tap and deionized distilled water samples for soaking and conditioning were conducted with additions of various amounts of calcium chloride that dissociated into  $\text{Cl}^-$  and  $\text{Ca}^{2+}$  ions. Relative averaged values indicate that the biological activity of a water exposed to a magnetic field depends on the calcium ion concentration, as shown in Fig. 5.1. It is interesting to note that similar concentrations of added calcium ions enhanced mobility of diatom algae in a magnetic field, as shown in Fig. 2.8.

These experiments demonstrate that a magnetic field can have an indirect effect on biological systems through a change of state of exposed water in the presence of calcium ions. This hypothesis was first set forth by Kislovsky (1971, 1982) and proved experimentally by Ayrapetyan *et al.* (1994).

- Akimov *et al.* (1998) measured the germination of tomato seeds soaked in various conditioned samples of distilled water to find that water conditioned in steel containers in front of a TV screen produced a reliable change in the seed growth pattern. These data imply, specifically, that water memorized exposure and stored this information for several hours after water conditioning to seed soaking.
- Gulyaev *et al.* (1997) observed metastable states of water set in it by electrolysis in an electrochemical cell with platinum electrodes separated by a semipermeable membrane. The DC density was  $50 \text{ A/m}^2$  at the electric field strength  $10^3\text{--}10^5 \text{ V/m}$ . In 10 min of electrolysis, the hydrogen ion exponent of the bidistilled water cathodic liquor peaked at  $\text{pH} \sim 14$ , over the common equilibrium level of  $\text{pH} \sim 7$ . Under natural conditions, this metastable state decayed over  $\sim 800 \text{ h}$ . In a membraneless electrochemical cell, this state decayed within several minutes at the stated current densities and even faster at higher current densities.

Special experiments indicated that this effect is not a consequence of water heating by electric current, nor does it refer to chemical impurities. Special properties of the membrane were found to be the necessary prerequisites for this unusual water. An appropriate type was a 2-mm-thick ceramic membrane with low permittivity. An irregular distribution of spatial charge over the electrolytic cell axis was noted. A relatively narrow field strength peak  $\sim 10^6\text{--}10^7 \text{ V/m}$  was offset from the membrane toward the cathode. The authors hypothesize that, in these experiments, the metastable state of water is due to  $(\text{H}_9\text{O}_4)^+$  ions in the cathodic liquor, which are responsible for water's strong antiviral activity.

- Colic and Morse (1998) demonstrated that the water memory of a 15-min 27-MHz RF field exposure is associated with the presence of gases dissolved in the water. They also studied various water systems, solutions, and suspensions prepared from common water solutions and solutions that were outgassed by a vacuum pump for 30 min.

The electrophoretic mobility in an RF-conditioned rutile suspension exhibited periodic  $\sim 100\%$  variations. Solutions outgassed before and after EM exposure yielded suspensions that did not show any electrophoretic variations. Similar results were obtained in forming and precipitating  $\text{CaCO}_3$  as measured by the turbidity of suspensions and by the grain size distribution of precipitated particles.

These experiments suggested that degassing of initial solutions eliminates long-term effects of EM exposure. An important observation also was that a permanent MF causes nanomoles to micromoles traces of hydrogen peroxide in the solution (spectrofluorometric measurements). Analysis of these observations and literature data led the authors to the conclusion that an EM exposure induces small amounts of ozone, superoxide, and active hydrogen in the solution. The authors believe that

the latter is retained by water for months, and heat treatment (whether freezing–thawing or boiling) fails to remove atomic hydrogen. It is assumed that the effect of EM field exposure on water is due to gas–liquid micro-interfaces surrounding hydrophobic impurities, specifically, atomic hydrogen.

- Goldsworthy *et al.* (1999) studied the effect of water conditioned by a modulated RF 100-kHz field for as long as 10 min on the growth rate of yeast cells. This water accelerated or decelerated cell growth depending on the length of conditioning and the degree of dilution of the irradiated samples. The RF field was assumed to act on the double electric layer surrounding colloid particles, causing the removal of structural calcium from the surface of biological membranes and thus enhancing membrane permeability to free calcium, which plays the role of a biochemical signal transducer.
- Stepanyan *et al.* (1999) observed linear 30-min variations of the specific conductivity of water in a measuring cell with electrodes. The cell was subjected to mechanical vibrations in a low-frequency range. The largest variations of conductivity were observed at a frequency of 4 Hz: for a fresh distillate,  $\sim 27\%$  and for a three-day distillate,  $\sim 15\%$ . The authors associated this effect with structural changes in water and with the processes of gas transfer at the interface. They believed that vibrations did not affect the measuring system. However it was reported (Belov *et al.*, 1997) that the water at the electrodes possesses its own electric properties, which could be disturbed by relative displacement of the electrodes and water caused by mechanical perturbations. Then the conclusion that bulk water changes its properties when subject to vibrations is poorly grounded. In any case, these experiments revealed a memory of water with a characteristic decay time of dozens of minutes.

Table 5.1 summarizes the literature data on water memory decay time. As can be seen there are many papers of (a) various authors made about (b) different methods, in (c) different time and in different places, all of which prove that water retains changes induced in it by exposure to an EM field for some time. Thus, *a long-time memory of water is a well-established fact.*

These experiments do not contradict the hypothesis that a water memory of EM field exposure is associated with structural defects of water and with processes at the water–gas interface. It is especially important to study how water is affected by permanent and low-frequency magnetic fields — the electric field component may be neglected. It has been repeatedly noted that the effect of magnetic fields on moving charges and microscopic magnetic moments is incomparable in energy terms with that of thermal fluctuations. In addition, the physical nature of water memory is not clear. Therefore, it is interesting to look into memory mechanisms that could be tested experimentally.

The idea of structural clusters in liquid water has been reiterated in the literature. Today it receives an experimental justification thanks to efforts of a team led by E. Fesenko. They predict *macroscopic* millimeter-size clusters in water. However, the concept of water clusters is yet to be defined. The concept has been

**Table 5.1.** Relaxation of metastable states and memory of water

Effect – property	Relaxation time
• EF – dielectric (Debye) relaxation	$\sim 10^{-11}$ s
• photolysis – dissociation of water	$10^{-4}$ s (Eisenberg and Kauzmann, 1969)
• MF – spin–lattice relaxation	$\approx 3$ s (Slichter, 1980)
• microwaves – optical refraction	tens of minutes (Berezhinsky <i>et al.</i> , 1993)
• microwaves – biochemical activity	tens of minutes (Fesenko <i>et al.</i> , 1995)
• microwaves – biological activity	tens of minutes (Devyatkov <i>et al.</i> , 1996; Katin, 1996)
• RF EMF – concentration of free radicals	tens of minutes (Colic and Morse, 1998)
• RF EMF – biological activity	tens of minutes (Goldsworthy <i>et al.</i> , 1999)
• mechanical perturbations – electric conductivity	tens of minutes (Stepanyan <i>et al.</i> , 1999)
• combined MF – fluorescence spectra	hours (Novikov <i>et al.</i> , 1999)
• microwaves – electric conductivity spectra	hours (Fesenko and Gluvstein, 1995)
• CRT radiation – biological activity	hours (Akimov <i>et al.</i> , 1998)
• microwaves – viscosity	hours (Khizhnyak and Ziskin, 1996)
• microwaves – reduction $[O_2]$	hours (Kazachenko <i>et al.</i> , 1999)
• mechanical perturbations – fluctuation spectra $\varepsilon$	hours (Belov <i>et al.</i> , 1997)
• radiation of organisms – corona discharge, biological activity	hours (Berden <i>et al.</i> , 1997)
• permanent MF – biological activity	days (Pandey <i>et al.</i> , 1996; Rai <i>et al.</i> , 1996)
• combined MF – biological activity	days (Ružič and Jerman, 1998)
• adsorption – spin-modified water, absorption spectra	minutes to months* (Konyukhov <i>et al.</i> , 1995)
• condensation – fluorescence spectra	hours to months* (Lobyshev <i>et al.</i> , 1995, 1999)
• electrolysis – reduction and oxygenation of water, biochemical activity	minutes to months* (Shirahata <i>et al.</i> , 1997)
• electrolysis – stoichiometry	months to years* (Gulyaev <i>et al.</i> , 1997; Binhi, 1998b)

\*Relaxation time strongly depends on external conditions.

introduced for the purpose of experimental interpretation without having to identify it structurally, geometrically, or physically. Therefore, it would be more appropriate to speak of a changed state of some domains of water or about macroscopic *metastable states* of water until information is obtained about the physical nature of those changes in water properties that segregate one cluster from another. For such states, dynamic phenomenological models which take into account only experimentally revealed properties of these states without having to define the origin of these properties are admissible. Phenomenological models, such as thermodynamics, are useful in the sense that they allow one to meaningfully plan the experiment and refine or disprove basic assumptions of the model. Having been proved many times, an assumption becomes a scientific fact that requires research into its microscopic nature.

Macroscopic states of water can be characterized by invariable quantities over the entire volume of water, i.e., by a spatial correlation on a macroscopic scale. Also, the information on the properties of the state in time is conserved; i.e. water does have a memory of some time coherence. As far back as 1990 it was hypothesized that macroscopic metastable states of water and water solutions exhibit quantum properties; specifically they can interfere upon the merging of two specimens (Binhi, 1990a, 1995a). This idea, which today is merely a phenomenological model, allows one to predict certain results of multiple repeated procedures like mixing and dilution. It also agrees with many known experimental data on water state behavior identified by this model with macroscopic quantum states. However, a review of these experiments and an expansion into the subject of quantum states of water would lead us far beyond the scope of this book.

We add also that, in a microscopic sense, clusters of water as more or less stable ensembles of molecules in a matrix of liquid water do not enjoy a direct spectroscopic proof. They exist merely as formations isolated from liquid, e.g., in a molecular jet of water. Such clusters possess characteristic spectra. For example, Liu *et al.* (1996a) studied a spectral band of  $81\text{ cm}^{-1}$  assigned to certain oscillations of a water pentamer, a ring cluster of five water molecules held together by hydrogen bonds so that oxygen atoms are approximately in one plane. The spectral band was assumed to be associated with the tunneling of protons, which are not involved in hydrogen bonding, from one side of the ring plane to the other, or with twisting and bending of the cluster oxygen skeleton. We note that there is no signal near  $81\text{ cm}^{-1}$  and also at other frequencies characteristic of  $n$ -dimensional clusters of water (Liu *et al.*, 1996b) in permittivity spectra of liquid water. Therefore, it is difficult to speak of small-size clusters in water as real objects that differ in their properties from the remaining water matrix. Measured in hydrogen bond energy units, the interaction energy of small-dimensional cluster is of order  $2n$ . This is the number of bonds between the cluster and the surrounding molecules of water. At the same time the cluster energy holding it together is obviously half as large. Therefore, the surrounding medium tears such a cluster into parts. Indeed, computer simulation of liquid water with both the molecular dynamic and Monte-Carlo methods (e.g., Belch and Rice, 1987) reveals such clusters only as virtual structures with a lifetime

on the order of dielectric relaxation time.

Cluster structures (predominantly pentamers and to a lesser degree hexamers) become more stable near hydrophobic objects, some ions, and molecular groups (Liu *et al.*, 1996b). The interaction of the medium with a hydrofuge stabilizes the coordination layer of water molecules around the hydrofuge. This disturbs the tetrahedral coordination of the hydrogen bonds, and the most energy favorable configuration of water molecules consists of contiguous five- and six-rings (by oxygen atoms) in the first coordination sphere. These are, for example, clathrate cages around molecules of inert gases.

On the one hand, such clusters do not have anything in common with the hypothetical cluster-forming of liquid water. On the other hand, various stable motives of hydrophobic hydration could be carriers of water memory. They possess almost equal energy and transitions between them are hampered due to a high barrier along the generalized transition coordinate.

Breakdown of the tetrahedral coordination of the hydrogen bond network is, expressed in terms of complementary concepts, a violation of the Bernal–Fowler rules. Therefore, generally speaking, hydration may be treated in terms of structural defects of water, and water memory may be ascribed to stable associates of such defects.

### 5.1.2 Stoichiometry and metastable behavior of water

Below we consider metastable states of liquid water, thus extending the subject of associates. These states are associated with stable changes in the organization of structural defects of water. These changes seem to be sensible to the impact of external EM fields (Binhi, 1998b). Below we demonstrate that the fact that these states exist can be verified by comparatively simple independent experiments.

#### 5.1.2.1 Defects of water structure

The structural organization of oxygen and hydrogen atoms in the network of hydrogen bonds is described by the Bernal–Fowler rules (Bernal and Fowler, 1933), which define that (a) every atom of oxygen has two hydrogen neighbors, and (b) each hydrogen bond (O–O line) contains one hydrogen atom.<sup>33</sup> Dissociation of water molecules in liquid water brings about an equilibrium concentration of hydroxyls  $\text{OH}^-$  and hydroxonium ions  $\text{OH}_3^+$



At  $T = 300\text{K}$ , the equilibrium concentration corresponds to  $\text{pH} \sim 7$  and yields  $\sim 10^{-7}\text{M/l}$ . The appearance of  $\text{OH}^-$  and  $\text{OH}_3^+$  ions violates rule (a) and causes so-called ionic defects in water structure. There exist defects associated with violation of rule (b). They are referred to as Bjerrum's orientation defects: a D-defect

---

<sup>33</sup>The Bernal–Fowler rules are well defined for ice. We will use these rules and the associated concepts for liquid water to illustrate nanosecond processes running within one or two coordination spheres.

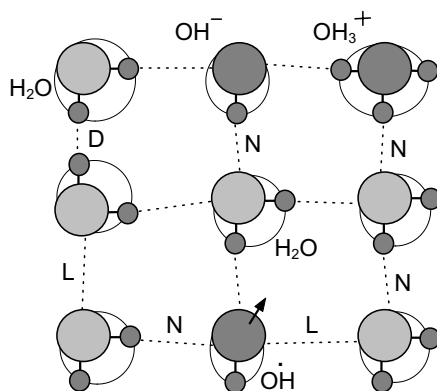


**Figure 5.2.** Ion defects  $\text{OH}_3^+$ ,  $\text{OH}^-$ , orientation D- and L-defects, and  $\dot{\text{O}}\text{H}$  radical defect of an ideal structure.

implies two protons on an O–O line, and an L-defect implies no protons on an O–O line (Eisenberg and Kauzmann, 1969), Fig. 5.2. These defects occur as a result of distortions of a regular orientation of water molecules in the hydrogen bond network,

$$2N \rightleftharpoons D + L ,$$

where N is the defectless hydrogen bond. An estimation of Bjerrum's defects in water  $< 10^{-6} \text{ M/l}$  may be found in the paper of Eigen and De Maeyer (1958). Bjerrum's defects carry opposite charges: L-defects are negative, and D-defects are positive.

The equilibrium of ion defects can be readily shifted by adding acid or alkali. The equilibrium of orientation defects is not connected directly with ionic defects. Rule (b) suggests that it may be shifted by changing the stoichiometry of water.

Some authors single out ion structures of the type  $(\text{H}_{2i+1}\text{O}_i)^+$ ,  $i = 1, 2, \dots$  in a network of hydrogen bonds. However, all these structures are model forms of the hydroxonium ion that exists in liquid water as a defect spread over a few water molecules. Saying it in other words, the hydroxonium is a perturbation of a network of hydrogen bonds associated with a local excessive proton density. This perturbation affects an area of the size of  $10\text{--}20 \text{ \AA}$ . This distribution is typical also for other structural defects.

The motion of defects occurs due to classic and quantum transitions of proton along and between hydrogen bonds (Eigen and De Maeyer, 1958). Figure 5.3 shows the states of water molecules in the first coordination sphere when a D-defect moves about. Davydov *et al.* used these representations of water defect motion due to proton jumps and rotations of molecules in their theory of solitons in molecular chains (e.g., Davydov, 1984b). Ionic defects of water structure are chemically active. For orientation defects, no reported data are available on their activity or non-activity. A disturbed equilibrium in dissociation of water molecules returns to the steady

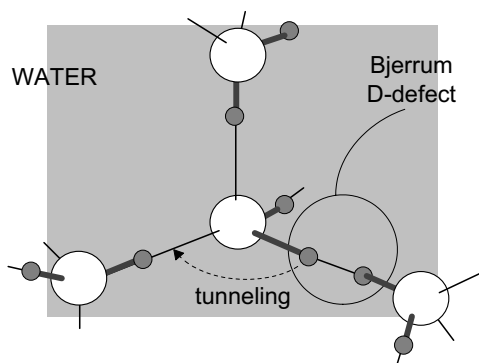


**Figure 5.3.** Movement of an orientation D-defect in a network of hydrogen bonds by proton tunneling to an adjacent bond.

state in about  $10^{-4}$  s. This is the characteristic time of diffusion of hydroxonium and hydroxyl ions to their first recombination contact. It is far shorter than the experimentally observed decay times of metastable states of changed water which persist for a month or longer. Therefore, one should look for other mechanisms to explain such long-lasting metastable states.

#### 5.1.2.2 Water defect mobility in a magnetic field

In a magnetic field, the mobility of these structural defects is changed owing to spin effects. They owe their existence to the spread of the proton wave functions to the adjacent potential wells of the hydrogen bond network. If the adjacent well is empty, then the probability of a quantum transition of the proton to this well is defined by the “wing” of the wave function overlapping this well. Various estimates suggest that classic and quantum transitions of protons over the network of hydrogen bonds are comparable in intensity. If the next well is occupied by another proton, then their wave functions overlap and there exists an exchange interaction which depends on the mutual orientation of their spins. In a section of molecular chain with a D-defect in a hydrogen bond, shown in Fig. 5.4, one of the D-defect protons can move in a quantum transition along the reaction coordinate  $x$ . The proton’s potential energy has a characteristic two-well profile. Two end particles are assumed to be fixed. The intricate interaction of the moving proton with stationary counterparts includes an exchange energy that depends on the mutual orientation of their spins. Figure 5.4 illustrates how the two-well potential changes in reflection to various orientations of proton’s spins. If the extreme spins have opposite orientations, the potential becomes asymmetric. The probability of proton quantum transitions from well to well depends upon the profile of this potential.

Under normal conditions, thermal energy is sufficient for transitions even in the absence of exchange interactions. To a first approximation, the contribution of the magnetic field in the intensity of transitions is proportional to the integral over

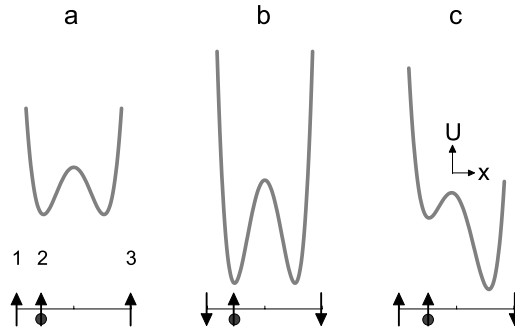


**Figure 5.4.** Potential energy of a D-defect tunneling proton as a function of three spin states.

the overlap of proton's wave functions and assumed to be sufficient to be observed experimentally. This contribution is modulated by the spin state, which evolves with the external magnetic field. The spin state may be controlled by this field. It is interesting to note that these variations leave a system's energy almost invariable because the energy of magnetic interaction is relatively small. On the other hand, the transition probabilities change and cause variations in the overall mobility of water defects.

The Hamiltonian of a model system includes the orbital, Zeeman, magnetic dipole–dipole, and exchange energies, the effective potential of the electron shell, and the relaxation interaction with the thermostat,

$$\mathcal{H} = \frac{1}{2M} \left( \mathbf{P}^{(2)} - \frac{e}{c} \mathbf{A}(t) \right)^2 - \gamma \left( \mathbf{I}^{(1)} + \mathbf{I}^{(2)} + \mathbf{I}^{(3)} \right) \mathbf{H}(t) + \sum_{\alpha, \beta} \mathcal{H}_{\text{dd}} \left( \mathbf{I}^{(\alpha)}, \mathbf{I}^{(\beta)} \right) + \sum_{\alpha, \beta} \mathcal{H}_{\text{exch}} \left( \mathbf{I}^{(\alpha)}, \mathbf{I}^{(\beta)} \right) + U \left( x^{(2)} \right) + \mathcal{H}_{\text{relax}} ,$$

where the superscript represents the particle running number. Owing to exchange interactions, two adjacent spins form two-particle singlet–triplet states  $\nu$ , and the third spin forms a single-particle state  $\psi$ . Denoting the orbital functions of the proton in one of the wells by  $\phi(x)$ , we can write the approximate eigenfunctions of the Hamiltonian unperturbed by magnetic and thermal interactions as

$$\Psi_0 = \frac{1}{\sqrt{2}} \left[ \phi(x) \psi^{(1)} \nu^{(23)} \pm \phi(-x) \nu^{(12)} \psi^{(3)} \right] .$$

As can be seen, these functions cannot be transformed into a product of functions of spatial and spin variables. This fact implies the presence of some effective interdependence between a proton coordinate and a system spin state. This interaction can be controlled by magnetic perturbation, i.e., by changing the spin state by an external magnetic field. This impact changes the probability of a particle

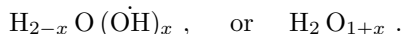
moving from well to well. A numerical analysis of this model may be found in a paper of Binhi (1998b).

### 5.1.2.3 Deviations from regular water stoichiometry

A possible mechanism of water memory may be by disturbing its regular stoichiometry. We consider this mechanism with reference to an electrolytic cell with a semipermeable membrane separating the areas of cathode and anode. The water stoichiometry is disturbed by evolving gases  $H_2$  and  $O_2$  at the cathode and anode, respectively, and by complex processes on the membrane. It would be logical to assume that the membrane is more permeable for one type of charge carrier and less permeable for the others. The fractions are neutral owing to respective changes in the concentrations of hydrated electrons, Fig. 5.5. In this case, the metastable state of water has the form



where  $x$  is the concentration of hydrated electrons per water molecule. It should be obvious that the relaxation of the metastable state of a water taken from the electrolytic cell is utterly hampered, since it can occur only due to gas transfer on the water surface. Under normal conditions, the partial pressures of atmospheric oxygen and hydrogen differ substantially. Therefore, the catholyte and anolyte fractions, differing in the sign at  $x$ , will relax at different rates. The negative values of  $x$  should be understood as a lack of electrons, that is, as a respective amount of ion-radicals. Removing a hydrogen atom from a water molecule leaves behind an electrically neutral ion-radical  $\dot{O}H$ . In this case, the metastable state is given as



A changed stoichiometry in water is a consequence of the fact that a certain balance is conserved while mass and charge are being transferred across the membrane. We assume that different types of charge carriers contribute to the membrane conductivity, namely, ionic  $O_i H_k^{(k-2i)}$  with the ion charge in parentheses, electrons  $e^-$ , and oxygen ion radicals  $\dot{O}^-$ . This type of writing for ion charge carriers covers both molecular ions such as hydroxonium and hydroxyl, and atomic ions such as  $H^+$  and  $O^{2-}$ . The neutral hydroxyl-radical  $\dot{O}H$  does not take part in the charge transfer across the membrane.

The current conservation law requires an identical amount of charge crossing the cathode, membrane, and anode per unit time in a stationary regime. Suppose that a charge equivalent to one electron passes a cross section of the circuit in time  $\tau$ . Denote by  $p$  the probability of an electron passing across the membrane to the anode in a time interval  $\tau$ . For an ion-radical and various hydro-ions, this probability will be denoted by  $p_r$  and  $p_{ik}$ , respectively. Now, a charge  $-e$  crossing the membrane may be represented in the form

$$\sum e(k-2i)p_{ik} - ep_r - ep = -e ,$$

where summation is over all  $i, k$ . This expression leads us to the formula that will be used later:

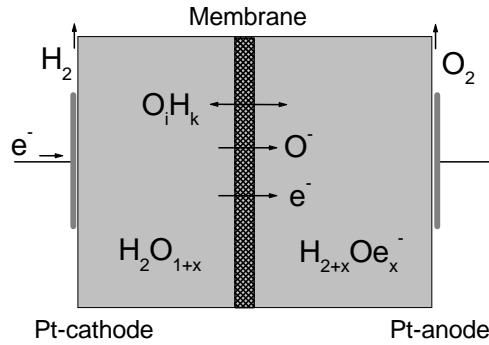
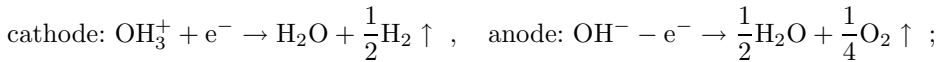


**Figure 5.5.** Electrolysis of water and formation of metastable states of water with changed stoichiometry in a membrane electrolyzer.

$$\sum kp_{ik} = p_r + p - 1 + 2 \sum ip_{ik} . \tag{5.1.2}$$

Prior to writing equations for mass transport we recall that reactions with the evolution of molecular gases take place at the electrodes:



that is, for each electron crossing the membrane it implies that one atom of hydrogen is removed from the cathodic liqueur and one half atom of oxygen is removed from the anolyte. Thus, each incoming electron removes

$$\left( \sum ip_{ik} + p_r \right) \text{O} + \left( \sum kp_{ik} + 1 \right) \text{H}$$

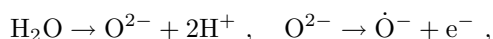
from the cathodic liqueur. Substituting the expression for (5.1.2) and performing simple transformations we arrive at the final expression for the amount of substance leaving the cathodic fraction. Similarly, we find the ingress of substance in the anolyte fraction, viz.,

$$\begin{aligned} \text{leaves catholyte: } & \left( \sum ip_{ik} + p_r \right) \text{H}_2\text{O} + \alpha \text{H} \\ \text{arrives into anolyte: } & \left( \sum ip_{ik} + p_r - \frac{1}{2} \right) \text{H}_2\text{O} + \alpha \text{H} \\ & \alpha = p - p_r . \end{aligned} \tag{5.1.3}$$

If  $p > p_r$ , which seems to be true because of a large size of the ion-radical, then  $\alpha > 0$  and the cathodic liqueur becomes depleted of protons. Conversely, the anolyte finds itself enriched with protons. The balance of mass over the whole liquid is negative, as it should be. Summing up the relations (5.1.3) with respective signs, we find that, with each electron passing through the circuit, the liquid is losing half

a molecule of water. These halves evolve at the electrodes in the form of molecular gases.

We note that under this mechanism, no protons pass from catholyte to anolyte and there will be no change in the stoichiometry unless the electron and ion-radical contributions into the membrane conductivity are taken into account. At the initial stage of electrolysis these charge carriers are almost absent, since they are associated with the breaking of covalent bonds O—H. The conductivity of the membrane is low compared to the ion conductivity of liquid water and the entire anode-cathode potential difference appears across the membrane. If the membrane is thin and the voltage across it is high, then the membrane may find itself subjected to considerable electric field strengths. At field strengths of the order of  $E \sim 10^6$ – $10^7$  V/m, ionization of water molecules begins in pores of the membrane,



thus bringing about electronic conductivity. In the anolyte area, electrons are present in a hydrated form, thus providing for the electrical neutrality of this fraction enriched by protons, that is, atomic hydrogen. This scheme illustrates the processes that change the stoichiometry of water. An in-depth analysis could be based on equations of plasma with chemical reactions which would be a convenient tool of study in this quasi-unidimensional case.

Thus, the cathodic fraction is characterized by a reduced relative number of protons, an alkali reaction, and, probably, a high content of dissolved molecular hydrogen. The anolyte fraction has an acidic reaction and enhanced concentrations of protons and dissolved molecular oxygen.

It is interesting to note that the hypothesis of non-stoichiometric water can be tested experimentally. The quantity  $x$  in the formula (5.1.1) can be measured from the NMR spectrum of water enriched by isotopes of oxygen  $^{17}\text{O}$ . For this purpose one needs to obtain the ratio of NMR signals of protons and  $^{17}\text{O}$  nuclei. This quantity should be proportional to a ratio of hydrogen and oxygen nuclei in water with a proportionality coefficient  $c$  depending on the NMR spectrometer alone:

$$W = c \frac{N_{\text{H}}}{N_{\text{O}}} .$$

As follows from (5.1.1) it is  $W_{\text{a}} = c(2 + x)$  for anolyte and  $W_{\text{k}} = c(2 - x)$  for catholyte. The ratio depends on parameter  $x$  alone, viz.,

$$\frac{W_{\text{a}}}{W_{\text{k}}} = \frac{2 + x}{2 - x} . \quad (5.1.4)$$

The deviation of this experimentally measured ratio from unity can be explained only by a deviation in water stoichiometry. One more prediction in the framework of the discussed mechanism concerns the dependence of the changed state relaxation rate on the gas exchange on the water surface. Specifically, such a water could retain its state however long if it is confined in a vessel with hydrogen-impermeable walls.

The presence of defects of liquid water structure at equilibrium is defined by a natural level of low-probable heat-activated processes of dissociation of molecules and the rotation of molecules into higher-energy metastable positions. We mentioned above that these defects can be explained by violations of the Bernal–Fowler rules. A necessary validity condition of these rules is an ideal stoichiometric composition of water expressed by the formula  $\text{H}_2\text{O}$ . The possibility for defects of water structure to occur as a result of water stoichiometry distortion has not been addressed in the literature. In this case, the concentration of defects would be proportional to the deviation from the stoichiometric composition multiplied by the Avogadro constant, that is, enormously high.

#### 5.1.2.4 Water–air ions and water stoichiometry

It would be interesting to combine the known phenomenon of biological activity of water–air ions with the deviation of the water formula from the familiar  $\text{H}_2\text{O}$ . The favorable effect of negative aeroions on living organisms found by A.L. Chizhevskii has been studied for more than half a century (Andreeva *et al.*, 1989). The mechanism of their therapeutic and biological activity has not been fully identified for model systems. One of the pertinent hypotheses relates the effect to an influx of electric charge introduced by ions into the living tissue, while other hypotheses treat the effect on the level of biochemical kinetics. Changes induced by water–air ions in the structure of water medium may also be hypothesized as a cause of further biochemical transformations.

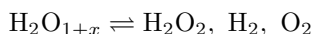
A fast drain of the excess electron from an aeroion  $\text{OH}^-$  introduced in water is equivalent to adding a neutral radical  $\text{OH}$  in water or, obviously, to extracting a neutral atom radical  $\text{H}$  from water. This defect of water structure, associated with a deviation from the stoichiometry, is very similar to Bjerrum’s L-defect. It differs from the latter in that it has been formed by the absence of a proton between a water molecule and an  $\text{OH}$  radical rather than between two water molecules. This defect has a lower mobility since a purely proton transfer is no longer viable. The radical recombination rate  $2\text{OH} \rightarrow \text{H}_2\text{O}_2$ , relatively slow due to the Coulomb repulsion of the associated L-defects, is further reduced due to their low mobility. At the same time the chemically active radical  $\text{OH}$  is capable of taking part in reactions of the next level. Kloss (1988) related the biological activity of water associated with its physical activation to the occurrence of radicals  $\text{OH}$ .

We estimate the number of added defects assuming that the solution absorbs all aeroions that hit its surface. Following Andreeva *et al.* (1989) we let the solution surface area be  $S = 1 \text{ cm}^2$ , the flow velocity  $V = 10^2 \text{ cm}\cdot\text{s}^{-1}$ , the ion concentration in the incident flow  $c = 2.5 \cdot 10^5 \text{ cm}^{-3}$ , and the time of blow  $t = 10^2 \text{ s}$  to obtain  $n \sim cVSt \approx 2.5 \cdot 10^9$ . This number of defects in a few cubic centimeters of solution approaches endogenous concentrations of enzymes, which corresponds to equilibrium concentrations of water defects and, therefore, is capable of producing a notable effect should Bjerrum’s defects and/or  $\text{OH}$  radicals be deemed chemically active. Water treated by  $\text{OH}^-$  aeroions is similar to the cathodic fraction of water from an electrochemical cell with membrane. In both cases, the stoichiome-

try deviates from equilibrium towards proton depletion  $\text{H}_{2-x}\text{O}(\dot{\text{O}}\text{H})_x = \text{H}_2\text{O}_{1+x}$ ,  $x > 0$ .

One may conclude that since negative water–air ions possess a positive therapeutic effect, then the catholyte water should also produce similar action. Excess L-defects of catholyte with net negative charge bind positive ions of hydroxonium, thus increasing the pH and additionally shifting the biochemical equilibria of reactions involving hydrogen.

Dissolving in water other molecules that consist of oxygen and hydrogen only, e.g., molecular gases or hydrogen peroxide, virtually does not disturb its stoichiometry or disturbs it slowly. Molecular covalent bonds, which are far stronger than hydrogen bonds, can be broken by an appropriate heating of such solution or in long storage. Kloss (1988) believes that the addition of hydrogen peroxide  $\text{H}_2\text{O}_2$  brings about a biological activity in the water due to dissociation of peroxide molecules yielding radicals. In this case, the natural relaxation time for a disturbed stoichiometric equilibrium



is relatively large. On the other hand, it is easier technically and faster to break covalent bonds by an electric field outside the water specimen when this is blown by water–air ions or inside the specimen on a membrane. Magnetic fields, addressed in preceding sections, seem to be capable of shifting the metastable stoichiometric equilibrium in water by changing its defect mobility and, thus, inducing a biological activity in water.

Isotopic studies with  $^2\text{H}$ - and  $^{17}\text{O}$ -enriched water–air ions could reveal the role of spin degrees of freedom in the processes of aeroion implementation into the network of water hydrogen bonds. Also, if the primary mechanism of aeroion activity, associated with violations of stoichiometry, is valid, then an addition of conditioned water to an incubation mixture could have qualitatively identical consequences with the case of an incubation mixture directly treated by ions.

#### 5.1.2.5 Experiments based on water electrolysis

Such free-radical oxidants as hydroxyl radical  $\dot{\text{O}}\text{H}$  and hydrogen peroxide  $\text{H}_2\text{O}_2$  dissociating into these radicals, superoxide anion-radical  $\dot{\text{O}}_2^-$ , and electron-excited singlet oxygen  $^1\text{O}_2$  are known to cause destruction of protein macromolecules, lipids, DNAs, enzymes, and lead to pathology and various diseases (Zhuravlev, 1982). Shirahata *et al.* (1997) used a common electrolytic cell to obtain water specimens possessing antioxidant activity from purified and salted, 0.1 g/l NaCl, water. The design of the electrolytic unit was not explained; however, the measured properties of fractions are comparable with the aforementioned properties of the catholyte and anolyte fractions of the membrane electrolytic unit.

After a sufficient treatment the cathodic liqueur exhibited an alkali reaction  $\text{pH} \sim 10\text{--}11$ , an enhanced concentration of dissolved molecular hydrogen  $\text{H}_2$  0.45–0.55 mg/l, a reduced concentration of dissolved oxygen  $\text{O}_2$  3.4–3.6 mg/l, and high negative values of redox potential  $-600$  to  $-800$  mV. This water also possessed a specific antioxidant activity determined by biochemical methods, Fig. 5.6. On

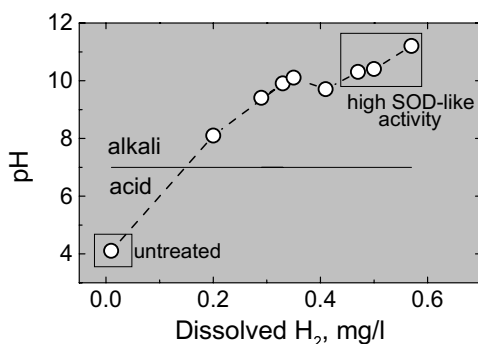


**Figure 5.6.** Hydrogen ion exponent (pH) of reduced water plotted versus the concentration of dissolved molecular hydrogen, after Shirahata *et al.* (1997).

the other hand, specific activity did not occur after the water had been saturated by molecular hydrogen in place of electrolysis, which suggests that this activity was caused by some independent quality of liquid water. Authors believed that the antioxidant activity of reduced water or catholyte was caused by an enhanced concentration of atomic hydrogen. The only argument in favor of this conclusion was that this activity disappeared after autoclaving in the presence of tungsten trioxide  $WO_3$ , which is an efficient absorber of atomic hydrogen.

It is instructive to note that, in the aforementioned scheme of the membrane electrolytic cell shown in Fig. 5.5, the abstract biological activity of catholyte was associated with a reduced, rather than enhanced, content of protons in water, whereas the other catholyte characteristics, such as pH and dissolved molecular hydrogen, correspond to those of reduced water (Shirahata *et al.*, 1997). It is not clear what has caused this discrepancy. One cannot measure the concentration of atomic hydrogen in a direct experiment; no relevant experimental methods have been reported. Unlike molecular hydrogen, active hydrogen cannot be imagined as a separate chemical substance dissolved in a matrix of "normal" water  $H_2O$ . Because of intense proton exchange, atomic hydrogen is closely interwoven in the net of hydrogen bonds to become an integral entity of this net and the water medium. This fact is reflected in the formulas of non-stoichiometric water, catholyte  $H_2O_{1+x}$ , and anolyte  $H_{2+x}O_{e_x}$ . The representations of these authors (Shirahata *et al.*, 1997) on the processes in an autoclave with salts and oxides, and especially on the concentration of dissolved active hydrogen in liquid water may need refinement. Also, the dependence of specific water activity on proton concentration may have a rather non-linear behavior.

Thus, the variation of water structural properties by a weak magnetic field seems to be associated with an exchange interaction of protons in the liquid water. EM field conditioning reduces the mobility of water structure defects — ionic,

orientation type, and free radical type — and shifts the biologically significant metastable equilibrium of various types of water defects, thus breaking down water stoichiometry. Water structural defects as well as the water proton subsystem in general are attractive objects in searching for targets of EM field impact. Relevant attractive points are as follows:

- The contribution of the spin magnetic moment to the magnetic Hamiltonian of a proton exceeds that of the orbital moment.
- The mechanical moment of a proton is equivalent to that of an electron. Electron spins participating in exchange interaction play a key role in chemical reactions. The exchange interaction of protons may in part control the mobility of water structure defects, thus affecting the solution kinetics.
- Protons are components of water media where biochemical processes usually proceed, and simultaneously they take part in many a biochemical reaction.
- Unlike free radicals, protons abound in water.
- Proton spins have long relaxation times — on the order of seconds — therefore they have sufficient time to adjust to or “feel” the external magnetic field.

## 5.2 BIOLOGICAL EFFECTS OF MICROWAVES AND ION INTERFERENCE

Investigations into biological effects of microwaves have been stimulated by the development of EM oscillators in this frequency range. In the USSR, relevant research began in the 1960s by a team of N. Devyatkov (Devyatkov, 1973; Devyatkov *et al.*, 1981; Devyatkov, 1999). Elsewhere early reports in this area were due to Webb and Dodds (1968) and Webb and Booth (1969). The features of biological effects of microwaves below thermal intensity are well known (Devyatkov *et al.*, 1981; Devyatkov and Betskii, 1994; Betskii *et al.*, 1998):

- The resonance response of biological systems to non-thermal,  $< 1 \text{ mW/cm}^2$ , microwaves, the resonant line width being  $10^{-2}$ – $10^{-3}$  of peak frequency.
- The resonant behavior of system response as a function of modulation frequency of the microwave carrier.
- A weak dependence of the effect on the radiation intensity, often beyond a threshold power.
- Physiological windows of the effect and sensitivity of spectra to the type of biological system and its physiological state.

A non-thermal nature of these effects is proved by the presence of resonances and the fact that biological responses to microwaves and heating are often of opposite sense (Webb and Booth, 1969; Pakhomov, 1993; Gapeyev *et al.*, 1994). Also, it is hard to relate the biological effects of extra weak microwaves (Grundler and Kaiser, 1992; Belyaev *et al.*, 1996) to thermal effects. Extended bibliographies on non-thermal effects of microwaves may be found in a book by Devyatkov *et al.* (1991), in review papers of Miller (1991) and Betskii (1994), and in a reference book by Polk and Postow (1997). One may also visit the Internet hyperlink database

<http://www.microwavenews.com>, devoted to various aspects of the subject associated predominantly with the potential physiological risk of using mobile phones.

### 5.2.1 Spectral measurements and theoretical concepts

Frequency spectra of microwave effects are most informative in providing insight into primary mechanisms. However, small-step frequency observations are time consuming and therefore relatively scarce. Also, the most valuable information can be obtained from spectral shifts that occur in response to varying experimental conditions.

Frequency selective action of microwaves has been observed on both living systems and proteins *in vitro*. Devyatkov *et al.* (1975) and Devyatkov (1978) pointed out that microwave exposure changed the state of the  $\text{Fe}^{2+}$  ion in the heme of the hemoglobin oxi-form Hb. Mössbauer spectra  $^{57}\text{Fe}$  isotope suggested that a part of iron ions in hemoglobin changed from the low spin state  $S = 0$  to the high spin state  $S = 2$ . The effect was frequency selective and changed sign depending on frequency, indicating a non-thermal mechanism of microwave action.

These findings were proved by Didenko *et al.* (1983) by measuring the width of a resonance signal at 42.173 GHz with intensity of  $4 \text{ mW/cm}^2$  and a long-time stability better than 1.3 MHz. The Mössbauer spectral parameters changed by about 15%. After an hour exposure to microwaves, the effect persisted for several hours. Several effective frequencies were determined with generally different qualitative effects. This difference indicates that different microwave frequencies may have different endpoint targets in a macromolecule.

Webb (1979) found that the lambda prophage synthesis in collibacillus cells conditioned by an unmodulated EM field was strongly dependent on field frequency and power density and on the oxygen content in the medium. A  $10^5$ -fold rise was detected at the optimal conditions of 70.4 GHz,  $0.25 \text{ mW/cm}^2$ . At  $0.6 \text{ mW/cm}^2$ , the effect fell to one-tenth of its peak level. The resonance band width was  $\sim 200$  MHz.

Bannikov and Ryzhov (1980) studied the frequency dependence of microwave effect on coli cells. They measured the induction of a  $\lambda$  phage by a *E. coli* K-12( $\lambda$ ) strain at power densities of  $0.1\text{--}0.2 \text{ mW/cm}^2$ . About 30 effective frequencies were found in the range 40–60 GHz. A spectral peak found at 41.268 GHz was about 1 MHz wide.

Grundler and Keilmann (1983), Grundler *et al.* (1992), and Grundler and Kaiser (1992) observed resonance peaks of yeast cell growth at 41.7 GHz. A frequency spectrum of microwave effect on the growth of *S. cerevisiae* cells in the range 41.65–41.83 GHz was obtained by Grundler and Keilmann (1983). The spectrum revealed many peaks about 8 MHz wide separated by intervals of about 16 MHz. Different irradiating antennas produced spectra that checked accurate to 1 MHz. A bioeffect threshold was found at  $1 \text{ mW/cm}^2$ . The generator radiation bandwidth was about 1 MHz.

Andreev *et al.* (1985) found that a  $1 \text{ mW/cm}^2$  radiation in the range 52.6–53.8 GHz applied to certain acupuncture points of the human body appreciably

changed the bioelectric activity of muscles in other parts of the body. The effect was found to be frequency dependent. This radiation range induced several response peaks about 100–200 MHz wide.

Aarholt *et al.* (1988) reported that a 18–20 h long exposure to a modulated 2-GHz field with power density around  $1 \mu\text{W}/\text{cm}^2$  caused a cataract (phacoscotasmus or eye lens fogging) in prepared bovine eye lens *in vitro*. The modulation frequency corresponded to that of NMR  $^1\text{H}$ , i.e., 2.13 kHz in a geomagnetic field of  $50 \mu\text{T}$ . The effect was found to be sensitive to both carrier and modulation frequencies. Microwaves at a frequency of 55 MHz with a bandwidth of 50 Hz caused a cataract at power densities attenuated to  $7.5 \text{ nW}/\text{cm}^2$ .

Belyaev *et al.* (1993) measured resonance peaks of *E. coli* cell's response to a microwave radiation of  $0.1 \text{ nW}/\text{cm}^2$  at  $41.324 \pm 0.001 \text{ GHz}$  and  $51.765 \pm 0.002 \text{ GHz}$ . Prophages inserted in the bacterial chromosome caused resonance peaks to shift as far as 0.05 GHz.

A frequency-dependent action of microwaves in the range 38–78 GHz on an ion current in the membrane of algae was reported by Kataev *et al.* (1993). A 1-h-long irradiation by  $5 \text{ mW}/\text{cm}^2$  microwaves caused a 100% reduction of ion currents of  $\text{Cl}^-$  at frequencies 41, 50, and 71 GHz and a similar increase when these frequencies were offset by  $\sim 1 \text{ GHz}$ . The endpoints of microwaves are assumed to be some links in the chain of biochemical regulation of channels, rather than ion channels themselves. A channel control agent density could be changed slowly by varying the radiation parameters.

Chemeris and co-workers (e.g., Gapeyev *et al.*, 1994) demonstrated that microwave radiation modulated by a key pattern affects the motility of *Paramecium caudatum* cells. The effect exhibited a resonance peak in the middle of the range 42.0–42.5 GHz. The radiation bandwidth was 10–20 MHz. Gapeyev *et al.* (1996) studied the frequency spectra of microwave effects in the range 41.5–42.7 GHz for a wide range of power densities and different radiator geometries to observe a few response peaks in mouse neutrophil activity.

Several authors reported power windows in biological effects of microwaves. In a review paper, Adey (1980) reported that a 450-MHz radiation modulated by 16 Hz caused the efflux of isotope tracer calcium ions of chicken cerebral hemispheres to peak at  $1 \text{ mW}/\text{cm}^2$  when the intensity varied in the range 0.05–5  $\text{mW}/\text{cm}^2$ . Dutta *et al.* (1984) found power windows in the response of brain tissues to microwave irradiation. A 915-MHz irradiated nerve cell culture showed an increased calcium ion yield at specific absorption rates of 0.05 and 1.0  $\text{mW}/\text{g}$ . This effect did not occur at lower or higher radiation intensities and was dependent on low-frequency modulation. Didenko *et al.* (1989) studied 77-K Mössbauer spectra of  $^{57}\text{Fe}$ -enriched polycrystalline rabbit hemoglobin. The Gunn diode generator frequency was  $42346.70 \pm 0.01 \text{ MHz}$  with a frequency stability of  $\sim 2.5 \cdot 10^{-8}$ . A power window was found in the range 0.5–2  $\text{mW}/\text{cm}^2$ . The lower threshold was explained by competition of acoustic mode accumulation and dissipation processes, the upper threshold being referred to as the non-linearity of these processes. Belyaev *et al.* (1996) demonstrated the effect of a 51.674-GHz radiation on the conformation state

of *E. coli* genome for a certain density of cell suspension when the radiation intensity was varied in the range  $10^{-11}$ – $1 \mu\text{W}/\text{cm}^2$ . It is instructive to note that this effect was absent at high radiation intensities.

The literature abounds in hypotheses on the physical nature of microwave biological effects. However, notwithstanding that microwave quanta are only one to three orders of magnitude weaker than  $\kappa\mathcal{I}$ , no unambiguously established and physical community-recognized mechanisms of this action have been reported. By way of example, some ideas exercised to explain this action are presented below.

### 5.2.1.1 High-Q molecular, subcellular, and cell oscillators

The frequency, wavelength, and propagation speed of vibrations (sound) in tissues are related by the simple formula  $f\lambda = v_s \sim 10^5 \text{ cm/s}$ . Consequently, various biophysical structures of the cell (organelles, membranes, and large macromolecules of size  $10^{-5}$ – $10^{-6} \text{ cm}$ ) treated as elastic elements are resonators at respective excitation frequencies  $10^{10}$ – $10^{11} \text{ Hz}$ . This fact has been the earliest harnessed to explain the biological effects of microwaves. Resonators considered were those carrying electric dipole moments to ensure coupling of microwaves with resonant oscillations.

For a possible mechanism of microwave impact on hemoglobin, Chernavsky (1973) assumed microwaves excite oscillations in the protein, which are accumulated as an elastic deformation of a unified generalized degree of freedom that involves the whole protein (“protein–machine” concept). Its natural frequency is estimated at around 100 GHz. The changed state of the protein entails a biological response.

Smolyanskaya *et al.* (1979) suggested that microwaves act on rotational states of molecular segments such as OH groups and amino acid radicals, which might be a probable explanation of a sharp resonance effect of microwaves in biological systems. These authors also briefly review earlier models of microwave biological mechanisms. Specifically, they address mechanical forces, which occur in an inhomogeneous medium immersed in a non-uniform EM field, wherein no frequency selectivity is present.

Sometimes frequency responses to microwave irradiation look like a comb with an almost regular sequence of effective frequencies (Grundler and Keilmann, 1983). This regular pattern of frequencies brings about an idea of classic multimode resonance systems reiterated in the literature. To illustrate, Golant (1989) speculated that cell membranes and their sections may be such high-quality multimode oscillators. In a normal state, they radiate EM waves of normal frequencies in the millimeter range — these are self-oscillations excited by metabolic processes. These EM fields are natural regulatory signals in both intra- and intercell interactions. Weak external EM fields synchronize the EM data transport and infer various types of biological response. This mechanism explains the resonance pattern of responses and the threshold profile of response with saturation of the biological effect by a rising EM power.

Mechanisms of direct microwave action on dipole resonators are hardly viable because these oscillations strongly attenuate and cannot accumulate a substantial

energy. An electric field  $E$  acting on a dipole  $d$  of size  $R$  exerts a force  $Ed/R$  of tension or compression depending on the mutual orientation of the field and the dipole moment. An alternating field  $E \cos \omega t$  sends the generalized coordinate  $r$  of a dipole oscillating. For the dimensionless coordinate  $x = r/R$ , the equation of a linear oscillator with attenuation may be written as

$$\ddot{x} + \gamma \dot{x} + \omega_0^2 x = \frac{Ed}{MR^2} \cos \omega t ,$$

where  $\omega_0$  is the oscillator natural frequency, and  $M$  is the dipole mass. It is not hard to find that at resonance when  $\omega = \omega_0$  the amplitude of forced oscillations  $a$  and their energy  $\epsilon$  are

$$a = \frac{Ed}{\gamma \omega MR^2} , \quad \epsilon = \frac{M}{2} \frac{(R\dot{x})^2}{(R\dot{x})^2} = \frac{E^2 d^2}{4\gamma^2 MR^2} = \frac{\pi P d^2}{c\gamma^2 MR^2} ,$$

where  $P$  is the flux of microwave energy. Chernavsky and Khurgin (1989) estimated these quantities for a real-size protein measuring  $5 \cdot 10^{-7}$  cm, sound attenuation of  $\sim 10^7 \text{ s}^{-1}$ , and  $P \sim 1 \text{ mW/cm}^2$ . The oscillation energy was  $\epsilon \sim 10^{-20}$  erg, which is about seven orders of magnitude lower than  $\kappa T$  at physiologic temperature. However, biological effects of microwaves were observed at radiation intensities far lower than those used in this estimation. This fact debases any discussion on mechanisms associated with microwave energy accumulation.

### 5.2.1.2 Collective modes of many-particle systems

Davydov (1984b) studied the transport of intramolecular oscillation energy along an  $\alpha$ -helix segment of protein macromolecules to find that the C=O oscillations in peptide groups are efficiently transported by soliton excitations deforming the molecule, see Addendum 6.5. It is assumed that the energy of ATP hydrolysis, used everywhere in the organism, might be transported to a consumer in the body, i.e. another reaction, in the form of C=O oscillations transported by a soliton. There exist other collective, exciton-type modes in macromolecules. Propagating excitons excite phonons and rapidly decay. They cannot be efficient transport vehicles for ATP energy quanta. Davydov and Eremko (1977) and Eremko (1984) demonstrated that an external EM field at a resonance frequency in the millimeter range causes dissociation of a soliton into a rapidly decaying exciton and a local deformation of the protein molecule, thus disturbing the efficient transport of hydrolysis energy and producing a biological response.

Hyland (1998) presented a brief review of biological effects of microwaves from the standpoint of an underlying phenomenon brought forth by Fröhlich (1968a), namely, coherent excitations of dipole structures. Coherence, or the ability of oscillations to retain their relative phase (phase difference) in time or space, may be illustrated as follows. Coherent excitations of ordered dielectrics in biophysical structures occur as a result of an electric dipole interaction of molecules forming these structures. Depending on the magnitude of the intermolecular dipole–dipole interaction, only low-energy collective oscillations can be excited at room temperature. The statistics of such excitations is substantially non-Boltzmann; rather, it

obeys the Bose–Einstein law. At temperatures below some critical point, called degeneration temperature, a phase transition, or Bose condensation, occurs in such systems whereby the energy of oscillations tends to move to the lowest oscillation mode. The stronger the interaction between the dipoles, the higher the degeneration temperature. An external EM field tends to enhance this interaction. It partly synchronizes individual oscillations. Dipoles become phased and their interaction energy increases. If the external stimulus is strong enough, the degeneration temperature is above room temperature, which causes condensation. Dipole oscillations become completely coherent; that is, a macroscopic oscillation of the dipole ensemble appears. The authors speculate that this oscillation is capable of causing a biological effect. Computer simulation experiments by Pokorný (1982) demonstrated that energy can accrue in several macroscopic oscillation states. The model predicts frequency selectivity and a microwave power threshold for the effect to appear.

Davydov (1984a) pointed out that a mechanism relating this type of collective excitation with cell metabolism is poorly defined. It is not obvious that a microscopically localized biochemical process can be sensitive to the presence of dipoles oscillating in phase yet far from the place of reaction. Chernavsky and Khurgin (1989) noted that, given a realistic attenuation, a microwave power density of  $\sim 1 \text{ mW/cm}^2$  is capable of exciting a mere  $\epsilon/hf \sim 10^{-4}$ – $10^{-5}$  additional quanta of collective elastic modes (see p. 357); this estimation casts doubt on the ability of microwave radiation to exercise an efficient control of intermode jumps. On the other hand, Fröhlich (1968b) notes that the energy of metabolism can be a source of external energy with respect to dipoles. If the flux of this energy is sufficiently intense, then the system may find itself close to a phase transition. Now, even a small increment of the flux due to an external EM field, say, could induce transition into a coherent state. By the time of writing this book, no experiments have been reported of unambiguously detecting condensation of collective dipole excitations in an artificially formulated dipole medium.

Blinowska *et al.* (1985) demonstrated that solutions of erythrocytes and their membranes exhibit virtually coinciding multiple-peak absorption spectra of a 35.5–37 GHz radiation. These spectra were assumed to be related with Fröhlich collective oscillations which, in this case, were localized in cell membranes.

The models of Davydov and Fröhlich enjoy independent experimental proofs: they received them from Raman spectra of scattering at microorganisms. At the same time, the hypotheses underlying these models have not received the status of reliably defined scientific facts.

Bohr *et al.* (1997) addressed the mechanism of microwave action associated with special excitations in biopolymer macromolecules, e.g., DNA. Such molecules are often characterized by the density of bending and twisting energy. Solving the Lagrange equations for the Hamilton function of such a chain to a continuum approximation yields twisting waves with natural frequencies of 12 GHz and bandwidths from 10 MHz to 10 GHz for a DNA double helix. Initiating the interaction of twisting and bending modes by an external EM field may, in view of chain topology, localize the bend by means of recoiling and, consequently, lead to a rup-

ture of the molecule. The authors assume that this mechanism is responsible for a microwave-induced hydrolysis of some proteins. This model predicts that the efficiency of hydrolysis will be dependent on a relationship between the RF frequency and polypeptide chain length.

#### 5.2.1.3 Enzyme reaction in an external field

Zubkus and Stamenkovich (1989) and Belousov *et al.* (1993) addressed variations of the rate of heat-activated enzyme reactions in an EM field at physiological temperatures. The effect of microwave fields boils down to reducing the activation energy by the interaction of the wave electric component with the dipole moment of the transition along the reaction coordinate. No estimates of effective field amplitudes were given; however, the effective frequencies may correspond to millimeter wavelengths.

#### 5.2.1.4 Convection of cytoplasm and intercellular fluid

Kazarinov *et al.* (1984) explain a monotonous growth of the Na<sup>+</sup> ion transport across the skin of a frog observed while a millimeter-wavelength radiation intensity was being increased in the range 0.1–100 mW/cm<sup>2</sup> by convective streams of water medium occurring near the skin. A proof in favor of this conclusion was obtained from the fact that the effect showed no frequency dependence when the CW radiation was varied in the wavelength range  $\lambda(7.2; 0.03; 8.5)$  mm. Khizhnyak and Ziskin (1996) reported that microconvective streams could be observed in water systems at as low a millimeter-wavelength intensity as 10  $\mu$ W/cm<sup>2</sup>.

#### 5.2.1.5 Metastable changes in properties of tissue water

The subject of microwave-induced variation of properties of a universal water medium where biological processes take place has been addressed by many workers. In recent time some experimental proofs to the point were reported, see Table 5.1. However, it would be premature to say that this could explain that part of biological effects of microwaves that exhibits sharp resonance peaks. To do so one would have to obtain similar resonance responses for water specimens having no connection with biological systems.

#### 5.2.1.6 Local microscale heating of the medium

Lyashchenko (1998) believes that biological effects of millimeter band waves may be explained by different dielectric permittivity  $\epsilon$  of water shells surrounding Na, Cl, K, and some other ions. Accordingly, microwaves heat these ions to different temperatures. These processes occur on membrane interfaces. This difference in  $\epsilon$  is especially sensible for ions with different signs of hydration: (+) H, K, Rb, Cs, NO<sub>3</sub>, Br, J; (–) Li, Na, Ca, Mg, SO<sub>4</sub>, CO<sub>3</sub>, Cu, and Ni (Devyatkov, 1978). Local heating is associated with probable phase transitions, e.g., in membrane structures (Ovchinnikova, 1993), which entail a biological response. These processes do not exhibit a strong frequency dependence which would be needed to explain resonance biological effects. Petrov and Betskii (1989) believe that microwave radiation is capable of changing the conformation of the quaternary structure of ATP proteins. The authors used known data about the protein conformation being dependent

on the number of water molecules bound with the protein by hydrogen bonds. In equilibrium, the number of bound water molecules is defined by the rate of the heat-activated reaction



On the other hand, the energy of a water molecule increases after absorption of a microwave quantum  $h\nu$ . A similar change in its energy occurs when the temperature of the medium rises by  $h\nu/\kappa \sim 2\text{--}3\text{ K}$ . An increase of effective temperature controlling the binding reaction suffices to affect operation of ATP systems.

Thompson *et al.* (2000) assumed that frequency and power windows of biological response to microwave irradiation might occur due to a phase transition in a system of abstract membrane EM field receptors related to Ca-binding membrane proteins. However, this model presumes an impact of the field on receptors, which should be on the order of  $kT$  and should be independent of field frequency and power. This circumstance leaves the model outside the realm of those suitable for solving the main problem of magnetobiology.

### 5.2.1.7 Change in concentration of dissolved gases

A fraction of gases dissolved in intercellular plasma is in the form of microscopic bubbles. Yemets (1999) demonstrated that these bubbles can grow in passing through a temperature gradient. As a consequence, the concentration of dissolved gases decreases and causes a cell reaction. Suitable temperature gradients can be created by a low-intensity microwave field above  $0.3\text{ mW/cm}^2$ . These intensities do not change the sample temperature to within  $0.2^\circ\text{C}$ . However, a temperature gradient induced by microwaves does not seem to be significantly dependent on frequency.

### 5.2.1.8 Quantum effects

The models due to Davydov and Fröhlich describe the quantum behavior of multi-particle systems. Biological effects of microwaves are also associated with quantum jumps whatever the microscopic structure of such systems could be. A general property of resonance quantum transitions manifests itself in a sharper resonance peak at lower irradiating intensities, see, e.g., Fig. 4.19. The peak decreases in width until a natural resonance width defined by the lifetime of the quantum states is reached.

Grundler and Kaiser (1992) studied the growth of yeast cells subjected to a millimeter waveband radiation,  $41.7\text{ GHz}$  modulated by  $8\text{ kHz}$ , at different powers in the interval from  $10\text{ mW/cm}^2$  to  $5 \cdot 10^{-6}\text{ }\mu\text{W/cm}^2$ . While the effect remained at a level of  $10\text{--}20\%$  a reduction of resonance peak widths was observed at lower radiation intensities.

Belyaev *et al.* (1996) also observed the narrowing of resonance peaks of biological effects on *E. coli* cells. When the power of  $51.755\text{ GHz}$  radiation was attenuated from  $100$  to  $10^{-10}\text{ }\mu\text{W/cm}^2$  the relative halfwidth of resonance peak decreased monotonously from  $\sim 2 \cdot 10^{-3}$  to  $\sim 10^{-4}$ , or, in absolute units, from  $200$  to  $5\text{--}6\text{ MHz}$ . A further  $1000$ -fold reduction of intensity did not reduce the peak width. The effect/power function has the form of a plot with a saturation plateau at

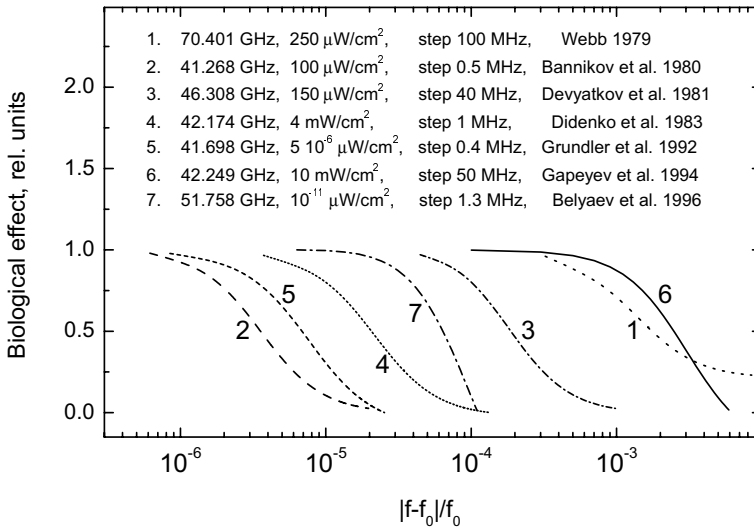


**Figure 5.7.** Resonance peaks of biological effects of microwaves: (1) induction of a prophage in *E. coli* cells (Webb, 1979); (2) same as in (1) (Bannikov and Ryzhov, 1980); (3) synthesis of penicillinase by staphylococci (Devyatkov *et al.*, 1981); (4) index of a Mössbauer spectrum of hemoglobin (Didenko *et al.*, 1983); (5) growth of yeast (Grunder and Kaiser, 1992); (6) motility of single-cell organisms (Gapeyev *et al.*, 1994); (7) state of the cell genome of *E. coli* (Belyaev *et al.*, 1996).

$10^{-11} \mu\text{W}/\text{cm}^2$  (this threshold changed its place depending on the density of cell suspension) — a profile typical for a dependence of quantum transition probability on resonance perturbation intensity. It is not clear yet whether the minimum bandwidth observed is associated with the lifetime of quantum states in the biological system or with the millimeter-wavelength generation bandwidth: the generator frequency bandwidth of  $\sim 1$  MHz coincided with the order of magnitude of the observed resonance peak width. Studying the biological effect of microwaves on *E. coli* cells, Bannikov and Ryzhov (1980) also noted the resonance peak width to be consistent with the generator bandwidth. Notably, the findings of Belyaev *et al.* (1996) correspond to the idea of resonance quantum transitions both qualitatively and quantitatively, namely, by a certain profile of the dependence of resonance halfwidth on pumped radiation power. From formulas describing the resonance in a two-level system, e.g. (4.4.11), it is not hard to derive that the peak halfwidth (disregarding the natural linewidth, i.e., at sufficiently large intensities) is proportional to the square root of pump power. A similar profile was observed by Belyaev *et al.* (1996) in attenuating the pump power from 100 down to  $10^{-2} \mu\text{W}/\text{cm}^2$ .

Figure 5.7 shows the Lorentzian approximations for some known results of the

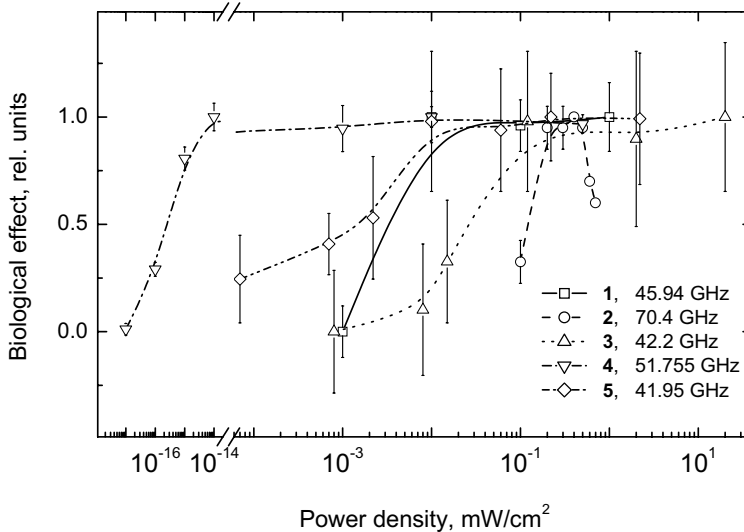


**Figure 5.8.** Dependence of the effects on microwave power: (1) colicine synthesis (Smolyanskaya *et al.*, 1979); (2)  $\lambda$ -phage induction on *E. coli* cells (Webb, 1979); (3) motility of single-cell *Paramecium caudatum* (Gapeyev *et al.*, 1994); (4) *E. coli* AB1157 genom conformational state (Belyaev *et al.*, 1996); (5) inhibition of neutrophile chemiluminescence (Gapeyev *et al.*, 1996).

frequency spectra of microwave biological effects. The data are normalized to unity. It should be obvious that the resonance linewidth correlates well with the generator tuning step rather than with the radiation power density. The frequency tuning step is naturally associated with the technical characteristics of the generator, above all with the radiation bandwidth.

Some authors reported relatively high threshold powers, fractions to units of  $\text{mW}/\text{cm}^2$ , of resonance biological effects of microwaves (Devyatkov *et al.*, 1981; Golant, 1989; Gapeyev *et al.*, 1994). This could be caused by inaccurate tuning to resonance. At lower pump intensities the radiation frequency may not fit the constricted resonance peak. Figure 5.8 shows familiar dependencies of resonance biological effects on microwave pump power normalized to unity. It should be obvious that the statement on threshold power in the said range is poorly grounded. Other workers reported the threshold at  $1 \mu\text{W}/\text{cm}^2$  (Gapeyev *et al.*, 1996),  $10^{-2} \mu\text{W}/\text{cm}^2$  (Aarholt *et al.*, 1988),  $5 \cdot 10^{-6} \mu\text{W}/\text{cm}^2$  (Grundler and Kaiser, 1992), and even at  $10^{-12} \mu\text{W}/\text{cm}^2$  (Belyaev *et al.*, 1996; Kuznetsov *et al.*, 1997). In the last case, the power of microwave radiation  $p$  taken up by cells was 5–6 orders of magnitude below the thermal radiated power  $P$ . The latter can be estimated roughly from the black body radiation law. The Planck formula for energy density in a unit frequency

interval is

$$\rho(\nu) = 8\pi h \left(\frac{\nu}{c}\right)^3 \left[ \frac{1}{\exp(h\nu/\kappa\mathcal{T}) - 1} \right].$$

For gigahertz frequencies  $\nu$  at room temperature, it may well be approximated by the Rayleigh–Jeans formula

$$\rho(\nu) = 8\pi \frac{\nu^2}{c^3} \kappa\mathcal{T}.$$

Substituting  $\nu \sim 50$  GHz and  $\Delta\nu \sim 5$  MHz we obtain the heat flux density

$$P = \Delta\nu c \rho(\nu) \sim 10^{-6} \mu\text{W}/\text{cm}^2.$$

The fact that  $p$  is much less than  $P$  represents the same paradox as in low-frequency magnetobiology — the “kT problem”. Now it is especially evident that the “kT problem” naturally forks in two equally important issues addressed in Section 3.12. The first concerns the mechanism of control of relatively strong,  $\sim \kappa\mathcal{T}$ , chemical processes by microwave quanta  $h\nu \ll \kappa\mathcal{T}$ , while the second concerns the mechanism of stability of such control in the background of thermal perturbations with intensity  $P \gg p$ .

Thus, there is sufficient ground to believe that some biological effects of microwaves are caused by quantum transitions between atom-like levels. On the other hand, Arber (1985) hypothesized that metalloproteins, specifically calcium-binding calmodulin, are the targets of microwave radiation in living tissues. To develop this hypothesis one should assume that microwave fields cause transitions between the quantum states of the ion confined in a binding cavity of the protein.

Liboff *et al.* (1987b), Alipov *et al.* (1994), Blank and Goodman (1997), Litovitz *et al.* (1997a), and Gapeyev *et al.* (1999) pointed out a remarkable analogy between biological effects caused by microwave radiation and low-frequency magnetic fields. These effects proved to be close in magnitude in one and the same biological systems. Both pumping methods require certain conditions to be met. Specifically, the time of invariable radiation parameters must exceed a certain threshold (Litovitz *et al.*, 1991, 1993). Both effects disappear when an additional low-frequency fluctuating magnetic field is applied (Litovitz *et al.*, 1997a). Penafiel *et al.* (1997) and Litovitz *et al.* (1994a) found close frequency spectra for exposure to a low-frequency magnetic field and a modulated millimeter-band radiation (dependencies on modulation frequency).

For example, Bawin *et al.* (1975) studied the efflux of  $^{45}\text{Ca}^{2+}$  ions from chicken brain tissue irradiated by an amplitude-modulated (AM) 0.5–35 Hz radiation of 147 MHz. The efflux increment peaked at 20% at a modulation frequency of 16 Hz, as shown in Fig. 5.10.

Penafiel *et al.* (1997) studied the effect of a  $\sim 1$  mW/cm<sup>2</sup>, 835-MHz microwave pumping on the activity of ornithine decarboxylase in L929 cells at various types of modulation. The most pronounced changes,  $\sim 90\%$ , were found for amplitude modulations with frequencies of 16 and 60 Hz after 8 h of exposure; the effect fell down to the initial level after 24 h of exposure. Other types of modulation, such as

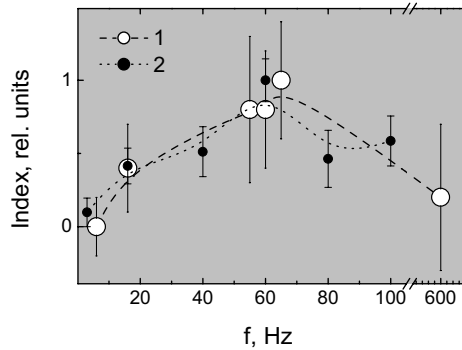


**Figure 5.9.** Dependence on microwave modulation frequency: (1) activity of ornithine decarboxylase in L929 cells (Penafiel *et al.*, 1997), and (2) inhibition of cytotoxicity of T-lymphocytes (Lyle *et al.*, 1983).

frequency, pulse, or voice modulation, were less effective or ineffective altogether. Figure 5.9 shows the effectiveness spectrum of modulation frequencies, at 8-h exposures, for a modulation factor of  $m = 0.23\%$ , computed from the AM signal power ratio  $P = P_0(1 + m^2/2)$ . The profile has an obvious extremum. Effective modulation frequencies correspond to the frequency range of the low-frequency magnetic fields that induce a similar biological effect in the same cell culture (Litovitz *et al.*, 1994a). A sensible effect, up to 60%, of AM 450-MHz microwaves on the same biological system was observed by Byus *et al.* (1988).

Lyle *et al.* (1983) found that an AM 450-MHz,  $1.5 \text{ mW/cm}^2$  radiation inhibits the toxicity of T-lymphocytes with respect to cancer cells. The dependence on modulation frequency exhibited an extremum at 60 Hz, as shown in Fig. 5.9. It was this frequency that produced the strongest inhibition effect when a low-frequency electric field was used as a conditioning agent (Lyle *et al.*, 1988).

Kuznetsov *et al.* (1997) used pulse-modulated microwave radiation in experiments with phasing cell cycles by external radiation. The maximum effect was obtained with a modulation frequency of around 10 Hz.

Grigoriev and Stepanov (2000) reported that a modulated 10-GHz radiation with intensity of  $40 \mu\text{W/cm}^2$  inhibited imprinting<sup>34</sup> in chicken embryos after merely a 5 min exposure. The effect was observed at modulation frequencies of 9–10 Hz and was absent at 1–3 and 40 Hz.

For all these experiments, neither the strength of a local permanent magnetic field nor its orientation with respect to the microwave field configuration was reported.

<sup>34</sup>Imprinting is the ability of animals to memorize the distinctive features of external stimuli in their infancy.

The noted similarity of the biological effects of microwaves and low-frequency magnetic fields suggests a possible common nature of the underlying physical processes. Since a number of magnetobiological effects induced by low-frequency magnetic fields lend themselves well to explanation by an ion interference theory, it seems reasonable to consider its behavior in a microwave field. An objective of such an analysis would be to derive the probability of dissociation of ion–protein complexes as a function of the amplitude modulation frequency of microwaves. These dependencies could be fairly simple to measure experimentally, for one would not need to vary the carrier frequency — a manipulation prone to artifacts (Khizhnyak and Ziskin, 1994; Gapeyev *et al.*, 1996), thus obtaining a convenient way for experimental verification of such theories. It should be noted also that the natural frequencies of quantum transitions of particles with parameters of Ca, Mg, and similar ions in the effective potential of radius  $R \sim 0.7 \text{ \AA}$ , corresponding to the binding site of calmodulin, are right in the millimeter-band of EM radiation, see Section 4.1. Moreover, as was recalled, experimenters often observe a number of close spectral maxima spaced 10–50 MHz from one another. This fact also agrees with the model of quantum levels sequentially excited by the scanning pump frequency. The splitting seems to owe its existence to an additional potential well with octahedral symmetry which perturbs the ideal spherical potential of the protein–ion cavity.

### 5.2.2 Interference in amplitude-modulated microwave fields

In this section, we will not discuss the interaction of a simple quantum system with a plane EM wave, for this interaction has been extensively reported (e.g., Davydov, 1973). Instead, we confine our consideration to studies of dissociation interference effects induced by an amplitude modulation of an irradiating carrier.

The state of the ion in a cavity is specified by the superposition of its fundamental states  $|k\rangle$

$$\Psi(r, \theta, \varphi) = \sum_k c_k(t) |k\rangle .$$

We assume that all states  $|k\rangle$  of the ion are numbered sequentially without reference to radial, azimuthal, or magnetic quantum numbers. In this notation, the density matrix takes the form

$$\sigma_{nk} = c_n^* c_k .$$

It obeys the Liouville quantum equation relating perturbation to a wideband amplitude-modulated EM radiation. After this definition, the equation can be derived in exactly the same way as outlined in the first half of Section 3.8.2 devoted to the parametric resonance in a three-level atomic system. Therefore, we retain the nomenclature and approximations of that section and begin right from Eq. (3.8.17) for the non-diagonal terms of the density matrix responsible for interference effects

$$\dot{\sigma}_{nk} = -(\Gamma_{nk} + i\omega_{nk}) \sigma_{nk} + F_{nk} .$$

Here,  $\Gamma_{nk}$  are the attenuation coefficients,  $\omega_{nk}$  are the frequency gaps between Zeeman sublevels, and the pumping matrix

$$F_{nk} \equiv \frac{2\pi E^2 \sigma_{00}}{\hbar^2} v_{0n}^* v_{0k}$$

includes the spectral density  $E$  of the EM field electric component, which is deemed to be invariable in time and independent of frequency, i.e.,  $E = E_\omega = \text{const}$ . This assumption is based on the fact that the bandwidth of microwave radiation is far wider than Zeeman's splitting even in very sophisticated generators.

In contrast to the case of modulation of a Zeeman gap bandwidth in a low-frequency magnetic field considered in Section 3.8.2, now we consider modulation of a microwave carrier intensity. In this case, the pump matrix becomes a function of time. Since the pump matrix is proportional to the spectral density squared, it can be readily expressed in terms of the density matrix  $F_{nk}$  in the absence of modulation (Alexandrov *et al.*, 1991),

$$F_{nk}(\epsilon) = F_{nk} (1 + \epsilon \cos \Omega t) ,$$

where  $\Omega$  is the frequency, and  $\epsilon$  is the modulation index. The equation for cross terms of the density matrix takes the form

$$\dot{\sigma} = -(\Gamma + i\omega) \sigma + F(1 + \epsilon \cos \Omega t) ,$$

and its solution is

$$\sigma = e^{ft} \left[ C + \int e^{-ft} g dt \right] , \quad f \equiv -\Gamma - i\omega , \quad g(t) \equiv F(1 + \epsilon \cos \Omega t) .$$

Here, for convenience, we temporarily drop the running subscripts  $n, k$ . We assume the initial conditions such that  $C = \text{const.} = 0$

$$\sigma = e^{ft} \int e^{-ft} g dt .$$

Having determined this integral, we obtain

$$\sigma = F \left[ \frac{1}{\Gamma + i\omega} + \frac{\epsilon}{2} \frac{\exp(i\Omega t)}{\Gamma + i(\omega + \Omega)} + \frac{\epsilon}{2} \frac{\exp(-i\Omega t)}{\Gamma + i(\omega - \Omega)} \right] . \quad (5.2.1)$$

The change of intensity of the re-emitted EM field that occurred when the modulation frequency and the frequency of difference between (Zeeman) levels coincide (this change is defined by elements of the density matrix (5.2.1)) is known as "beet resonance" (Alexandrov *et al.*, 1991). We, however, will be interested in the variation in the internal distribution of particle density affecting the probability of its escape from the binding site.

We write the wave function using the approximations and notation of Section 4.1

$$\Psi = \sum_{klm} d_{klm} R_{kl} P_l^m \Phi_m .$$

In contrast to (4.1.5), the coefficients  $d_{klm}$  depend on time because of transitions caused by microwaves. Now, the probability density for the ion to be in a certain angular state is

$$\begin{aligned} p(t, \varphi_0) &= \langle \Psi(t, \varphi_0) | \Psi(t, \varphi_0) \rangle_{r, \theta} \\ &= \sum_{kk' ll' mm'} d_{klm}^* d_{k'l'm'} \langle R_k | R_{k'} \rangle \langle P_l^m | P_{l'}^{m'} \rangle \Phi_m(\varphi_0)^* \Phi_{m'}(\varphi_0) \\ &= \sum_{mm'} \sigma_{mm'} a_{mm'} e^{-i(m-m')\varphi_0} , \end{aligned} \quad (5.2.2)$$

where

$$\sigma_{mm'} a_{mm'} \equiv \sum_{kk' ll'} d_{klm}^* d_{k'l'm'} \langle R_k | R_{k'} \rangle \langle P_l^m | P_{l'}^{m'} \rangle .$$

Here, the coefficients  $a_{mm'}$ , defining the initial conditions, explicitly follow from the density matrix  $\sigma$ . We substitute the found density matrix (5.2.1) in the expression for probability density (5.2.2) and take into account that the leading constant term in (5.2.1) is not of interest for this consideration. The phenomenological damping coefficients in the density matrix make sense in connection with the earlier introduced lifetime of magnetic modes. We assume that they all are identical and equal to  $\Gamma_{mm'} = \Gamma = 1/T$ . We suppress also the constant factor  $\frac{1}{2}$  immaterial for the subsequent analysis. Returning the subscripts to (5.2.1), we can write the probability density in the form

$$p = \sum_{mm'} a_{mm'} \left[ \frac{F\epsilon \exp(i\Omega t)}{\Gamma + i(\omega_{mm'} + \Omega)} + \frac{F\epsilon \exp(-i\Omega t)}{\Gamma + i(\omega_{mm'} - \Omega)} \right] \exp(i\Delta m \varphi_0) .$$

For a Zeeman multiplet,  $\omega_{mm'} = \omega_0 \Delta m$ . Denote

$$\omega_+ = \omega_0 \Delta m + \Omega , \quad \omega_- = \omega_0 \Delta m - \Omega .$$

The probability density takes the form

$$p(t, \varphi_0) = F\epsilon \sum_{mm'} a_{mm'} \left[ \frac{\exp(i\Omega t)}{\Gamma + i\omega_+} + \frac{\exp(-i\Omega t)}{\Gamma + i\omega_-} \right] \exp(i\Delta m \varphi_0) . \quad (5.2.3)$$

In contrast to (4.1.8) the probability density (5.2.3) oscillates at a single frequency  $\Omega$ . Therefore, in this case, there is no need for selecting slow-oscillation components by taking a smoothing average.

The sum (5.2.3) has complex conjugated terms, namely,  $mm'$ , and  $m'm$ . After multiplication and averaging, these terms have a non-zero contribution. To illustrate, we write a pair of such terms:

$$a_{mm'} \left[ \frac{\exp(i\Omega t)}{\Gamma + i\omega_+} + \frac{\exp(-i\Omega t)}{\Gamma + i\omega_-} \right] \exp(i\Delta m \varphi_0)$$

$$a_{m'm} \left[ \frac{\exp(-i\Omega t)}{\Gamma - i\omega_+} + \frac{\exp(i\Omega t)}{\Gamma - i\omega_-} \right] \exp(-i\Delta m \varphi_0) .$$

All the products of other pairs that do not produce a permutation  $m \leftrightarrow m'$  vanish due to averaging over an arbitrary angle  $\varphi_0$ . Thus, the squared density  $p(t, \varphi_0)$  will be the sum of products of designated terms. We multiply these terms and average the product over time, i.e., discard the terms with exponents depending on  $t$ , to obtain

$$P \equiv \overline{p^2(t, \varphi_0)} = F^2 \epsilon^2 \sum_{mm'} |a_{mm'}|^2 \left( \frac{1}{\Gamma^2 + \omega_+^2} + \frac{1}{\Gamma^2 + \omega_-^2} \right) .$$

Since we study the case of  $\Omega \sim \omega$ , that is, the one with  $\omega_- \rightarrow 0$ ,  $\omega_+ \rightarrow 2\Omega$ , one of the two terms introduces only a small correction to the results. Therefore, we omit it from our further consideration. The final formula for the field-dependent probability of dissociation is

$$P = \sum_{mm'} |a_{mm'}|^2 \frac{F^2 \epsilon^2}{T^{-2} + (\omega_0 \Delta m - \Omega)^2} , \quad (5.2.4)$$

or, rewritten in dimensionless variables accurate to a factor, it becomes

$$P = \sum_{mm'} |a_{mm'}|^2 \frac{\epsilon^2}{1 + [(\Delta m/2 - f')\Xi]^2} . \quad (5.2.5)$$

A quadratic dependence of the effect on modulation index  $\epsilon$  immediately leaps to the eye. However, in view of a generally non-linear behavior of the biological effect to a growing stimulus, this dependence would be hard to verify experimentally.

The frequencies of effect peaks make up a series similar to the case of a low-frequency magnetic field, viz.,

$$f' = \Delta m / 2 . \quad (5.2.6)$$

Now,  $f' = \Omega/\Omega_c$  is the relative modulation frequency of microwaves. Thus, *if the biological effect of AM microwave radiation is the consequence of interference of ion states, then the dependence on modulation frequency has maxima whose frequencies are directly proportional to a local static magnetic field.* This prediction (Binhi, 1999c) can be verified experimentally.

Figure 5.10 shows the experimental data (Bawin *et al.*, 1975) that have not been interpreted in the literature. It also plots a calculation with the interference model. Since the DC magnetic field was not measured during the experiment, the calculation is based on a probable MF strength of  $H_{DC} = 50 \mu\text{T}$ . The other parameters were the same as in the calculations for calcium. A qualitative agreement between theory and experiment is evident.

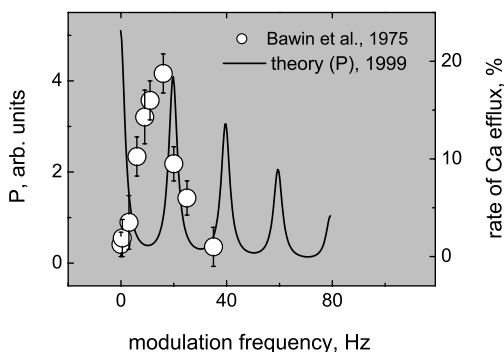


**Figure 5.10.** Experimental data (Bawin *et al.*, 1975) on  $^{45}\text{Ca}^{2+}$  efflux from brain tissue and a theory describing the behavior of these ions in the field  $H_{\text{DC}} = 50 \mu\text{T}$ ,  $\Xi = \Omega_c T = 20$ .

### 5.2.2.1 Interference in unmodulated RF fields

The outlined mechanism fails to predict effects in the absence of modulation ( $\epsilon = 0$ ) of microwave pumping. This fact is at variance with abundant observations of biological effects for unmodulated RF fields. We present here, without giving an underlying theory, a statement that the ion-interference mechanism allows these effects to occur as a result of rotation of ion-protein complexes. In Section 4.5 we demonstrated that the rotation of complexes in a steady magnetic field causes effects similar to the action of alternating magnetic fields in the background of a permanent field. The effects observed were obtained only with those rotations of complexes that were matched in rate with the magnetic field. On the other hand, for microwave irradiation, we presume that the role of modulating agent will be played by the natural rotation of ion-protein complexes. If this is the case, then *the resonance peaks of the unmodulated-RF-induced biological effect disappear when the biological system performs macroscopic rotation. Changing the strength of the permanent magnetic field causes the earlier observed resonance peaks to disappear and new peaks to appear at other frequencies.* It was this behavior of the microwave spectra of a biological effect that was observed by Gapeyev *et al.* (1999). They measured the activity of mouse neutrophils from the chemiluminescence of a sonde in response to a CW  $50 \mu\text{W}/\text{cm}^2$  radiation. When the local magnetic field was increased in strength from 50 to  $100 \mu\text{T}$  the effect (absolute level at about 25%) changed sign and position of the spectral maximum from 41.95 to 42.00 GHz.

Gapeyev *et al.* (1994) reported that the biological effect depends on the keying modulation frequency 0.091–0.102 Hz, which is one-tenth to one-hundredth the relevant ion frequency. It seems that effects of continuous microwave radiation did occur on the primary level, but in order to occur on the biological level they needed to strike resonance with some internal rhythms with a period around 1 s, e.g., with oscillations in the concentration of cellular calcium suggested by these authors.

Gapeyev *et al.* (1997) observed an intricate behavior of the effect as a function of the carrier frequency and the modulation frequency including the effect's sign alternations. However, in this case as well, the characteristic modulation frequency was rather low — around 1 Hz. This fact justifies the conclusion drawn by these workers saying that a system of coupled biochemical reactions with characteristic frequencies in this range was involved in the reception of microwaves. On the other hand, the primary reception could occur independently of whether a modulation is used. Thus, the action of microwaves on biological systems, just as the action of low-frequency magnetic fields, may be latent and may therefore lead, like chemical agents do, to unpredictable remote consequences.

### 5.2.3 Dissociation in circularly polarized EM fields

Now we turn to consider dissociation in a field of circularly polarized radiation. We dwell on changes that need be made in the derivation of the equation for non-diagonal elements of the density matrix outlined in Section 3.8.2. Here we demonstrate that, compared to the case of plane polarized radiation, the changes will involve the pumping matrix alone.

Let  $\mathbf{e}_x$ ,  $\mathbf{e}_y$ , and  $\mathbf{e}_z$  be the unit normal vectors of a Cartesian system of coordinates. A plane polarized wave, e.g., in the  $y = 0$  plane, propagating along the  $z$  axis may be written as

$$\mathbf{E}_x = \mathbf{e}_x \cos \omega t = \frac{1}{2} \mathbf{e}_x (e^{i\omega t} + e^{-i\omega t}) . \quad (5.2.7)$$

Here, a unit wave intensity  $\overline{\mathbf{E}\mathbf{E}}$  is assumed, and the term  $kz$  reflecting variations of the phase in space and immaterial in this section is suppressed from the phase representation  $\omega t - kz$ . A circularly polarized wave, whose vector traces a right- or left-hand helix in space, can be represented as a superposition of two coherent waves plane-polarized in different planes with a certain phase shift, viz.,

$$\mathbf{E}_+ = \frac{1}{\sqrt{2}}(\mathbf{e}_x \cos \omega t - \mathbf{e}_y \sin \omega t) , \quad \mathbf{E}_- = \frac{1}{\sqrt{2}}(\mathbf{e}_x \cos \omega t + \mathbf{e}_y \sin \omega t) ,$$

where the wave is again normalized to unit intensity. It is convenient to represent such waves in a special basis with so-called cyclic unit vectors

$$\mathbf{e}_+ = -\frac{1}{\sqrt{2}}(\mathbf{e}_x + i\mathbf{e}_y) , \quad \mathbf{e}_- = \frac{1}{\sqrt{2}}(\mathbf{e}_x - i\mathbf{e}_y) , \quad \mathbf{e}_0 = \mathbf{e}_z .$$

Then we may represent a circularly polarized wave in a form close to (5.2.7):

$$\mathbf{E}_+(t) = \mathbf{e}_- \int E_\omega \exp(-i\omega t - i\varphi_\omega) d\omega - \mathbf{e}_+ \int E_\omega \exp(i\omega t + i\varphi_\omega) d\omega .$$

In contrast to the case of plane polarized waves, now the complex conjugates in Eq. (3.8.8) have different polarizations. In the subsequent derivation of the density

matrix equation, we will use only one of these summands since the other is associated with rapidly oscillating terms whose contribution may be neglected. Therefore, the matrix elements  $v_{0k}$  from (3.8.12), which are also terms of the pump matrix (3.8.16), can be written as

$$v_{0k} = \langle 0 | \mathbf{d} \mathbf{e}_- | k \rangle .$$

Alexandrov *et al.* (1991) demonstrated that, in a cyclic basis, the matrix elements of the dipole moment operator have the form

$$\langle n | \mathbf{d} | k \rangle = \mathbf{e}_\nu d_{kn} ,$$

where  $d_{kn}$  are coefficients depending on the quantum numbers of states  $n, k$ , and  $\nu = m_k - m_n$  is the difference of the projections of the total magnetic moment on the quantization axis. The unit vectors  $\mathbf{e}$  do not affect the wave functions and can be factored out of the quantum bracket; therefore the matrix elements  $v_{0k}$  become

$$v_{0k} = d_{k0} \mathbf{e}_\nu \mathbf{e}_- .$$

In the pumping matrix, these elements occur as the combination  $v_{0n}^* v_{0k}$ . Without any loss of generality, allowance for the possibility of circular polarization boils down to a replacement of the pump matrix in the equation for density matrix

$$F_{nk} \rightarrow F_{nk} |\mathbf{e}_\nu \mathbf{e}_-|^2 .$$

From the scalar product of vectors, the pumping peaks at  $\mathbf{e}_\nu = \mathbf{e}_+$  and vanishes at  $\mathbf{e}_\nu = \mathbf{e}_-$ . These selection rules, dictating the conservation of the sum of projections of the total moment of the atomic system and a photon in a dipole transition, define which polarization, right-hand or left-hand, of external radiation will be efficient. While the dissociation of the atom-like system, considered in Section 5.2.2, is associated with a dipole transition from the ground state to an excited state with the total moment differing by one unit, then the probability of dissociation (5.2.4) will be non-zero for microwaves of only one, right- or left-hand, circular polarization. Linearly polarized radiation, which is a coherent superposition of opposite circularly polarized waves, will also be efficient. The power of one circular component is half the power of linearly polarized radiation. However, since the pump matrix, directly proportional to the radiation power, enters the expression for dissociation probability as  $F^2$ , then the linearly polarized radiation will produce one-quarter as large a dissociation effect as a circularly polarized radiation of equal power.

A similar dependence of biological effects of a SHF radiation of  $10\text{--}200 \mu\text{W}/\text{cm}^2$  on the state of its polarization was observed by Belyaev *et al.* (2000). In the range 41.25–41.50 GHz where the effect peaked, left-hand almost circularly polarized microwaves produced a 10–20% statistically significant effect in preliminarily X-rayed *E. coli* cells. Right-hand polarized microwaves were ineffective and linearly polarized microwaves produced an intermediate effect. Conversely, the other spectral maximum at 51.76–51.78 GHz could be observed with right-hand polarization

only. It was concluded that quantum transitions with helical selection rules were involved in the biological reception of microwaves.

It should be noted that at lower RF intensities, the semiclassical approximation — in which the quantum atomic system interacts with a classical EM radiation — becomes, generally speaking, inapplicable. However, in this specific case, conclusions boil down mainly to stating the angular momentum conservation law, which holds independently of a selected model, i.e., a semiclassical formalism or quantum electrodynamics. Therefore the conclusions of this section are equally applicable in the range of very low microwave intensities where biological effects are also observed, as shown in Fig. 3.1. In this case, the RF radiation can adequately be described by the helicity of EM quanta, specifically, the quantum number ( $\pm 1$ ) characterizing the projection of the photon spin on its momentum.

### 5.2.4 Raman scattering at organisms and RF field effects

Quantum theory treats Raman or combination scattering of light as a two-stage process. In the first stage, the quantum system absorbs a photon of energy  $\hbar\omega$  to assume a virtual state. In the second stage, it emits a photon of energy  $\hbar\omega'$  and either returns to the ground state or jumps into an excited state. The energy of the scattered photon may be identical to that of the incident photon  $\omega' = \omega$ , then one speaks of Rayleigh scattering. The incident photon may share its energy with the quantum system  $\omega' = \omega - \Omega$ , to produce a line shifted towards lower frequencies in the scattering spectrum — this is Stokes scattering. Conversely, if the scattered photon carries away some energy of the quantum system, this is anti-Stokes scattering. These processes in a quantum system scattering EM radiation and giving rise to Rayleigh, Stokes, and anti-Stokes lines in the scattering spectrum are illustrated in Fig. 5.11. As a result of Stokes or anti-Stokes scattering, the quantum system is carried into a different state. In the Stokes process, the system moves from the ground to an excited state, while in the anti-Stokes process, it returns from an excited state to the ground state. Since at thermal equilibrium the populations of the excited and ground states are related by  $n_1/n_0 = \exp[-\hbar\Omega/\kappa\mathcal{T}]$  the intensities of Stokes and anti-Stokes lines are generally different. If the splitting  $\Delta E = \hbar\Omega$  is far below the thermal energy  $\kappa\mathcal{T}$ , then the levels are equally populated and the Raman lines have identical intensities.<sup>35</sup> Otherwise, as this usually happens with electron terms of molecules, the anti-Stokes component is far weaker than its Stokes counterpart.

Most often than not the quantum system is characterized by many levels of different structures. Then the spectrum of scattered EM radiation exhibits multiple lines corresponding to transitions between these levels — combination transitions. The position and intensity of these lines give information about the structure and

---

<sup>35</sup>Since the intensity of radiation is  $\sim \omega'^4$ , a more accurate relation of intensities far from the frequencies of resonance scattering  $\omega$  is given by  $I_{\text{as}}/I_{\text{st}} = \exp[-\hbar\Omega/\kappa\mathcal{T}] (\omega + \Omega)^4/(\omega - \Omega)^4$ .

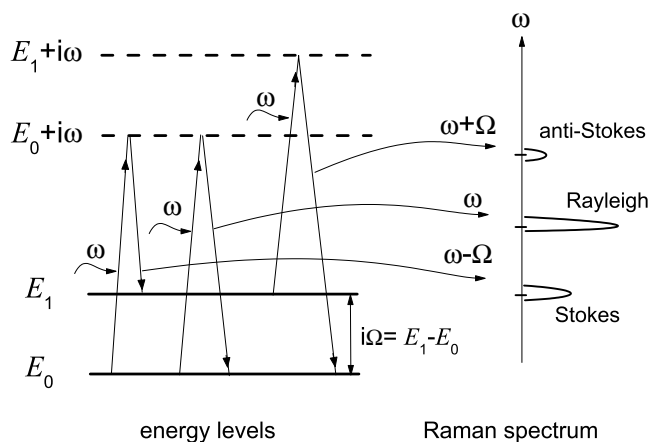


**Figure 5.11.** Quantum transitions in Raman scattering of EM radiation and the Raman spectrum including Rayleigh, Stokes, and anti-Stokes lines.

state of the system. Therefore Raman scattering is an informative probe for studying molecular processes *in vitro* including macromolecular processes.

Webb (1980) reviewed a number of their studies on Raman scattering at biological cells conducted *in vivo* in various metabolic states since 1971. The cells studied included those of *B. megaterium*, *E. coli*, and mammal carcinoma. In the range  $0\text{--}3400\text{ cm}^{-1}$  they found multiple Raman lines which appeared only when cells were in a metabolically active state. Raman spectra, positions of lines, and their intensities changed as the cells were proceeding through their evolution stages. The general pattern of the spectra was replicated in different specimens of cell culture. Several tens of lines with frequencies above  $300\text{ cm}^{-1}$  tend to shift to high frequencies, whereas those lying below  $300\text{ cm}^{-1}$  (about a dozen of lines) shift towards the Rayleigh line. A strong line of scattering at *E. coli* was shifted for an hour at an average rate of  $0.5\text{ cm}^{-1}$  per minute from  $158$  to  $126\text{ cm}^{-1}$ . Over a cell lifecycle, some lines disappeared and reappeared with a period of  $3\text{--}5$  min. Thus, spectra of Raman scattering at biological systems studied *in vivo* provide information about cell metabolism and reflect the physiological state of the cell.

Raman scattering with similar properties were reported by Drissler (1988) for *Clorella pyrenoidosa* algae and by Bannikov *et al.* (1980) for *B. megaterium* cells.

The thermal energy  $\kappa\mathcal{T}$  has its equivalent frequency  $\kappa\mathcal{T}/2\pi\hbar c$  or around  $230\text{ cm}^{-1}$ . Therefore, as we said above, at thermal equilibrium, anti-Stokes lines with frequencies significantly above  $230\text{ cm}^{-1}$  should be sensibly weaker than their Stokes counterparts while those with frequencies above  $500\text{ cm}^{-1}$  should not be visible altogether. Nonetheless, this is not always the case. Scattering at weed cells (Drissler, 1988) gives strong anti-Stokes lines in this range. Moreover, anti-Stokes

lines near  $1000\text{ cm}^{-1}$  are stronger than their Stokes satellites. The range below  $200\text{ cm}^{-1}$  shows its specific features. For lines in the range  $100\text{--}200\text{ cm}^{-1}$ , the equilibrium anti-Stokes/Stokes intensity ratio must be within  $0.65\text{--}0.42$  at physiological temperatures. However, for scattering at *E. coli*, Webb (1980) reported a pair of lines with almost equal intensities at  $\pm 130\text{ cm}^{-1}$ . The population of the excited level computed from the relative intensities of  $\pm 868\text{ cm}^{-1}$  lines reported by Drissler (1988) exceeded the thermal population 2.6 times. This inconsistency of expected and measured relative intensities of Raman satellites suggests that excitations at which scattering occurs are not thermalized; that is, they decay before they would come to thermal equilibrium with the surroundings. Alternatively, such excitations obey other statistics than Boltzmann.

Let us consider the quantum effect governing the intensities of Raman scattering lines. We assume that, in terms of population, the number of excitation quanta on the excited level (level 1 in Fig. 5.11) is  $n$ , and that in the ground level is  $m$ . The Stokes process increases  $n$  by one unit, and decreases  $m$  by one unit. This process may be thought of as action of a birth operator  $a^+$  on  $|n\rangle$  and an annihilation operator  $b$  on  $|m\rangle$ . The result will be the state  $|n+1, m-1\rangle$  occurring from the state  $|n, m\rangle$ . In accord with the normalization rules of these representation we have

$$a^+b|n, m\rangle = \sqrt{n+1}\sqrt{m}|n+1, m-1\rangle.$$

The intensity of this process is proportional to the square of the respective matrix element, i.e.,  $(n+1)m$ . The second part of the perturbation operator  $a^+b + b^+a$ , inducing transitions in these levels, conversely, reduces  $n$  by 1 and increases  $m$  by 1, thus representing the anti-Stokes process:

$$b^+a|n, m\rangle = \sqrt{n}\sqrt{m+1}|n-1, m+1\rangle.$$

The intensity of this process is  $n(m+1)$ . Thus, if thermal and, possibly metabolic, processes sustain the populations of these states at  $n$  and  $m$  quanta, respectively, the intensity ratio is  $I_{\text{as}}/I_{\text{st}} = n(m+1)/m(n+1)$ . The ground state is usually populated so that  $m \gg 1$ , therefore,

$$\frac{I_{\text{as}}}{I_{\text{st}}} = \frac{n}{n+1}.$$

If the Boltzmann statistics gives that  $n = 0$  with a large probability, but experiment gives  $I_{\text{as}}/I_{\text{st}} \sim 1$ , then the statistics of excitations is other than Boltzmann. Indeed, the collective oscillation modes are bosons and obey a Bose–Einstein distribution

$$\overline{n_k} = \left[ e^{(E_k - \mu)/\kappa\mathcal{T}} - 1 \right]^{-1}, \quad (5.2.8)$$

where  $\overline{n_k}$  is the average number of excitation quanta (or particles) in mode  $k$  with energy  $E_k$ ,  $\mu(\mathcal{T}) \leq 0$  is the chemical potential such that  $\mu \rightarrow 0$  for  $\mathcal{T} \rightarrow \mathcal{T}_0$ , and

$\mathcal{T}_0$  is the degeneration temperature. For  $\mathcal{T}_0 \ll \mathcal{T}$ , the average number of particles in mode  $k$

$$\bar{n}_k \approx \exp(\mu - E_k)/\kappa\mathcal{T}$$

obeys a Boltzmann law. However, if  $\mathcal{T} < \mathcal{T}_0$ , then only a part of the particles is distributed to the (5.2.8) formula. The other part proportional to  $1 - (\mathcal{T}/\mathcal{T}_0)^{2/3}$  resides in the state with  $E_k = 0$ , i.e., undergoes a Bose–Einstein condensation.

In the general case, levels 0 and 1 in Fig. 5.11 are not levels of a certain quantum number. It is assumed that level 1 can be ground in some series  $n_k$  of levels of collective excitation. If the number of excitation quanta on this level is large, then  $I_{\text{as}}/I_{\text{st}} = 1$ . Fröhlich (1968b), Wu (1994, 1996), and many other workers treat the equality of intensities of Stokes and anti-Stokes lines at  $130\text{ cm}^{-1}$  observed in scattering at *E. coli* cells (Webb, 1980) — and in general anomalies of Raman scattering at metabolic cells — as an indication of a Bose condensation caused by metabolism, i.e., a sharp growth of excitation quanta in lower oscillation modes.

Opinions differ as to the nature of those quantum excitations on living systems that are responsible for Raman lines. Scott (1981) analyzed Webb data on Raman lines in the range  $45\text{--}182\text{ cm}^{-1}$  excited by a  $5145\text{-\AA}$  laser radiation in *E. coli* cells. He pointed out that a series of these lines is close to a series of combination frequencies formed from the computed frequencies of internal vibrations of the Davydov soliton  $17$  and  $125\text{ cm}^{-1}$ , see Addendum 6.5. Zabusky and Kruskal (1965) demonstrated that solitons often behave like particles, conserving their individual properties, i.e., shape, in collisions with one another. Therefore it would be wise to treat them as excitation quanta in interactions with excitations of other origin — phonons and photons. Scott believes low-frequency Raman lines from metabolic cells owe their existence to scattering at Davydov solitons. The fact that these lines shift to low frequencies during the life cycle of cells reflects a reduction of soliton propagation speed in aging cells.

For electromagnetobiology, it would be most interesting to study Raman lines in the range  $1\text{--}3\text{ cm}^{-1}$ , i.e.,  $30\text{--}90\text{ GHz}$ , since these lines are likely associated with excitations responsible for biological effects of microwaves. However, for laser-excited Raman spectra, the usual resolution of  $2\text{--}5\text{ cm}^{-1}$  is insufficient for reliable recording of such spectra. In addition, with laser excitation, this range is overlapped by an intense tail of a Rayleigh line. A way to probe excitations in this range was found by exposing the objects to microwaves and measuring re-emitted waves in a far lower decimeter range. Essentially, this is a spontaneous luminescence in an RF range.

### 5.2.5 Radio wave luminescence of water and organisms

Luminescence is a superfluous radiation, as compared to thermal radiation, that may be caused by a variety of physicochemical influences. Radiating centers are commonly atoms and molecules that emit from the visible range to the infrared. At the same time, nothing prevents some collective atom–molecular excitations from being sources of characteristic emissions that should be at far lower frequencies. A

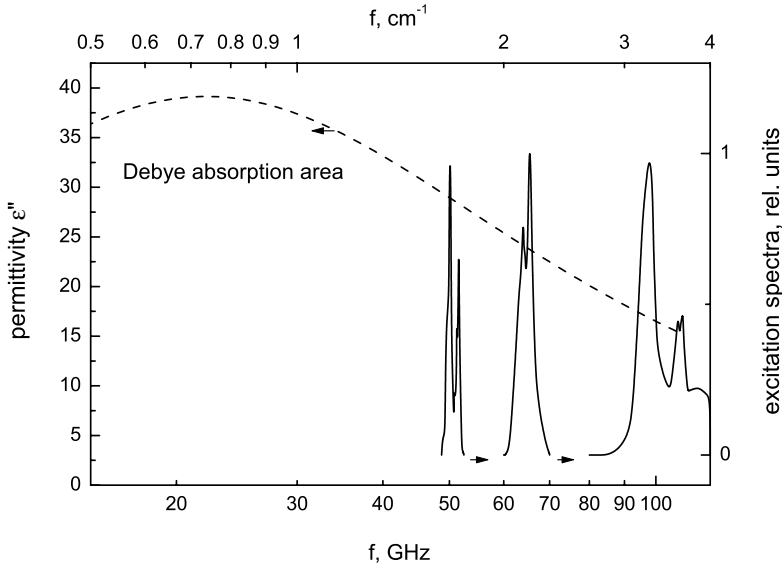


**Figure 5.12.** Excitation spectra of RF luminescence of water, after Petrosyan *et al.* (1995), and the spectrum of a reactive permittivity component responsible for the Debye absorption of radio waves.

team led by Yu. Gulyaev (see Petrosyan *et al.*, 1995) found out that liquid media and biological objects irradiated by microwaves begin emitting EM waves in the decimeter range above the thermal level. The response of the object to an RF radiation was measured by a microwave radiometer at 0.4 or 1 GHz in a frequency band of 50 MHz. The radiometer sensitivity was 0.3 K, its time constant was  $\sim 1$  s. They measured luminescence excitation spectra by scanning excitation frequency in a range 4–120 GHz. The spectra exhibited sharp peaks with fine structure at 51, 65, and 103 GHz, as shown in Fig. 5.12.

The figure also displays the frequency dependence of the permittivity imaginary part responsible for attenuation. In this range, the permittivity can be approximately described by the Debye formula

$$\varepsilon(\omega) = \varepsilon_{\infty} + \frac{\varepsilon_0 - \varepsilon_{\infty}}{1 + i\omega\tau},$$

where  $\varepsilon_0 \approx 80$  is the static dielectric permittivity,  $\varepsilon_{\infty} \approx 1.7$  is the dielectric permittivity at optical frequencies, and  $\tau \approx 0.7 \cdot 10^{-11}$  s is a parameter — the time of dielectric relaxation of water at room temperature. As can be seen, the absorption does not correlate with excitation spectra of water RF luminescence.

The spectra were obtained with a pump power density of  $\sim 1 \mu\text{W}/\text{cm}^2$ . At higher pump intensities, these spectra were hard to detect because the luminescence was non-stationary. Since the frequency of 1 GHz corresponds to a wavelength of 30 cm,

the authors assume that the RF emission owes its existence to excitation of the whole water volume. At the same time, the Debye absorption of the microwave pump by water was rather strong, as can be seen in Fig. 5.12. The absorption coefficient in this range was several tens of centimeters<sup>-1</sup>, and the exciting radiation was almost completely absorbed by a surface water layer as thin as 0.1cm. The mechanism to convert excitation energy into RF radiation is not clear. The radiation power detected by the radiometer was substantially above the thermal background but many orders of magnitude below the absorbed power with an RF power density of  $\sim 1 \mu\text{W}/\text{cm}^2$ . Therefore, the energy conversion mechanism is obviously inefficient. We note that this mechanism is not connected with the general heating of the water specimen however small and with a rise of thermal radiation in the RF range by this reason. Heating of water by microwaves does not possess a frequency selectivity whereas the effective excitation spectra are frequency sensitive.

RF luminescence spectra of water and different tissues are similar in having peaks in the same frequency intervals at 51, 65, and 103 GHz. The authors believe this is an implication of the fact that living tissues are several tens of percent water. At the same time, the fine structure of luminescence spectra depends on the physiological state of the organism, thus allowing one to use this phenomenon for medical diagnosis (Sinityn *et al.*, 1998).

An important observation to the point was that the magnetic field splits the peak at 50 GHz into a Zeeman doublet. In a field of  $H = 50 \text{ G}$ , the splitting was as large as  $\Delta f \sim 1 \text{ GHz}$ . The equivalent magnetic moment  $\mu$  is related to these quantities by the formula  $2\mu H = 2\pi\Delta f\hbar$  and is equal to  $\mu \sim 7 \cdot 10^{-20} \text{ erg/G}$ , which is almost ten times the spin magnetic moment of the electron. We note that the splitting of the peak could be caused by orbital motion of electrons or other charged particles. Thus, hypothetical collective modes, responsible for the excitation of the luminescence should possess (a) natural frequencies in the RF range, (b) an electric dipole moment, (c) a magnetic moment, and, consequently, an angular mechanical momentum of the transitions. The nature of such excitations is not yet known. Petrosyan *et al.* (1996) believe that such excitations could be caused by collective oscillations of bound hexagonal rings formed from six water molecules by hydrogen bonds. It should be noted that the ring binding energy, i.e., the energy of 6 hydrogen bonds, is half as large as the interaction energy of such a ring with the surroundings of almost 12 hydrogen bonds. Therefore, it is highly unlikely that such a hypothetical construction of water molecules could exist in liquid water as a self-sustained structure.

Thus far no information is available on the RF luminescence decay time. One could not exclude that the metastable states of water induced by magnetic fields and EM radiation are related to collective excitations that manifest themselves in this interesting phenomenon.

### 5.3 GENERAL IDEAS IN ELECTROMAGNETOBIOLOGY

Del Giudice *et al.* (1988) have been developing a quantum-field theory of biological

matter, specifically its polarization theory. The Lagrangian describing the polarization field of the medium is invariant with respect to transformations of a continuous group of rotations because of an assumption that the medium is initially isotropic. However, the ground state of the medium, which is a solution to dynamic Lagrangian equations, may have no symmetry of the Hamiltonian and have instead a lower symmetry due to a state with spontaneous polarization — an electret state. It is assumed that, at physiological temperatures, a biological tissue containing a large number of molecules with dipole moments may be in different *sets* of states with non-zero macroscopic polarization  $P$ . The latter plays the role of an order parameter for electret states. Each set is defined on its space of states in accordance with the value of  $P$ , and is characterized by its dynamics or a Lagrangian. Transitions between sets of states are induced by the interaction with the exterior medium. Thus a “two-dimensional” dynamics occurs: the system evolves within each set of states in agreement with a certain Lagrangian dynamics and, forced by external factors such as heat or metabolic energy, undergoes transitions between different sets. This behavior leads to a correlation in oscillations of dipoles and manifests itself as waves of macroscopic polarization — dipole waves. This scenario reveals Fröhlich coherent excitations substantiated in the framework of a quantum-field approach.

In a complementary description, dipole waves correspond to massless particles — quanta obeying a Bose–Einstein statistics. An order or coherence occurs in the system as a consequence of a Bose condensation of particles in the ground state. Since the bosons do not have mass, maintaining a coherent state does not require an additional energy input from outside. Vitiello (1992) uses that as a basis to explain one of the enigmas of biology — conservation of an organism as it stands, i.e., maintaining a macroscopic coherence under conditions when the external source of energy does not contain information about any sort of order.

An external EM field changes the nature of polarization waves in the medium, for such a medium is non-linear with respect to EM fields. The specific interaction of an external EM field with polarization waves, or dipole modes, has an important implication. Waves propagating in such a medium are not described by d’Alembert’s wave equation, following from Maxwell’s equations, viz.,

$$\square A_\mu = j_\mu, \quad \square = -\frac{\partial^2}{\partial x_\mu \partial x^\mu},$$

where  $A_\mu$  is the 4-potential of the EM field, and  $j_\mu$  is the 4-tuple of current density. The behavior of an EM field in the medium is described by

$$\square A_\mu + M^2 A_\mu = j_\mu, \quad M^2 \sim P. \quad (5.3.1)$$

These equations have a number of corollaries important for the interpretation of general biological regularities. For example, an EM field propagating as described by Eqs. (5.3.1) is confined by thin-thread-like margins so that high EM gradients occur at the edges. These field gradients separate and condense different ions, molecules,

and molecular groups. Therefore, thread-like propagation of EM fields in a medium with spontaneous polarization becomes a *structure-forming* or morphological factor and may describe, e.g., the occurrence of such structures as microtubules of a cytoskeleton.

That idea is likely to have an indirect relation to magnetobiology. Del Giudice *et al.* (1988) supposed that liquid water is a dipole medium which gives birth to polarization waves. By affecting the spin magnetic moments of water protons, a low-frequency magnetic field controls, to some degree, the proton mobility, thus affecting the probabilities of different orientations of water molecules. Thus, a magnetic field could affect the properties of polarization waves and produce a resulting biological effect.

#### 5.4 MOLECULAR INTERFERING GYROSCOPE

A long lifetime of angular modes is the sole serious idealization underlying the mechanism of ion interference. This idealization would be hard to substantiate with the ion-in-protein-capsule model. One would have to assume that the ion forms bound states of the polaron type with capsule walls. In turn, justification of a large lifetime of polaron angular modes would require new idealizations. A “vicious circle” that one could not leave without having to substantially change the model itself occurs. Thus, despite the obvious advantages of the ion-in-capsule model, namely, simplicity and a high forecasting skill, we have to recognize its limitations and seek other solutions.

One of them hinges on the use of conservation laws in the dynamics of rotating solids. The rotation of a solid is described by the equation

$$\frac{d\mathbf{L}}{dt} = \mathbf{K} , \quad (5.4.1)$$

where  $\mathbf{L}$  is the angular momentum, and  $\mathbf{K}$  is the sum of torques acting on the solid. Consider for simplicity a symmetric top or gyro rotating around one of its main axes of inertia with a force  $\mathbf{F}$  acting on its point of support, as shown in Fig. 5.13. The moment of this force about the shown axis is obviously zero. From Eq. (5.4.1) we have

$$\mathbf{L} = \mathbf{L}_0 + d\mathbf{L} , \quad d\mathbf{L} = \mathbf{K} dt = \mathbf{r} \times \mathbf{F} dt .$$

Since  $\mathbf{K} \perp \mathbf{F}$ , then  $d\mathbf{L} \perp \mathbf{F}$ ; i.e., the force caused an orthogonal displacement of the axis of rotation. Also, the vector  $\mathbf{r}$  is directed along the axis of rotation; therefore the vector  $d\mathbf{L}$  is also orthogonal with  $\mathbf{L}_0$ .

Thus, a continuously acting force  $\mathbf{F}$  causes a forced precession of the gyro about the direction  $\mathbf{F}$  with an angular velocity defined by the angle through which the gyro axis of rotation deviates per unit time, viz.,

$$\Omega_{\text{precession}} = \frac{d\mathbf{L}/L_0}{dt} = \frac{K}{L_0} = \frac{rF}{L_0} .$$

The length of vector  $\mathbf{r}$  is defined by the gyro-locking conditions. If point B is fixed, then the origin of  $\mathbf{r}$  coincides with B. If point B is free, then the origin of  $\mathbf{r}$  is on

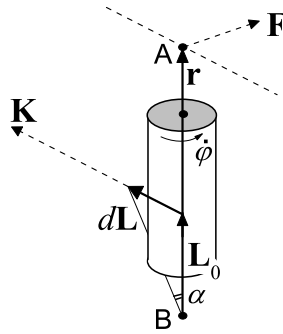


**Figure 5.13.** Forces, moments of forces, and angular momenta in rotation of a top.

line AB and depends on the gyro parameters. For estimation, it is important that  $r$  has the order of magnitude of gyro length.

Let the gyro be a model of a rigid molecule free to move and constrained by the thermal oscillations of one of the points of support (e.g., A) alone. We estimate the mean gyro axis deviation angle for a random force  $\mathbf{F}$  causing chaotic oscillations of its point of support. It should be noted that the gyro gravity energy  $\sim MgR$  is many orders of magnitude below its kinetic energy  $\sim L^2/2I$  and the effects of gravity may be neglected. In the last formulas,  $M$ ,  $R$ , and  $I$  are the gyro mass, size, and moment of inertia, and  $g$  is the acceleration due to gravity.

The energy of natural gyro rotation is  $\varepsilon_0 = L_0^2/2I$ . The gyro energy including chaotic rotations is  $\varepsilon_0 + \kappa\mathcal{T}$ . On the other hand, the mean energy with allowance for orthogonality of  $\mathbf{L}_0$  and  $d\mathbf{L}$  is

$$\langle \frac{1}{2I}(\mathbf{L}_0 + d\mathbf{L})^2 \rangle = \frac{1}{2I} \{ L_0^2 + 2\langle \mathbf{L}_0 d\mathbf{L} \rangle + \langle d^2\mathbf{L} \rangle \} = \varepsilon_0 + \frac{\langle d^2L \rangle}{2I},$$

where brackets mean averaging over the ensemble. Then  $\langle d^2L \rangle/2I \sim \kappa\mathcal{T}$ . Denoting the average deviation angle by  $\alpha = \sqrt{\langle d^2L \rangle}/L_0$  yields  $\alpha^2 \sim 2I\kappa\mathcal{T}/L_0^2$ . The smaller  $L_0$ , the larger the random deviations of a molecule caused by thermal perturbations of its support. Such a support is the covalent bond with the body of the protein molecule. Low bound estimates of  $L_0$  follow from the Heisenberg uncertainty principle which, for a complementary pair of non-commuting operators of angular variable  $\varphi$  and angular momentum  $\mathcal{L} \sim d/d\varphi$ , can be written as

$$\Delta L \Delta\varphi \sim \hbar/2.$$

Since  $\Delta\varphi \sim \pi$ , then  $\Delta L \sim \hbar/2\pi$ ; thus the angular momentum cannot be smaller than its uncertainty, i.e.,  $L_0 \sim \hbar/2\pi$ . Finally, we have

$$\alpha^2 \sim 8\pi^2 \frac{I\kappa\mathcal{T}}{\hbar^2}.$$

As can be seen deviations increase with the size of the molecule; however, even for small molecules, the estimate of deviation is unrealistically large. It implies that, in lower rotation states, molecules will “lay aside” in response to the perturbation of their support and, consequently, the angular momentum will not be conserved. It should be noted that we are interested only in angular states with small quantum numbers. Otherwise the interference patterns to be discussed below become fine grained and are unlikely to be reflected in measured properties.

Thus, in order to be immune to thermal displacements of supports, the gyro has to have its second support also fixed in the protein matrix. The configuration of a rotating solid with supports fixed in the rim is one of the types of *gyroscope*, i.e., a device for measuring angular displacements and velocities. What we consider is essentially a molecular gyro: a relatively large molecular group is placed in a protein cavity and its two edges form covalent bonds (supports) with the cavity walls. It is important to note that thermal oscillations of the supports produce only zero moments of forces about the natural group rotation axis. Therefore, the gyroscopic degree of freedom  $\varphi$  is not thermalized. This does not imply that the energy of the gyro degree of freedom does not dissipate.

#### 5.4.1 Relaxation time of the molecular gyroscope

Suitable molecules for studying molecular interference in magnetic fields should possess an electric moment, e.g., a dipole moment. In such molecules, the reasons of gyro energy relaxation are inter alia radiation damping or Lorentz friction force. The loss of angular momentum by a system of charges as a result of dipole radiation is described by the equation (Landau and Lifshitz, 1976a)

$$\frac{d\mathbf{L}}{dt} = -\frac{2}{3c^3} \dot{\mathbf{d}} \times \ddot{\mathbf{d}} \quad (5.4.2)$$

( $\mathbf{d}$  is the dipole moment of the system), which is valid, as well as the approximation of classical electrodynamics, under the conditions

$$\omega \ll Mc^2/\hbar, \quad \Omega_c \ll Mc^2/\hbar,$$

where  $\omega$  is the radiation frequency, and  $M$  is the mass of the radiating particle. For masses of the size of molecular masses, the characteristic frequency  $Mc^2/\hbar$  has the order of magnitude  $> 10^{20}$  rad/s; therefore both inequalities hold with a margin.

Let the dipole be rotated in the  $xy$  plane:

$$\mathbf{d} = d(\mathbf{n}_x \cos \omega t + \mathbf{n}_y \sin \omega t).$$

By differentiating and substituting in Eq.(5.4.2) we obtain, with allowance for  $L = I\omega$ , the equation

$$\dot{L} = -a(L + \dot{L}t)^3, \quad a = \frac{2d^2}{3c^3 I^3},$$

whose solution  $aL^3t + L = L_0$  (neglecting the terms  $\sim \ddot{L}$  and higher order terms) defines implicitly a dependence of the angular momentum on time. The quantity

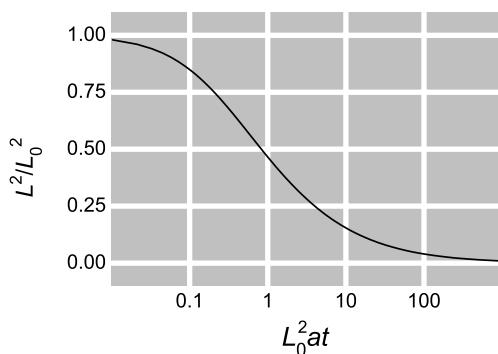


**Figure 5.14.** Relaxation of angular momentum energy due to dipole radiation.

$L^2/L_0^2$  is a relative energy of molecular rotation. The dependence of the relative energy on the dimensionless parameter  $L_0^2 a t$  is plotted in Fig. 5.14. This plot shows that the damping time scale  $\tau$  is governed by the equality  $L_0^2 a \tau \sim 1$ , whence, using the estimate  $L_0$ , we have

$$\tau \sim \frac{1}{aL_0^2} = 6\pi^2 \frac{c^3 I^3}{d^2 \hbar^2}.$$

The order of magnitude of radiation damping time can be readily determined by the approximate equalities  $I \sim MR^2$ ,  $d \sim eR$ . For a molecule with a mass of a hundred protons having a dipole moment  $e \cdot 5 \text{ \AA}$ , this is a time on the order of  $10^{11}$  s. Here, radiation damping is virtually zero.

The contribution to the relaxation by the long-range van der Waals forces induced by vibrations of the walls may be roughly estimated as follows. The interaction of the gyro with the walls is described by the Lennard–Jones potential; it decreases as the size of the cavity increases as  $1/r^6$ . At the same time, the wall cavity surface increases as  $r^2$ . Consequently, the contribution of van der Waals interactions is proportional to  $1/r^4$ . The transfer of energy rapidly decreases as the size of the cavity increases. Usually the relaxation time varies inversely with the intensity of energy transfer and, for atom–molecular motions, is on the order of  $10^{-10}$  s in a size of  $1 \text{ \AA}$ . Then, for a  $100\text{-\AA}$  cavity, the gyro relaxation time will be on the order of  $0.01$  s.

Thus, thermal perturbations of the supports of a molecular gyro does not thermalize its rotation degree of freedom, and for cavities measuring about  $100 \text{ \AA}$ , the radiation damping is low and the damping due to van der Waals forces is also small. Therefore, the coherence time of the rotational degree of freedom  $\sim 0.01$  s is sufficient to obtain detectable manifestations of interference effects.

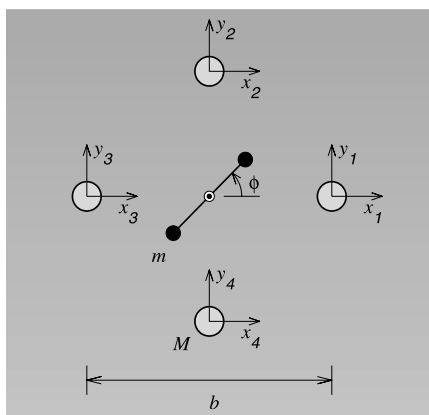


**Figure 5.15.** A two-dimensional model of a gyro in a molecular cavity of diameter  $b$  formed by four heavy particles of mass  $M$ .

#### 5.4.2 Estimating relaxation time from molecular dynamics

Computer simulation of molecular gyro behavior indicates that, for relaxation times of order 0.1 s, the size of the cavity should be about  $30 \text{ \AA}$ .<sup>36</sup> This seems to be a far more reasonable size for protein cavities.

We consider the amino acid residue phenylalanine, (Phe)  $C_\alpha C_6H_5$ , as a gyro and look at the revolution of its benzene ring  $C_6H_5$  about the valence bond  $C_\alpha - C_\beta$ . This revolution may be thought of as a rotation in one plane of two rigidly bound point masses  $m = 26 m_p$ , spaced  $a = 2.42 \text{ \AA}$  from one another, about their common center of gravity.

We model the cavity by four heavy particles of mass  $M \geq m$  placed in the corners of a square (diagonal  $b > a$ ) centered on the gyro axis, Fig. 5.15. We assume that these particles oscillate in the gyro rotation plane  $xy$ . Each particle moves in the potential well  $U(x_i, y_i)$ , where  $x_i, y_i$  is the deviation of particle  $i$  from its equilibrium state. The Hamilton function for this system has the form

$$H = \frac{1}{2} I \dot{\phi}^2 + \sum_{i=1}^4 \left[ \frac{1}{2} M (\dot{x}_i^2 + \dot{y}_i^2) + V(\phi, x_i, y_i) + U(x_i, y_i) \right], \quad (5.4.3)$$

where  $I = \frac{1}{2} m a^2$  is the gyro moment of inertia, and  $\phi$  is its revolution angle.

The potential of interaction of particle  $i$  with the gyro is the sum of two Lennard-Jones potentials

$$V(\phi, x_i, y_i) = \epsilon \{ [(r_0/r_1)^6 - 1]^2 + [(r_0/r_2)^6 - 1]^2 \},$$

<sup>36</sup>The author is grateful to A.V. Savin for conducting these computations.

where  $r_0$  is the equilibrium arm between a heavy and a light particle,  $r_1$  is the instantaneous distance of a heavy particle  $i$  to the first particle of the gyro, and  $r_2$  is the distance to the second particle.

The interaction of carbon atoms in polymeric macromolecules is commonly described by Lennard–Jones potentials of the form

$$V_{LJ}(r) = 4\epsilon_0[(\sigma/r)^{12} - (\sigma/r)^6]$$

with  $\sigma = 3.8 \text{ \AA}$  and  $\epsilon_0 = 0.4937 \text{ kJ/mol}$  (Savin and Manevitch, 1998). Recognizing that each particle of the gyro consists of two carbon atoms, we let  $\epsilon = 1 \text{ kJ/mol} \approx 2\epsilon_0$  and  $r_0 = 4.5 \text{ \AA} \approx 2^{1/6}\sigma$ .

The carrier potential for each heavy particle is taken in the form

$$U(x, y) = \frac{1}{2}K \frac{x^2 + y^2}{1 - (x^2 + y^2)/R_0},$$

where  $K$  is the rigidity in particle–carrier interaction, and  $R_0$  is the maximum possible deviation radius of a heavy particle. In a protein macromolecule, the rigidity of atomic displacements is  $K = 4 \text{ N/m}$ . We consider two maximum displacement values:  $R_0 = 1 \text{ \AA}$  and  $R_0 = \infty$ .

Assuming that heavy particles alone are connected with the thermostat, we obtain the Langevin equations of motion in the form

$$\begin{aligned} I\ddot{\phi} &= -\frac{\partial H}{\partial \phi}, \\ M\ddot{x}_i &= -\frac{\partial H}{\partial x_i} - \Gamma M\dot{x}_i + \xi_i, \\ M\ddot{y}_i &= -\frac{\partial H}{\partial y_i} - \Gamma M\dot{y}_i + \eta_i, \\ & i = 1, 2, 3, 4, \end{aligned} \tag{5.4.4}$$

where the system's Hamilton function is given by Eq. (5.4.3),  $\xi_i$  and  $\eta_i$  are random normally distributed forces (white noise) describing the interaction of a heavy particle  $i$  with the thermostat,  $\Gamma = 1/t_r$  is the friction factor, and  $t_r$  is the particle velocity relaxation time.

The correlation functions of random forces are

$$\begin{aligned} \langle \xi_i(t_1)\xi_j(t_2) \rangle &= 2M\Gamma\kappa\mathcal{T}\delta_{ij}\delta(t_1 - t_2), \\ \langle \eta_i(t_1)\eta_j(t_2) \rangle &= 2M\Gamma\kappa\mathcal{T}\delta_{ij}\delta(t_1 - t_2), \\ \langle \xi_i(t_1)\eta_j(t_2) \rangle &= 0. \end{aligned}$$

Here,  $\kappa$  is the Boltzmann constant, and  $\mathcal{T}$  is the thermostat temperature.

The equation system (5.4.4) was integrated by the Runge–Kutta method to the fourth order of accuracy with a constant integration step  $\Delta t$ . In this computation, the delta function  $\delta(t)$  is 0 for  $|t| > \Delta t/2$  and  $1/\Delta t$  for  $|t| < \Delta t/2$ , that is, the

integration step corresponds to the correlation time of random force. Therefore, to use a system of Langevin equations, we need that  $\Delta t \ll t_r$ : the relaxation time was  $t_r = 0.2$  ps, and the numerical integration step was  $\Delta t = 0.0025$  ps.

Let in the initial moment of time  $t = 0$  the system be in the fundamental state. Thus, at time zero, the molecular gyro is not thermalized. Our objective is to estimate the average time of gyro thermalization. It corresponds to the relaxation time of gyro rotation in a thermalized molecular system. For this purpose, we numerically integrate the equations of motion (5.4.4) subject to appropriate initial conditions.

The gyro thermalization at time  $t$  is characterized by its current temperature.

$$\mathcal{T}_1(t) = \frac{I}{\kappa} \langle \dot{\phi}^2(t) \rangle ,$$

where brackets  $\langle \cdot \rangle$  imply averaging over independent realizations of random forces  $\xi_i(t)$ ,  $\eta_i(t)$ ,  $i = 1, 2, 3, 4$ . To obtain the average value, the system (5.4.4) was integrated more than 10,000 times. Now, the thermalization of a system of heavy particles is characterized by its current temperature

$$\mathcal{T}_2(t) = \frac{M}{8\kappa} \sum_{i=1}^4 \langle \dot{x}_i^2(t) + \dot{y}_i^2(t) \rangle .$$

At  $t = 0$ , the temperatures are  $\mathcal{T}_1(0) = \mathcal{T}_2(0) = 0$ . Further on the time coordinate, they monotonously approach the thermostat temperature  $\mathcal{T} = 300$  K. The molecular subsystem is assumed to be completely thermalized if its current temperature exceeds  $0.99 \mathcal{T}$ ; i.e., thermalization time  $t_i$  is a solution of the equation  $\mathcal{T}_i(t) = 0.99 \mathcal{T}$ .

We analyzed the behavior of the system for a set of model parameters. The dependence of gyro thermalization time on cavity diameter  $b$  is shown in Fig. 5.16. It is evident that the thermalization time increases exponentially with  $b$ . If we extrapolate this dependence to the range of large  $b$ , we see that, at  $b = 28\text{--}32$  Å, the thermalization time, and hence the gyro relaxation time, will be on the order of seconds. With this size of cavity, the molecular gyro will revolve almost freely.

### 5.4.3 Interference of the gyroscope

Rotations of large molecules is much slower a process than electron and oscillatory processes. Therefore, we think of the rotating molecular group as a rigid system of charged point masses — atoms and molecules with partially polarized chemical bonds. To illustrate, we point to molecules of amino acids which could be built into rather spacious protein cavities, forming chemical bonds at the extreme ends of the molecule, thus forming a molecular gyroscope. Amino acids are links of polymeric protein macromolecules and also occur in a bioplasm as free monomers. The general formula of amino acids is well known

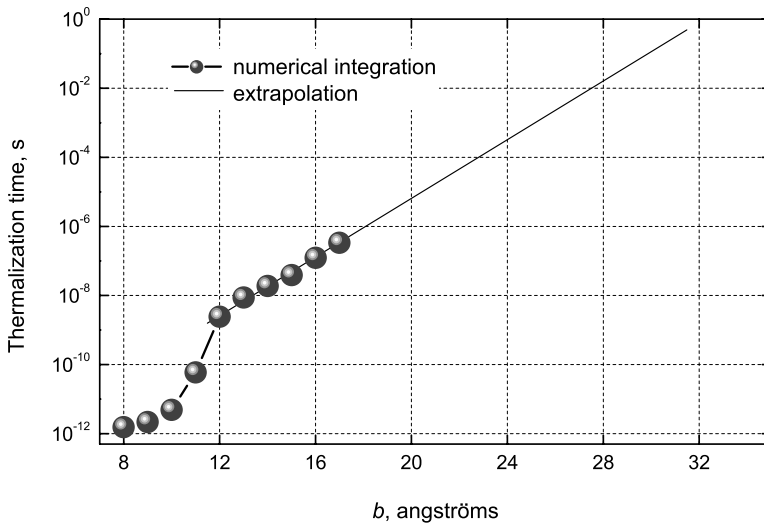
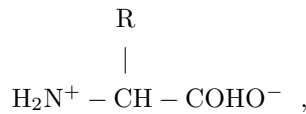


**Figure 5.16.** Gyro thermalization time  $t_1$  computed as a function of molecular cavity diameter  $b$  at  $M = m$ , and extrapolation of this function to large  $b$ .



where R is a radical that differs one molecule from another. Polarities of the groups are shown in a water solution. By way of example, the radical of amino glutaric acid consists of three links  $-\text{CH}_2 - \text{CH}_2 - \text{COOH}$ , as shown in Fig. 5.17. Fixed on either side of a cavity, such a molecule, treated as a dynamic unit, has one degree of freedom — a polar angle  $\varphi$ , which simplifies analysis of its behavior in a magnetic field.

For small velocities, the Lagrange function of one charge particle has the form

$$\mathcal{L} = \frac{Mv^2}{2} + \frac{q}{c} \mathbf{A}\mathbf{v} - qA_0 , \quad (5.4.5)$$

where  $\mathbf{v}$  is the particle velocity, and  $q$  is a charge. Let the magnetic field  $\mathbf{H} = (0, 0, H)$  be directed along the  $z$  axis, and the particle be bounded by a holonomic constraint causing its circumferential motion in the  $xy$  plane. In spherical coordinates, the constraints can be written in the form

$$r = R = \text{const.} , \quad \theta = \pi/2 . \quad (5.4.6)$$

We choose the vector potential in the form

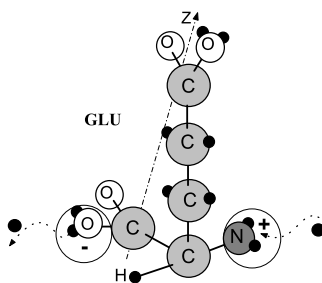


**Figure 5.17.** An amino glutaric acid molecule with potentially ionizing groups. The  $z$  axis is the main axis of inertia. Rotation of charges distributed over the molecule in a magnetic field leads to interference of its quantum angular states.

$$\mathbf{A} = \left( -\frac{1}{2}Hy, \frac{1}{2}Hx, 0 \right). \quad (5.4.7)$$

With allowance for constraints (5.4.6), the velocity of a particle in spherical coordinates will be  $v = R\dot{\varphi}$ , and the velocity vector in Cartesian coordinates is

$$\mathbf{v} = (-R\dot{\varphi} \sin(\varphi), R\dot{\varphi} \cos(\varphi), 0). \quad (5.4.8)$$

Substituting this expression in Eq. (5.4.5), we obtain the Lagrange function in spherical coordinates

$$\mathbf{L} = \frac{MR^2\dot{\varphi}^2}{2} + \frac{qH}{2c}R^2\dot{\varphi} - qA_0. \quad (5.4.9)$$

Now, the generalized momentum  $l = \partial\mathbf{L}/\partial\dot{\varphi}$ , and the Hamilton function  $\mathbf{H} = l\dot{\varphi} - \mathbf{L}$  are

$$l = \frac{\partial\mathbf{L}}{\partial\dot{\varphi}} = MR^2\dot{\varphi} + \frac{qH}{2c}R^2, \quad (5.4.10)$$

$$\mathbf{H} = l\dot{\varphi} - \mathbf{L} = MR^2\dot{\varphi}^2 + \frac{qH}{2c}R^2\dot{\varphi} - \frac{1}{2}MR^2\dot{\varphi}^2 - \frac{qH}{2c}R^2\dot{\varphi} + qA_0 = \frac{1}{2}MR^2\dot{\varphi}^2 + qA_0.$$

We need to express  $\mathbf{H}$  in generalized coordinates. From Eq. (5.4.10) we see

$$\left( l - \frac{qH}{2c}R^2 \right)^2 = M^2R^4\dot{\varphi}^2, \\ (\mathbf{H} - qA_0) = \frac{1}{2}MR^2\dot{\varphi}^2 = \frac{1}{2MR^2} (M^2R^4\dot{\varphi}^2) = \frac{1}{2MR^2} \left( l - \frac{qH}{2c}R^2 \right)^2.$$

Then

$$\mathbf{H} = \frac{1}{2MR^2} \left( l - \frac{qH}{2c}R^2 \right)^2 + qA_0. \quad (5.4.11)$$

In the absence of an electromagnetic field  $\mathbf{H} = l^2/2MR^2$ , and it is obvious that  $l$  is the angular momentum of the particle. The Hamiltonian operator repeats (5.4.11) with the difference that here  $l$  is the angular momentum operator  $\mathcal{L} = -i\hbar\partial/\partial\varphi$ .

Let us now rotate a few particles and, in a spherical system of coordinates, the constraints for particle  $i$  be

$$r_i = \text{const.}, \quad \theta_i = \text{const.}$$

Then, for a system of particles in a uniaxial magnetic field, the Lagrange function can be written following the derivation of formula (5.4.9) as

$$L = \frac{I}{2}\dot{\varphi}^2 + \frac{HQ}{2c}\dot{\varphi} - \sum_i q_i A_0(r_i, \theta_i, \varphi_i), \quad (5.4.12)$$

where

$$I = \sum_i M_i r_i^2 \sin^2(\theta_i), \quad Q = \sum_i q_i r_i^2 \sin^2(\theta_i) \quad (5.4.13)$$

is the moment of inertia and the ‘‘charge moment of inertia’’ of the system about the axis of rotation. As can be seen, the Lagrange function of the system follows from the Lagrange function (5.4.9) after formal replacement of  $MR^2$  with  $I$ ,  $qR^2$  with  $Q$ , and  $qA_0$  with the respective sum. Therefore, the Hamiltonian of the system immediately follows from Eq. (5.4.11) after similar substitutions

$$\mathcal{H} = \frac{1}{2I} \left( \mathcal{L} - \frac{QH}{2c} \right)^2 + \sum_i q_i A_0(r_i, \theta_i, \varphi_i).$$

We assume further that the electric field is absent, i.e., let  $A_0 = 0$ :

$$\mathcal{H} = \frac{1}{2I} \left( \mathcal{L} - \frac{QH}{2c} \right)^2.$$

In addition to  $\mathcal{L}^2/2I$  we find here two more operators. There are certain grounds to neglect the term proportional to squared  $H$ . From the ratios of coefficients at the quadratic and linear terms in  $H$  we obtain

$$\frac{QH}{4c\hbar} \sim 10^{-7}, \quad (5.4.14)$$

where, for estimation purposes, we let  $Q \sim eR^2$ ,  $R \sim 10^{-7}$  cm,  $H \sim 1$  G. Dropping this term and using the notation

$$\omega = \frac{QH}{2Ic}, \quad (5.4.15)$$

we write the Hamiltonian in a convenient form

$$\mathcal{H} = \frac{\mathcal{L}^2}{2I} - \omega(t)\mathcal{L}. \quad (5.4.16)$$

The eigenfunctions and energies of the time-independent part of Hamiltonian (5.4.16) are

$$|m\rangle = \frac{1}{\sqrt{2\pi}} \exp(im\varphi) , \quad m = 0, \pm 1, \dots , \quad \varepsilon_m = \frac{\hbar^2}{2I} m^2 .$$

The solution of the time-dependent Schrödinger equation with Hamiltonian (5.4.16) is virtually similar to that of (4.1.5), viz.,

$$\Psi = \sum_m a_m \exp \left[ im \int \omega(\tau) d\tau \right] \exp \left( -\frac{i}{\hbar} \varepsilon_m t \right) |m\rangle . \quad (5.4.17)$$

Equation (5.4.17) includes the energies  $\varepsilon_m$  since, unlike the polar mode of a charge in a central potential, rotation of a rotator is quantized in the absence of a magnetic field as well.

For some value of the angular coordinate, the wave function probability density is ( $\Delta m = m' - m$ )

$$\begin{aligned} p(\varphi_0, t) &= |\Psi(\varphi_0, t)|^2 \\ &= \sum_{mm'} a_{mm'} \exp \left[ i\Delta m \varphi_0 - i\frac{\hbar}{2I} (m'^2 - m^2)t + i\Delta m \int \omega(\tau) d\tau \right] . \end{aligned}$$

Denote

$$\omega = \omega_0 + \omega_1 \cos(\Omega t) , \quad \omega_0 = \frac{QH_{DC}}{2Ic} , \quad \omega_1 = \frac{QH_{AC}}{2Ic} . \quad (5.4.18)$$

This nomenclature is similar to the respective notation for Larmor frequencies (4.1.8), except that the place of charge  $q$  and mass  $M$  is occupied by their rotation equivalents  $Q$  and  $I$ , respectively. By calculating the moving average over the time interval  $T$  we obtain a formula coinciding with Eq. (4.1.12), where the coefficients of  $z$  and  $\alpha z$  are

$$z = \Delta m \frac{\omega_1}{\Omega} , \quad \alpha z = \Delta m \frac{\omega_0}{\Omega} - \frac{\hbar}{2I\Omega} (m'^2 - m^2) . \quad (5.4.19)$$

In Section 4.1, a slow passage of ion's probability density maxima at the gates was associated with a rising probability of dissociation of the ion-protein complex. We assume that electrochemical processes, protein synthesis, and biochemical processes are not indifferent to the "freezing" of the interference distribution of the rotating group angular probability density. We resort to the methods of Section 4.1 to identify the conditions for efficient "freezing". It is important to note that the molecule does not cease rotating. In these circumstances, that is, at optimal magnetic field parameters, the molecule rotates irregularly, residing for a long time in fixed angular positions. This residence probably facilitates chemical processes. For example, the molecule of amino acid, generally speaking, has three potentially active end groups capable of forming a chemical bond. If two of them are used in gyro supports, then, keeping its irregular rotation, the remaining group can "hover" over certain hypothetically active sites of the shell to form a chemical bond with them, thus modifying the activity of the entire protein.

Thus, we write for the rotating molecular group Eq. (4.1.19), and substituting from (5.4.19) transform it to dimensionless variables:

$$P = \sum_{mm'n} |a_{mm'}|^2 \left( \frac{\sin \left[ \left( \frac{\Delta m}{2} + n f' - \Lambda(m'^2 - m^2) \right) \Xi \right]}{\left( \frac{\Delta m}{2} + n f' - \Lambda(m'^2 - m^2) \right) \Xi} \right)^2 J_n^2 \left( \frac{\Delta m}{2} \frac{h'}{f'} \right). \quad (5.4.20)$$

Here we see a new dimensionless parameter  $\Lambda$ , since the distribution of system charges represented by  $Q$  turns out to be as important as the rotational equivalent of the particle mass, that is, the system's moment of inertia  $I$ . In this formula, the dimensionless frequency  $f' = \Omega/\Omega_r$  and "a coupling parameter"  $\Xi = \Omega_r T$  relating the probability density to chemical events are defined with respect to frequency

$$\Omega_r = \frac{QH_{DC}}{Ic}, \quad (5.4.21)$$

which can be conveniently called a gyral frequency. An order of magnitude for  $\Omega_r$  may be obtained by estimating spin inertias  $I$  and  $Q$

$$I \sim MR^2, \quad Q = eR^2.$$

In Eq. (5.4.13),  $Q$  is represented as a product of the electronic charge by the square of effective radius  $R$  about the size of the molecule, and  $M$  is the mass of the molecule. Then  $\Omega_r \sim eH_{DC}/Mc$ , i.e., close to the cyclotron frequency in the common sense. For amino acids immersed in magnetic fields of fractions of a gauss, this quantity will be several hertz high. The parameter  $\Lambda$  is

$$\Lambda = \frac{\hbar}{2I\Omega_r} = \frac{c\hbar}{2QH_{DC}} \sim 10^6-10^7. \quad (5.4.22)$$

As can be seen from Eq. (5.4.20), the positions of effect maxima follow from putting the denominator  $\sin(x)/x$  to 0, viz.,

$$f'_{\max} = \frac{1}{n} \left[ \Lambda(m'^2 - m^2) - \frac{\Delta m}{2} \right]. \quad (5.4.23)$$

In case of interference of modes  $m' \neq |m|$ , the peak frequencies, in view of large  $\Lambda$ , are determined by

$$f'_{\max} = \frac{1}{n} \Lambda(m'^2 - m^2)$$

and occur in the microwave range. In this case, Eq. (5.4.7), derived for the vector potential of a uniaxial magnetic field, is inapplicable and in order to study the microwave spectrum of a molecular interference, one has to derive the Hamiltonian anew. Similarity of the biological effects of microwaves and low-frequency magnetic fields have been noted by many authors, see Section 5.2.

We consider here the interference of states  $m' = -m$ , which gives rise to effects in a low-frequency range. Since in this case  $m'^2 - m^2 = 0$ , the peak frequencies in this range will be given by

$$f'_{\max} = -\frac{\Delta m}{2n} = \frac{m}{n}, \quad (5.4.24)$$

and the effect formula boils down to

$$P = \sum_{mn} |a_m|^2 \left( \frac{\sin [(m + nf') \Xi]}{(m + nf') \Xi} \right)^2 J_n^2 \left( m \frac{h'}{f'} \right). \quad (5.4.25)$$

While the spectrum (5.4.24) repeats the main properties of the frequency spectrum (4.1.26) of the base model of an ion in a protein cavity, it determines only possible locations of extrema. A real form of the spectrum depends on the initial conditions specified by coefficients  $a_m$ , i.e., on the population of levels of different rotational quantum number  $m$ . It is important to note that the amplitude spectrum (5.4.25) also coincides with the amplitude spectrum of the base model.

It is instructive to note that the molecule need not have a dipole moment  $\sum_i q_i \mathbf{r}_i$  for this effect to appear. Rather, it is important that the “charge moment of inertia”  $Q$  be other than 0. This can be the case in the absence of the dipole moment, e.g., for the ionic rather than the zwitterionic form of the molecule.

We note that the interference of a molecular gyro has salient features that differ from those of the ion interference. Firstly, the peak frequencies are defined with respect to the gyral frequency — a rotation equivalent of cyclotron frequency (5.4.21). Peak frequencies depend on the distribution of electric charges over the molecule and may deviate from the harmonics and subharmonics of the cyclotron frequency. Secondly, the gyro rotation axis is fixed with respect to the shell, which introduces, in the general case, one more averaging parameter in the model. However, these features are not of principal significance. The main properties of interference are identical in both cases, namely, multiple peaks in the amplitude and frequency spectra, dependence of frequency peaks on the magnetic field intensity, etc. In Chapter 4 we demonstrate that the specific properties of the interference can always be calculated for any configuration of magnetic and electric fields, for rotation of the biological systems and macromolecules involved, etc.

The molecular interfering gyroscope is a challenger for solving the “kT problem” as a probable mechanism of magnetobiological effects. Indeed, the walls of a protein cavity do not interfere with the gyro degree of freedom directly via short-range chemical bonds. For cavities larger than  $30 \text{ \AA}$  in size, the contribution to the relaxation from the van der Waals electromagnetic forces, induced by wall oscillations, is small. Radiation damping is negligibly small. Finally, the oscillations of gyro supports produce a zero moment of forces about the axis of rotation and do not affect the angular momentum. The gyro degree of freedom is very slow to thermalize, its dynamic behavior is coherent, which gives rise to slow interference effects. Of course, whether some more or less water-free cavities of the size of  $30 \text{ \AA}$  and larger

do exist remains an open question, but, what is essential, is that this is no longer a paradox.

The role of molecular gyros could probably be played by short sections of polypeptides and nucleic acids built inside globular proteins or in cavities between associated globules. In this respect it is interesting to look at Watson–Crick pairs of nitrous bases (adenine–thymine and guanine–cytosine) which bind DNA strands into a double helix as well as some other hydrogen-bound complexes of nitrous bases. Their rotations are hampered by steric factors. However, in the realm of activity of special DNA enzymes, steric constraints may be lifted to allow a relatively free rotation of molecular complexes. It is not yet clear whether the gyro type of molecular structures exists. They are unlikely to be detected by X-ray methods since these require crystallization of proteins for structural analysis. In this state, the rotation would likely be frozen. Should a rotation be allowed, the mobile groups would not give clearcut reflections. Some other methods that would work with native forms of proteins avoiding distortions due to crystallization are needed.

Generally speaking, the fact that the molecular gyro model gives a physically consistent explanation of MBEs proves indirectly its real grounds. Further studies should verify whether this conclusion is correct. In any case, today, the interfering molecular gyroscope is a single available mechanism to provide explanations that would be physically transparent and generally agreeable with experiments.

## 5.5 MAGNETOBIOLOGICAL PROBLEMS TO SOLVE

Even within a relatively simple model of ion interference, there are a large number of factors governing the profile of amplitude and frequency spectra. In the general case, the more evident of these factors are as follows:

- non-linearity in the energy conversion of a signal from the prime target of the magnetic field in the chain of biophysical and biochemical transformations,
- different signs of response from different ion targets under specific magnetic conditions,
- different mechanisms of magnetoreception acting simultaneously in the conditioned biological system, and
- a dependence on the initial conditions imposed on the ion in the macromolecular capsule, which in turn depend on the conformational state of the molecule, i.e., on such physical quantities as temperature and pressure; other aspects controlling the conformational state and metabolism are genetic modifications within one biological species, concentrations of substances, and targets for magnetic fields.

In the environment of many affecting factors and their intricate relationships, observation of a predicted magnetobiological effect becomes an experimental success, in a certain sense an ingenious finding of the experimenter. It is important therefore to seek experimental models virtually insensitive to factors other than magnetic fields. Such biological systems could provide on a regular basis improvement of our knowledge about the physical nature of MBEs.

Unfortunately, it should be recognized that most of the available experimental MBE models are of limited applicability for those wishing a better insight into the physical nature of these effects. Also, one should not expect much of the known theoretical models. A suitable theoretical model should provide for a *correct* explanation of the nature of a specific magnetobiological effect. As explained above, given that this model is physically consistent, a correct explanation follows from agreement with only a limited number of specially engineered experiments.

Today it could be safe to say that the main characteristic traits of MBEs, reliably established in numerous experiments and successfully repeated in different experimental models under different magnetic conditions, are as follows:

- multiple peak profiles of both frequency and amplitude MBE spectra,
- biological efficiency of magnetic vacuum,
- effective frequencies proportionate to the harmonics and subharmonics of cyclotron and sometimes NMR frequencies of various atom ions, and
- paradoxically small energy of magnetic fields causing biochemical and biological responses.

The theory of ion-molecular interference proved capable of explaining these general regularities of magnetobiological reception. This ability is based on the assumption that the angular quantum states of atom ions and rotational states of molecules in a magnetic field are involved in MBE. These states are de Broglie waves in the space of angular coordinate fitted to a microscopic scale which can interfere with one another, forming slowly rotating nodes and antinodes of the particle. The fact that the interference pattern is stable with respect to thermal oscillations of the medium may be due to their interaction with the angular and rotational states. The ion-molecule interference theory gives some general “field-effect” formulas which lend themselves to experimental verification. Estimations made with these formulas for magnetic conditions of a number of familiar experiments check well with their results.

Now, it is more or less clear why, in contrast to weak magnetic fields, relatively strong magnetic fields seldom induce sensible biological effects. This is associated with the fact that the magnetic field never produces a force action on the particles. Stronger fields result in larger frequency shifts in the phases which do not coincide in order of magnitude with the natural frequencies of ions and therefore does not entail a new quality in the system. For example, Glaser *et al.* (1998) have conducted a fundamental study of the action of EM fields on the membrane calcium pump in human erythrocytes. In a low-frequency range, for magnetic fields stronger than 1 mT, no pronounced biological effects were found. Fields of such intensity are likely to carry the system outside possible interference mechanisms, Fig. 5.18.

It is natural that a single mechanism, or even a group of mechanisms, based on one idea would hardly explain all the variety of collected experimental data. It is probable that different principles of magnetic reception in biological objects are active in different ranges of magnetic field intensity. For example, for relatively strong magnetic fields above 1 mT, probable mechanisms would hinge on magneti-

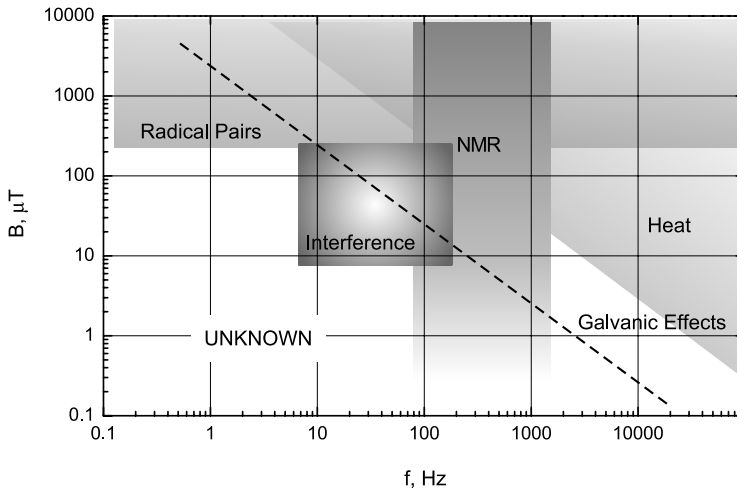


**Figure 5.18.** Approximate amplitude–frequency bounds of possible mechanisms of MBE.

cally sensitive reactions with free radicals. It should be noted that this idea expects its verification in dedicated experiments.

From the data presented in this book one may infer that the physical problems of magnetobiology yet to be solved include:

- identification of targets of magnetic fields in well-reproducible MBEs,
- mechanisms of biological action of moderate permanent magnetic fields,
- role of water and water memory in MBEs,
- mechanisms of ion interference stability against thermal perturbations in the medium,
- mechanisms of biological action of very weak, under  $1\ \mu\text{T}$ , magnetic fields,
- acceptable proportioning of background magnetic fields in social environments with frequency- and amplitude-sensitive mechanisms of magnetoreception,
- targeted action of EM fields on selected physiological/biochemical subsystems,
- transport of sophisticated magnetic fields to local areas in biological systems,
- general methods of correction of immune processes by low-frequency magnetic fields,
- development of methods of active protection from harmful background radiation, and
- specific mechanisms of magnetic action on biological communication processes — intercellular, population, interspecific, etc. — and their application to population control.

A common drawback of magnetobiological experiments is a relatively small number of measurements in varying magnetic field parameters. Generally speaking, this drawback prevents one from drawing reliable conclusions on the presence of spectral peaks of the effect, since there exists a possibility that the interval between two adjacent points contains a spectral feature that might be revealed with appropriate experiments. A few relevant experiments that comply with the acceptable rules of spectral measurements in physics are known. Therefore, regular spectral measurements that could be reliably approximated by smooth curves remain one of the unsolved problems of magnetic biology.

Very few experiments that have been engineered for an unambiguous answer to a question about the physical processes of the primary act of magnetoreception are known. Most experiments giving unambiguous proofs of MBEs provide insignificant information about the physics of the relevant processes. It would be advisable to use the experience of physical experimenting and statistical physical hypothesis testing in magnetobiology. A methodologically correct formulation of the hypothesis should be such that the results of the experiments unambiguously identify one of two equiprobable physical situations. A number of interesting experiments have been suggested by Engström and Fitzsimmons (1999). They were engineered to establish the general characteristics of the physical processes of magnetoreception, such as rate, nature of the acting field, and spatial distribution of magnetic field targets. Formulating similar uniquely interpretable experiments could lead to a quick resolution of the magnetobiological challenge.

During the preparation of this manuscript the author of this book has looked through several thousand papers on EM biology and related fields. The list of literature appended at the end of the book contains about seven hundred items. A paper qualified to be in the list if it contained results essential for the considered subject. No other selection criteria were used. Accordingly, this list of references could serve as a basis for a small statistical analysis. It would be interesting to look into the distribution of research over time. It usually gives a clue to how the discipline has developed. We should keep in mind also a wane of social significance of works with a characteristic period of 15 to 20 years and hence a natural decay of citing rate. However, the subject of this book, the physics of magnetoreception in biological systems, enjoys absolute novelty today. Therefore, this field does not contain obsolete publications, and the time distribution of papers is indicative of the evolution of the discipline — from a false doctrine to front-end research which, with some effort, finds its way to the pages of established scientific journals.

Figure 5.19 indicates how the density of publications has increased with time. An exponential growth in recent decades reflects a regular variation. This profile is typical of many natural social processes at the early stage of their evolution when no constraints are in view. Later the process may enter into a phase of relative stabilization or even a decline in intensity. This change occurs due to many a reason, specifically due to a loss of social significance by this field of research in connection with a successful resolution of the problem, or conversely, in connection with a series of failures in attempting its solution. I think that this field had an absolute peak

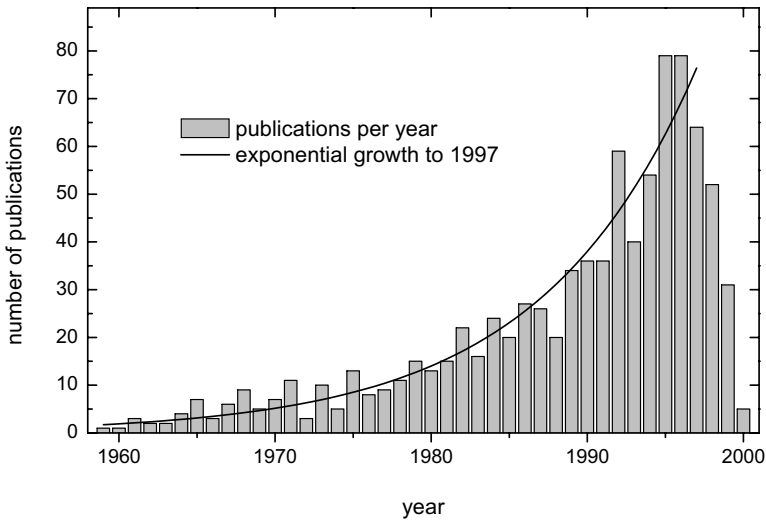


**Figure 5.19.** The distribution of the number of annually published papers has been constructed from the bibliography of this book. In the interval preceding 1997, the distribution is approximated by an exponent.

of activity in 1995–1996. This implies that a decline in intensity of publications in recent years reflects not only a natural 2–3 year delay in citing typical of scientific literature, but also the research status of the fundamental processes of magnetoreception in biological systems. The phase of extensive accumulation of experimental data seems to be completing. The biological regularities in the action of EM fields have been identified in general. On the other hand, the accumulated knowledge is totally empirical, without understanding of the nature of established regularities. This drawback should be due to the fact that most research has been heavily biological rather than directed at evaluating the physical nature of the interaction of EM fields and living systems. In this respect it is indicative to refer to the contents of the large annual conference BEMS-2000 in Munich. Of 100 reports and 220 wall papers, it was only the report of the author along these lines that presented a theory of the prime mechanisms of biological sensitivity to weak EM fields.

Magnetobiology, as a developing field of science, is faced with a number of objective hardships. Difficulties stem from a considerable underdevelopment of magnetobiological *theory*. In his presentation of the history of discovery of the Belousov–Zhabotinsky oscillatory chemical reaction, Shnoll (1997) writes “We note and declare as a phenomenon only what we understand and for what a theory has been developed. However, to build a theory, one needs to have a ‘request for proposal’ — an unexplained phenomenon. Breaking this vicious circle requires tremen-

dous intellectual and ethic efforts.” These words seem to be equally applicable to magnetobiology. A natural way out of this “vicious” situation would be parallel, hand-in-hand development of theory and experiments. Today we see a considerable domination of magnetobiological experiments over theory.

Academic interest in magnetobiology is restrained by the absence of a clearcut physical explanation. Therefore, this field is mainly supported by funds from interested manufacturers of equipment operating with EM emissions. The interest of these companies focuses on demonstrating harmlessness of, e.g., mobile phones and household electrical equipment, or conversely, a high therapeutic efficacy of biomedical EM technologies. In both cases, targeted research confines the area of EM modes studied into rather narrow limits. The leading journal of the field, *Bioelectromagnetics*, abounds in papers on biological effects of electromagnetic fields at industrial frequencies of 50 and 60 Hz and some gigahertz frequencies of mobile communications. It should be obvious that both the orientation of research and its frequency and amplitude constraints prevent the physical nature of magnetobiological effects from being efficiently investigated.

Finally, one more stumbling block is associated with the fact that magnetobiology, on the one hand, occurs simultaneously in the realms of physics and biology, but, on the other hand, does not fit either of these sciences completely. This circumstance hampers publication of papers devoted to physical aspects of magnetobiology. Biology journals, as a rule, find it hard to review submitted papers that are essentially physical in their research. This explains why they publish obviously weak papers on mechanisms of biological effects. On the other hand, physics journals remain skeptical about the possibility of weak EM fields affecting biological systems. The sole argument of physicists that have a negative respect of the subject is that the effects explained in reviewed papers are infamous for their poor replication, and thus they cannot identify a subject for analysis. Still, physics journals have begun publishing positive papers on mechanisms of magnetobiological effects (Moggia *et al.*, 1997).

The very concept of magnetobiology implies, in a certain sense, that physics and biology have to be equally represented in it. However, the modern state of the area is such that the physical involvement is at its infancy and the biological contribution dramatically outperforms its physical counterpart. This imbalance is the main stimulating force of magnetobiology. The magnetobiological discipline of theoretical biophysics has come to be formed. Among priorities one will find generalization of accumulated findings, formulating hypotheses on biophysical mechanisms of magnetoreception, and engineering experiments on determining primary physical processes converting electromagnetic signals into biochemical signals. I would deem the objective of this book reached if it gave a useful stimulus for further research in this field.

# 6

## ADDENDA

### 6.1 ANGULAR MOMENTUM OPERATORS

Transformations of spherical and Cartesian coordinate systems have the form

$$x = r \sin \theta \cos \varphi, \quad y = r \sin \theta \sin \varphi, \quad z = r \cos \theta$$

and

$$r = \sqrt{x^2 + y^2 + z^2}, \quad \theta = \arccos \frac{z}{r}, \quad \tan \varphi = \frac{y}{x}.$$

Differentiating equations for  $x, y, z$  successively with respect to  $r, \theta, \varphi$  gives

$$\frac{\partial(x, y, z)}{\partial(r, \theta, \varphi)} = \begin{vmatrix} \sin \theta \cos \varphi & r \cos \theta \cos \varphi & -r \sin \theta \sin \varphi \\ \sin \theta \sin \varphi & r \cos \theta \sin \varphi & r \sin \theta \cos \varphi \\ \cos \theta & -r \sin \theta & 0 \end{vmatrix}.$$

Differentiating equations for  $r, \theta, \varphi$  successively with respect to  $x, y, z$  gives

$$\frac{\partial(r, \theta, \varphi)}{\partial(x, y, z)} = \begin{vmatrix} \sin \theta \cos \varphi & \sin \theta \sin \varphi & \cos \theta \\ \frac{1}{r} \cos \theta \cos \varphi & \frac{1}{r} \cos \theta \sin \varphi & -\frac{1}{r} \sin \theta \\ -\frac{\sin \varphi}{r \sin \theta} & \frac{\cos \varphi}{r \sin \theta} & 0 \end{vmatrix}. \quad (6.1.1)$$

By definition, the angular momentum is  $\mathcal{L} = -i\mathbf{r} \times \nabla$ :

$$\mathcal{L}_x = -i \left( y \frac{\partial}{\partial z} - z \frac{\partial}{\partial y} \right), \quad \mathcal{L}_y = -i \left( z \frac{\partial}{\partial x} - x \frac{\partial}{\partial z} \right), \quad \mathcal{L}_z = -i \left( x \frac{\partial}{\partial y} - y \frac{\partial}{\partial x} \right).$$

Using (6.1.1), we get

$$\begin{aligned} \mathcal{L}_x &= i \sin \varphi \frac{\partial}{\partial \theta} + i \cos \varphi \cot \theta \frac{\partial}{\partial \varphi}, & \mathcal{L}_y &= -i \cos \varphi \frac{\partial}{\partial \theta} + i \sin \varphi \cot \theta \frac{\partial}{\partial \varphi}, \\ \mathcal{L}_z &= -i \frac{\partial}{\partial \varphi}, & \mathcal{L}_{\pm} &= \mathcal{L}_x \pm i \mathcal{L}_y = e^{\pm i \varphi} \left( \pm \frac{\partial}{\partial \theta} + i \cot \theta \frac{\partial}{\partial \varphi} \right), \end{aligned}$$

where we also used the formula

$$\frac{\partial}{\partial x_i} = r'_{x_i} \frac{\partial}{\partial r} + \theta'_{x_i} \frac{\partial}{\partial \theta} + \varphi'_{x_i} \frac{\partial}{\partial \varphi}.$$

## 6.2 THE LANDE FACTOR FOR IONS WITH A NUCLEAR SPIN

The factor of magnetic splitting in relatively weak MFs, or the Lande factor, for ions with a nuclear spin, is dependent on the charge, mass, spin, and magnetic moment of an ion. In a central potential, the spin-orbit operator varies with the product of the operators of the nuclear spin  $\mathbf{I}$  and the orbital mechanical (angular) momentum  $\mathbf{L}$ . Such an operator is given by a linear combination of the operators of squared spin, orbital, and total ( $\mathbf{J} = \mathbf{I} + \mathbf{L}$ ) momenta; i.e., it commutes with each of them. Therefore, the eigenfunctions of the Hamiltonian of an ion in a central potential subject to spin-orbit interaction can be taken to be common for the specified operators: for spin-orbit and squared momenta, and also for the component  $\mathcal{J}_z$  of the total momentum that commutes with them. Let such functions be  $|lijm\rangle$ , where  $l, i, j, m$  are quantum numbers of the orbit, spin, and total momenta, and also of the component of the total momentum. The ion magnetic Hamiltonian has the form  $-\mathbf{MH}$ , and the ion magnetic moment operator will be

$$\mathbf{M} = \hbar(b\mathbf{L} + \gamma\mathbf{I}) = \hbar b(\mathbf{L} + 2\Gamma\mathbf{I}),$$

where  $\Gamma$  is the ion-isotope constant. Following the procedure as laid down say in Davydov (1973), we will represent the operator  $\mathbf{M}$  as  $\mathbf{M} = \mathcal{G}\mathbf{J}$ , i.e., as the product of the total momentum operator and some scalar operator  $\mathcal{G}$ , which is yet to be found. We have the operator equality

$$\mathcal{G}\mathbf{J} = \hbar b(\mathbf{L} + 2\Gamma\mathbf{I}).$$

Since  $\mathbf{J} = \mathbf{I} + \mathbf{L}$ , we get

$$\mathcal{G}\mathbf{J} = \hbar b(\mathbf{J} + (2\Gamma - 1)\mathbf{I}).$$

Multiplying the last equality in a scalar manner by  $\mathbf{J}$  yields

$$\mathcal{G} = \hbar b \left[ 1 + (2\Gamma - 1) \frac{(\mathbf{J}\mathbf{I})}{\mathcal{J}^2} \right].$$

By virtue of the operator identity,

$$2\mathbf{J}\mathbf{I} = \mathcal{J}^2 + \mathbf{I}^2 - \mathcal{L}^2,$$

which is obtained by squaring the expression  $\mathcal{L} = \mathbf{J} - \mathbf{I}$ , the relationship for  $\mathcal{G}$  becomes

$$\mathcal{G} = \hbar b \left[ 1 + (2\Gamma - 1) \frac{\mathcal{J}^2 + \mathbf{I}^2 - \mathcal{L}^2}{2\mathcal{J}^2} \right].$$

Since  $|lijm\rangle$  are eigenfunctions for the operators that enter into that expression, they will be such for the operator  $\mathcal{G}$  as well. In a homogeneous MF  $H_z$  the ion magnetic Hamiltonian is  $-\mathbf{MH} = -\mathcal{M}_z H_z = -\mathcal{G}\mathcal{J}_z H_z$ . Clearly, its matrix elements

are diagonal, and corrections to energy levels that define their splitting in an MF will be

$$\Delta\varepsilon_{lijm} = \langle lijm | -\mathcal{G}\mathcal{J}_z H_z | lijm \rangle = -mb\hbar g H_z, \quad (6.2.1)$$

where the Lande factor  $g$  can be derived by substituting for the operator  $\mathcal{G}$  its eigenvalues:

$$g = \left[ 1 + (2\Gamma - 1) \frac{j(j+1) + i(i+1) - l(l+1)}{2j(j+1)} \right]. \quad (6.2.2)$$

It differs from the g-factor for an atomic electron in that it has the coefficient  $2\Gamma - 1$  at the fraction in (6.2.2). For an electron we have  $\Gamma = \mu M c / \hbar S q = 1$ , which reduces (6.2.2) to the standard definition.

The ion–isotope constants, which are needed to compute the Lande factor, along with other properties important for the functioning of biological systems, are provided in Table 6.1. The quantities in the table are in the CGS system.

The values of the Lande factor for some biologically significant ions with a nuclear spin are given in the tables below.

• ${}^1\text{H}$ , $i = \frac{1}{2}$ , $\Gamma = 2.80$	$l \setminus j$	$\frac{1}{2}$	$\frac{3}{2}$	$\frac{5}{2}$	$\frac{7}{2}$
	0	5.6			
	1	-0.533		2.533	
	2	0.08		1.92	
	3	0.343		1.657	

• ${}^7\text{Li}$ , $i = \frac{3}{2}$ , $\Gamma = 7.55$	$l \setminus j$	$\frac{1}{2}$	$\frac{3}{2}$	$\frac{5}{2}$	$\frac{7}{2}$	$\frac{9}{2}$
	0	15.1				
	1	24.5		11.34		9.46
	2	-13.1		3.82		6.237
	3	-7.46		1.403		4.357
	3	-7.46		1.403		5.7

• ${}^{23}\text{Na}$ , $i = \frac{3}{2}$ , $\Gamma = 16.88$	$l \setminus j$	$\frac{1}{2}$	$\frac{3}{2}$	$\frac{5}{2}$	$\frac{7}{2}$	$\frac{9}{2}$
	0	33.76				
	1	55.6		25.02		20.66
	2	-31.76		7.552		13.17
	3	-18.66		1.936		8.8
	3	-18.66		1.936		11.92

• ${}^{25}\text{Mg}$ , $i = \frac{5}{2}$ , $\Gamma = -2.124$	$l \setminus j$	$\frac{1}{2}$	$\frac{3}{2}$	$\frac{5}{2}$	$\frac{7}{2}$	$\frac{9}{2}$	$\frac{11}{2}$
	0	-4.248					
	1	-6.347		-3.648		-2.749	
	2	-11.25		-3.548		-2.449	
	3	9.747		0.65		-0.649	
	3	9.747		0.65		-0.649	
	3	9.747		0.65		-0.649	
	3	9.747		0.65		-0.649	

**Table 6.1.** Magnetic characteristics of some cations

at. No. Ion $I$	$M/q$	C, $T_{1/2}$	$\omega_0$	$f_c/f_N$	$\frac{\mu}{\mu_N}/\Gamma$
$^1\text{H}_{1/2}$	1.008/1	99.99	4781	1522/4261	2.793/2.80
$^2\text{H}_1$	2.014	0.016	2393	761.7/654	0.8574/0.86
$^3\text{H}_{1/2}$	3.016	12.32 y	1598	508.7/4544	2.979/8.93
$^6\text{Li}_1$	6.015/1	7.59	801.2	255.0/627	0.822/2.46
$^7\text{Li}_{3/2}$	7.016	92.41	686.9	218.7/1656	3.256/7.57
$^{22}\text{Na}_3$	21.99/1	2.61 y	219.2	69.8/444	1.746/6.36
$^{23}\text{Na}_{3/2}$	22.99	100	209.6	66.7/1128	2.218/16.9
$^{24}\text{Na}_4$	23.99	14.96 h	200.9	63.9/322	1.690/5.04
$^{24}\text{Mg}$	23.99/2	78.99	401.8	127.9	
$^{25}\text{Mg}_{5/2}$	24.99	10.0	385.7	122.8/ <b>261</b>	<b>0.855/2.12</b>
$^{26}\text{Mg}$	25.98	11.01	371.0	118.1	
$^{35}\text{Cl}_{3/2}$	34.97/ <b>1</b>	75.78	<b>137.8</b>	<b>43.9</b> /418	0.8219/ <b>9.53</b>
$^{37}\text{Cl}_{3/2}$	36.97	24.22	<b>130.4</b>	<b>41.5</b> /348	0.6841/ <b>8.38</b>
$^{39}\text{K}_{3/2}$	38.96/1	93.26	123.7	39.4/199	0.3915/5.06
$^{40}\text{K}_4$	39.96	0.0117	120.6	38.4/ <b>248</b>	<b>1.298/6.45</b>
$^{41}\text{K}_{3/2}$	40.96	6.73	117.7	37.5/109	0.215/2.92
$^{40}\text{Ca}$	39.96/2	96.94	241.2	76.8	
$^{43}\text{Ca}_{7/2}$	42.96	0.145	224.4	71.4/ <b>287</b>	<b>1.317/4.02</b>
$^{45}\text{Ca}_{7/2}$	44.96	163 d	214.4	68.2/ <b>289</b>	<b>1.327/4.23</b>
$^{55}\text{Mn}_{5/2}$	54.94/2	100	175.4	55.8/1053	3.453/18.86
$^{59}\text{Co}_{7/2}$	58.93/2	100	163.6	52.1/1008	4.627/19.37
$^{63}\text{Cu}_{3/2}$	62.93/1	69.17	76.6	24.4/1130	2.223/46.37
$^{65}\text{Cu}_{3/2}$	64.93	30.83	74.2	23.6/1211	2.382/51.26
$^{64}\text{Zn}$	63.93/2	48.63	150.8	48.0	
$^{66}\text{Zn}$	65.93	27.90	146.2	46.5	
$^{67}\text{Zn}_{5/2}$	66.93	4.10	144.0	45.8/267	0.8755/5.83
$^{85}\text{Rb}_{5/2}$	84.91/1	72.17	56.8	18.1/413	1.355/22.88
$^{87}\text{Rb}_{3/2}$	86.91	27.83	55.5	17.7/1399	2.751/79.25
$^{133}\text{Cs}_{7/2}$	132.9/1	100	36.2	11.5/563	2.582/48.78

$I$ , the ion nuclear spin;  $M, q$ , the mass in a.m.u. and the charge of an ion; C, the isotopic abundance in %;  $T_{1/2}$ , the half-life;  $\mu$ , the nuclear magnetic moment; the frequencies ( $\omega_0$ , the Larmor frequency;  $f_c$ , the cyclotron frequency; and  $f_N$ , the NMR frequency) are given for an MF of 1 G (100  $\mu\text{T}$ );  $\Gamma = \Omega_N/\Omega_c$ , the ion-isotope constant. The negative numbers are in boldface.

	$l \setminus j$	$\frac{1}{2}$	$\frac{3}{2}$	$\frac{5}{2}$	$\frac{7}{2}$	$\frac{9}{2}$
• $^{39}\text{K}$ , $i = \frac{3}{2}$ , $\Gamma = 5.055$	0		10.11			
	1	16.18	7.681	6.466		
	2	-8.11	2.822	4.384	4.904	
	3		-4.47	1.26	3.169	4.037

### 6.3 MAGNETIC RESONANCE

The wave function of a particle with spin  $\frac{1}{2}$  is a spinor of first rank  $\psi = \begin{pmatrix} \psi^1 \\ \psi^2 \end{pmatrix}$  with components  $\psi^1$  and  $\psi^2$ . Like other mathematical objects, spinors are known to be transformed in a peculiar way under rotations of a coordinate system. The spinor components  $\psi$  in a turned system will be defined as

$$\psi' = U\psi ,$$

where  $U$  is a unit matrix  $U^+ = U^{-1}$  with a unit determinant. The operator for the rotation through the angle  $\varphi$  about the direction  $\mathbf{n}$  for a wave function with spin  $\mathbf{S}$  is (Landau and Lifshitz, 1977)

$$U_{\mathbf{n}}(\varphi) = \exp(i\varphi\mathbf{n}\mathbf{S}) .$$

Specifically, for spin  $\frac{1}{2}$  the operator of rotation about the axis  $a = x, y, z$  is  $U_a(\varphi) = \exp(i\varphi\sigma_a/2)$ , where the Pauli matrices  $\sigma = 2\mathbf{S}$  have the form

$$\sigma_x = \begin{pmatrix} 0 & 1 \\ 1 & 0 \end{pmatrix} , \quad \sigma_y = \begin{pmatrix} 0 & -i \\ i & 0 \end{pmatrix} , \quad \sigma_z = \begin{pmatrix} 1 & 0 \\ 0 & -1 \end{pmatrix} .$$

Expanding the exponential function into a series and noting that all the even powers of the Pauli matrices are identity transformations, and the odd ones are equal to  $\sigma_a$ , we obtain

$$U_x = \begin{pmatrix} \cos \frac{\varphi}{2} & i \sin \frac{\varphi}{2} \\ i \sin \frac{\varphi}{2} & \cos \frac{\varphi}{2} \end{pmatrix} , \quad U_y = \begin{pmatrix} \cos \frac{\varphi}{2} & \sin \frac{\varphi}{2} \\ -\sin \frac{\varphi}{2} & \cos \frac{\varphi}{2} \end{pmatrix} , \quad U_z = \begin{pmatrix} e^{i\varphi/2} & 0 \\ 0 & e^{-i\varphi/2} \end{pmatrix} . \quad (6.3.1)$$

The magnetic resonance described by

$$i\hbar\dot{\Psi} = \mathcal{H}\Psi , \quad \mathcal{H} = -\gamma\hbar\mathbf{S}\mathbf{H} = -\frac{1}{2}\gamma\hbar\sigma\mathbf{H} \quad (6.3.2)$$

occurs in a so-called precessing magnetic field

$$H_x = h \cos(\omega t) , \quad H_y = h \sin(\omega t) , \quad H_z = H ,$$

where  $H$  is the magnitude of a DC MF, and  $h$  is the amplitude of an AC MF. It is convenient to go over into a coordinate system that rotates around the  $z$  axis with

frequency  $\omega$ . The operator of that rotation, which for convenience will be denoted by one letter, has the form

$$U_z(\omega t) = Z = \begin{pmatrix} e^{i\omega t/2} & 0 \\ 0 & e^{-i\omega t/2} \end{pmatrix} .$$

The spinor  $\Psi$  will then become

$$\Psi' = Z\Psi .$$

Substituting this into (6.3.2), we arrive at the dynamic equation for a spin in a rotating coordinate system:

$$\dot{\Psi}' = \mathcal{H}'\Psi' , \quad \mathcal{H}' = -\frac{i}{\hbar}Z\mathcal{H}Z^{-1} + \dot{Z}Z^{-1} . \quad (6.3.3)$$

Note that in the new coordinate system the Hamiltonian  $\mathcal{H}'$ , just like the MF, is time-independent. Therefore, the equation has a simpler solution. Multiplying the matrices gives

$$\dot{\Psi}' = \frac{i}{2}A\Psi' , \quad A = \begin{pmatrix} a & b \\ b & -a \end{pmatrix} , \quad a = \gamma H + \omega , \quad b = \gamma h . \quad (6.3.4)$$

The eigenvectors of the matrix  $A$  are

$$\begin{aligned} \eta_0 &= \begin{pmatrix} b \\ -f \end{pmatrix} , \quad \eta_1 = \begin{pmatrix} f \\ b \end{pmatrix} , \quad f = a - \lambda \\ \lambda &= \sqrt{a^2 + b^2} , \quad \lambda_0 = \lambda , \quad \lambda_1 = -\lambda . \end{aligned} \quad (6.3.5)$$

Here  $\lambda_{0,1}$  are eigenvectors. The solution to the equation is a superposition

$$\Psi' = \sum_k c_k e^{i\lambda_k t/2} \eta_k ,$$

and the wave function in the initial coordinate system is

$$\Psi = Z^{-1}\Psi' = \sum_k c_k e^{i\lambda_k t/2} Z^{-1}\eta_k . \quad (6.3.6)$$

Out of the four real quantities that define the complex factors  $c_k$ , only three are independent, since they obey the normalization condition  $|\Psi|^2 = 1$ . Further, the common phase of the factors has no physical meaning. The choice of the two remaining quantities is dictated by the initial condition of the spin wave function. Let at  $t = 0$  the spin state coincide with the eigenfunction  $\psi_1 = \begin{pmatrix} 1 \\ 0 \end{pmatrix}$  of the operator  $\sigma_z$ . In that state the  $z$  component of the spin is  $\frac{1}{2}$ . From the equalities

$$\Psi(0) = c_0\eta_0 + c_1\eta_1 = c_0 \begin{pmatrix} b \\ -f \end{pmatrix} + c_1 \begin{pmatrix} f \\ b \end{pmatrix} = \begin{pmatrix} 1 \\ 0 \end{pmatrix}$$

we find

$$c_0 = b/\rho , \quad c_1 = f/\rho , \quad \rho = f^2 + b^2 .$$

The normalization of  $\Psi(t)$  is taken care of by the fact that the initial state function is normalized. We now find the time dependence of the probability for the spin

to be found at state  $\psi_0$ . That is clearly the squared magnitude of the appropriate factor in the expansion of the wave function  $\Psi(t)$  into a superposition of  $\psi_0$  and  $\psi_1$ :

$$p_0 = |\langle \psi_0 | \Psi(t) \rangle|^2 .$$

Computation<sup>37</sup> of that quantity gives

$$p_0 = \frac{2f^2b^2}{\rho^2}(1 - \cos \lambda t) = \frac{b^2}{2\lambda^2}(1 - \cos \lambda t) , \quad (6.3.7)$$

where the equality  $fb/\rho = -b/2\lambda$  was used. It follows from (6.3.4) and (6.3.5) that the oscillation frequency for the probability of spin states, the Rabi frequency, is

$$\lambda = \sqrt{(\gamma H + \omega)^2 + (\gamma h)^2} .$$

The oscillation amplitude attains a maximum (magnetic resonance), when the Rabi frequency is minimal. The frequency of an external field will then be equal to the frequency of spin-free precession in an MF  $H$ :

$$\omega = -\gamma H = \omega_0 .$$

We now find the quantum-mechanical mean values for the operators of various spin components

$$\langle \mathcal{S}_i \rangle = \frac{1}{2} \langle \Psi(t) | \sigma_i | \Psi(t) \rangle = \frac{1}{2} \sum_{km} c_k^* c_m e^{-i(\lambda_k - \lambda_m)t/2} \langle \eta_k | Z \sigma_i Z^{-1} | \eta_m \rangle . \quad (6.3.8)$$

Skipping, as before, intermediate computations, we write the result for the magnetic resonance situation:

$$\begin{aligned} \langle \mathcal{S}_x \rangle &= \frac{1}{2} \sin \omega_0 t \sin(\gamma h t) \\ \langle \mathcal{S}_y \rangle &= \frac{1}{2} \cos \omega_0 t \sin(\gamma h t) \\ \langle \mathcal{S}_z \rangle &= \frac{1}{2} \cos(\gamma h t) . \end{aligned} \quad (6.3.9)$$

The imaginary “spin vector” with the components  $\langle \mathcal{S}_i \rangle$  rotates around the  $z$  axis, so that its end describes spiral paths on the spherical surface of radius  $\frac{1}{2}$ .

It is possible to refer to a spin vector only in a conventional or statistical sense. Since various spin components do not commute, the appropriate observables cannot take on definite values simultaneously. Quantum-mechanically, the spin vector is thus not an observable quantity. We note that there are more than a dozen various systems of quantum-mechanical postulates or interpretations that are the subject of investigations in so-called quantum metaphysics (Sudbery, 1986). Interpretations differ in their substance and ratios of non-observable quantities and are in

---

<sup>37</sup>The scalar  $\langle \psi | \xi \rangle$  is calculated following the rule  $\langle \psi | \xi \rangle = \psi^+ \xi = (\psi^1)^* \xi^1 + (\psi^2)^* \xi^2$ .

essence attempts at circumventing the inherent difficulties of the theory — the so-called paradoxes of quantum mechanics. It is important that all the interpretations give identical predictions for observables. One quantum-mechanical interpretation ascribes to the spin vector, which is not observable experimentally, a status of real state. However, measuring any of its components invariably destroys the very state, thus making measuring other components impossible. We further assume the statistical meaning of the term “spin vector” and use it without the inverted commas.

Classically, the derivative of the angular momentum of a system equals the moment of forces acting on the system. The mechanical angular momentum  $\hbar\mathbf{S}$  connected to the spin vector  $\mathbf{S}$  is exposed in a DC MF  $\mathbf{H}$  to the moment  $\mathbf{M} \times \mathbf{H}$ , where  $\mathbf{M} = \gamma\hbar\mathbf{S}$  is the “vector” of the spin magnetic moment. Therefore

$$\dot{\mathbf{S}} = \omega_0 \mathbf{n} \times \mathbf{S}, \quad \omega_0 = -\gamma H,$$

where  $\mathbf{n}$  is a unit vector along  $\mathbf{H}$ . The equation implies that the vector  $\mathbf{S}$  rotates with the angular velocity  $\omega_0$  about the orientation of an MF, the vector magnitude and angle it forms with the MF orientation remaining unchanged. Such motion is called precession, and in the case of the precession of a system’s orbital momentum it is referred to as the Larmor precession. Generally speaking, the orbital and spin momenta, e.g., those of an electron, precess with different frequencies,  $eH/2m_e c$  and  $\gamma H = eH/m_e c$ , respectively. In the literature, spin precession is often called Larmor precession as well.

If at some moment  $t_0$  an AC field is switched off, the phases  $\gamma ht$  in (6.3.9) will assume some fixed values  $\vartheta = \gamma ht_0$ . The further motion of the spin is described by the equations

$$\langle \mathcal{S}_x \rangle = \frac{1}{2} \sin \omega_0 t \sin \vartheta, \quad \langle \mathcal{S}_y \rangle = \frac{1}{2} \cos \omega_0 t \sin \vartheta, \quad \langle \mathcal{S}_z \rangle = \frac{1}{2} \cos \vartheta.$$

It is easily seen that these expressions correspond to the precession of a vector with components  $\langle \mathcal{S}_i \rangle$  around the direction of an MF along the  $z$  axis at an angle  $\vartheta$ , thus justifying the use of the vector model for the spin.

In the general case, we can write the spin states at which the spin component along an arbitrary direction  $\theta$ ,  $\varphi$  has definite values  $\pm \frac{1}{2}$ ,

$$|+\rangle = \begin{pmatrix} \cos \frac{\theta}{2} \\ e^{i\varphi} \sin \frac{\theta}{2} \end{pmatrix}, \quad |-\rangle = \begin{pmatrix} -e^{-i\varphi} \sin \frac{\theta}{2} \\ \cos \frac{\theta}{2} \end{pmatrix}, \quad (6.3.10)$$

which are eigenstates of the spin operator

$$\mathcal{S}_{\theta, \varphi} = \frac{1}{2} \begin{pmatrix} \cos \theta & e^{-i\varphi} \sin \theta \\ e^{i\varphi} \sin \theta & -\cos \theta \end{pmatrix}. \quad (6.3.11)$$

That operator is obtained from  $\mathcal{S}_z$  by appropriate turns. If the spin state in the old coordinate system was defined so that its  $z$  component was  $\frac{1}{2}$ , then in order that in the new coordinate system the state would have a component in the  $\theta, \varphi$  direction equal to  $\frac{1}{2}$ , the coordinate system will have to be turned about the  $z$  axis through

the angle  $-\varphi$  and further around the new  $y'$  axis through the angle  $-\theta$ . The spin operators  $\mathcal{S}_i$  after the first rotation become  $\mathcal{S}'_i = U_z(-\varphi)\mathcal{S}_iU_z^{-1}(-\varphi)$ , where  $U_z$  is defined in (6.3.1). The second rotation yields the desired operator (we will have to take into consideration that  $\mathcal{S}'_z = \mathcal{S}_z$ )

$$\mathcal{S}_{\theta,\varphi} = U_{y'}(-\theta)\mathcal{S}_zU_{y'}^{-1}(-\theta), \quad U_{y'}(-\theta) = \exp(-i\theta\mathcal{S}'_y).$$

Computations yield (6.3.10), (6.3.11). It is only natural that at  $\theta = 0$  we return to the initial operator  $\mathcal{S}_z = \sigma_z/2$  and its eigenfunctions.

The factors  $c_k$  in (6.3.6) are associated with the selection of the wave function at the initial moment of time. In the general case, it should be taken in the form, say,  $|+\rangle$ . In this state, the value of the spin's component along  $\theta$ ,  $\varphi$  is  $\frac{1}{2}$ . This corresponds to a situation where the spin ensemble has not been prepared in some special manner; i.e., the prior state of a spin is in a way arbitrary. Then

$$\Psi(0) = c_0\eta_0 + c_1\eta_1 = c_0 \begin{pmatrix} b \\ -f \end{pmatrix} + c_1 \begin{pmatrix} f \\ b \end{pmatrix} = \begin{pmatrix} \cos \frac{\theta}{2} \\ e^{i\varphi} \sin \frac{\theta}{2} \end{pmatrix}.$$

Hence the general expression for the factors  $c_k$  is

$$c_0 = \frac{1}{\rho} \left( b \cos \frac{\theta}{2} - f \sin \frac{\theta}{2} e^{i\varphi} \right), \quad c_1 = \frac{1}{\rho} \left( b \sin \frac{\theta}{2} e^{i\varphi} + f \cos \frac{\theta}{2} \right).$$

Substituting that into (6.3.8), we obtain

$$\begin{aligned} \langle \mathcal{S}_z \rangle &= \frac{b^2 - f^2}{2\rho^2} [(b^2 - f^2) \cos \theta - 2bf \sin \theta \cos \varphi] \\ &\quad + \frac{bf}{\rho^2} [2bf \cos \theta \cos \tau + b^2 \sin \theta \cos(\varphi - \tau) - f^2 \sin \theta \cos(\varphi + \tau)], \end{aligned}$$

where  $\tau = \lambda t$ . We will rewrite the time-dependent part as

$$\begin{aligned} \langle \mathcal{S}_z \rangle &= r \frac{bf}{\rho^2} \sin(\tau + \xi), \quad r^2 = (b^2 + f^2)^2 x + 4b^2 f^2 y + 2bf(b^2 - f^2) z, \\ x &= \sin^2 \theta, \quad y = \cos^2 \theta - \sin^2 \theta \cos \varphi, \quad z = \sin 2\theta \cos \varphi. \end{aligned}$$

It can be shown that extrema of the oscillation amplitude are defined by the solutions to the following equation in  $p = f/b$

$$p^6 - 3\frac{z}{x}p^5 + (1 + 8\frac{y}{x})p^4 + 10\frac{z}{x}p^3 - (1 + 8\frac{y}{x})p^2 - 3\frac{z}{x}p - 1 = 0 \quad (6.3.12)$$

and in the general case they do not coincide with the common condition for a resonance  $f = -b$ , which follows from the set of equalities  $\omega = -\gamma H \rightarrow a = 0 \rightarrow \lambda = b \rightarrow f = -b$ , see (6.3.4), (6.3.5). At  $\theta = 0$  the equation reduces to  $p^2 = 1$ . One of the solutions of that equation is exactly the common condition for a resonance. If then, for instance,  $\theta = \pi/2$ ,  $\varphi = 0$ , the oscillation amplitude with  $f = -b$  will be

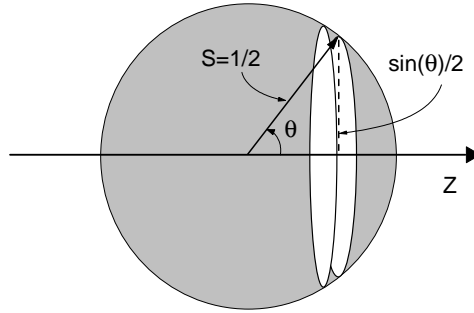


**Figure 6.1.** On the derivation of the probability density for the spin orientation at an angle  $\theta$  to the  $z$  axis.

zero. It attains maxima at other frequencies. They can be found from the solution to (6.3.12) for given angle values:  $(f/b)^2 = 3 \pm 2\sqrt{2}$ .

Spin motion for arbitrary initial conditions is quite complicated. If the frequency of an external field coincides with the natural frequency of spin precession, then  $f = -b$ , and

$$\langle \mathcal{S}_z \rangle = \frac{1}{2}(\cos \theta \cos \tau - \sin \theta \sin \varphi \sin \tau) . \quad (6.3.13)$$

Significantly, the oscillation amplitude of the spin  $z$  component is dictated by the initial conditions. Note that if we would take account of the random phase  $\zeta$  of the precession of an external MF, then it would enter the last expression as an additional term in one of the arguments. Instead of  $\tau = \omega t$  we would have to write  $\omega t + \zeta$ .

In a DC MF similar to the geomagnetic field, Zeeman splitting  $\hbar\omega_0$  is many orders of magnitude smaller than  $\kappa\mathcal{T}$ , which suggests that in the absence of prior information on the state of a particle all the possible spin states have equal probabilities. Put another way, this means that each spin in an ensemble may be aligned in whatever direction with equal probability. We now find the probability density of various values  $\theta$  and  $s \equiv \langle \mathcal{S}_z \rangle$ .

The probability for a spin to have a definite angle to the  $z$  axis from  $\theta$  to  $\theta + d\theta$  is a relative solid angle cut out by the difference of cones aligned along  $\theta$  and  $\theta + d\theta$ , respectively, Fig.6.1,

$$dP = \frac{2\pi \sin \theta d\theta}{4\pi} = \frac{1}{2} \sin \theta d\theta . \quad (6.3.14)$$

Hence we immediately find the probability density for values of  $\theta$

$$f(\theta) \equiv \frac{dP}{d\theta} = \frac{1}{2} \sin \theta . \quad (6.3.15)$$

If the spin is aligned at an angle  $\theta$  to the  $z$  axis, then

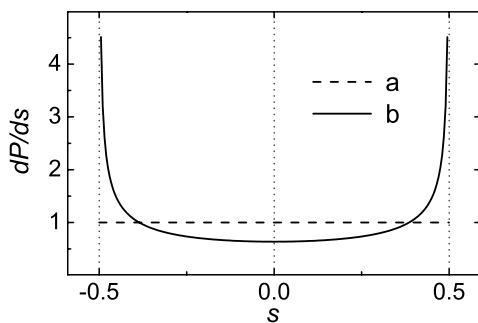


**Figure 6.2.** The distribution density of the values of spin  $z$  components  $s = \langle S_z \rangle$  at (a) thermodynamic equilibrium and (b) magnetic resonance.

$$\langle S_z \rangle = \frac{1}{2} \cos \theta, \quad ds = -\frac{1}{2} \sin \theta d\theta = -dP. \quad (6.3.16)$$

Thus, substituting (6.3.14),

$$\frac{dP}{ds} = 1, \quad -\frac{1}{2} \leq s \leq \frac{1}{2}. \quad (6.3.17)$$

The minus sign is omitted, since its only purpose is to indicate that  $\langle S_z \rangle$  decreases as the angle  $\theta$  grows. It is seen in Fig. 6.2-a that the quantity  $\langle S_z \rangle = \frac{1}{2} \cos \theta$  is uniformly distributed within the interval  $[-0.5, 0.5]$ .

Let a spin system now be in resonance with an AC MF. If the initial state of the spin is defined, then the oscillations  $s \equiv \langle S_z \rangle$  are a sinusoidal process (6.3.13) with the random phase  $\zeta \in [0, 2\pi)$ , whose distribution function, equal to (Korn and Korn, 1961)

$$\frac{dP}{ds} = \frac{2}{\pi\sqrt{1-4s^2}}, \quad (6.3.18)$$

is shown in Fig. 6.2-b. It differs markedly from the equilibrium distribution, the spin vector being predominantly aligned along the MF axis. If the initial state is not defined, then in (6.3.13) random quantities are not only  $\tau(\zeta)$ , but also the angles  $\theta$  with distribution (6.3.15), and  $\varphi$  with equilibrium distribution. It can be shown that in this case the distribution  $dP/ds$  is similar to the equilibrium distribution in Fig. 6.2-a. It follows that the MBE mechanism could, in principle, be connected with the changes in the distribution function  $dP/ds$  at magnetic resonance. It is possible, however, only if there is a measure of certainty in relation to spin states. Such a certainty occurs in a number of cases in reactions involving free radicals exposed to an MF (Buchachenko *et al.*, 1978).

## 6.4 ESTIMATION OF EF GRADIENTS ON THE CELL SURFACE

To assess the EF gradients caused by an external field, we will employ the toolkit of the electrodynamics of continuous media. The latter deals with physical quantities averaged over “physically infinitesimal” volume elements. That is to say, changes of the field owing to the atomic structure of matter are not taken into consideration; the fields are considered averaged on scales that significantly exceed a molecule’s size of the matter.

Specifically, this approximation is convenient to assess the behavior of an EF near biological cells in a plasmatic solution. EF gradients induced by an external field near the surface of cell membranes can affect the ion–protein complexes located there.

One model of a biological cell in a cytoplasm can be a dielectric cylinder in a dielectric medium. Let the cylinder length  $L$  be much larger than its radius  $R$ , which enables estimations to be obtained for some special cylinder orientations.

To begin with, we will consider the case where the axis ( $y$ ) of the cylinder is perpendicular to an applied field  $\mathbf{G} \parallel z$ . The condition  $L \gg R$  allows one to deal with two-dimensional cases. We will distinguish between an external EF  $\mathbf{G}$ , and a field  $\mathbf{E}$ , which is a superposition of the external field and the field produced by the cylinder polarized in it. We will introduce the index  $e$  to denote quantities pertaining to the medium and the index  $i$  for the space within the cylinder. It was shown (Landau and Lifshitz, 1960) that the field potentials within and without the cylinder have the form

$$\varphi^e(\mathbf{r}) = -\mathbf{G}\mathbf{r} + A\mathbf{G}\mathbf{r}/r^2, \quad \varphi^i(\mathbf{r}) = -B\mathbf{G}\mathbf{r}, \quad (6.4.1)$$

where  $\mathbf{r}$  is the vector radius marked off from a point on the cylinder axis, and  $A, B$  are constants. Only such potentials meet the two-dimensional Laplace equation for potentials within and without a cylinder with the necessary boundary conditions.

On the interface of two dielectrics the well-known conditions of the continuity of the potential and that of the EF component  $\mathbf{D} = \varepsilon\mathbf{E}$  normal to the interface, where  $\varepsilon$  is a permittivity, must be obeyed. That is, in our case

$$\varphi^e(\mathbf{R}) = \varphi^i(\mathbf{R}), \quad \varepsilon^e\mathbf{E}^e(\mathbf{R}) = \varepsilon^i\mathbf{E}^i(\mathbf{R}),$$

where  $\mathbf{R}$  is a vector of a specified length  $R$ . The first condition yields  $B = 1 - A/R^2$ , and hence

$$\mathbf{E}^i(\mathbf{r}) = -\nabla\varphi^i(\mathbf{r}) = \mathbf{G}(1 - A/R^2).$$

The electric field outside of the cylinder is

$$\mathbf{E}^e(\mathbf{r}) = -\nabla\varphi^e(\mathbf{r}) = \mathbf{G} - A\nabla(\mathbf{G}\mathbf{r}/r^2).$$

Since

$$\nabla(\mathbf{G}\mathbf{r}/r^2) = (\mathbf{G}\nabla)\mathbf{r}/r^2 = r^{-2}\mathbf{G} - 2r^{-4}(\mathbf{r}\mathbf{G})\mathbf{r},$$

then

$$\mathbf{E}^e(\mathbf{r}) = \mathbf{G}(1 - A/r^2) + (\mathbf{r}\mathbf{G})\mathbf{r}2A/r^4. \quad (6.4.2)$$

The quantity  $A$  follows from the condition that the normal components of the induction  $\mathbf{D}$  on the interface be equal. The induction normal component within the cylinder is

$$D_n^i(\mathbf{r}) = \mathbf{D}^i(\mathbf{r})\mathbf{r}/r = \varepsilon^i \mathbf{E}^i(\mathbf{r})\mathbf{r}/r = \varepsilon^i(1 - A/R^2)\mathbf{G}\mathbf{r}/r. \quad (6.4.3)$$

The induction normal component outside of the cylinder will be

$$D_n^e(\mathbf{r}) = \mathbf{D}^e(\mathbf{r})\mathbf{r}/r = \varepsilon^e \mathbf{E}^e(\mathbf{r})\mathbf{r}/r.$$

Substituting here  $\mathbf{E}^e(\mathbf{r})$  from (6.4.2) gives

$$D_n^e(\mathbf{r}) = \varepsilon^e(\mathbf{G}\mathbf{r})(1 + A/r^2)/r. \quad (6.4.4)$$

Equating (6.4.3) to (6.4.4) at  $\mathbf{r} = \mathbf{R}$ , we get

$$\frac{A}{R^2} = \frac{\varepsilon^i - \varepsilon^e}{\varepsilon^i + \varepsilon^e}. \quad (6.4.5)$$

We can obtain the EF gradients on the surface of the cylinder  $\mathbf{r} = \mathbf{R}$ . We now work them out for two special cases where the vector  $\mathbf{r}$  is aligned along the  $z$  axis,  $\mathbf{r} = (0, 0, R)$ , and along the  $x$  axis,  $\mathbf{r} = (R, 0, 0)$ . In both cases we only have the  $z$  components of the field  $\mathbf{E}^e$ . In the  $x$  direction we have from (6.4.2) and (6.4.5)  $E^e(r) = G(1 - A/r^2)$ , hence

$$(E_z)'_x = \frac{2G}{R} \frac{\varepsilon^i - \varepsilon^e}{\varepsilon^i + \varepsilon^e}.$$

Similarly, we find the field gradient in the  $z$  direction

$$(E_z)'_z = -\frac{2G}{R} \frac{\varepsilon^i - \varepsilon^e}{\varepsilon^i + \varepsilon^e}.$$

When  $\varepsilon^e \gg \varepsilon^i$ , a case for biopolymers ( $\varepsilon^i \sim 3$ ) in an aqueous solution ( $\varepsilon^e \sim 80$ ), the gradients will have the following order of magnitude

$$E' \sim 2G/R. \quad (6.4.6)$$

Let us now turn to the case where the cylinder is aligned with the field. Of interest here is the magnitude of the gradient on the lateral face, since the relative area of the end planes is small. The field  $\mathbf{E}$  of such a cylinder polarized by an external field  $\mathbf{G}$  is close to a dipole field. The charge density in a dielectric is defined by the relationship  $\rho = -\nabla\mathbf{P}$ , where  $\mathbf{P}$  is the medium polarization vector or the dipole moment of a unit volume of a dielectric. It follows that the surface charge density  $\sigma$  at the interface of the two dielectrics is equal to the sum of the normal components of the polarization vector:  $\sigma = P_n^i + P_n^e$ . For a long cylinder,

the polarization  $\mathbf{P}$  of the dielectrics is parallel with the cylinder lateral surface. Therefore, the surface charge density is zero and the outside field  $\mathbf{E}$  is the sum of the homogeneous external field  $\mathbf{G}$  and the field of a polarized cylinder with effective charges  $q$  on the end faces. The gradients are clearly dictated by the latter field, which is close to a dipole field, i.e., produced by the charges  $\pm q$  at a distance  $L$ .

For the surface charge on the end faces we can write

$$\mathbf{P}^{i,e} = \frac{\varepsilon^{i,e} - 1}{4\pi} \mathbf{G}, \quad \Rightarrow \quad \sigma = \frac{\varepsilon^e - \varepsilon^i}{4\pi} G.$$

Therefore, the effective charge on the end faces will be

$$q = \pi R^2 \sigma = GR^2(\varepsilon^e - \varepsilon^i)/4.$$

We can readily work out the dependence of an EF on the distance  $r$  to the dipole axis

$$E_r = \frac{2q}{\varepsilon^e} r(r^2 + L^2/4)^{-3/2}.$$

Taking a derivative and substituting  $q$ , we find

$$(E_z)'_x = \frac{4G}{L} \frac{\varepsilon^e - \varepsilon^i}{\varepsilon^e} \left(\frac{R}{L}\right)^2 + o\left(\frac{R}{L}\right)^3.$$

If  $\varepsilon^e \gg \varepsilon^i$ , we then obtain

$$E' \sim \frac{4G}{L} \left(\frac{R}{L}\right)^2. \quad (6.4.7)$$

Comparing it with (6.4.6), we conclude that for parallel cylinder alignment the gradients will be significantly, by a factor of  $(R/L)^2 \ll 1$ , smaller than those for a cylinder normally oriented to a field.

## 6.5 DAVYDOV SOLITON

The concept of the Davydov soliton is concerned with the transportation of excitation energy of the C=O bond of peptide groups along  $\alpha$ -spiral areas of protein chains. Protein macromolecules are composed of sequences of 20 amino acids of residues connected by so-called peptide groups  $-\text{C}:\text{O}-\text{N}\cdot\text{H}-$ . One of the possible conformations of a polypeptide chain with the minimal potential energy is the so-called Pauling-Cori  $\alpha$ -spiral. The conformational energy of the chain is determined by hydrogen bonds of chain atoms that are valence-unbound. Each peptide group forms a hydrogen bond with an identical group, the fourth one starting from a given group. The spatial arrangement of peptide groups is shown in Fig. 6.3. For some reasons a polypeptide chain can be deformed, and the peptide groups displaced by a distance  $\beta_n$  from their equilibrium positions  $a_n$ .

Infrared vibrational oscillations of C=O peptide groups of  $\alpha$ -spirals with frequencies near  $1650 \text{ cm}^{-1}$ , which came to be known as Amid I, feature a significant

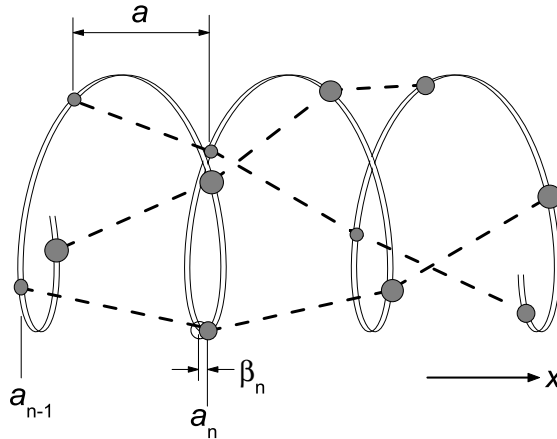


**Figure 6.3.** The arrangement of peptide groups in a molecule of  $\alpha$ -spiral. Hydrogen bonds between the groups are shown by dash lines. There are 3.6 peptide groups per one spiral turn; therefore the hydrogen bond chains, of which there are three, form spirals with a large constant.

dipole moment,  $d \sim 0.3$  Debye. Therefore, Amid I oscillations interact with neighboring peptide groups, thus causing collective perturbations. Since dipole interaction is strongly dependent on distance,  $\sim r^{-3}$ , then the deformation of the peptide chain and the propagation of C=O excitations appear to be interconnected.

The probability amplitude of Amid I oscillations in peptide groups with number  $n$  is described by the function  $\varphi_n(t)$ . In continuum approximation the distribution of these probabilities along the chain and over time can conveniently be described by a plane wave

$$\Phi(x, t) \exp [i(kx - Et/\hbar)] ,$$

where  $E$  is the excitation energy, and  $k$  is a wave number. In the idealized infinite chain, owing to its translational symmetry, the velocity  $V$  of an excitation propagating along the chain is conserved. Therefore, it is convenient to go over to a traveling coordinate system  $\xi = x - Vt$ . Davydov indicated (e.g., Davydov, 1984b) that Amid I stationary excitations are described by the non-linear Schrödinger's equation

$$\frac{\hbar^2}{2m} \frac{d^2}{d\xi^2} \Phi(\xi) + G\Phi^3(\xi) = \Lambda\Phi(\xi) , \quad m = \frac{\hbar^2}{2a^2J} , \quad G = \frac{\chi^2}{\kappa(1-s^2)} . \quad (6.5.1)$$

Here  $J = 2d^2/a^3 \sim 7.8 \text{ cm}^{-1}$  is the resonance interaction energy for Amid I oscillations,  $\chi \sim 10^{-10} \text{ N}$  is the coupling constant between Amid I oscillations and displacements  $\beta$ ,  $\kappa \sim 19 \text{ N/m}$  is the spiral elasticity factor,  $s$  is the ratio of the

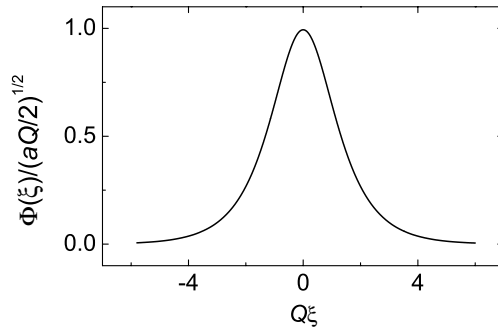


**Figure 6.4.** The form of the soliton solution to the non-linear Schrödinger's equation.

excitation travel velocity  $V$  and the sound velocity in the chain, and  $a = 4.5 \text{ \AA}$  is the space period of peptide groups.

The solutions (6.5.1) are envelopes  $\Phi(\xi)$  and the corresponding values of the spectral parameter  $\Lambda$ . If the velocity  $V$  is higher than the speed velocity, i.e.,  $s^2 > 1$ , then there are so-called exciton solutions

$$\Phi(\xi) = 1/\sqrt{N}, \quad \Lambda = -G/N,$$

where  $N \gg 1$  is the number of chain elements. The distribution of Amid I excitations is described by plane waves. The wave packet formed by excitons smears out with time; they cannot serve as energy carriers.

For low velocities  $V$ ,  $s^2 < 1$ , in addition to the exciton one there is also a soliton solution in the form of hyperbolic secant  $\text{sch}(x) = 2/[\exp(x) + \exp(-x)]$ ,

$$\Phi(\xi) = \sqrt{aQ/2} \text{sch}(Q\xi), \quad \Lambda = \frac{\hbar^2 Q^2}{2m}, \quad Q = \frac{maG}{2\hbar^2}.$$

The form of this function is shown in Fig. 6.4. Unlike excitons, a soliton travels at a velocity that is smaller than the sound speed, and therefore it does not emit phonons and does not slow down. An excitation travels without losing its shape. It is important that the energy of a low-velocity soliton is smaller than the energy of an exciton. The energy difference corresponds to the MM range of electromagnetic radiations (Eremko, 1984).

A more realistic model assumes that corresponding to the Pauling–Cori spiral is not one, but rather three interacting spiral chains of hydrogen bonds, Fig. 6.3. A soliton excitation travels along three chains simultaneously, with, as was shown (Scott, 1981) by computer simulation, the excitation energy from time to time migrating from one chain to another. The Davydov soliton thus possesses internal vibrations with a frequency of about  $17 \text{ cm}^{-1}$ . There are also vibrations in the IR range,  $\sim 125 \text{ cm}^{-1}$ , owing to the polypeptide chain being discrete.

The question of the stability of a Davydov soliton at physiological temperatures has not received a proper theoretical treatment as yet, see p. 206. A critique of the Davydov soliton concept is available in Ivić *et al.* (1996), where it is shown that quantum fluctuations hinder a Davydov soliton from being an effective intramolecular energy carrier.

## 6.6 FRÖHLICH MODEL OF COHERENT DIPOLE EXCITATIONS

A model (Fröhlich, 1968a) for describing a quantum system of collective dipole excitations in a medium, which interact with a thermostat and an external EMF, uses the occupation number representation. We will begin by explaining an individual quantum oscillator in that picture. The initial Hamiltonian of the oscillator has the form

$$\mathcal{H} = \frac{\mathcal{P}^2}{2M} + \frac{M\omega^2 x^2}{2},$$

where  $\omega$  and  $M$  are the natural frequency and mass of an oscillator. If we introduce the operator

$$a = \frac{1}{\sqrt{2\hbar}} \left( x\sqrt{M\omega} + i\frac{\mathcal{P}}{\sqrt{M\omega}} \right)$$

and use the commutator  $\{x, \mathcal{P}\} = i\hbar$ , we can write the Hamiltonian in the form (e.g., Landau and Lifshitz, 1977)

$$\mathcal{H} = \hbar\omega \left( a^+ a + \frac{1}{2} \right), \quad (6.6.1)$$

where  $a^+$  is a Hermitian conjugate operator to the operator  $a$ . The term  $\frac{1}{2}$ , which represents the energy of zero oscillations, is omitted where it is immaterial. The spectrum of eigenvalues of the Hamiltonian is

$$\epsilon = \hbar\omega \left( n + \frac{1}{2} \right).$$

It is seen that the number  $n$  can be regarded as the number of excitation quanta  $\hbar\omega$  or as the occupation number for a state represented by an oscillator, and the operator  $a^+ a$  as the operator of the number of excitation quanta. In the occupation number picture,  $n$  is an independent variable. The wave functions of that representation are dependent on  $n$ , with operators operating on these numbers. The Hamiltonian eigenstates (6.6.1), denoted, for instance, as  $|n\rangle$ , obey the recurrence relations

$$a^+ |n\rangle = \sqrt{n+1} |n+1\rangle, \quad a |n\rangle = \sqrt{n} |n-1\rangle. \quad (6.6.2)$$

The operators  $a^+$  and  $a$  are, therefore, referred to as the creation and the destruction operators, respectively, for excitation quanta, or the raising and the lowering operators. A description of quantum systems in the occupation number representation in many cases features a higher degree of generality, which enables algebraic

techniques to be used to solve quantum mechanics problems. The Hamiltonian of a system is then not derived, but rather written immediately in a form similar to (6.6.1). What is important is that for two arbitrarily interacting identical quantum systems described by Hamiltonians proportional to  $a^+a$  and  $b^+b$ , the interaction operator can be written as an expansion in  $a, a^+, b, b^+$ , the first term having the form  $ab^+ + a^+b$ . Its physical meaning is obvious — it is an exchange of excitation quanta between systems.

One well-known result of the condensed state theory is that the dynamics of a many-particle system is described in terms of collective excitations. The complicated motion of a many-particle system can be pictured as a superposition of normal collective modes. Each of such normal oscillations is distinguished by the fact that the motion of all the particles of the system is ordered and is a wave. One example is sound waves in solids.

Fröhlich addressed the dynamics of bound dipole systems. Many biophysical constructs, such as polyamino acids, membranes, and cytoskeleton tubulin filaments, are suitable objects for simulation using idealized dipole systems. If a system is sufficiently large, the frequencies of its natural collective modes form a fairly dense and limited series  $\omega_i$ . The Hamiltonian of such a system can be written by assigning to each collective mode an oscillator with a corresponding natural frequency:  $\sum_i \hbar\omega_i a_i^+ a_i$ . For oscillators of a thermostat and an external electromagnetic field, with which dipoles interact, similar Hamiltonians  $\sum_k \hbar\Omega_k b_k^+ b_k$  and  $\sum_l \hbar\nu_l p_l^+ p_l$  can be written. The interaction of dipole modes with a thermostat is represented by the sum of Hamiltonians of the form

$$\sum_{i,j,k} (a_i b_j^+ b_k + a_i^+ b_j b_k^+) \quad (6.6.3)$$

and

$$\sum_{i,j,k} (a_i a_j^+ b_k + a_i^+ a_j b_k^+) . \quad (6.6.4)$$

The former describes a process in which a quantum of dipole modes vanishes, which is accompanied by the disappearance of a thermostat quantum of one mode and the appearance of a thermostat quantum of another mode, and vice versa. Clearly, that Hamiltonian contains terms of the form  $a_i b_i^+ + a_i^+ b_i$  as a special case. By virtue of energy conservation we have  $\omega_i = \Omega_j - \Omega_k$ ; therefore summation here is over two indices. The second Hamiltonian takes account of processes, in which two dipole mode quanta and one thermostat quantum take part. The remaining terms of the interaction operator, which correspond to the two-quantum exchanges  $\sim a_i a_j$  and  $\sim a_i^+ a_j^+$ , were shown by Wu and Austin (1978) to be immaterial. Interaction of an external source with dipole modes will accordingly be proportional to  $\sum_i (a_i p_i^+ + a_i^+ p_i)$ .

Using the Hamiltonian  $\mathcal{H}$  of a system interacting with a thermostat and an external field, i.e., the sum of the terms cited above, we can arrive at the wave

function of a system  $\Psi(t)$  and work out the variation rate for the mean number of quanta of the  $i$ th dipole mode  $n_i = \langle \Psi(t) | \mathcal{N}_i | \Psi(t) \rangle$

$$\dot{\mathcal{N}}_i = -\frac{i}{\hbar} \{ \mathcal{N}_i, \mathcal{H} \}, \quad \mathcal{N}_i = a_i^+ a_i,$$

which has been carried out by Wu and Austin (1977). Fröhlich derived the kinetic equation for  $n_i$  phenomenologically. We would like to show how that could be done.

The rate of the process, which, when operated on by  $a^+$ , has its occupation number  $n$  increased by one, is proportional to the squared matrix element

$$\langle n+1 | a^+ | n \rangle = \sqrt{n+1},$$

which follows from (6.6.2), i.e., varies with  $n+1$ . Also, for  $a$  the rate varies with  $n$ . Therefore, if  $n_i$  and  $m_j$  are mean occupation numbers of appropriate dipole modes and thermostat modes, then the rate of the variation of  $n_i$  with single-quantum exchange (6.6.3) is proportional to

$$\dot{n}_i \sim \sum_{j,k} [n_i(m_j+1)m_k - (n_i+1)m_j(m_k+1)].$$

The minus sign here is due to the fact that two terms in (6.6.3) act in the opposite direction. Using the Planck distribution for mean occupation numbers  $m_j$  of thermostat quantum oscillators,

$$m_j = \frac{1}{e^{\hbar\Omega_j/\kappa\mathcal{T}} - 1},$$

subject to energy conservation  $\omega_i = \Omega_j - \Omega_k$ , we can reduce this expression to the form

$$\dot{n}_i \sim \phi(\omega_i, \mathcal{T}) [n_i e^{\beta\omega_i} - (n_i+1)], \quad (6.6.5)$$

where  $\phi$  is a function of the absolute temperature and frequency,  $\beta = \hbar/\kappa\mathcal{T}$ . Similarly, the variation rate  $n_i$  due to two-quantum exchange (6.6.4) varies with

$$\dot{n}_i \sim \sum_j \lambda(\omega_i, \omega_j, \mathcal{T}) [n_i(n_j+1)e^{\beta\omega_i} - (n_i+1)n_j e^{\beta\omega_j}], \quad (6.6.6)$$

where conservation law is used in the form  $\omega_j - \omega_i = \Omega_k$ . One simplification is that the functions  $\phi$  and  $\lambda$  are taken to be constants:

$$\dot{n}_i = s_i - \phi [n_i e^{\beta\omega_i} - (n_i+1)] - \lambda \sum_j [n_i(n_j+1)e^{\beta\omega_i} - (n_i+1)n_j e^{\beta\omega_j}], \quad (6.6.7)$$

where  $s_i$  is the growth rate for quanta of the  $i$ th mode due to an external source. Under stationary conditions  $\dot{n}_i = 0$  a formal solution to this equation with respect to  $n_i$  is

$$n_i = \frac{c + s_i}{e^{\beta\omega_i} [\phi + \lambda \sum_j (n_j + 1)] - c}, \quad c = \phi + \lambda \sum_j n_j e^{\beta\omega_j}, \quad (6.6.8)$$

where for convenience the summation index is dropped. Fröhlich gives the following analysis of that expression, which can be rewritten as

$$n_i = \left(1 + \frac{s_i}{c}\right) \frac{1}{e^{\beta(\omega_i - \mu)} - 1}, \quad e^{-\beta\mu} = \frac{\phi + \lambda \sum (n_j + 1)}{c}. \quad (6.6.9)$$

It follows that in the absence of pumping, i.e., at  $s_i = 0$ , the distribution turns, as should be the case, into the thermally equilibrium distribution

$$n_i^T = \frac{1}{e^{\beta\omega_i} - 1}. \quad (6.6.10)$$

Here  $\mu$  has the meaning of chemical potential, which vanishes at  $s_i = 0$ . If we introduce an excess  $m_i = n_i - n_i^T$  of the mean quantum number over the equilibrium distribution, the definition  $\mu$  becomes

$$e^{\beta\mu} = 1 + \frac{\lambda \sum m_j (e^{\beta\omega_j} - 1)}{\phi + \lambda \sum (n_j + 1)}. \quad (6.6.11)$$

This suggests that  $\mu \geq 0$ . On the other hand, since the number of quanta is always positive, it follows that  $\mu \leq \omega_0$ , where  $\omega_0$  is the smallest frequency of dipole excitations. Using the definition of  $\mu$  from (6.6.9), we get

$$\frac{s_i}{c} = \frac{s_i e^{-\beta\mu}}{\phi + \lambda \sum (n_j + 1)}.$$

By (6.6.11)

$$\phi + \lambda \sum (n_j + 1) = \frac{\lambda \sum m_j (e^{\beta\omega_j} - 1)}{e^{\beta\mu} - 1},$$

then

$$\frac{s_i}{c} = \frac{s_i (1 - e^{-\beta\mu})}{\lambda \sum m_j (e^{\beta\omega_j} - 1)}.$$

We would now like to re-sum the expression (6.6.7) over  $i$  under steady-state conditions,

$$S = \sum s_i = \sum \phi [n_i e^{\beta\omega_i} - (n_i + 1)] = \phi \sum m_i (e^{\beta\omega_i} - 1), \quad (6.6.12)$$

where the definition for the excess of quanta  $m_i$  is used. Referring to that equality, we write the previous equation as

$$\frac{s_i}{c} = \frac{s_i \phi}{S \lambda} (1 - e^{-\beta\mu}).$$

Returning to (6.6.9), we can write it in the form

$$n_i = \left[1 + \frac{s_i \phi}{S \lambda} (1 - e^{-\beta\mu})\right] \frac{1}{e^{\beta(\omega_i - \mu)} - 1}. \quad (6.6.13)$$

Summing  $n_i = n_i^T + m_i$  gives  $\sum n_i = N + N^T$ , where  $N = \sum m_i$  is the excess of quanta (mean number summed over the states) over its equilibrium value  $N^T = \sum n_i^T$ . Now we sum (6.6.13) using the inequalities  $s_i < S$  and  $\mu < \omega_0$ :

$$N + N^T \leq \left[ 1 + \frac{\phi}{\lambda} (1 - e^{-\beta\omega_0}) \right] \sum \frac{1}{e^{\beta(\omega_i - \mu)} - 1}. \quad (6.6.14)$$

It follows from the definition  $S$  (6.6.12) that

$$S = \phi \sum m_i (e^{\beta\omega_i} - 1) < \phi N (e^{\beta\omega_{\max}} - 1);$$

i.e., the mean number of quanta  $N$  must grow with pumping power  $S$ . However, by virtue of (6.6.14), this is only possible if  $\mu$  approaches  $\omega_0$ , since  $0 \leq \mu \leq \omega_0$ . Clearly, the population of the lowest state  $n_0 \sim [e^{\beta(\omega_0 - \mu)} - 1]^{-1}$  grows faster than that of others. It becomes very large, when pumping is fairly large, so that  $\mu \approx \omega_0$ . This implies that a process similar to Bose condensation takes place. A phase transition to a new state is here caused not by a temperature drop, but rather by an increase in energy flux through a system. The new state is a macroscopic synchronous oscillation of all the dipole moments with frequency  $\omega_0$ , a so-called coherent excitation. Fröhlich's analysis of Eqs. (6.6.8) is a piece of elegance and art of physical reasoning.

There is a correlation between Davydov's and Fröhlich's models. Tuszynski *et al.* (1984) have shown that initial Hamiltonians for both models can be reduced to the same form. The equations of motion for that general Hamiltonian admit, specifically, of two types of solutions that describe the localization of an excitation either in coordinate space — Davydov's model — or in quasi-momentum space — Fröhlich's model. It is assumed that these effects in complicated dipole systems could represent various aspects of one and the same phenomenon.

## 6.7 QUANTIZATION OF MAGNETIC FLUX AND JOSEPHSON EFFECTS

It is common knowledge that superconductors are absolute diamagnetics. A magnetic field does not penetrate a superconductor. Surface currents are organized so that they completely compensate for an MF within a superconductive area (Meissner effect). It is also known that charge carriers in a superconductor are electron pairs, with charge  $q = 2e$ , at the same quantum state. Therefore, a superconductor's state is described by a one-particle wave function that obeys Schrödinger's equation. These idealizations are justified theoretically and in many cases they find a convincing experimental support (White and Geballe, 1979). Using them, we can readily show that a magnetic flux confined to some superconductive doubly connected region can only assume a discrete set of values.

Let a superconductor have an arbitrary shape, e.g., that of a deformed ring, and let it be placed in an external DC MF  $\mathbf{H}$ . Consider the superconductor state

within a ring, where there is no MF. In that region  $\mathbf{H} = \nabla \times \mathbf{A} = 0$ ; i.e., a vector potential can be represented as the gradient of some scalar function  $w$ :

$$\mathbf{A} = \nabla w . \quad (6.7.1)$$

The Schrödinger equation for a one-particle state in an MF looks like

$$i\hbar\dot{\Psi} = \mathcal{H}\Psi , \quad \mathcal{H} = \frac{1}{2M} \left( \mathbf{P} - \frac{q}{c} \mathbf{A} \right)^2 + qA_0 .$$

The vector potential is defined up to gauge transformation. The transformation

$$\mathbf{A} \rightarrow \mathbf{A}' = \mathbf{A} + \nabla f , \quad A_0 \rightarrow A'_0 = A_0 - \dot{f}/c , \quad (6.7.2)$$

where  $f$  is a single-valued continuous function of coordinates and time, leaves the observables unchanged. The wave function can only change by a phase factor. The Schrödinger equation is invariant under simultaneous substitutions of (6.7.2) and

$$\Psi \rightarrow \Psi' = \Psi \exp \left( \frac{iq}{\hbar c} f \right) .$$

In fact, the transformation

$$\Psi \rightarrow \mathcal{A}\Psi , \quad \mathcal{H} \rightarrow \mathcal{A}\mathcal{H}\mathcal{A}^{-1} + i\hbar\dot{\mathcal{A}}\mathcal{A}^{-1}$$

leaves the equation unchanged. Let the operator  $\mathcal{A}$  be the phase shift operator  $\mathcal{A} = \exp(-i\alpha f)$ , where  $\alpha$  is a factor, and  $f$  is a single-valued differentiable function. It can easily be shown that the following operator equalities hold:

$$\begin{aligned} \left( \mathbf{P} - \frac{q}{c} \mathbf{A} \right) e^{i\alpha f} &= e^{i\alpha f} \left( \mathbf{P} - \frac{q}{c} \mathbf{A}' \right) , \\ \left( \mathbf{P} - \frac{q}{c} \mathbf{A} \right)^2 e^{i\alpha f} &= e^{i\alpha f} \left( \mathbf{P} - \frac{q}{c} \mathbf{A}' \right)^2 , \quad \mathbf{A}' = \mathbf{A} - \frac{c}{q} \alpha \hbar \nabla f . \end{aligned}$$

Using these equalities, we arrive at the transformed Hamiltonian:

$$\begin{aligned} \mathcal{A}\mathcal{H}\mathcal{A}^{-1} + i\hbar\dot{\mathcal{A}}\mathcal{A}^{-1} &= \frac{1}{2M} e^{-i\alpha f} \left( \mathbf{P} - \frac{q}{c} \mathbf{A} \right)^2 e^{i\alpha f} + qA_0 + \alpha \hbar \dot{f} \\ &= \frac{1}{2M} \left( \mathbf{P} - \frac{q}{c} \mathbf{A}' \right)^2 + qA'_0 , \quad A'_0 = A_0 + \frac{\alpha \hbar}{q} \dot{f} . \end{aligned}$$

$\alpha = -q/c\hbar$  gives the standard form of gauge transformation (6.7.2).

Putting  $f = -w$ , we reduce the Hamiltonian to the case  $\mathbf{A} = 0$ . Therefore, the Schrödinger equation has the form

$$\Psi = \Psi' \exp \left( \frac{iq}{\hbar c} w \right) = \Psi|_{\mathbf{A}=0} \exp \left( \frac{iq}{\hbar c} w \right) . \quad (6.7.3)$$

We now integrate  $\mathbf{H} = \nabla \times \mathbf{A}$  over a surface bounded by a contour  $L$  within a superconductor, Fig. 6.5, and reduce the result to a contour integral using the Stokes theorem:

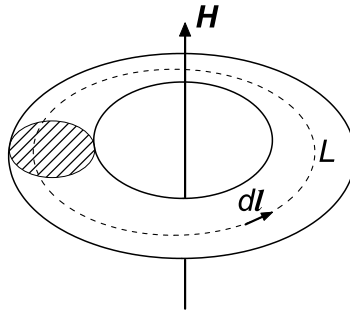


**Figure 6.5.** A superconductive ring in an MF  $\mathbf{H}$ . Shown is the integration contour  $L$  within the ring.

$$\Phi = \int \nabla \times \mathbf{A} ds = \oint \mathbf{A} dl = \oint \nabla w dl = \oint dw(l) = \Delta w . \quad (6.7.4)$$

The magnetic flux  $\Phi$  equals the increment of the function  $w$  in tracing the contour  $L$ . However, the wave function (6.7.3) being single-valued, i.e.,  $\Psi(l) = \Psi(l + L)$ , where  $L$  is the contour length, and since  $w(l + L) = w(l) + \Delta w$ , we obtain

$$\exp\left(\frac{iq\Delta w}{\hbar c}\right) = 1 .$$

That is,  $\Delta w q/\hbar c = 2\pi n$ . The magnetic flux through the contour  $L$  will thus be an integer number of quanta

$$\Phi_0 = 2\pi\hbar\frac{c}{q} = \frac{\hbar c}{2e} = 2.0679 \cdot 10^{-7} \text{ G}\cdot\text{cm}^2 .$$

This quantity is known as fluxoid.

Josephson (1962) showed that as electron pairs tunnel through a thin isolator or a weak current passes through a non-superconductive layer between two superconductors, no voltage occurs across the barrier. Also the phase jump of the wave function of paired electrons is dictated by the value of the current,

$$I = I_0 \sin \Delta\varphi , \quad (6.7.5)$$

which is the underlying idea of the *stationary* or DC Josephson effect. This underpins the workings of so-called SQUIDS, i.e., meters of hyperweak MFs.

It is seen from (6.7.3) that the scalar function  $w$  coincides up to a factor with the phase change of the wave function in the field of a vector potential within a superconductor:

$$\varphi = \frac{q}{\hbar c} w = \frac{2\pi}{\Phi_0} w . \quad (6.7.6)$$

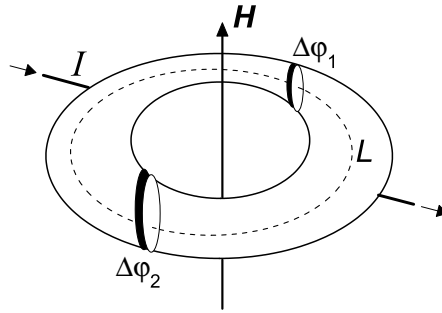


**Figure 6.6.** SQUID in an MF  $H$ . Across Josephson junctions the wave function of superconductive electrons exhibits phase jumps  $\Delta\varphi_1$  and  $\Delta\varphi_2$ .

We now would like to consider a device shown in Fig. 6.6: a ring composed of two superconductors separated by two Josephson junctions. The total current  $I$  through the SQUID is

$$I = I_0(\sin \Delta\varphi_1 + \sin \Delta\varphi_2) . \tag{6.7.7}$$

On the other hand, integrating  $w$  along the contour  $L$  now yields, in addition to the progression  $\Delta w = \Phi_0 n$ , considered above, additional phase shifts  $\Delta\varphi_1$  and  $\Delta\varphi_2$ , which have to be taken with signs corresponding to the tracing direction. Using (6.7.6), instead of (6.7.4), we write

$$\Phi = \Phi_0 n + \frac{\Phi_0}{2\pi}(\Delta\varphi_2 - \Delta\varphi_1) , \quad \text{or} \quad \Delta\varphi_2 - \Delta\varphi_1 = 2\pi \frac{\Phi}{\Phi_0} - 2\pi n .$$

Applying this to (6.7.7), we find that the current along the ring oscillates as the magnetic flux through the ring changes:

$$I \sim \cos \left( \pi \frac{\Phi}{\Phi_0} - \pi n \right) .$$

The separation between neighboring maxima of the function is  $2\Phi_0$ , which for a ring of area  $1 \text{ cm}^2$  defines an MF  $H \sim 4 \cdot 10^{-7} \text{ G}$ . The maximum location is generally measured to within 1–0.1%; therefore the minimal detectable MF is about  $10^{-9} \text{ G}$  or  $10^{-13} \text{ T}$ .<sup>38</sup>

If the current  $I$  in (6.7.5) exceeds a critical value  $I_0$ , a voltage is engendered across the junction. This is known as the *non-stationary* or AC Josephson effect. For a fixed potential difference  $V$  across the junction, the phase difference and current oscillate at frequency  $\omega = 2eV/\hbar$ . On passing through the junction, an electron pair loses the energy  $\hbar\omega = 2eV$ , which is emitted as an EMF quantum.

<sup>38</sup>SQUID magnetometers are sensitive to a magnetic field within  $10^{-9}$ – $10^{-10} \text{ GHz}^{-1/2}$ .

At laboratory voltages the radiation frequency falls within the microwave range; at 1 mV the frequency is 483.6 GHz.

The phenomena just considered are to a large measure conditioned by the fact that an MF does not penetrate a superconductor; consequently, the vector potential can be represented as the gradient of some function  $\mathbf{A} = \nabla w$  (6.7.1). That gives rise to interesting phase effects. There is another phenomenon, which is not connected with superconductivity — the Aharonov–Bohm effect (Aharonov and Bohm, 1959) — in which unusual phase relationships are dictated by the gradient representation of a vector potential. The Aharonov–Bohm effect consists of the motion variables of a charged quantum particle depending on the MF magnitude in the region where no particles can reside. At first sight, this is a paradox.

Let us consider the states of a quantum particle near a long solenoid with magnetic flux  $\Phi$ . One convenient idealization is that the solenoid is infinitely long and thin. The first assumption provides that an MF outside of the solenoid is zero, the second, that the probability for a particle to be within the solenoid, where there is the MF, is zero. If the solenoid is aligned along the  $z$  axis, the vector potential only has the  $\varphi$  component, since  $\mathbf{H} = \nabla \times \mathbf{A}$ . Thus since  $\oint \mathbf{A} \cdot d\mathbf{l} = A_\varphi 2\pi r = \Phi$ , the flux  $\Phi$  being finite, the vector potential will be

$$A_\varphi = \frac{\Phi}{2\pi r}$$

everywhere, except for the point  $r = 0$ . Let the particle motion be confined to the contour bounding the solenoid, e.g., a circumference of radius  $r$ . The Hamiltonian of the particle will then become

$$\mathcal{H} = \varepsilon_0 \left( -i \frac{\partial}{\partial \varphi} - \frac{\Phi}{\Phi_0} \right)^2, \quad \varepsilon_0 = \frac{\hbar^2}{2Mr^2}.$$

The eigenfunctions of the Hamiltonian are  $\sim \exp(im\varphi)$ , the eigenvalues of the component of the momentum operator along the motion path are  $m = 0, \pm 1, \dots$ , and hence the energy spectrum is

$$\varepsilon = \varepsilon_0 \left( m - \frac{\Phi}{\Phi_0} \right)^2.$$

It is readily seen that the spectrum depends on the MF flux within the solenoid. If the solenoid lies outside of the particle motion contour, then  $\Phi = 0$  and the spectrum assumes a form that is common for a rotator.

This dependence is no corollary of an overidealization of an infinitely long and thin solenoid and is general in nature (e.g., Skarzhinsky, 1985). The question of how a particle “feels” an MF where it never turns up has caused a multitude of publications of a metaphysical nature. What was discussed was in essence whether the EMF potentials are primary entities in relation to electric and magnetic fields. Owing to the gauge invariance of the dynamic equations for the observables, the potentials themselves are not observable. However, gauge invariant quantities associated with the potentials are observable. These are (1) local quantities, such as

strengths of EM fields, i.e., derivatives of the potentials, and (2) non-local quantities, such as integrals of the potentials along closed paths, which are dictated by the space–temporal distribution of EM fields. The former quantities determine local force actions on a particle; the latter, non-local non-force actions that are specific to quantum mechanics. One proof of the fact that non-local interactions are a real thing are the so-called quantum-mechanical paradoxes, e.g., the Einstein–Podolsky–Rosen paradox. One spectacular manifestation of non-local interactions are experiments on so-called quantum teleportation (Sudbery, 1997; Furusawa *et al.*, 1998).

The special role played by the vector potential in magnetobiology was discussed by Trukhanov (1975). An experimental scheme was proposed to observe the Aharonov–Bohm effect on a biological system that enveloped a toroidal solenoid with a magnetic field trapped inside. Note that, orthodoxically, the action of a solenoid’s vector potential on a biological system is only plausible where a quantum system — a target for an EMF — envelops the solenoid’s magnetic flux, i.e., is macroscopic. Throughout the book we only consider localized microscopic quantum targets for an MF. At physiological temperatures, the presence of macroscopic one-particle quantum states in biological systems is unlikely. That brings us back to the weakly justified idea of the so-called biological superconductivity. At the same time, there are experiments pointing to a long-range intercellular communication. It is quite likely that it can be described in terms of one-particle quantum states. Therefore, the experiment proposed in Trukhanov (1975) is still not without a heuristic meaning.

A simpler experiment to reveal the role of the vector potential relies on exposing a biological system to an inhomogeneous MF, e.g., to that of a current-carrying ring. Assuming the integration contour  $\mathbf{A}$  to be infinite and to include the ring axis, we can readily see that  $\mathbf{A} = 0$  throughout the ring axis. At the same time, an MF on the axis of a ring of radius  $R$  with current  $I$  is<sup>39</sup>

$$H = \frac{2\pi IR^2}{c(R^2 + h^2)^{3/2}},$$

where  $h$  is the distance from the ring plane. It follows that if an experiment reveals a specific dependence of an MBE on  $h$ , this is evidence that it is precisely the inhomogeneity of the vector potential (i.e., an MF), rather than its magnitude, that is detected by a biological system. Such assays are known. So, Blackman *et al.* (1994), and de Seze *et al.* (2000) placed organisms at various places along the axes of solenoid exposure systems and observed biological effects. At the same time, such experiments by no means prove that the magnitude of a vector potential cannot show up where it is distinct from zero (Baurov, 1993).

---

<sup>39</sup>A point magnetic moment  $\boldsymbol{\mu}$  produces at a distance  $r$  in a direction  $\mathbf{n}$  a vector potential  $\mathbf{A} = (\boldsymbol{\mu} \times \mathbf{n})/r^2$  and an MF  $[3\mathbf{n}(\boldsymbol{\mu} \cdot \mathbf{n}) - \boldsymbol{\mu}]/r^3$ .

## Bibliography

---

- Aarholt, E., Flinn, E., and Smith, C. (1982). Magnetic fields affect the lac operon system. *Phys. Med. Biol.* **27**(4), 606–610.
- Aarholt, E., Jaberansari, M., Jafary-Asl, A., Marsh, P., and Smith, C. (1988). NMR conditions and biological systems. In *Modern Bioelectricity* (A. Marino, Ed.), pp. 75–105. Marcel Dekker, New York.
- Able, K., and Able, M. (1995). Interactions in the flexible orientation system of a migratory bird. *Nature* **375**, 230–232.
- Achimowicz, J., Cader, A., Pannert, L., and Wojcik, E. (1979). Quantum cooperative mechanism of enzymatic activity. *Phys. Lett. A* **60**, 383–394.
- Achimowicz, J. (1982). Quantum solid state mechanisms of biological effects of electromagnetic radiation with emphasis on local superconductivity. *Radio Sci.* **17**(5S), 23S–27S.
- Adair, R. (1991). Constraints on biological effects of weak extremely low frequency electromagnetic fields. *Phys. Rev. A* **43**, 1039–1048.
- Adair, R. (1992). Criticism of Lednev's mechanism for the influence of weak magnetic fields on biological systems. *Bioelectromagnetics* **13**, 231–235.
- Adey, W., and Bowin, S. (1982). Binding and release of brain calcium by low-level electromagnetic fields: A review. *Radio Sci.* **17**(5S), 149S–157S.
- Adey, W., and Sheppard, A. (1987). Cell surface ionic phenomena in transmembrane signaling to intracellular enzyme systems. In *Mechanistic Approaches to Interactions of Electric and Electromagnetic Fields with Living Systems* (M. Blank, and E. Findl, Eds.), pp. 365–387. Plenum, New York.
- Adey, W. (1980). Frequency and power windowing in tissue interactions with weak electromagnetic fields. *Proc. IEEE* **68**(1), 119–125.
- Adey, W. (1988). Cell membranes: The electromagnetic environment and cancer promotion. *Neurochem. Res.* **13**(7), 671–677.
- Adey, W. (1992). Collective properties of cell membranes. In *Interaction Mechanisms of Low-Level Electromagnetic Fields in Living Systems* (B. Norden, and C. Ramel, Eds.), pp. 47–77. Oxford Univ. Press, Oxford.
- Adey, W. (1993). Biological effects of electromagnetic fields. *J. Cell Biochem.* **51**, 410–416.

- Adey, W. (Ed.) (1997). *Extremely-Low-Frequency Electric and Magnetic Fields*, Vol. 3 of *Reports of the NCRP Scientific Committee 89*. NCRP.
- Agadzhanyan, N., and Vlasova, I. (1992). Influence<sup>40</sup> of an infra-low-frequency magnetic field on the rhythm of nerve cells and their stability to hypoxia. *Biofizika* **37**(4), 681–689. [In Russian].
- Aharonov, Y., and Bohm, D. (1959). Significance of electromagnetic potentials in quantum theory. *Phys. Rev.* **115**, 485–491.
- Ahmed, N., Calderwood, J., Fröhlich, H., and Smith, C. (1975). Evidence for collective magnetic effects in an enzyme likelihood of room temperature superconductive regions. *Phys. Lett. A* **53**(2), 129–130.
- Aho, A.-C., Donner, K., Hyden, C., Larsen, L., and Reuter, T. (1988). Low retinal noise in animals with low body temperature allows high visual sensitivity. *Nature* **334**, 348–350.
- Akasofu, S.-I., and Chapman, S. (1972). *Solar-Terrestrial Physics*. Clarendon Press, Oxford.
- Akerstedt, T., Arnets, B., Ficca, G., and Paulsson, L.-E. (1997). Low frequency electromagnetic fields suppress SWS. *J. Sleep Res.* **26**, 260–266.
- Akhiezer, A., and Berestetskii, V. (1965). *Quantum Electrodynamics*, Vol. 11 of *Interscience Monographs and Texts in Physics and Astronomy*. Interscience, New York.
- Akhmanov, S., Diakov, Y., and Chirkin, A. (1981). *Introduction to Statistical Radio Wave Physics and Optics*. Nauka, Moscow. [In Russian].
- Akimenko, V., and Voznesenskii, S. (1997). Effect of CRT electrostatic fields on aeroion and radon decay products in air. In *Abst. First International Congress Weak and Hyperweak Fields and Radiations in Biology and Medicine*, pp. 221–222, St. Petersburg.
- Akimine, T., Muramatsu, H., Hamada, H., and Sakou, T. (1985). Effects of pulsed electromagnetic field on growth and differentiation of embryonal carcinoma cells. *J. Cell. Physiol.* **124**, 247–254.
- Akimov, A., Binhi, V., and Lazareva, N. (1998). Change in the biological activity of a liquid water by a TV set irradiation. *Soznanie Fiz. Realnost* **3**(1), 72–74.
- Akimov, A., Shipov, G., and Binhi, V. (1997). New approach to the problem of electromagnetobiology. In *Abst. 2 World Congress Elect. Magn. Biol. Med.*, pp. 185–186, Bologna, Italy. BEMS.
- Akimov, A., Tarasenko, V., and Shipov, G. (1995). Torsion fields as a cosmophysical factor. *Biofizika* **40**(4), 938–943.
- Aksenov, S. (1990). *Water in Regulation of Biological Processes*. Nauka, Moscow. [In Russian].
- Aldrich, T., Laborde, D., and Griffith, J. (1992). A meta-analysis of the epidemiological evidence regarding human health risk associated with exposure to electromagnetic fields. *Electro Magnetobiol.* **11**(2), 127–143.

---

<sup>40</sup>The titles of Russian books and papers in Russian and Ukrainian journals, such as *Biofizika*, *Usp. Fiz. Nauk SSSR*, and *Ukr Fiz. Zh.*, have been translated in English for convenience.

- Alexander, M. (1996). Effect of VHF and high-amplitude alternating EMF on the growth of bacteria *Xanthomonas campestris*. *Electro Magnetobiol.* **15**(1), 57–62.
- Alexandrov, V. (1995). Electro-kinetic fields of aquatic organisms. biorhythms of locomotive activity. relation to geomagnetism. *Biofizika* **40**(4), 771–777.
- Alexandrov, Y., Khvostenko, G., and Chaika, M. (1991). *Interference of Atomic States*. Nauka, Moscow. [In Russian].
- Alipov, Y., Belyaev, I., and Aizenberg, O. (1994). Systemic reaction of *Escherichia coli* cells to weak electromagnetic fields of extremely low frequency. *Bioelectroch. Bioener.* **34**, 5–12.
- Alipov, Y., and Belyaev, I. (1996). Difference in frequency spectrum of extremely-low-frequency effects on the genom's conformal state of AB1157 and EMG2 *E. coli* cells. *Bioelectromagnetics* **17**, 384–387.
- Andreeva, L., Bakaneva, V., Grigorenko, Y., and Kondrashova, M. (1989). Negatively charged hydroaeroions effect on electromechanical properties of the *Rana Ridibunda* ear. *Biofizika* **34**, 306.
- Andreev, E., Belyi, M., and Sitko, S. (1985). Human response to mm-band irradiation. *Vestnik AN SSSR* (1), 24–33.
- Andryushechkin, B., Eltsov, K., Shevlyuga, V., and Yurov, V. (1998). Atomic structure of saturated chlorine monolayer on Ag(111) surface. *Surf. Sci.* **407**, L633–L639.
- Antonchenko, V. Y., Davydov, A., and Iliin, V. (1991). *Principal Physics of Water*. Naukova Dumka, Kiev. [In Russian].
- APS Statement (1995). Statement on power line fields and public health. Available at <http://www.aps.org/statements/95.2.html>.
- Arber, S. (1985). Microwave enhancement of membrane conductance: Calmodulin hypothesis. *Physiol. Chem. Phys. Med. NMR* **17**, 227–233.
- Asashima, M., Shimada, K., and Pfeiffer, C. (1991). Magnetic shielding induces early developmental abnormalities in the Newt, *Cynops pyrrhogaster*. *Bioelectromagnetics* **12**, 215–224.
- Ashcroft, N., and Mermin, N. (1976). *Solid State Physics*. Holt, Rinehart and Winston, New York.
- Ashkaliev, Y., Drobzhev, V., Somsikov, V., and Turkeeva, B. (1995). Effect of heliogeophysical factors on ecological conditions. *Biofizika* **40**(5), 1031–1037.
- Astumian, R., Weaver, J., and Adair, R. (1995). Rectification and signal averaging of weak electric fields by biological cells. *Proc. Natl. Acad. Sci. USA* **92**, 3740–3743.
- Ayrapetyan, S., Grigorian, K., Avanesyan, A., and Stamboltsian, K. (1994). Magnetic fields alter electrical properties of solutions and their physiological effects. *Bioelectromagnetics* **15**, 133–142.
- Babu, Y., Bugg, C., and Cook, W. (1988). Structure of calmodulin refined at 2.2 Å resolution. *J. Mol. Biol.* **204**(1), 191–204.
- Ball, P. (1993). New horizons in inner space. *Nature* **361**, 297.

- Bannikov, V., Bezruchko, S., Grishankova, Y., Kuzmin, S., Mityagin, Y., Orlov, R., Rozhkov, S., and Sokolina, V. (1980). The Raman scattering study in *B. megaterium* bacteria. *Dokl. Acad. Nauk SSSR* **253**(2), 479–480.
- Bannikov, V., and Ryzhov, S. (1980). Resonance absorption of millimeter waves by *E. coli* K-12( $\lambda$ ) bacterial cells. *Dokl. Acad. Nauk SSSR* **255**(3), 746–748.
- Barnes, F. (1998). A model for detection of weak ELF electric and magnetic fields. *Bioelectroch. Bioener.* **47**, 207–212.
- Barnothy, J. (1956). Influence of a magnetic field upon the leukocytes of the mouse. *Nature* **177**, 577–578.
- Bassett, C. (1984). The development and application of pulsed electromagnetic fields (pemfs) for ununited fractures and arthrodeses. *Orthop. Clin. N. Am.* **15**(1), 61–87.
- Bastian, J. (1994). Electrosensory organisms. *Phys. Today* **47**(2), 30–37.
- Bates, D. (1994). *Environmental Health Risks and Public Policy: Decision-Making in Free Societies*. Univ. of Washington Press, Seattle.
- Baumgartner, C., Deecke, L., Stroink, G., and Williamson, S. (Eds.) (1995). *Bio-magnetism: Fundamental Research and Clinical Applications*, Vol. 7 of *Studies in Applied Electromagnetics and Mechanics*. IOS Press, Amsterdam.
- Baurov, Y. (1993). Space magnetic anisotropy and a new interaction in nature. *Phys. Lett. A* **181**(4), 283.
- Bawin, S., Adey, W., and Sabbot, I. (1978). Ionic factors in release of  $^{45}\text{Ca}^{2+}$  from chicken cerebral tissue by electromagnetic fields. *Proc. Natl. Acad. Sci. USA* **75**, 6314–6318.
- Bawin, S., and Adey, W. (1976). Sensitivity of calcium binding in cerebral tissue to weak environmental electric fields oscillating at low frequency. *Proc. Natl. Acad. Sci. USA* **73**, 1999–2003.
- Bawin, S., Kazmarek, L., and Adey, W. (1975). Effects of modulated VHF fields on the central nervous system. *Ann. NY Acad. Sci.* **247**, 74–81.
- Beason, R., and Brennan, W. (1986). Natural and induced magnetization in the bobolink (Icteridae: *Dolichonyx oryzivorus*). *J. Exp. Biol.* **125**, 49–56.
- Beason, R. (1989). Use of an inclination compass during migratory orientation by the bobolink (*Dolichonyx oryzivorus*). *Ethology* **81**, 291–299.
- Becker, G. (1965). Zur magnetfeld-orientierung von dipteren. *Z. Vgl. Physiol.* **51**(2), 135.
- Beischer, D. (1965). Biomagnetics. *Ann. NY Acad. Sci.* **134**(1), 454.
- Beischer, D. (1971). The null magnetic field as reference for the study of geomagnetic directional effects in animals and man. *Ann. NY Acad. Sci.* **188**, 324–330.
- Belch, A., and Rice, S. (1987). The distribution of rings of hydrogen-bonded molecules in a model of liquid water. *J. Chem. Phys.* **86**(10), 5676–5682.
- Belisheva, N., Popov, A., Petukhova, N., Pavlova, L., Osipov, K., Tkachenko, S., and Baranova, T. (1995). Effect of geomagnetic field variations on the human brain functional status: qualitative and quantitative estimations. *Biofizika* **40**(5), 1005–1012.

- Belousov, A., Kovarskii, V., Merlin, Y., and Yastrebov, B. (1993). Enzyme reactions in external magnetic fields. *Biofizika* **38**(4), 619–626.
- Belov, A., Konyukhov, V., Logvinenko, V., and Tikhonov, V. (1996). Determination of permittivity of spin-modified water. *Bull. Lebedev Phys. Inst., Allerton Press, New York* (3), 38–42.
- Belov, A., Konyukhov, V., and Stepanov, A. (1997). Permittivity fluctuations in water at thermal and mechanical perturbations. *Bull. Lebedev Phys. Inst., Allerton Press, New York* (7–8), 74–80.
- Belyaev, I., Alipov, Y., and Harms-Ringdahl, M. (1997). Effects of zero magnetic field on the conformation of chromatin in human cells. *Biochim. Biophys. Acta* **1336**, 465–473.
- Belyaev, I., Alipov, Y., Matronchik, A., and Radko, S. (1995). Cooperativity in E.coli cell response to resonance effect of weak extremely low frequency electromagnetic field. *Bioelectroch. Bioener.* **37**, 85–90.
- Belyaev, I., Alipov, Y., Polunin, V., and Shcheglov, V. (1993). Evidence for dependence of resonant frequency of millimeter wave interaction with Escherichia coli K12 cells on haploid genome length. *Electro Magnetobiol.* **12**(1), 39–49.
- Belyaev, I., Matronchik, A., and Alipov, Y. (1994). The effect of weak static and alternating magnetic fields on the genome conformational state of E.coli cells: The evidence for model of phase modulation of high frequency oscillations. In *Charge and Field Effects in Biosystems - 4* (M. Allen, Ed.), pp. 174–184. World Scientific, Singapore.
- Belyaev, I., Shcheglov, V., Alipov, Y., and Polunin, V. (1996). Resonance effect of millimeter waves in the power range from  $10^{-19}$  to  $3 \times 10^{-3}$  W/cm<sup>2</sup> on Escherichia coli cells at different concentrations. *Bioelectromagnetics* **17**, 312–321.
- Belyaev, I., Shcheglov, V., Alipov, Y., and Ushakov, V. (2000). Nonthermal effects of extremely high-frequency microwaves on chromatin conformation in cells *in vitro* — dependence on physical, physiological, and genetic factors. *IEEE Trans. Microwave Theory* **48**(11), 2172–2179.
- Belyavskaya, N., Fomicheva, V., Govorun, R., and Danilov, V. (1992). Structure and functional organization of meristematic cells of pease, lentil, and flax roots at geomagnetic field shielding. *Biofizika* **37**(4), 759–768.
- Benninghoff, W., and Benninghoff, A. (1982). Airborne biological particles and electric fields. *Radio Sci.* **17**(5S), 13S–15S.
- Benzi, R., Sutera, A., and Vulpiani, A. (1981). The mechanism of stochastic resonance. *J. Phys. A* **14**, L453–L457.
- Berden, M., Jerman, I., and Škarja, M. (1997). Indirect instrumental detection of ultraweak, presumably electromagnetic radiation from organisms. *Electro Magnetobiol.* **16**(3), 249–266.
- Berestetskii, V., Lifshitz, E., and Pitaevskii, L. (1982). *Quantum Electrodynamics*, second ed. Pergamon, Oxford.

- Berezhinsky, L., Gridina, N., Dovbeshko, G., Lisitsa, M., and Litvinov, G. (1993). Visualization of the effect of mm wavelengths on blood plasma. *Biofizika* **38**(2), 378–384.
- Bergethon, P. (1998). *The Physical Basis of Biochemistry: The Foundations of Molecular Biophysics*. Springer-Verlag, New York.
- Berg, H., and Zhang, L. (1993). Electrostimulation in cell biology by low-frequency electromagnetic fields. *Electro Magnetobiol.* **12**(2), 147–163.
- Berg, H. (1993). Electrostimulation of cell metabolism by low-frequency electric and electromagnetic fields. *Bioelectroch. Bioener.* **31**, 1–25.
- Berg, H. (1995). Possibilities and problems of low frequency weak electromagnetic fields in cell biology. *Bioelectroch. Bioener.* **38**, 153–159.
- Berk, S., Srikanth, S., Mahajan, S., and Ventrice, C. (1997). Static uniform magnetic fields and amoebae. *Bioelectromagnetics* **18**, 81–84.
- Berman, E., Chacon, L., House, D., Koch, B., Koch, W., Leal, J., Løvtrup, S., Mantiply, E., Martin, A., Martucci, G., Mild, K., Monahan, J., Sandström, M., Shamsaifar, K., Tell, R., Trillo, M., Ubeda, A., and Wagner, P. (1990). Development of chicken embryos in a pulsed magnetic field. *Bioelectromagnetics* **11**, 169–187.
- Bernal, J., and Fowler, R. (1933). A theory of water and ionic solution, with particular reference to hydrogen and hydroxyl ions. *J. Chem. Phys.* **1**(8), 515–548.
- Bersani, F., Marinelli, F., Ognibene, A., Matteucci, A., Cecchi, S., Santi, S., Squarzone, S., and Maraldi, N. (1997). Intramembrane protein distribution in cell cultures is affected by 50 Hz pulsed magnetic fields. *Bioelectromagnetics* **18**(7), 463–469.
- Bersani, F. (Ed.) (1999). *Electricity and Magnetism in Biology and Medicine*. Kluwer/Plenum, London.
- Berzhanskaya, L. Y., Berzhanskii, V., Beloplotova, O., Pilnikova, T., and Metlyaev, T. (1995). Bioluminescent activity of bacteria as an indicator of geomagnetic perturbations. *Biofizika* **40**(4), 778–781.
- Beschkov, V., and Peeva, L. (1994). Effects of electric current passing through the fermentation broth of a strain *Acetobacter suboxydans*. *Bioelectroch. Bioener.* **34**, 185–188.
- Bethune, D., Johnson, R., Salem, J., M.S. de V., and Yannoni, C. (1993). Atoms in carbon cages: The structure and properties of endohedral fullerenes. *Nature* **366**, 123–128.
- Betskii, O., Devyatkov, N., and Kislov, V. (1998). Low intensity millimeter waves in medicine and biology. *Biomed. Radioelektron.* (4), 13–29.
- Betskii, O. (1994). Electromagnetic millimeter waves and living organisms. In *Biological Aspects of Low Intensity Millimeter Waves* (N. Devyatkov, and O. Betskii, Eds.), pp. 8–38. Seven Plus, Moscow.
- Bezrukov, S., and Vodyanoy, I. (1997a). Stochastic resonance at the single-cell level. *Nature* **388**, 632–633.

- Bezrukov, S., and Vodyanoy, I. (1997b). Stochastic resonance in non-dynamical systems without response thresholds. *Nature* **385**, 319–321.
- Bingman, V. (1983). Magnetic field orientation of migratory savannah sparrows with different first summer experience. *Behaviour* **87**, 43–53.
- Binhi, V., Alipov, Y., and Belyaev, I. (2001). Effect of static magnetic field on E. coli cells and individual rotations of ion-protein complexes. *Bioelectromagnetics* **22**(2), 79–86.
- Binhi, V., and Goldman, R. (2000). Ion-protein dissociation predicts “windows” in electric field-induced wound-cell proliferation. *Biochim. Biophys. Acta* **1474**(2), 147–156.
- Binhi, V. (1990a). Metastable states of water: Quantum mechanisms. Dep.VINITI, N5743-B90, Moscow. [In Russian].
- Binhi, V. (1990b). Proton dynamics in one-dimensional special potential. Interpretation of “magnetic” effects in water and ice. In *Relaxation Processes and Phenomena in Active Media*, pp. 74–85. State Inst. Phys. Tech. Problems, Moscow. [In Russian].
- Binhi, V. (1991a). “Current” states of the proton in water. *Zh. Fiz. Khim.* **65**(7), 2002–2008.
- Binhi, V. (1991b). Induction of water metastable states. Preprint No.3, CISE VENT, Moscow. [In Russian].
- Binhi, V. (1992). Biomagnetic correlations and the hypothesis of current states of a proton in water. *Biofizika* **37**(3), 596–600.
- Binhi, V. (1995a). Can aqueous solutions possess macroscopic quantum properties? In *Abst. 2 Int. Symp. “Mechanisms of Ultra-low Dose Effects”*, p. 87, Moscow. Inst. Biochem. Phys. [In Russian].
- Binhi, V. (1995b). Nuclear spins in primary mechanisms of biomagnetic effects. *Biofizika* **40**(3), 677–691.
- Binhi, V. (1995c). On the ion channel — magnetic coil model. *Biofizika* **40**(3), 561–562.
- Binhi, V. (1996). Spin mechanisms of biological effects of weak magnetic fields. In *Abst. 4 Int. Symp. “Relation of Biol. and Physicochem. Processes with Space and Helio-geophys. Factors”*, pp. 124–125, Pushchino. Inst. Theor. Exp. Biophys. [In Russian].
- Binhi, V. (1997a). A formula for frequency and amplitude windows of some ELF and null MF bioeffects follows from the Schrödinger equation. In *Abst. 2 World Congress Elect. Magn. Biol. Med.*, pp. 184–185, Bologna, Italy. BEMS.
- Binhi, V. (1997b). Interference of ion quantum states within a protein explains weak magnetic field’s effect on biosystems. *Electro Magnetobiol.* **16**(3), 203–214.
- Binhi, V. (1997c). The mechanism of magnetosensitive binding of ions by some proteins. *Biofizika* **42**(2), 338–342.
- Binhi, V. (1997d). Shift of spectral peaks of some magnetobiological effects under rotation of biological sample in ELF magnetic field. In *The 1997 Annual Review of Research on Biol. Effects of Elect. Magn. Fields, San Diego, California*, p. 78, Frederick MD. BEMS, W/L Associates.

- Binhi, V. (1998a). Interference mechanism for some biological effects of pulsed magnetic fields. *Bioelectroch. Bioener.* **45**(1), 73–81.
- Binhi, V. (1998b). On structural defects of liquid water in magnetic and electric fields. *Biomed. Radioelektron.* (2), 7–16.
- Binhi, V. (1999a). An analytical survey of theoretical studies in the area of magnetoreception. In *Electromagnetic Fields: Biological Effects and Hygienic Standardization* (M. Repacholi, N. Rubtsova, and A. Muc, Eds.), pp. 155–170. World Health Organization, Geneva, Switzerland.
- Binhi, V. (1999b). A formula for frequency and amplitude windows of some ELF and null MF bioeffects follows from the Schrödinger equation. In *Electricity and Magnetism in Biology and Medicine* (F. Bersani, Ed.), pp. 417–421. Kluwer/Plenum, London.
- Binhi, V. (1999c). Ion interference mechanism for biological effects of the amplitude modulated microwaves. In *Abst. 21 BEMS Meeting*, pp. 216–217, Long Beach, California. BEMS.
- Binhi, V. (2000). Amplitude and frequency dissociation spectra of ion-protein complexes rotating in magnetic fields. *Bioelectromagnetics* **21**(1), 34–45.
- Binhi, V. (2001). Theoretical concepts in magnetobiology. *Electro Magnetobiol.* **20**(1), 47–62.
- Blackman, C., Benane, S., Blanchard, J., and House, D. (1997). PC-12 cell response to parallel AC and DC magnetic fields tuned for calcium ions. In *Abst. 2 World Congress Elect. Magn. Biol. Med.*, p. 151, Bologna, Italy. BEMS.
- Blackman, C., Benane, S., Elliott, D., Wood, A., House, D., and Pollock, M. (1988). Influence of electromagnetic fields on the efflux of calcium ions from brain tissue in vitro: A three-model analysis consistent with the frequency response up to 510 Hz. *Bioelectromagnetics* **9**, 215–227.
- Blackman, C., Benane, S., House, D., and Elliott, D. (1990). Importance of alignment between local DC magnetic field and an oscillating magnetic field in responses of brain tissue in vitro and in vivo. *Bioelectromagnetics* **11**, 159–167.
- Blackman, C., Benane, S., and House, D. (1991). The influence of temperature during electric- and magnetic-field-induced alteration of calcium-ion release from in vitro brain tissue. *Bioelectromagnetics* **12**, 173–182.
- Blackman, C., Benane, S., and House, D. (1993). Evidence for direct effect of magnetic fields on neurite outgrowth. *FASEB J.* **7**, 801–806.
- Blackman, C., Benane, S., and House, D. (1995a). Frequency-dependent interference by magnetic fields of nerve growth factor-induced neurite outgrowth in PC-12 cells. *Bioelectromagnetics* **16**, 387–395.
- Blackman, C., Benane, S., and House, D. (2001). The influence of 1.2  $\mu$ T, 60 Hz magnetic fields on melatonin- and tamoxifen-induced inhibition of MCF-7 cell growth. *Bioelectromagnetics* **22**(2), 122–128.
- Blackman, C., Benane, S., Rabinowitz, J., House, D., and Joines, W. (1985). A role for the magnetic field in the radiation-induced efflux of calcium ions from brain tissue in vitro. *Bioelectromagnetics* **6**, 327–337.

- Blackman, C., Blanchard, J., Benane, S., and House, D. (1994). Empirical test of an ion parametric resonance model for magnetic field interactions with PC-12 cells. *Bioelectromagnetics* **15**, 239–260.
- Blackman, C., Blanchard, J., Benane, S., and House, D. (1995b). The ion parametric resonance model predicts magnetic field parameters that affect nerve cells. *FASEB J.* **9**, 547–551.
- Blackman, C., Blanchard, J., Benane, S., and House, D. (1996). Effect of AC and DC magnetic field orientation on nerve cells. *Biochem. Biophys. Res. Co.* **220**, 807–811.
- Blackman, C., Blanchard, J., Benane, S., and House, D. (1999). Experimental determination of hydrogen bandwidth for the Ion Parametric Resonance model. *Bioelectromagnetics* **20**(1), 5–12.
- Blackman, C., Elder, J., Weil, C., Benane, S., Eichinger, D., and House, D. (1979). Induction of calcium ion efflux from brain tissue by radio frequency radiation. *Radio Sci.* **14**, 93–98.
- Blakemore, R. (1975). Magnetotactic bacteria. *Science* **190**(4212), 377–379.
- Blanchard, J., and Blackman, C. (1994). Clarification and application of an ion parametric resonance model for magnetic field interactions with biological systems. *Bioelectromagnetics* **15**, 217–238.
- Blanchard, J., House, D., and Blackman, C. (1995). Evaluation of whole-animal data using the ion parametric resonance model. *Bioelectromagnetics* **16**, 211–215.
- Blank, M., and Goodman, R. (1997). Do electromagnetic fields interact directly with DNA? *Bioelectromagnetics* **18**, 111–115.
- Blank, M., Soo, L., Lin, H., Henderson, A., and Goodman, R. (1992). Changes in transcription in HL-60 cells following exposure to alternating currents from electric fields. *Bioelectroch. Bioener.* **28**, 301–309.
- Blank, M., and Soo, L. (1990). Ion activation of the Na,K-ATPase in alternating currents. *Bioelectroch. Bioener.* **24**, 51–61.
- Blank, M., and Soo, L. (1996). The threshold for Na,K-ATPase stimulation by electromagnetic fields. *Bioelectroch. Bioener.* **40**, 63–65.
- Blank, M., and Soo, L. (1998). Frequency dependence of cytochrome oxidase activity in magnetic fields. *Bioelectroch. Bioener.* **46**, 139–143.
- Blank, M. (Ed.) (1995). *Electromagnetic fields: Biological Interactions and Mechanisms*. Advances in Chemistry – 250. Am. Chem. Soc., Washington, DC.
- Blinowska, K., Lech, W., and Wittlin, A. (1985). Cell membrane as a possible site of Fröhlich's coherent oscillations. *Phys. Lett. A* **109**(3), 124–126.
- Blokhintsev, D. (1983). *Fundamentals of Quantum Mechanics*. Nauka, Moscow. [In Russian].
- Bohr, H., Brunak, S., , and Bohr, J. (1997). Molecular wring resonances in chain molecules. *Bioelectromagnetics* **18**, 187–189.
- Bookman, M. (1977). Sensitivity of the homing pigeon to an Earth-strength magnetic field. *Nature* **267**, 340–342.

- Boorman, G., McCormick, D., Ward, J., Haseman, J., and Sills, R. (2000). Magnetic fields and mammary cancer in rodents: A critical review and evaluation of published literature. *Radiat. Res.* **153**, 617–626.
- Bowman, J., Thomas, D., London, S., and Peters, J. (1995). Hypothesis: The risk of childhood leukemia is related to combinations of power-frequency and static magnetic fields. *Bioelectromagnetics* **16**, 48–59.
- Brawn, G., and Iliinsky, O. (1984). *Physiology of Electrorceptors*. Nauka, Leningrad. [In Russian].
- Breus, T., Halberg, F., and Kornelissen, J. (1995). Solar activity impact on physiological rhythms of biological systems. *Biofizika* **40**(4), 737–748.
- Brocklehurst, B., and McLauchlan, K. A. (1996). Free radical mechanism for the effects of environmental electromagnetic fields on biological systems. *Int. J. Radiat. Biol.* **69**(1), 3–24.
- Broers, D., Kraepelin, G., Lamprecht, I., and Schulz, O. (1992). *Mycotypha africana* in low-level athermic elf magnetic fields. *Bioelectroch. Bioener.* **27**, 281–291.
- Buchachenko, A., Sagdeev, R., and Salikhov, K. (1978). *Magnetic and Spin Effects in Chemical Reactions*. Nauka, Novosibirsk. [In Russian].
- Burlakova, E. (1994). Effect of extremely small additions. *Vestn. Ross. Akad. Nauk. Ser. Biol.* **64**(5), 425–431.
- Busby, D. (1968). Space biomagnetics. *Space Life Sci.* **1**(1), 23–63.
- Butlerov, A. (1882). *Antimaterialism in Science. Neural Analysis by Ieger and Homeopathy — by Non-homeopath*. Suvorin, St. Petersburg. [In Russian].
- Byus, C., Kartun, K., Pieper, S., and Adey, W. (1988). Increased ornithine decarboxylase activity in cultured cells exposed to low energy modulated microwave fields and phorbol ester tumor promoters. *Cancer Res.* **48**, 4222–4226.
- Byus, C., Lundak, R., Fletcher, R., and Adey, W. (1984). Alterations in protein kinase activity following exposure of cultured lymphocytes to modulated microwave fields. *Bioelectromagnetics* **5**, 34–51.
- Careri, G., Buontempo, U., Galluzzi, F., Scott, A., Gratton, E., and Shyamsunder, E. (1984). Spectroscopic evidence for Davydov-like solitons in acetanilide. *Phys. Rev. B* **30**(8), 4689–4702.
- Carlo, G. (Ed.) (2000). *Wireless Phones and Health II. State of the Science*. Kluwer/Plenum, New York.
- Carpenter, D., and Ayrapetyan, S. (Eds.) (1994). *Biological Effects of Electric and Magnetic Fields: Sources and Mechanisms*, Vol. 1. Academic Press, New York.
- Cavopoli, A., Wamil, A., Holcomb, R., and McLean, M. (1995). Measurement and analysis of static magnetic fields that block action potentials in cultured neurons. *Bioelectromagnetics* **16**, 197–206.
- Cheng, K., and Goldman, R. (1998). Electric fields and proliferation in a dermal wound model: Cell cycle kinetics. *Bioelectromagnetics* **19**, 68–74.
- Chernavsky, D., and Khurgin, Y. (1989). Physical mechanisms responsible for the interaction of protein macromolecules with RF radiation. In *Millimeter Waves in Medicine and Biology* (N. Devyatkov, Ed.), pp. 227–235. Institute of Radio

- Engineering and Electronics, USSR Academy of Sciences, Moscow. [In Russian].
- Chernavsky, D. (1973). Scientific session of the Department of general physics and astronomy of the Soviet Academy of Sciences. *Usp. Fiz. Nauk* **110**(3), 469.
- Chetaev, D., and Yudovich, V. (1970). Directional analysis of magnetotelluric observations. *Izv. Akad. Nauk SSSR, Geofiz.* (12), 61.
- Chew, G., and Brown, G. (1989). Orientation of rainbow trout (*Salmo gairdneri*) in normal and null magnetic fields. *Can. J. Zool.* **67**, 641–643.
- Chew, W. (1984). Dielectric enhancement and electrophoresis due to an electrochemical double layer: A uniform approximation. *J. Chem. Phys.* **80**(9), 4541–4552.
- Chiabrera, A., Bianco, B., Caratozzolo, F., Giannetti, G., Grattarola, M., and Viviani, R. (1985). Electric and magnetic field effects on ligand binding to the cell membrane. In *Interaction Between Electromagnetic Fields and Cells* (A. Chiabrera, C. Nicolini, and H. Schwan, Eds.), pp. 253–280. Plenum, New York.
- Chiabrera, A., Bianco, B., Kaufman, J., and Pilla, A. (1991). 1. Quantum dynamics of ions in molecular crevices under electromagnetic exposure. 2. Quantum analysis of ion binding kinetics in electromagnetic bioeffects. In *Electromagnetics in Medicine and Biology* (C. Brighton, and S. Pollack, Eds.), pp. 21–26; 27–31. San Francisco Press, San Francisco.
- Chiabrera, A., and Bianco, B. (1987). The role of the magnetic field in the em interaction with ligand binding. In *Mechanistic Approaches to Interactions of Electric and Electromagnetic Fields with Living Systems* (M. Blank, and E. Findl, Eds.), pp. 79–95. Plenum, New York.
- Chiabrera, A., Grattarola, M., and Viviany, R. (1984). Interaction between electromagnetic fields and cells: Microelectrophoretic effect of ligands and surface receptors. *Bioelectromagnetics* **5**, 173.
- Chibrikin, V., Kashinskaya, I., and Udalltsova, N. (1995a). Social processes and geomagnetic activity. 2. Geomagnetic response in money emissions. *Biofizika* **40**(5), 1054–1059.
- Chibrikin, V., Samovichev, E., Kashinskaya, I., and Udalltsova, N. (1995b). Social processes and geomagnetic activity. 1. Periodic component in the Moscow total criminal record. *Biofizika* **40**(5), 1050–1053.
- Chizhevskii, A. (1976). *The Earth Echo of Solar Storms*. Mysl, Moscow. [In Russian].
- Cho, M., Thatte, H., Lee, R., and Golan, D. (1996). Reorganization of microfilament structure induced by ac electric fields. *FASEB J.* **10**, 1552–1558.
- Coghill, R. (1996). Low frequency electric and magnetic fields at the beds of children with leukemia. *Biofizika* **41**(4), 798–806.
- Colic, M., and Morse, D. (1998). Mechanism of the long-term effects of electromagnetic radiation on solutions and suspended colloids. *Langmuir* **14**(4), 783–787.
- Collett, T., and Baron, J. (1994). Biological compasses and the coordinate frame of landmark memories in honeybees. *Nature* **368**, 137–140.

- Congress EMBM (1997). *Abst. 2 World Congress for Electricity and Magnetism in Biology and Medicine, Bologna, Italy*, Frederick MD. BEMS, W/L Associates. Pages 47, 57, 62, 87, 112, 134, 171, 174, 199, 203, 204, 209, 221, 228, 231, 232, 256, 268, 299, 301, 302, 303, 304, 306, 319, 322.
- Congress WRBM (1997). *Abst. 1 Int. Congress Weak Hyperweak Fields Radiat. Biol. Med.*, St. Petersburg, Russia. Inst. Analyt. Instr. Industry.
- Conley, C. (1969). Effect of near-zero-magnetic field upon biological systems. In *Biological Effects of Magnetic Fields* (M. Barnothy, Ed.), Vol. 2, p. 29. Plenum, New York.
- Conti, P., Gigante, G., Alesse, E., Cifonte, M., Fieschi, C., Reale, M., and Angeletti, P. (1985). A role for  $\text{Ca}^{2+}$  in the effect of very low frequency electromagnetic field on blastogenesis of human lymphocytes. *FEBS Lett.* **181**, 28–32.
- Conti, R., Caracciolo, L., and Sartore, L. (1997). Residential exposure to power frequency electric and magnetic fields generated by italian electrical system components. In *Abst. 2 World Congress Elect. Magn. Biol. Med.*, p. 181, Bologna, Italy. BEMS.
- Cook, D., Ma, D., Pon, N., and Hearst, J. (1992). Dynamics of DNA supercoiling by transcription in *Escherichia coli*. *Proc. Natl. Acad. Sci. USA* **89**, 10,603–10,607.
- Cope, F. (1973). Biological sensitivity to weak magnetic fields due to biological superconductive Josephson junctions. *Physiol. Chem. Phys.* **5**, 173–176.
- Cope, F. (1981). On the relativity and uncertainty of electromagnetic energy measurement at a superconductive boundary: application to perception of weak magnetic fields by living systems. *Physiol. Chem. Phys.* **13**, 231–239.
- Costato, M., Milani, M., and Spinoglio, L. (1996). Quantum mechanics: A breakthrough into biological system dynamics. *Bioelectroch. Bioener.* **41**, 27–30.
- Coulton, L., and Barker, A. (1993). Magnetic fields and intercellular calcium: Effects on lymphocytes exposed to conditions for “cyclotron resonance”. *Phys. Med. Biol.* **38**, 347–360.
- Cramer, H. (1946). *Mathematical Methods of Statistics*. Princeton Univ. Press, Princeton, NJ.
- Cremer-Bartels, G., Krause, K., Mitoskas, G., and Brodersen, D. (1984). Magnetic field of the Earth as additional zeitgeber for endogenous rhythms. *Naturwissenschaften* **71**, 567–574.
- Crommie, M., Lutz, C., and Eigler, D. (1993a). Confinement of electrons to quantum corrals on a metal surface. *Science* **262**, 218–220.
- Crommie, M., Lutz, C., and Eigler, D. (1993b). Imaging standing waves in a two-dimensional electron gas. *Nature* **363**, 524–527.
- Cruseiro, L., Halding, J., Christiansen, P., Skovguard, O., and Scott, A. (1988). Temperature effects on the Davydov soliton. *Phys. Rev. A* **37**(3), 880–887.
- Daniel, H., and Adibi, S. (1995). Selective effect of zinc on uphill transport of oligopeptides into kidney brush border membrane vesicles. *FASEB J.* **9**, 1112–1117.

- Davis, A., and Rawls, W. (1987). The effects of the two poles on the living system. In *Magnetism and Its Effects on the Living System*, pp. 25–33. Exposition Press, Smithtown, NY.
- Davydov, A., and Eremko, A. (1977). Radiation lifetime of solitons in molecular crystals. *Ukr. Fiz. Zh.* **22**(6), 881–893.
- Davydov, A. (1973). *Quantum Mechanics*. Nauka, Moscow. [In Russian].
- Davydov, A. (1984a). *Nonlinear Biophysics*. Preprint No. 171, Theor. Phys. Inst. Ukr. Acad. Sci., Kiev. [In Russian].
- Davydov, A. (1984b). *Solitons in Molecular Systems*. Naukova Dumka, Kiev. [In Russian].
- Davydov, A. (1987). Quantum theory of quasiparticle movement in a molecular chain under thermal oscillations. 2. Self-localized states. *Ukr. Fiz. Zh.* **32**(3), 352–360.
- Davydov, A. (1994). Energy and electron transport in biological systems. In *Bioelectrodynamics and Biocommunication* (M.-W. Ho, F.-A. Popp, and U. Warnke, Eds.), pp. 411–430. World Scientific, Singapore.
- Delgado, J., Leal, J., Monteagudo, J., and Garcia, M. (1982). Embryological changes induced by weak, extremely low frequency electromagnetic fields. *J. Anat.* **134**, 553–561.
- Del Giudice, E., Doglia, S., Milani, M., Smith, C., and Vitiello, G. (1989). Magnetic flux quantization and Josephson behaviour in living systems. *Phys. Scripta* **40**, 786–791.
- Del Giudice, E., Doglia, S., Milani, M., and Vitiello, G. (1988). Structures, correlations and electromagnetic interactions in living matter: Theory and applications. In *Biological Coherence and Response to External Stimuli* (H. Fröhlich, Ed.), pp. 49–64. Springer-Verlag, Berlin.
- Deryugina, O., Pisachenko, T., and Zhadin, M. (1996). Combined action of ac and dc magnetic fields on the behavior of rats in “open field”. *Biofizika* **41**(3), 762–764.
- de Seze, R., Tuffet, S., Moreau, J.-M., and Veyret, B. (2000). Effects of 100 mT time varying magnetic fields on the growth of tumors in mice. *Bioelectromagnetics* **21**(2), 107–111.
- Devyatkov, N., Betskii, O., Gellvich, E., Golant, M., Makhov, A., Rebrova, T., Sevastyanova, L., and Smolyanskaya, A. (1981). Effect of mm-band EM fields on biological systems. *Radiobiologiya* **21**(2), 163–171.
- Devyatkov, N., and Betskii, O. (Eds.) (1994). *Biological Aspects of Low Intensity Millimeter Waves*. Seven Plus, Moscow.
- Devyatkov, N., Golant, M., and Betskii, O. (1991). *Millimeter EM Waves and Their Role in Physiological Processes*. Radio i Svyaz, Moscow. [In Russian].
- Devyatkov, N., Khrapov, V., Garibov, R., Kudryashova, V., Gaiduk, V., Bakaushina, G., Khrapko, A., Andreeva, A., and Levina, A. (1975). Effect of low intensity mm-waves on gamma-resonance spectra of hemoglobin. *Dokl. Akad. Nauk SSSR* **225**(4), 962–965.

- Devyatkov, N., Kislov, V., Kislov, V., Kolesov, V., Smirnov, V., and Chigin, E. (1996). Normalization of the physiological state of human's internal organs by a mm-wave conditioned water. Detection of the effect. *Millimetr. Volny Biol. Med.* (8), 65–68.
- Devyatkov, N. (1973). Effect of a SHF (mm-band) radiation on biological objects. *Usp. Fiz. Nauk* **110**(3), 453–454.
- Devyatkov, N. (1978). Interaction of a mm-band radiation with biologically active compounds and polar liquids. *Radiotekh. Elektron.* (9), 1882–1890.
- Devyatkov, N. (1999). Evolution of medical electronics in Russia. *Biomed. Radioelektron.* (5), 3–12.
- Didenko, N., Zelentsov, V., Falkovich, V., and Fedorov, N. (1989). Resonance response of a hemoglobin molecule as a function of mm-wave intensity. In *Millimeter Waves in Medicine and Biology* (N. Devyatkov, Ed.), pp. 220–226, Moscow. Inst. Radio Engineering and Electronics. [In Russian].
- Didenko, N., Zelentsov, V., Kositsyn, V., and Chan, V. (1983). Moessbauer spectra of the hemoglobin interaction with EM fields: resonance frequency bandwidth. In *Proceedings of Institute of Nuclear. Issue 10: Nuclear-Physical Methods for Substance Analysis* (A. Didenko, and G. Glukhov, Eds.), pp. 81–84, Moscow. Tomsk Polytech. Inst., Energoatomizdat. [In Russian].
- Dorfman, Y. (1971). Physical phenomena in living objects exposed to static magnetic fields. In *Effects of Magnetic Fields on Biological Objects*, pp. 15–23. Nauka, Moscow. [In Russian].
- Drissler, F. (1988). Physical aspects of plant photosynthesis. In *Biological Coherence and Response to External Stimuli* (H. Fröhlich, Ed.), pp. 114–138. Springer-Verlag, Berlin.
- Dubrov, A. (1969). Effect of heliogeophysical factors on the membrane permeability and diurnal rhythm of organic excretions from plant roots. *Dokl. Akad. Nauk SSSR* **187**(6), 1429.
- Dubrov, A. (1978). *The Geomagnetic Field and Life. Geomagnetobiology*. Plenum, New York.
- Dutta, S., Das, K., Ghosh, B., and Blackman, C. (1992). Dose dependence of acetylcholinesterase activity in neuroblastoma cells exposed to modulated radio-frequency electromagnetic radiation. *Bioelectromagnetics* **13**, 317–322.
- Dutta, S., Subramoniam, A., Ghosh, B., and Parshad, R. (1984). Microwave radiation-induced calcium efflux from brain tissue, in vitro. *Bioelectromagnetics* **5**, 71–78.
- Dutta, S., Verma, M., and Blackman, C. (1994). Frequency-dependent alterations in enolase activity in escherichia coli caused by exposure to electric and magnetic fields. *Bioelectromagnetics* **15**, 377–383.
- Dwight, H. (1961). *Tables of Integrals and Other Mathematical Data*, fourth ed. Macmillan, New York.
- Dyke, J. V., and Halpern, M. (1965). Observations on selected life processes in null magnetic field. *Anat. Rec.* **151**(3), 480.

- Edmiston, J. (1975). Effect of exclusion of the earth's magnetic field on the germination and growth of seeds of white mustard *Sinapis alba*. *Biochem. Physiol. Pflanzen* **167**(1), 97–100.
- Edmonds, D. (1993). Larmor precession as a mechanism for the detection of static and alternating magnetic fields. *Bioelectroch. Bioener.* **30**, 3–12.
- Edmonds, D. (1996). A sensitive optically detected magnetic compass for animals. *Proc. R. Soc. London B* **263**, 295–298.
- Eichwald, C., and Kaiser, F. (1995). Model for external influences on cellular signal transduction pathways including cytosolic calcium oscillations. *Bioelectromagnetics* **16**, 75–85.
- Eigen, M., and De Maeyer, L. (1958). Self-dissociation and protonic charge transport in water and ice. *Proc. R. Soc. London A* **247**, 505.
- Eisenberg, D., and Kauzmann, W. (1969). *The Structure and Properties of Water*. Clarendon, Oxford.
- Engström, S., and Fitzsimmons, R. (1999). Five hypotheses to examine the nature of magnetic field transduction in biological systems. *Bioelectromagnetics* **20**(7), 423–430.
- Engström, S. (1996). Dynamic properties of Lednev's parametric resonance mechanism. *Bioelectromagnetics* **17**, 58–70.
- Eremenko, S., Denisov, I., and Vainer, L. (1981). Anomalous surface conductivity of phospholipid membranes. *Biofizika* **26**(6), 1011–1016.
- Eremenko, T., Esposito, C., Pasquarelli, A., Pasquali, E., and Volpe, P. (1997). Cell-cycle kinetics of friend erithroleukemia cells in a magnetically shielded room and in a low-frequency/low-intensity magnetic field. *Bioelectromagnetics* **18**, 58–66.
- Eremko, A. (1984). Dissociation of Davydov solitons in an EM field. *Dokl. Akad. Nauk Ukr. SSR* **A**(3), 52–55.
- Espinar, A., Píera, V., Carmona, A., and Guerrero, J. (1997). Histological changes during development of the cerebellum in the chick embryo exposed to a static magnetic field. *Bioelectromagnetics* **18**, 36–46.
- Farrell, J., Litovitz, T., Penafiel, M., Montrose, C., Doinov, P., Barber, M., Brown, K., and Litovitz, T. (1997). The effect of pulsed and sinusoidal magnetic fields on the morphology of developing chick embryos. *Bioelectromagnetics* **18**(6), 431–438.
- Fefer, A. (1967). USSR Inventor Certificate No. 445438 of 12.01.1967. [In Russian].
- Fermi, E. (1960). *Notes on Quantum Mechanics*. Univ. of Chicago Press, Chicago.
- Fesenko, E., Geletyuk, V., Kazachenko, V., and Chemeris, N. (1995). Preliminary microwave irradiation of water solutions changes their channel-modifying activity. *FEBS Lett.* **366**, 49–52.
- Fesenko, E., and Gluvstein, A. (1995). Changes in the state of water, induced by radiofrequency electromagnetic fields. *FEBS Lett.* **367**, 53–55.
- Fesenko, E., Novikov, V., and Shvetsov, Y. (1997). Molecular mechanisms of biological effect of weak magnetic fields. *Biofizika* **42**(3), 742–745.

- Feychting, M., Schulgen, G., Olsen, J., and Ahlbom, A. (1995). Magnetic fields and childhood cancer — A pooled analysis of two Scandinavian studies. *Eur. J. Cancer* **31A**(12), 2035–2039.
- Fitzsimmons, R., Farley, J., Adey, W., and Baylink, D. (1989). Frequency dependence of increased cell proliferation, in vitro, in exposure to a low-amplitude, low-frequency electric field: Evidence for dependence on increased mitogen activity released into culture medium. *J. Cell. Physiol.* **139**(3), 586–591.
- Fitzsimmons, R., Ryaby, J., Mohan, S., Magee, F., and Baylink, D. (1995). Combined magnetic fields increase insulin-like growth factor-II in TE-85 human osteosarcoma bone cell cultures. *Endocrinology* **136**(7), 3100–3106.
- Fomicheva, V., Govorun, R., and Danilov, V. (1992a). Proliferating activity and cell reproduction in root systems of pea, lentils and flax exposed to a screened geomagnetic field. *Biofizika* **37**(4), 745–749.
- Fomicheva, V., Zaslavskii, V., Govorun, R., and Danilov, V. (1992b). Dynamics of RNA and protein synthesis in cells of the root meristems of pea, lentils, and flax. *Biofizika* **37**(4), 750–758.
- Forsen, S., and Lindman, B. (1981). Calcium and magnesium NMR in chemistry and biology. *Ann. R. NMR S.* **11A**, 183–226.
- Foster, K., and Schwan, H. (1996). Dielectric Properties of Tissues. In *Handbook of Biological Effects of Electromagnetic Fields* (C. Polk, and E. Postow, Eds.). CRC Press, Boca Raton, FL.
- Frankel, R., Blakemore, R., de Araujo, F. T., Esquivel, D., and Danon, J. (1981). Magnetotactic bacteria at the geomagnetic equator. *Science* **212**, 1269–1270.
- Frankel, R., Blakemore, R., and Wolfe, R. (1979). Magnetite in freshwater magnetotactic bacteria. *Science* **203**(4387), 1355–1357.
- Franks, F. (Ed.) (1972–1982). *Water. A Comprehensive Treatise*, Vols. 1–7. Plenum, London.
- Fröhlich, H. (1968a). Bose condensation of strongly excited longitudinal electric modes. *Phys. Lett. A* **26**, 402–403.
- Fröhlich, H. (1968b). Long-range coherence and energy storage in biological systems. *Int. J. Quantum Chem.* **2**(5), 641–649.
- Furusawa, A., Sørensen, J., Braunstein, S., Fuchs, C., Kimble, H., and Polzik, E. (1998). Unconditional quantum teleportation. *Science* **282**, 706–709.
- Gabriel, S., Lau, R., and Gabriel, C. (1996). The dielectric properties of biological tissues: Measurements in the frequency range 10 Hz – 20 GHz. *Phys. Med. Biol.* **41**, 2251–2269.
- Galvanovskis, J., Sandblom, J., Bergqvist, B., Galt, S., and Hammerius, Y. (1999). Cytoplasmic Ca<sup>2+</sup> oscillations in human leukemia T-cells are reduced by 50 Hz magnetic fields. *Bioelectromagnetics* **20**, 269–276.
- Galvanovskis, J., and Sandblom, J. (1998). Periodic forcing of intracellular calcium oscillators. Theoretical studies of the effects of low frequency fields on the magnitude of oscillations. *Bioelectroch. Bioener.* **46**, 161–174.

- Gandhi, O., Kang, G., Wu, D., and Lazzi, G. (2001). Currents induced in anatomic models of the human for uniform and nonuniform power frequency magnetic fields. *Bioelectromagnetics* **22**(2), 112–121.
- Gandhi, O. (Ed.) (1997). *Modulated Radiofrequency Fields*, Vol. 4 of *Rep. NCRP Sci. Comm. 89*. NCRP.
- Gapeyev, A., Chemeris, N., Fesenko, E., and Khramov, R. (1994). Resonance effects of a low-energy modulated RF field. Changes in motion activity of single-cell *Paramecium caudatum*. *Biofizika* **39**(1), 74–82.
- Gapeyev, A., Safronova, V., Chemeris, N., and Fesenko, E. (1996). Modification of activity of mice peritoneal neutrophils by mm-band waves in the radiator's far and near fields. *Biofizika* **41**(1), 205–219.
- Gapeyev, A., Yakushina, V., Chemeris, N., and Fesenko, E. (1997). Modulated SHF radiation of low intensity activates or inhibits respiratory upsurge of neutrophils as a function of modulation frequency. *Biofizika* **42**(5), 1125–1134.
- Gapeyev, A., Yakushina, V., Chemeris, N., and Fesenko, E. (1999). Static magnetic field modifies the frequency-dependent effect of the EHF EMR on immune system cells. In *Electromagnetic Fields: Biological Effects and Hygienic Standardization* (M. Repacholi, N. Rubtsova, and A. Muc, Eds.), pp. 261–273. World Health Organization, Geneva.
- Garcia-Sancho, J., Montero, M., Alvarez, J., Fonteriz, R., and Sanchez, A. (1994). Effects of extremely-low-frequency electromagnetic fields on ion transport in several mammalian cells. *Bioelectromagnetics* **15**, 579–588.
- Garkavi, L., Kvakina, Y., and Shikhlyarova, A. (1990). Role of frequency keying in the tumor-suppressing mechanism of EM fields. In *Novel Approaches in Oncology* (Y. Sidorenko, Ed.), pp. 38–45. Gertsen Oncology Institute, Moscow. [In Russian].
- Geletyuk, V., Kazachenko, V., Chemeris, N., and Fesenko, E. (1995). Dual effects of microwaves on single  $\text{Ca}^{2+}$ -activated  $\text{K}^+$  channels in cultured kidney cells *Ver. FEBS Lett.* **359**, 85–88.
- Glaser, R., Michalsky, M., and Schramek, R. (1998). Is the  $\text{Ca}^{2+}$  transport of human erythrocytes influenced by ELF- and MF-electromagnetic fields? *Bioelectroch. Bioener.* **47**, 311–318.
- Glasstone, S., Laidler, K., and Eyring, H. (1941). *The Theory of Rate Processes*. McGraw-Hill, London.
- Gleizer, S., and Khodorkovskii, V. (1971). Experimental detection of geomagnetic reception in European eel. *Dokl. Akad. Nauk SSSR* **201**(4), 964.
- Gnevyshev, M., and Oll, A. (Eds.) (1971). *Effects of Solar Activity on the Earth Atmosphere and Biosphere*. Nauka, Moscow. [In Russian].
- Gnevyshev, M., and Oll, A. (Eds.) (1982). *Effect of Solar Activity on the Biosphere. Cosmic Biology Issues*, Vol. 43. Nauka, Moscow. [In Russian].
- Golant, M. (1989). On resonance action of coherent mm-band EM radiations on living organisms. *Biofizika* **34**(2), 339–348.

- Goldbeter, A., Dupont, G., and Berridge, M. (1990). Minimal model for signal-induced  $\text{Ca}^{2+}$  oscillations and for their frequency encoding through protein phosphorylation. *Proc. Natl. Acad. Sci. USA* **87**, 1461–1465.
- Goldman, R., and Pollack, S. (1996). Electric fields and proliferation in a chronic wound model. *Bioelectromagnetics* **17**, 450–457.
- Goldsworthy, A., Whitney, H., and Morris, E. (1999). Biological effects of physically conditioned water. *Water Res.* **33**(7), 1618–1626.
- Golovkov, V. (1990). Terrestrial magnetism. In *Physical Encyclopedia*, 2, pp. 81–82. Sovetskaya Entsiklopediya, Moscow. [In Russian].
- Goodman, E., Greenebaum, B., and Marron, M. (1993a). Altered protein synthesis in a cell-free system exposed to a sinusoidal magnetic field. *Biochim. Biophys. Acta* **1202**, 107–112.
- Goodman, E., Greenebaum, B., and Marron, M. (1995). Effects of electromagnetic fields on molecules and cells. *Int. Rev. Cytol.* **158**, 279–338.
- Goodman, R., Bassett, C., and Henderson, A. (1983). Pulsing electromagnetic fields induce cellular transcription. *Science* **220**, 1283–1285.
- Goodman, R., Chizmadzhev, Y., and Henderson, A. (1993b). Electromagnetic fields and cells. *J. Cell Biochem.* **51**, 436–441.
- Goodman, R., and Henderson, A. (1988). Exposure of salivary gland cells to low-frequency electromagnetic fields alters polypeptide synthesis. *Proc. Natl. Acad. Sci. USA* **85**, 3928–3932.
- Goodman, R., and Henderson, A. (1990). Exposure to extremely low-frequency electromagnetic fields: Relationship to malignancy? *Cancer Cells* **2**(11), 355–359.
- Goodman, R., and Henderson, A. (1991). Transcription and translation in cells exposed to extremely low frequency electromagnetic fields. *Bioelectroch. Bioener.* **25**, 335–355.
- Goodman, R., Wey, L.-X., Xu, J.-C., and Henderson, A. (1989). Exposure of human cells to low frequency electromagnetic fields results in quantitative changes in transcripts. *Biochim. Biophys. Acta* **1009**, 216–220.
- Gould, J., Kirschvink, J., Deffeyes, K., and Brines, M. (1980). Orientation by demagnetized bees. *J. Exp. Biol.* **86**, 1–8.
- Gould, J., Kirschvink, J., and Deffeyes, K. (1978). Bees have magnetic remanence. *Science* **201**(4360), 1026–1028.
- Govorun, R., Danilov, V., Fomicheva, V., Belyavskaya, N., and Zinchenko, S. (1992). Effect of fluctuations of the geomagnetic field and its screening on early growth phases of higher plants. *Biofizika* **37**(4), 738–744.
- Greene, J., Skowronski, W., Mullins, J., Nardone, R., Penafiel, M., and Meister, R. (1991). Delineation of electric and magnetic field effects of extremely low frequency electromagnetic radiation on transcription. *Biochem. Biophys. Res. Co.* **174**(2), 742–749.
- Green, A., and Halpern, M. (1966). Response of tissue culture cells to low magnetic fields. *Aerosp. Med.* **37**(3), 251–253.

- Grigoriev, Y., and Stepanov, V. (2000). Microwave effect on embryo brain: Dose dependence and the effect of modulation. In *Radio Frequency Radiation Dosimetry* (B. Klauenberg, and D. Miklavcic, Eds.), pp. 31–37. Kluwer/Plenum, London.
- Grigoriev, Y. (1994). Extremely weak impacts of medium's physical factors from the magnetobiology standpoint. *Magnitobiologiya* (1), 6–7.
- Grissom, C. (1995). Magnetic field effects in biology: A survey of possible mechanisms with emphasis on radical-pair recombination. *Chem. Rev.* **95**(1), 3–24.
- Grundler, W., Kaiser, F., Keilmann, F., and Walleczek, J. (1992). Mechanisms of electromagnetic interaction with cellular systems. *Naturwissenschaften* **79**, 551–559.
- Grundler, W., and Kaiser, F. (1992). Experimental evidence for coherent excitations correlated with cell growth. *Nanobiology* **1**, 163–176.
- Grundler, W., and Keilmann, F. (1983). Sharp resonances in yeast growth prove nonthermal sensitivity to microwaves. *Phys. Rev. Lett.* **51**(13), 1214–1216.
- Guliyellmi, A., and Troitskaya, V. (1973). *Geomagnetic Pulsations and Diagnostics of Magnetosphere*. Nauka, Moscow. [In Russian].
- Gulyaev, Y., Yeregin, S., and Markov, I. (1997). Structure and energy modification of water exposed to an EM field in a inhomogeneous system. Report to an ad hoc meeting devoted to “Water and electromagnetic fields”, Pushchino, Institute of Cell Biology.
- Gurfinkell, Y., Kuleshova, V., and Oraevskii, V. (1998). Assessing the effect of geomagnetic storms on the frequency of acute cardiovascular pathologies. *Biofizika* **43**(4), 654–658.
- Gurfinkell, Y., Lyubimov, V., Oraevskii, V., Parfenova, L., and Yuriev, A. (1995). Effect of geomagnetic perturbations on the capillary blood stream in ischemic patients. *Biofizika* **40**(4), 793–799.
- Gurney, J., Davis, S., Schwartz, S., Mueller, B., Kaune, W., and Stevens, R. (1995). Childhood cancer occurrence in relation to power line configurations: A study of potential selection bias in case-control studies. *Epidemiology* **6**, 31–35.
- Gustavsson, M., Lindgren, M., Galt, S., and Hamnerius, Y. (1999). Statistical comparison of independently replicated cellular ELF experiments. In *Electricity and Magnetism in Biology and Medicine* (F. Bersani, Ed.). Kluwer/Plenum, London.
- Hafemeister, D. (1996). Biological effects of low-frequency electromagnetic fields. *Am. J. Phys.* **64**(8), 974–981.
- Halpern, M., and Van Dyke, J. (1966). Very low magnetic fields: Biological effects and their implication for space exploration. *Aerosp. Med.* **37**(3), 281–284.
- Hämäläinen, M., Hari, R., Ilmoniemi, R., Knuutila, J., and Lounasmaa, O. (1993). Magnetoencephalography — theory, instrumentation, and applications to non-invasive studies of the working human brain. *Rev. Mod. Phys.* **65**(2), 413–497.
- Harland, J., and Liburdy, R. (1997). Environmental magnetic fields inhibit the antiproliferative action of tamoxifen and melatonin in a human breast cancer cell line. *Bioelectromagnetics* **18**(8), 555–562.

- Hays, J. (1971). Faunal extinctions and reversals of the Earth's magnetic field. *Geol. Soc. Am. Bull.* **82**, 2433–2447.
- Heath, C. (1996). Electromagnetic field exposure and cancer: A review of epidemiologic evidence. *CA. Cancer J. Clin.* **46**(1), 29–44.
- Henshaw, D., Ross, A., Fews, A., and Preece, A. (1996). Enhanced deposition of radon daughter nuclei in the vicinity of power frequency electromagnetic fields. *Int. J. Rad. Biol.* **69**(1), 25–38.
- Hitchcock, R., and Patterson, R. (1995). *Radiofrequency and ELF Electromagnetic Energies: A Handbook for Health Professionals*. Van Nostrand Reinhold, New York.
- Ho, M.-W., Stone, T., Jerman, I., Bolton, J., Bolton, H., Goodwin, B., Saunders, P., and Robertson, F. (1992). Brief exposures to weak static magnetic field during early embryogenesis cause cuticular pattern abnormalities in *Drosophila* larvae. *Phys. Med. Biol.* **37**(5), 1171–1179.
- Hoelzel, R., and Lamprecht, J. (1994). Electromagnetic fields around biological cells. *Neural Netw. World* **4**, 327.
- Höjeric, P., Sandblom, J., Galt, S., and Hamnerius, Y. (1995). Ca<sup>2+</sup> ion transport through patch-clamped cells exposed to magnetic fields. *Bioelectromagnetics* **16**, 33–40.
- Huang, R., Peng, L., and Hertz, L. (1997). Effects of low-voltage static electric field on energy metabolism in astrocytes. *Bioelectromagnetics* **18**, 77–80.
- Hughes, M. (1996). *Computers, Antennas, Cellular Telephones and Power Lines Health Hazards*. Hughes Press, Washington, DC.
- Hyland, G., Bastide, M., Youbicier-Simo, J., Faivre-Bonhomme, L., Coghill, R., Miyata, M., Catier, J., Canavan, A., Fillion-Robin, M., Marande, J., and Clements-Croome, D. (1999). Electromagnetic biocompatibility at workplace: Protection principles, assessment and tests. Results of an EMF protective compensation technology in humans and in animals. In *Nichtionisierende Strahlung: mit ihr Leben in Arbeit und Umwelt* (N. Krause, M. Fischer, and H.-P. Steimel, Eds.), pp. 213–240. Köln. IRPA, TÜV-Verlag.
- Hyland, G. (1998). Non-thermal bioeffects induced by low-intensity microwave irradiation of living systems. *Engineering Sci. Educ. J.* **7**, 261–269.
- Ivić, Z., Pržulj, Ž., Kapor, D., and Škrinjar, M. (1996). On the relevance of self-trapping as the mechanism for charge and energy transfer in biological system. *Bioelectroch. Bioener.* **41**, 43–46.
- Ivlev, A., Panteleev, N., Knyazev, Y., Logachev, M., and Miller, Y. (1994). Diurnal variations of the carbon isotope composition in CO<sub>2</sub> exhaled by humans with some metabolic disorders. *Biofizika* **39**(2), 393–399.
- Ivlev, A. (1985). Distribution of carbon isotopes in amino acids of the protein fraction of microorganisms as a sounding means of cell biosynthesis. *Biokhimiya* **50**(10), 1607–1615.
- Jacobson, B., Laties, G., Smith, B., Epstein, S., and Laties, B. (1970). Cyanide-induced transition from endogenous carbohydrate to lipid oxidation as indi-

- cated by the carbon-13 content of respiratory CO<sub>2</sub>. *Biochim. Biophys. Acta* **216**(2), 295–304.
- Jacobson, J. (1991). A look at the possible mechanism and potential of magnetotherapy. *J. Theor. Biol.* **149**, 97–120.
- Jacobson, J. (1994). Pineal-hypothalamic tract mediation of picotesla magnetic fields in the treatment of neurological disorders. *FASEB J.* **8**(5), A656.
- Jafary-Asl, A., Solanki, S., Aarholt, E., and Smith, C. (1983). Dielectric measurements on live biological material under magnetic resonance condition. *J. Biol. Phys.* **11**, 15–22.
- Jenrow, K., Smith, C., and Liboff, A. (1995). Weak extremely-low-frequency magnetic fields and regeneration in the planarian *Dugesia tigrina*. *Bioelectromagnetics* **16**, 106–112.
- Jerman, I., Berden, M., and Ružič, R. (1996). Biological influence of ultraweak supposedly EM radiation from organisms mediated through water. *Electro Magnetobiol.* **15**(3), 229–244.
- Josephson, B. (1962). Possible new effects in superconductive tunnelling. *Phys. Lett.* **1**(7), 251–253.
- Jungerman, R., and Rosenblum, B. (1980). Magnetic induction for the sensing of magnetic fields. *J. Theor. Biol.* **87**, 25.
- Juutilainen, J., Kumlin, T., Alhonen, L., Janne, J., Komulainen, H., Kosma, V.-M., Lang, S., Pasanen, M., Rytömaa, T., and Servomaa, K. (1996). Effects of UV radiation and 50 Hz magnetic fields in ODC-transgenic mice: Skin tumor development and ODC and polyamine levels. In *Abst. 3 EBFA Congress*, p. 230, Nancy. Univ. Henri Poincaré.
- Juutilainen, J., Lang, S., and Rytömaa, T. (2000). Possible cocarcinogenic effects of ELF electromagnetic fields may require repeated long-term interaction with known carcinogenic factors. *Bioelectromagnetics* **21**(2), 122–128.
- Juutilainen, J. (1986). Effects of low frequency magnetic fields on chick embryos. dependence on incubation temperature and storage of the eggs. *Z. Naturforsch. C* **41**, 1111–1115.
- Kadantsev, V., Lupichev, L., and Savin, A. (1988). Formation of soliton states in a molecular chain subjected to thermal oscillation quanta. *Ukr. Fiz. Zh.* **33**(8), 1135–1139.
- Kaiser, F. (1996). External signals and internal oscillation dynamics: biophysical aspects and modeling approaches for interactions of weak electromagnetic fields at the cellular level. *Bioelectroch. Bioener.* **41**, 3–18.
- Kalmijn, A. (1978). Experimental evidence of geomagnetic orientation in elasmobranch fishes. In *Animal Migration, Navigation, and Homing* (K. Schmidt-Koenig, and W. Keeton, Eds.), pp. 347–353. Springer-Verlag, New York.
- Kalmijn, A. (1982). Electric and magnetic field detection in elasmobranch fishes. *Science* **218**, 916.
- Kamenir, E., and Kirillov, A. (1995). Effects of cosmophysical factors on the germination of wheat seeds conditioned in a corona discharge field. *Biofizika* **40**(4), 765–770.

- Karnaukhov, A. (1994). Dissipative structures in weak magnetic fields. *Biofizika* **39**(6), 1009–1014.
- Kashulin, P., and Pershakov, L. (1995). Experimental study of the subarctic magnetosphere as a possible exogenous factor for northern biota. *Biofizika* **40**(4), 782–785.
- Kataev, A., Alexandrov, A., Tikhonova, L., and Berestovskii, G. (1993). Frequency dependent effect of mm-band EM waves on ion currents of *Nitellopsis* algae. Nonthermal effects. *Biofizika* **38**(3), 446–462.
- Katin, A. (1996). Duration of the effect of a water conditioned by mm-band radiation on human organism. *Millimetr. Volny Biol. Med.* (8), 63–64.
- Kato, M., Honma, K., Shigemitsu, T., and Shiga, Y. (1993). Effects of exposure to a circularly polarized 50-Hz magnetic field on plasma and pineal melatonin levels in rats. *Bioelectromagnetics* **14**, 97–106.
- Kato, M., Honma, K., Shigemitsu, T., and Shiga, Y. (1994). Recovery of nocturnal melatonin concentration takes place within one week following cessation of 50 Hz circularly polarized magnetic field exposure for six weeks. *Bioelectromagnetics* **15**, 489–492.
- Kato, M., and Shigemitsu, T. (1996). Effects of exposure to 50 Hz magnetic field of melatonin in rats. In *Biological Effects of Magnetic and Electromagnetic Fields* (S. Ueno, Ed.). Kluwer/Plenum, New York.
- Kato, R., Kamada, H., and Asashima, M. (1989). Effects of high and very low magnetic fields on the growth of hairy roots of *Daucus carota* and *Atropa belladonna*. *Plant Cell Physiol.* **30**(4), 605–608.
- Kato, R. (1988). Effects of a magnetic field on the growth of primary roots of *Zea mays*. *Plant Cell Physiol.* **29**(7), 1215–1219.
- Katsir, G., Baram, S., and Parola, A. (1998). Effect of sinusoidal magnetic fields on cell proliferation and adenosine deaminase specific activity. *Bioelectromagnetics* **19**(1), 46–52.
- Kavaliers, M., and Ossenkopp, K. (1985). Tolerance to morphine-induced analgesia in mice: Magnetic fields function as environmental specific cues and reduced tolerance development. *Life Sci.* **37**, 1125–1135.
- Kavaliers, M., and Ossenkopp, K. (1986). Magnetic field inhibition of morphine-induced analgesia and behavioral activity in mice: Evidence for involvement of calcium ions. *Brain Res.* **379**, 30–38.
- Kavaliers, M., Prato, F., and Thomas, A. (1996). ELF magnetic field increase opioid-induced analgesia in the land snail consistent with the predictions of the paramagnetic resonance model (PRM) for  $K^+$ . In *Abst. 18th BEMS Meeting*, pp. 64–65, Victoria, Canada.
- Kazachenko, V., Deryugina, O., Kochetkov, K., and Fesenko, E. (1999). Effect of admixtures on reduction of  $[O_2]$  in water exposed to a millimeter radiation. *Biofizika* **44**(5), 796–805.
- Kazarinov, K., Sharov, V., Putvinskii, A., and Betskii, O. (1984). Effect of CW low-intensity mm-waves on  $Na^+$  ion transport in frog skin. *Biofizika* **29**(3), 480–482.

- Keeton, W., Larkin, T., and Windsor, D. (1974). Normal fluctuations in the earth's magnetic field influence pigeon orientation. *J. Comp. Physiol.* **95**, 95–103.
- Khizhnyak, E., and Ziskin, M. (1994). Heating patterns in biological tissue phantoms caused by millimeter wave electromagnetic irradiation. *IEEE Trans. Biomed. Eng.* **41**(9), 865–873.
- Khizhnyak, E., and Ziskin, M. (1996). Temperature oscillations in liquid media caused by continuous (unmodulated) millimeter wavelength electromagnetic irradiation. *Bioelectromagnetics* **17**, 223–229.
- Khodorkovskii, V., and Polonnikov, R. (1971). Studies of hyperweak magnetic field reception in fish. In *Fish Behavior*, p. 72. Kaliningrad State Univ. [In Russian].
- Kholodov, Y., Kozlov, A., and Gorbach, A. (1990). *Magnetic Fields of Biological Systems*. Nauka, Moscow. [In Russian].
- Kholodov, Y., and Lebedeva, N. (1992). *Human Neural Responses to Electromagnetic Fields*. Nauka, Moscow. [In Russian].
- Kholodov, Y. (1975). *Response of Nervous System to EM Fields*. Nauka, Moscow. [In Russian].
- Kholodov, Y. (1982). *Brain in EM Fields*. Nauka, Moscow. [In Russian].
- Kholodov, Y. (1986). Basic problems of electromagnetic biology. In *Electromagnetic Fields and Biomembranes* (M. Markov, and M. Blank, Eds.), pp. 109–116. Plenum, New York.
- Kirschvink, J., Jones, D., and MacFadden, B. (Eds.) (1985). *Magnetite Biomineralization and Magnetoreception in Organisms. A New Biomagnetism*. Plenum, New York.
- Kirschvink, J., Kobayashi-Kirschvink, A., Diaz-Ricci, J., and Kirschvink, S. (1992). Magnetite in human tissues: A mechanism for the biological effects of weak ELF magnetic fields. *Bioelectromagnetics* **1**(S12), S101–S114.
- Kislovsky, L. (1971). On a possible molecular mechanism of solar activity transduced in biospheric processes. In *Effect of Solar Activity on the Earth Atmosphere and Biosphere*, pp. 147–164. Nauka, Moscow. [In Russian].
- Kislovsky, L. (1982). Response of the biological system to adequate weak low-frequency EM fields. In *Space Biology Issues Vol. 43. Effect of Solar Activity on the Biosphere* (V. Chernigovsky, Ed.), pp. 148–166. Nauka, Moscow. [In Russian].
- Klassen, V. (1973). *Water and Magnet*. Nauka, Moscow. [In Russian].
- Klassen, V. (1982). *Magnetic Conditioning of Water Systems*. Khimiya, Moscow. [In Russian].
- Klochek, N., Palamarchuk, L., and Nikonova, M. (1995). Preliminary results of studies into the effects of non-EM space radiation on physical and biological systems. *Biofizika* **40**(4), 889–896.
- Kloss, A. (1988). Electron-radical dissociation and a mechanism of water activation. *Dokl. Akad. Nauk. SSSR* **303**(6), 1403–1407.
- Kobayashi, A., Kirschvink, J., and Nesson, M. (1995). Ferromagnetism and EMFs. *Nature* **374**, 123.

- Kogan, A., and Tikhonova, N. (1965). Effect of a static magnetic field on motion of paramecia. *Biofizika* **10**(2), 292–296.
- Konyukhov, V., Logvinenko, V., and Tikhonov, V. (1995). Separation of water to its spin modifications and determination of the spin conversion time of water molecules. *Kratk. Soobsh. Fiz. FIAN* (5–6), 83–86. [Translated into English as *Bull. Lebedev Phys. Inst., Allerton, New York*].
- Konyukhov, V., and Tikhonov, V. (1995). Adsorption of water molecules on cluster surface under the conditions of proton NMR in weak magnetic fields. *Kratk. Soobshch. Fiz. FIAN* (1–2), 12–18. [Translated into English as *Bull. Lebedev Phys. Inst., Allerton, New York*].
- Kopanev, V., and Shakula, A. (1986). *Effect of a Hypomagnetic Field on Biological Systems*. Nauka, Moscow. [In Russian].
- Kopylov, A., and Troitskii, M. (1982). Effect of magnetic fields on radiosensitivity in mice. Effect of weak low-frequency magnetic fields on the survival rate of x-rayed animals. *Radiobiologiya* **22**, 687–690.
- Korn, G., and Korn, T. (1961). *Mathematical Handbook*. McGraw-Hill, New York.
- Krasnogorskaya, N. (Ed.) (1984). *Electromagnetic Fields in the Biosphere*, Vols. 1–2. Nauka, Moscow. [In Russian].
- Krasnogorskaya, N. (Ed.) (1991–1992). *Current Issues of Biosphere Preservation and Research*, Vols. 1–3. Gidrometeoizdat, Moscow. [In Russian].
- Kroto, H., Heath, J., O'Brien, S., Curl, R., and Smalley, R. (1985). C<sub>60</sub>: Buckminsterfullerene. *Nature* **318**, 162–163.
- Kruglikov, I., and Dertinger, H. (1994). Stochastic resonance as a possible mechanism of amplification of weak electric signals in living cells. *Bioelectromagnetics* **15**, 539–547.
- Krylov, A., and Tarakanova, G. (1960). Magnetotropism of plants and its nature. *Plant Physiol.* **7**, 156–160.
- Kuznetsov, A., Golant, M., and Bozhanova, T. (1997). Exposure of a cell culture to an RF field with intensity below that of background noise. In *Millimeter Waves in Biology and Medicine*, pp. 145–147. Inst. Radio Engineering Electronics, Moscow. [In Russian].
- Kuznetsov, A., Kshutashvili, T., Kolokolov, A., and Lazarev, A. (1990). Quasi-resonance dependencies of arrhythmogenic action of low-frequency magnetic fields on contraction of a myocardium. *Izv. Akad. Nauk. SSSR, Biol.* (2), 178–183. [In Russian].
- Kuznetsov, A., and Vanag, V. (1987). Mechanisms of the magnetic field effect on biological systems. *Izv. Akad. Nauk SSSR Biol.* (6), 814–827.
- Lacroix, M., Mosora, F., Pontus, M., Lefebvre, P., Luyckx, A., and Lopez-Habib, G. (1973). Glucose naturally labeled with carbon-13: Use for metabolic studies in man. *Science* **181**(4098), 445–446.
- Lacy-Hulbert, A., Wilkins, R., Hesketh, T., and Metcalfe, J. (1995). Cancer risk and electromagnetic fields. *Nature* **375**(6526), 22–23.

- Lai, H., and Carino, M. (1999). 60 Hz magnetic fields and central cholinergic activity: Effects of exposure intensity and duration. *Bioelectromagnetics* **20**, 284–289.
- Lai, H., and Singh, N. (1997a). Acute exposure to a 60 Hz magnetic field increases DNA strand breaks in rat brain cells. *Bioelectromagnetics* **18**, 156–165.
- Lai, H., and Singh, N. (1997b). Melatonin and a spin-trap compound block radiofrequency electromagnetic radiation-induced DNA strand breaks in rat brain cells. *Bioelectromagnetics* **18**, 446–454.
- Landau, L., and Lifshitz, E. (1960). *Electrodynamics of Continuous Media*, Vol. 8 of *Theoretical Physics*. Pergamon, Oxford.
- Landau, L., and Lifshitz, E. (1976a). *The Classical Theory of Fields*, Vol. 2 of *Theoretical Physics*. Pergamon, Oxford.
- Landau, L., and Lifshitz, E. (1976b). *Fluid Mechanics*, Vol. 6 of *Theoretical Physics*. Pergamon, Oxford.
- Landau, L., and Lifshitz, E. (1977). *Quantum Mechanics*, Vol. 3 of *Theoretical Physics*. Pergamon, Oxford.
- Lathrop, J. (1996). Realtors' Association Contributes. *EMF Health & Safety Digest* **14**(2), 3.
- Lawrence, A., McDaniel, J., Chang, D., Pierce, B., and Birge, R. (1986). Dynamics of the Davydov model in  $\alpha$ -helical proteins: Effects of the coupling parameter and temperature. *Phys. Rev. A* **33**(2), 1188–1201.
- Lednev, V., Srebnitskaya, L., Ilyasova, E., Rozhdestvenskaya, Z., Klimov, A., Belova, N., and Tiras, H. (1996a). Magnetic parametric resonance in biosystems: Experimental proof of the theoretical predictions using regenerating planaria *Dugesia tigrina* as a test system. *Biofizika* **41**(4), 815–825.
- Lednev, V., Srebnitskaya, L., Ilyasova, E., Rozhdestvenskaya, Z., Klimov, A., and Tiras, H. (1996b). Weak combined magnetic field set in parametric resonance of nuclear spins of hydrogen atoms increases proliferation of neoblasts in regenerating planaria. *Dokl. Ross. Akad. Nauk* **348**, 830–833.
- Lednev, V., Srebnitskaya, L., Ilyasova, E., Rozhdestvenskaya, Z., Klimov, A., and Tiras, K. (1997).  $H^+$ -tuned combined magnetic field decreases the rate of regeneration of planarians. In *Abst. 2 World Congress Elect. Magn. Biol. Med.*, pp. 257–258, Bologna, Italy. BEMS.
- Lednev, V. (1991). Possible mechanism for the influence of weak magnetic fields on biological systems. *Bioelectromagnetics* **12**, 71–75.
- Lednev, V. (1996). Bioeffects of weak combined, static, and alternating magnetic fields. *Biofizika* **41**(1), 224–232.
- Lee, J., Stormshak, J., Thompson, J., Hess, D., and Foster, D. (1995). Melatonin and puberty in female lambs exposed to EMF: A replicate study. *Bioelectromagnetics* **16**, 119–123.
- Lei, C., and Berg, H. (1998). Electromagnetic window effects on proliferation rate of *Corynebacterium glutamicum*. *Bioelectroch. Bioener.* **45**, 261–265.
- Lerchl, A., Nonaka, K., and Reiter, R. (1990). Pineal gland “magnetosensitivity” is a consequence of induced electric eddy currents. *J. Pineal Res.* **10**, 109–116.

- Lerchl, A., Reiter, R., Howes, K., Nonaka, K., and Stokkan, K. (1991). Evidence that extremely low frequency Ca(2+)-cyclotron resonance depresses pineal melatonin synthesis in vitro. *Neurosci. Lett.* **124**(2), 213–215.
- Lester, D., and Blumfeld, V. (1991). Divalent cation-induced changes in conformation of protein kinase C. *Biophys. Chem.* **39**, 215–224.
- Leucht, T. (1987). Effects of weak magnetic fields on background adaptation in *Xenopus laevis*. *Naturwissenschaften* **74**, 192–194.
- Li, C., Chiang, H., Fu, Y., Shao, B., Shi, J., and Yao, G. (1999). Effects of 50 Hz magnetic fields on gap junctional intercellular communication. *Bioelectromagnetics* **20**, 290–294.
- Liboff, A., Jr., T. W., Strong, D., and Jr., R. W. (1984). Time varying magnetic fields: Effect on DNA synthesis. *Science* **223**(4638), 818–820.
- Liboff, A., and Parkinson, W. (1991). Search for ion-cyclotron resonance in an Na<sup>+</sup>-transport system. *Bioelectromagnetics* **12**, 77–83.
- Liboff, A., Rozek, R., Sherman, M., McLeod, B., and Smith, S. (1987a). Ca<sup>2+</sup>-45 cyclotron resonance in human lymphocytes. *J. Bioelect.* **6**, 13–22.
- Liboff, A., Smith, S., and McLeod, B. (1987b). Experimental evidence for ion cyclotron resonance mediation of membrane transport. In *Mechanistic Approaches to Interactions of Electric and Electromagnetic Fields with Living Systems* (M. Blank, and E. Findl, Eds.), pp. 109–132. Plenum, New York.
- Liboff, A., Smith, S., and McLeod, B. (1995). Comments on “Clarification and application of an Ion Parametric Resonance model for magnetic field interactions with biological systems,” by Blanchard and Blackman. *Bioelectromagnetics* **16**, 272–273.
- Liboff, A. (1985). Geomagnetic cyclotron resonance in living cells. *J. Biol. Phys.* **13**, 99–102.
- Liboff, A. (1997). Electric-field ion cyclotron resonance. *Bioelectromagnetics* **18**, 85–87.
- Liburdy, R. (1992). Calcium signaling in lymphocytes and ELF fields. *FEBS Lett.* **301**(1), 53–59.
- Lifshitz, Y., and Pitaevsky, L. (1978). *Statistical Physics – 2*, Vol. 9 of *Theoretical Physics*. Nauka, Moscow. [In Russian].
- Lindauer, M., and Martin, H. (1968). Die Schwerorientierung der Bienen unter dem Einfluss des Erdmagnetfeldes. *Z. Vgl. Physiol.* **60**(3), 219–243.
- Lindgren, M., Gustavsson, M., Hamnerius, Y., and Galt, S. (2001). ELF magnetic fields in a city environment. *Bioelectromagnetics* **22**(2), 87–90.
- Lindstrom, E., Lindstrom, P., Berglund, A., Lundgren, E., and Mild, K. (1995). Intracellular calcium oscillations in a T-cell line after exposure to extremely-low-frequency magnetic fields with variable frequencies and flux densities. *Bioelectromagnetics* **16**, 41–47.
- Lin, H., Blank, M., Jin, M., and Goodman, R. (1996). Electromagnetic field stimulation of biosynthesis changes in *c-myc* transcript levels during continuous and intermittent exposures. *Bioelectroch. Bioener.* **39**, 215–220.

- Lin, H., and Goodman, R. (1995). Electric and magnetic noise blocks the 60 Hz magnetic field enhancement of steady state *c-myc* transcript levels in human leukemia cells. *Bioelectroch. Bioener.* **36**, 33–37.
- Lin, J., and Chou, C.-K. (Eds.) (1997). *Biological Effects and Exposure Criteria for Radiofrequency Electromagnetic Fields*, Vol. 5 of *Rep. NCRP Sci. Comm.* 89. NCRP.
- Lin, J., Singleton, G., Schaeffer, J., Hong, C.-Z., and Meltzer, R. (1985). Geophysical variables and behavior: XXVII. Magnetic necklace: Its therapeutic effectiveness on neck and shoulder pain: 2. Psychological assessment. *Psychol. Rep.* **56**(2), 639–649.
- Lissmann, H., and Machin, K. (1963). Electric receptors in a nonelectric fish. *Nature* **199**, 88–90.
- Litovitz, T., Krause, D., Montrose, C., and Mullins, J. (1994a). Temporally incoherent magnetic fields mitigate the response of biological systems to temporally coherent magnetic fields. *Bioelectromagnetics* **15**, 399–409.
- Litovitz, T., Krause, D., and Mullins, J. (1991). Effect of coherence time of the applied magnetic field on the enhancement of ornithine decarboxylase activity. *Biochem. Biophys. Res. Co.* **178**(3), 862–865.
- Litovitz, T., Krause, D., Penafiel, M., Elson, E., and Mullins, J. (1993). The role of coherence time in the effect of microwaves on ornithine decarboxylase activity. *Bioelectromagnetics* **14**, 395–403.
- Litovitz, T., Montrose, C., Doynov, P., Brown, K., and Barber, M. (1994b). Superimposing spatially coherent electromagnetic noise inhibits field induced abnormality in developing chick embryos. *Bioelectromagnetics* **15**, 105–113.
- Litovitz, T., Penafiel, L., Farrel, J., Krause, D., R.Meister, and Mullins, J. (1997a). Bioeffects induced by exposure to microwaves are mitigated by superposition of ELF noise. *Bioelectromagnetics* **18**, 422–430.
- Litovitz, T., Penafiel, M., Krause, D., Zhang, D., and Mullins, J. (1997b). The role of temporal sensing in bioelectromagnetic effects. *Bioelectromagnetics* **18**, 388–395.
- Liu, K., Brown, M., Cruzan, J., and Saykally, R. (1996a). Vibration-rotation tunneling spectra of the water pentamer: Structure and dynamics. *Science* **271**, 62–64.
- Liu, K., Cruzan, J., and Saykally, R. (1996b). Water clusters. *Science* **271**, 929–933.
- Lobyshev, V., Ryzhikov, B., and Shikhliinskaya, R. (1995). Luminescence of water conditioned by its structure polymorphism. *Vestnik Mosk. Gos. Univ., Fiz. Astron.* **36**(2), 48–54.
- Lobyshev, V., Shikhliinskaya, R., and Ryzhikov, B. (1999). Experimental evidence for intrinsic luminescence of water. *J. Mol. Liquids* **82**, 73–81.
- Lohmann, K. (1993). Magnetic compass orientation. *Nature* **362**, 703.
- Lomdahl, P., and Kerr, W. (1985). Do Davydov soliton exist at 300K? *Phys. Rev. Lett.* **55**(11), 1235–1238.

- Loscher, W., Wahnschaffe, U., Mevissen, M., Lerchl, A., and Stamm, A. (1994). Effects of weak alternating magnetic fields on nocturnal melatonin production and mammary carcinogenesis in rats. *Oncology* **51**, 288–295.
- Luben, R., Cain, C., Chen, M.-Y., Rosen, D., and Adey, W. (1982). Effects of electromagnetic stimuli on bone and bone cells in vitro: Inhibition of responses to parathyroid hormone by low energy low frequency fields. *Proc. Natl. Acad. Sci. USA* **79**, 4180–4184.
- Luben, R., Mild, K., and Blank, M. (1996). BEMS Presidents' letter goes to Congress following strong urging from members. *Bioelectromagn. Newslett.* **131**, 1–4.
- Luben, R. (1991). Effects of low-energy electromagnetic fields (pulsed and DC) on membrane signal transduction processes in biological systems. *Health Phys.* **61**(1), 15–28.
- Lyashchenko, A. (1998). Structure of water and water solutions, relaxation processes and a mechanism of mm-band waves action on biological objects. *Biomed. Radioelektron.* (2), 17–22.
- Lyle, D., Ayotte, R., Sheppard, A., and Adey, W. (1988). Suppression of T-lymphocyte cytotoxicity following exposure to 60 Hz sinusoidal electric fields. *Bioelectromagnetics* **9**(3), 303–313.
- Lyle, D., Schechter, P., Adey, W., and Lundak, R. (1983). Suppression of T-lymphocyte cytotoxicity following exposure sinusoidally amplitude-modulated fields. *Bioelectromagnetics* **4**, 281–292.
- Lyle, D., Wang, X., Ayotte, R., Sheppard, A., and Adey, W. (1991). Calcium uptake by leukemic and normal T-lymphocytes exposed to low frequency magnetic fields. *Bioelectromagnetics* **12**, 145–156.
- Lyskov, E., Chernyshev, M., Mikhailov, V., Kozlov, A., Makarova, T., Vasil'eva, Y., Druzin, M., Sokolov, G., and Vishnevskii, A. (1996). Effect of a 50 Hz magnetic field on rat behavior depends on the direct current component. *Biofizika* **41**(4), 870–875.
- Machlup, S., and Blackman, C. (1997). Two ions oscillating coherently: A conjecture to illuminate the beautiful agreement of IPR model with cell-culture data. In *Abst. 2 World Congress Elect. Magn. Biol. Med.*, p. 186, Bologna, Italy. BEMS.
- Mahlum, D. (Ed.) (1997). *Biological Effects of Static Magnetic Fields*, Vol. 1 of *Rep. NCRP Sci. Committee 89*. NCRP.
- Makarevich, A. (1999). Effect of magnetoplast's magnetic fields on growth of microorganisms. *Biofizika* **44**(1), 70–74.
- Makeev, V. (1993). Stochastic resonance and its possible role in living nature. *Biofizika* **38**(1), 194–201.
- Malko, J., Constantinidis, I., Dillehay, D., and Fajman, W. (1994). Search for influence of 1.5 Tesla magnetic field on growth of yeast cells. *Bioelectromagnetics* **15**, 495–501.
- Mamar-Bachi, A., and Cox, J. (1987). Quantitative analysis of the free energy coupling in the system calmodulin, calcium, smooth muscle myosin light chain kinase. *Cell Calcium* **8**, 473–482.

- Markin, V., Liu, D., Gisma, J., Strobel, R., Rosenberg, M., and Tsong, T. (1992). Ion channel enzyme in an oscillating electric field. *J. Membr. Biol.* **126**, 137–145.
- Markov, M., Muehsam, D., and Pilla, A. (1998). A possible model for the static  $\mu\text{T}$ -level magnetic field modulation of calcium binding to calmodulin in cell-free myosin phosphorylation. In *Abst. 20th BEMS Annual Meeting, St. Pete Beach, Florida*, pp. 143–144, Frederick MD. BEMS, W/L Associates.
- Markov, M., Ryaby, J., Kaufman, J., and Pilla, A. (1992). Search for weak electromagnetic fields effects in cell-free myosin light chain phosphorylation. In *Charge and Field Effects in Biosystems - 3* (M. Allen, S. Cleary, A. Sowers, and D. Shillady, Eds.), p. 62. Birkhauser, Boston.
- Markx, G., and Davey, C. (1999). The dielectric properties of biological cells at radiofrequencies: Applications in biotechnology. *Enzyme Microb. Tech.* **25**, 161–171.
- Martin, H., and Lindauer, M. (1977). Der Einfluss der Erdmagnetfelds und die Schwerorientierung der Honigbiene. *J. Comp. Physiol.* **122**, 145–187.
- Martynyuk, V. (1992). On the phasing effect of infra-low-frequency magnetic fields on biological systems. *Biofizika* **37**(4), 669–673.
- Mather, J., and Baker, R. (1981). Magnetic sense of direction in woodmice for route-based navigation. *Nature* **291**, 152–155.
- Matronchik, A., Alipov, Y., and Belyaev, I. (1996a). A phase modulation model of high-frequency oscillations of a nucleotide in the response of E.coli cells to weak static and low-frequency magnetic fields. *Biofizika* **41**(3), 642–649.
- Matronchik, Y., Belyaev, I., Alipov, Y., Kravchenko, V., and Harms-Ringdahl, M. (1996b). Effect of weak magnetic fields on the conformation of chromatin in living cells and its possible physical explanation. In *Abst. III International Congress EBBA, Nancy, France*.
- Mazzoleni, A., Siskin, B., and Kahler, R. (1986). Conductivity values of tissue culture medium from 20°C to 40°C. *Bioelectromagnetics* **7**, 95–99.
- McGivern, R., Sokol, R., and Adey, W. (1990). Prenatal exposure to a low-frequency electromagnetic field demasculinized adult scent marking behavior and increases accessory sex organ weight in rats. *Teratology* **41**, 1–8.
- McLeod, B., Liboff, A., and Smith, S. (1992a). Biological systems in transition: sensitivity to extremely low-frequency fields. *Electro Magnetobiol.* **11**(1), 29–42.
- McLeod, B., Liboff, A., and Smith, S. (1992b). Electromagnetic gating in ion channels. *J. Theor. Biol.* **158**(1), 15–32.
- McLeod, B., Smith, S., and Liboff, A. (1987a). Calcium and potassium cyclotron resonance curves and harmonics in diatoms. *J. Bioelec.* **6**(2), 153–168.
- McLeod, K., Lee, R., and Ehrlich, H. (1987b). Frequency dependence of electric field modulation of fibroblast protein synthesis. *Science* **236**, 1465–1469.
- McNamara, B., and Wiesenfeld, K. (1989). Theory of stochastic resonance. *Phys. Rev. A* **39**(9), 4854–4869.

- Milham, Jr, S. (1982). Mortality from leukemia in workers exposed to electrical and magnetic fields (letter). *N. England J. Med.* **307**, 249.
- Miller, D. (1991). Useful perspective on the relation between biological and physical descriptions of phenomena. *J. Theor. Biol.* **152**, 341–355.
- Miller, J., Serio, G., Howard, R., Bear, J., Evans, J., and Kimball, A. (1979). Subunit localizations of zinc(II) in DNA-dependent RNA polymerase from *Escherichia coli* B. *Biochim. Biophys. Acta* **579**, 291–297.
- Mir, L., Orłowski, S., Jr., J. B., Teissie, J., Rols, M., Sersa, G., Miklavcic, D., Gilbert, R., and Heller, R. (1995). Biomedical applications of electric pulses with special emphasis on antitumor electrochemotherapy. *Bioelectroch. Bioener.* **38**, 203–207.
- Misakian, M., and Kaune, W. (1990). Optimal experimental design for in vitro studies with ELF magnetic fields. *Bioelectromagnetics* **11**, 251–255.
- Miyamoto, H., Yamaguchi, H., Ikehara, T., and Kinouchi, Y. (1996). Effects of electromagnetic fields on  $K^+(Rb^+)$  uptake by HeLa Cells. In *Biological Effects of Magnetic and Electromagnetic Fields* (S. Ueno, Ed.). Plenum, New York.
- Moggia, E., Chiabrera, A., and Bianco, B. (1997). Fokker-Planck analysis of the Langevin-Lorentz equation: Application to ligand-receptor binding under electromagnetic exposure. *J. Appl. Phys.* **82**(9), 4669–4677.
- Mooney, N., Smith, R., and Watson, B. (1986). Effect of extremely-low-frequency pulsed magnetic fields on the mitogenic response of peripheral blood mononuclear cells. *Bioelectromagnetics* **7**, 387–394.
- Moore, R. (1979). Biological effects of magnetic fields: Studies with microorganisms. *Can. J. Microbiol.* **25**, 1145–1151.
- Moses, A., and Basak, A. (Eds.) (1996). *Nonlinear Electromagnetic Systems*, Vol. 10 of *Studies in Applied Electromagnetics and Mechanics*. IOS Press, Amsterdam.
- Moulder, J. (2000). The Electric and Magnetic Fields Research and Public Information Dissemination (EMF-RAPID) Program. *Radiat. Res.* **153**, 613–616.
- Muehsam, D., and Pilla, A. (1994). Weak magnetic field modulation of ion dynamics in a potential well: mechanistic and thermal noise considerations. *Bioelectroch. Bioener.* **35**, 71–79.
- Mullins, J., Krause, D., and Litovitz, T. (1993). Simultaneous application of a spatially coherent noise field blocks response of cell cultures to 60 Hz EMF. In *Electricity and Magnetism in Biology and Medicine* (M. Blank, Ed.), pp. 345–346. San Francisco Press, San Francisco.
- Muzalevskaya, N., and Uritskii, V. (1997). Tumor-suppressing action of weak ELF stochastic magnetic field with an 1/f spectrum. *Biofizika* **42**(4), 961–970.
- Nakagawa, M. (1997). A study on extremely low-frequency electric and magnetic fields and cancer: Discussion of EMF safety limits. *J. Occupat. Health* **39**, 18–28.
- Nazar, A., Paul, A., and Dutta, S. (1996). Frequency-dependent alteration of enolase activity by elf fields. *Bioelectroch. Bioener.* **39**, 259–262.
- Nikollskaya, K., Shtemler, V., Savonenko, A., Osipov, A., and Nikollskii, S. (1996). Weak magnetic fields and cognitive activity. *Biofizika* **41**(4), 887–893.

- Noji, H., Yasuda, R., Yoshida, M., and Kinosita, J. (1997). Direct observation of the rotation of F1-ATPase. *Nature* **386**, 299–302.
- Nordensen, I., Mild, K., Andersson, G., and Sandstrom, M. (1994). Chromosomal aberrations in human amniotic cells after intermittent exposure to fifty hertz magnetic fields. *Bioelectromagnetics* **15**, 293–301.
- Novikov, V., and Karnaukhov, A. (1997). Mechanism of action of weak electromagnetic fields on ionic currents in aqueous solutions of amino acids. *Bioelectromagnetics* **18**(1), 25–27.
- Novikov, V., Kuvichkin, V., and Fesenko, E. (1999). Effect of weak combined dc and ac low-frequency magnetic fields on natural fluorescence of proteins in water solutions. *Biofizika* **44**(2), 224–230.
- Novikov, V., Novikova, N., and Kachan, A. (1996). Cooperative effects of weak magnetic fields on tumor forming processes in vivo. *Biofizika* **41**(4), 934–938.
- Novikov, V., and Zhadin, M. (1994). Combined effect of weak static and alternating low-frequency fields on ionic currents in aqueous solutions of amino acids. *Biofizika* **39**(1), 45–49.
- Novikov, V. (1994). Weak magnetic fields initiate formation of molecular bonds in water solutions of amino acids. *Biofizika* **39**(5), 825–830.
- Novikov, V. (1996). Cooperative effect of resonance enhancement of ion current in water solutions of amino acids under weak electromagnetic exposures. *Biofizika* **41**(5), 973–978.
- NRC (1997). *Possible Health Effects of Exposure to Residential Electric and Magnetic Fields*. Rep. Committee on the Possible Eff. Electromagn. Fields on Biol. Syst. of the Natl. Res. Council. National Academy Press, Washington, USA.
- Opalinskaya, A., and Agulova, L. (1984). *Effect of Natural and Artificial EM Fields on Physico-chemical and Elementary Biological Systems*. Tomsk Univ., Tomsk. [In Russian].
- Opdyke, N., Glass, B., Hays, J., and Foster, J. (1966). Paleomagnetic study of antarctic deep-sea cores. *Science* **154**(3747), 349.
- Oraevskii, V., Golyshev, S., Levitin, A., Breus, T., Ivanova, S., Komarov, F., and Rapoport, S. (1995). Parameters of “electromagnetic weather” in the near-Earth space, which control its biotropic properties. *Biofizika* **40**(4), 813–821.
- Ossenkopp, K., Kavaliers, M., and Hirst, M. (1983). Reduced nocturnal morphine analgesia in mice following a geomagnetic disturbance. *Neurosci. Lett.* **40**, 321–325.
- Ossenkopp, K., Kavaliers, M., Prato, F., Teskey, G., Sestini, E., and Hirst, M. (1985). Exposure to nuclear magnetic resonance imaging procedures attenuates morphine-induced analgesia in mice. *Life Sci.* **37**, 1507–1514.
- Ossenkopp, K., and Ossenkopp, M. (1983). Geophysical variables and behavior. XI. Open-field behaviors in young rats exposed to ELF rotating magnetic field. *Psychol. Rep.* **52**, 343–350.
- Ovchinnikova, G. (1993). Restructuring and charge transfer in model and biological membranes under microwave exposure. *Biologich. Membr.* **10**(5), 551–560.

- Pakhomov, A. (1993). Nonthermal action of microwaves on the function of nerve fibers. *Biofizika* **38**(2), 367–371.
- Pandey, S., Garg, T., Singh, K., and Rai, S. (1996). Effect of magnetically induced water structure on the oestrous cycles of albino female mice *Mus musculus*. *Electro Magnetobiol.* **15**(2), 133–140.
- Panth, H., Brenner, M., and Wu, F. (1991). <sup>1</sup>H NMR study of the interaction of ATP with *Escherichia coli* RNA polymerase containing in vivo-incorporated Co(II). *Arch. Biochem. Biophys.* **291**, 307–310.
- Pasechnik, V. (1985). Cytoskeleton and mechanoreception thresholds. *Biofizika* **30**(5), 858.
- Pavlovich, S., and Sluvko, A. (1975). Effect of magnetic field screening *Staphylococcus aureus*. In *Proc. 3rd All-Union Symp. "Effects of Magnetic Fields on Biological Systems"*, p. 56. Kaliningrad State Univ., Kaliningrad. [In Russian].
- Pavlovich, S. (1985). *Magnetic Susceptibility of Organisms*. Nauka i Tekhnika, Minsk. [In Russian].
- Penafiel, L., Litovitz, T., Krause, D., Desta, A., and Mullins, J. (1997). Role of modulation on the effect of microwaves on ornithine decarboxylase activity in L929 cells. *Bioelectromagnetics* **18**, 132–141.
- Persson, B., and Stahlberg, F. (1989). *Health and Safety of Clinical NMR Examinations*. CRC Press, Boca Raton, FL.
- Pestryaev, V. (1994). Controlled action of a pulsed EM field on the central nervous system. *Biofizika* **39**(3), 515–518.
- Petrosyan, V., Gulyaev, Y., Zhiteneva, E., Yelkin, V., and Sinitsyn, N. (1995). Shf electromagnetic waves interaction with physical and biological objects. *Radiotekh. Elektr.* **40**(1), 127–134. [In Russian].
- Petrosyan, V., Zhiteneva, E., Gulyaev, Y., Devyatkov, N., Yelkin, V., and Sinitsyn, N. (1996). Physics of the interaction mm-band waves with different living systems. *Radiotekhnika* (9), 20–31.
- Petrov, I., and Betskii, O. (1989). On the biological mechanism of low-energy mm-band electromagnetic radiation. In *Millimeter Waves in Medicine and Biology* (N. Devyatkov, Ed.), pp. 242–248, Moscow. Inst. Radio Engineering Electronics, Russian Academy of Sciences. [In Russian].
- Pfau, T., Spälter, S., Kurtsiefer, C., Ekstrom, C., and Mlynek, J. (1994). Loss of spatial coherence by a single spontaneous emission. *Phys. Rev. Lett.* **73**(9), 1223–1226.
- Phillips, J., Haggren, W., Thomas, W., Ishida-Jones, T., and Adey, W. (1992). Magnetic field-induced changes in specific gene transcription. *Biochim. Biophys. Acta* **1132**, 140–144.
- Phillips, J., and McChesney, L. (1991). Effect of 72 Hz pulsed magnetic field exposure on macromolecular synthesis in CCRF-CEM cells. *Cancer Biochem. Biophys.* **12**, 1–7.
- Phillips, J., Rutledge, L., and Winters, W. (1986a). Transferring binding to two human colon carcinoma cell lines: Characterization and effect of 60-Hz electromagnetic fields. *Cancer Res.* **46**, 239–244.

- Phillips, J., Winters, W., and Rutledge, L. (1986b). In vitro exposure to electromagnetic fields: Changes in tumor cell properties. *Int. J. Radiat. Biol.* **49**, 463.
- Picazo, M., Vallejo, D., and Bardasano, J. (1994). An introduction to the study of ELF magnetic field effects on white blood cells in mice. *Electro Magnetobiol.* **13**(1), 77–84.
- Piccardi, G. (1962). *The Chemical Basis of Medical Climatology*. Charles C. Thomas, Illinois.
- Pilla, A., Nasser, P., and Kaufman, J. (1994). Gap junction impedance, tissue dielectrics and thermal noise limits for electromagnetic field bioeffects. *Bioelectroch. Bioener.* **35**, 63–69.
- Piruzyan, L., and Kuznetsov, A. (1983). Effect of static and low-frequency magnetic fields on biological systems. *Dokl. Akad. Nauk SSSR, Biol.* (6), 805–821.
- Piruzyan, L., Lazarev, A., Kshutashvili, T., Uliyankin, I., and Kuznetsov, A. (1984). Influence of low-frequency magnetic fields on the Na current in myocardial cells. *Dokl. Akad. Nauk SSSR, Biol.* **274**(4), 952.
- Pittman, U., and Ormrod, D. (1970). Physiological and chemical features of magnetically treated winter wheat seeds and resultant seedlings. *Can. J. Plant Sci.* **50**, 211–217.
- Plekhanov, G. (1990). *Main Regularities of Low-Frequency Electromagnetobiology*. Tomsk State Univ., Tomsk. [In Russian].
- Plusnina, T., Riznichenko, G., Aksenov, S., and Chernyakov, G. (1994). Effect of a weak electric field on the trigger system of the transmembrane ion transfer. *Biofizika* **39**(2), 345–350.
- Pohl, H., and Pollock, J. (1986). Orbitally magnetized organic solids. *J. Biol. Phys.* **14**(1), 9–14.
- Pokorný, J. (1982). Multiple Fröhlich coherent states in biological systems: Computer simulation. *J. Theor. Biol.* **98**, 21–27.
- Polk, C., and Postow, E. (Eds.) (1997). *Handbook of Biological Effects of Electromagnetic Fields*, second ed. CRC Press, Boca Raton, FL.
- Polk, C. (1986). Physical mechanisms by which low-frequency magnetic fields can affect the distribution of counterions on cylindrical biological cell surfaces. *J. Biol. Phys.* **14**(1), 3–8.
- Polk, C. (1989). Nuclear precessional magnetic resonance as a cause for biological effects of time varying electric or magnetic fields in the presence of an earth-strength static magnetic field. In *Proc. Eleventh Ann. Meet. Bioelectromagnet. Soc.*, Frederic, MD. BEMS.
- Polk, C. (1991). Biological effects of low-level low-frequency electric and magnetic fields. *IEEE Trans. Educat.* **34**(3), 243–249.
- Pool, R. (1990a). Electromagnetic fields: The biological evidence. *Science* **249**, 1378–1381.
- Pool, R. (1990b). Is there an EMF-cancer connection? *Science* **249**, 1096–1098.
- Popp, F. (Ed.) (1979). *Electromagnetic Bioinformation*. Urban and Schwarzenberg, Vienna.

- Porschke, D., and Grell, E. (1995). Electric parameters of  $\text{Na}^+/\text{K}^+$ -ATPase by measurements of the fluorescence-detected electric dichroism. *Biochim. Biophys. Acta* **1231**, 181–188.
- Portier, C., and Wolfe, M. (Eds.) (1998). *Assessment of Health Effects from Exposure to Power-Line Frequency Electric and Magnetic Fields. Working Group Report*. No. 98-3981. NIEHS/NIH, PO Box 12233, Res. Triangle Park, NC 27709.
- Prato, F., Carson, J., Ossenkopp, K., and Kavaliers, M. (1995). Possible mechanism by which extremely low frequency magnetic fields affect opioid function. *FASEB J.* **9**, 807–814.
- Prato, F., Kavaliers, M., Carson, J., and Ossenkopp, K. (1993). Magnetic field exposure at 60 Hz attenuates endogenous opioid-induced analgesia in a land snail consistent with the quantum mechanical predictions of the Lednev model. In *Abst. 15th BEMS Meeting*, Los Angeles, CA. BEMS. A-1-1.
- Prato, F., Kavaliers, M., Cullen, A., and Thomas, A. (1997). Light-dependent and -independent behavioral effects of extremely low frequency magnetic fields in a land snail are consistent with a parametric resonance mechanism. *Bioelectromagnetics* **18**, 284–291.
- Prato, F., Kavaliers, M., and Thomas, A. (1996). ELF magnetic fields both increase and decrease opioid-induced analgesia in the land snail consistent with the predictions of the parametric resonance model (PRM) for  $\text{Ca}^{2+}$ . In *Abst. 18th BEMS Meeting*, pp. 133–134, Victoria, Canada.
- Presman, A. (1970). *Electromagnetic Fields and Life*. Plenum, New York.
- Preston-Martin, S., Navidi, W., Thomas, D., Lee, P.-J., Bowman, J., and Pogoda, J. (1996). Los Angeles study of residential magnetic fields and childhood brain tumors. *Am. J. Epidemiol.* **143**(2), 105–119.
- Prigogine, I. (1980). *From Being to Becoming: Time and Complexity in the Physical Sciences*. Freeman, San Francisco.
- Privalov, P. (1968). Water and its role in biological systems. *Biofizika* **13**(1), 163–177.
- Purich, D. L., and Allison, R. D. (2000). *Handbook of Biochemical Kinetics*. Academic Press, San Diego.
- Pushchino (1992). Proc. 2nd All-Union Symp. “Cosmophysical Fluctuations in Biological and Physico-chemical Systems”. Pushchino, Nov. 1990. *Biofizika* **37**(3–4).
- Pushchino (1995). Proc. 3rd Int. Symp. “Cosmogeophysical Correlations in Biological and Physico-chemical Processes”. Pushchino, Nov. 1993. *Biofizika* **40**(4–5).
- Pushchino (1998). Proc. 4th Int. Symp. “Cosmogeophysical Correlations in Biological and Physico-chemical Processes”. Pushchino, Sep. 1996. *Biofizika* **43**(4).
- Quinn, T., Merrill, R., and Brannon, E. (1981). Magnetic field detection in sockeye salmon. *J. Exp. Zool.* **217**, 137–142.
- Rai, S., Garg, T., and Vashistha, H. (1996). Possible effect of magnetically induced water structures on photosynthetic electron transport chains of a green alga *Chlorella vulgaris*. *Electro Magnetobiol.* **15**(1), 49–55.

- Rai, S., Singh, U., Singh, K., and Singh, A. (1994). Germination responses of fungal spores to magnetically restructured water. *Electro Magnetobiol.* **13**(3), 237–246.
- Ramirez, E., Monteagudo, J., Garcia-Gracia, M., and Delgado, J. (1983). Oviposition and development of *Drosophila* modified by magnetic fields. *Bioelectromagnetics* **4**(4), 315–326.
- Ramundo-Orlando, A., Morbiducci, U., Mossa, G., and D’Inzeo, G. (2000). Effect of low frequency, low amplitude magnetic fields on the permeability of cationic liposomes entrapping carbonic anhydrase. *Bioelectromagnetics* **21**, 491–498.
- Rapoport, S. (1968). *Medical Biochemistry*. Mir, Moscow.
- Raskmark, P., and Kwee, S. (1996). The minimizing effect of electromagnetic noise on the changes in cell proliferation caused by ELF magnetic fields. *Bioelectroch. Bioener.* **40**, 193–196.
- Rea, W., Pan, Y., Fenyves, E., Sujisawa, I., Samadi, N., and Ross, G. (1991). Electromagnetic field sensitivity. *J. Bioelectricity* **10**, 241–256.
- Reese, J., Fraizer, M., Morris, J., Buschbom, R., and Miller, D. (1991). Evaluation of changes in diatom mobility after exposure to 16-Hz electromagnetic fields. *Bioelectromagnetics* **12**, 21–25.
- Reinbold, K., and Pollack, S. (1997). Serum plays a critical role in modulating  $[Ca^{2+}]_c$  of primary culture bone cells exposed to weak ion-resonance magnetic fields. *Bioelectromagnetics* **18**, 203–214.
- Reiter, R., and Robinson, J. (1993). *Melatonin: Your Body’s Natural Wonder Drug*. Bantam, New York.
- Reiter, R. (1992). Changes in circadian melatonin synthesis in the pineal gland of animals exposed to extremely low frequency electromagnetic radiation: A summary of observations and speculation on their implications. In *Electromagnetic Fields and Circadian Rhythmicity* (M. Moore-Ede, S. Campbell, and R. Reiter, Eds.), pp. 13–25. Birkhauser, Boston.
- Reiter, R. (1998). Melatonin in the context of the reported bioeffects of environmental electromagnetic fields. *Bioelectroch. Bioener.* **47**, 135–142.
- Repacholi, M., and Greenebaum, B. (1999). Interaction of static and extremely low frequency electric and magnetic fields with living systems: Health effects and research needs. *Bioelectromagnetics* **20**(3), 133–160.
- Richards, P., Persinger, M., and Koren, S. (1996). Modification of semantic memory in normal subjects by application across the temporal lobes of a weak (1 microT) magnetic field structure that promotes long-term potentiation in hippocampal slices. *Electro Magnetobiol.* **15**(2), 141–148.
- Robinson, K. (1985). The responses of cells to electrical fields: A review. *J. Cell Biol.* **101**, 2023–2027.
- Romanovsky, Y., Stepanova, N., and Chernavsky, D. (1984). *Mathematical Biophysics*. Nauka, Moscow. [In Russian].
- Ross, S. (1990). Combined DC and ELF magnetic fields can alter cell proliferation. *Bioelectromagnetics* **11**, 27–36.

- Rozek, R., Sherman, M., Liboff, A., McLeod, B., and Smith, S. (1987). Nifedipine is an antagonist to cyclotron resonance enhancement of  $^{45}\text{Ca}$  incorporation in human lymphocytes. *Cell Calcium* **8**, 413–427.
- Rubakov, V. (2000). On the book “A theory of physical vacuum” by G.I. Shipov. *Usp. Fiz. Nauk* **170**(3), 351–352.
- Ruhenstroth-Bauer, G., Hoffmann, G., Vogl, S., Baumer, H., Kulzer, R., Peters, J., and Staub, F. (1994). Artificial simulation of naturally occurring, biologically active atmospheric fields. *Electro Magnetobiol.* **13**(1), 85–92.
- Ružič, R., Jerman, I., and Gogala, N. (1998). Water stress reveals effects of ELF magnetic fields on the growth of seedlings. *Electro Magnetobiol.* **17**(1), 17–30.
- Ružič, R., Jerman, I., Jeglič, A., and Fefer, D. (1992). Electromagnetic stimulation of buds of *Castanea sativa*, Mill. in tissue culture. *Electro Magnetobiol.* **11**(2), 145–153.
- Ružič, R., Jerman, I., Jeglič, A., and Fefer, D. (1993). Various effects of pulsed and static magnetic fields on the development of *Castanea sativa* Mill. in tissue culture. *Electro Magnetobiol.* **12**(2), 165–177.
- Ružič, R., and Jerman, I. (1998). Influence of  $\text{Ca}^{2+}$  in biological effects of direct and indirect ELF magnetic field stimulation. *Electro Magnetobiol.* **17**(2), 205–216.
- Ryabyh, T., and Mansurova, L. (1992). Relation between the sector structure of the interplanetary magnetic field and hematological indexes in normal and tumor processes. *Biofizika* **37**(4), 716–719.
- Ryaby, J. (1998). Clinical effects of electromagnetic and electric fields on fracture healing. *Clin. Orthop.* **355**(Suppl.), 205–215.
- Saali, K., Juutilainen, J., and Lahtinen, T. (1986). Effects of low frequency magnetic fields on chick embryos and embryonal chick tibia. In *Electromagnetic Fields and Biomembranes* (M. Markov, and M. Blank, Eds.). Plenum, New York.
- Sagan, L. (1996). *Electric and Magnetic Fields: Invisible Risks?* Gordon and Breach, New York.
- Sage, C., and Sampson, M. (1996). *Epidemiology for decisionmakers: A visual guide to residential and occupational EMF epidemiological results.* Sage Associates, Santa Barbara, CA.
- Salikhov, K., Molin, Y., Sagdeev, R., and Buchachenko, A. (1984). *Spin Polarization and Magnetic Effects in Radical Reactions.* Elsevier, Amsterdam.
- Sandweiss, J. (1990). On the cyclotron resonance model of ion transport. *Bioelectromagnetics* **11**, 203–205.
- Sapogov, A. (1992). On poor repeatability of magnetobiological experiments. *Biofizika* **37**(4), 769–771.
- Sasamori, R., Okaue, Y., Isobe, T., and Matsuda, Y. (1994). Stabilization of atomic hydrogen in both solution and crystal at room temperature. *Science* **265**, 1691–1693.
- Sastre, A., Cook, M., and Graham, C. (1998). Nocturnal exposure to intermittent 60 Hz magnetic fields alters human cardiac rhythm. *Bioelectromagnetics* **19**(2), 98–106.

- Satyshur, K., Rao, S., Pyzalska, D., Drendel, W., Greaser, M., and Sundaralingam, M. (1988). Refined structure of chicken skeletal muscle troponin C in the two-calcium state at 2-Å resolution. *J. Biol. Chem.* **263**(4), 1628–1647.
- Saunders, M., Jimenez-Vazquez, H., Cross, R., Mroczkowski, S., Freedberg, D., and Anet, F. (1994). Probing the interior of fullerenes by  $^3\text{He}$  NMR spectroscopy of endohedral  $^3\text{He}@C_{60}$  and  $^3\text{He}@C_{70}$ . *Nature* **367**, 256–258.
- Savin, A., and Manevitch, L. (1998). Solitons in crystalline polyethylene: A chain surrounded by immovable neighbors. *Phys. Rev. B* **58**(17), 11386–11400.
- Schimmelpfeng, J., and Dertinger, H. (1997). Action of a 50 Hz magnetic field on proliferation of cells in culture. *Bioelectromagnetics* **18**, 177–183.
- Schwartz, J.-L., House, D., and Mealing, G. (1990). Exposure of frog heats to CW or amplitude-modulated VHF fields: Selective efflux of calcium ions at 16 Hz. *Bioelectromagnetics* **11**, 349–358.
- Scott, A. (1981). The laser-Raman spectrum of a Davydov soliton. *Phys. Lett. A* **86**(1), 60–62.
- Semikin, V., and Golubeva, M. (1975). Diurnal biorhythm in the optical activity of plants screened from the local magnetic field. In *Proc. 3rd All-Union Symp. "Effect of Magn. Fields on Biol. Objects"*, p. 183, Kaliningrad. Kaliningrad State Univ. [In Russian].
- Semm, P., and Beason, R. (1990). Responses to small magnetic variations by the trigeminal system of the bobolink. *Brain Res. Bull.* **25**(5), 735–740.
- Serpersu, E., and Tsong, T. (1983). Stimulation of a ouabain-sensitive  $\text{Rb}^+$  uptake in human erythrocytes with an electric field. *J. Membrane Biol.* **74**, 191–201.
- Serpersu, E., and Tsong, T. (1984). Activation of electrogenic  $\text{Rb}^+$  transport of Na, K-ATPase by an electric field. *J. Biol. Chem.* **259**, 7155–7162.
- Shaya, S., and Smith, C. (1977). The effects of magnetic and radiofrequency fields on the activity of lysozyme. *Coll. Phenom.* **2**, 215–218.
- Shemii-Zade, A. (1992). Conversion of a pulse of solar-geomagnetic activity into perturbations of radon and aeroion fields of the planet. *Biofizika* **37**(4), 690–699.
- Shiga, T., Okazaki, M., Maeda, N., and Seiyama, A. (1996). Effects of static magnetic fields on erythrocyte rheology. In *Biological Effects of Magnetic and Electromagnetic Fields* (S. Ueno, Ed.). Plenum, New York.
- Shilov, V., Rabinovich, E., and Kuznetsov, A. (1983). Influence of a static magnetic field on chemiluminescence of a skin at destruction. *Biofizika* **28**(5), 863–865.
- Shipov, G. (1998). *A Theory of Physical Vacuum. A New Paradigm*, third ed. GART, Moscow.
- Shirahata, S., Kabayama, S., Nakano, M., Miura, T., Kusumoto, K., Gotoh, M., Hayashi, H., Otsubo, K., Morisawa, S., and Katakura, Y. (1997). Electrolyzed-reduced water scavenges active oxygen species and protects DNA from oxidative damage. *Biochem. Biophys. Res. Comm.* **234**, 269–274.
- Shnoll, S. (1995a). 3rd Int. Symp. "Cosmogeophys. Correlations in Biological and Physico-chemical Processes. Pushchino, 26 Sept. – 1 Oct. 1993". *Biofizika* **40**(4), 725–731.

- Shnoll, S. (1995b). Spectra of states realized in macroscopic fluctuations depend on the rotation of the Earth. *Biofizika* **40**(4), 865–875.
- Shnoll, S. (1997). *Heroes and Villains in Russian Science*. Kron-Press, Moscow. [In Russian].
- Shrager, L. (1975). Cytogenetic effect of attenuated magnetic fields on right and left isomers of onion. In *Proc. 3rd All-Union Symp. "Influence of Magnetic Fields on Biological Objects"*, p. 194, Kaliningrad. Kaliningrad State Univ. [In Russian].
- Shuvalova, L., Ostrovskaya, M., Sosunov, E., and Lednev, V. (1991). The effect of a weak magnetic field in the parametric resonance mode on the rate of the calmodulin-dependent phosphorylation of myosin in solution. *Dokl. Akad. Nauk SSSR* **317**(1), 227–230.
- Sidyakin, V. (1992). Influence of solar activity fluctuations on biological systems. *Biofizika* **37**(4), 647–652.
- Sienkiewicz, Z., Haylock, R., Bartrum, R., and Saunders, R. (1998). 50 Hz magnetic field effects on the performance of a spatial learning task by mice. *Bioelectromagnetics* **19**(8), 486–493.
- Simkó, M., Kriehuber, R., and Lange, S. (1998). Micronucleus formation in human amnion cells after exposure to 50 Hz MF applied horizontally and vertically. *Mutation Res.* **418**, 101–111.
- Simonov, A., Livshitz, V., and Kuznetsov, A. (1986). Static magnetic field effect on formation of two-layer lipid membranes. *Biofizika* **31**(5), 777–780.
- Simon, N. (1992). *Biological Effects of Static Magnetic Fields: A Review*. Int. Cryogen. Mat. Commission, Boulder, CO.
- Singh, S., Rai, S., Rai, A., Tewary, S., Singh, S., Samarketu, and Abraham, J. (1994). Athermal physiological effects of microwaves on a cyanobacterium *Nostoc muscorum*: evidence for EM-memory bits in water. *Biomed. Biol. Eng. Comput.* **32**, 175–180.
- Sinitsyn, N., Petrosyan, V., Yelkin, V., Devyatkov, N., Gulyaev, Y., and Betsky, O. (1998). Particular role of the system “millimeter waves — water medium” in nature. *Biomed. Radioelektron.* (1), 5–23.
- Sisken, J., Shahidain, R., and Sisken, B. (1996). Failure to detect effects of exogenous ELF EMF on baseline  $[Ca^{2+}]_i$  and spontaneous calcium spiking activity in ROS 17/2.8 cells. In *Abst. 18th BEMS Meeting*, pp. 8–9, Victoria, Canada.
- Sizov, Y., Tsyullnik, L., Kanonidi, K., Oraevskii, V., Glukhov, D., Kimlyk, M., Komarov, F., Ushakov, I., and Shalimov, P. (1997). Heliogeophysical factors among possible causes flight accidents and catastrophes. In *Abst. 1 Int. Congress Weak and Hyperweak Fields Radiat. Biol. Med.*, pp. 259–260, St. Petersburg.
- Skarzhinsky, V. (1985). Aharonov–Bohm effect: theory and interpretation. In *Group Theory, Gravitation and Physics of Elementary Particles*, pp. 139–161. Nauka, Moscow. [In Russian].
- Skiles, D. (1985). Geomagnetic field: its nature, history, and significance for biology. In *Magnetite Biomineralization and Magnetoreception in Organisms. A New*

- Biomagnetism* (J. Kirschvink, D. Jones, and B. MacFadden, Eds.). Plenum, New York.
- Slichter, C. (1980). *Principles of Magnetic Resonance*, second ed. Springer-Verlag, Berlin.
- Sluvko, A. (1975). Variation of corinobacteria of diphtheria conditioned in a permalloy chamber. In *Proc. 3rd All-Union Symp. "Influence of Magn. Fields on Biol. Objects"*, p. 61, Kaliningrad. Kaliningrad State Univ. [In Russian].
- Smith, O., Goodman, E., Greenebaum, B., and Tipnis, P. (1991). An increase in the negative surface charge of U937 cells exposed to a pulsed magnetic field. *Bioelectromagnetics* **12**, 197–202.
- Smith, R. (1988). Lithium as a normal metabolite: some implications for cyclotron resonance of ions in magnetic fields. *Bioelectromagnetics* **9**, 387–391.
- Smith, S., McLeod, B., Liboff, A., and Cooksey, K. (1987). Calcium cyclotron resonance and diatom mobility. *Bioelectromagnetics* **8**, 215–227.
- Smith, S., McLeod, B., and Liboff, A. (1992). Effects of ion resonance tuned magnetic fields on n-18 murine neuroblastoma cells. In *Charge and Field Effects in Biosystems - 3* (M. Allen, S. Cleary, A. Sowers, and D. Shillady, Eds.), p. 64. Birkhauser, Boston.
- Smith, S., McLeod, B., and Liboff, A. (1995). Testing the ion cyclotron resonance theory of electromagnetic field interaction with odd and even harmonic tuning for cations. *Bioelectroch. Bioener.* **38**, 161–167.
- Smolyanskaya, A., Gelvich, E., Golant, M., and Makhov, A. (1979). Resonance phenomena in biological objects under millimeter EM wave exposure. *Usp. Sovrem. Biol.* **87**(3), 381–392.
- Sollazzo, V., Massari, L., Caruso, A., Mattei, M. D., and Pezzetti, F. (1996). Effects of low-frequency pulsed electromagnetic fields on human osteoblast-like cells in vitro. *Electro Magnetobiol.* **15**(1), 75–83.
- Sontag, W. (1998). Action of extremely low frequency electric fields on the cytosolic calcium concentration of differentiated HL-60 cells: Nonactivated cells. *Bioelectromagnetics* **19**(1), 32–40.
- Sontag, W. (2000). Modulation of cytokine production by interferential current in differentiated HL-60 cells. *Bioelectromagnetics* **21**(3), 238–244.
- Spadinger, I., Agnew, D., and Palcic, B. (1995). 3T3 cell motility and morphology before, during, and after exposure to extremely-low-frequency magnetic fields. *Bioelectromagnetics* **16**, 178–187.
- Steiner, U., and Ulrich, T. (1989). Magnetic field effects in chemical kinetics and related phenomena. *Chem. Rev.* **89**(1), 51–147.
- Stepanov, E., Milyaev, V., and Selivanov, Y. (2000). Laser orthomolecular medical diagnostics. *Usp. Fiz. Nauk* **170**(4), 458–462.
- Stepanyan, R., Ayirapetyan, G., Arakelyan, A., and Ayirapetyan, S. (1999). Effect of mechanical oscillations on electrical conductivity of water. *Biofizika* **44**(2), 197–202.
- Stern, D. (1996). A brief history of magnetospheric physics during the space age. *Rev. Geophys.* **34**(1), 1–31.

- Stern, S., and Laties, V. (1998). 60 Hz electric fields and incandescent light as aversive stimuli controlling the behavior of rats responding under concurrent schedules of reinforcement. *Bioelectromagnetics* **19**(4), 210–221.
- Stevens, R., Wilson, B., and Anderson, L. (Eds.) (1997). *The Melatonin Hypothesis: Breast Cancer and Use of Electric Power*. Battelle Press, Columbus, OH.
- Stillings, D. (1997). The history of electricity in life as reflected in the collections of the Bakken Library. In *Abst. 2 World Congress Elect. Magn. Biol. Med.*, p. 237, Bologna, Italy. BEMS.
- Strand, J., Abernethy, C., Skalski, J., and Genoway, R. (1983). Effects of magnetic field exposure on fertilization success in rainbow trout *Salmo gairdneri*. *Bioelectromagnetics* **4**, 295–301.
- Suckling, C., Gibson, C., and Pitt, A. (Eds.) (1998). *Enzyme Chemistry: Impact and Applications*, third ed. Kluwer, Dordrecht.
- Sudbery, A. (1986). *Quantum Mechanics and the Particles of Nature. An Outline for Mathematicians*. Cambridge Univ. Press, Cambridge.
- Sudbery, T. (1997). The fastest way from A to B. *Nature* **390**, 551–552.
- Sushkov, F. (1975). Equivalence of some response of culture tissue cells to increase and decrease of a magnetic field. In *Physical, Mathematical and Biological Problems of the Action of Magnetic Fields and Ionization of Air*, Vol. 2, pp. 112–113. Nauka, Moscow. [In Russian].
- Suvorov, G., Paltsev, Y., Khundanov, L., Rubtsova, N., Nikonova, K., and Pokhodzei, L. (1998). *Non-ionizing Electromagnetic Radiation and Fields (Environmental and Hygienic Aspects)*. Vooruzheniye. Politika. Konversiya, Moscow.
- Sybesma, C. (1989). *Biophysics: An Introduction*. Kluwer/Plenum, Dordrecht.
- Takahashi, K., Kaneko, I., Date, M., and Fukada, E. (1986). Effect of pulsing electromagnetic fields on DNA synthesis in mammalian cells in culture. *Experientia* **42**, 185–186.
- Tang, Q., Chen, G., and Zhao, N. (1998). Effects of ELF electric field on proliferation of mouse osteoblastic cells. *Bioelectroch. Bioener.* **47**(2), 349–353.
- Taoka, S., Padmakumar, R., Grissom, C., and Banerjee, R. (1997). Magnetic field effects on coenzyme B<sub>12</sub>-dependent enzymes: Validation of ethanolamine ammonia lyase results and extension to human methylmalonyl CoA mutase. *Bioelectromagnetics* **18**, 506–513.
- Taubes, G. (1993). EMF-cancer links: Yes, No, and Maybe. *Science* **262**, 649.
- Taylor, R., and Walton, D. (1993). The chemistry of fullerenes. *Nature* **363**, 685–693.
- Temuriyants, N., Makeev, V., and Malygina, V. (1992a). Influence of weak ELF magnetic fields on infradyan rhymes of sympathoadrenalic system of rats. *Biofizika* **37**(4), 653–655.
- Temuriyants, N., Vladimirkii, B., and Troshkin, O. (1992b). *Extremely Low Frequency Electromagnetic Signals in Biological World*. Naukova Dumka, Kiev. [In Russian].

- Tenforde, T., and Kaune, W. (1987). Interaction of extremely low frequency electric and magnetic fields with humans. *Health Phys.* **53**, 585–607.
- Tenforde, T. (1992). Biological interactions and potential health effects of extremely-low-frequency magnetic fields from power lines and other common sources. *Annu. Rev. Public. Health.* **13**, 173–196.
- Theriault, G., Goldberg, M., Miller, A., Armstrong, B., Guenel, P., Deadman, J., Imbernon, E., To, T., Chevalier, A., Cyr, D., and Wall, C. (1994). Cancer risks associated with occupational exposure to magnetic fields among electric utility workers in Ontario and Quebec, Canada, and France: 1970–1989. *Am. J. Epidem.* **139**(6), 550–572.
- Thomas, J., Schrot, J., and Liboff, A. (1986). Low-intensity magnetic fields alter operant behavior in rats. *Bioelectromagnetics* **7**, 349–357.
- Thompson, C., Yang, Y., Anderson, V., and Wood, A. (2000). A cooperative model for  $\text{Ca}^{++}$  efflux windowing from cell membranes exposed to electromagnetic radiation. *Bioelectromagnetics* **21**, 455–464.
- Tofani, S., Ferrara, A., Anglesio, L., and Gilli, G. (1995). Evidence for genotoxic effects of resonant ELF magnetic fields. *Bioelectroch. Bioener.* **36**, 9–13.
- Tolstoi, N., and Spartakov, A. (1990). A new type of magnetism — Arhomagnetism. *Pis'ma Zh. Eksp. Teor. Fiz.* **52**(3), 796–799.
- Trillo, M., Ubeda, A., Blanchard, J., House, D., and Blackman, C. (1996). Magnetic fields at resonant conditions for the hydrogen ion affect neurite outgrowth in PC-12 cells: A test of the Ion Parametric Resonance model. *Bioelectromagnetics* **17**(1), 10–20.
- Trukhanov, K. (1975). On the possible role of the Aharonov–Bohm effect in biological effect of magnetic fields. In *Physical, Mathematical, and Biological Foundations of the Action of EM Fields and Air Ionization*, pp. 151–152. Nauka, Moscow. [In Russian].
- Tsong, T. (1992). Molecular recognition and processing of periodic signals in cells: study of activation of membrane ATPases by alternating electric fields. *Biochim. Biophys. Acta* **1113**, 53–70.
- Tuszynski, J., Paul, R., Chatterjee, R., and Sreenivasan, S. (1984). Relationship between Fröhlich and Davydov models of biological order. *Phys. Rev. A* **30**(5), 2666–2675.
- Tyasto, M., Ptitsyna, N., Kopytenko, Y., Voronov, P., Kopytenko, E., Villorezi, J., and Yuchchi, N. (1995). Influence of natural and anthropogenic EM fields on the occurrence rate of pathologies in St. Petersburg. *Biofizika* **40**(4), 839–847. [In Russian].
- Ueno, S. (Ed.) (1996). *Biological Effects of Magnetic and Electromagnetic Fields*. Kluwer/Plenum, New York.
- Uffen, R. (1963). Influence of the Earth's core on the origin and evolution of life. *Nature* **198**, 143–144.
- Usacheva, M. (1981). *Use of dc Magnetic Fields in Skin Surgery*. Meditsina, Moscow. [In Russian].

- Valberg, P. (1995). Designing EMF experiments: What is required to characterize "Exposure"? *Bioelectromagnetics* **16**(6), 396–401.
- Valet, J.-P., and Meynadier, L. (1993). Geomagnetic field intensity and reversals during the past four million years. *Nature* (6452), 234.
- Vanag, V., and Kuznetsov, A. (1988). Magnetic spin effects in biological systems. *Izv. Akad. Nauk SSSR, Biol.* (2), 215–228.
- Verreault, R., Weiss, N., Hollenbach, K., Strader, C., and Daling, J. (1990). Use of electric blankets and risk of testicular cancer. *Am. J. Epidemiol.* **131**, 759–762.
- Villoresi, J., Breus, T., Dorman, L., Yuchi, N., and Rapoport, S. (1995). Influence of interplanetary and geomagnetic perturbations on the rate of clinically severe pathologies (hard attacks and strokes). *Biofizika* **40**(5), 983–993.
- Vitiello, G. (1992). Coherence and electromagnetic fields in living matter. *Nanobiology* **1**, 221–228.
- Vladimirskii, B., Narmanskii, V., and Temuriyants, N. (1995). Global rhythmic activity of the solar system in the terrestrial biosphere. *Biofizika* **40**(4), 749–754.
- Vladimirskii, B., Volynskii, A., Vinogradov, S., Brodovskaya, Z., Temuriyants, N., Achkasova, Y., Rosenberg, V., and Chelkova, Z. (1971). Experimental studies of the effect of ELF EM fields on hemothermals and microorganisms. In *Effect of Solar Activity on the Terrestrial Atmosphere and Biosphere*, pp. 224–233. Nauka, Moscow. [In Russian].
- Vladimirskii, B. (1971). On possible factors of solar activity affecting processes in the biosphere. In *Effect of Solar Activity on the Terrestrial Atmosphere and Biosphere*, pp. 126–141. Nauka, Moscow. [In Russian].
- Vladimirskii, B. (1995). "Solar activity — biosphere" — The historically first interdisciplinary large-scale problem. *Biofizika* **40**(5), 950–958. [In Russian].
- Volkenstein, M. (1983). *General Biophysics*. Academic Press, New York.
- Vvedenskii, V., and Ozhogin, V. (1986). *Supersensitive Magnetometry and Biomagnetism*. Nauka, Moscow. [In Russian].
- Wagner, M., Huang, R., Eglin, J., and Dye, J. (1994). An electrified ring with a large six-electron ring. *Nature* **368**, 726–729.
- Walcott, C., Gould, J., and Kirschvink, J. (1979). Pigeons have magnets. *Science* **205**(4410), 1027–1029.
- Walleczek, J., and Budinger, T. (1992). Pulsed magnetic field effects on calcium signaling in lymphocytes: dependence on cell status and field intensity. *FEBS Lett.* **314**(3), 351–355.
- Walleczek, J. (1992). Electromagnetic field effects on cells of the immune system: The role of calcium signaling. *FASEB J.* **6**, 3176–3185.
- Warnke, U., and Popp, F. (1979). Some aspects of magnetic influences on biological systems. In *Electromagnetic Bio-Information* (F. Popp, G. Becker, H. König, and W. Peschka, Eds.), pp. 195–199. Urban & Schwarzenberg, München.
- Watterson, J. (1988). The role of water in cell architecture. *Mol. Cell. Biochem.* **79**(2), 101–105.

- Weaver, J., and Astumian, R. (1990). The response of living cells to very weak electric fields: The thermal noise limit. *Science* **247**, 459–462.
- Webb, S., and Booth, A. (1969). Absorption of microwaves by microorganisms. *Nature* **222**, 1199–1200.
- Webb, S., and Dodds, D. (1968). Microwave inhibition of bacterial growth. *Nature* **218**(5139), 374–375.
- Webb, S. (1979). Factors affecting the induction of lambda prophages by millimeter microwaves. *Phys. Lett. A* **73**(2), 145–148.
- Webb, S. (1980). Laser-Raman spectroscopy of living cells. *Phys. Rep.* **60**(4), 201–224.
- West, R., Hinson, W., and Swicord, M. (1996). Anchorage-independent growth with JB6 cells exposed to 60 Hz magnetic fields at several flux densities. *Bioelectroch. Bioener.* **39**, 175–179.
- Wever, R. (1973). Human circadian rhythms under the influence of weak electric fields and the different aspects of these studies. *Int. J. Biometeor.* **17**(3), 227–232.
- White, R., and Geballe, T. (1979). *Long Range Order in Solids*. Academic Press, New York.
- White, R. (1970). *Quantum Theory of Magnetism*. McGraw-Hill, New York.
- Whitson, G., Carrier, W., Francis, A., Shih, C., Georghiou, S., and Regan, J. (1986). Effects of extremely low frequency (ELF) electric fields on cell growth and DNA repair in human skin fibroblasts. *Cell Tissue Kinet.* **19**(1), 39–47.
- Wiesenfeld, K., and Moss, F. (1995). Stochastic resonance and the benefits of noise: from ice ages to crayfish and SQUIDS. *Nature* **373**, 33–36.
- Williams, M., Goodfellow, J., and Thornton, J. (1994). Buried waters and internal cavities in monomeric proteins. *Protein Sci.* **3**, 1224–1235.
- Wilson, B., Anderson, L., Hilton, D., and Phillips, R. (1981). Chronic exposure to 60 Hz fields: Effect on pineal function in the rat. *Bioelectromagnetics* **2**, 371–380.
- Wilson, B., Stevens, R., and Anderson, L. (Eds.) (1990). *Extremely Low Frequency Electromagnetic Fields: The Question of Cancer*. Battelle Press, Columbus, OH.
- Wiltschko, W., Nohr, D., Fuller, E., and Wiltschko, R. (1986). Pigeon homing: The use of magnetic information in position finding. In *Biophysical Effects of Steady Magnetic Fields* (G. Maret, N. Boccara, and J. Kiepenheuer, Eds.), pp. 154–162. Springer-Verlag, New York.
- Winfrey, A. (1994). Persistent tangled vortex rings in generic excitable media. *Nature* **371**(6494), 233–236.
- Wolff, D., Poirier, P., Brostrom, C., and Brostrom, M. (1977). Divalent cation binding properties of bovine brain  $\text{Ca}^{2+}$ -dependent regulator protein. *J. Biol. Chem.* **252**, 4108–4117.
- Wu, T., and Austin, S. (1977). Bose condensation in biosystems. *Phys. Lett. A* **64**(1), 151–152.

- Wu, T., and Austin, S. (1978). Cooperative behavior in biological systems. *Phys. Lett. A* **65**(1), 74–76.
- Wu, T. (1994). Fröhlich's theory of coherent excitations — A retrospective. In *Bioelectrodynamics and Biocommunication* (M.-W. Ho, F.-A. Popp, and U. Warnke, Eds.), pp. 387–409. World Scientific, Singapore.
- Wu, T. (1996). Quantum mechanical concepts of coherent states in biological systems. *Bioelectroch. Bioener.* **41**, 19–26.
- Yano, A., Hidaka, E., Fujiwara, K., and Iimoto, M. (2001). Induction of primary root curvature in radish seedlings in a static magnetic field. *Bioelectromagnetics* **22**(3), 194–199.
- Yeagley, H. (1947). A preliminary study of a physical basis of bird navigation. *J. Appl. Phys.* **18**, 1035–1063.
- Yemets, B. (1999). On the physical mechanism of low intensity EM radiation acting on biological cells. *Biofizika* **44**(3), 555–558.
- Yen-Patton, G., Patton, W., Beer, D., and Jacobson, B. (1988). Endothelial cell response to electromagnetic fields: Stimulation of growth rate and angiogenesis in vitro. *J. Cell Physiol.* **134**, 37–46.
- Yost, M., and Liburdy, R. (1992). Time-varying and static magnetic fields act in combination to alter calcium signal transduction in the lymphocyte. *FEBS Lett.* **296**, 117–122.
- Youbicier-Simo, B., Lebecq, J., and Bastide, M. (1998). Damage of chicken embryos by EMFs from mobile phones: Protection by a compensation antenna. In *Abst. 20th BEMS Annual Meeting, Florida*, pp. 102–104. BEMS.
- Zabusky, N., and Kruskal, M. (1965). Interaction of solitons in a collisionless plasma and the recurrence of initial states. *Phys. Rev. Lett.* **1S**, 240–243.
- Zettle, A. (1993). Making waves with electrons. *Nature* **363**, 496–497.
- Zhadin, M., and Fesenko, E. (1990). Ion cyclotron resonance in biomolecules. *Biomedical Sci.* **1**(3), 245–250.
- Zhadin, M. (1996). Magnetic field effect on the ion motion in a macromolecule: Theoretical analysis. *Biofizika* **41**(4), 832–849.
- Zhadin, M. (2001). Review of Russian literature on biological action of DC and low-frequency AC magnetic fields. *Bioelectromagnetics* **22**(1), 27–45.
- Zhuravlev, A. (1982). Developmetn of B.N. Tarusov's ideas on chain processes biology. In *Bioantioxidizers in Regulation of Metabolism in Healthy and Pathological States* (O. Gulikova, Ed.), pp. 3–37. Nauka, Moscow. [In Russian].
- Zillberman, M. (1992). Effect of geomagnetic activity on the density of true predictions in mass lotteries. *Biofizika* **37**(3), 566–571. [In Russian].
- Zoeger, J., Dunn, J., and Fuller, M. (1981). Magnetic material in the head of the common Pacific dolphin. *Science* **213**(4510), 892–894.
- Zolotaryuk, A., Pnevmatikos, S., and Savin, A. (1991). Charge transport in hydrogen-bonded materials. *Phys. Rev. Lett.* **67**(6), 707–710.
- Zubkus, V., and Stamenkovich, S. (1989). Kinetics of enzyme reactions in alternating electric fields. *Biofizika* **34**(4), 541–544.

## AUTHOR INDEX

- Aarholt, E., 64, 95, 204, 313, 355  
 Adair, R.K., 112, 181, 186  
 Adey, W.R., 50, 69, 76, 111, 355  
 Agadzhanyan, N.A., 108  
 Agulova, L.P., 88  
 Akerstedt, T., 109  
 Akimov, A.E., 339  
 Aksenov, S.I., 334  
 Alexandrov, E.B., 211  
 Andreev, E.A., 354  
 Arber, S.L., 69, 363  
 Asashima, M., 46  
 Astumian, R.D., 126, 133  
 Ayrapetyan, S.N., 339
- Bannikov, V.S., 354  
 Barnes, F.S., 127  
 Bawin, S.M., 50, 69, 76, 98, 319, 363  
 Beischer, D.E., 46  
 Belousov, A.V., 188, 359  
 Belyaev, I.Ya., 28, 41, 47, 59, 182, 204, 302, 317, 355, 371  
 Belyavskaya, N.A., 45  
 Berden, M., 337  
 Berezhinsky, L.I., 334  
 Berg, H., 98, 107, 111, 158, 320  
 Berman, E., 246  
 Bersani, F., 10, 247  
 Beschkov, V.N., 322  
 Betskii, O.V., 353, 359  
 Blackman, C.F., 50, 51, 56, 74, 77, 100, 154, 180, 231, 254, 264, 290, 312  
 Blanchard, J.P., 308  
 Blank, M., 9, 30, 67, 98, 100, 108, 319  
 Bohr, H., 358  
 Boorman, G.A., 9  
 Bowman, J.D., 51  
 Brocklehurst, B., 199  
 Broers, D., 23  
 Burlakova, E.V., 334
- Carlo, G.L., 5  
 Cavopol, A.V., 48  
 Chemeris, N.K., 355  
 Chernavsky, D.S., 356, 358  
 Chew, W.C., 320  
 Chiabrera, A., 51, 155, 168, 181, 185
- Chizhevskii, A.L., 84, 350  
 Cho, M.R., 102  
 Colic, M., 339  
 Collett, T.S., 42  
 Conti, R., 5  
 Cremer-Bartels, G., 51
- Danilov, V.I., 45  
 Davis, A.R., 48  
 Davydov, A.S., 156, 206, 344, 357, 413  
 de Seze, R., 424  
 Del Giudice, E., 157, 377  
 Delgado, J.M.R., 108  
 Deryugina, O.N., 72  
 Devyatkov, N.D., 10, 336, 353  
 Didenko, N.P., 354  
 Dorfman, Ya.G., 151  
 Drissler, F., 373  
 Dubrov, A.P., 43, 84  
 Dutta, S.K., 355
- Edmonds, D.T., 118, 152  
 Eichwald, C., 130  
 Engström, S., 395  
 Eremko, A.A., 357
- Farrell, J.M., 246  
 Fesenko, E.E., 118, 334, 336  
 Feychting, M., 7  
 Fillion-Robin, M., 11  
 Fitzsimmons, R., 100, 319  
 Fomicheva, V.M., 45  
 Fröhlich, H., 156, 357, 375, 415
- Galvanovskis, J., 130  
 Gandhi, Om P., 21  
 Gapeyev, A.B., 355  
 Garcia-Sancho, J., 61, 264, 309  
 Garkavi, L.K., 11  
 Glaser, R., 393  
 Golant, M.B., 353  
 Goldman, R., 319, 321  
 Goodman, R., 53, 248  
 Greene, J.J., 154  
 Greenebaum, B., 40  
 Grigoriev, Yu.G., 6, 364  
 Grundler, W., 118, 130, 199, 204, 354

- Gulyaev, Yu.V., 339, 376  
Gurfinkel, Yu.I., 85
- Heath, C.W., 8  
Henshaw, D.L., 90  
Hoelzel, R., 158  
Hojerik, P., 69  
Huang, R., 103
- Jacobson, J.I., 108  
Jafary-Asl, A.H., 93  
Jenrow, K.A., 69, 154  
Jerman, I., 48  
Jungerman, R.L., 126  
Juutilainen, J.P., 8, 153
- Kaiser, F., 117  
Kalmijn, A.J., 126  
Kashulin, P.A., 46, 89  
Kataev, A.A., 355  
Kato, M., 108  
Kato, R., 44  
Katsir, G., 66  
Kavaliers, M., 73  
Kazachenko, V.N., 335  
Kazarinov, K.D., 359  
Keeton, W.T., 108  
Khizhnyak, E.P., 337, 359  
Kholodov, Yu.A., 10  
Kirschvink, J.L., 41, 116  
Kislovsky, L.D., 69, 339  
Klassen, V.I., 334  
Kobayashi, A.K., 152  
Konyukhov, V.K., 95, 335  
Kopanev, V.I., 43  
Kuznetsov, A.N., 52, 113, 150  
Kvakina, Ye.B., 11
- Lednev, V.V., 47, 51, 72, 76, 96, 172, 173,  
184, 231, 305, 310, 316  
Lee, J.M., 8  
Leucht, Th., 41  
Liboff, A.R., 43, 51, 72, 128, 153, 162, 172,  
237, 307  
Liburdy, R.P., 109  
Lin, H., 289  
Lin, J.C., 9, 48  
Lindstrom, E., 58  
Lissmann, H., 320  
Litovitz, T.A., 65, 253, 289  
Lobyshev, V.I., 336  
Lohmann, K.J., 42  
Luben, R.A., 9  
Lyashchenko, A.K., 359  
Lyle, D.B., 55, 364
- Lyskov, E.B., 51
- Makarevich, A.V., 50  
Malko, J.A., 40  
Markin, V.S., 136  
Markov, M.S., 41  
McLeod, B.R., 52, 73, 228  
McLeod, K.J., 98, 319  
Mild, K.H., 9  
Milham, S. (Jr), 6  
Miller, D.A., 156, 353  
Mooney, N.A., 316  
Moulder, J., 9  
Mullins, J.M., 289  
Muzalevskaya, N.I., 11, 65
- Nakagawa, M., 6  
Nazar, A.S.M.I., 102, 319  
Novikov, V.V., 7, 62, 108
- Opalinskaya, A.M., 88  
Oraevsky, V.N., 86  
Ossenkopp, K.P., 96
- Pandey, S., 336  
Penafiel, L.M., 363  
Petrosyan, V.I., 377  
Phillips, J.L., 248  
Picazo, M.L., 61  
Piccardi, G., 84  
Pilla, A.A., 127  
Piruzyan, L.A., 79, 111  
Plekhanov, G.F., 50  
Plyusnina, T.Yu., 130  
Pokorný, J., 358  
Polk, C., 111, 117, 154, 353  
Popp, F.A., 8  
Prato, F.S., 55, 154, 306, 308  
Presman, A.S., 107, 204  
Prigogine, I., 129
- Rai, S., 49, 334, 336  
Ramundo-Orlando, A., 74  
Raskmark, P., 290  
Rea, W.R., 108  
Reese, J.A., 53  
Reinbold, K.A., 65  
Reiter, R.J., 39  
Repacholi, M.A., 40  
Robinson, K.R., 136  
Ross, S.M., 154, 244, 307  
Ružič, R., 48, 75, 338  
Ruhenstroth-Bauer, G., 89  
Ryaby, J.T., 11

- Saali, K., 51  
Sage, C.L., 7  
Savin, A.V., 206  
Schimmelpfeng, J., 98, 154, 243  
Scott, A.C., 375, 414  
Semm, P., 42, 148  
Serpersu, E.H., 97  
Shakula, A.V., 43  
Shaya, S.Y., 94  
Shemii-Zade, A.E., 90  
Sheppard, A., 10  
Shilov, V.N., 48  
Shirahata, S., 337, 351  
Shnoll, S.E., 91  
Sienkiewicz, Z.J., 264  
Simko, M., 30  
Simon, N.J., 113  
Sisken, J.E., 71  
Sitko, S.P., 354  
Smith, C.W., 94  
Smith, O.M., 315  
Smith, R.F., 290  
Smith, S.D., 52, 70, 78  
Smolyanskaya, A.Z., 356  
Sollazzo, V., 248  
Sontag, W., 105  
Spadinger, I., 61  
Stoneham, M.E., 373
- Takahashi, K., 246  
Tenforde, T.S., 6  
Thomas, J.R., 74, 77, 290  
Thompson, C.J., 360  
Tofani, S., 59  
Trillo, M.A., 75, 231, 313  
Trukhanov, K.A., 424  
Tsong, T.Y., 134  
Tuszynski, J.A., 419  
Tyasto, M.U., 89
- Ueno, S., 9  
Usacheva, M.D., 48
- Villoresi, G., 87  
Vitiello, G., 378  
Vladimirkii, B.M., 91
- Walleczek, J., 247  
Warnke, U., 8  
Weaver, J.C., 136  
Webb, S.J., 353, 373  
West, R.W., 109  
Wilson, B., 8  
Wu, T.M., 118, 375
- Yano, A., 49  
Youbicier-Simo, B.J., 109
- Zhadin, M.N., 118, 185  
Ziskin, M., 337  
Zolotaryuk, A.V., 206  
Zubkus, V.E., 188, 359

## SUBJECT INDEX

- aeroions, 6
- alpha-spiral, 206, 412
- amino acids, 34, 63, 92, 122, 356, 385, 412
- approximation
  - continuum, 115
  - semiclassical, 23, 124, 189, 228, 372
- atmospherics, 89
  
- Bernal–Fowler rules, 343, 350
- biological rhythms, 30, 36, 46, 52, 85, 87, 88, 91, 369
- biomembrane, 69, 97, 106, 109, 118, 125, 131, 132, 135, 136, 147, 154, 157, 247, 272, 280, 334, 340, 355, 356, 358, 359, 393, 410
  
- cancer, 7, 84, 90, 109
- cells
  - E. coli*, 41, 47, 59, 64, 78, 183, 302, 318, 354, 361, 373
  - cancer, 55, 61, 84, 97, 364
- coherent excitations, 357, 378, 415
- conductivity, 22, 341
  - amino acid, 63
  - electronic, 159, 349
  - ion channel, 68, 133, 148
  - ionic, 281, 349
  - medium, 21, 102, 106, 131, 159, 320
  - membrane, 131, 347
  - super, 156, 423
  - water, 121, 340
  
- de Broglie wave, 210, 215, 393
- defects of water structure, 336, 340, 343, 345, 350
  
- density
  - current, 99, 106, 155, 319, 339, 378
  - MF energy, 203
  - probability, 189, 207, 212, 215, 408
- density matrix, 173, 219, 365
- diamagnetism, 149, 156, 161
- dipole field, 283, 424
- distribution
  - Boltzmann, 133, 144, 149, 150, 357, 374, 375
  - Bose–Einstein, 358, 374, 378
  - Planck, 417
  
- eddy currents, 19, 113, 153, 186, 244
- effect
  - Aharonov–Bohm, 423
  - biological, for rotation in an MF, 273
  - Josephson, 156, 421
  - Kirlian, 337
  - Mössbauer, 354
  - Meissner, 419
  - Paschen–Back, 192
  - Stark, 25, 275
  - Zeeman, 25, 316
    - abnormal, 192, 294
    - normal, 192
- Einstein relation, 281
- electrochemical EMF effects, 19, 22, 98, 117, 136, 155, 244
- electromagnetic pollution, 3
- electron, 17, 47, 92, 114, 120, 147, 149, 151, 157, 163, 173, 180, 188, 190, 193, 195, 211, 284, 303, 325, 334, 347, 350, 377, 401, 406, 419, 422
- EM safety standards, 5, 11, 22, 244
- enzyme, 1, 8, 30, 64, 65, 67, 68, 94, 100, 102, 107, 118, 131, 135, 188, 203, 214, 253, 267, 289, 314, 319, 321, 323, 337, 350
  
- equation(s)
  - Arrhenius, 144
  - continuity, 155
  - d’Alembert, 378
  - Dirac, 189
  - Hill, 169
  - Langevin, 186, 206, 384
  - Liouville, 174
  - Mathieu, 187
  - Maxwell, 19, 123
  - Pauli, 292
  - Schrödinger, 23, 389, 420
    - non-linear, 331, 413
    - van’t Hoff, 134
- equilibrium
  - biochemical, 79, 121, 172, 351
  - dynamic, 117, 128, 142, 180, 225
  - stoichiometric, 351
  - thermodynamic, 125, 133, 149, 203, 227, 372, 409

- Faraday cage, 285
- field gradient  
   electric, 206, 277, 280, 281, 292, 319, 320, 378, 410  
   magnetic, 39, 48, 58, 76
- fluxoid, 421
- formula  
   Langevin, 150  
   Nyquist, 125, 127, 136  
   of experiment, 39  
   Planck, 362  
   Rayleigh–Jeans, 363
- frequency  
   cyclotron, 2, 119, 128, 162, 227, 237, 254, 267, 285, 326  
   gyral, 390  
   Larmor, 170, 187, 219, 232, 253, 266, 268, 270  
   NMR, 63, 77, 78, 94, 120, 297, 326  
   Rabi, 197, 405
- fullerenes, 213
- gauge transformation, 23, 420
- geoelectric field, 285
- geomagnetic field, 8, 14, 17, 36, 41, 43, 63, 77, 80, 84, 106, 171, 193, 203, 253, 408
- GMF vector orientation, 43, 82, 253
- gravity, 380
- gyro, 379
- gyromagnetic ratio, 161, 217, 299
- harmonics, subharmonics, 52, 68, 71, 73, 100, 130, 163, 178, 248, 253, 277, 325, 393
- helicity, 372
- homeopathy, 11, 333
- hydroaeroions, 350
- hydrogen, 77, 80, 166, 246, 290, 297, 301, 313, 316, 326, 343, 347, 351  
   atomic, 214, 338, 339, 349
- hydrogen peroxide, 339, 351
- hydrophobic forces, hydration, 171, 340, 343, 359
- hyperweak MF, 107, 156, 270, 421
- interaction  
   Coulomb, 194, 284, 350  
   dipole–dipole, 95, 206, 346, 357  
   hyperfine, 197  
   spin–orbit, 189, 191, 192, 206, 293, 400
- ion  
   QM object, 212, 215, 224  
   radical, 196, 347, 351  
   zwitter, 64, 391
- ion channel, 68, 69, 73, 102, 116, 125, 133, 147, 164, 334, 355
- ion mobility, 206, 281, 292, 379
- ion–isotope constant, 191–193, 297, 400
- isotopes, 68, 92, 97, 191, 326, 349, 354
- Larmor theorem, 118, 187
- Lennard–Jones potential, 384
- liquid crystals, 113, 152
- Lorentz force, 115, 159, 160, 162, 165, 169, 182, 185, 189
- magnetic storms, 6, 10, 80, 85, 87, 108, 122
- magnetic susceptibility, 149, 161, 218
- magnetic vacuum, 2, 17, 44, 213, 239, 270, 271, 316, 393
- magnetoreception, 14
- magnetotropism, 49
- MBE maximum reversal, 237
- measurement, 120, 167, 179, 205, 211, 298
- melatonin, 8, 109, 199
- metastable state, 95, 113, 121, 206, 207, 213, 214, 225, 329, 332, 342, 343, 347, 353, 377
- microwaves, 10, 15, 27, 28, 30, 50, 69, 110, 115, 118, 123, 289, 292, 330, 334, 336, 341, 353, 390, 423
- mobility of ion, 353
- moment  
   electric dipole, 25, 134, 145, 159, 173, 276, 282, 320, 356, 357, 371, 378, 379, 381, 411, 413, 416  
   induced, 149, 153, 284  
   magnetic, 17, 120, 148, 152, 190, 192, 298, 340, 424  
   orbital, 192, 256  
   spin, 92, 192, 206, 217, 292, 316, 377, 379, 400, 406  
   total, 371
- momentum  
   angular, 331, 372, 379, 399  
   orbital, 161, 218  
   total, 191, 293
- near zone, 19, 27
- noise, 29, 128, 136, 137, 322  
   electric, 125, 322  
   magnetic, 4, 89, 286  
   thermal, 117, 127, 204  
   white, 65, 145, 384
- nucleic acids, 32, 46, 107, 134, 153, 154, 183, 186, 246, 248, 267, 318–320, 325, 358
- orthomolecular diagnostics, 92

- paramagnetism, 151  
permeability, 17  
permittivity, 22, 26, 93, 106, 126, 131, 283,  
320, 337, 342, 359, 376, 410  
peroxide oxidation of lipids, 48, 351  
polarizability, 284  
precession, 195, 299, 300, 379, 405  
proton, 75, 93, 121, 188, 205, 211, 274, 292,  
297, 298, 301, 319, 333, 336,  
342, 344, 353, 379
- radiation  
  circularly polarized, 108, 263, 370  
  damping, 381  
  thermal, 362, 376  
  wideband, 173, 179, 360, 365  
radon, 6, 90  
random process, 59, 80, 125, 137, 187, 238,  
286, 287, 322, 380  
relaxation  
  Debye, 341, 343, 376  
  spin, 144, 206, 225, 292  
rotations, 19, 95, 149–151, 187, 207, 240,  
282, 300, 335, 356, 378, 405  
  biosystems, 271, 274, 369  
  coordinate system, 213, 267, 403  
  macromolecules, 120, 267, 285, 312, 319,  
323, 369  
  magnetic field, 38, 256, 263, 268, 403
- singlet–triplet states, 95, 194, 346, 351  
soliton, 156, 206, 331, 344, 357, 375  
spin, 77, 92, 118, 120, 144, 149, 188, 191,  
205, 218, 298, 300, 345, 351,  
354, 400, 403  
  electron, 194, 195  
  nuclear, 121, 124, 190, 218, 327, 333  
SQUID, 142, 156, 421  
superposition of quantum states, 173, 207,  
210, 226, 260, 293, 404
- theoretical predictions, 228, 249, 265, 271,  
273, 274, 285, 289, 297, 368, 369  
thermalization, 206, 385  
torque, 116, 148, 153, 161, 282, 379
- uncertainty principle, 166, 211, 380
- van der Waals forces, 382  
vector potential, 23, 26, 190, 386, 390, 420,  
424
- water, 340, 359, 376, 379  
  *n*-dimensional clusters, 121, 342  
  non-stoichiometric, 349  
  spin-modified, 96, 336  
  Watson–Crick pairs, 392